Aus dem Physiologischen Institut der
Justus-Liebig-Universität Gießen
Direktor: Prof. Dr. med. Dr. h.c. Rainer Schulz

Die Pathophysiologie des chronisch druckbelasteten Myokards: Neue Therapieoptionen der hypertensiven Herzkrankheit

Habilitationsschrift
zur Erlangung der Venia legendi
des Fachbereichs Medizin
der Justus-Liebig-Universität Gießen

vorgelegt von
Dr. med. Rolf Schreckenberg
Gießen 2020

Inhaltsverzeichnis

Abkürzungsverzeichnis

CaSR	**Calcium-sensing Rezeptor**
GRK	**G-Protein gekoppelte Rezeptorkinase**
HFpEF	**Herzinsuffizienz mit erhaltener Auswurffraktion**
HFrEF	**Herzinsuffizienz mit reduzierter Auswurffraktion**
IPC	**ischämisches pre-conditioning**
IPoC	**ischämisches post-conditioning**
LOX	**Lysyloxidase**
NO	**Stickstoffmonoxid**
PAH	**pulmonal-arterielle Hypertonie**
PKA	**Proteinkinase A**
PKC	**Proteinkinase C**
PTH	**Parathormon**
PTHrP	**Parathormon related Peptide**
RAAS	**Renin-Angiotensin-Aldosteron-System**
RAMP	**Receptor Activity Modifying Protein**
ROS	**reaktive Sauerstoffspezies**
SOD	**Superoxiddismutase**
TNF-α	**Tumornekrosefaktor alpha**

1. Einleitung

1.1 Die hypertensive Herzkrankheit

Als zentrales Organ des Blutkreislaufs ist das Herz maßgeblich an der Aufrechterhaltung und Stabilität der Hämodynamik in den arteriellen und venösen Abschnitten des Gefäßsystems beteiligt. Diese Aufgabe muss das Herz über 24 Stunden täglich, ohne Unterbrechung erfüllen. In dieser Zeit schlägt es ca. 115.000-mal und befördert so etwa 8000 Liter Blut durch seine beiden Herzkammern.[1]

Um diese Leistung erbringen zu können werden besondere Anforderungen an das Herz gestellt: Die Kontraktion und Relaxation des Myokards sollen rasch und autonom erfolgen, gleichzeitig müssen die Herzrate, die Auswurffraktion sowie der entwickelte Druck stets den Bedürfnissen der Peripherie angepasst werden. Hauptrisikofaktor für die kardiale Funktion: Die arterielle Hypertonie.

Die Pathogenese der hypertensiven Herzkrankheit

Aktuellen Schätzungen zufolge wird die Zahl hypertensiver Patienten im Jahr 2025 auf weltweit ca. 1,6 Mrd. ansteigen. Die chronische arterielle Hypertonie zählt somit zu den wichtigsten eigenständigen Risikofaktoren für das gesamte Herz-Kreislaufsystem und ist von zentraler Bedeutung für die kardio-vaskuläre Morbidität und Mortalität.[2]

Ausgangspunkt zahlreicher Herz-Kreislauferkrankungen ist häufig ein strukturell umgebautes und geschädigtes Gefäßbett.[3] Das Ausmaß des vaskulären Remodelings korreliert direkt mit dem kardio-vaskulären Risikoprofil betroffener Patienten. Basierend auf einer Vielzahl epidemiologischer und klinischer Studien konnte die arterielle Hypertonie als wichtigster Risikofaktor für atherosklerotische Gefäßveränderungen in der Peripherie sowie der Koronarstrombahn identifiziert werden.[4,5] Darüber hinaus verursacht die chronische Blutdruckerhöhung in beiden Ventrikeln eine myokardiale Hypertrophie, auf Ebene der Vorhöfe häufig eine Dilatation. In ihrer Gesamtheit lassen sich die Hypertonie-bedingten kardialen Schädigungen unter der Bezeichnung „ICD-10 Code I11“ bzw. „hypertensive Herzkrankheit“ zusammenfassen.[6,7]

Die komplexe Symptomatik der hypertensiven Herzkrankheit manifestiert sich klinisch als Herzinsuffizienz oder Angina pectoris und kann darüber hinaus die Inzidenz ventrikulärer

Rhythmusstörungen erhöhen und den plötzlichen Herztod verursachen. Ätiologisch liegen den unterschiedlichen Krankheitsbildern und Verlaufsformen strukturelle und funktionelle Schädigungen des Myokards zugrunde, die durch Co-Morbiditäten, prädisponierende Risikofaktoren und die Familienanamnese beeinflusst werden.

Vaskulär begünstigt die arterielle Hypertonie sowohl die Arteriosklerose der epikardial gelegenen Makrostrombahn als auch die endotheliale Dysfunktion der Mikrozirkulation, die sich vorrangig durch eine Mediawandverdickung sowie eine perivaskuläre Fibrose auszeichnet. Die klinische Manifestation dieser vaskulären Umbauvorgänge entspricht der koronaren Herzkrankheit, die bereits im Frühstadium aufgrund endothelialer Dysfunktionen die koronare Flussreserve signifikant einschränkt.[8,9]

Die Zunahme des peripheren Gefäßwiderstandes als pathomorphologisches Korrelat der arteriellen Hypertonie führt hämodynamisch unmittelbar zum Anstieg der kardialen Nachlast; das Myokard reagiert auf die systolische Druckbelastung sowie die daraus resultierende Erhöhung der ventrikulären Wandspannung mit der Ausbildung einer konzentrischen Hypertrophie.

Die chronische Überfunktion des hypertrophen Myokards verursacht auf myozytärer Ebene subletale Zellschädigungen sowie zur Stabilisierung der Funktion die Bildung neuer, parallel angeordneter Sarkomere.

Wird das kritische Herzgewicht durch anhaltende Wachstumsstimuli (Wandspannung, neurohumorale Mediatoren) überschritten, kann es zur Dekompensation der bislang adaptiven Prozesse kommen.[10] Das Koronarsystem ist außer Stande, den Energiebedarf des hypertrophierten Myokards zu decken; die Leistungsreserven werden bereits in Ruhe maximal ausgeschöpft, bei zusätzlicher Belastung kann die Perfusion nicht mehr adäquat gesteigert werden. Das Risiko kardio-vaskulärer Ereignisse ist bei Hypertonikern mit diagnostizierter linksventrikulärer Hypertrophie um das 2-fache erhöht, das Mortalitätsrisiko je nach klinischer Studie um den Faktor zwei bis vier.[11]

Die chronische Herzinsuffizienz

In ca. 80 % der Fälle wird die Kombination aus arterieller Hypertonie und koronarer Herzkrankheit als Ursache für die Entwicklung einer chronischen Herzinsuffizienz

verantwortlich gemacht. Unter pathophysiologischen Gesichtspunkten lässt sich die Herzinsuffizienz als komplexes Syndrom definieren, dem ursächlich eine Funktionsstörung des Myokards zugrunde liegt. Als unmittelbare Konsequenz resultiert das Unvermögen des Herzmuskels, die Gewebe mit ausreichend Blut und damit auch Sauerstoff zu versorgen. Die Folgen dieser ungenügenden Körper- bzw. Organperfusion führen zu den charakteristischen, nicht jedoch spezifischen Symptomen wie Dyspnoe, Leistungsabnahme, Müdigkeit und Flüssigkeitsretention (klinische Definition der Herzinsuffizienz).

Zu Beginn einer chronischen Herzinsuffizienz wird das Herzminutenvolumen durch unterschiedliche Adaptionsmechanismen aufrechterhalten, die kurzfristig zu einer Kompensation beitragen können, langfristig jedoch in einem Circulus vitiosus enden und selbst zur Progression und Dekompensation der Herzinsuffizienz beitragen können. Zu den initialen Kompensationsmechanismen zählen ein Anstieg der Herzrate sowie die dauerhafte Aktivierung des Frank-Starling-Mechanismus.[10,12]

In dem bereits insuffizienten Myokard führt diese Situation allerdings unmittelbar zu einer Steigerung des Sauerstoffbedarfs bei gleichzeitig reduzierter kapillärer Durchblutung, da besonders subendokardial gelegene Gefäße durch die hohen Füllungsdrücke während der Diastole komprimiert werden. Darüber hinaus kann die zunächst funktionelle Dilatation des Herzmuskels in eine „Gefügedilatation“ übergehen, die durch ein strukturell umgebautes Myokard mit reduzierter Elastizität sowie Kontraktilität gekennzeichnet ist.[12]

Wichtige Neuerungen in den Leitlinien der Europäischen Gesellschaft für Kardiologie (ESC) zur Diagnostik und Behandlung der akuten und chronischen Herzinsuffizienz betreffen nicht nur Anpassungen bestehender Definitionen, zuletzt wurde die Terminologie um eine dritte Entität erweitert, der Herzinsuffizienz mit mäßiggradig eingeschränkter Ejektionsfraktion (HFmrEF). Per Definition erfordert die Diagnose einer Herzinsuffizienz mit reduzierter Ejektionsfraktion (HFrEF) eine entsprechende klinische Symptomatik sowie eine linksventrikuläre Auswurffraktion <40 %; die Kriterien zur Diagnose einer HFmrEF umfassen eine Auswurffraktion von 40-49 % und darüber hinaus das Vorliegen erhöhter BNP-Spiegel, struktureller Schädigungen sowie diastolischer Funktionsstörungen. Die HFpEF wird bei vergleichbaren Kriterien und einer Ejektionsfraktion ≥50 % diagnostiziert.[13,14]

Das akute Koronarsyndrom

Noch immer lassen sich 20 % aller Todesfälle in Europa auf eine Form der ischämischen Herzerkrankung zurückführen.[15] Pathophysiologisch liegt den kardialen Ereignissen das akute Koronarsyndrom zugrunde, das die Entitäten Nicht-ST-Hebungsinfarkt (NSTEMI), ST-Hebungsinfarkt (STEMI) sowie instabile Angina pectoris (instabile AP) umfasst.[16]

Die koronare Perfusionsstörung verursacht zunächst unter körperlicher Belastung, mit zunehmender Progression bereits in Ruhe die typische Symptomatik einer Angina pectoris mit „Engegefühl und Druck“ in der Brust sowie Kurzatmigkeit und Luftnot.

Die sichere Abgrenzung der Angina pectoris zu NSTEMI bzw. STEMI erfordert diagnostisch die Beurteilung der klinischen Symptomatik, die Bestimmung kardialer Biomarker (vorzugsweise kardiales Troponin; [cTn]) sowie die Auswertung des EKGs. Im Gegensatz zum Myokardinfarkt sind die Laborbefunde bei instabiler AP unauffällig. Ein Anstieg des kardialen Troponins über die 99th Perzentile des oberen Sollwerts in Verbindung mit thorakalen Beschwerden und Auffälligkeiten im EKG weisen auf ein akutes atherothrombotisches Ereignis hin. Ein Myokardverlust sowie Wandbewegungsstörungen in der kardialen Bildgebung oder der Nachweis eines intrakoronaren Thrombus in der Koronarangiografie sichern die Diagnose ab.[17,18]

Die Klassifikation des Myokardinfarktes nach Thygesen et al. umfasst fünf Typen; im klinischen Alltag spielt hinsichtlich der zu treffenden Therapiemaßnahmen die Unterscheidung zwischen Typ 1 und Typ 2 Infarkten eine wichtige Rolle.[19,20]

Im Gegensatz zum „klassischen“ Myokardinfarkt (Typ 1), der durch eine akute Plaqueerosion bzw. Plaqueruptur sowie ein thrombotisches Ereignis verursacht wird, können dem Typ 2 Infarkt zahlreiche Ursachen zugrunde liegen, die ein Missverhältnis zwischen myokardialem Sauerstoffangebot (Hypoxämie, Anämie, endotheliale Dysfunktion, Koronarspasmen) und Sauerstoffbedarf (Tachykardie, hypertensive Krise, Sepsis) hervorrufen.[21,22]

1.2 Der Risikofaktor Bluthochdruck

Eine der Hauptursachen für die hohe Inzidenz der Herz-Kreislauferkrankungen in den westlichen Industrieländern liegt in der hohen Prävalenz der arteriellen Hypertonie. Aktuelle Studien gehen davon aus, dass weltweit annähernd ein Drittel der erwachsenen Bevölkerung

entsprechend den Grenzwerten aktueller Leitlinien einen Bluthochdruck aufweist.[23] Die arterielle Hypertonie steht als Hauptrisikofaktor in direktem Zusammenhang mit der Pathogenese der koronaren Herzkrankheit, der Herzinsuffizienz und des Myokardinfarktes. Mit einer konsequenten antihypertensiven Therapie ließe sich folglich die kardio-vaskuläre Morbidität und Mortalität der Patienten entscheidend reduzieren. Neben einer medikamentösen Intervention wird als Grundlage einer antihypertensiven Therapie generell eine entsprechende Anpassung der Lebensweise empfohlen.

In den USA bereits seit 2017 auf 130/80 mmHg gesenkt, hat sich die etablierte Definition des Bluthochdrucks in Europa nach Vorgaben der ESC/ESH auch in den Leitlinien des Jahres 2018 nicht verändert.[24-26] Wie zuvor differenziert die aktuelle Leitlinie zwischen einem optimalen Blutdruckbereich (<120/80 mmHg), einem normalen (120-129/80-84 mmHg) und einem hochnormalen (130-139/85-89 mmHg). Ebenfalls unverändert wird der Beginn einer antihypertensiven Therapie bei Druckwerten von ≥140/90 mmHg empfohlen – und das zunächst ausschließlich über Lebensstil-modifizierende Maßnahmen. Erst bei Werten ≥160/100 mmHg sollte die medikamentöse Therapie unmittelbar initiiert werden; die Ausnahme bilden Patienten mit sehr hohem kardio-vaskulären Risiko, bei denen eine medikamentöse Therapie ab Blutdruckwerten von 135-139/85-89 mmHg indiziert ist .[27]

Als Reaktion auf die Ergebnisse der SPRINT-Studie haben die europäischen Fachgesellschaften den Zieldruckkorridor jedoch signifikant reduziert. Unabhängig vom Alter sowie bestehender Begleiterkrankungen sollen diastolische Druckwerte von 70-80 mmHg angestrebt werden; systolisch wurde der Zielbereich für Patienten unter 65 Jahren um 10 mmHg auf 120-130 mmHg gesenkt.[28] Übereinstimmend haben zahlreiche neue Metaanalysen eine optimale Risikoreduktion kardio-vaskulärer Ereignisse innerhalb des neu definierten Zielbereichs bestätigen können.[29-31]

Sowohl europäische als auch US-amerikanische Fachgesellschaften empfehlen zur medikamentösen Therapie des Bluthochdrucks weiterhin AT_1-Rezeptorblocker, ACE-Hemmer, Calciumantagonisten, Diuretika sowie Betablocker.[24,26]

Die Therapieschemata sind jedoch einem radikalen Strategiewechsel unterzogen worden; bereits die Initialbehandlung soll aus einer 2-fach-Kombination bestehen, die, falls erforderlich, um ein drittes Medikament erweitert werden müsse. Patienten, die unter ausreichend hoch dosierter 3-fach-Kombination den neu definierten Zielbereich nicht

erreichen, werden als therapieresistent eingestuft und sollen zusätzlich den Aldosteronantagonisten Spironolacton erhalten.

Zur Verbesserung der Therapietreue wird darüber hinaus die Verwendung von Fixdosis-Kombinationen, sog. „single pill combinations“ (2-3 blutdrucksenkende Substanzen in einer Tablette) empfohlen.[32]

Unter Berücksichtigung einer hohen Dunkelziffer wird die Hälfte aller Hypertoniepatienten nicht oder nicht ausreichend behandelt.[33,34]

1.3 Zukünftige Therapiestrategien – individuell statt allgemein

Als Reaktion auf die zuvor beschriebenen strukturellen und funktionellen Schädigungen des chronisch druckbelasteten Myokards werden vom Körper Kompensationsmechanismen initiiert, die eine Aufrechterhaltung des Blutdrucks und der Organperfusion sicherstellen sollen. Neben dem sympathischen Anteil des vegetativen Nervensystems wird insbesondere das Renin-Angiotensin-Aldosteron-System, kurz RAAS, aktiviert.[35] Darüber hinaus werden die Synthese und Sekretion (neuro-) humoraler Faktoren induziert, die bzgl. ihrer Effekte zur Gruppe der Vasokonstriktoren, Vasodilatatoren und der Zytokine gezählt werden. Während der Progression einer Herzinsuffizienz überwiegt generell der Anteil an Mediatoren, die vasokonstriktorische sowie positiv chronotrope und inotrope Effekte vermitteln.[36]

Eine unproportionale und dauerhafte Aktivitätssteigerung des RAAS bzw. des sympathischen Nervensystems soll der nachlassenden Pumpfunktion des Myokards entgegenwirken. Vermag die Aktivierung dieser Systeme zwar kurzfristig zur Kompensation beitragen, induzieren sie jedoch langfristig ein funktionelles und strukturelles Remodeling, das die Progression der kardialen Insuffizienz zusätzlich beschleunigt.

Hohe Angiotensin II- und Aldosteron-Spiegel erhöhen nicht nur durch Steigerung der Vor- und Nachlast den Energiebedarf des insuffizienten Myokards, über direkte Stimulation ihrer jeweiligen Rezeptoren beschleunigen sie lokal die Progression kardialer Umbauvorgänge. Eine dauerhafte Sympathikusaktivierung steigert ebenfalls den Energieverbrauch, reduziert durch Anstieg der Herzrate die Perfusionszeit der Koronarien und hat darüber hinaus arrhythmogene Wirkung.

Über die Hemmung Angiotensin II-abhängiger Effekte senken ACE-Inhibitoren und AT_1-Antagonisten sowohl Vor- als auch Nachlast und verringern indirekt die Synthese von Aldosteron. Ihr kardioprotektives Potential vermitteln beide Wirkstoffgruppen nicht nur über ihren Einfluss auf die Hämodynamik, durch Reduktion der lokalen Angiotensin- und Aldosteronwirkungen verbessern sie das kardiale Remodeling auch auf zellulärer Ebene.[37,38]

Die genauen Mechanismen, über die β_1-spezifische Rezeptorblocker ihre Effekte vermitteln, sind bis heute nur unvollständig verstanden. Zu den gut dokumentierten kardioprotektiven Wirkungen zählen ihre negativ chronotropen und anti-arrhythmogenen Eigenschaften. Über die reine Blockade β_1-adrenerger Rezeptoren hinaus, tragen Betablocker möglicherweise zu einer Resensitivierung des kardialen beta-adrenergen Systems bei; ein Mechanismus, der ebenfalls zur Verbesserung der klinischen Symptomatik beitragen könnte.[39]

Zusammen mit den Mineralkortikoid-Rezeptorantagonisten und den Angiotensin-Rezeptor-Neprilysin-Inhibitoren stehen somit Vertreter aus fünf Substanzklassen zur Verfügung, die alleine oder in Kombination verabreicht, aktuell das Fundament der medikamentösen Herzinsuffizienztherapie bilden.[40]

Ihre Effizienz bzgl. Gesamtmortalität, kardio-vaskulärer Mortalität und Hospitalisierung wurde in großen klinischen Studien sowohl an Kollektiven herzinsuffizienter Patienten als auch an Patienten nach Myokardinfarkt unlängst nachgewiesen.

2. Hypothese und Zielsetzung

Mit dem aktuellen Repertoire an medikamentösen Therapieoptionen lassen sich die systemischen und lokalen Effekte des vegetativen Nervensystems sowie des RAAS dauerhaft reduzieren; spezifische Pathomechanismen innerhalb des Myokards, die an der Pathogenese und Progression der kardialen Symptomatik maßgeblich beteiligt sind, werden jedoch nicht oder nur unzureichend erfasst.

HINTERGRUND

- ***Für Patienten mit diagnostizierter HFpEF steht aktuell keine effiziente Medikation zur Verfügung.***[41,42]
- ***Für das post-ischämische Myokard stellen besonders die ersten Minuten nach Beginn der Revaskularisation einen relevanten Interventionszeitraum dar, in dem zugrunde liegende Signalmechanismen des Reperfusionsschadens effizient beeinflusst werden können; die Frühphase der Reperfusion ist als therapeutisches Fenster klinisch noch immer ungenutzt.***[43,44]
- ***Zahlreiche Therapiestrategien für den insuffizienten rechten Ventrikel sind ohne Nachweis ihrer therapeutischen Effizienz aus den Leitlinien zum linken Ventrikel übernommen worden.***[45]

HYPOTHESE

Jeder Verlaufsform der hypertensiven Herzkrankheit liegen spezifische Signalwege und Schlüsselmechanismen zugrunde, die maßgeblich am funktionellen und strukturellen Remodeling des Myokards beteiligt sind. Über die Erforschung molekularer und zellphysiologischer Pathomechanismen lassen sich therapeutische Targets identifizieren, die eine effiziente Therapie der individuellen Symptomatik ermöglichen. Nach eingehender Diagnostik und erfolgter Klassifikation führt eine zielgerichtete Intervention in Verbindung mit der aktuell empfohlenen (Basis-) Therapie zu einer signifikanten Verbesserung der Prognose kardio-vaskulärer Erkrankungen.

FORSCHUNGSZIEL

Die Zielsetzung dieser Arbeit besteht darin, an Modellen der Links- (HFrEF, HFpEF) bzw. Rechtsherzinsuffizienz sowie der myokardialen Ischämie und Reperfusion spezifische Pathomechanismen zu identifizieren, die zur Entwicklung neuer und innovativer Behandlungsstrategien der hypertensiven Herzkrankheit beitragen können.

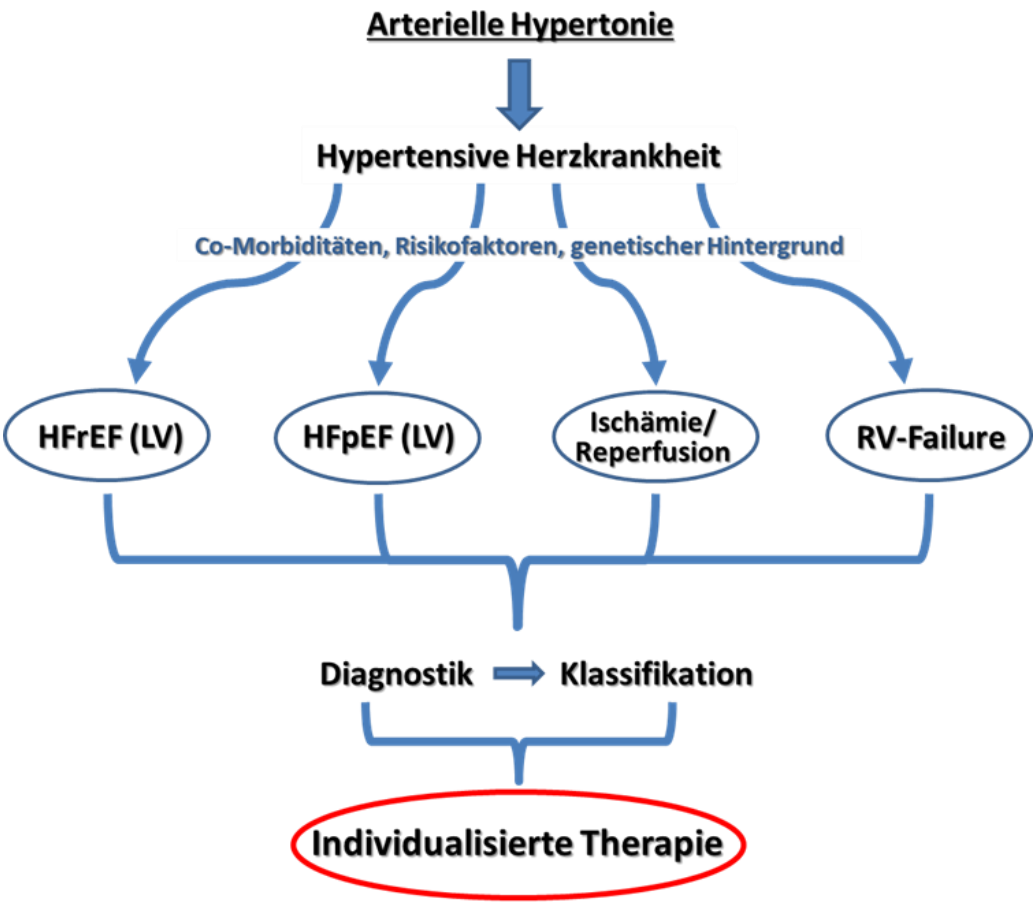

Abb. 1: Die Symptomatik der hypertensiven Herzkrankheit. Individuelle Pathomechanismen der unterschiedlichen Verlaufsformen eröffnen neue Perspektiven für kardiale Therapiekonzepte.

Die Habilitationsschrift fokussiert in vier eigenständigen, identisch aufgebauten Kapiteln auf die wichtigsten Entitäten der hypertensiven Herzkrankheit (siehe Abb. 1). Die Überschriften sämtlicher Abschnitte, in denen eigene Befunde präsentiert und diskutiert werden, weisen durch den Zusatz der entsprechenden Referenzen (Ref.: RS1 bis RS20) auf die zugrunde liegenden Originalarbeiten hin.

Aufgrund der heterogenen klinischen Symptomatik erfolgt in jedem Kapitel sowohl eine Darstellung des jeweiligen Krankheitsbildes als auch der verwendeten Methoden und Modelle, anhand derer spezifische, an der Pathogenese und Progression der jeweiligen Verlaufsform beteiligte Signalwege und Schlüsselmechanismen identifiziert werden konnten.

Die einleitende Abbildung (Abb. 1) wird in der abschließenden Zusammenfassung um die eigenen Befunde ergänzt (siehe Abb. 8) und leitet in die Schlussfolgerung über.

3. Ergebnisse und Diskussion (Synopsis der Originalarbeiten)

3.1 Die Herzinsuffizienz mit reduzierter Auswurffraktion (HFrEF)

Die Framingham-Herz-Studie hat als wichtigste Auslöser bzw. Risikofaktoren einer Herzinsuffizienz in absteigender Reihenfolge bzgl. ihrer Prävalenz die Hypertonie, die koronare Herzerkrankung, den Diabetes mellitus, Herzklappenerkrankungen und die linksventrikuläre Hypertrophie identifiziert.[46]

Zur Aufrechterhaltung einer bedarfsgerechten Durchblutung der gesamten Peripherie wird die kardiale Funktion permanent an die jeweils erforderliche Situation angepasst. Neben autonomen Regelmechanismen (Frank-Starling, Bowditch) wird die Herzfunktion durch eine intensive autonome Innervation sowie durch zahlreiche humorale Faktoren kontinuierlich beeinflusst. Ca^{2+}-Ionen und das Ca^{2+}-Sensing spielen dabei im gesamten kardio-vaskulären System eine entscheidende Rolle. Fundierte Kenntnisse über die zellulären und molekularen Regulationsmechanismen des Ca^{2+}-Haushalts stellen wiederum die Grundvoraussetzung dafür, spezifische Pathomechanismen und darüber hinaus Interventionsmöglichkeiten zu identifizieren, die zur Aufrechterhaltung und Stabilität der Hämodynamik im Herz-Kreislaufsystem unerlässlich sind.[RS5]

Im Gegensatz zu den gut charakterisierten Eigenschaften klassischer Ca^{2+}-Handlingproteine ist der Einfluss des kardial exprimierten Calcium-sensing Rezeptors (CaSR) auf funktionelle und metabolische Prozesse des Myokards weitestgehend unbekannt.

Die Pathogenese einer HFrEF

Für die Herzinsuffizienz mit reduzierter systolischer Pumpfunktion gibt es eine weitreichende Übereinstimmung bzgl. der zugrunde liegenden Pathomechanismen. Schädigende Stimuli wie eine Ischämie, inflammatorische Prozesse oder zelltoxische Mediatoren wirken auf das Myokard und induzieren auf zellulärer Ebene ein Remodeling, das direkt die Kontraktion und metabolische Funktion des einzelnen Myozyten beeinträchtigt.

Der gestörte Zellstoffwechsel, eine erhöhte Radikalbildung und Veränderungen im Ca^{2+}-Haushalt führen mittel- und langfristig zu einer erhöhten myozytären Apoptose- und Nekroserate sowie einer Induktion der Autophagozytose. Im weiteren Verlauf induzieren auto- und parakrine Faktoren sowie (neuro-) humorale Mediatoren des RAAS und

autonomen Nervensystems in Kardiomyozyten, Endothelzellen und Fibroblasten ein Remodeling, das die Progression der Herzinsuffizienz im Sinne eines Circulus vitiosus weiter beschleunigt.

KAPITEL 3.1 – KEY POINTS

Im folgenden Kapitel werden zunächst die Struktur und die Funktionsweise des CaSR sowie seine Rolle bei der Aufrechterhaltung einer globalen Ca^{2+}-Homöostase beschrieben. Das spezifische Aufgabenspektrum des CaSR innerhalb des kardio-vaskulären Systems sowie sein Stellenwert als therapeutisches Target werden in den nachfolgenden Abschnitten erläutert und diskutiert.

FRAGESTELLUNG

Trägt der Einfluss des CaSR auf die myozytäre Ca^{2+}-Homöostase zur Aufrechterhaltung und Stabilisierung der kardialen Funktion bei?

METHODIK

Akute und chronische Effekte einer CaSR Stimulation haben wir in unseren Arbeiten vorrangig am Modell der isolierten ventrikulären Herzmuskelzelle sowie im Myokard NO-defizienter, hypertensiver Ratten untersucht.

EIGENE BEFUNDE

- ***Die Aktivierung des CaSR stellt eine positiv inotrope Intervention dar, die die systolische Ca^{2+}-Konzentration sukzessiv auf ein neues Niveau anhebt.***
- ***Die CaSR vermittelte Aktivitätssteigerung der SERCA unterstützt die Relaxation des Myokards während der Diastole.***
- ***Im Modell NO-defizienter Ratten erweist sich die gesteigerte Expression des CaSR als endogener Protektionsmechanismus, der einen entscheidenden Beitrag zur Stabilisierung der kardialen Funktion leistet.***
- ***Durch seine membranstabilisierenden Eigenschaften vermittelt die Induktion des CaSR anti-arrhythmische Effekte.***
- ***RAMP-1 interagiert direkt mit dem CaSR, erhöht dessen Rezeptoraktivität und verbessert die intrazelluläre Signaltransduktion.***

Die Rolle des CaSR an der Aufrechterhaltung der Ca^{2+}-Homöostase

Zahlreiche Zelltypen in den unterschiedlichsten Organen besitzen die Fähigkeit, bereits kleinste Veränderungen extrazellulärer Ca^{2+}-Konzentrationen zu detektieren. Die Bedeutung des Ca^{2+} als „First Messanger“ wurde von Edward M. Brown bereits postuliert und beschrieben, bevor er zusammen mit Herbert et al. den Rezeptor identifizierte, dem das Prinzip des „Calcium Sensings“ zugrunde liegt.[47,48]

Die Konzentration der freien Ca^{2+}-Ionen im Extrazellulärraum unterliegt einer exakten Regulation und wird stets in einer Spanne zwischen 1,0 und 1,3 mmol/l gehalten. Wichtigster Baustein zur Aufrechterhaltung einer konstanten Ca^{2+}-Homöostase bildet dabei der CaSR, dessen Expression in sämtlichen Zellen bzw. Organen, die unmittelbar an der Regulation des Ca^{2+}-Haushalts beteiligt sind, nachgewiesen werden konnte.[49]

Doch selbst 25 Jahre nach seiner Erstbeschreibung werden für den CaSR noch immer neue Funktionen und Mechanismen beschrieben, die über eine reine Aufrechterhaltung physiologischer Ca^{2+}-Konzentrationen weit hinausgehen.[50] Darüber hinaus wurden in zahlreichen Studien neben Ca^{2+} weitere Agonisten identifiziert, so dass der ursprünglich gewählte Name „Calcium-sensing Rezeptor“ der Bedeutung und dem Stellenwert dieses Rezeptors nach heutigem Kenntnisstand bei weitem nicht mehr gerecht wird.

Durch seine Fähigkeit freies Ca^{2+} zu detektieren, übernimmt der CaSR eine zentrale Stellung in der Regulation der Ca^{2+}-Homöostase.[51] Seine Aktivierung in der Nebenschilddrüse erfolgt durch den Anstieg freien Serum-Ca^{2+}, in dessen Folge die Freisetzung und Synthese des Parathormons (PTH) gehemmt, gleichzeitig jedoch die Sekretion von Calcitonin aus den C-Zellen der Schilddrüse gefördert wird – umgekehrt führt eine Hypocalcämie zu einer gesteigerten PTH-Sekretion. Sinkt die Plasma-Ca^{2+} Konzentration auf 1 mmol/l, wird die maximale PTH-Sekretionsrate erreicht, ab einem Wert von 1,25 mmol/l wird die PTH-Sekretion auf das Minimum zurückgefahren.

Der exakte Sekretionsmechanismus des PTHs ist nicht vollständig entschlüsselt, wird jedoch aller Wahrscheinlichkeit nach $G_{q/11}$-vermittelt reguliert. Eine Aktivierung des CaSR veranlasst durch Bildung von IP_3 einen Anstieg des zytosolischen Ca^{2+}, ein Prozess, der normalerweise die Vesikelfusion mit der Zellmembran induziert und somit die Freisetzung von Proteohormonen fördert.[52] Einzig in den Hauptzellen der Nebenschilddrüse sinkt nach Ca^{2+}-

induzierter Aktivierung des CaSR die Sekretionsrate des PTH, ein Prozess, dem möglicherweise eine IP_3-vermittelte Hemmung der Adenylatcyclase zugrunde liegt.[53]

An Niere und Knochengewebe üben sowohl PTH als auch Calcitonin als Gegenspieler im Ca^{2+}-Haushalt überwiegend direkte Effekte an ihren Zielzellen aus. Die Regulation der enteralen Ca^{2+}-Resorption im terminalen Ileum wird hingegen vorrangig durch Vitamin D3 (Calcitriol) gesteuert. Dessen Synthese hängt wiederum entscheidend von der Aktivität der 1α-Hydroxylase ab, die als Schlüsselenzym der Calcitriol-Biosynthese vorrangig in der Niere unter Kontrolle des PTH steht.[47]

Fazit: Der CaSR registriert bereits kleinste Schwankungen des Serum-Ca^{2+} und veranlasst daraufhin eine bedarfsgerechte Synthese und Sekretion der calcitropen Hormone PTH, Calcitonin und Calcitriol. Die wichtigsten Zielorgane für die Ca^{2+}-regulierenden Hormone sind das Knochengewebe, die Niere und der Darm.

Hierbei ist jedoch zu berücksichtigen, dass ein Teil der Zellen, die unter der Regulation calcitroper Hormone stehen, ebenfalls den CaSR exprimieren, so dass die lokale Ca^{2+}-Konzentration die endokrin-induzierten Signalmechanismen in den Zielzellen moduliert und beeinflusst.[54]

Struktur und Funktionsmechanismen des CaSR

Das Gen des CaSR ist auf dem langen Arm des Chromosom 3 (3q13.3-21) lokalisiert, umfasst ca. 103 kb und ist in 8 Exons organisiert.[55-57] Der CaSR wird als klassischer G-Protein gekoppelter Rezeptor entsprechend der aktuellen Klassifizierung in die Gruppe II der Familie C eingeordnet.[58]

An der Zelloberfläche wird der CaSR größtenteils als Dimer exprimiert. Die Zusammenlagerung zweier Monomere erfolgt bereits im endoplasmatischen Retikulum durch hydrophobe Wechselwirkungen sowie die Ausbildung kovalenter Disulfidbrücken.[59,60]

Im Gegensatz zu vielen anderen Rezeptoren verbleibt der CaSR im Anschluss an die post-translationalen Modifikationen zunächst im endoplasmatischen Retikulum bzw. Golgi-Apparat und wird erst durch Aktivierungssignale entsprechender extrazellulärer Agonisten zeitnah mobilisiert und an die Zellmembran transportiert[61]. So induziert ein Anstieg der extrazellulären Ca^{2+}-Konzentration einen raschen anterograden Transport des CaSR an die

Zelloberfläche, an der sich die Rezeptordichte solange auf ein neues Level einstellt, bis sich die Konzentration des Agonisten wieder ändert. Eine Desensitivierung des CaSR kann sowohl durch β-Arrestin als auch durch G-Protein gekoppelte Rezeptorkinasen (GRKs) hervorgerufen werden.[62] Hingegen führen eine Absenkung des extrazellulären ph-Wertes sowie eine reduzierte Ionenkonzentration ebenso wie L-Phenylalanin als allosterischer Aktivator zu einer Sensitivierung des CaSR.[63-66]

Die Internalisierung durch Endozytose läuft konstitutiv ab, unterliegt jedoch keiner nennenswerten Regulation. Der Großteil internalisierter Rezeptoren wird dem Lysosom zugeführt und abgebaut, ein Recycling findet beim CaSR praktisch nicht statt.[62,67,68] Durch seine fünf Phosphorylierungsstellen für die Proteinkinase C (PKC) bzw. zwei für die Proteinkinase A (PKA) besteht jedoch die Möglichkeit, Funktion und intrazelluläre Kopplung zu modulieren.[55,69]

Einfluss von RAMP-1 auf die Signaltransduktion des CaSR an der Herzmuskelzelle (Ref.: RS2)

Über weitestgehend unerforschte, komplexe Interaktionen können alle drei Isoformen der „Receptor Activity Modifying Proteins“, kurz RAMPs, Einfluss auf die intrazellulären Transportschritte, die zellspezifische Membran-Expression sowie die Ligandenspezifität des CaSR nehmen.[70,71]

Die Bedeutung von RAMP-1 für die intrazelluläre Kopplung des CaSR haben wir *in vivo* am Modell eines chronischen Defizits an Stickstoffmonoxid (NO) nachweisen können. Nach vierwöchiger Trinkwasser-Applikation des NO-Synthase-Inhibitors L-NAME wiesen die Ventrikel drei Monate alter Wistar Ratten eine signifikante Zunahme ihrer RAMP-1-Expression auf. Unter diesen Bedingungen wird die CaSR-vermittelte intrazelluläre Signaltransduktion erheblich verbessert und liefert einen entscheidenden Beitrag zur Aufrechterhaltung der systolischen Pumpfunktion (Mechanismus s. Seite 17).[RS2]

Ca^{2+}-Homöostase im kardio-vaskulären System

Die Rolle des CaSR im vaskulären System

Die Aufgabe des kardio-vaskulären Systems besteht in der Aufrechterhaltung und Stabilität der Hämodynamik im Gefäßsystem. Zur Regulation des arteriellen Blutdrucks werden

zahlreiche Presso-, Volumen- und Chemorezeptoren benötigt, die kontinuierlich aktuelle Kreislaufparameter messen und ihre Informationen zur Verarbeitung an zentral gelegene Kreislaufzentren in der Medulla oblongata weiterleiten. Nach komplexer Verschaltung und unter dem Einfluss übergeordneter vegetativer Zentren werden peripherer Widerstand und Organperfusion zeitnah durch die Aktivität des vegetativen Nervensystems beeinflusst. Die langfristige Blutdruckregulation wird vorrangig über den Volumenhaushalt gesteuert.

Neben diesen zentralen Steuerungsmechanismen, die mittels neuronaler Innervation bzw. durch Hormonsekretion vermittelt werden, sind die Blutgefäße jedoch auch selbstständig in der Lage, durch lokale Mechanismen ihre Perfusion zu steuern.[72]

Bereits lange vor Entdeckung des CaSR wurden Zusammenhänge zwischen der extrazellulären Ca^{2+}-Konzentration und dem Relaxationsvermögen arterieller Blutgefäße beschrieben.[73]

Obwohl die exakten Funktionsmechanismen des CaSR in den unterschiedlichen Abschnitten des Gefäßsystems sowie das Zusammenspiel der beteiligten Zelltypen noch nicht vollständig geklärt sind, erfolgt die Regulation des Gefäßtonus und somit die Modulation des Blutdrucks unter direkter Beteiligung des CaSR und seiner Agonisten.

Die pulmonal-arterielle Hypertonie (PAH) ist durch einen erhöhten Druck in den Lungenarterien gekennzeichnet, der in Ruhe über 25 mmHg und bei Belastung über 30 mmHg liegt (Normwerte: 10-15 mmHg). Der erhöhte Druck in der Lungenstrombahn führt an den Lungengefäßen langfristig zu einem Remodeling, das durch Proliferation der Endothelzellen sowie der glatten Muskelzellen charakterisiert ist. Die Obliteration der Lungenstrombahn führt im Krankheitsverlauf zu einer progredienten Belastung des rechten Ventrikels, so dass die Rechtsherzinsuffizienz bzw. das Rechtsherzversagen die häufigsten Todesursachen der PAH darstellen.[74]

Im Gegensatz zu den überwiegend vasorelaxierenden Eigenschaften des CaSR in der Kreislaufperipherie wird dem CaSR in der Lungenstrombahn sowohl eine Beteiligung an der hypoxischen Vasokonstriktion als auch am vaskulären Remodeling während der Entstehung und Progression einer PAH zugeschrieben.[75-77] Darüber hinaus können Calcilytics, die am CaSR eine antagonistische Wirkung hervorrufen, die Umbauprozesse der Lungengefäße bei PAH signifikant verbessern.[78,79]

Die Bedeutung des CaSR für das Myokard (Ref.: RS1,RS4)

„Calcium controls cardiac function – by all means!“, so lautet ein Artikel von Ole M. Sejersted publiziert im Journal of Physiology.[80]

Betrachtet man die zellulären Mechanismen, die an der Steuerung und Umsetzung eines Herzschlags beteiligt sind, wird sehr schnell deutlich, welche Bedeutung das Ca^{2+}-Ion für den regulären Ablauf der Herzmuskelkontraktion hat. Als klassischer second messenger spielt Ca^{2+} eine wichtige Rolle bei zahlreichen intrazellulären Signalschritten. Durch seine Interaktion mit dem CaSR übernimmt Ca^{2+} jedoch auch die Aufgabe eines first messengers und reguliert so Zellfunktionen, die unmittelbar die Ca^{2+}-Homöostase beeinflussen.[RS1]

Den ersten Nachweis für die Präsenz des CaSR in Herzmuskelzellen haben Wang et al. im Jahr 2003 durch den Nachweis von mRNA in atrialen und ventrikulären Myozyten erbracht.[81]

Das Expressionsmuster des CaSR im Rattenherz haben wir in unseren Studien auf Protein Ebene getrennt für den linken und rechten Ventrikel sowie für die Vorhöfe untersucht; das linksventrikuläre Myokard weist die höchste, das Vorhofgewebe die niedrigste Konzentration an CaSR Protein auf.[RS4]

Einfluss des CaSR auf die kardiale Elektrophysiologie (Ref.: RS3)

Bereits die elektrische Herzaktivität, dessen Ursprung im Sinusknoten liegt, steht sowohl unter der Kontrolle von Ca^{2+} bzw. Ca^{2+}-Kanälen als auch der des CaSR.

Das Aktionspotential der einzelnen Herzmuskelzelle beginnt mit einer Öffnung schneller N^{+}-Kanäle, die es N^{+}-Ionen ermöglichen, entsprechend ihrer chemischen und elektrostatischen Gradienten in die Zelle einzuströmen. Etwas verzögert öffnen sich K^{+}-Kanäle (K_{lto}) und leiten so durch den Ausstrom von K^{+}-Ionen bereits partiell wieder die Repolarisation ein. Überlagert werden diese Ionenströme von einem lang anhaltenden, depolarisierenden Ca^{2+}-Einstrom über spannungsgesteuerte L-Typ-Ca^{2+}-Kanäle, der die Membran vor einer voranschreitenden Repolarisation bewahrt und für die charakteristische Plateauphase (bis zu 400 ms) der Aktionspotentiale im Arbeitsmyokard verantwortlich ist. Die Repolarisation wird durch den massiven Ausstrom von K^{+} über iK, iK_1 und K_{lto} Kanäle bewerkstelligt.

Durch seinen direkten Einfluss auf die Expression des iK_1 Kanals kann der CaSR an Kardiomyozyten indirekt membranstabilisierende Effekte ausüben, da iK_1 Kanäle nicht nur

bei der Repolarisation, sondern auch bei der Aufrechterhaltung eines stabilen Ruhemembranpotentials eine entscheidende Rolle spielen.[82]

Bereits 1990 berichteten Tagliavini et al. über die anti-arrhythmischen Eigenschaften von Putrescin, die auf seine membranstabilisierenden und antioxidativen Eigenschaften zurückgeführt wurden.[83] Darüber hinaus haben Zhao et al. nachweisen können, dass die effiziente Applikation eines ischämischen pre-conditionings (IPC) eine ausreichend hohe Polyaminkonzentration voraussetzt, die ggf. eine exogene Zufuhr von Spermin erforderlich macht.[84] Da sowohl Putrescin als auch Spermin potente CaSR Agonisten darstellen, muss folglich bei sämtlichen kardioprotektiven Effekten, die durch Polyamine induziert werden, eine CaSR Stimulation in Betracht gezogen werden.

Bzgl. seiner Rolle im post-ischämischen Myokard haben wir das Expressionsmuster des CaSR sieben Tage nach 30-minütiger LAD Ligatur im links- und rechtsventrikulären Myokard männlicher Wistar Ratten untersucht. Während die Expression im linken Ventrikel signifikant abnahm, wurde sie im rechten Ventrikel 4-fach induziert.[RS3]

Im reperfundierten Myokard tragen besonders in den ersten Tagen nach einem Infarkt die membranstabilisierenden Eigenschaften einer CaSR Stimulation zur Kardioprotektion bei. Vor diesem Hintergrund stellt die Herabregulation des CaSR im post-ischämischen linken Ventrikel einen potentiellen Risikofaktor dar, der sowohl anti-arrhythmische Ereignisse als auch Formen einer kardialen Dysfunktion in hohem Maße begünstigen kann.

Einfluss des CaSR auf die zellulären Mechanismen der Herzmuskelkontraktion (Ref.: RS4)

$G_{q/11}$-abhängig kann der CaSR sowohl die Kontraktion als auch die Relaxation der Herzmuskelzelle beeinflussen. Die wichtigsten Untersuchungsbefunde in unseren Studien haben gezeigt, dass eine Aktivierung des CaSR an isolierten ventrikulären Herzmuskelzellen adulter Ratten zu einer progredienten Erhöhung des Ca^{2+}-Transienten führt.[RS4]

Nach seiner Stimulation ist der CaSR über die Aktivierung der Phospholipase C zur Bildung der Second Messenger Inositoltrisphosphat (IP_3) und Diacylglycerin (DAG) befähigt.

Das Phospholipid IP_3 kann durch Bindung an seinen spezifischen Rezeptor Ca^{2+} aus intrazellulären Speichern freisetzen. IP_3-Rezeptoren sind unspezifische Kationenkanäle, die bei ihrer Öffnung eine schnelle Freisetzung von Ca^{2+}-Ionen aus dem SR und damit einen

Anstieg der zytoplasmatischen Ca^{2+}-Konzentration bewirken können. Die IP_3-induzierte Freisetzung sarkoplasmatischen Ca^{2+} erhöht die RyR2-vermittelte zytoplasmatische Ca^{2+}-Konzentration und induziert somit einen positiv inotropen Effekt.

Über die Bereitstellung des DAG, das lokal in der Plasmamembran verbleibt, wird eine wichtige Voraussetzung zur Aktivierung der PKC geschaffen. Derzeit sind mindestens zwölf Isoformen der PKC beschrieben worden, die sich in ihrer Aminosäurensequenz und ihren Regulationsmechanismen unterscheiden. Aufgrund dieser Unterschiede werden sie in vier Subfamilien zusammengefasst: classical, novel, eccentric und atypical. Für die klassischen PKC Isoformen stellt wiederum das Ca^{2+} einen wichtigen Co-Faktor dar, der die Translokation des Enzyms an die Plasmamembran fördert und somit die Aktivierung des Enzyms mittels DAG unterstützt.

Die simultane Aktivierung der PKC führt über eine verstärkte Phosphorylierung des Phospholambans an Ser10 und Ser16 zu einer gesteigerten Aktivität der SERCA, die Ca^{2+}-Ionen schneller wieder in ihre intrazellulären Speicher zurückpumpt. An der isolierten Herzmuskelzelle spiegelt sich dieser Mechanismus in einer unveränderten diastolischen Ca^{2+}-Konzentration sowie einer erhöhten Relaxationsgeschwindigkeit wider.

In unserem Modell stellt die Aktivierung des CaSR eine positiv inotrope Intervention dar, die die systolische Ca^{2+}-Konzentration sukzessiv und moderat auf ein neues Niveau anhebt. Die gesteigerte Aktivität der SERCA unterstützt darüber hinaus die Relaxation während der Diastole. An der isolierten Herzmuskelzelle zeigen die Funktionsparameter keine typischen Nachteile anderer positiv inotrop wirkender Substanzen; dies schließt sowohl die gestörte Relaxation einiger Calciumsensitizer als auch die pro-arrhythmogene Wirkung der Katecholamine mit ein.[RS4]

Der Einfluss des CaSR auf die myokardiale Hypertrophie (Ref.: RS2)

Zunächst beschrieben Tfelt-Hansen et al. am Modell neonataler Kardiomyozyten, dass die Aktivierung des CaSR zu einer Reduktion der DNA-Synthese führe und schlussfolgerten daraus potentiell antihypertrophe Effekte.[85] In der Folgezeit wurden jedoch weitere Studien durchgeführt, die dem CaSR vorrangig prohypertrophe Eigenschaften bescheinigten.[86,87] Der überwiegende Einsatz neonataler Kardiomyozyten stellt jedoch eine methodische

Limitierung dar, da sich hypertrophe Signalmechanismen in diesem Zellstadium nur eingeschränkt auf die adulte Kardiomyozyte übertragen lassen.

In Fortführung an unsere erste Studie haben wir die funktionellen Auswirkungen einer CaSR Stimulation am Modell der Endothelin-induzierten Hypertrophie adulter Kardiomyozyten der Ratte untersucht. Endothelin, ein Peptidhormon, das hauptsächlich von Endothelzellen produziert und sezerniert wird, vermittelt seine kardialen Effekte über den ETA Rezeptor sowie die beiden Splicevarianten ETB_1 und ETB_2.

Die Befunde zeigen, dass die Stimulation des ETA und ETB_1 Rezeptors zur Ausbildung einer überwiegend adaptiven linksventrikulären Hypertrophie beiträgt, die sich unter anderem durch eine Heraufregulation des CaSR auszeichnet. Unter diesen Bedingungen ist der CaSR am hypertrophen Wachstum selbst nicht beteiligt, trägt jedoch entscheidend zum Funktionserhalt der Kardiomyozyten bei. Der ETB_2 Rezeptor, dessen Funktionsweise am Herzen weitgehend unerforscht ist, verursacht bei selektiver Stimulation die Ausbildung einer kontraktilen Dysfunktion ohne das Wachstum der Myozyten zu beeinflussen.[RS2]

Fazit: Im chronisch druckbelasteten Herzen stellt die gesteigerte Expression des CaSR einen endogenen Protektionsmechanismus dar, der einen entscheidenden Beitrag zur Stabilisierung und Aufrechterhaltung der kardialen Funktion leistet.

Kardioprotektion durch CaSR Aktivierung

Sun und Murphy untersuchten an Langedorff-perfundierten Mausherzen den Stellenwert des CaSR für ein IPC. Während der Applikation des IPC wurden die Herzen mit NPS-2143, einem selektiven CaSR Antagonisten perfundiert. Die IPC-vermittelte Induktion kardioprotektiver Kinasen (ERK1/2, AKT und GSK3) blieb unter CaSR Hemmung aus; positive Effekte auf die Infarktgröße sowie die post-ischämische Funktionserholung waren ebenfalls aufgehoben.[88] Bai et al. untersuchten die Pathomechanismen einer dilatativen Kardiomyopathie (DCM) in diabetischen Ratten und machten eine gestörte Ca^{2+}-Homöostase der Kardiomyozyten für die Funktionseinschränkung des Myokards verantwortlich. Als Ursache fanden sie eine reduzierte Expression des CaSR und schlussfolgerten, dass eine Aktivierung bzw. Induktion des CaSR als neue Therapieoption der DCM in Betracht gezogen werden müsste.[89] Diese Interpretation entspricht den bereits vorgestellten eigenen

Untersuchungsbefunden, die eine Heraufregulation des CaSR als adaptiven Mechanismus werten, der zur Stabilisierung der kardialen Funktion beiträgt.

Der CaSR im kardio-vaskulären System

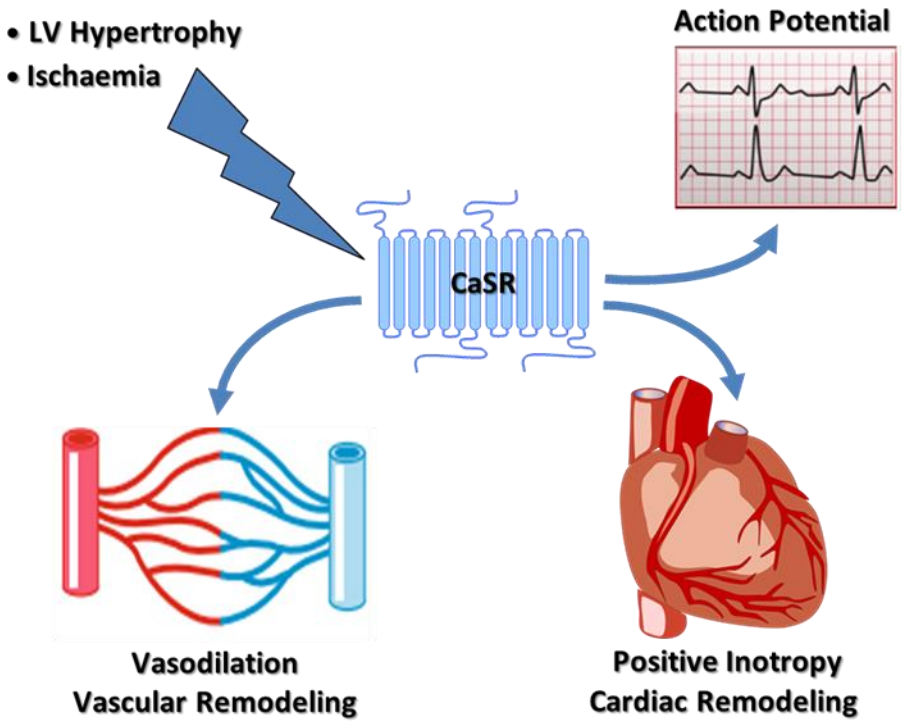

Abb. 2: Seine kardioprotektiven Eigenschaften vermittelt der CaSR durch anti-arrhythmische, vasodilatierende und positive inotrope Effekte.

Der CaSR als therapeutisches Target einer HFrEF (Ref.: RS1)

Aufgrund seines weitreichenden Aufgabenspektrums sowie seiner Beteiligung an zahlreichen physiologischen und pathophysiologischen Signalmechanismen werden je nach Funktion sowohl die selektive Aktivierung als auch Hemmung des CaSR als vielversprechende Therapieoptionen diskutiert.

Calcimimetika (Cinacalcet, Etelcalcetide) sind allosterische Modulatoren des CaSR, die über eine Konformationsänderung der Tertiärstruktur die Empfindlichkeit des Rezeptors erhöhen. Calcilytika (NPS-2143, ATF-936, AXT-914) hingegen wirken als Antagonisten am CaSR.[90-93]

Die beiden einzigen derzeit zugelassenen Agonisten des CaSR, Cinacalcet und Etelcalcetide, sind zur Behandlung des sekundären Hyperparathyreoidismus bei chronischer

Niereninsuffizienz bzw. dialysepflichtigem Nierenversagen sowie der Hypercalcämie beim Nebenschilddrüsenkarzinom indiziert. Für Etelcalcetide, das durch die U.S. Food and Drug Administration im Februar 2017 zugelassen wurde, zählen Übelkeit, Erbrechen, Durchfall sowie Muskelspasmen zu den häufigsten Nebenwirkungen. Gelegentlich bzw. selten führte die Einnahme zur Hypotonie sowie zu einer Verlängerung des QT-Intervalls.[94,95]

Strukturell den Calcimimetics sehr ähnlich, wurden in den letzten Jahren negative allosterische Modulatoren (Calcilytics) des CaSR entwickelt, die vorrangig zur Behandlung der autosomal dominanten Hypocalcämie sowie der Osteoporose postmenopausaler Frauen vorgesehen sind. NPS-2143 bzw. seine Weiterentwicklung SB423557, ronacaleret und JTT-305/MK-5442 sowie NPSP795 waren in den bisher durchgeführten Phase II bzw. Phase III Studien der jeweiligen Standardtherapie nicht überlegen – eine Zulassung erfolgte bislang nicht. Generell attestieren jedoch die klinischen Daten den Calcilytics sowohl eine gute Verträglichkeit als auch ein günstiges Sicherheitsprofil.[90,96]

Neuere Studien weisen darauf hin, dass die Indikation einer calcilytischen Therapie zukünftig auf die Behandlung des Asthma Bronchiale sowie der PAH ausgeweitet wird.[79,97]

Zahlreiche Studien und Arbeiten zum CaSR empfehlen abschließend die medikamentöse Aktivierung bzw. Hemmung des Rezeptors zur Prävention oder Therapie vaskulärer bzw. kardialer Erkrankungen. Für den jeweils untersuchten Zelltyp bzw. die aufgereinigte Zellkultur sind diese Empfehlungen durchaus valide und nachvollziehbar. Nur bestehen sowohl Blutgefäße als auch das Myokard aus unterschiedlich differenzierten Zellen, die in einem funktionellen Zellverband fest verbunden sind.

Die Wahl einer Therapiestrategie (Calcimimetikum vs. Calcilytikum) wird bereits dadurch erschwert, dass Organfunktionen je nach untersuchtem Zelltyp mitunter gegensätzlich reguliert werden (Vasorelaxation des Endothels vs. Vasokonstriktion glatter Muskelzellen). Darüber hinaus werden dem CaSR in benachbarten Zellen sowohl protektive als auch nachteilige Eigenschaften (Ca^{2+}-Homöostase in Myozyten vs. Proliferation kardialer Fibroblasten) zugeschrieben.

Für den CaSR lässt die aktuelle Datenlage (mit Ausnahme der PAH) noch keine konkreten Rückschlüsse auf allgemeingültige Therapiestrategien innerhalb des Herz-Kreislaufsystems zu.[RS1]

3.2 Die Herzinsuffizienz mit erhaltener Auswurffraktion (HFpEF)

Die chronische Herzinsuffizienz basiert häufig auf einer multifaktoriellen Genese und setzt in vielen Fällen das Zusammentreffen verschiedener Risikofaktoren voraus. Bei nahezu 50 % der Patienten mit diagnostizierter Herzinsuffizienz liegt die Ursache der kardialen Funktionsstörung in der Diastole, also der Füllungsphase des Herzzyklus, während die systolische Pumpfunktion vollständig erhalten ist (HFpEF). Die langfristige Prognose dieser Patienten unterscheidet sich nur unwesentlich von Patienten, deren Funktionsstörung mit einer reduzierten Auswurfleistung des Herzmuskels (HFrEF) einhergeht.[98]

Kapitel 3.2 – Key Points

In diesem Kapitel werden zunächst mögliche Risikofaktoren und Pathomechanismen der HFpEF vorgestellt, die allerdings aufgrund fehlender experimenteller Daten weitestgehend auf theoretischen Annahmen basieren. Anschließend werden anhand unseres Tiermodells, das in vielen Aspekten die kardiale Symptomatik einer HFpEF aufweist, charakteristische Untersuchungsbefunde und potentielle Therapieoptionen vorgestellt.

Fragestellung

Liegen der kardialen Dysfunktion einer HFpEF extramyozytäre Pathomechanismen zugrunde, die vorrangig ein Remodeling der extrazellulären Matrix verursachen?

Methodik

Durch zusätzliche hämodynamische Belastung zeichnet sich unser SHR Modell durch klinische Symptome und molekularbiologische Befunde aus, die bei vielen Patienten mit diagnostizierter HFpEF beschrieben werden.

Eigene Befunde

- ***Unter hämodynamischer Belastung entwickelt die spontan hypertensive Ratte eine diastolische Funktionsstörung bei gleichzeitig erhaltener systolischer Pumpfunktion.***
- ***Als Ursache konnte die Induktion der Lysyloxidase identifiziert werden, die zu einer gesteigerten Vernetzung der Matrixproteine und einer massiven Steigerung der Kollagen III-Expression führte.***
- ***Unsere Befunde liefern darüber hinaus wichtige Hinweise auf eine kausale Beteiligung des Aldosteronmetabolismus an der Pathogenese der HFpEF.***

Die eigenständige Pathophysiologie der HFpEF

Erst in den letzten Jahren haben die Ergebnisse verschiedener Studien dazu geführt, die diastolische Herzinsuffizienz mit erhaltener systolischer Funktion und die Herzinsuffizienz mit reduzierter Auswurfleistung als eigenständige Krankheitsbilder zu betrachten. Diese Neubewertung basiert auf der Annahme, dass beiden Funktionsstörungen grundsätzlich unterschiedliche Pathomechanismen zugrunde liegen. Doch besonders bei der Herzinsuffizienz mit einer primär diastolischen Funktionsstörung basieren die Erkenntnisse mangels geeigneter Tiermodelle und eingeschränkter Verfügbarkeit humanen Probenmaterials auf nur wenigen Studien.[99]

Das unzureichende Verständnis über die Pathophysiologie der HFpEF erschwert ebenfalls die Wahl einer effizienten therapeutischen Strategie, zumal verschiedene klinische Studien gezeigt haben, dass sich die effektive Medikation der HFrEF mit Inhibitoren des RAAS nicht erfolgreich auf die Behandlung der HFpEF übertragen lässt.[100-102]

Risikofaktoren und Pathomechanismen der HFpEF

Anhand neuer Evidenzen, die überwiegend in klinischen Studien gewonnen wurden, wird das Myokard nicht als Ausgangspunkt für die Entwicklung einer HFpEF verantwortlich gemacht, sondern im Laufe eines vaskulär-inflammatorischen Prozesses sekundär geschädigt.[103]

Als Auslöser dieses inflammatorischen Geschehens beschreiben Paulus und Tschöpe in ihrem Reviewartikel ein Zusammenspiel verschiedener Co-Morbiditäten, die häufig zusammen mit einer HFpEF diagnostiziert werden. Neben der arteriellen Hypertonie werden ein Typ 2 Diabetes, die Adipositas, chronische Nierenerkrankungen und Anämien für die vaskulären Schäden verantwortlich gemacht. Eine reduzierte Bioverfügbarkeit von NO zusammen mit einem Anstieg freier Radikale sollen daraufhin die Induktion einer endothelialen Dysfunktion und die Inflammation der Mikrostrombahn von Herz und Lunge auslösen.[103]

Nach dieser neuen Modellvorstellung erfolgt das strukturelle und funktionelle Remodeling des Myokards zeitlich verzögert als Folge dieser intrakoronaren Prozesse. Ein daraus resultierender Verlust der inhibitorischen Einflüsse von NO/cGMP auf profibrotische und

prohypertrophe Mediatoren könnte unmittelbar die Entwicklung einer diastolischen Funktionsstörung induzieren.[104]

Zu berücksichtigen ist jedoch, dass es sich bei dem hier beschriebenen Szenario über die Pathogenese einer HFpEF „lediglich“ um eine (aktuelle) Hypothese handelt, dessen kausale Zusammenhänge größtenteils unbewiesen sind. So ist der Stellenwert der oben aufgezählten Begleiterkrankungen unbestritten, doch findet sich ein vergleichbares Bild an Co-Morbiditäten auch bei der HFrEF wieder. Damit ist zum gegenwärtigen Zeitpunkt völlig unklar, welche Faktoren für die individuelle Ausprägung der kardialen Funktionsstörung (HFrEF vs. HFpEF) vor dem Hintergrund identischer Risikofaktoren verantwortlich sind.[105]

Der vollzogene Paradigmenwechsel, die HFpEF als Folge eines vaskulär-inflammatorischen Geschehens zu betrachten, eröffnet in mancher Hinsicht neue Perspektiven und Erklärungsansätze für das spezifische Remodeling des insuffizienten Myokards, obgleich die Applikation antiinflammatorischer Wirkstoffe den klinischen Verlauf einer HFpEF nicht signifikant verbessern konnte.[106,107]

HFpEF – Standardmedikation unwirksam?

In 2013 schlussfolgerte Desai, dass weder ACE-Inhibitoren noch AT_1-Rezeptorblocker für Patienten mit diagnostizierter HFpEF von therapeutischem Nutzen seien.[104]

Nachdem im Jahr 2014 der Angiotensin-Rezeptor-Neprilysin-Inhibitor Sacubitril/Valsartan den primären Endpunkt (Hospitalisierung/kardio-vaskuläre Mortalität) im PARADIGM-HF trial (mittleres Alter: 64 Jahre, EF: ≤40 %) erreicht bzw. übertroffen hatte und somit die Prognose der Patienten mit HFrEF signifikant verbessern konnte, wurde unter Beibehaltung identischer Einschlusskriterien der PARAGON-HF trial initiiert – einzige Ausnahme, die linksventrikuläre Auswurffraktion durfte nicht unter 45 % liegen.[108] Mit den jüngst veröffentlichen Studienergebnissen musste erneut ein Rückschlag auf der Suche nach einer effizienten Therapieoption der HFpEF hingenommen werden; in der Subgruppenanalyse erwies sich die Kombination Sacubitril/Valsartan gegenüber der alleinigen Medikation mit Valsartan allenfalls bei Patienten mit „mittelgradig“ eingeschränkter Ejektionsfraktion als überlegen.[109]

In 2020/21 werden die Ergebnisse des EMPEROR-PRESERVED bzw. DELIVER trials erwartet, mit deren Hilfe Aussagen zur Wirksamkeit der SGLT-2 Inhibitoren bei HFpEF Patienten getroffen werden können.[110] Das kardioprotektive Potential der SGLT-2 Inhibitoren, die unlängst im Therapieschema zur Behandlung des Typ 2 Diabetes etabliert sind, hatte sich bereits in früheren Studien abgezeichnet. Für Dapagliflozin konnte darüber hinaus im DAPA-HF trial eine signifikante Verringerung der kardio-vaskulären Mortalität bzw. Progression der Herzinsuffizienz bei Patienten mit HFrEF nachgewiesen werden – unabhängig davon, ob ein Diabetes vorlag oder nicht.[111] Der zugrunde liegende Mechanismus ist nicht bekannt, über den diuretischen Effekt allein lässt sich die therapeutische Effizienz sicher nicht erklären.

Bereits vielfach nachgewiesen und gut dokumentiert sind die Effekte einer medikamentösen Blockade der Mineralkortikoid-Rezeptoren, die bei diagnostizierter HFrEF sowohl die klinische Symptomatik als auch die Prognose der Patienten entscheidend verbessern. Neben einer Reduktion der kardialen Vor- bzw. Nachlast zählen antihypertrophe sowie antifibrotische Effekte zu den wichtigsten Eigenschaften dieser Medikamentenklasse.[112,113]

Das vielversprechende pharmakologische Profil der Aldosteronantagonisten war Anlass, die Wirksamkeit von Spironolacton auf klinisch relevante Endpunkte einer HFpEF in multizentrischen, randomisierten Studien zu untersuchen.

Im OPTIMIZE-HF trial wurde die therapeutische Effizienz von Spironolacton auf die Gesamtmortalität und die Hospitalisierung an einem 48.612 Patienten umfassenden Kollektiv (mittleres Alter: 80 Jahre, mittlere EF: 54 %) über 2,4 Jahre geprüft. Spironolacton konnte weder den klinischen Verlauf noch die definierten Endpunkte innerhalb dieser Studie positiv beeinflussen.[114]

In den Jahren 2006 bis 2013 wurde im TOPCAT trial der therapeutische Nutzen von Spironolacton an 3.445 Patienten (mittleres Alter: 69 Jahre, mittlere EF: 56 %) über einen Zeitraum von 3,3 Jahren untersucht. Einzig die Rate der Hospitalisierung war gegenüber der Placebo-Gruppe signifikant verbessert.[115]

Entsprechend den Schlussfolgerungen von Patel et al. belegen die Ergebnisse der aktuellen klinischen Studien erneut, dass eine effiziente medikamentöse Therapie nur möglich ist, wenn fundierte Kenntnisse über die Genese und die zugrunde liegenden Pathomechanismen einer Erkrankung vorliegen.[114]

Die signifikante Reduktion der Hospitalisierung durch Spironolacton im TOPCAT trial sollte Anlass geben, die komplexe Pathophysiologie der HFpEF intensiver zu erforschen um potentielle Interventionsmöglichkeiten wie den Aldosteronmetabolismus therapeutisch effizienter nutzen zu können.[116] Zu dieser Schlussfolgerung gelangen ebenfalls Li et al., die in ihrer Metaanalyse klinischer HFpEF Studien festgestellt haben, dass ausschließlich die Applikation des Aldosteronantagonisten Spironolacton zu einer signifikanten Verbesserung diastolischer Funktionsparameter führte.[117]

Die HFpEF im Tiermodell (Ref.: RS6)

Die Prävalenz und Inzidenz einer chronischen Herzinsuffizienz nimmt in vielen westlichen Ländern kontinuierlich zu. Allein in Deutschland sind nach aktuellen Schätzungen 1,8 Millionen Menschen betroffen.

Für einen großen Anteil dieser Patienten, bei denen die Ursache der kardialen Funktionsstörung in der Füllungsphase des Herzzyklus liegt, ist bis heute keine effiziente Therapie möglich. Einzig die positiven Ergebnisse des Rezeptorantagonisten Spironolacton bzgl. Lebensqualität und Hospitalisierung geben wichtige Hinweise auf eine kausale Beteiligung des Aldosteronmetabolismus an der Pathogenese der HFpEF.

Im Langzeitmodell entwickelt die spontan hypertensive Ratte (SHR) durch zusätzliche hämodynamische Belastung einen kardialen Phänotyp, der sich durch klinische Symptome und Befunde auszeichnet, die bei vielen Patienten mit diagnostizierter HFpEF beschrieben werden.[RS6]

Neben der Untersuchung grundlegender Pathomechanismen bietet unser Tiermodell erstmals die Möglichkeit, die Wirkung der Aldosteronantagonisten auf einen typischen Symptomkomplex der HFpEF auf molekularer und zellphysiologischer Ebene zu untersuchen.

Das Modell der spontan hypertensiven Ratte (SHR) (Ref.: RS8,RS9)

Weltweit werden SHRs als favorisiertes Tiermodell zur Untersuchung der essentiellen Hypertonie eingesetzt. Der Bluthochdruck spontan hypertensiver Ratten wird polygenetisch mit einer Beteiligung von mindestens drei Major-Genen vererbt, die zugrunde liegenden Quantitative trait loci (QTLs) befinden sich auf den Chromosomen 1, 10 und 18.[118-120] Bis zur

8. Lebenswoche weisen SHR normotensive Blutdruckwerte von 125/80 mmHg auf. Im weiteren Verlauf entwickelt sich über einen Zeitraum von 2 Monaten eine arterielle Hypertonie mit Werten von 175/115 mmHg (weibliche Tiere).

Vorrangig die Untersuchungsergebnisse von Rebelo et al. lassen darauf schließen, dass seneszente SHR mit etabliertem Hochdruck zusätzliche Lauf- bzw. Sport-bedingte hämodynamische Belastungen nicht kompensieren und somit nicht von entsprechenden zellulären Adaptionsmechanismen profitieren können. Im Vordergrund der klinischen und pathomorphologischen Befunde dieser Studien stehen eine massive leistungsinduzierte Myokardhypertrophie sowie ein verschlechtertes Ca^{2+}-Handling.[RS8,RS9]

Die prähypertensive SHR als Modell einer HFpEF (Ref.: RS6)

In weiterführenden Studien haben wir die Auswirkungen eines 6-monatigen Laufradtrainings auf das Herz-Kreislaufsystem untersucht, bevor und während sich in jungen, 1½Monate alten SHR ein Bluthochdruck etablierte.

Ohne die zeitliche Entwicklung und die Höhe des Blutdrucks zu beeinflussen, verursacht ein freiwilliges Laufradtraining junger SHR ein funktionelles und strukturelles kardiales Remodeling, das der klinischen Symptomatik einer primär diastolischen Herzinsuffizienz mit erhaltener Ejektionsfraktion entspricht. Als Ursache konnte die kardiale Induktion der Lysyloxidase identifiziert werden, die zu einer gesteigerten Vernetzung der Matrixproteine und einer massiven Steigerung der Kollagen III-Expression führte.[RS6]

Die Lysyloxidase (LOX)

Codiert wird die Lysyloxidase vom LOX-Gen, das sich beim Menschen auf Chromosom 5 im Genlocus q23.3 bis q31.2 befindet. Die gesamte LOX-Familie umfasst fünf Mitglieder, die LOX sowie die Isoformen LOX-like-1 bis 4. Die katalytisch aktive Domäne liegt stets in der hochkonservierten C-terminalen Region; N-terminal weisen die unterschiedlichen Isoformen hingegen eine große interindividuelle Variabilität auf.[121]

Die ca. 50 kDa schweren Pre-Proenzyme werden im endoplasmatischen Retikulum zunächst durch N-Glykosylierung post-translational modifiziert und nach Abspaltung ihres jeweiligen Signalpeptids in den Extrazellulärraum transportiert. Die als Pro-LOX bezeichnete sezernierte

Form wird vorrangig durch die Prokollagen C-Proteinase proteolytisch in die 32 kDa schwere LOX sowie das Pro-Peptid LOX-PP gespalten.[122]

Als Kupfer-abhängige amine Oxidasen katalysieren die LOX Isoformen vorrangig die extrazelluläre Polymerisation monomerer Matrixproteine. Intrazellulär beeinflusst die LOX neben der Zelladhäsion und -migration spezifisch die Genexpression der Kollagen III Isoform.[123]

Die Induktion der LOX und ihr Einfluss auf das extrazelluläre Remodeling (Ref.: RS6,RS7)

Die Kollagenisoformen werden zunächst als Monomere in den Extrazellulärraum sezerniert und erst durch post-translationale Modifikation zu stabilen Polymeren aufgebaut. Der initiale Schritt dieser Aggregatbildung, die oxidative Deamination von epsilon Aminogruppen, wird durch die katalytisch aktive Form der LOX realisiert.[124] Eine erhöhte Expression der kardialen LOX resultiert folglich in einer gesteigerten Vernetzung der Kollagen (und Elastin) Isoformen und wurde bereits durch Lopez et al. als Ursache für eine erhöhte Ventrikelsteifigkeit mit den daraus resultierenden Symptomen einer Herzinsuffizienz beschrieben.[125] Darüber hinaus beeinflusst die pre-LOX intrazellulär die Genexpression der Kollagen III Isoform, indem sie spezifisch den COL3A1 Promotor aktiviert.[126]

Die kardiale Fibrose der SHR ist nach drei Monaten Versuchsdauer funktionell noch nicht relevant, nach sechs Monaten steigt das E/A ratio jedoch auf einen Wert ≥2 und entspricht damit dem Stadium 3 einer restriktiven Füllungsstörung.[127] Beide Eigenschaften der LOX, die gesteigerte Vernetzung der Matrixproteine und die Steigerung der Kollagen III-Expression müssen für die diastolische Funktionsstörung verantwortlich gemacht werden.

Innerhalb der Versuchsgruppen lässt sich eine signifikante Korrelation zwischen der LOX-Expression und der Expression der Kollagen III Isoform sowie der linksventrikulären Masse herleiten. Auf eine ursächliche Beteiligung der Kollagen III Isoform an der diagnostizierten Relaxationsstörung trainierter SHR weist vorrangig die signifikante Korrelation des echokardiographisch ermittelten E/A ratios und der Kollagen III-Expression hin.

Cytokine wie TGF-beta und CTGF sowie eine Zunahme freier Radikale sind nicht nur ursächlich an der Entwicklung einer Herzinsuffizienz beteiligt, sie zählen ebenfalls zu den wichtigsten Mediatoren, die zur Induktion der LOX-Expression beitragen.[RS6,RS7,125]

Unabhängig von diesen klassischen Stimuli müssen für die gesteigerte Expression der LOX während des Ausdauertrainings noch alternative Mechanismen in Betracht gezogen werden. Im Myokard herzinsuffizienter Patienten sowie in kardialen Fibroblasten wurde sowohl die Expression als auch die Aktivität der LOX durch Osteopontin bzw. Osteopontin-abhängige Signalwege induziert.[128] In unserer Studie liefert die signifikante Korrelation zwischen der LOX- und der Osteopontin-Expression im linksventrikulären Myokard Hinweise auf einen vergleichbaren Regulationsmechanismus.

Das „nicht-klassische" Remodeling einer HFpEF

Osteopontin, ein saures, hochphosphoryliertes Glykoprotein für das bereits klinisch relevante pleiotrope Effekte innerhalb des kardio-vaskulären Systems beschrieben worden sind, wurde bereits von Lopez et al. als direkter Stimulus für eine gesteigerte LOX-Expression identifiziert.[128,129] Zusammenfassend lässt sich die Situation im linken Ventrikel der SHR wie folgt beschreiben: Adaptive Mechanismen verhindern im Myokard der Läufer das „klassische" Remodeling des chronisch druckbelasteten Herzens. Stattdessen induziert die Lauf- und Hypertonie-bedingte Aktivierung des Sympathikus bzw. des RAAS über Angiotensin II die Expression des Osteopontins und nachfolgend der LOX, die spezifisch den Kollagen III Promotor aktiviert und durch Quervernetzung die Steifigkeit des Ventrikels erhöht.[130-132] Darüber hinaus konnte für das Osteopontin bereits gezeigt werden, dass es ursächlich an der Entstehung einer kardialen Hypertrophie beteiligt ist, so dass die Ausbildung der linksventrikulären Hypertrophie ebenfalls als Folge dieses „nicht-klassischen" Remodelings in Betracht gezogen werden muss.[133,134]

Fazit: Die zusätzliche hämodynamische Belastung des Lauftrainings induziert in jungen, spontan hypertensiven Ratten eine diastolische Funktionsstörung bei gleichzeitig erhaltener systolischer Pumpfunktion. Die Aufklärung zugrunde liegender zellulärer und molekularer Mechanismen der kardialen Dysfunktion am Modell hämodynamisch belasteter SHR könnte zukünftig einen Beitrag zum besseren Verständnis bzgl. der Genese und Pathophysiologie einer HFpEF leisten.

Besonders hervorzuheben sind in diesem Zusammenhang die Befunde von Lavall et al., die in ihren Studien zum Vorhofflimmern das atriale Remodeling auf eine Aldosteron-induzierte Heraufregulation der LOX zurückführten. Die zugrunde liegenden Signalmechanismen liefen

unter Beteiligung des CTGFs sowie der RhoA/Rho Kinase ab; durch die Applikation von Spironolacton sowie einem Rhokinase-Inhibitor ließ sich die Induktion der LOX effizient verhindert.[135]

Der Einfluss von Spironolacton auf die HFpEF Symptomatik in SHR

In Kooperation mit der Kerckhoff-Klinik sowie dem Kerckhoff-Herzforschungsinstitut wurden bereits erste Versuchsserien initiiert, in denen der Einfluss des Aldosteronantagonisten Spironolacton auf den Blutdruck sowie das funktionelle und strukturelle Remodeling des Myokards am Modell einer Lauf-induzierten HFpEF Symptomatik untersucht werden soll. Die Applikation von Spironolacton erfolgt als therapeutische Intervention vier Monate nach Versuchsbeginn über einen Zeitraum von 20 Wochen.

Erste Ergebnisse und Befunde zeigen, dass sich die zurückgelegte Laufstrecke drei Wochen nach Therapiebeginn stabilisiert hat, während die Leistungsfähigkeit unbehandelter SHR aufgrund der kardialen Symptomatik kontinuierlich abnimmt. Darüber hinaus verringert der Aldosteronantagonist signifikant die Anzahl proinflammatorischer Zellen im venösen Blut und reduziert sowohl die Adhäsion als auch die Migration natürlicher Killerzellen an den Gefäßwänden. Diese Veränderungen spiegeln sich in einer signifikanten Verbesserung sämtlicher echokardiographisch erhobener Funktionsparameter wider.

Die LOX als Ursache einer HFpEF

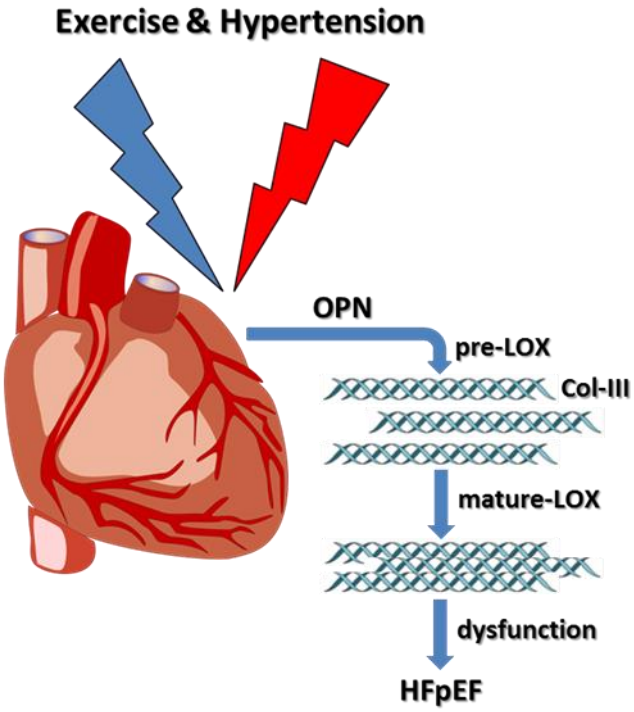

Abb. 3: Die spezifische Induktion des Osteopontins (OPN) verursacht durch gesteigerte Expression der Lysyloxidase (LOX) die linksventrikuläre Symptomatik einer HFpEF.

Die LOX als therapeutisches Target einer HFpEF

Udelson beschreibt in seinem Review die HFpEF als eine Form der Herzinsuffizienz, die aufgrund ihrer Risikofaktoren und Pathomechanismen als eigenständige Krankheitsentität zu betrachten sei, die folgerichtig eine spezifische und leitliniengerechte Therapie unabdingbar macht. Basierend auf der aktuellen Datenlage sollte der Fokus bei der Suche nach neuen therapeutischen Targets einer HFpEF verstärkt auf den Extrazellulärraum gelegt werden.[105]

Übereinstimmend wird eine Steigerung der LOX Aktivität bei zahlreichen Erkrankungen beschrieben, deren pathophysiologisches Korrelat in einer Fibrose der extrazellulären Matrix zu finden ist. Die Induktion der LOX wird sowohl für die Akkumulation als auch die effizientere Vernetzung sowie eine gestörte Degradation extrazellulärer Fasern verantwortlich gemacht. In zahlreichen Veröffentlichungen konnten Fibrose-assoziierte Erkrankungen der Lunge[136,137], der Leber[138,139], der Haut[140] und nicht zuletzt des Herzens[141-143] und der Blutgefäße[144,145] auf die Induktion der LOX bzw. der LOX-like Enzyme zurückgeführt werden. Darüber hinaus wurde die LOX als Ursache für bestimmte Formen der

Myelofibrose sowie für die gehäufte Metastasierung verschiedener Tumore identifiziert.[146-149] Basierend auf diesen Befunden wurde der Einsatz allgemeiner sowie Isoform-spezifischer LOX-Inhibitoren für zahlreiche Indikationen vorgeschlagen. Für die beiden Wirkstoffe β-Aminopropionitril und Tetrathiomolybdat ist die inhibitorische Effizienz hinreichend bewiesen, ihr Nebenwirkungsprofil verhindert jedoch den Einsatz *in vivo*.[150-152]

Aufgrund der zahlreichen Anwendungsmöglichkeiten befinden sich derzeit sowohl small molecule Inhibitoren[153] als auch monoklonale Antikörper[154,155] in der Entwicklung. Beide Ansätze verfolgen das Ziel, sowohl selektiv einzelne Isoformen als auch unspezifisch alle fünf Mitglieder der LOX Familie zu hemmen. Der Einsatz monoklonaler Antikörper würde ausschließlich die extrazellulären Metabolite der LOX neutralisieren, während die small molecule Inhibitoren darüber hinaus die intrazelluläre Aktivität der LOX hemmen.

Abgesehen vom individuellen Nebenwirkungsprofil könnte jedoch eine generelle bzw. unverhältnismäßig starke Inhibition der LOX zu Struktur- und Funktionsstörungen verschiedener Organsysteme führen. Die LOX knock-out Maus stirbt bereits perinatal aufgrund schwerwiegender kardio-vaskulärer Fehlbildungen. Für das Herz-Kreislaufsystem spielt eine ausreichend hohe LOX-Aktivität jedoch auch in allen folgenden Lebensabschnitten eine wichtige Rolle. Innerhalb der Ventrikel und der Gefäße trägt sie nicht nur zur Normalisierung der Wandspannung bei, sie spielt nach neusten Erkenntnissen darüber hinaus eine wichtige Rolle bei der Stabilisierung arteriosklerotischer Plaques.[156,157]

Die Entwicklung neuer LOX-Inhibitoren hat bereits begonnen, die Chancen ihrer klinischen Anwendbarkeit zur Behandlung Fibrose-assoziierter sowie neoplastischer Erkrankungen sind gut.[158] Die Indikation zur adjuvanten Therapie restriktiver Funktionsstörungen des Herzmuskels kann auf Basis der vorliegenden Daten gestellt werden; die Charakterisierung der jeweils beteiligten Isoformen sowie die Identifikation spezifischer Interaktionspartner sind jedoch unabdingbare Voraussetzungen für die zukünftige Anwendung selektiver LOX-Inhibitoren bei ausgewählten Formen der Herzinsuffizienz.

3.3 Das funktionelle und strukturelle Remodeling des post-infarzierten Myokards

Das akute Koronarsyndrom basiert fast immer auf einer plötzlich einsetzenden, lokalen Durchblutungsstörung, die das Gewebe und die Struktur des Herzmuskels unmittelbar schädigen kann. Klinisch nicht sicher zu differenzieren, werden dem Syndrom die instabile

AP, der Myokardinfarkt sowie der plötzliche Herztod subsumiert.[16] Pathophysiologisch liegt der Perfusionsstörung die koronare Herzkrankheit zugrunde, die durch arteriosklerotische Gefäßwandveränderungen, Plaqueablagerungen sowie ein reduziertes intravasales Lumen charakterisiert ist.

Ein langjähriger Bluthochdruck und Nikotinkonsum, erhöhte Cholesterinwerte, ein Diabetes mellitus und nicht zuletzt die familiäre Belastung zählen zu den wichtigsten Risikofaktoren für die Entwicklung einer sog. Koronarsklerose. Der bereits eingeschränkte Blutfluss in derart vorgeschädigten Gefäßen kann durch ein entstandenes Blutgerinnsel plötzlich und vollständig unterbrochen werden. Darüber hinaus besteht die Gefahr, dass an der Oberfläche instabiler Plaques durch Einrisse in der Fibrinschicht die intravasale Blutgerinnung sowie die Bildung von Thromben initiiert werden.[159] Bereits 15 Minuten nach Unterbrechung der Blutzufuhr entstehen irreparable Schäden am Myokard, die nach ca. 4 Stunden mikroskopisch als Koagulationsnekrosen sowie Hyperkontraktionsbänder sichtbar werden.[160]

Die unter Umständen akut lebensbedrohliche Situation erfordert eine sofortige Intervention, deren Ziel es ist, durch Wiedereröffnung des verschlossenen Koronargefäßes sowohl Durchblutung als auch Reoxygenierung des betroffenen Areals sicherzustellen.

Die katheterinterventionelle oder chirurgische Revaskularisation begrenzen durch die Wiederherstellung des Blutflusses den Ischämie-bedingten Gewebsschaden; die unmittelbar einsetzende Durchblutung eines zuvor infarzierten Areals kann jedoch unter Umständen den bereits entstandenen Schaden zunächst noch vergrößern. Dieses paradox klingende Phänomen wird in der Medizin als „Reperfusionsschaden“ bezeichnet.[161]

Strategien der Myokardprotektion

Voraussetzung für die Verbesserung der langfristigen Prognose eines akuten Myokardinfarktes ist neben einer erfolgreichen Reperfusion die Reduktion des myokardialen Reperfusionsschadens und die Induktion eines positiven Remodelings. Zu den derzeit effizientesten Strategien der Myokardprotektion zählen kurze repetitive Ischämie/Reperfusionszyklen, die als ischämisches pre-conditioning (IPC) und ischämisches post-conditioning (IPoC) beschrieben werden.[162,163] Beide Interventionen greifen, obwohl sie an gegenüberliegenden Seiten der Ischämie angewandt werden, auf gemeinsame

Signalwege zurück, die als RISK oder SAFE pathways bezeichnet werden.[164,165] In wieweit diese Protektion auch langfristig zu einer besseren Prognose führt, hängt im Wesentlichen von ihrem Einfluss auf die unmittelbar einsetzenden Umbauprozesse des post-ischämischen Myokards ab.

Therapeutisch bietet die Applikation zum Zeitpunkt der Reperfusion eine relevante Interventionsmöglichkeit, so dass im klinischen Alltag ein IPoC die favorisierte Protektionsstrategie darstellt.[166]

Das kardioprotektive Potential einer Konditionierung

Die Effizienz beider Strategien hinsichtlich ihres kardioprotektiven Potentials konnte bereits in zahlreichen experimentellen Studien an unterschiedlichen Modellen gezeigt werden. An isolierten *ex vivo* perfundierten Herzen sowie an isolierten und kultivierten Herzmuskelzellen wurden die zugrunde liegenden Signalwege charakterisiert, die durch ein IPC bzw. IPoC aktiviert werden.[167,168] Anhand dieser Modelle können jedoch aufgrund der eingeschränkten Überlebenszeit der Gewebe keine Aussagen über eine langfristige Funktionsverbesserung bzw. ein positives Remodeling getroffen werden. Darüber hinaus wird in klassischen *in vivo* Kurzzeitmodellen überwiegend die Infarktgrößenreduktion als relevanter Endpunkt der Myokardprotektion gewählt, die jedoch häufig nicht von einer entsprechenden Funktionserholung begleitet wurde.[169,170]

Folglich ist zum heutigen Zeitpunkt weitgehend unklar, in wieweit das konditionierte Herz auch mittel- bzw. langfristig von einer der beiden Protektionsstrategien profitiert. Für beide Applikationen konnte bereits gezeigt werden, dass sowohl vorab durchgeführte medikamentöse Interventionen als auch bestehende Vorerkrankungen (Diabetes mellitus, Herzinsuffizienz) zu einer Reduktion ihres kardioprotektiven Potentials beitragen.[171-173]

Der Einfluss von IPC und IPoC auf die Funktion kardialer Rezeptoren (Ref.: RS10,RS16)

Eine wichtige Komponente für das funktionelle und strukturelle Remodeling und somit die langfristige Prognose des Patienten spielt das spezifische Rezeptor-vermittelte Signaling des post-ischämischen Herzens. Obwohl die Reduktion der Infarktgröße durch IPC und IPoC auf die Aktivierung identischer Signalwege und Schlüsselenzyme zurückzuführen ist, scheint die

Regulation und das Ansprechverhalten kardialer Rezeptoren durch die beiden Protokolle in unterschiedlicher Weise beeinflusst zu werden.[RS10,RS16] Watanabe postulierte bereits 2006, dass die Protektion durch ein IPC lediglich temporär erfolgt, das hinzugewonnene Zeitfenster jedoch durch eine gezielte medikamentöse Therapie effizient genutzt werden kann.[174] Eine effektive Medikation im Anschluss an ein IPC oder IPoC setzt jedoch fundierte Kenntnisse über den Rezeptorstatus des konditionierten post-ischämischen Myokards voraus.[175]

Kapitel 3.3 – Key Points

In den beiden folgenden Abschnitten wird zunächst der Stellenwert des PTHrP- und des beta-adrenergen Rezeptors für das post-ischämische Myokard sowie ihre Beeinflussung durch ein IPC bzw. IPoC beschrieben. Die Relevanz des Argininmetabolismus für das funktionelle und strukturelle Remodeling des reperfundierten Myokards wird im dritten Abschnitt dieses Kapitels erläutert.

Fragestellung

Lässt sich durch gezielte pharmakologische Intervention unmittelbar nach Revaskularisation das Ausmaß des Reperfusionsschadens reduzieren und die Entwicklung einer kardialen Dysfunktion verhindern?

Methodik

Akute und chronische Folgen eines Myokardinfarktes wurden in vivo, ex vivo am isoliert perfundierten Langendorff-Herzen sowie in vitro am Modell isolierter Herzmuskelzellen untersucht.

Eigene Befunde

- ***Verminderte NO-Spiegel, ein Östrogenmangel sowie die myokardiale Ischämie reduzieren das kardioprotektive Potential des PTHrPs in der frühen Reperfusion durch Herabregulation des korrespondierenden PTH1 Rezeptors.***
- ***Trotz seiner kardioprotektiven Effekte zu Beginn der Reperfusion verursacht die Applikation eines IPoCs durch Stabilisierung der GRK2 langfristig eine kardiale Dysfunktion mit eingeschränkter inotroper Funktionsreserve.***
- ***Über die Hemmung der Arginase unmittelbar zu Beginn der Reperfusion lässt sich die Ischämie-bedingte Dysbalance im Argininmetabolismus normalisieren und die kardiale Funktion stabilisieren.***

1) Das PTHrP/PTH1 Rezeptor System – Regulationsmechanismen und funktionelle Bedeutung im reperfundierten Myokard (Ref.: RS17,RS18)

Das Parathormon related Peptide (PTHrP) konnte 1987 erstmals als Ursache für das Syndrom der „hypercalcemia of malignancy“ identifiziert werden.[176] Sowohl in seiner Struktur als auch in seiner Wirkungsweise zeigt es ähnliche Charakteristika wie das PTH und das TIP39. Innerhalb des kardio-vaskulären Systems wird PTHrP in Glattmuskelzellen, Endothelzellen und im Vorhofmyokard exprimiert. Über para- und autokrine Mechanismen beeinflusst es durch Aktivierung des PTH1 Rezeptors die Kontraktilität und die Proliferation glatter Muskelzellen.[177-179] Ebenfalls Rezeptor-vermittelt zählt die vasorelaxierende Wirkung auf Koronargefäße zu den wichtigsten kardioprotektiven Eigenschaften des PTHrPs; auf molekularer Ebene konnten sowohl Sutliff als auch Abdallah et al. die Induktion des endothelium-derived hyperpolarizating factors sowie eine Cyclooxygenase-abhängige Freisetzung von Prostaglandinen nachweisen; an isolierten Endothelzellen führte die Applikation von PTHrP darüber hinaus zu einer Freisetzung von NO.[180-182]

Die spezifischen Wirkungen des PTHrPs auf kardiale Funktionsparameter sind noch immer Gegenstand der aktuellen Forschung[RS17]; es beeinflusst sowohl die Chronotropie als auch die Inotropie und trägt zum hypertrophen Wachstum ventrikulärer Herzmuskelzellen bei.[183] Eine Hypoxie-induzierte Freisetzung von PTHrP verbessert nicht nur die Inotropie des reperfundierten Myokards[RS18], seine vasodilatierenden Eigenschaften führen darüber hinaus zu einer signifikanten Verbesserung der post-ischämischen Perfusion.[184,185]

Aktuell existieren nur wenige gesicherte Befunde zu den Regulationsmechanismen der PTHrP-Expression sowie den spezifischen kardio-vaskulären Effekten von PTHrP unter physiologischen und pathophysiologischen Bedingungen.

Der Einfluss von NO auf das kardio-vaskuläre Risikoprofil

Bei Frauen nimmt die Prävalenz kardialer Ereignisse im Klimakterium und in der Menopause deutlich zu. Diesem Umstand liegt eine kontinuierliche Abnahme der kardioprotektiv wirkenden weiblichen Geschlechtshormone zugrunde.[186,187] Verschiedene Studien konnten übereinstimmend zeigen, dass eine Hormonersatztherapie zahlreiche Risikofaktoren der koronaren Herzerkrankung signifikant reduziert. Beeinflusst werden der arterielle Blutdruck,

die Glattmuskelzell-Proliferation, die Serum-Lipidspiegel sowie der Glukose- und Insulinmetabolismus.[188,189]

Für den Anstieg des kardio-vaskulären Risikoprofils in der Postmenopause wird unter anderem ein Absinken der NO-Spiegel verantwortlich gemacht. Eine Substitution mit Östrogenen führt zu einem Anstieg der NO-Produktion durch Aktivierung und Expressionssteigerung der endothelialen NO-Synthasen.[190,191] Darüber hinaus wurde bereits in zwei Studien anhand von *in vivo* Modellen gezeigt, dass sinkende Östrogenspiegel direkt die Expression von PTHrP beeinflussen können.[192,193]

Die NO-abhängige Kardioprotektion durch PTHrP (Ref.: RS15,RS16,RS18)

Die kardialen Regulationsmechanismen des PTHrP Systems haben wir sowohl am Modell eines chronischen NO-Defizits in weiblichen Ratten (L-NAME) als auch an ovarektomierten Mäusen mit und ohne Hormonersatztherapie untersucht.[RS15]

Beide Tiermodelle liefern übereinstimmende Ergebnisse bzgl. der kardio-vaskulären Effekte von PTHrP und seines Rezeptors.

Verminderte NO-Spiegel führen zu einem Verlust der inotropen und chronotropen Wirkung, deren Ursache wir auf eine Herabregulation des PTH1 Rezeptors in (linksventrikulären) Kardiomyozyten zurückführen konnten. Die gefäßrelaxierenden Eigenschaften von PTHrP werden unter diesen Bedingungen nicht beeinflusst. Für die Regulation des Rezeptors in Kardiomyozyten haben wir TGF-beta als wichtigen Mediator identifizieren können; die endotheliale Regulation findet hingegen TGF-beta-unabhängig statt. Zur Wiederherstellung einer normalen Rezeptor-Expression am linken Ventrikel stellt die Applikation von Östrogenen in ovarektomierten Mäusen eine effiziente Therapieoption dar.[RS15]

Basierend auf den Ergebnissen dieser Studie führt ein derart verändertes Wirkprofil von PTHrP unter den Bedingungen verminderter NO-Spiegel zu einer Verschlechterung des kardialen Risikoprofils. Während eine Verbesserung der Koronarperfusion auch in NO-defizienten Tieren zu beobachten ist, würde sich die reduzierte Ansprechbarkeit ventrikulärer Myozyten negativ auf eine post-ischämische Funktionserholung des Herzens auswirken. Das während einer Ischämie/Hypoxie endothelial freigesetzte PTHrP verbessert am post-ischämischen Myokard direkt die kontraktile Funktion. Eine verminderte Expression

des myokardialen PTH1 Rezeptors schwächt somit einen wichtigen endogenen Protektionsmechanismus in der Reperfusion.[RS16,RS18,194,195]

Einfluss von Ischämie und Reperfusion auf den PTH1 Rezeptor (Ref.: RS16)

Bereits in 2007 untersuchten Ross et al. die Regulationsmechanismen kardial exprimierter PTHrP Rezeptoren und beschrieben eine kontinuierliche Desensitivierung des PTH1 Rezeptors im Verlauf einer prolongierten Ischämie.[196] Die einsetzende Hypoxie induziert andererseits die endotheliale Sekretion von PTHrP, ein Mechanismus, der zu Beginn der Reperfusion sowohl die Inotropie als auch die koronare Perfusion signifikant verbessern könnte. Ließen sich Desensitivierung bzw. Internalisierung des PTH1 Rezeptors verhindern, könnten die kardioprotektiven Eigenschaften des endogen freigesetzten PTHrP die Funktionserholung des reperfundierten Myokards unmittelbar unterstützen.

Signalmechanismen, die sowohl an der Internalisierung als auch an der intrazellulären Kopplung membranständiger Rezeptoren beteiligt sind, laufen häufig unter Beteiligung der PI3-Kinase ab. Als essentieller Bestandteil des RISK pathways sollten daher sowohl IPC als IPoC Einfluss auf die Regulation des PTH1 Rezeptors nehmen können.

Am Modell *ex vivo* perfundierter Langendorff-Herzen haben wir zeigen können, dass eine Desensitivierung des PTHrP Rezeptors während einer 45-minütigen no-flow Ischämie durch ein IPoC, nicht aber durch ein IPC verhindert werden kann. Durch selektive Inhibition konnte die Beteiligung der PI3-Kinase bestätigt werden; die PKC, ebenfalls wichtiger Bestandteil des RISK pathways, spielt auf Basis unserer Befunde dbzgl. keine Rolle.[RS16]

Kardioprotektive Mechanismen des PTHrP/PTH1 Rezeptor Systems

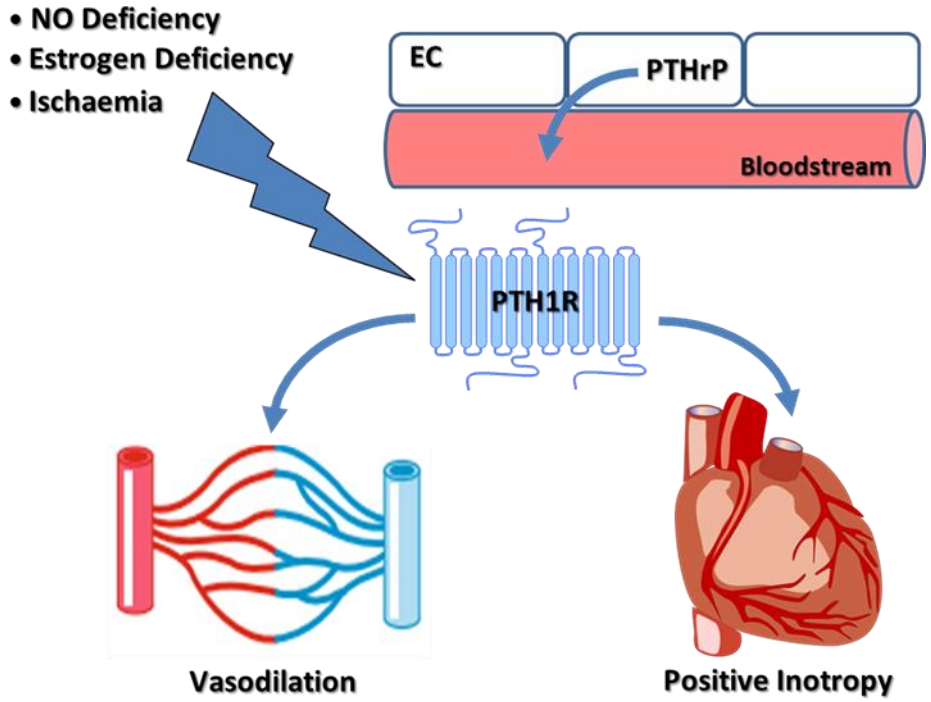

Abb. 4: Das endothelial (EC) freigesetzte PTHrP verbessert durch Aktivierung des PTH1 Rezeptors sowohl die Koronarperfusion als auch die Kontraktilität des post-ischämischen Myokards.

Das Parathormon related Peptide als therapeutisches Target im reperfundierten Myokard (Ref.: RS15,RS16)

Zur Umsetzung seiner protektiven Effekte ist das endogen freigesetzte PTHrP auf eine ausreichend hohe Expression des PTH1 Rezeptors im post-ischämischen Myokard angewiesen. In unseren Studien haben wir ein chronisches NO-Defizit, einen persistierenden Östrogenmangel sowie die myokardiale Ischämie als Ursachen einer verminderten Rezeptor-Expression im Herz identifizieren können.[RS15,RS16]

Therapeutisch können wir in unseren Modellen die Suppression des PTH1 Rezeptors durch Applikation einer Hormonersatztherapie sowie eines IPoC verhindern. Experimentell lässt sich sowohl die endotheliale Freisetzung des PTHrPs als auch die gezielte Stimulation des PTH1 Rezeptors innerhalb des kardio-vaskulären Systems nur schwer umsetzen. Vor dem Hintergrund, das therapeutische Potential des endogenen PTHrPs möglichst effizient nutzen zu können, sollte das Ziel zukünftiger Studien darin bestehen, den Einfluss zugelassener Standardtherapien auf die Expression des PTH1 Rezeptors hin zu untersuchen.

Detaillierte Kenntnisse zur Regulation des PTH1 Rezeptors im kardio-vaskulären System sind auch im Hinblick auf die Entwicklung neuer PTHrP Analoga (1-36, 1-34 BA058) zur Behandlung der (postmenopausalen) Osteoporose zwingend erforderlich.[197,198]

2) Der Einfluss von IPC und IPoC auf die Aktivierbarkeit und intrazelluläre Kopplung des β_1-adrenergen Rezeptors

Die Aufrechterhaltung sowie die bedarfsgerechte Anpassung der Herzfunktion stehen vorrangig unter Kontrolle β-adrenerger Rezeptoren. Neben der Aktivität des Sinus- und AV-Knotens beeinflussen sie maßgeblich die Inotropie und Lusitropie und sind darüber hinaus für die Sicherstellung der Myokardperfusion durch Dilatation insbesondere der kleineren Koronargefäße verantwortlich.

Das Verhältnis von β_1 zu β_2 Rezeptoren beträgt im Herzen ca. 70:30. Funktionell wirken sie überwiegend synergistisch, jedoch überwiegt der Einfluss des β_1 Rezeptors am Myokard und der des β_2 Rezeptors an der glatten Muskulatur der Gefäße. Quantitativ spielt der β_3 Rezeptor im Herz eine untergeordnete Rolle, doch werden ihm besonders im insuffizienten Myokard protektive Effekte zugeschrieben.[199]

Die Dichte sowie das Signaling kardialer β-Rezeptoren ändern sich im Verlauf vieler kardio-vaskulärer Erkrankungen. Im reperfundierten Myokard findet nach initialer Zunahme der β-Rezeptoren langfristig eine signifikante Herabregulation statt. Die Aktivierbarkeit und intrazelluläre Kopplung des β_1-adrenergen Rezeptors hingegen wird besonders in der post-ischämischen Frühphase inadäquat erhöht.[200-202]

Derzeit unbekannt sind die Effekte der beiden Interventionsstrategien IPC und IPoC auf die Funktion kardialer β-Rezeptoren, die als wichtige Komponenten des funktionellen und strukturellen Remodelings maßgeblich am Funktionserhalt des post-ischämischen Myokards beteiligt sind und somit die Effizienz einer Konditionierungsstrategie grundlegend beeinflussen können.

IPoC – Ergebnisse aktueller Langzeitstudien

Die Resultate klinischer Studien liefern für das IPoC hinsichtlich Effizienz und Sicherheit bisher kein einheitliches Bild.[203] Vielmehr wurden im Jahr 2013 von Freixa et al. in einer

single-centre Studie neben einer geringfügig eingeschränkten Pumpfunktion (EF (%), IPoC vs. Controls: 44.3±10.4 vs. 47.5± 9.1, p=0.28) nach Ablauf von 6 Monaten eine signifikante Verschlechterung der myocardial salvage und des myocardial salvage index festgestellt.[204] Diese Ergebnisse entsprechen den von Hahn et al. veröffentlichen Daten einer 700 Patienten umfassenden multi-centre Studie (POST trial), die zwischen 2009 und 2012 durchgeführt wurde.[205] Darüber hinaus wurden in 2017 von Engström et al. die Ergebnisse des DANAMI-3–iPOST trial veröffentlicht; die Anwendung eines IPoC nach erfolgter perkutaner Koronarintervention beeinflusste nach 38 Monaten follow-up weder die Gesamtmortalität noch die Hospitalisierung.[206]

Das kardioprotektive Potential eines IPC bzw. IPoC wurde in vielen tierexperimentellen Studien innerhalb weniger Stunden nach Beginn der Reperfusion vorrangig über ihren Einfluss auf die Infarktgröße, die Apoptoserate, die Radikalproduktion, die pH Stabilisierung und das Infarktödem nachgewiesen.[163,175,207]

Die Reduktion von Infarktgröße und metabolischer Störung durch Applikation eines IPC oder IPoC sollten auf Grundlage einer verbesserten kurzfristigen Ausgangssituation auch langfristig das funktionelle und strukturelle Remodeling des post-ischämischen Myokards verbessern. Zu den möglichen Ursachen und Gründen der unerwartet schlechten Resultate klinischer Langzeitstudien liegen aktuell keine gesicherten Daten vor.

Vor diesem Hintergrund haben wir in unseren Arbeiten unter Verwendung etablierter IPC und IPoC Algorithmen das Remodeling des reperfundierten Myokards am Modell der Ratte sowohl akut als auch nach Ablauf von 7 Tagen untersucht.

Funktionelle und molekularbiologische Analysen wurden vor allem unter Berücksichtigung des beta-adrenergen Systems *in vivo*, *ex vivo* sowie *in vitro* am Modell isolierter Herzmuskelzellen durchgeführt.

Die GRK2-induzierte Desensitivierung β-adrenerger Rezeptoren (Ref.: RS10)

Die Applikation eines IPoC führt, im Gegensatz zu der eines IPC, trotz kurzfristiger Kardioprotektion nicht zum langfristigen Funktionserhalt des post-ischämischen Myokards, so der zentrale Untersuchungsbefund unserer Studie.[RS10]

Die spezifische Induktion der GRK2 im postkonditionierten Herz verursacht in Verbindung mit einer reduzierten Expression β-adrenerger Rezeptoren ein molekulares Remodeling, das als pathophysiologisches Korrelat einer kontraktilen Funktionsstörung den Beginn einer systolischen Herzinsuffizienz kennzeichnet. Die GRK2-induzierte Desensitivierung β-adrenerger Rezeptoren betrifft jedoch ausschließlich das Myokard und reduziert somit 'nur' das positiv inotrope sowie lusitrope Potential des Ventrikels. Die Schrittmacherzellen werden durch die Applikation nicht beeinflusst, so dass eine (wünschenswerte) Frequenzkontrolle nicht zu beobachten ist. Ausgenommen von einer Desensitivierung sind ebenfalls die Koronargefäße, die somit durch Erhalt der β-adrenerg-vermittelten Gefäßdilatation weiterhin eine bedarfsgerechte Myokardperfusion gewährleisten können.[RS10]

GRKs – Klassifikation und Aufgabenspektrum

Säugetiere verfügen über sieben Isoformen G-Protein gekoppelter Rezeptorkinasen (GRKs). Die Klassifikation basiert auf der jeweiligen Funktion, den Interaktionspartnern sowie der Gewebespezifität und umfasst drei Subgruppen: GRK1 und GRK7 werden als „visuelle“ GRKs ausschließlich in Zellen der Retina exprimiert, GRK2 und GRK3, die beiden Vertreter der zweiten Subgruppe, werden als sog. β-adrenerge Rezeptorkinasen (β-ARKs) nahezu ubiquitär exprimiert. Die GRK4, deren Vorkommen fast ausschließlich auf das Hodengewebe beschränkt ist, bildet zusammen mit den Isoformen GRK5 und GRK6 die dritte Subgruppe.[208,209]

Obgleich für die jeweiligen Isoformen durchaus hochspezifische Charakteristika identifiziert werden konnten, weisen alle sieben GRK Mitglieder eine nahezu identische Struktur auf: eine zentral gelegene, hochkonservierte katalytische Domäne wird jeweils von variablen C- und N-terminalen Enden flankiert.[210]

Für die einzelnen Isoformen wurden mitunter zahlreiche Interaktionspartner beschrieben, so dass den GRKs ein breites Aufgabenspektrum zuteil wird, das weit über die Regulation G-Protein gekoppelter Rezeptoren hinausgeht: Sie beeinflussen die Aktivität von Rezeptor-Tyrosinkinasen und ihren downstream Elementen, interagieren mit wichtigen Kinasen der Signaltransduktion (p38Mapk, AMPK, PI3K/Akt, MEK1) und nehmen direkt Einfluss auf die

Aktivität verschiedener Transkriptionsfaktoren (Smad2/3, IκBα). Diese multifunktionalen Eigenschaften werden vor allem der kardial dominierenden Isoform GRK2 zugeschrieben.[208]

Bereits im Frühstadium einer Insuffizienz kennzeichnet die Induktion der GRK2 den Beginn des kardialen Remodelings auf molekularer Ebene. Darüber hinaus wird hohen GRK2-Spiegeln eine ursächliche Beteiligung an der Pathogenese und Progression wichtiger kardiovaskulärer Risikofaktoren zugeschrieben. Durch medikamentöse Hemmung ließe sich folglich nicht nur die kardiale Symptomatik unmittelbar verbessern, nach aktuellem Kenntnisstand sind ebenfalls positive Effekte auf Co-Morbiditäten wie Glukoseintoleranz, arterielle Hypertonie sowie eine bestehende Obesitas zu erwarten.[211-214]

Zur Verbesserung der klinischen Diagnostik verglichen Iaccarino und Wen-Qian et al. an zwei unabhängigen Patientenkollektiven nach linksventrikulärem Infarkt bzw. diagnostizierter Herzinsuffizienz die kardiale GRK2-Expression mit der in zirkulierenden Lymphozyten. In beiden Fällen spiegelten die Zellen des peripheren Blutes die Änderungen im Herzen wider. Die Bestimmung der GRK2-Expression/Aktivität in zirkulierenden Lymphozyten könnte somit als potentieller Surrogatmarker herangezogen werden, mit dessen Hilfe Änderungen der kardialen GRK2-Expression nachvollzogen werden können.[215,216]

Einfluss der GRK2 auf die kardiale Funktion (Ref.: RS11)

Entscheidend am Regulationsmechanismus der intrazellulären Kopplung β-adrenerger Rezeptoren im Myokard beteiligt ist die β-adrenerge Rezeptorkinase 1 (GRK2), die durch Phosphorylierung an Serin und Threonin Resten intrazellulärer Domänen des Rezeptors die Anlagerung von β-Arrestin vermittelt, dass seinerseits die Aktivierung der Gs-Untereinheit verhindert bzw. die Internalisierung des Rezeptors induzieren kann.[RS11,210]

Ursprünglich wurde postuliert, dass eine Erhöhung der GRK2-Spiegel während der Progression einer Herzinsuffizienz einen sinnvollen Protektionsmechanismus darstellen könnte, der das Herz vor exzessiver Katecholaminexposition schützt.[217] Auch für das post-infarzierte Herz könnte eine schnelle und transiente Erhöhung bzw. Aktivierung der GRK2 den Reperfusionsschaden reduzieren und das Myokard vor Hyperkontrakturen schützen. Eine langfristige und dauerhafte Heraufregulation der GRK2 mit einer daraus resultierenden Desensitivierung bzw. Entkopplung β-adrenerger Rezeptoren führt jedoch unweigerlich zur kardialen Funktionseinschränkung und dem Verlust der positiv inotropen Reserve.[218-221] Im

transgenen Mausmodell beschrieben sowohl Harding als auch Tevaearai et al., dass eine kardial-spezifische Überexpression des GRK2-Inhibitors βARKct nicht nur die basale und Katecholamin-stimulierte Herzfunktion verbessert, sie führt darüber hinaus in verschiedenen Modellen der Herzinsuffizienz zu einer signifikanten Reduktion der kardialen Dysfunktion sowie der Mortalität.[222,223] Rockman et al. konnten diese Ergebnisse mit Hilfe kardial-spezifischer heterozygoter GRK2 knock-out Mäuse bestätigen, die ebenfalls nach Induktion einer Herzinsuffizienz eine signifikant bessere Prognose aufwiesen.[224]

Regulationsmechanismen der GRK2

Zum gegenwärtigen Zeitpunkt existieren nur wenige gesicherte Befunde über die genauen Regulationsmechanismen der GRK2 innerhalb des kardio-vaskulären Systems. Die Steuerung der Expression erfolgt wie von Penela et al. beschrieben sowohl auf Ebene der Transkription als auch durch Beeinflussung der Degradation und somit der Stabilisierung des Proteins.[225] Das exakte Zusammenspiel zwischen Synthese und Abbau unter physiologischen und pathophysiologischen Bedingungen ist weitgehend unbekannt, doch kommt dem Abbau der GRK2 über eine Ubiquitinierung mit nachfolgendem proteasomalen Abbau eine nicht unerhebliche Rolle zu.[226] An diesem Prozess sind sowohl das β-Arrestin als auch die E3-ubiquitin ligase Mdm2 beteiligt, die nach Befunden von Salcedo et al. über eine Komplexbildung den Abbau der GRK2 über das Proteasom initiiert.[227]

β-Arrestin werden innerhalb dieser Regelmechanismen ebenfalls verschiedene Funktionen zugeschrieben. Zusammen mit der GRK2 ist es direkt an der Entkopplung sowie Internalisierung G-Protein gekoppelter Rezeptoren beteiligt. Darüber hinaus kann es in Abwesenheit einer Rezeptorstimulation die GRK2-Mdm2 Interaktion und somit den Abbau der GRK2 inhibieren, andererseits bei Rezeptorstimulation die Komplexbildung und somit die Degradation der GRK2 fördern.[228]

Die signifikante Zunahme der GRK2-Spiegel in den postkonditionierten Herzen unserer Studie ist aufgrund der vorliegenden Befunde auf eine gestörte Degradation zurückzuführen, deren Ursache in einer verstärkten Phosphorylierung des Mdm2 zu finden ist. Phosphoryliertes Mdm2 translociert verstärkt in den Kern und steht somit nicht mehr für die Ubiquitinierung der GRK2 im Zytosol zur Verfügung. Darüber hinaus wird eine gestörte

Interaktion des phosphorylierten Mdm2 mit der GRK2 postuliert, das folglich nicht mehr dem Proteasom zugeführt werden kann.[227]

Da PI3-Kinase (RISK pathway) und Mdm2 bereits als direkte Interaktionspartner beschrieben wurden, sollte in den postkonditionierten Herzen vorrangig der PI3/Akt-Mdm2 Signalweg für eine Stabilisierung der GRK2 verantwortlich sein.[229-233]

Der Einfluss eines IPoC auf die Kopplung kardialer β-Rezeptoren

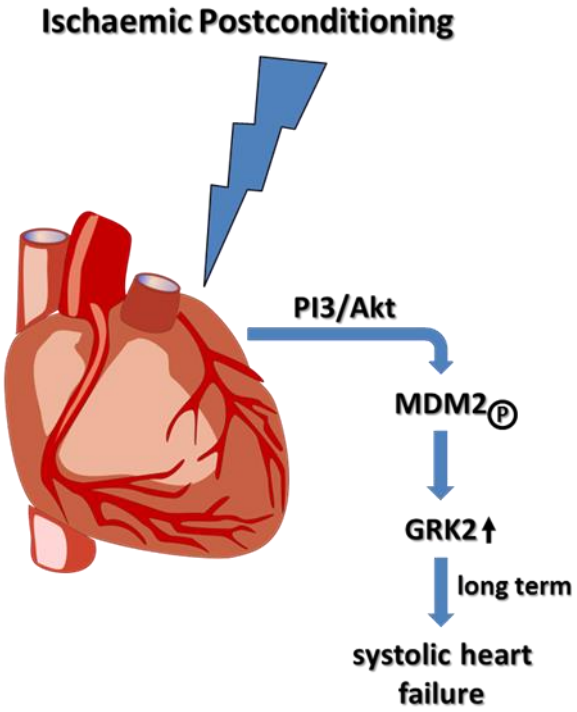

Abb. 5: Die IPoC-induzierte Stabilisierung der GRK2 führt durch Verlust der positiv inotropen Funktion kardialer β-Rezeptoren zum funktionellen Bild einer systolischen Herzinsuffizienz.

Die GRK2 als therapeutisches Target im reperfundierten Myokard

Die Ergebnisse unserer Studie haben erstmalig gezeigt, dass die Applikation einer ischämischen Postkonditionierung eine Desensitivierung bzw. Entkopplung β-adrenerger Rezeptoren hervorruft, in dessen Folge eine kardiale Dysfunktion mit eingeschränkter inotroper Funktionsreserve induziert wird. Bei vergleichbaren kardioprotektiven Eigenschaften unmittelbar nach dem Infarkt gewährleistet ein IPC, ohne das beta-adrenerge System zu beeinträchtigen, auch langfristig den Funktionserhalt des post-ischämischen

Myokards. Die vorliegenden Befunde müssen als mögliche Ursachen der bislang enttäuschenden Resultate klinischer Langzeitstudien in Betracht gezogen werden und erfordern, die klinische Anwendung eines IPoC kritisch zu überdenken.

Zusammen mit dem kardioprotektiven Potential unmittelbar nach Beginn der Reperfusion könnte jedoch durch selektive Hemmung der GRK2 auch langfristig eine signifikante Funktionsverbesserung des postkonditionierten Myokards erzielt werden.

Mit dem Ziel, die Aktivität der GRK2 effizient zu reduzieren, werden derzeit in zahlreichen Studien vielversprechende Therapieansätze und Wirkstoffkandidaten auf ihre klinische Anwendung hin untersucht.

Sowohl der GRK2 Knock-out als auch das adeno- bzw. lentiviral-induzierte Silencing sowie die Überexpression selektiver GRK2-Inhibitorpeptide haben in den letzten Jahren wichtige Erkenntnisse bzgl. der potentiellen Anwendungsmöglichkeiten zukünftiger GRK2-Inhibitoren geliefert. Ein klinischer Transfer dieser experimentellen „Therapiestrategien“ lässt sich derzeit allerdings nicht realisieren.

Small molecule Inhibitoren

Identifiziert durch Takeda, stabilisieren die beiden heterocyclische Verbindungen CMPD101 und CMPD103A selektiv die katalytischen Domänen der GRK2 und GRK3 in einem nahezu geschlossenen Zustand. Die klinische Anwendung misslang aller Wahrscheinlichkeit nach durch zu geringe Bioverfügbarkeit *in vivo*.[234]

Basierend auf den Erkenntnissen, dass der FDA zugelassene Serotonin-Wiederaufnahme-Hemmer Paroxetin die Aktivität der GRK2 reduzieren kann, wurden mit dem Ziel einer verbesserten Selektivität und Effizienz aussichtsreiche strukturverwandte Verbindungen identifiziert. Doch sowohl für GSK180736A als auch für CCG-224406 und 14as sind bisher keine klinischen Studien initiiert worden. Aktuell wird jedoch der Einfluss von Paroxetin (20 mg QD per os über 12 Wochen, anschließend 10 mg für eine Woche) an einem 50 Patienten umfassenden Kollektiv auf das Remodeling des post-infarzierten Myokards untersucht. Erste Studienergebnisse werden im Laufe des Jahres 2020 erwartet.[235,236]

Aptamere

Für die GRK2 wurde das hochselektive RNA Aptamer C13 entwickelt, dass durch Bindung an die katalytische Domäne die Struktur in einer inaktiven Konfiguration stabilisiert. Die Applikation RNA basierter Aptamere ist zurzeit auf *in vitro* Modelle beschränkt; bis zur klinischen Anwendbarkeit müssen noch umfangreiche Modifikationen zur Verbesserung ihrer Resorption und Stabilität durchgeführt werden.[237]

Peptide

Peptid-basierte Inhibitoren bieten bzgl. Selektivität und Nebenwirkungsprofil Vorteile gegenüber den small molecule Inhibitoren. Die Bioverfügbarkeit nach oraler Applikation sowie der frühzeitige Abbau durch Endo- und Exonukleasen limitieren jedoch ihre klinische Anwendbarkeit. KRX-683107 und KRX-683124 hemmen die GRK2 *in vitro* sowie nach parenteraler Gabe *in vivo*. Mit der Entwicklung cyclischer Peptide (9b and 10d) soll zukünftig die Halbwertszeit signifikant verlängert werden.[238]

Hemmung der GRK2-Gβγ Interaktion

Durch Überexpression des C-terminalen Fragments der GRK2 (βARKct) ist es gelungen, selektiv die Anlagerung der Isoform GRK2 an freie Gβγ-Untereinheiten zu blockieren. Sowohl für die Translokation als auch die Aktivierung der GRK2 hat sich die GRK2-Gβγ Interaktion als unabdingbare Voraussetzung erwiesen. Auf diesem Mechanismus basierend, konnte für die beiden small molecule Inhibitoren M119 und Gallein bereits *in vivo* gezeigt werden, dass sie durch Hemmung der GRK2-Gβγ Interaktion die Progression einer Herzinsuffizienz sicher verhindern können.[239,240]

Die vorgestellten Wirkstoffkandidaten haben in den sog. „rhodopsin/tubulin *in vitro* phosphorylation assays“ ihre Effizienz und Selektivität gegenüber der Isoform GRK2 unter Beweis gestellt. Darüber hinaus wurde in zahlreichen Tiermodellen nachgewiesen, dass die unterschiedlichen Interventionsstrategien durch Hemmung der GRK2 die Progression kardio-vaskulärer Erkrankungen signifikant reduzieren. Mit Ausnahme von Paroxetin, dessen Einfluss auf das post-ischämische Myokard zurzeit in der Phase 2 Studie „CARE-AMI“

untersucht wird, verfügen die oben aufgeführten Wirkstoffe (noch) nicht über ein ausreichendes klinisch-pharmakologisches Profil.

3) Der Einfluss des Argininmetabolismus auf die Funktionserholung des post-ischämischen Myokards (Ref.: RS12,RS13)

Die Entwicklung einer Herzinsuffizienz als Folge eines Myokardinfarktes ist auch nach erfolgreicher Reperfusion oftmals unvermeidlich. Prognostische Relevanz haben sowohl Umfang und Schweregrad des akut entstandenen Gewebeschadens als auch die unmittelbar einsetzenden Umbauprozesse des post-ischämischen Myokards; beide Einflussgrößen werden entscheidend durch die Bioverfügbarkeit von NO sowie die Konzentration reaktiver Sauerstoffspezies (ROS) geprägt. Ein Schlüsselenzym, dessen Induktion unmittelbar die NO/ROS-Balance stört und infolge dessen für zahlreiche Dysregulationen innerhalb des Herz-Kreislaufsystems verantwortlich gemacht wird, ist das manganhaltige Metalloenzym Arginase.[RS12,RS13] Im letzten Schritt des Harnstoffzyklus katalysiert das Enzym Arginase durch hydrolytische Abspaltung der Guanidinogruppe aus L-Arginin die beiden Reaktionsprodukte L-Ornithin und Isoharnstoff. In direkter Konkurrenz zur Arginase stehen die NO-produzierenden Enzyme, die über eine zweistufige 5-Elektronen-Redoxreaktion L-Arginin zu NO und L-Citrullin umsetzen.[241,242]

Der Einfluss von Stickstoffmonoxid auf die kardiale Funktion und das Remodeling des post-ischämischen Myokards

Die NO-Produktion wird überwiegend enzymatisch mit Hilfe der drei NOS Isoformen 1-3 aufrechterhalten. Quantitativ entfällt der größte Anteil auf die konstitutiv aktivierte NOS-3 des Endothels. Herzmuskelzellen selbst verfügen sowohl über die NOS-1 als auch die NOS-3, die Spezies-abhängig zu unterschiedlichen Anteilen ihren Beitrag zur myozytären NO-Produktion liefern.[243]

In niedriger Konzentrationen (nM Bereich) verursacht NO positiv inotrope Effekte, die auf eine Hemmung der PDEIII bzw. Aktivierung der Adenylatcyclase, einen Anstieg der cAMP Konzentration sowie eine gesteigerte PKA-Aktivität zurückzuführen sind. Im Bereich mikromolarer Konzentrationen überwiegen hingegen die negativ inotropen Eigenschaften

des NO; ausgelöst durch eine Aktivierung der Proteinkinase G wird die Aktivität spannungsgesteuerter Ca^{2+}-Kanäle inhibiert und die Ca^{2+}-Sensitivität des Troponinkomplexes durch TnI- Phosphorylierung herabgesetzt.[244,245]

In der Frühphase einer myokardialen Ischämie können die NO-Spiegel aufgrund gesteigerter Enzymaktivitäten für wenige Minuten zunächst ansteigen; kurz darauf inhibiert jedoch die beginnende Gewebsazidose sowohl Expression als auch Aktivität der NO-Synthasen, so dass sich mit zunehmender Dauer der Ischämie das NO-Defizit kontinuierlich ausweitet.

Nach einem kurzen Anstieg zu Beginn der Reperfusion verursachen langfristig überwiegend neurohumorale Mediatoren eine signifikante Reduktion der enzymatischen NO-Produktion. Als Folge des Substratmangels übertragen die NO-Synthasen im Anschluss an eine prolongierte Ischämie zunehmend freie Elektronen auf molekularen Sauerstoff und leisten somit einen entscheidenden Beitrag zur Produktion freier Radikale. Unter diesen Bedingungen gewinnt die „nicht-enzymatische“ NO-Produktion aus Nitrit, die selbst im sauren Milieu und deutlich reduzierten Sauerstoffpartialdrücken abläuft, zunehmend an Bedeutung.[246] Mit Ausnahme weniger Arbeiten werden dem gasförmigen Transmitter NO zahlreiche kardioprotektive Eigenschaften zugeschrieben. Jones und Bolli beschreiben in ihrem Reviewartikel die Situation wie folgt: “... whether NO is beneficial or detrimental to the ischemic myocardium is no longer an issue and the basic premise of this mini-review is undemanding: NO protects the heart against ischemia-reperfusion injury”.[247]

Die NO-vermittelte Protektion des ischämischen bzw. post-ischämischen Myokards erfolgt auf drei Ebenen: Die Koronarperfusion wird über eine vaskuläre Dilatation, eine Hemmung der Thrombozytenaggregation sowie eine reduzierte Adhäsion neutrophiler Monozyten verbessert; die Vitalität bzw. Integrität kardialer Zellen wird durch antiinflammatorische bzw. antiapoptotische Signalmechanismen sowie einen verringerten Sauerstoffbedarf aufrecht erhalten; das Myokard zeichnet sich durch eine verbesserte Ischämietoleranz aus, die sich in einer Reduktion des Infarktareals, einer verbesserten Funktion und einer verringerten Arrhythmieneigung widerspiegelt.[248,249]

Einfluss der Arginase auf die NO/ROS-Homöostase (Ref.: RS12)

Sowohl eine zelluläre Hypoxie (via c-Jun/AP1 pathway) als auch freie Radikale (via Rho/ROCK pathway) führen über jeweils unterschiedliche Signalwege zu einer Aktivierung sowie

Expressionssteigerung der Arginase.[250,251] Eine unverhältnismäßig hohe Arginaseaktivität wiederum entzieht den NO-Synthasen ihr Substrat (L-Arignin) und überführt es in den Polyaminstoffwechsel. Gleichzeitig tragen oxidativer Stress sowie die Arginase selbst zur Entkopplung der NO-Synthasen bei.[250] In dieser Konformation liefern sämtliche NO-produzierenden Enzyme, insbesondere die NOS-3 (eNOS), einen nicht unerheblichen Beitrag zur ROS-Produktion und sind neben der Ausbildung einer myokardialen Hypertrophie mittelfristig am funktionellen und strukturellen Remodeling des Myokards beteiligt.[252] Darüber hinaus verhindert eine Herabregulation des reduzierenden Co-Faktors Tetrahydrobiopterin die Rückkopplung der NO-Synthasen und beschleunigt somit die weitere Produktion von Radikalen.[252] Basierend auf Befunden, die vorwiegend in experimentellen Arbeiten sowie ersten klinischen Studien erhoben wurden, sollte eine pharmakologische Hemmung der Arginase über die Rebalancierung des L-Arginins die NO-Produktion normalisieren und parallel die ROS-Freisetzung reduzieren.[253,254]

Im Verlauf einer myokardialen Ischämie und Reperfusion dürfen der Arginase jedoch keineswegs ausschließlich nachteilige Eigenschaften zugesprochen werden. Aus den zuvor beschriebenen Mechanismen lassen sich für die Induktion bzw. Aktivierung der Arginase im Verlauf einer prolongierten Ischämie wichtige kardioprotektive Effekte herleiten. Wie zuvor beschrieben, tragen sämtliche NO-produzierenden Enzyme als direkte Folge der Ischämie/Hypoxie in zunehmendem Maße zur Akkumulation freier Radikale bei. Die Induktion der Arginase übernimmt in dieser Phase die Rolle eines endogenen, antioxidativen Schutzmechanismus, der den NO-Synthasen ihr Substrat (L-Arginin) entzieht und gleichzeitig deren Aktivität hemmt.[RS12]

Unmittelbar zu Beginn der Reperfusion entwickelt sich jedoch die bis dato protektive Dysbalance innerhalb kürzester Zeit zu einem kardio-vaskulären Risikofaktor für das post-ischämische Myokard.

Mit Beginn der Reoxygenierung werden sämtliche Voraussetzungen geschaffen, die zur Wiederaufnahme der enzymatischen NO-Produktion notwendig sind. Die supprimierte Expression sowie die reduzierte Aktivität der NO-Synthasen in Verbindung mit einem geringen Substratangebot verhindern jedoch den Aufbau ausreichend hoher NO-Spiegel in der Reperfusion.[255] Vor dem Hintergrund, das kardio-vaskuläre Remodeling durch Steigerung der endogenen NO-Produktion zu verbessern, erhielten Patienten im VINTAGE-MI trial täglich 3-mal 3 Gramm L-Arginin per os über einen Zeitraum von sechs Monaten nach

diagnostiziertem ST-Hebungsinfarkt. Die alleinige Supplementation von L-Arginin verbesserte in Anbetracht der zuvor beschriebenen Enzymkonstellationen weder vaskuläre noch kardiale Funktionsparameter; aufgrund einer erhöhten Mortalität in der Verumgruppe musste die Studie vorzeitig beendet werden.[256]

Expression und Regulation der Arginase

Isoformen der Arginase werden in nahezu allen prokaryonten und eukaryonten Organismengruppen exprimiert. Im Säugetier kodieren zwei unterschiedliche Gene die beiden Isoformen Arginase I und II, die nur geringe Unterschiede bzgl. ihrer katalytischen Eigenschaften aufweisen, anhand ihrer intrazellulären Kompartimentierung und Gewebeverteilung jedoch eindeutig zu differenzieren sind. Speziesunabhängig weisen die untersuchten Isoformen vor allem im Bereich der katalytischen Domäne eine ausgeprägte Sequenzkonservierung auf.[257,258]

Arginasen werden zu homo-trimeren Komplexen aufgebaut, deren Sekundärstruktur aus acht parallel angeordneten beta-Faltblatt-Strängen besteht, die von mehreren alpha-helikalen Domänen umgeben sind. Jede Untereinheit bindet in ihrem Zentrum zwei Mn(II)-Ionen in Form eines binuklearen Mangan-Clusters; die beiden Mn(II)-Ionen richten das Hydroxid-Ion zwischen sich aus, orientieren und stabilisieren das gesamte Molekül und ermöglichen den nukleophilen Angriff am Guanidin-Kohlenstoff des L-Arginins.[259,260]

Die Arginase I katalysiert als “hepatische” Isoform im Zytosol der Leberzellen den fünften und damit letzten Schritt des Harnstoffzyklus. Auf Chromosom 6 (6q.23) kodiert, wird ihre Aktivität vorrangig über die Expression gesteuert. Die ursprüngliche Annahme, Transkription und Translation der Arginase I seien ausschließlich der Leberzelle vorbehalten, musste zwischenzeitlich revidiert werden; ihr Nachweis in extra-hepatischem Gewebe schließt ebenfalls zahlreiche Zelltypen des kardio-vaskulären Systems ein.[261,262]

Der Arginase II werden vorrangig regulatorische Aufgaben innerhalb des Zellmetabolismus zugeschrieben; ihr zugehöriger Genlocus liegt auf dem langen Arm von Chromosom 14 (14q.24.1). Exprimiert wird die Arginase II sowohl in Hepatozyten als auch in Zellen, die keinen Harnstoffzyklus betreiben können. Vorrangig in den Mitochondrien lokalisiert, ist die Arginase II durch Bereitstellung von L-Ornithin direkt an der Prolin- und Polyaminsynthese beteiligt.[261,262]

Einfluss der Arginase auf die Funktion des post-ischämischen Myokards (Ref.: RS12-RS14)

Mit der Zielsetzung, Interventionsmöglichkeiten innerhalb des kardialen Argininmetabolismus zu identifizieren, haben wir am isoliert perfundierten Langendorff-Herzen sowie *in vivo* am closed chest Modell drei unterschiedliche Therapieansätze verglichen.

Expressionsanalysen am post-ischämischen linksventrikulären Myokard haben die zuvor postulierte Induktion Arginase-assoziierter Signalwege zu Lasten NO-produzierender Enzyme bestätigt. Eine unmittelbar zu Beginn der Reperfusion induzierte Hemmung der Arginase mittels Nor-NOHA führt bereits innerhalb von zwei Stunden zu einer signifikanten Verbesserung der post-ischämischen Funktion. Sowohl die Applikation des ACE-Hemmers Captopril als auch die Hemmung TNF-α-abhängiger Signalwege normalisieren den kardialen Argininmetabolismus und stabilisieren die Herzfunktion innerhalb der ersten 24 Stunden post Infarkt.[RS13,RS14]

Sowohl Induktion als auch Aktivierung der Arginase können im Verlauf einer myokardialen Ischämie durch zahlreiche Mediatoren ausgelöst werden; identifiziert wurden Interleukine (IL4, IL10, IL13), Interferone (IF-γ), microRNAs (miR-17-5p) sowie reaktive Sauerstoff- und Stickstoff-Verbindungen.[253]

Ausgelöst durch Ischämie und Reperfusion verursachen Ca^{2+}-Oszillationen innerhalb der Herzmuskelzellen irreversible, fokale Hyperkontrakturen, die unmittelbar die zelluläre Integrität und Vitalität der betroffenen sowie angrenzenden Kardiomyozyten beeinträchtigen. Infolgedessen können kleine, zytosolische RNA Fragmente (eRNAs) mittels auto- oder parakriner Stimulation die membranständige Sheddase TACE (TNF-α converting enzyme oder kurz “ADAM17”) aktivieren.[263] Der Tumornekrosefaktor alpha (TNF-α) wird zunächst als 26 kDa schweres, membrangebundenes Typ-2-Protein translatiert, das erst nach proteolytischer Spaltung durch die Metalloprotease TACE freigesetzt wird. TNF-α kann die Expression der Arginase sowohl über den c-Jun/AP1 als auch den PKC/Rho/ROCK Signalweg induzieren.[264,265] Durch Applikation des TACE-Inhibitors TAPI lässt sich die Induktion der Arginase sowie die Suppression der eNOS vollständig verhindern. Befunde von Flesch et al. haben darüber hinaus gezeigt, dass TNF-α-induzierte Signalmechanismen unter direkter Beteiligung des RAAS umgesetzt werden.[266] In Bezug auf die untersuchten Parameter erzielt

die frühzeitige Applikation des ACE-Hemmers Captopril vergleichbare Effekte wie der TACE-Inhibitor TAPI.

Die Induktion der Arginase mittels TAPI oder Captopril zu verhindern hat sich als effiziente Intervention erwiesen, die jedoch mit einer gewissen Verzögerung die Ischämie-bedingte Dysbalance im Argininmetabolismus normalisiert und infolge dessen die kardiale Funktion stabilisiert. Demgegenüber hat die Applikation des Arginase-Inhibitors Nor-NOHA zu Beginn der Reperfusion die Funktion des reperfundierten Myokards unmittelbar verbessern können.

Die therapeutische Effizienz einer direkten Arginasehemmung ist jedoch auf ein schmales Zeitfenster zu Beginn der Reperfusion begrenzt; in experimentellen Studien leicht umzusetzen, erschwert dieser Umstand den Transfer in die klinische Anwendung: protektioniert die Arginase noch während einer Ischämie das Myokard durch Hemmung der Radikalproduktion, werden ihr bereits 12 bis 24 Stunden nach Beginn der Reperfusion wichtige antiinflammatorische Effekte während der Reparaturprozesse infarzierter Areale zugeschrieben.[RS12]

Einfluss der Arginase auf die myokardiale Ischämie und Reperfusion

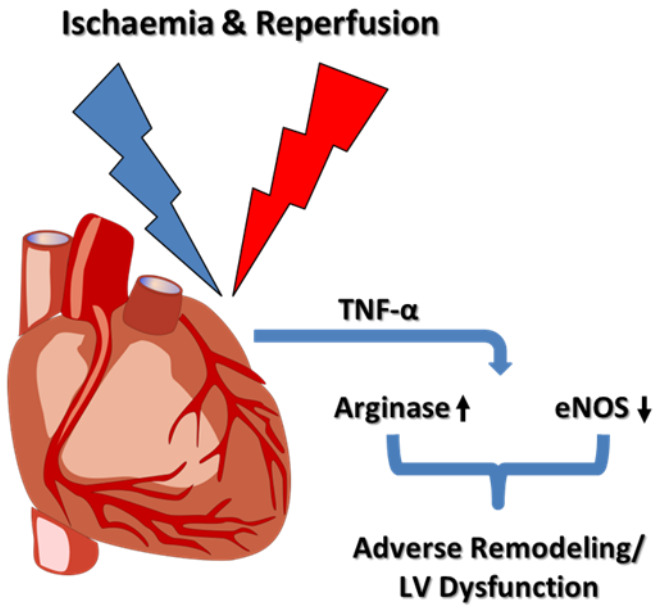

Abb. 6: TNF-α-abhängige Signalmechanismen induzieren im reperfundierten Myokard die Heraufregulation der Arginase sowie die Entkopplung NO-produzierender Enzyme.

Die Arginase als therapeutisches Target im reperfundierten Myokard

In ihren beiden Reviewartikeln haben sowohl Yang als auch Pernow et al. die Induktion der Arginase als Ursache zahlreicher Erkrankungen innerhalb des Herz-Kreislaufsystems identifizieren können und prognostizieren zukünftigen Arginase-Inhibitoren großes Potential.[250,253]

Direkte Arginase-Inhibitoren

Aktuelle Erkenntnisse zu Therapiestrategien basieren überwiegend auf *in vitro* Modellen sowie tierexperimentellen Studien unter Verwendung transgener und pharmakologischer Methoden. In begrenztem Umfang haben erste klinische Studien das therapeutische Potential des Arginase-Inhibitors Nor-NOHA in Bezug auf vaskuläre Funktionsparameter bestätigen können.

Aktuell verfügbare Inhibitoren weisen noch immer keine Isoformspezifität auf; die Arginase I knock-out Maus stirbt postnatal innerhalb von zwei Wochen.[267] Bzgl. der Pathogenese und Progression kardio-vaskulärer Erkrankungen konnte bislang keine eindeutige Differenzierung der beteiligten Isoformen getroffen werden.[268,269] Darüber hinaus erschweren sowohl Zeitpunkt als auch Therapiedauer die sichere Applikation pharmakologischer Arginase-Inhibitoren (siehe oben).

Zwei klinische Studien, in denen eine verbesserte Gefäßprotektion durch direkte Hemmung der Arginase erzielt werden sollte, sind erfolgreich abgeschlossen worden; die primären Endpunkte wurden erreicht.[270]

Substitutionstherapien

Die alleinige Substitution mit L-Arginin ist auf Basis unterschiedlichster Indikationen bereits an zahlreichen (Patienten-) Kollektiven untersucht worden. Die perorale Medikation im Anschluss an einen linksventrikulären Infarkt wurde jedoch ausschließlich im VINTAG-MI trial (siehe oben) durchgeführt; vaskuläre und kardiale Funktionsparameter zeigten keine Unterschiede im Vergleich zur Placebo-Gruppe.[256]

Die Befunde aktueller präklinischer Studien favorisieren im Hinblick auf eine Normalisierung der NOS/Arginase-Dysbalance die Substitution mit L-Citrullin bzw. die Kombination L-

Citrullin/L-Arginin. Die Aminosäure L-Citrullin kann bei Bedarf über die Argininosuccinat Synthetase und die Argininosuccinat Lyase zu L-Arginin metabolisiert werden und stellt somit ein abrufbares Substratreservoir dar, das sämtliche NO-Synthasen nutzen können; als entscheidender Vorteil gegenüber Arginin hat sich die effiziente Citrullin-induzierte Hemmung der Arginase erwiesen.[271-275] Erste klinische Studien, in denen kardio-vaskuläre Funktionsparameter nach oraler L-Citrullin Substitution untersucht worden sind, lieferten vielversprechende Ergebnisse.

Hemmung der Arginaseinduktion

Unabhängig von der Cholesterinsenkung werden zahlreiche gefäßprotektive Effekte der Statine durch pleiotrope Mechanismen vermittelt. Für Simvastatin und Atorvastatin konnte bereits gezeigt werden, dass sie durch Hemmung der GTPase RhoA sowohl die Induktion der Arginase verhindern als auch die Kopplung der NO-Synthasen stabilisieren.[268,276,277] Experimentell und klinisch ließen sich vergleichbare Effekte durch Hemmung des mTORC1-S6K1 Signalwegs sowie der p38MAP Kinase erzielen.[278,279] Die Effizienz dieses Therapieansatzes konnten wir in unserer Studie am reperfundierten Myokard durch die gezielte Hemmung TNF-α-abhängiger Signalwege verifizieren.

Die Aktivität der Arginase zu reduzieren bzw. ihre Induktion zu verhindern, haben sowohl in tierexperimentellen als auch in klinischen Studien kardio-vaskuläre Funktionsparameter signifikant verbessern können; eine favorisierte Strategie hat sich aus den vorgestellten Therapieansätzen bis heute (noch) nicht durchsetzen können.

3.4 Die Insuffizienz des rechtsventrikulären Myokards

Die Erforschung der rechtsventrikulären Physiologie sowie die Identifizierung spezifischer Pathomechanismen einer Rechtsherzinsuffizienz wurden über viele Jahre vernachlässigt, da nach gängiger Lehrmeinung die Funktion des rechten Ventrikels für die Aufrechterhaltung des Blutkreislaufs von untergeordneter Bedeutung sei. Wenige klinische Studien sowie eine begrenzte Auswahl therapeutischer Optionen stehen jedoch im Widerspruch zur Häufigkeit

und Prognose der Rechtsherzinsuffizienz, die sich dbzgl. nur unwesentlich von der Linksherzinsuffizienz unterscheidet.[280]

KAPITEL 3.4 – KEY POINTS

Der erste Teil dieses Kapitels beschreibt die zentrale Bedeutung sowie häufige Beteiligung des rechten Ventrikels an zahlreichen kardio-vaskulären Erkrankungen und unterstreicht die Notwendigkeit, die rechtsventrikuläre Pathophysiologie als eigenständige Entität zu betrachten, die sich nicht einfach von der des linken Ventrikels ableiten lässt. Im zweiten Teil werden Signalwege und Pathomechanismen vorgestellt, die wir an unserem Modell der Rechtsherzinsuffizienz identifiziert haben und zukünftig einen wichtigen Beitrag zur Entwicklung neuer und spezifischer Therapieoptionen leisten können.

FRAGESTELLUNG

Ist ein Transfer der gut dokumentierten Befunde zum linken Ventrikel hinsichtlich seiner Pathophysiologie uneingeschränkt auf den rechten Ventrikel zulässig?

METHODIK

Durch orale Applikation des NO-Synthase-Inhibitors L-NAME konnten wir ein nicht-invasives Modell einer Rechtsherzinsuffizienz entwickeln, an dem sich das kardiale Remodeling des rechten Ventrikels über einen Zeitraum von mehreren Wochen in vivo nachverfolgen lässt.

EIGENE BEFUNDE

- ***Die Applikation von L-NAME induziert ausschließlich im rechten Ventrikel ein Remodeling, das morphologisch und funktionell dem Bild einer dilatative Kardiomyopathie entspricht.***
- ***Der rechte Ventrikel verfügt nicht über die erforderlichen Adaptionsmechanismen zur Bewältigung oxidativer Stresssituationen.***
- ***Der linke Ventrikel ist imstande, über eine Induktion von Nrf-2 und dessen downstream Target SOD2 sein antioxidatives Potential entscheidend zu erhöhen.***
- ***Sowohl SOD Mimetics als auch Mitochondria-targeted Antioxidants könnten in Zukunft einen wichtigen Stellenwert im Therapieschema der Rechtsherzinsuffizienz einnehmen.***

Die Pathophysiologie des rechten Ventrikels

Das “National Heart, Lung, and Blood Institute” formulierte die Situation in einem Special-Report zum rechten Ventrikel wie folgt: „…, right ventricular failure cannot be understood simply by extrapolating data and experience from left ventricular failure.”…„The Right Ventricle Is Different From the Left Ventricle.”[281]

Lange Zeit bestand in der biomedizinischen Forschung der Konsens, dass der rechte Ventrikel zur Aufrechterhaltung und Stabilität der Hämodynamik im Blutkreislauf des Erwachsenen keinen nennenswerten Beitrag leiste. Diese (Fehl-) Einschätzung hatte zur Folge, dass die Erforschung der rechtsventrikulären Physiologie und darüber hinaus die Identifizierung spezifischer Pathomechanismen über viele Jahre außer Acht gelassen und nur wenige randomisierte klinische Studien zur Rechtsherzinsuffizienz initiiert worden sind.

Das Spektrum an therapeutischen Interventionen entspricht daher weitestgehend dem der Linksherzinsuffizienz und zielt vorwiegend auf eine Vasodilatation und somit eine Senkung der Nachlast ab.[282]

Darüber hinaus haben die Ergebnisse des CORE trial gezeigt, dass die isolierte Rechtsherzinsuffizienz oder die Beteiligung des rechten Ventrikels an der kardialen Symptomatik im Vergleich zu einer rein linksventrikulären Insuffizienz mit einer schlechteren Prognose assoziiert ist.[283] Die Rechtsherzinsuffizienz kann isoliert oder in Kombination mit einer Linksherzinsuffizienz auftreten; zugrunde liegende Ursachen können sowohl kardialen als auch extrakardialen Ursprungs sein.

Die Kardiogenese des rechten Ventrikels

Die chronische Herzinsuffizienz lässt sich als polyätiologisches Syndrom definieren, dem häufig eine komplexe Pathophysiologie zugrunde liegt. Jedoch lassen sich die bereits gut dokumentierten molekularen und zellphysiologischen Mechanismen des linken Ventrikels nicht ohne weiteres auf das rechte Herz übertragen. Dieser Umstand lässt sich bereits mit der spezifischen Kardiogenese des rechten Ventrikels begründen, dessen zellulärer Ursprung zusammen mit dem Septum und Ausflusstrakt auf das sekundäre oder vordere Herzfeld zurückzuführen ist. Die Vorhöfe sowie der gesamte linke Ventrikel entstammen hingegen einer Population Progenitorzellen, die sich zum sog. primären Herzfeld formiert haben.[284,285]

Die Rechtsherzinsuffizienz – eine eigenständige Krankheitsentität

Generell zeichnet sich der rechte Ventrikel durch eine hohe Plastizität aus. Stellt er noch intrauterin bei geöffnetem Ductus arteriosus die Körperperfusion sicher, wird diese Aufgabe von Geburt an auf die linke Herzhälfte übertragen.[286] Das Myokard des rechten Ventrikels passt sich postpartal seiner neuen Funktion an und zeichnet sich fortan bei geringer Wandstärke durch eine hohe Elastizität aus. Struktur und Geometrie sind auf Volumenarbeit ausgelegt und können leichter an eine erhöhte Vorlast als an einen Anstieg der Nachlast adaptieren.[286]

Der Beitrag des rechten Ventrikels an der Aufrechterhaltung einer bedarfsgerechten Blutzirkulation wurde lange Zeit unterschätzt und die Erforschung seiner spezifischen Physiologie vernachlässigt. Sein hoher Stellenwert für das gesamte Herz-Kreislaufsystem lässt sich jedoch allein damit erklären, dass die körperliche Leistungsfähigkeit stärker mit der rechtsventrikulären als der linksventrikulären Funktion korreliert.[287]

Darüber hinaus haben Gulati et al. eine rechtsventrikuläre Dysfunktion bei 30 % der Patienten mit nicht-ischämischer dilatativer Kardiomyopathie diagnostiziert und als unabhängigen Risikofaktor identifiziert, der mit einer 4-fach höheren Gesamtmortalität assoziiert war.[288] Vergleichbare Ergebnisse haben Metha et al. für die Beteiligung des rechten Ventrikels beim linksventrikulären Myokardinfarkt festgestellt und beschrieben eine erhöhte Rate post-ischämischer Komplikationen und Todesfälle.[283]

Für die PAH konnten Handoko et al. die Rechtsherzfunktion sogar als entscheidenden Prädiktor für eine frühzeitige Mortalität identifizieren, obwohl der rechte Ventrikel das Potential besitzt, sich langfristig an eine pathologisch erhöhte Nachlast durch kompensatorische Hypertrophie anzupassen.[74]

Das chronische NO-Defizit als Risikofaktor

Auf molekularer und zellphysiologischer Ebene werden die Pathogenese und Progression einer chronischen Herzinsuffizienz häufig auf eine reduzierte Bioverfügbarkeit von NO, erhöhten Radikalstress und endotheliale Dysfunktionen zurückgeführt.[289-291]

So wird die erhöhte Rate an kardio-vaskulären Ereignissen bei chronischen Nierenerkrankungen oder dem Typ 2 Diabetes mellitus unter anderem auf ein allgemeines

Defizit an NO zurückgeführt. Vergleichbare Befunde erklären das erhöhte kardiale Risikoprofil bei Frauen in der Postmenopause. In klinischen Studien und diversen Tiermodellen konnte die genomische und nicht-genomische Wirkung der Östrogene auf die endotheliale NO-Synthase als Ursache für einen Teil der protektiven Eigenschaften einer Hormonersatztherapie festgestellt werden.[292,293]

Die vielfach beschriebenen Effekte des NO innerhalb des Herz-Kreislaufsystems dürfen jedoch nicht allein auf seine vasodilatierenden und damit blutdrucksenkenden Eigenschaften reduziert werden. Vielmehr interagiert NO ubiquitär auf zellulärer und subzellulärer Ebene u.a. mit Signalmechanismen des RAAS, des sympathischen Nervensystems und der Mitochondrien und beeinflusst somit direkt und indirekt die Funktion und Struktur des Myokards.[294-296]

Die chronische L-NAME Applikation als nicht-invasives Modell einer Rechtsherzinsuffizienz (Ref.: RS20)

Der Zustand chronisch reduzierter Bioverfügbarkeit von NO stellt für das gesamte Herz-Kreislaufsystem einen Risikofaktor dar, der auf erhöhten hämodynamischen, oxidativen und inflammatorischen Stress zurückzuführen ist. In unserer Studie wurden die Voraussetzungen für ein entsprechendes Szenario in 3 Monate alten weiblichen Wistar Ratten durch die Verfütterung von L-NAME geschaffen. Im Anschluss an den vierwöchigen Behandlungszeitraum erfolgte die Charakterisierung des kardialen Remodelings getrennt für den rechten und linken Ventrikel unter Berücksichtigung struktureller und funktioneller Anpassungsreaktionen. [RS20]

Zur Differenzierung direkter und indirekter NO-abhängiger Effekte wurde die reine L-NAME Substitution um zwei weitere Applikationen ergänzt. In Form einer therapeutischen Intervention erhielt eine Behandlungsgruppe in der dritten und vierten Woche zusätzlich den ACE-Hemmer Captopril, eine weitere den Radikalfänger bzw. das SOD-Mimetikum Tempol. Neben seiner Interaktion mit dem RAAS und der daraus resultierenden Verringerung Angiotensin II-abhängiger Effekte besitzt Captopril über eine abspaltbare Sulfhydryl-(SH-) Gruppe direkte antioxidative Eigenschaften.[297,298] Durch den separaten Einsatz von Tempol lassen sich somit protektive Effekte identifizieren, die allein auf eine Reduktion von ROS zurückzuführen sind. [RS20]

Die vorrangige Zielsetzung dieses Versuchsaufbaus bestand darin, Schlüsselenzyme und Pathomechanismen zu identifizieren, die vor dem gemeinsamen Hintergrund des NO-Defizits für den jeweiligen Ventrikel spezifisch und in unterschiedlicher Weise reguliert werden.

Oxidativer Stress vs. antioxidative Kapazität (Ref.: RS20)

Der rechte Ventrikel verfügt -im Gegensatz zum linken- nicht über die erforderlichen Adaptionsmechanismen zur Bewältigung oxidativer Stresssituationen, so der wesentliche Untersuchungsbefund unserer Studie. Die L-NAME-induzierte Radikalbelastung des rechtsventrikulären Myokards führt zur Ausbildung einer dilatativen Kardiomyopathie mit ausgeprägter kontraktiler Dysfunktion. Das endogen vorhandene antioxidative Potential verhindert im linken Ventrikel ein entsprechendes strukturelles und funktionelles Remodeling. Durch adjuvante Therapie mit dem SOD-Mimetikum Tempol oder dem ebenfalls antioxidativ wirkenden Captopril lässt sich im rechten Ventrikel der Circulus vitiosus bestehend aus Radikalbildung, Fibrose und funktioneller Dysfunktion durchbrechen.[RS20]

Bei der chronischen Applikation von L-NAME über das Trinkwasser handelt es sich um ein etabliertes Modell der arteriellen Hypertonie. Der erhöhte Gefäßwiderstand sowie das vaskuläre Remodeling werden über eine Reduktion der NO-Spiegel und Aktivierung der systemischen und lokalen Renin-Angiotensin-Systeme sowie durch vermehrten oxidativen Stress induziert.[299] Der therapeutische Einsatz des ACE-Hemmers Captopril führte zu einer signifikanten Senkung des systolischen Blutdrucks, während das antioxidativ wirkende Tempol lediglich einen weiteren Anstieg verhindern konnte.

Die Beteiligung freier Sauerstoffradikale am L-NAME-induzierten Hypertonus konnte bereits durch Kumar et al. gezeigt werden, die durch orale Applikation von Syringic Acid, einem natürlichen Antioxidans, den Blutdruck signifikant senken konnten.[300]

Da sich L-NAME in der verwendeten Konzentration weder auf die Perfusion der Lungenstrombahn auswirkt (keine PAH!) noch auf die Funktion des linken Ventrikels (moderate kompensatorische Hypertrophie), bietet das Modell die Möglichkeit, Mechanismen und Signalwege einer „eigenständigen“ Rechtsherzinsuffizienz zu untersuchen und vor diesem Hintergrund neue und spezifische Therapieoptionen zu entwickeln.[301]

Die Bedeutung der Superoxiddismutase 2 (SOD2) für das rechtsventrikuläre Remodeling (Ref.: RS20)

Histologische und molekulare Befunde unserer Studie weisen darauf hin, dass der rechtsventrikulären Dysfunktion ein massiver ROS-Anstieg zugrunde liegt. Als potentielle Quellen einer übermäßigen Radikalproduktion unter chronischer L-NAME Applikation konnten sowohl von Kumar als auch Suda et al. die NADPH oxidase, die Xathinoxidase sowie das Renin-Angiotensin-System identifiziert werden.[300,302] Darüber hinaus beschreibt Dikalov et al., dass ROS, generiert durch NADPH oxidasen, die Bildung reaktiver Sauerstoffintermediate in Mitochondrien induziert, die ihrerseits wieder die Radikalproduktion im Zytosol stimulieren und somit Teil eines selbstunterhaltenden Circulus vitiosus bilden.[303] Shen et al. konnten durch gezielte pharmakologische Intervention mit Substanzen, deren antioxidatives Potential spezifisch auf mitochondriales ROS ausgerichtet ist, diesen feed-forward cycle effizient unterbrechen.[304]

Dieser therapeutische Ansatz entspricht der endogenen Heraufregulation der SOD2 im linken Ventrikel L-NAME behandelter Tiere unserer Studie. Die Typ 2 Isoform, auch als manganhaltige Dismutase (Mn-SOD) bezeichnet, katalysiert die Bildung von Wasserstoffperoxid aus Superoxid-Anionen spezifisch in den Mitochondrien. Verschiedene Arbeitsgruppen haben bereits übereinstimmend gezeigt, dass vorrangig die Transkriptionsfaktoren PGC1α, Nrf-2 und Sirt1, dessen mRNA-Spiegel ausschließlich im linksventrikulären Myokard induziert waren, die SOD2-Expression regulieren.[305-307]

Als direkte Folge der rechtsventrikulären Radikalbelastung stellt die Induktion des Cytokins TGF-beta einen Schlüsselmechanismus dar, der für die Entstehung der Fibrose und die Progression der Rechtsherzinsuffizienz verantwortlich ist.[290,291,308]

Die fehlende Heraufregulation der SOD2 zusammen mit der Akkumulation freier Radikale haben darüber hinaus zu einem selektiven Anstieg von Peroxynitrit im rechtsventrikulären Myokard geführt. Diese hochreaktive Verbindung verursacht im Verlauf verschiedener Herz-Kreislauferkrankungen Schäden auf zellulärer und subzellulärer Ebene.[309-311] Im Herzgewebe identifizierten Wang et al. die Protease MMP2, die u. a. für einen proteolytischen Abbau von Troponin I verantwortlich ist, als direktes Ziel von Peroxynitrit.[312,313] In Folge der hohen Peroxynitrit-Spiegel stieg auch die MMP2-Expression ausschließlich im rechtsventrikulären Myokard L-NAME gefütterter Tiere signifikant an. [RS20]

Risikofaktoren der Rechtsherzinsuffizienz (Ref.: RS19,RS20)

Zusammenfassend zeigen die Ergebnisse unserer Studie erstmalig, dass oxidativer Stress für den rechten Ventrikel einen weitaus größeren Risikofaktor darstellt als für den linken. Molekulare und zellphysiologische Befunde weisen darauf hin, dass entscheidende Signalwege und Schlüsselenzyme im rechten und linken Ventrikel unterschiedlich aktiviert und reguliert werden.[RS19] Vor diesem Hintergrund lassen sich die Befunde dieser Studie auf kardiale Erkrankungen übertragen, die mit erhöhtem oxidativen Stress einhergehen und folglich die Entwicklung einer Rechtherzinsuffizienz induzieren können.[305] Ohne selbst Ausgangspunkt der Symptomatik zu sein, besteht für den rechten Ventrikel somit ein erhöhtes Risiko, durch vermehrt anfallendes ROS während einer Linksherzinsuffizienz oder eines linksventrikulären Infarktes sekundär geschädigt zu werden.

Das Unvermögen des rechten Ventrikels, seine antioxidative Kapazität unter pathophysiologischen Bedingungen entsprechend anzupassen, führt zu einer gesteigerten ROS-Bildung, einem erhöhtem Anteil oxidierten Tropomyosins und einer verstärkten Bildung von Peroxynitrit. Die Ursachen für eine daraus resultierende kardiale Dysfunktion basieren sowohl auf einem strukturell umgebauten Ventrikel mit signifikant erhöhtem Anteil von Kollagen als auch auf einer Funktionseinschränkung der rechtsventrikulären Kardiomyozyten selbst. Die restriktive Komponente dieser kardialen Symptomatik führt durch Blutrückstau in die Leber zu einem Anstieg der Lebertransaminasen GOT/GPT.[RS20]

Das begrenzte Potential des rechten Ventrikels, seine endogene antioxidative Kapazität in ausreichendem Maße zu erhöhen, muss bei der gezielten Entwicklung neuer Therapiestrategien der Rechtsherzinsuffizienz berücksichtigt werden. Seine zentrale Bedeutung sowie häufige Beteiligung an zahlreichen kardio-vaskulären Erkrankungen unterstreichen die Notwendigkeit, die Pathophysiologie des rechten Ventrikels als eigenständige Entität zu betrachten, die sich nicht einfach von der des linken Ventrikels ableiten lässt.

Die unzureichende antioxidative Kapazität des rechten Ventrikels

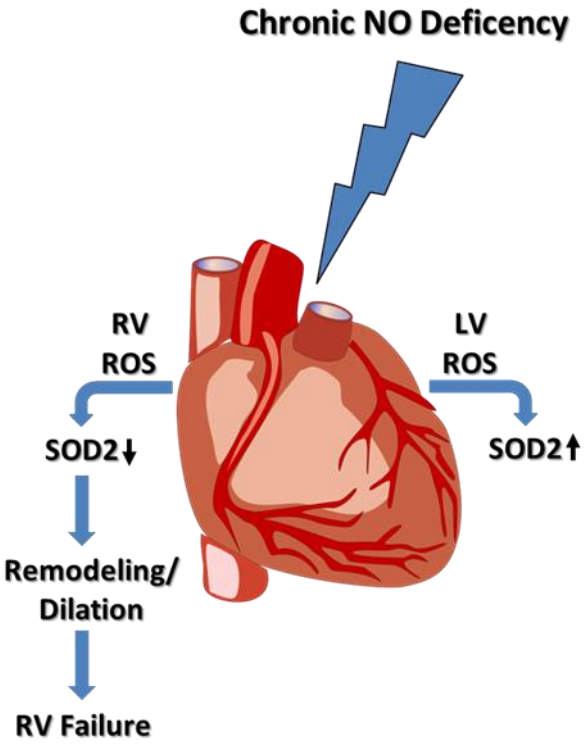

Abb. 7: Die eingeschränkte antioxidative Kapazität (SOD2) des rechten Ventrikels (RV) verursacht durch Akkumulation freier Radikale die Entwicklung einer dilatativen Kardiomyopathie.

Das eingeschränkte antioxidative Potential des rechten Ventrikels als therapeutisches Target für die Rechtsherzinsuffizienz (Ref.: RS19,RS20)

Anhand von humanem Biopsiematerial des rechten und linken Ventrikels verglichen Borchi et al. die oxidative Belastung sowie das antioxidative Potential des insuffizienten Myokards und diagnostizierten eine im direkten Vergleich reduzierte Protektion gegenüber freien Radikalen im rechten Ventrikel.[305] Das generelle NO-Defizit in unserem Modell induziert ausschließlich im rechtsventrikulären Myokard ein Remodeling, das morphologisch und funktionell dem Bild einer dilatativen Kardiomyopathie entspricht. Abermals kann die unzureichende Kapazität antioxidativer Abwehrsysteme für die rechtsventrikuläre Symptomatik verantwortlich gemacht werden.[RS19,RS20]

Diese Befunde müssen zukünftig bei der Ausarbeitung spezifischer, leitliniengerechter Therapien der Rechtsherzinsuffizienz berücksichtigt werden.

Im Folgenden werden drei Therapieoptionen vorgestellt, die aufgrund der vorliegenden Befunde zur Prävention und Behandlung einer Rechtsherzinsuffizienz indiziert erscheinen.

ACE-Inhibitoren

In unserem Modell wurde als therapeutische Intervention in der dritten und vierten Woche des Versuchszeitraums der ACE-Hemmer Captopril appliziert. Die Wirkstoffgruppe der ACE-Hemmer hat bereits seit vielen Jahren ihren festen Platz in der Therapie des Bluthochdrucks und der chronischen Herzinsuffizienz. Über die Hemmung des Angiotensin Converting Enzyme reduzieren ACE-Hemmer die Konzentration an Angiotensin II, senken auf diese Weise sowohl Vor- als auch Nachlast und verringern indirekt die Synthese von Aldosteron. Ihr kardioprotektives Potential vermitteln die ACE-Hemmer jedoch nicht nur allein über ihre Wirkung auf die Hämodynamik, durch die Reduktion der lokalen Angiotensin- und Aldosteronwirkungen sowie durch Hemmung des Bradykininabbaus verbessern sie das kardiale Remodeling auch auf zellulärer Ebene.[298,314]

Unter sämtlichen derzeit zugelassenen ACE-Inhibitoren verfügen jedoch ausschließlich Captopril und Zofenopril über abspaltbare Sulfhydryl-(SH-) Gruppen und somit über zusätzliche antioxidative Eigenschaften.

Die antioxidative Kapazität liegt bei Zofenopril im Vergleich zu Captopril um ein Vielfaches höher; gegenüber allen anderen Vertretern zeichnet sich Zofenopril darüber hinaus durch eine besonders lipophile Struktur aus, diese wirkt sich positiv auf Membrangängigkeit und Halbwertszeit aus.[315]

Eine weitere kardioprotektive Eigenschaft der ACE-Hemmer besteht in ihrer stimulierenden Wirkung auf die NO-Produktion; je nach Wirkstoff allerdings mit deutlich unterschiedlicher Effizienz.[316] Für Zofenopril haben Donnarumma et al. unlängst zeigen können, dass nach dessen Applikation nicht nur die NO-Spiegel um ein Vielfaches ansteigen, parallel nimmt auch die Bioverfügbarkeit von H_2S signifikant zu. Für die zytoprotektiven Eigenschaften beider Transmitter werden vor allem ihre antioxidativen Wirkungen verantwortlich gemacht.[317]

Fazit: Sein ausgezeichnetes pharmakologisches Profil spricht für den ACE-Hemmer Zofenopril als Therapieoption der ersten Wahl bei kardio-vaskulären Erkrankungen mit Beteiligung des rechten Ventrikels.

Vor allem die ausgebliebene Induktion der SOD2 im Myokard des rechten Ventrikels hat uns veranlasst, als zweite medikamentöse Therapieoption das SOD Mimetikum 4-Hydroxy-TEMPO oder kurz 'TEMPOL' zu verwenden.

SOD Mimetics

Die SOD bzw. ihre drei Isoformen sind 1969 von Irwin Fridovich erstmals isoliert und charakterisiert worden. Die Familie der SODs zeichnet sich durch seine einzigartige Fähigkeit aus, freie Radikale direkt zu neutralisieren, d.h. anfallende Superoxid-Anionen zu Sauerstoff und Wasserstoffperoxid umzusetzen. Ihr besonderer Stellenwert in der Aufrechterhaltung einer ausbalancierten Redoxhomöostase lässt sich allein damit erklären, dass sämtliche Lebewesen unseres Planeten über mindestens eine SOD Isoform verfügen. Bereits Fridovich beschrieb eine Kupfer/Zink haltige SOD (SOD1), die vorzugsweise im Zytoplasma, sowie eine mangan- bzw. eisenhaltige Isoform (SOD2), die ausschließlich in den Mitochondrien lokalisiert ist. Die SOD3, auch als extrazelluläre SOD bezeichnet, zählt ebenfalls zu den Kupfer/Zink haltigen Isoformen, unterscheidet sich jedoch strukturell von ihren intrazellulären Verwandten.[318,319]

Vor allem die Bedeutung der SOD2 für die Pathogenese und Progression zahlreicher Erkrankungen hat dazu geführt, speziell diese Isoform als therapeutische Intervention im Tier überzuexprimieren bzw. Vektor-basiert zu applizieren. Bzgl. ihrer pharmakologischen Effizienz überzeugte die SOD2 sowohl in Modellen der Ischämie-Reperfusion und Inflammation als auch im Verlauf neoplastischer, neurodegenerativer und metabolischer Erkrangungen.[318,319]

Die Verwendung des nativen Proteins hat sich klinisch jedoch als nicht praktikabel erwiesen. Die geringe Membranpermeabilität in Verbindung mit einer sehr kurzen Halbwertszeit sowie einem hohen immunogenen Potential haben dazu geführt, sog. SOD Mimetics zu entwickeln. Bei vergleichbaren pharmakodynamischen Eigenschaften sowie einer überlegenen Kinetik sollen zukünftig small molecules die katalytischen Reaktionen der SOD2 übernehmen; klinische Studien sind bereits initiiert.[320,321]

Mitochondria-targeted Antioxidants

Die Atmungskette der inneren Mitochondrienmembran zählt zu den wichtigsten intrazellulären Quellen freier Radikale. Bereits unter physiologischen Bedingungen verlassen ca. 2 % der Elektronen die Transportkette an den Proteinkomplexen I und III und reagieren mit molekularem Sauerstoff zu Superoxid-Anionen.[303] Einigen Kandidaten der sog. „Mitochondria-targeted Antioxidants“ wird bereits heute großes Potential eingeräumt, da sie gezielt die mitochondriale Phospholipiddoppelschicht überqueren und ROS direkt an der Quelle neutralisieren können.[322] Vorgesehene Indikationen entsprechen weitestgehend denen der SOD Mimetics; für SKQ1, SS-31, MitoQ und Methylene blue sind bereits klinische Studien angelaufen, deren Fokus überwiegend auf kardio-vaskuläre sowie neurologische Erkrankungen gelegt wurde.[323-325]

Sowohl SOD Mimetics als auch Mitochondria-targeted Antioxidants könnten zukünftig einen wichtigen Stellenwert im Therapieschema der Rechtsherzinsuffizienz einnehmen. Der Einfluss von MitoQ auf die diastolische Herzfunktion wird derzeit an 60 gesunden Probanden untersucht; erste Ergebnisse sind im Jahr 2020 bzw. 2021 zu erwarten.

4. Zusammenfassung

Der besondere Stellenwert des Bluthochdrucks als kardialer Risikofaktor hat dazu geführt, die komplexe Symptomatik des chronisch druckbelasteten Myokards zusammengefasst als „hypertensive Herzkrankheit“ zu bezeichnen. Beeinflusst durch primäre und sekundäre Risikofaktoren, Co-Morbiditäten sowie die Familienanamnese kann sich die hypertensive Herzkrankheit klinisch auf unterschiedliche Weise manifestieren. Die kardiale Symptomatik kann, zunächst auf einen Ventrikel beschränkt, im weiteren Krankheitsverlauf das gesamte Herz betreffen; funktionell lassen sich diastolische, systolische oder kombinierte Störungen diagnostizieren; abhängig vom Ausmaß der Koronarsklerose kann zwischen akutem oder chronischem Verlauf differenziert werden.

Die aktuellen Therapieoptionen basieren unabhängig von der jeweils dominierenden Symptomatik vorrangig auf einer Hemmung des Sympathikus sowie der Effekte, die durch Angiotensin und Aldosteron verursacht werden.

Mit der Zielsetzung, die Prognose kardio-vaskulärer Erkrankungen weiter zu verbessern, wurden in dieser Arbeit spezifische Pathomechanismen identifiziert, die zur Entwicklung neuer und individueller Therapiestrategien beitragen können.

An isolierten Kardiomyozyten, *ex vivo* perfundierten Herzen sowie an Tiermodellen wurden die unterschiedlichen Verlaufsformen einer hypertensiven Herzkrankheit auf beteiligte Signalwege und Schlüsselmechanismen hin untersucht. Über die selektive Aktivierung bzw. Hemmung ausgewählter Zielkandidaten ließen sich sowohl die kardiale Funktion, die Perfusion als auch strukturelle Umbauvorgänge mitunter signifikant verbessern (s. Abb. 8).

Die vorgestellten Ergebnisse liefern die Grundvoraussetzung für die Entwicklung neuer und individualisierter Therapieansätze, beschleunigen deren Transfer in die klinische Routine und tragen dazu bei, die Rekonvaleszenz kardio-vaskulär erkrankter Patienten signifikant zu verkürzen.

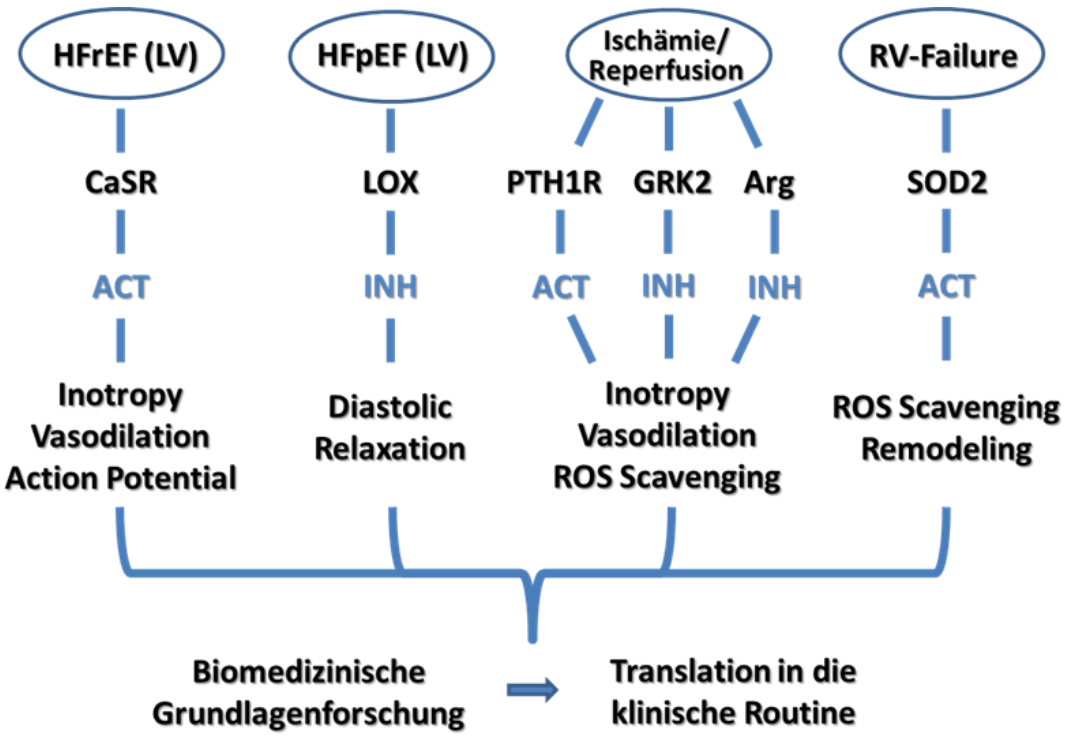

Abb. 8: Individuelle Therapieoptionen der hypertensiven Herzkrankheit (ACT, Aktivierung; INH, Inhibierung).

5. Schlussfolgerung und Ausblick

Das Spektrum an effizienten pharmakologischen Therapieoptionen zur Behandlung kardio-vaskulärer Erkrankungen hat sich in den letzten Jahren kontinuierlich verbessert. Aufgrund der stetig wachsenden Weltbevölkerung sowie der demographischen Entwicklung wird sich die absolute Anzahl kardial-bedingter Erkrankungen und Todesfälle zukünftig jedoch weiter erhöhen.

Das Potential der hämodynamisch orientierten Therapieansätze scheint weitestgehend erschöpft; die aktuellen Therapiestrategien zur Behandlung und Prävention kardio-vaskulärer Risikofaktoren stoßen bereits in vielen Bereichen an ihre Grenzen. Für die Herzinsuffizienz mit erhaltener Auswurffraktion, die Rechtsherzinsuffizienz sowie den Reperfusionsschaden liegen derzeit keine evidenzbasierten Therapieempfehlungen vor.

Die Ergebnisse dieser Arbeit belegen, dass die Entwicklung neuer und effizienter Therapieoptionen möglich ist, wenn fundierte Kenntnisse über die Genese und die zugrunde liegenden Pathomechanismen der jeweiligen Erkrankung verfügbar sind.

Die erfolgreiche Integration der vorgestellten molekularen und zellphysiologischen Befunde in eine patientenorientierte Forschung sowie deren Translation in leitlinienrelevante klinische Studien werden es der kardio-vaskulären Medizin ermöglichen, die Prognose Herz-Kreislauf-assoziierter Erkrankungen durch individuelle Behandlungskonzepte auch zukünftig weiter zu verbessern.

6. Verzeichnis der Originalpublikationen zur kumulativen Habilitationsschrift

Publikationen zu Kapitel *3.1 „Die Herzinsuffizienz mit reduzierter Auswurffraktion (HFrEF)“*

RS1 ***Schreckenberg R**, Schlüter KD. Calcium sensing receptor expression and signalling in cardiovascular physiology and disease. Vascul Pharmacol, 1537-1891 (2018).*

RS2 *Dyukova E, **Schreckenberg R**, Arens C, Sitdikova G, Schlüter KD. The Role of Calcium-Sensing Receptors in Endothelin-1-Dependent Effects on Adult Rat Ventricular Cardiomyocytes: Possible Contribution to Adaptive Myocardial Hypertrophy. J Cell Physiol **232**, 2508-2518 (2017).*

RS3 *Dyukova E, **Schreckenberg R**, Sitdikova G, Schlüter KD. Influence of Ischemic Pre- and Post-Conditioning on Cardiac Expression of Calcium-Sensing Receptor. Bio Nano Science **7**, 112-114 (2017).*

RS4 ***Schreckenberg R**, Dyukova E, Sitdikova G, Abdallah Y, Schlüter KD. Mechanisms by which calcium receptor stimulation modifies electromechanical coupling in isolated ventricular cardiomyocytes. Pflugers Arch **467**, 379-388 (2015).*

RS5 ***Schreckenberg R**, Wenzel S and Schlüter KD. Role of Extracellular Calcium Control, Calcium Sensing, and Regulation of Calcium Regulating Hormones in Heart Failure. Open Heart Fail J **3**, 16-24 (2010).*

Publikationen zu Kapitel *3.2 „Die Herzinsuffizienz mit erhaltener Auswurffraktion (HFpEF)“*

RS6 ***Schreckenberg R**, Horn AM, da Costa Rebelo RM, Simsekyilmaz S, Niemann B, Li L, Rohrbach S, Schlüter KD. Effects of 6-months' Exercise on Cardiac Function, Structure and Metabolism in Female Hypertensive Rats-The Decisive Role of Lysyl Oxidase and Collagen III. Front Physiol **8**, 556 (2017).*

RS7 *Koncsos G, Varga ZV, Baranyai T, Boengler K, Rohrbach S, Li L, Schlüter KD, **Schreckenberg R**, Radovits T, Oláh A, Mátyás C, Lux Á, Al-Khrasani M, Komlódi T, Bukosza N, Máthé D, Deres L, Barteková M, Rajtík T, Adameová A, Szigeti K, Hamar P, Helyes Z, Tretter L, Pacher P, Merkely B, Giricz Z, Schulz R, Ferdinandy P. Diastolic dysfunction in prediabetic male rats: Role of mitochondrial oxidative stress. Am J Physiol Heart Circ Physiol **311**, 927-943 (2016).*

RS8 *da Costa Rebelo RM, **Schreckenberg R**, Schlüter KD. Adverse cardiac remodelling in spontaneously hypertensive rats: acceleration by high aerobic exercise intensity. J Physiol **590**, 5389-5400 (2012).*

RS9 *Schlüter KD, **Schreckenberg R**, da Costa Rebelo RM. Interaction between exercise and hypertension in spontaneously hypertensive rats: a meta-analysis of experimental studies. Hypertens Res **33**, 1155-1161 (2010).*

Publikationen zu Kapitel *3.3 „Das funktionelle und strukturelle Remodeling des post-infarzierten Myokards“*

RS10 ***Schreckenberg R**, Bencsik P, Weber M, Abdallah Y, Csonka C, Gömöri K, Kiss K, Pálóczi J, Pipis J, Sárközy M, Ferdinandy P, Schulz R, Schlüter KD. Adverse effects on β-adrenergic receptor coupling: Ischemic postconditioning failed to preserve long-term cardiac function. J Am Heart Assoc **6** (2017).*

RS11 *Nippert F, **Schreckenberg R**, Hess A, Weber M, Schlüter KD. The Effects of Swiprosin-1 on the Formation of Pseudopodia-Like Structures and β-Adrenoceptor Coupling in Cultured Adult Rat Ventricular Cardiomyocytes. PLoS One **11**, e0167655 (2016).*

RS12 *Schlüter KD, Schulz R, **Schreckenberg R**. Arginase induction and activation during ischemia and reperfusion and functional consequences for the heart. Front Physiol **6**, 65 (2015).*

RS13 ***Schreckenberg R**, Weber P, Cabrera-Fuentes HA, Steinert I, Preissner KT, Bencsik P, Sárközy M, Csonka C, Ferdinandy P, Schulz R, Schlüter KD. Mechanism and consequences of the shift in cardiac arginine metabolism following ischaemia and reperfusion in rats. Thromb Haemost **113**, 482-493 (2015).*

RS14 *Mörlein C, **Schreckenberg R**, Schlüter KD. Basal ornithine decarboxylase activity modifies apoptotic and hypertrophic marker expression in post-ischemic hearts. Open Heart Fail J **3**, 31-37 (2010).*

RS15 ***Schreckenberg R**, Wenzel S, da Costa Rebelo RM, Röthig A, Meyer R, Schlüter KD. Cell-specific effects of nitric oxide deficiency on parathyroid hormone-related peptide (PTHrP) responsiveness and PTH1 receptor expression in cardiovascular cells. Endocrinology **150**, 3735-3741 (2009).*

RS16 ***Schreckenberg R**, Maier T, Schlüter KD. Post-conditioning restores pre-ischaemic receptor coupling in rat isolated hearts. Br J Pharmacol **156**, 901-908 (2009).*

RS17 *Schlüter KD, **Schreckenberg R**. Ischemic injury and the parathyroid hormone-related protein system: friend or foe? Basic Res Cardiol **104**, 424-426 (2009).*

RS18 *Tastan I, **Schreckenberg R**, Mufti S, Abdallah Y, Piper HM, Schlüter KD. Parathyroid hormone improves contractile performance of adult rat ventricular cardiomyocytes at low concentrations in a non-acute way. Cardiovasc Res **82**, 77-83 (2009).*

Publikationen zu Kapitel *3.4 „Die Insuffizienz des rechtsventrikulären Myokards“*

RS19 *Schlüter KD, Kutsche HS, Hirschhäuser C, **Schreckenberg R**, Schulz R. Review on Chamber-Specific Differences in Right and Left Heart Reactive Oxygen Species Handling. Front Physiol **9**, 1799 (2018).*

RS20 ***Schreckenberg R**, da Costa Rebelo M, Deten A, Weber M, Rohrbach S, Pipicz M, Csonka C, Ferdinandy P, Schulz R, Schlüter KD. Specific Mechanisms underlying Right Heart Failure: The missing Upregulation of Superoxide Dismutase-2 and its decisive Role in Antioxidative Defense. Antioxid Redox Signal **23**, 1220-1232 (2015).*

7. Literaturverzeichnis

1. Schreckenberg, R. Endogenous Mechanisms for Regulating Myocardial Contractility. Pages 135-163. Cardiomyocytes – Active Players in Cardiac Disease. (ed. Schlüter, K.-D.) (Springer, 2016).
2. Forouzanfar, M.H.*, et al.* Global Burden of Hypertension and Systolic Blood Pressure of at Least 110 to 115 mm Hg, 1990-2015. *JAMA* **317**, 165-182 (2017).
3. Intengan, H.D. & Schiffrin, E.L. Vascular remodeling in hypertension: roles of apoptosis, inflammation, and fibrosis. *Hypertension* **38**, 581-587 (2001).
4. Collaborators, G.B.D.R.F. Global, regional, and national comparative risk assessment of 84 behavioural, environmental and occupational, and metabolic risks or clusters of risks for 195 countries and territories, 1990-2017: a systematic analysis for the Global Burden of Disease Study 2017. *Lancet* **392**, 1923-1994 (2018).
5. Rapsomaniki, E.*, et al.* Blood pressure and incidence of twelve cardiovascular diseases: lifetime risks, healthy life-years lost, and age-specific associations in 1.25 million people. *Lancet* **383**, 1899-1911 (2014).
6. Georgiopoulou, V.V., Kalogeropoulos, A.P., Raggi, P. & Butler, J. Prevention, diagnosis, and treatment of hypertensive heart disease. *Cardiol Clin* **28**, 675-691 (2010).
7. Tackling, G. & Borhade, M.B. Hypertensive Heart Disease. in *StatPearls* (Treasure Island (FL), 2019).
8. Konukoglu, D. & Uzun, H. Endothelial Dysfunction and Hypertension. *Adv Exp Med Biol* **956**, 511-540 (2017).
9. Bolad, I. & Delafontaine, P. Endothelial dysfunction: its role in hypertensive coronary disease. *Curr Opin Cardiol* **20**, 270-274 (2005).
10. Messerli, F.H., Rimoldi, S.F. & Bangalore, S. The Transition From Hypertension to Heart Failure: Contemporary Update. *JACC Heart Fail* **5**, 543-551 (2017).
11. Aronow, W.S. Hypertension and left ventricular hypertrophy. *Ann Transl Med* **5**, 310 (2017).
12. Drozdz, D. & Kawecka-Jaszcz, K. Cardiovascular changes during chronic hypertensive states. *Pediatr Nephrol* **29**, 1507-1516 (2014).
13. McMurray, J.J.*, et al.* ESC Guidelines for the diagnosis and treatment of acute and chronic heart failure 2012: The Task Force for the Diagnosis and Treatment of Acute and Chronic Heart Failure 2012 of the European Society of Cardiology. Developed in collaboration with the Heart Failure Association (HFA) of the ESC. *Eur Heart J* **33**, 1787-1847 (2012).
14. Ponikowski, P.*, et al.* 2016 ESC Guidelines for the diagnosis and treatment of acute and chronic heart failure: The Task Force for the diagnosis and treatment of acute and chronic heart failure of the European Society of Cardiology (ESC)Developed with the special

contribution of the Heart Failure Association (HFA) of the ESC. *Eur Heart J* **37**, 2129-2200 (2016).
15. Townsend, N.*, et al.* Cardiovascular disease in Europe: epidemiological update 2016. *Eur Heart J* **37**, 3232-3245 (2016).
16. Singh, A. & Grossman, S.A. Acute Coronary Syndrome. in *StatPearls* (Treasure Island (FL), 2019).
17. Kumar, A. & Cannon, C.P. Acute coronary syndromes: diagnosis and management, part I. *Mayo Clin Proc* **84**, 917-938 (2009).
18. Kumar, A. & Cannon, C.P. Acute coronary syndromes: Diagnosis and management, part II. *Mayo Clin Proc* **84**, 1021-1036 (2009).
19. Thygesen, K.*, et al.* Third universal definition of myocardial infarction. *Circulation* **126**, 2020-2035 (2012).
20. Landes, U.*, et al.* Type 2 myocardial infarction: A descriptive analysis and comparison with type 1 myocardial infarction. *J Cardiol* **67**, 51-56 (2016).
21. Lopez-Cuenca, A.*, et al.* Comparison between type-2 and type-1 myocardial infarction: clinical features, treatment strategies and outcomes. *J Geriatr Cardiol* **13**, 15-22 (2016).
22. Baron, T.*, et al.* Impact on Long-Term Mortality of Presence of Obstructive Coronary Artery Disease and Classification of Myocardial Infarction. *Am J Med* **129**, 398-406 (2016).
23. Mills, K.T.*, et al.* Global Disparities of Hypertension Prevalence and Control: A Systematic Analysis of Population-Based Studies From 90 Countries. *Circulation* **134**, 441-450 (2016).
24. Whelton, P.K.*, et al.* 2017 ACC/AHA/AAPA/ABC/ACPM/AGS/APhA/ASH/ASPC/NMA/PCNA Guideline for the Prevention, Detection, Evaluation, and Management of High Blood Pressure in Adults: Executive Summary: A Report of the American College of Cardiology/American Heart Association Task Force on Clinical Practice Guidelines. *Hypertension* **71**, 1269-1324 (2018).
25. Mancia, G.*, et al.* 2013 ESH/ESC guidelines for the management of arterial hypertension: the Task Force for the Management of Arterial Hypertension of the European Society of Hypertension (ESH) and of the European Society of Cardiology (ESC). *Eur Heart J* **34**, 2159-2219 (2013).
26. Williams, B.*, et al.* 2018 ESC/ESH Guidelines for the management of arterial hypertension. *Eur Heart J* **39**, 3021-3104 (2018).
27. Vidal-Petiot, E.*, et al.* Cardiovascular event rates and mortality according to achieved systolic and diastolic blood pressure in patients with stable coronary artery disease: an international cohort study. *Lancet* **388**, 2142-2152 (2016).
28. Group, S.R.*, et al.* A Randomized Trial of Intensive versus Standard Blood-Pressure Control. *N Engl J Med* **373**, 2103-2116 (2015).
29. Ettehad, D.*, et al.* Blood pressure lowering for prevention of cardiovascular disease and death: a systematic review and meta-analysis. *Lancet* **387**, 957-967 (2016).
30. Thomopoulos, C., Parati, G. & Zanchetti, A. Effects of blood pressure lowering on outcome incidence in hypertension: 7. Effects of more vs. less intensive blood pressure lowering and different achieved blood pressure levels - updated overview and meta-analyses of randomized trials. *J Hypertens* **34**, 613-622 (2016).
31. Bohm, M.*, et al.* Achieved blood pressure and cardiovascular outcomes in high-risk patients: results from ONTARGET and TRANSCEND trials. *Lancet* **389**, 2226-2237 (2017).
32. Egan, B.M.*, et al.* Initial monotherapy and combination therapy and hypertension control the first year. *Hypertension* **59**, 1124-1131 (2012).
33. Oliveria, S.A.*, et al.* Physician-related barriers to the effective management of uncontrolled hypertension. *Arch Intern Med* **162**, 413-420 (2002).
34. Ho, P.M.*, et al.* Importance of therapy intensification and medication nonadherence for blood pressure control in patients with coronary disease. *Arch Intern Med* **168**, 271-276 (2008).
35. Zucker, I.H., Xiao, L. & Haack, K.K. The central renin-angiotensin system and sympathetic nerve activity in chronic heart failure. *Clin Sci (Lond)* **126**, 695-706 (2014).

36. Spinarova, L. & Vitovec, J. Neurohumoral changes in chronic heart failure. *Biomed Pap Med Fac Univ Palacky Olomouc Czech Repub* **151**, 201-207 (2007).
37. Ferrario, C.M. Cardiac remodelling and RAS inhibition. *Ther Adv Cardiovasc Dis* **10**, 162-171 (2016).
38. Wang, Y.*, et al.* Effects of the Angiotensin-Receptor Neprilysin Inhibitor on Cardiac Reverse Remodeling: Meta-Analysis. *J Am Heart Assoc* **8**, e012272 (2019).
39. Dominguez, R.F.*, et al.* Hypertensive heart disease: Benefit of carvedilol in hemodynamic, left ventricular remodeling, and survival. *SAGE Open Med* **7**, 2050312118823582 (2019).
40. Burnett, H.*, et al.* Thirty Years of Evidence on the Efficacy of Drug Treatments for Chronic Heart Failure With Reduced Ejection Fraction: A Network Meta-Analysis. *Circ Heart Fail* **10**(2017).
41. Roh, J., Houstis, N. & Rosenzweig, A. Why Don't We Have Proven Treatments for HFpEF? *Circ Res* **120**, 1243-1245 (2017).
42. Iliesiu, A.M. & Hodorogea, A.S. Treatment of Heart Failure with Preserved Ejection Fraction. *Adv Exp Med Biol* **1067**, 67-87 (2018).
43. Zhang, Y. & Huo, Y. Early reperfusion strategy for acute myocardial infarction: a need for clinical implementation. *J Zhejiang Univ Sci B* **12**, 629-632 (2011).
44. Davidson, S.M.*, et al.* Multitarget Strategies to Reduce Myocardial Ischemia/Reperfusion Injury: JACC Review Topic of the Week. *J Am Coll Cardiol* **73**, 89-99 (2019).
45. Konstam, M.A.*, et al.* Evaluation and Management of Right-Sided Heart Failure: A Scientific Statement From the American Heart Association. *Circulation* **137**, e578-e622 (2018).
46. Hajar, R. Framingham Contribution to Cardiovascular Disease. *Heart Views* **17**, 78-81 (2016).
47. Brown, E.M. Extracellular Ca2+ sensing, regulation of parathyroid cell function, and role of Ca2+ and other ions as extracellular (first) messengers. *Physiol Rev* **71**, 371-411 (1991).
48. Brown, E.M.*, et al.* Cloning and characterization of an extracellular Ca(2+)-sensing receptor from bovine parathyroid. *Nature* **366**, 575-580 (1993).
49. Tfelt-Hansen, J. & Brown, E.M. The calcium-sensing receptor in normal physiology and pathophysiology: a review. *Crit Rev Clin Lab Sci* **42**, 35-70 (2005).
50. Alfadda, T.I., Saleh, A.M., Houillier, P. & Geibel, J.P. Calcium-sensing receptor 20 years later. *Am J Physiol Cell Physiol* **307**, C221-231 (2014).
51. Smajilovic, S. & Tfelt-Hansen, J. Calcium acts as a first messenger through the calcium-sensing receptor in the cardiovascular system. *Cardiovasc Res* **75**, 457-467 (2007).
52. Stenovec, M., Goncalves, P.P. & Zorec, R. Peptide hormone release monitored from single vesicles in "membrane lawns" of differentiated male pituitary cells: SNAREs and fusion pore widening. *Endocrinology* **154**, 1235-1246 (2013).
53. Ritter, C.S., Pande, S., Krits, I., Slatopolsky, E. & Brown, A.J. Destabilization of parathyroid hormone mRNA by extracellular Ca2+ and the calcimimetic R-568 in parathyroid cells: role of cytosolic Ca and requirement for gene transcription. *J Mol Endocrinol* **40**, 13-21 (2008).
54. Egbuna, O.*, et al.* The full-length calcium-sensing receptor dampens the calcemic response to 1alpha,25(OH)2 vitamin D3 in vivo independently of parathyroid hormone. *Am J Physiol Renal Physiol* **297**, F720-728 (2009).
55. Garrett, J.E.*, et al.* Molecular cloning and functional expression of human parathyroid calcium receptor cDNAs. *J Biol Chem* **270**, 12919-12925 (1995).
56. Janicic, N.*, et al.* Mapping of the calcium-sensing receptor gene (CASR) to human chromosome 3q13.3-21 by fluorescence in situ hybridization, and localization to rat chromosome 11 and mouse chromosome 16. *Mamm Genome* **6**, 798-801 (1995).
57. Hendy, G.N., Guarnieri, V. & Canaff, L. Calcium-sensing receptor and associated diseases. *Prog Mol Biol Transl Sci* **89**, 31-95 (2009).
58. Brauner-Osborne, H., Wellendorph, P. & Jensen, A.A. Structure, pharmacology and therapeutic prospects of family C G-protein coupled receptors. *Curr Drug Targets* **8**, 169-184 (2007).

59. Bai, M., Trivedi, S., Kifor, O., Quinn, S.J. & Brown, E.M. Intermolecular interactions between dimeric calcium-sensing receptor monomers are important for its normal function. *Proc Natl Acad Sci U S A* **96**, 2834-2839 (1999).
60. Pidasheva, S.*, et al.* Calcium-sensing receptor dimerizes in the endoplasmic reticulum: biochemical and biophysical characterization of CASR mutants retained intracellularly. *Hum Mol Genet* **15**, 2200-2209 (2006).
61. Grant, M.P., Stepanchick, A., Cavanaugh, A. & Breitwieser, G.E. Agonist-driven maturation and plasma membrane insertion of calcium-sensing receptors dynamically control signal amplitude. *Sci Signal* **4**, ra78 (2011).
62. Pi, M.*, et al.* Beta-arrestin- and G protein receptor kinase-mediated calcium-sensing receptor desensitization. *Mol Endocrinol* **19**, 1078-1087 (2005).
63. Brown, E.M. & MacLeod, R.J. Extracellular calcium sensing and extracellular calcium signaling. *Physiol Rev* **81**, 239-297 (2001).
64. Nemeth, E.F.*, et al.* Calcimimetics with potent and selective activity on the parathyroid calcium receptor. *Proc Natl Acad Sci U S A* **95**, 4040-4045 (1998).
65. Conigrave, A.D., Quinn, S.J. & Brown, E.M. L-amino acid sensing by the extracellular Ca2+-sensing receptor. *Proc Natl Acad Sci U S A* **97**, 4814-4819 (2000).
66. Lee, H.J.*, et al.* Allosteric activation of the extracellular Ca2+-sensing receptor by L-amino acids enhances ERK1/2 phosphorylation. *Biochem J* **404**, 141-149 (2007).
67. Breitwieser, G.E. The calcium sensing receptor life cycle: trafficking, cell surface expression, and degradation. *Best Pract Res Clin Endocrinol Metab* **27**, 303-313 (2013).
68. Ray, K. Calcium-Sensing Receptor: Trafficking, Endocytosis, Recycling, and Importance of Interacting Proteins. *Prog Mol Biol Transl Sci* **132**, 127-150 (2015).
69. Bosel, J., John, M., Freichel, M. & Blind, E. Signaling of the human calcium-sensing receptor expressed in HEK293-cells is modulated by protein kinases A and C. *Exp Clin Endocrinol Diabetes* **111**, 21-26 (2003).
70. Bouschet, T., Martin, S. & Henley, J.M. Regulation of calcium sensing receptor trafficking by RAMPs. *Adv Exp Med Biol* **744**, 39-48 (2012).
71. Bouschet, T., Martin, S. & Henley, J.M. Regulation of calcium-sensing-receptor trafficking and cell-surface expression by GPCRs and RAMPs. *Trends Pharmacol Sci* **29**, 633-639 (2008).
72. Smajilovic, S. & Tfelt-Hansen, J. Novel role of the calcium-sensing receptor in blood pressure modulation. *Hypertension* **52**, 994-1000 (2008).
73. Bukoski, R.D., Bian, K., Wang, Y. & Mupanomunda, M. Perivascular sensory nerve Ca2+ receptor and Ca2+-induced relaxation of isolated arteries. *Hypertension* **30**, 1431-1439 (1997).
74. Handoko, M.L.*, et al.* Perspectives on novel therapeutic strategies for right heart failure in pulmonary arterial hypertension: lessons from the left heart. *Eur Respir Rev* **19**, 72-82 (2010).
75. Tang, H.*, et al.* Pathogenic role of calcium-sensing receptors in the development and progression of pulmonary hypertension. *Am J Physiol Lung Cell Mol Physiol* **310**, L846-859 (2016).
76. Peng, X.*, et al.* Involvement of calcium-sensing receptors in hypoxia-induced vascular remodeling and pulmonary hypertension by promoting phenotypic modulation of small pulmonary arteries. *Mol Cell Biochem* **396**, 87-98 (2014).
77. Zhang, J.*, et al.* Extracellular calcium-sensing receptor is critical in hypoxic pulmonary vasoconstriction. *Antioxid Redox Signal* **17**, 471-484 (2012).
78. Yamamura, A., Ohara, N. & Tsukamoto, K. Inhibition of Excessive Cell Proliferation by Calcilytics in Idiopathic Pulmonary Arterial Hypertension. *PLoS One* **10**, e0138384 (2015).
79. Yamamura, A., Yagi, S., Ohara, N. & Tsukamoto, K. Calcilytics enhance sildenafil-induced antiproliferation in idiopathic pulmonary arterial hypertension. *Eur J Pharmacol* **784**, 15-21 (2016).
80. Sejersted, O.M. Calcium controls cardiac function--by all means! *J Physiol* **589**, 2919-2920 (2011).

81. Wang, R., *et al.* Calcium and polyamine regulated calcium-sensing receptors in cardiac tissues. *Eur J Biochem* **270**, 2680-2688 (2003).
82. Liu, C.H., Chang, H.K., Lee, S.P. & Shieh, R.C. Activation of the Ca(2+)-sensing receptors increases currents through inward rectifier K(+) channels via activation of phosphatidylinositol 4-kinase. *Pflugers Arch* **468**, 1931-1943 (2016).
83. Tagliavini, S., Genedani, S., Bertolini, A. & Bazzani, C. Ischemia- and reperfusion-induced arrhythmias are prevented by putrescine. *Eur J Pharmacol* **194**, 7-10 (1991).
84. Zhao, Y.J., *et al.* Role of polyamines in myocardial ischemia/reperfusion injury and their interactions with nitric oxide. *Eur J Pharmacol* **562**, 236-246 (2007).
85. Tfelt-Hansen, J., *et al.* Calcium receptor is functionally expressed in rat neonatal ventricular cardiomyocytes. *Am J Physiol Heart Circ Physiol* **290**, H1165-1171 (2006).
86. Wang, L.N., *et al.* Involvement of calcium-sensing receptor in cardiac hypertrophy-induced by angiotensinII through calcineurin pathway in cultured neonatal rat cardiomyocytes. *Biochem Biophys Res Commun* **369**, 584-589 (2008).
87. Liu, L., *et al.* Suppression of calciumsensing receptor ameliorates cardiac hypertrophy through inhibition of autophagy. *Mol Med Rep* **14**, 111-120 (2016).
88. Sun, J. & Murphy, E. Calcium-sensing receptor: a sensor and mediator of ischemic preconditioning in the heart. *Am J Physiol Heart Circ Physiol* **299**, H1309-1317 (2010).
89. Bai, S.Z., *et al.* Decrease in calcium-sensing receptor in the progress of diabetic cardiomyopathy. *Diabetes Res Clin Pract* **95**, 378-385 (2012).
90. Filopanti, M., Corbetta, S., Barbieri, A.M. & Spada, A. Pharmacology of the calcium sensing receptor. *Clin Cases Miner Bone Metab* **10**, 162-165 (2013).
91. Harrington, P.E. & Fotsch, C. Calcium sensing receptor activators: calcimimetics. *Curr Med Chem* **14**, 3027-3034 (2007).
92. Ward, D.T. & Riccardi, D. New concepts in calcium-sensing receptor pharmacology and signalling. *Br J Pharmacol* **165**, 35-48 (2012).
93. Letz, S., *et al.* Amino alcohol- (NPS-2143) and quinazolinone-derived calcilytics (ATF936 and AXT914) differentially mitigate excessive signalling of calcium-sensing receptor mutants causing Bartter syndrome Type 5 and autosomal dominant hypocalcemia. *PLoS One* **9**, e115178 (2014).
94. Parsabiv New FDA Drug Approval, CenterWatch. (www.centerwatch.com).
95. Parsabiv - Incidence of adverse reactions from controlled clinical studies. (www.medicines.org.uk).
96. Hannan, F.M., Babinsky, V.N. & Thakker, R.V. Disorders of the calcium-sensing receptor and partner proteins: insights into the molecular basis of calcium homeostasis. *J Mol Endocrinol* **57**, R127-142 (2016).
97. Penn, R.B. Physiology. Calcilytics for asthma relief. *Science* **348**, 398-399 (2015).
98. Borlaug, B.A. & Paulus, W.J. Heart failure with preserved ejection fraction: pathophysiology, diagnosis, and treatment. *Eur Heart J* **32**, 670-679 (2011).
99. Owan, T.E., *et al.* Trends in prevalence and outcome of heart failure with preserved ejection fraction. *N Engl J Med* **355**, 251-259 (2006).
100. Massie, B.M., *et al.* Irbesartan in patients with heart failure and preserved ejection fraction. *N Engl J Med* **359**, 2456-2467 (2008).
101. Cleland, J.G., *et al.* The perindopril in elderly people with chronic heart failure (PEP-CHF) study. *Eur Heart J* **27**, 2338-2345 (2006).
102. Yusuf, S., *et al.* Effects of candesartan in patients with chronic heart failure and preserved left-ventricular ejection fraction: the CHARM-Preserved Trial. *Lancet* **362**, 777-781 (2003).
103. Paulus, W.J. & Tschope, C. A novel paradigm for heart failure with preserved ejection fraction: comorbidities drive myocardial dysfunction and remodeling through coronary microvascular endothelial inflammation. *J Am Coll Cardiol* **62**, 263-271 (2013).
104. Desai, A.S. Heart failure with preserved ejection fraction: time for a new approach? *J Am Coll Cardiol* **62**, 272-274 (2013).
105. Udelson, J.E. Heart failure with preserved ejection fraction. *Circulation* **124**, e540-543 (2011).

106. Mann, D.L*., et al.* Targeted anticytokine therapy in patients with chronic heart failure: results of the Randomized Etanercept Worldwide Evaluation (RENEWAL). *Circulation* **109**, 1594-1602 (2004).
107. Chung, E.S*., et al.* Randomized, double-blind, placebo-controlled, pilot trial of infliximab, a chimeric monoclonal antibody to tumor necrosis factor-alpha, in patients with moderate-to-severe heart failure: results of the anti-TNF Therapy Against Congestive Heart Failure (ATTACH) trial. *Circulation* **107**, 3133-3140 (2003).
108. McMurray, J.J*., et al.* Angiotensin-neprilysin inhibition versus enalapril in heart failure. *N Engl J Med* **371**, 993-1004 (2014).
109. Solomon, S.D*., et al.* Angiotensin-Neprilysin Inhibition in Heart Failure with Preserved Ejection Fraction. *N Engl J Med* (2019).
110. Anker, S.D*., et al.* Evaluation of the effects of sodium-glucose co-transporter 2 inhibition with empagliflozin on morbidity and mortality in patients with chronic heart failure and a preserved ejection fraction: rationale for and design of the EMPEROR-Preserved Trial. *Eur J Heart Fail* (2019).
111. McMurray, J.J.V*., et al.* Dapagliflozin in Patients with Heart Failure and Reduced Ejection Fraction. *N Engl J Med* (2019).
112. Fraccarollo, D., Galuppo, P. & Bauersachs, J. Mineralocorticoid receptor antagonism and cardiac remodeling in ischemic heart failure. *Curr Med Chem Cardiovasc Hematol Agents* **2**, 287-294 (2004).
113. Bauersachs, J. & Fraccarollo, D. Aldosterone antagonism in addition to angiotensin-converting enzyme inhibitors in heart failure. *Minerva Cardioangiol* **51**, 155-164 (2003).
114. Patel, K*., et al.* Aldosterone antagonists and outcomes in real-world older patients with heart failure and preserved ejection fraction. *JACC Heart Fail* **1**, 40-47 (2013).
115. Shah, A.M*., et al.* Cardiac structure and function in heart failure with preserved ejection fraction: baseline findings from the echocardiographic study of the Treatment of Preserved Cardiac Function Heart Failure with an Aldosterone Antagonist trial. *Circ Heart Fail* **7**, 104-115 (2014).
116. Gustafsson, F., Azizi, M., Bauersachs, J., Jaisser, F. & Rossignol, P. Targeting the aldosterone pathway in cardiovascular disease. *Fundam Clin Pharmacol* **26**, 135-145 (2012).
117. Li, S*., et al.* Effects of spironolactone in heart failure with preserved ejection fraction: A meta-analysis of randomized controlled trials. *Medicine (Baltimore)* **97**, e11942 (2018).
118. Yen, T.T., Yu, P.L., Roeder, H. & Willard, P.W. A genetic study of hypertension in Okamoto-Aoki spontaneously hypertensive rats. *Heredity (Edinb)* **33**, 309-316 (1974).
119. Tanase H, S.Y. „Strain difference and genetic determination of blood pressure in rats.“ *Exp Animals (Japan)* 1-5 (1971).
120. Kovacs, P., Voigt, B. & Kloting, I. Novel quantitative trait loci for blood pressure and related traits on rat chromosomes 1, 10, and 18. *Biochem Biophys Res Commun* **235**, 343-348 (1997).
121. Hamalainen, E.R*., et al.* Molecular cloning of human lysyl oxidase and assignment of the gene to chromosome 5q23.3-31.2. *Genomics* **11**, 508-516 (1991).
122. Gacheru, S.N*., et al.* Structural and catalytic properties of copper in lysyl oxidase. *J Biol Chem* **265**, 19022-19027 (1990).
123. Kagan, H.M. & Li, W. Lysyl oxidase: properties, specificity, and biological roles inside and outside of the cell. *J Cell Biochem* **88**, 660-672 (2003).
124. Rodriguez, C*., et al.* Regulation of lysyl oxidase in vascular cells: lysyl oxidase as a new player in cardiovascular diseases. *Cardiovasc Res* **79**, 7-13 (2008).
125. Lopez, B*., et al.* Role of lysyl oxidase in myocardial fibrosis: from basic science to clinical aspects. *Am J Physiol Heart Circ Physiol* **299**, H1-9 (2010).
126. Giampuzzi, M*., et al.* Lysyl oxidase activates the transcription activity of human collagene III promoter. Possible involvement of Ku antigen. *J Biol Chem* **275**, 36341-36349 (2000).
127. Oh, J.K., Park, S.J. & Nagueh, S.F. Established and novel clinical applications of diastolic function assessment by echocardiography. *Circ Cardiovasc Imaging* **4**, 444-455 (2011).

128. Lopez, B.*, et al.* Osteopontin-mediated myocardial fibrosis in heart failure: a role for lysyl oxidase? *Cardiovasc Res* **99**, 111-120 (2013).
129. Collins, A.R.*, et al.* Osteopontin modulates angiotensin II-induced fibrosis in the intact murine heart. *J Am Coll Cardiol* **43**, 1698-1705 (2004).
130. Matsui, Y.*, et al.* Role of osteopontin in cardiac fibrosis and remodeling in angiotensin II-induced cardiac hypertrophy. *Hypertension* **43**, 1195-1201 (2004).
131. Nakayama, H.*, et al.* Association between osteopontin promoter variants and diastolic dysfunction in hypertensive heart in the Japanese population. *Hypertens Res* **34**, 1141-1146 (2011).
132. Lorenzen, J.M.*, et al.* Osteopontin is indispensible for AP1-mediated angiotensin II-related miR-21 transcription during cardiac fibrosis. *Eur Heart J* **36**, 2184-2196 (2015).
133. Graf, K.*, et al.* Myocardial osteopontin expression is associated with left ventricular hypertrophy. *Circulation* **96**, 3063-3071 (1997).
134. Xie, Z., Singh, M. & Singh, K. Osteopontin modulates myocardial hypertrophy in response to chronic pressure overload in mice. *Hypertension* **44**, 826-831 (2004).
135. Lavall, D.*, et al.* The mineralocorticoid receptor promotes fibrotic remodeling in atrial fibrillation. *J Biol Chem* **289**, 6656-6668 (2014).
136. Wang, J.*, et al.* Lysyl oxidase promotes epithelial-to-mesenchymal transition during paraquat-induced pulmonary fibrosis. *Mol Biosyst* **12**, 499-507 (2016).
137. Tjin, G.*, et al.* Lysyl oxidases regulate fibrillar collagen remodelling in idiopathic pulmonary fibrosis. *Dis Model Mech* **10**, 1301-1312 (2017).
138. Liu, S.B.*, et al.* Lysyl oxidase activity contributes to collagen stabilization during liver fibrosis progression and limits spontaneous fibrosis reversal in mice. *FASEB J* **30**, 1599-1609 (2016).
139. Ikenaga, N.*, et al.* Selective targeting of lysyl oxidase-like 2 (LOXL2) suppresses hepatic fibrosis progression and accelerates its reversal. *Gut* **66**, 1697-1708 (2017).
140. Rimar, D.*, et al.* Brief report: lysyl oxidase is a potential biomarker of fibrosis in systemic sclerosis. *Arthritis Rheumatol* **66**, 726-730 (2014).
141. Adam, O.*, et al.* Inhibition of aldosterone synthase (CYP11B2) by torasemide prevents atrial fibrosis and atrial fibrillation in mice. *J Mol Cell Cardiol* **85**, 140-150 (2015).
142. Rosin, N.L., Sopel, M.J., Falkenham, A., Lee, T.D. & Legare, J.F. Disruption of collagen homeostasis can reverse established age-related myocardial fibrosis. *Am J Pathol* **185**, 631-642 (2015).
143. El Hajj, E.C., El Hajj, M.C., Ninh, V.K. & Gardner, J.D. Inhibitor of lysyl oxidase improves cardiac function and the collagen/MMP profile in response to volume overload. *Am J Physiol Heart Circ Physiol* **315**, H463-H473 (2018).
144. Nave, A.H.*, et al.* Lysyl oxidases play a causal role in vascular remodeling in clinical and experimental pulmonary arterial hypertension. *Arterioscler Thromb Vasc Biol* **34**, 1446-1458 (2014).
145. Bank, R.A. & van Hinsbergh, V.W. Lysyl oxidase: new looks on LOX. *Arterioscler Thromb Vasc Biol* **22**, 1365-1366 (2002).
146. Leiva, O.*, et al.* A Novel Lysyl Oxidase Inhibitor Attenuates Bone Marrow Fibrosis and Decreases Spleen Size in a Mouse Model of Primary Myelofibrosis. *Blood* **130**, 4214-4214 (2017).
147. Erler, J.T.*, et al.* Lysyl oxidase is essential for hypoxia-induced metastasis. *Nature* **440**, 1222-1226 (2006).
148. Salvador, F.*, et al.* Lysyl Oxidase-like Protein LOXL2 Promotes Lung Metastasis of Breast Cancer. *Cancer Res* **77**, 5846-5859 (2017).
149. Johnston, K.A. & Lopez, K.M. Lysyl oxidase in cancer inhibition and metastasis. *Cancer Lett* **417**, 174-181 (2018).
150. Yilmaz, M., Suer, I., Karatas, O.F., Cansiz, H. & Ozen, M. Differential expression of LOXL4 in normal and tumour tissue samples of laryngeal squamous cell carcinoma. *Clin Otolaryngol* **41**, 206-210 (2016).

151. Gorogh, T*., et al.* Functional analysis of the 5' flanking domain of the LOXL4 gene in head and neck squamous cell carcinoma cells. *Int J Oncol* **33**, 1091-1098 (2008).
152. Kumar, P*., et al.* Tetrathiomolybdate inhibits head and neck cancer metastasis by decreasing tumor cell motility, invasiveness and by promoting tumor cell anoikis. *Mol Cancer* **9**, 206 (2010).
153. Buson, A*., et al.* Inhibition Of LOXL2: Pharmaxis' Small Molecule Approach To Treat Fibrosis. in *C30. LATE BREAKING ABSTRACTS IN DISEASE TREATMENT AND CLINICAL OUTCOMES* A6669-A6669.
154. Rodriguez, H.M*., et al.* Modulation of lysyl oxidase-like 2 enzymatic activity by an allosteric antibody inhibitor. *J Biol Chem* **285**, 20964-20974 (2010).
155. Gorogh, T*., et al.* Lysyl oxidase like-4 monoclonal antibody demonstrates therapeutic effect against head and neck squamous cell carcinoma cells and xenografts. *Int J Cancer* **138**, 2529-2538 (2016).
156. Maki, J.M*., et al.* Inactivation of the lysyl oxidase gene Lox leads to aortic aneurysms, cardiovascular dysfunction, and perinatal death in mice. *Circulation* **106**, 2503-2509 (2002).
157. Lee, V.S*., et al.* Loss of function mutation in LOX causes thoracic aortic aneurysm and dissection in humans. *Proc Natl Acad Sci U S A* **113**, 8759-8764 (2016).
158. Trackman, P.C. Lysyl Oxidase Isoforms and Potential Therapeutic Opportunities for Fibrosis and Cancer. *Expert Opin Ther Targets* **20**, 935-945 (2016).
159. Saleh, M. & Ambrose, J.A. Understanding myocardial infarction. *F1000Res* **7**(2018).
160. Basso, C. & Thiene, G. The pathophysiology of myocardial reperfusion: a pathologist's perspective. *Heart* **92**, 1559-1562 (2006).
161. Granfeldt, A., Lefer, D.J. & Vinten-Johansen, J. Protective ischaemia in patients: preconditioning and postconditioning. *Cardiovasc Res* **83**, 234-246 (2009).
162. Hausenloy, D.J. & Yellon, D.M. Survival kinases in ischemic preconditioning and postconditioning. *Cardiovasc Res* **70**, 240-253 (2006).
163. Zhao, Z.Q*., et al.* Inhibition of myocardial injury by ischemic postconditioning during reperfusion: comparison with ischemic preconditioning. *Am J Physiol Heart Circ Physiol* **285**, H579-588 (2003).
164. Heusch, G. Molecular basis of cardioprotection: signal transduction in ischemic pre-, post-, and remote conditioning. *Circ Res* **116**, 674-699 (2015).
165. Hausenloy, D.J., Tsang, A. & Yellon, D.M. The reperfusion injury salvage kinase pathway: a common target for both ischemic preconditioning and postconditioning. *Trends Cardiovasc Med* **15**, 69-75 (2005).
166. Staat, P*., et al.* Postconditioning the human heart. *Circulation* **112**, 2143-2148 (2005).
167. Shahzad, T*., et al.* Mechanisms involved in postconditioning protection of cardiomyocytes against acute reperfusion injury. *J Mol Cell Cardiol* **58**, 209-216 (2013).
168. Lacerda, L., Somers, S., Opie, L.H. & Lecour, S. Ischaemic postconditioning protects against reperfusion injury via the SAFE pathway. *Cardiovasc Res* **84**, 201-208 (2009).
169. van Vuuren, D., Genis, A., Genade, S. & Lochner, A. Postconditioning the isolated working rat heart. *Cardiovasc Drugs Ther* **22**, 391-397 (2008).
170. Couvreur, N*., et al.* Differential effects of postconditioning on myocardial stunning and infarction: a study in conscious dogs and anesthetized rabbits. *Am J Physiol Heart Circ Physiol* **291**, H1345-1350 (2006).
171. Ferdinandy, P., Schulz, R. & Baxter, G.F. Interaction of cardiovascular risk factors with myocardial ischemia/reperfusion injury, preconditioning, and postconditioning. *Pharmacol Rev* **59**, 418-458 (2007).
172. Ferdinandy, P., Hausenloy, D.J., Heusch, G., Baxter, G.F. & Schulz, R. Interaction of risk factors, comorbidities, and comedications with ischemia/reperfusion injury and cardioprotection by preconditioning, postconditioning, and remote conditioning. *Pharmacol Rev* **66**, 1142-1174 (2014).

173. Lecour, S*., et al.* ESC working group cellular biology of the heart: position paper: improving the preclinical assessment of novel cardioprotective therapies. *Cardiovasc Res* **104**, 399-411 (2014).
174. Watanabe, K*., et al.* Attenuated cardioprotection by ischemic preconditioning in coronary stenosed heart and its restoration by carvedilol. *Cardiovasc Res* **71**, 537-547 (2006).
175. Ovize, M*., et al.* Postconditioning and protection from reperfusion injury: where do we stand? Position paper from the Working Group of Cellular Biology of the Heart of the European Society of Cardiology. *Cardiovasc Res* **87**, 406-423 (2010).
176. Burtis, W.J*., et al.* Identification of a novel 17,000-dalton parathyroid hormone-like adenylate cyclase-stimulating protein from a tumor associated with humoral hypercalcemia of malignancy. *J Biol Chem* **262**, 7151-7156 (1987).
177. Schluter, K*., et al.* Expression, release, and biological activity of parathyroid hormone-related peptide from coronary endothelial cells. *Circ Res* **86**, 946-951 (2000).
178. Bui, T.D*., et al.* Parathyroid hormone related peptide gene expression in human fetal and adult heart. *Cardiovasc Res* **27**, 1204-1208 (1993).
179. Deftos, L.J., Burton, D.W. & Brandt, D.W. Parathyroid hormone-like protein is a secretory product of atrial myocytes. *J Clin Invest* **92**, 727-735 (1993).
180. Sutliff, R.L*., et al.* Vasorelaxant properties of parathyroid hormone-related protein in the mouse: evidence for endothelium involvement independent of nitric oxide formation. *Endocrinology* **140**, 2077-2083 (1999).
181. Abdallah, Y., Ross, G., Dolf, A., Heinemann, M.P. & Schluter, K.D. N-terminal parathyroid hormone-related peptide hyperpolarizes endothelial cells and causes a reduction of the coronary resistance of the rat heart via endothelial hyperpolarization. *Peptides* **27**, 2927-2934 (2006).
182. Kalinowski, L., Dobrucki, L.W. & Malinski, T. Nitric oxide as a second messenger in parathyroid hormone-related protein signaling. *J Endocrinol* **170**, 433-440 (2001).
183. Halapas, A., Diamanti-Kandarakis, E., Kremastinos, D. & Koutsilieris, M. The PTHrP/PTH.1-R bioregulation system in cardiac hypertrophy: possible therapeutic implications. *In Vivo* **20**, 837-844 (2006).
184. Jansen, J*., et al.* Parathyroid hormone-related peptide improves contractile function of stunned myocardium in rats and pigs. *Am J Physiol Heart Circ Physiol* **284**, H49-55 (2003).
185. Schluter, K.D., Weber, M. & Piper, H.M. Effects of PTH-rP(107-111) and PTH-rP(7-34) on adult cardiomyocytes. *J Mol Cell Cardiol* **29**, 3057-3065 (1997).
186. Huang, C.H., Li, C.L., Kor, C.T. & Chang, C.C. Menopausal symptoms and risk of coronary heart disease in middle-aged women: A nationwide population-based cohort study. *PLoS One* **13**, e0206036 (2018).
187. Anagnostis, P*., et al.* Menopausal hormone therapy and cardiovascular risk. Where are we now? *Curr Vasc Pharmacol* (2018).
188. Balci, H*., et al.* Effects of transdermal estrogen replacement therapy on plasma levels of nitric oxide and plasma lipids in postmenopausal women. *Maturitas* **50**, 289-293 (2005).
189. Miller, V.M. & Duckles, S.P. Vascular actions of estrogens: functional implications. *Pharmacol Rev* **60**, 210-241 (2008).
190. Nevzati, E*., et al.* Estrogen induces nitric oxide production via nitric oxide synthase activation in endothelial cells. *Acta Neurochir Suppl* **120**, 141-145 (2015).
191. Loyer, X*., et al.* 17beta-estradiol regulates constitutive nitric oxide synthase expression differentially in the myocardium in response to pressure overload. *Endocrinology* **148**, 4579-4584 (2007).
192. Holt, E.H., Lu, C., Dreyer, B.E., Dannies, P.S. & Broadus, A.E. Regulation of parathyroid hormone-related peptide gene expression by estrogen in GH4C1 rat pituitary cells has the pattern of a primary response gene. *J Neurochem* **62**, 1239-1246 (1994).
193. Cros, M*., et al.* Estrogen stimulates PTHrP but not PTH/PTHrP receptor gene expression in the kidney of ovariectomized rat. *J Cell Biochem* **70**, 84-93 (1998).

194. Ross, G. & Schluter, K.D. Cardiac-specific effects of parathyroid hormone-related peptide: modification by aging and hypertension. *Cardiovasc Res* **66**, 334-344 (2005).
195. Grohe, C*., et al.* Sex-specific differences in ventricular expression and function of parathyroid hormone-related peptide. *Cardiovasc Res* **61**, 307-316 (2004).
196. Ross, G., Heinemann, M.P. & Schluter, K.D. Vasodilatory effect of tuberoinfundibular peptide (TIP39): requirement of receptor desensitization and its beneficial effect in the post-ischemic heart. *Peptides* **28**, 878-886 (2007).
197. Augustine, M. & Horwitz, M.J. Parathyroid hormone and parathyroid hormone-related protein analogs as therapies for osteoporosis. *Curr Osteoporos Rep* **11**, 400-406 (2013).
198. Horwitz, M.J*., et al.* A comparison of parathyroid hormone-related protein (1-36) and parathyroid hormone (1-34) on markers of bone turnover and bone density in postmenopausal women: the PrOP study. *J Bone Miner Res* **28**, 2266-2276 (2013).
199. Niu, X*., et al.* Cardioprotective effect of beta-3 adrenergic receptor agonism: role of neuronal nitric oxide synthase. *J Am Coll Cardiol* **59**, 1979-1987 (2012).
200. Strasser, R.H. & Marquetant, R. Sensitization of the beta-adrenergic system in acute myocardial ischaemia by a protein kinase C-dependent mechanism. *Eur Heart J* **12 Suppl F**, 48-53 (1991).
201. Bartels, L.A., Clifton, G.D. & Szabo, T.S. Influence of myocardial ischemia and reperfusion on beta-adrenoceptor subtype expression. *J Cardiovasc Pharmacol* **31**, 484-487 (1998).
202. Anthonio, R.L*., et al.* Beta-adrenoceptor density in chronic infarcted myocardium: a subtype specific decrease of beta1-adrenoceptor density. *Int J Cardiol* **72**, 137-141 (2000).
203. Hausenloy, D.J*., et al.* Translating cardioprotection for patient benefit: position paper from the Working Group of Cellular Biology of the Heart of the European Society of Cardiology. *Cardiovasc Res* **98**, 7-27 (2013).
204. Freixa, X*., et al.* Ischaemic postconditioning revisited: lack of effects on infarct size following primary percutaneous coronary intervention. *Eur Heart J* **33**, 103-112 (2012).
205. Hahn, J.Y*., et al.* Long-term effects of ischemic postconditioning on clinical outcomes: 1-year follow-up of the POST randomized trial. *Am Heart J* **169**, 639-646 (2015).
206. Engstrom, T*., et al.* Effect of Ischemic Postconditioning During Primary Percutaneous Coronary Intervention for Patients With ST-Segment Elevation Myocardial Infarction: A Randomized Clinical Trial. *JAMA Cardiol* **2**, 490-497 (2017).
207. Yellon, D.M. & Downey, J.M. Preconditioning the myocardium: from cellular physiology to clinical cardiology. *Physiol Rev* **83**, 1113-1151 (2003).
208. Murga, C*., et al.* G Protein-Coupled Receptor Kinase 2 (GRK2) as a Potential Therapeutic Target in Cardiovascular and Metabolic Diseases. *Front Pharmacol* **10**, 112 (2019).
209. Cannavo, A., Liccardo, D. & Koch, W.J. Targeting cardiac beta-adrenergic signaling via GRK2 inhibition for heart failure therapy. *Front Physiol* **4**, 264 (2013).
210. Woodall, M.C., Ciccarelli, M., Woodall, B.P. & Koch, W.J. G protein-coupled receptor kinase 2: a link between myocardial contractile function and cardiac metabolism. *Circ Res* **114**, 1661-1670 (2014).
211. Cannavo, A*., et al.* GRK2 as a therapeutic target for heart failure. *Expert Opin Ther Targets* **22**, 75-83 (2018).
212. Cusi, K. Role of obesity and lipotoxicity in the development of nonalcoholic steatohepatitis: pathophysiology and clinical implications. *Gastroenterology* **142**, 711-725 e716 (2012).
213. Mayor, F., Jr*., et al.* G Protein-coupled receptor kinase 2 (GRK2): A novel modulator of insulin resistance. *Arch Physiol Biochem* **117**, 125-130 (2011).
214. Izzo, R*., et al.* Enhanced GRK2 expression and desensitization of betaAR vasodilatation in hypertensive patients. *Clin Transl Sci* **1**, 215-220 (2008).
215. Iaccarino, G*., et al.* Elevated myocardial and lymphocyte GRK2 expression and activity in human heart failure. *Eur Heart J* **26**, 1752-1758 (2005).
216. Gao, W.Q*., et al.* GRK 2 level in peripheral blood lymphocytes of elderly patients with acute myocardial infarction. *J Geriatr Cardiol* **10**, 281-285 (2013).

217. Matkovich, S.J., *et al.* Cardiac-specific ablation of G-protein receptor kinase 2 redefines its roles in heart development and beta-adrenergic signaling. *Circ Res* **99**, 996-1003 (2006).
218. Koch, W.J., *et al.* Cardiac function in mice overexpressing the beta-adrenergic receptor kinase or a beta ARK inhibitor. *Science* **268**, 1350-1353 (1995).
219. Lymperopoulos, A. GRK2 and beta-arrestins in cardiovascular disease: Something old, something new. *Am J Cardiovasc Dis* **1**, 126-137 (2011).
220. Raake, P.W., *et al.* Cardiac G-protein-coupled receptor kinase 2 ablation induces a novel Ca2+ handling phenotype resistant to adverse alterations and remodeling after myocardial infarction. *Circulation* **125**, 2108-2118 (2012).
221. Siryk-Bathgate, A., Dabul, S. & Lymperopoulos, A. Current and future G protein-coupled receptor signaling targets for heart failure therapy. *Drug Des Devel Ther* **7**, 1209-1222 (2013).
222. Harding, V.B., Jones, L.R., Lefkowitz, R.J., Koch, W.J. & Rockman, H.A. Cardiac beta ARK1 inhibition prolongs survival and augments beta blocker therapy in a mouse model of severe heart failure. *Proc Natl Acad Sci U S A* **98**, 5809-5814 (2001).
223. Tevaearai, H.T., Walton, G.B., Keys, J.R., Koch, W.J. & Eckhart, A.D. Acute ischemic cardiac dysfunction is attenuated via gene transfer of a peptide inhibitor of the beta-adrenergic receptor kinase (betaARK1). *J Gene Med* **7**, 1172-1177 (2005).
224. Rockman, H.A., *et al.* Control of myocardial contractile function by the level of beta-adrenergic receptor kinase 1 in gene-targeted mice. *J Biol Chem* **273**, 18180-18184 (1998).
225. Penela, P., *et al.* Mechanisms of regulation of G protein-coupled receptor kinases (GRKs) and cardiovascular disease. *Cardiovasc Res* **69**, 46-56 (2006).
226. Penela, P., Ruiz-Gomez, A., Castano, J.G. & Mayor, F., Jr. Degradation of the G protein-coupled receptor kinase 2 by the proteasome pathway. *J Biol Chem* **273**, 35238-35244 (1998).
227. Salcedo, A., Mayor, F., Jr. & Penela, P. Mdm2 is involved in the ubiquitination and degradation of G-protein-coupled receptor kinase 2. *EMBO J* **25**, 4752-4762 (2006).
228. Nogues, L., Salcedo, A., Mayor, F., Jr. & Penela, P. Multiple scaffolding functions of {beta}-arrestins in the degradation of G protein-coupled receptor kinase 2. *J Biol Chem* **286**, 1165-1173 (2011).
229. Mayo, L.D. & Donner, D.B. A phosphatidylinositol 3-kinase/Akt pathway promotes translocation of Mdm2 from the cytoplasm to the nucleus. *Proc Natl Acad Sci U S A* **98**, 11598-11603 (2001).
230. Feng, J., *et al.* Stabilization of Mdm2 via decreased ubiquitination is mediated by protein kinase B/Akt-dependent phosphorylation. *J Biol Chem* **279**, 35510-35517 (2004).
231. Ogawara, Y., *et al.* Akt enhances Mdm2-mediated ubiquitination and degradation of p53. *J Biol Chem* **277**, 21843-21850 (2002).
232. Tsang, A., Hausenloy, D.J., Mocanu, M.M. & Yellon, D.M. Postconditioning: a form of "modified reperfusion" protects the myocardium by activating the phosphatidylinositol 3-kinase-Akt pathway. *Circ Res* **95**, 230-232 (2004).
233. Zhu, M., *et al.* Ischemic postconditioning protects remodeled myocardium via the PI3K-PKB/Akt reperfusion injury salvage kinase pathway. *Cardiovasc Res* **72**, 152-162 (2006).
234. Homan, K.T. & Tesmer, J.J. Molecular basis for small molecule inhibition of G protein-coupled receptor kinases. *ACS Chem Biol* **10**, 246-256 (2015).
235. Schumacher, S.M., *et al.* Paroxetine-mediated GRK2 inhibition reverses cardiac dysfunction and remodeling after myocardial infarction. *Sci Transl Med* **7**, 277ra231 (2015).
236. Powell, J.M., Ebin, E., Borzak, S., Lymperopoulos, A. & Hennekens, C.H. Hypothesis: Paroxetine, a G Protein-Coupled Receptor Kinase 2 (GRK2) Inhibitor Reduces Morbidity and Mortality in Patients With Heart Failure. *J Cardiovasc Pharmacol Ther* **22**, 51-53 (2017).
237. Mayer, G., *et al.* An RNA molecule that specifically inhibits G-protein-coupled receptor kinase 2 in vitro. *RNA* **14**, 524-534 (2008).
238. Sorriento, D., Ciccarelli, M., Cipolletta, E., Trimarco, B. & Iaccarino, G. "Freeze, Don't Move": How to Arrest a Suspect in Heart Failure - A Review on Available GRK2 Inhibitors. *Front Cardiovasc Med* **3**, 48 (2016).

239. Casey, L.M.*, et al.* Small molecule disruption of G beta gamma signaling inhibits the progression of heart failure. *Circ Res* **107**, 532-539 (2010).
240. Salazar, N.C.*, et al.* GRK2 blockade with betaARKct is essential for cardiac beta2-adrenergic receptor signaling towards increased contractility. *Cell Commun Signal* **11**, 64 (2013).
241. Mori, M. & Gotoh, T. Regulation of nitric oxide production by arginine metabolic enzymes. *Biochem Biophys Res Commun* **275**, 715-719 (2000).
242. Forstermann, U. & Sessa, W.C. Nitric oxide synthases: regulation and function. *Eur Heart J* **33**, 829-837, 837a-837d (2012).
243. Schulz, R., Rassaf, T., Massion, P.B., Kelm, M. & Balligand, J.L. Recent advances in the understanding of the role of nitric oxide in cardiovascular homeostasis. *Pharmacol Ther* **108**, 225-256 (2005).
244. Kojda, G.*, et al.* Low increase in cGMP induced by organic nitrates and nitrovasodilators improves contractile response of rat ventricular myocytes. *Circ Res* **78**, 91-101 (1996).
245. Rassaf, T.*, et al.* Positive effects of nitric oxide on left ventricular function in humans. *Eur Heart J* **27**, 1699-1705 (2006).
246. Schulz, R., Kelm, M. & Heusch, G. Nitric oxide in myocardial ischemia/reperfusion injury. *Cardiovasc Res* **61**, 402-413 (2004).
247. Jones, S.P. & Bolli, R. The ubiquitous role of nitric oxide in cardioprotection. *J Mol Cell Cardiol* **40**, 16-23 (2006).
248. Totzeck, M., Hendgen-Cotta, U.B. & Rassaf, T. Nitrite-Nitric Oxide Signaling and Cardioprotection. *Adv Exp Med Biol* **982**, 335-346 (2017).
249. Strijdom, H., Chamane, N. & Lochner, A. Nitric oxide in the cardiovascular system: a simple molecule with complex actions. *Cardiovasc J Afr* **20**, 303-310 (2009).
250. Yang, Z. & Ming, X.F. Arginase: the emerging therapeutic target for vascular oxidative stress and inflammation. *Front Immunol* **4**, 149 (2013).
251. Singh, M., Padhy, G., Vats, P., Bhargava, K. & Sethy, N.K. Hypobaric hypoxia induced arginase expression limits nitric oxide availability and signaling in rodent heart. *Biochim Biophys Acta* **1840**, 1817-1824 (2014).
252. Moens, A.L.*, et al.* Reversal of cardiac hypertrophy and fibrosis from pressure overload by tetrahydrobiopterin: efficacy of recoupling nitric oxide synthase as a therapeutic strategy. *Circulation* **117**, 2626-2636 (2008).
253. Pernow, J. & Jung, C. Arginase as a potential target in the treatment of cardiovascular disease: reversal of arginine steal? *Cardiovasc Res* **98**, 334-343 (2013).
254. Zhu, C., Yu, Y., Montani, J.P., Ming, X.F. & Yang, Z. Arginase-I enhances vascular endothelial inflammation and senescence through eNOS-uncoupling. *BMC Res Notes* **10**, 82 (2017).
255. Hein, T.W.*, et al.* Ischemia-reperfusion selectively impairs nitric oxide-mediated dilation in coronary arterioles: counteracting role of arginase. *FASEB J* **17**, 2328-2330 (2003).
256. Schulman, S.P.*, et al.* L-arginine therapy in acute myocardial infarction: the Vascular Interaction With Age in Myocardial Infarction (VINTAGE MI) randomized clinical trial. *JAMA* **295**, 58-64 (2006).
257. Jenkinson, C.P., Grody, W.W. & Cederbaum, S.D. Comparative properties of arginases. *Comp Biochem Physiol B Biochem Mol Biol* **114**, 107-132 (1996).
258. Takiguchi, M., Matsubasa, T., Amaya, Y. & Mori, M. Evolutionary aspects of urea cycle enzyme genes. *Bioessays* **10**, 163-166 (1989).
259. Dowling, D.P., Di Costanzo, L., Gennadios, H.A. & Christianson, D.W. Evolution of the arginase fold and functional diversity. *Cell Mol Life Sci* **65**, 2039-2055 (2008).
260. Kanyo, Z.F., Scolnick, L.R., Ash, D.E. & Christianson, D.W. Structure of a unique binuclear manganese cluster in arginase. *Nature* **383**, 554-557 (1996).
261. Grody, W.W.*, et al.* Differential expression of the two human arginase genes in hyperargininemia. Enzymatic, pathologic, and molecular analysis. *J Clin Invest* **83**, 602-609 (1989).
262. Ash, D.E. Structure and function of arginases. *J Nutr* **134**, 2760S-2764S; discussion 2765S-2767S (2004).

263. Cabrera-Fuentes, H.A*., et al.* RNase1 prevents the damaging interplay between extracellular RNA and tumour necrosis factor-alpha in cardiac ischaemia/reperfusion injury. *Thromb Haemost* **112**, 1110-1119 (2014).
264. Gao, X*., et al.* TNF-alpha contributes to endothelial dysfunction by upregulating arginase in ischemia/reperfusion injury. *Arterioscler Thromb Vasc Biol* **27**, 1269-1275 (2007).
265. Zhang, C., Wu, J., Xu, X., Potter, B.J. & Gao, X. Direct relationship between levels of TNF-alpha expression and endothelial dysfunction in reperfusion injury. *Basic Res Cardiol* **105**, 453-464 (2010).
266. Flesch, M*., et al.* Activation and functional significance of the renin-angiotensin system in mice with cardiac restricted overexpression of tumor necrosis factor. *Circulation* **108**, 598-604 (2003).
267. Iyer, R.K*., et al.* Mouse model for human arginase deficiency. *Mol Cell Biol* **22**, 4491-4498 (2002).
268. Durante, W. Role of arginase in vessel wall remodeling. *Front Immunol* **4**, 111 (2013).
269. Caldwell, R.B., Toque, H.A., Narayanan, S.P. & Caldwell, R.W. Arginase: an old enzyme with new tricks. *Trends Pharmacol Sci* **36**, 395-405 (2015).
270. Kovamees, O., Shemyakin, A. & Pernow, J. Effect of arginase inhibition on ischemia-reperfusion injury in patients with coronary artery disease with and without diabetes mellitus. *PLoS One* **9**, e103260 (2014).
271. Figueroa, A*., et al.* Impact of L-citrulline supplementation and whole-body vibration training on arterial stiffness and leg muscle function in obese postmenopausal women with high blood pressure. *Exp Gerontol* **63**, 35-40 (2015).
272. Morita, M*., et al.* Oral supplementation with a combination of L-citrulline and L-arginine rapidly increases plasma L-arginine concentration and enhances NO bioavailability. *Biochem Biophys Res Commun* **454**, 53-57 (2014).
273. Suzuki, T., Morita, M., Hayashi, T. & Kamimura, A. The effects on plasma L-arginine levels of combined oral L-citrulline and L-arginine supplementation in healthy males. *Biosci Biotechnol Biochem* **81**, 372-375 (2017).
274. Tsuboi, T., Maeda, M. & Hayashi, T. Administration of L-arginine plus L-citrulline or L-citrulline alone successfully retarded endothelial senescence. *PLoS One* **13**, e0192252 (2018).
275. Wijnands, K.A*., et al.* Citrulline Supplementation Improves Organ Perfusion and Arginine Availability under Conditions with Enhanced Arginase Activity. *Nutrients* **7**, 5217-5238 (2015).
276. Laufs, U. & Liao, J.K. Direct vascular effects of HMG-CoA reductase inhibitors. *Trends Cardiovasc Med* **10**, 143-148 (2000).
277. Holowatz, L.A., Santhanam, L., Webb, A., Berkowitz, D.E. & Kenney, W.L. Oral atorvastatin therapy restores cutaneous microvascular function by decreasing arginase activity in hypercholesterolaemic humans. *J Physiol* **589**, 2093-2103 (2011).
278. Toque, H.A*., et al.* p38 Mitogen-activated protein kinase (MAPK) increases arginase activity and contributes to endothelial dysfunction in corpora cavernosa from angiotensin-II-treated mice. *J Sex Med* **7**, 3857-3867 (2010).
279. Yepuri, G*., et al.* Positive crosstalk between arginase-II and S6K1 in vascular endothelial inflammation and aging. *Aging Cell* **11**, 1005-1016 (2012).
280. Kevin, L.G. & Barnard, M. Right ventricular failure. *BJA Education* **7**, 89-94 (2007).
281. Voelkel, N.F*., et al.* Right ventricular function and failure: report of a National Heart, Lung, and Blood Institute working group on cellular and molecular mechanisms of right heart failure. *Circulation* **114**, 1883-1891 (2006).
282. Markel, T.A*., et al.* The right heart and its distinct mechanisms of development, function, and failure. *J Surg Res* **146**, 304-313 (2008).
283. Mehta, S.R*., et al.* Impact of right ventricular involvement on mortality and morbidity in patients with inferior myocardial infarction. *J Am Coll Cardiol* **37**, 37-43 (2001).
284. Verzi, M.P., McCulley, D.J., De Val, S., Dodou, E. & Black, B.L. The right ventricle, outflow tract, and ventricular septum comprise a restricted expression domain within the secondary/anterior heart field. *Dev Biol* **287**, 134-145 (2005).

285. Zaffran, S., Kelly, R.G., Meilhac, S.M., Buckingham, M.E. & Brown, N.A. Right ventricular myocardium derives from the anterior heart field. *Circ Res* **95**, 261-268 (2004).
286. Hines, R. Right ventricular function and failure: a review. *Yale J Biol Med* **64**, 295-307 (1991).
287. Baker, B.J., Wilen, M.M., Boyd, C.M., Dinh, H. & Franciosa, J.A. Relation of right ventricular ejection fraction to exercise capacity in chronic left ventricular failure. *Am J Cardiol* **54**, 596-599 (1984).
288. Gulati, A.*, et al.* The prevalence and prognostic significance of right ventricular systolic dysfunction in nonischemic dilated cardiomyopathy. *Circulation* **128**, 1623-1633 (2013).
289. Cannon, R.O., 3rd. Role of nitric oxide in cardiovascular disease: focus on the endothelium. *Clin Chem* **44**, 1809-1819 (1998).
290. Jain, M.*, et al.* Mitochondrial reactive oxygen species regulate transforming growth factor-beta signaling. *J Biol Chem* **288**, 770-777 (2013).
291. Lijnen, P.J., Petrov, V.V. & Fagard, R.H. Induction of cardiac fibrosis by transforming growth factor-beta(1). *Mol Genet Metab* **71**, 418-435 (2000).
292. Baylis, C. Nitric oxide deficiency in chronic kidney disease. *Am J Physiol Renal Physiol* **294**, F1-9 (2008).
293. Tessari, P.*, et al.* Nitric oxide synthesis is reduced in subjects with type 2 diabetes and nephropathy. *Diabetes* **59**, 2152-2159 (2010).
294. Gaucher, C., Boudier, A., Dahboul, F., Parent, M. & Leroy, P. S-nitrosation/denitrosation in cardiovascular pathologies: facts and concepts for the rational design of S-nitrosothiols. *Curr Pharm Des* **19**, 458-472 (2013).
295. Pacher, P., Beckman, J.S. & Liaudet, L. Nitric oxide and peroxynitrite in health and disease. *Physiol Rev* **87**, 315-424 (2007).
296. Soetkamp, D.*, et al.* S-nitrosation of mitochondrial connexin 43 regulates mitochondrial function. *Basic Res Cardiol* **109**, 433 (2014).
297. Misik, V., Mak, I.T., Stafford, R.E. & Weglicki, W.B. Reactions of captopril and epicaptopril with transition metal ions and hydroxyl radicals: an EPR spectroscopy study. *Free Radic Biol Med* **15**, 611-619 (1993).
298. Benzie, I.F. & Tomlinson, B. Antioxidant power of angiotensin-converting enzyme inhibitors in vitro. *Br J Clin Pharmacol* **45**, 168-169 (1998).
299. Gonzalez, W.*, et al.* Molecular plasticity of vascular wall during N(G)-nitro-L-arginine methyl ester-induced hypertension: modulation of proinflammatory signals. *Hypertension* **36**, 103-109 (2000).
300. Kumar, S., Prahalathan, P. & Raja, B. Syringic acid ameliorates (L)-NAME-induced hypertension by reducing oxidative stress. *Naunyn Schmiedebergs Arch Pharmacol* **385**, 1175-1184 (2012).
301. Sekiguchi, F.*, et al.* Endothelium-dependent relaxation in pulmonary arteries of L-NAME-treated Wistar and stroke-prone spontaneously hypertensive rats. *J Smooth Muscle Res* **38**, 131-144 (2002).
302. Suda, O.*, et al.* Long-term treatment with N(omega)-nitro-L-arginine methyl ester causes arteriosclerotic coronary lesions in endothelial nitric oxide synthase-deficient mice. *Circulation* **106**, 1729-1735 (2002).
303. Dikalov, S. Cross talk between mitochondria and NADPH oxidases. *Free Radic Biol Med* **51**, 1289-1301 (2011).
304. Shen, X., Zheng, S., Metreveli, N.S. & Epstein, P.N. Protection of cardiac mitochondria by overexpression of MnSOD reduces diabetic cardiomyopathy. *Diabetes* **55**, 798-805 (2006).
305. Borchi, E.*, et al.* Enhanced ROS production by NADPH oxidase is correlated to changes in antioxidant enzyme activity in human heart failure. *Biochim Biophys Acta* **1802**, 331-338 (2010).
306. Buelna-Chontal, M.*, et al.* Nrf2-regulated antioxidant response is activated by protein kinase C in postconditioned rat hearts. *Free Radic Biol Med* **74**, 145-156 (2014).
307. Do, M.T., Kim, H.G., Choi, J.H. & Jeong, H.G. Metformin induces microRNA-34a to downregulate the Sirt1/Pgc-1alpha/Nrf2 pathway, leading to increased susceptibility of wild-

type p53 cancer cells to oxidative stress and therapeutic agents. *Free Radic Biol Med* **74**, 21-34 (2014).
308. Bujak, M. & Frangogiannis, N.G. The role of TGF-beta signaling in myocardial infarction and cardiac remodeling. *Cardiovasc Res* **74**, 184-195 (2007).
309. Andreadou, I.*, et al.* The role of gasotransmitters NO, H2S and CO in myocardial ischaemia/reperfusion injury and cardioprotection by preconditioning, postconditioning and remote conditioning. *Br J Pharmacol* **172**, 1587-1606 (2015).
310. Ferdinandy, P. & Schulz, R. Nitric oxide, superoxide, and peroxynitrite in myocardial ischaemia-reperfusion injury and preconditioning. *Br J Pharmacol* **138**, 532-543 (2003).
311. Ferdinandy, P. Peroxynitrite: just an oxidative/nitrosative stressor or a physiological regulator as well? *Br J Pharmacol* **148**, 1-3 (2006).
312. Wang, W., Sawicki, G. & Schulz, R. Peroxynitrite-induced myocardial injury is mediated through matrix metalloproteinase-2. *Cardiovasc Res* **53**, 165-174 (2002).
313. Wang, W.*, et al.* Intracellular action of matrix metalloproteinase-2 accounts for acute myocardial ischemia and reperfusion injury. *Circulation* **106**, 1543-1549 (2002).
314. Gauthier, K.M., Cepura, C.J. & Campbell, W.B. ACE inhibition enhances bradykinin relaxations through nitric oxide and B1 receptor activation in bovine coronary arteries. *Biol Chem* **394**, 1205-1212 (2013).
315. Evangelista, S. & Manzini, S. Antioxidant and cardioprotective properties of the sulphydryl angiotensin-converting enzyme inhibitor zofenopril. *J Int Med Res* **33**, 42-54 (2005).
316. Comini, L.*, et al.* Therapeutic modulation of the nitric oxide: all ace inhibitors are not equivalent. *Pharmacol Res* **56**, 42-48 (2007).
317. Donnarumma, E.*, et al.* Zofenopril Protects Against Myocardial Ischemia-Reperfusion Injury by Increasing Nitric Oxide and Hydrogen Sulfide Bioavailability. *J Am Heart Assoc* **5**(2016).
318. Younus, H. Therapeutic potentials of superoxide dismutase. *Int J Health Sci (Qassim)* **12**, 88-93 (2018).
319. Borgstahl, G.E.O. & Oberley-Deegan, R.E. Superoxide Dismutases (SODs) and SOD Mimetics. *Antioxidants (Basel)* **7**(2018).
320. Bonetta, R. Potential Therapeutic Applications of MnSODs and SOD-Mimetics. *Chemistry* **24**, 5032-5041 (2018).
321. Batinic-Haberle, I., Reboucas, J.S. & Spasojevic, I. Superoxide dismutase mimics: chemistry, pharmacology, and therapeutic potential. *Antioxid Redox Signal* **13**, 877-918 (2010).
322. Oyewole, A.O. & Birch-Machin, M.A. Mitochondria-targeted antioxidants. *FASEB J* **29**, 4766-4771 (2015).
323. Rossman, M.J.*, et al.* Chronic Supplementation With a Mitochondrial Antioxidant (MitoQ) Improves Vascular Function in Healthy Older Adults. *Hypertension* **71**, 1056-1063 (2018).
324. Broome, S.C., Woodhead, J.S.T. & Merry, T.L. Mitochondria-Targeted Antioxidants and Skeletal Muscle Function. *Antioxidants (Basel)* **7**(2018).
325. Ahmed, E., Donovan, T., Yujiao, L. & Zhang, Q. Mitochondrial Targeted Antioxidant in Cerebral Ischemia. *J Neurol Neurosci* **6**(2015).

8. Danksagung

Mein besonderer Dank gilt Herrn Prof. Schulz und Herrn Prof. Schlüter, die durch ihre fachliche Kompetenz, ihr persönliches Engagement und nicht zuletzt durch ihre kollegiale und freundschaftliche Zusammenarbeit die Umsetzung dieser Arbeit ermöglicht haben.

Für die herausragenden Befunde zum myokardialen Reperfusionsschaden, die in Kooperation mit der Semmelweis Universität Budapest sowie dem Institut für Pharmakologie der Universität Budapest erhoben worden sind, möchte ich mich bei Herrn Prof. Ferdinandy ganz herzlich bedanken.

9. Anlage: Originalpublikationen der kumulativen Habilitationsschrift

Vascular Pharmacology 107 (2018) 35–42

Contents lists available at ScienceDirect

Vascular Pharmacology

journal homepage: www.elsevier.com/locate/vph

Review

Calcium sensing receptor expression and signalling in cardiovascular physiology and disease

Rolf Schreckenberg*, Klaus-Dieter Schlüter

Justus-Liebig-Universität Gießen, Physiologisches Institut, Germany

ARTICLE INFO

Keywords:
Calcium sensing receptor
Endothelial cells
Vascular smooth muscle cells
Blood pressure
Cardiomyocytes

ABSTRACT

Initially identified in the parathyroidea, the calcium sensing receptor (CaSR) is now recognized as an ubiquitously expressed receptor that exerts specific functions in multiple organs including the cardiovascular system. This review will focus on the role that CaSR plays in vascular and cardiac tissues. In the vasculature, CaSR is expressed in endothelial and smooth muscle cells. CaSR of endothelial cells participates in part to the regulation of local perfusion by linkage of CaSR activation to endothelial hyperpolarization and nitric oxide release. CaSR of smooth muscle cells is involved in the control of proliferation. In the pulmonary vasculature, however, CaSR participates in the onset of pulmonary hypertension, making CaSR antagonism a therapeutic option in this case. In the heart, CaSR is expressed in cardiac fibroblasts and myoyctes, contributing to normal cardiac function and composition of extracellular matrix. More important, activation of CaSR may participate in the cardiac protective effects of ischaemic pre-conditioning. In conclusion, CaSR plays an important physiological role in many regulatory pathways of the cardiovascular system, but due to the complex interaction between various cardiovascular cells and cell-specific effects, use of activators or inhibitors of CaSR for treatment of specific disease forms is yet not on the way.

1. Introduction

Many cell types are able to detect even the smallest of changes in extracellular Ca^{2+} concentrations under specific physiologic or pathophysiologic conditions. The importance of Ca^{2+} as a first messenger had already been postulated and described by Edward M. Brown before he, together with Herbert and colleagues, identified the receptor that underpins Ca^{2+} sensing [1,2].

The concentrations of free Ca^{2+} in the extracellular space are precisely regulated and are always kept between 1.0 and 1.3 mmol/L at physiological pH. The most important sensing element is the calcium-sensing receptor (CaSR), the expression of which has been verified in all cells or organs that are directly involved in the regulation of the Ca^{2+} balance, primarily in the parathyroid glands [3].

Even 25 years after its first description, new functions and mechanisms are still being attributed to the CaSR that go well beyond simply sensing physiological Ca^{2+} concentrations. Many studies have also identified agonists other than Ca^{2+}, meaning that the original name of 'calcium-sensing receptor' no longer reflects the importance or the relevance of this receptor based on our current knowledge.

The focus of this review is on the importance of CaSR for the cardiovascular system and describes its influence on functional and metabolic processes in vascular cells, atrial and ventricular cardiomyocytes. CaSR activity is directly involved in regulating vascular tone and thus has a direct effect on the blood pressure. The heart and blood vessels, however, do not directly influence the extracellular Ca^{2+} homeostasis, which means that the expression 'calcium sensing' primarily describes the various signalling mechanisms that can be initiated by the first messenger Ca^{2+} under both physiological and pathophysiological conditions throughout the cardiovascular system [4].

1.1. Structure and functional mechanisms of CaSR

In humans, the gene for CaSR is located on the long arm of chromosome 3 (3q13.3-21), in rats on chromosome 11 and in mice on chromosome 16. It is about 103 kb in size and is organized into 8 exons [5–7]. Exon II and VII have been partly translated and exons III to VI have been completely translated and together they form the full-length protein for CaSR. Exons II to VI and the start of exon VII code for the extracellular domain (ECD) while the information for the transmembrane (TMD) and intracellular domains (ICD) are located on exon VII alone. The fully processed mRNA for CaSR encodes for 1078 amino acids (AA): The hydrophilic ECD is made up of 612 AA and forms the N-terminus that is responsible for ligand binding. The hydrophobic TMD

* Corresponding author at: Physiologisches Institut, Aulweg 129, D-35392 Gießen, Germany.
E-mail address: rolf.schreckenberg@physiologie.med.uni-giessen.de (R. Schreckenberg).

https://doi.org/10.1016/j.vph.2018.02.007
Received 2 November 2017; Received in revised form 18 January 2018; Accepted 21 February 2018
Available online 04 March 2018

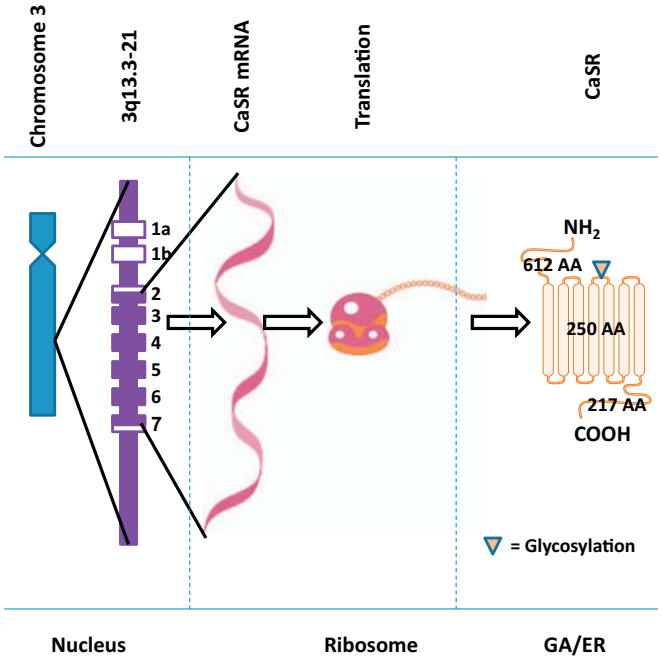

Fig. 1. Molecular organisation of the CaSR. CaSR gene is located on chromosome 3 and organized in 8 exons. Parts of exon 2, exon 3–6 and part of exon 7 represent the coding information. After splicing, CaSR mRNA in translated into a 1078 amino acid long protein that is stored in the endoplasmic reticulum (ER) or golgi apparatus (GA) and target of subsequent glycosylation.

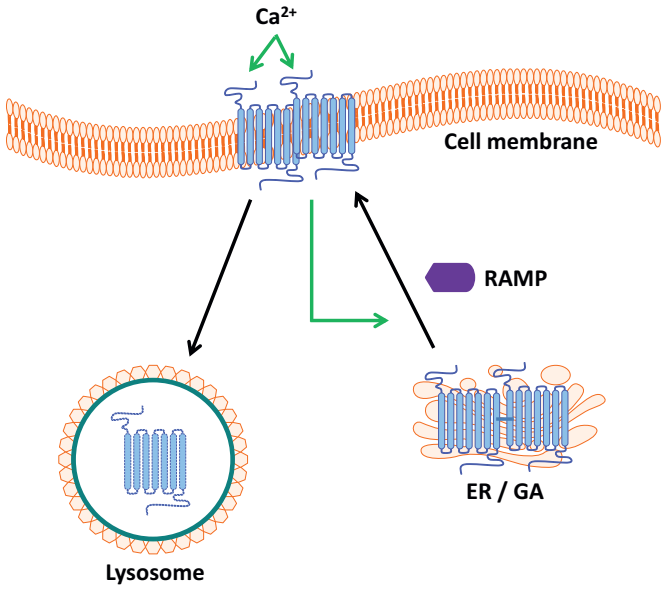

Fig. 2. Intracellular transport of CaSR. CaSR is located at the plasma membrane as dimer. Retrograde transport to lysosoms with subsequent degradation of the receptor is constitutive. Anterograde transport of the receptor from the endoplasmic reticulum (ER) or golgi apparatus (GA) requires receptor activator modifying proteins (RAMPs). Anterograde transport is regulated by agonist stimulation and determines the level of receptor expression at the plasma membrane.

with its seven helices is made up of 250 AA. The exceptionally long cytosolic section (ICD) of CaSR is made up of 217 AA and forms the carboxyl terminus [8]. Fig. 1 summarizes the organisation of CaSR gene and protein.

As a classic G-protein coupled receptor (GPCR), the CaSR belongs to group II of family C of the GPCRs as defined in the current classification [9].

The protein structure of CaSR has numerous post-translational modifications. Binding sites for carbohydrate side chains are first glycosylated in the endoplasmic reticulum (ER) and then in the golgi apparatus (GA). The molecular weight accordingly varies between 130 kDa for the immature form and 150 kDa for the mature form of the receptor. The importance of the complex glycosylation has not yet been fully clarified but there are indications that the sugar residues primarily affect intracellular transport or expression on the cell surface rather than the protein's intrinsic activity or function [10].

CaSR is largely expressed as a dimer on the cell surface. Two monomers aggregate in the ER as a result of hydrophobic interactions and the formation of covalent disulfide bridges [11,12].

Unlike many other GPCRs, CaSR remains in the ER or the GA upon completion of the post-translational modifications and is only mobilised by activation signals from relevant extracellular agonists and then transported to the cell membrane [13]. In this way, an increase in the extracellular Ca^{2+} concentration thus induces rapid anterograde transport of CaSR to the cell surface where the receptor density remains at the new level until the concentration of the agonist changes again (Fig. 2). Desensitization of CaSR can be induced by either β-arrestin or the G-protein coupled receptor kinases [14]. On the other hand, a drop in the extracellular pH and a reduction in the ion concentration also lead, just as for L-phenylalanine, to sensitisation of CaSR by means of allosteric activation [15–18].

Internalisation by endocytosis is constitutive and is not subject to any noteworthy regulation. Most of the internalised receptors are transported to the lysosome where they are degraded with practically no recycling of CaSR taking place [14,19,20]. Its five phosphorylation sites for PKC and its two phosphorlyation sites for PKA, however, mean that there is the possibility of modulating the function and intracellular coupling [5,21].

In a complex and as yet largely unexplored manner, all three isoforms of the receptor activity modifying proteins, or RAMPs, affect the intracellular transport steps, cell-specific membrane expression and ligand specificity of CaSR, however [22,23].

With the identification of CaSR in many cell types and organs that are not involved in the regulation of systemic Ca^{2+} homeostasis, the range of activities carried out by the receptor has grown continuously. Up to now, CaSR activation has been linked to cell proliferation, differentiation, chemotaxis and apoptosis in various cell types [3,24].

This broad spectrum of intracellular effects mediated by CaSR activation is based on the ability of CaSR to couple to different G proteins which can in turn activate or regulate various ligand- and tissue-specific signalling pathways. CaSR can interact with multiple G-proteins, namely $G\alpha_{q/11}$, $G\alpha_{i/0}$, $G\alpha_{12/13}$, and $G\alpha_s$.

CaSR can activate phospholipases C and D (PLC, PLD) when interacting with $G\alpha_{q/11}$. PLC leads to the formation of the second messenger inositol triphosphate (IP_3) and diacylglycerol (DAG), which consequently leads to the release of Ca^{2+} ions from intracellular storage via activation of IP_3 receptors and subsequent activation of PKC isoforms. PLD preferentially hydrolyses the membrane phospholipid phosphatidylcholine to form phosphatidic acid and choline. Downstream of PLC and PLD, $G\alpha_{q/11}$-mediated activation of CaSR leads to induction of extracellular regulated kinase (ERK)1/2 (also known as p42- and p44-MAP Kinase) and the phospholipase A2, which primarily releases arachidonic acid from membrane lipids [25,26].

Interaction of CaSR with $G\alpha_{12/13}$ induces the activation of monomeric Rho GTPases, which can modulate cytoskeletal functions as well as the contraction of smooth muscle cells, using Rho GTPase guanine nucleotide exchange factor (RhoGEF) [27].

$G\alpha_{i/0}$ and $G\alpha_s$ respectively inhibit or activate adenylate cyclase and thus regulate the formation of the second messenger cAMP. $G\alpha_{i/0}$ also induces the opening of K^+ channels and reduces the open probability of Ca^{2+} channels [28,29].

1.2. The role of CaSR in maintaining Ca^{2+} homeostasis

Thanks to its ability to detect free Ca^{2+}, CaSR has a key role in the regulation of Ca^{2+} homeostasis [4]. In the parathyroid gland CaSR is activated by a rise in free plasma Ca^{2+}. This activation subsequently inhibits the release and synthesis of parathormone (PTH) while simultaneously boosting the secretion of calcitonin from C cells in the thyroid gland – hypocalcaemia on the other hand leads to an increase in PTH secretion. If the plasma Ca^{2+} concentration drops to ≤ 1 mmol/L, the maximal rate of PTH secretion is reached whereas Ca^{2+} concentrations ≥ 1.25 mmol/L minimize PTH secretion. In addition, PTH secretion and CaSR expression is also affected by extracellular Mg^{2+} concentration, specifically as long as Ca^{2+} concentration is low, an effect that is of clinical importance in patients receiving Mg^{2+}-containing phosphate binders [30].

The precise secretory mechanism for parathormone has not been fully determined but is in all likelihood regulated by CaSR-dependent activation of $G\alpha_{q/11}$ pathways. Activation of CaSR triggers an increase in cytosolic Ca^{2+} by formation of IP_3, a process that normally induces vesicle fusion with the cell membrane and thus stimulates the release of proteohormones [31]. Uniquely in the primary cells of the parathyroid gland, after Ca^{2+}-induced activation of CaSR, the rate of secretion of PTH drops, a process that is possibly based on IP_3-mediated inhibition of adenylate cyclase [32]. The release of PTH from cells of the parathyroidea is probably mediated by Mg^{2+}.

In the kidneys and bones, both PTH regulates Ca^{2+} balance predominantly by direct effects on its target cells. The regulation of enteral Ca^{2+} resorption in the terminal ileum, however, is controlled primarily by vitamin D_3 (calcitriol) [1]. The synthesis of calcitriol depends on the activity of 1α-hydroxylase, which as a key enzyme in calcitriol biosynthesis is largely regulated by PTH in the kidneys [1]. Therefore, in kidneys and bones CaSR indirectly affects Ca^{2+} homeostasis by regulating PTH secretion from the parathyroidea. Apart from this effect, CaSR is also directly involved in Ca^{2+} homeostasis because CaSR is expressed in the thick ascending limb of the loop of Henle and involved in Ca^{2+} reabsorption and secretion in the kidney by affecting the paracellular pathway permeability [33].

In summary, CaSR can detect even the smallest fluctuations in the plasma Ca^{2+} levels and subsequently initiates adequate synthesis and secretion of the calciotropic hormones PTH, calcitonin and calcitriol. The most important target organs for the Ca^{2+}-regulating hormones are the bones, kidneys and intestines. However, some of the cells that are regulated by calciotropic hormones also express CaSR, meaning that the local Ca^{2+} concentration modulates and influences the endocrine signalling mechanisms in the target cells [34]. As the extracellular Ca^{2+} concentration directly affects the tonus of smooth muscle cells, these effects are of importance for maintenance of a regular blood pressure.

1.3. Agonists of CaSR

The extensive range of functions carried out by CaSR can be attributed not least to the properties of its ECD, which can bind di-, tri- and polyvalent cations in addition to its classical agonists Ca^{2+} and Mg^{2+}. Its physiological endogenous ligands include the polyamines putrescine, spermidine and spermine, L-amino acids, primarily the aromatic amino acids, including L-phenylalanine and L-tryptophan, as well as poly-L-arginine and β-amyloid peptide.

It has been attempted over the last few decades to exert positive effects primarily on the course of psychiatric disorders (depression, seasonal affective disorder, bulimia, attention deficit hyperactivity disorder) by substituting aromatic amino acids [35,36]. The results of animal trials and human studies have not delivered a uniform picture regarding the efficiency. However, there are no concrete data available about effects that can be attributed to interactions with CaSR.

The most important non-physiological agonists include the cations Al^{3+}, Ba^{2+} and Gd^{3+} as well as antibiotics of the aminoglycoside type (e.g. neomycin) [37,38].

1.4. Expression and function in different organs/tissues

Since its initial description, both the expression and the functional relevance of CaSR have been demonstrated in many cells in different organs that are not directly involved in Ca^{2+} regulation:

In the gastrointestinal tract CaSR takes on the role of a 'food sensor': In the parietal and G cells of the stomach it is involved in gastric acid production and gastrin secretion, it influences the exocrine pancreas and regulates fluid retention in the large intestine. Via its expression in the myenteric and submucosal plexus of the enteric nervous system, it also affects intestinal motility [39–44].

In the kidneys, it regulates the release of renin along with the secretion of Ca^{2+} and phosphate, thus modulating blood pressure and fluid balance [33,45–47].

In bones, CaSR participates in the regulation of mineralization and it controls the differentiation, proliferation and activity of osteoblasts [48–50].

In the central and peripheral nervous system, expression of CaSR has been confirmed in neurons, oligodendrocytes and microglial cells. Which tasks it carries out in the olfactory bulb, the cerebellum, the hippocampus and the pituitary gland are largely unknown but the secretion of adrenocorticotropic hormones (ACTH) and PTH-related protein (PTHrP) are directly influenced by CaSR [28,51–55].

Furthermore, CaSR is also expressed in breast tissue, the ovaries, the uterus, testes and the prostate; likewise, its expression has been detected in the tongue, the lens epithelium and the bone marrow. Its function in erythrocytes, monocytes/macrophages and B cells is largely unknown. In the placenta it plays an important role in supplying the foetus with Ca^{2+} [15,56].

In addition to these roles of CaSR in various tissues, CaSR plays an important role in cardiocascular biology, as explained in the next chapter.

2. Ca^{2+} homeostasis in the cardiovascular system

2.1. The role of CaSR in the vascular system

The regulation of the arterial blood pressure requires baroreceptors and chemoreceptors that continuously measure the circulatory parameters and transmit their information to centrally located circulatory centres in the medulla oblongata for processing. After complex switching and under the influence of upstream vegetative centres, the peripheral resistance and organ perfusion are tightly modulated by the activity of the vegetative nervous system. Long-term blood pressure regulation is controlled primarily by the volume balance.

Along with these central control mechanisms, which are mediated by neuronal innervation and hormone secretion, blood vessels are also able to independently control their perfusion using local mechanisms [57].

Interactions between the extracellular Ca^{2+} concentration and the relaxation of arterial blood vessels had been described long before the discovery of CaSR. Four years after the first discovery of CaSRs, Bukoski et al. were able to demonstrate the presence of CaSR in the perivascular nerves of mesenteric arteries and subsequently also in the nerve endings of renal, cerebral and coronary arterial vessels [58]. For the first time, a mechanism was described for Ca^{2+}-induced vasorelaxation: The activation of CaSR induces neuronal release of a vasodilatory substance, which is mostly likely cannabinoid (Fig. 3A). Via the cannabinoid receptor, endothelium-independent hyperpolarisation of vascular smooth muscle cells (VSMC) is induced with subsequent relaxation of the arteries [59].

Weston et al. demonstrated the expression of CaSR in coronary endothelial cells in pigs [60]. Activation by Ca^{2+} or by the direct CaSR agonist calindol leads to opening of the Ca^{2+}-sensitive K^+ channel

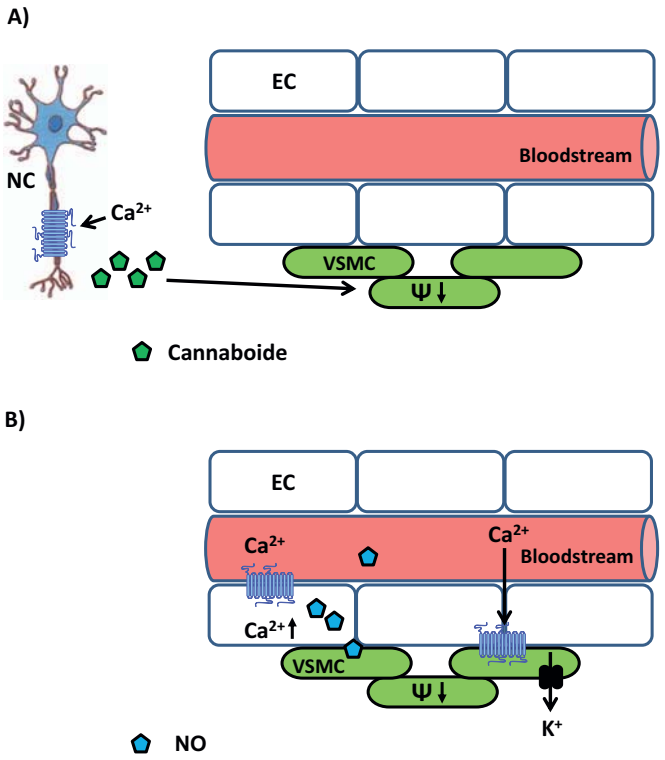

Fig. 3. Vascular effects of CaSR stimulation. A) Sensory nerve-dependent Ca^{2+}-induced relaxation. Activation of CaSR in nerve cells (NC) subsequently leads to the release of cannaboides that subsequently cause hyperpolarisation in smooth muscle cells (VSMC). B) Endothelial-dependent and endothelial-independent vasodilation in vessels. Stimulation of CaSR in endothelial cells (EC) causes an increase in intracellular Ca^{2+} inducing the release of NO. In the same vessels agonists of CaSR can also directly stimulate VSMCs thereby inducing the opening of Ca^{2+}-dependent K^+ channels that hyperpolarize the cells.

(IKCa) which also induces hyperpolarisation of VSMCs. The same group were able demonstrate that the vascular expression of CaSR is significantly reduced in type 2 diabetes using a Zucker Diabetic Fatty (ZDF) rat model [61]. Reduced vasorelaxation by low CaSR expression may play a role in the complications of diabetic vasculopathy.

The expression of CaSR in endothelial cells was confirmed in the human aorta. Here it was shown, that activation of CaSR by spermine led to an increase in the intracellular Ca^{2+} concentration which decreased the vascular tone by increasing nitric oxide (NO) production [62]. Greenberg et al. were able to verify that the two CaSR signalling mechanisms, IKCa-induced hyperpolarisation and endothelial NO release, proceed in parallel in mesenteric arteries and are responsible for vasorelaxation (Fig. 3B) [63].

In contrast to the expression of CaSR in endothelial cells, the expression or functional relevance of CaSR in VSMCs is the subject of considerable controversy. Wonneberger et al. describe vasoconstrictive effects as a response to increasing extracellular Ca^{2+} concentrations that were induced by direct stimulation of CaSR in VSMCs [64]. This finding correspond to the results obtained by Schepelmann et al. who described a significant reduction in vascular tone following cell-specific knock-out of CaSR in smooth muscle cells [65]. Smajilovic et al. were also able to confirm the expression of CaSR in VSMCs in rat aortas and showed that an increase in the extracellular Ca^{2+} concentration induced ERK1/2 phosphorylation and subsequently led to an increase in proliferation with no increase in the IP_3 level [66]. However, Farzaneh-Far et al. were not able to detect CaSR expression in VSMCs but suggest that the Ca^{2+} sensing in VSMCs is carried out by an alternative Ca^{2+}-detecting protein, the matrix Gla protein [67].

Although the precise functional mechanism of CaSR in the various parts of the vascular system and the interaction between the different cell types has not yet been fully clarified, it is generally accepted that CaSR activity participates in the modulation of the blood pressure by direct interaction with vascular cells.

Additional vasoprotective properties are also attributed to the CaSR. Masih-ul Alam et al. showed that a reduced expression of CaSR in human VSMCs in vitro and in vivo is associated with vascular calcification [68]. According to results obtained by Mary et al., an adequate calcitriol level prevents down-regulation of CaSR in the vasculature and thus protects against excessive VSMC mineralization [69]. Molostvov et al. showed that physiological pulsation also maintains stable expression of CaSR in VSMCs [70]. Thus, expression of CaSR in VSMC is required to maintain vascular elasticity.

The CaSR is also involved in this antiproliferating effects of hydrogen sulphide (H_2S) as its activation modifies the vascular production of H_2S [71,72].

2.2. CaSR in pulmonary hypertension

Pulmonary arterial hypertension (PAH) is characterised by increased pressure in the pulmonary arteries that is greater than 25 mmHg at rest and greater than 30 mmHg under load (standard values: 10–15 mmHg). The increased pressure in the pulmonary circulation leads over the long term to a remodelling of the pulmonary vessels that is characterised by proliferation of endothelial cells and smooth muscle cells. Obliteration of the pulmonary circulation as the disease advances leads to progressive loading of the right ventricle with right ventricular failure or right heart failure being the most common causes of death associated with PAH [73].

Unlike the largely protective properties of CaSR in the peripheral vascular system, such as vasorelaxtion, maintenance of elasticity, and anti-proliferative effects, vascular effects of CaSR activation in the pulmonary circulation are considered as non-protective. Recent work shows that CaSR is involved in hypoxic vasoconstriction but also in vascular remodelling during the development and progression of PAH [74–76].

Furthermore, it has previously been demonstrated that calcilytics that exert an antagonist effect at the CaSR can significantly improve the remodelling process of the lung vessels in cases of PAH [77,78].

2.3. CaSR and the myocardium

'Calcium controls cardiac function – by all means!' is the name of an article by Ole M. Sejersted that was published in the Journal of Physiology outlining the role of Ca^{2+} for cardiac function as first and second messenger [79]. The first evidence of CaSR expression in cardiomyocytes that may mediate the effects of Ca^{2+} as a first messenger was provided by Wang et al. in 2003. They detected CaSR mRNA in atrial and ventricular myocytes [80]. These initial studies were confirmed also on the level of protein expression. In our own work, we analyzed the expression of CaSR on the protein level separately for left and right ventricles and for the atria; the left-ventricular myocardium has the highest concentration of CaSR protein while the atria have the lowest concentration [81].

2.3.1. Influence of CaSR on electromechanical coupling

CaSR can influence both the contraction and the relaxation of the cardiomyocytes dependent on $G\alpha_{q/11}$ pathways. The most direct experimental finding showed that activation of CaSR in isolated ventricular cardiomyocytes from adult rats leads to a progressive increase in the Ca^{2+} transients and therefore cell shortening. Via an IP_3-dependent mechanism, Ca^{2+} is released from the SR and this is responsible for an improvement in the cell shortening by increasing the systolic Ca^{2+}. Along with the increased supply of IP_3, DAG is formed in parallel, which is a condition for the activation of PKC. PKC is in turn able to phosphorylate phospholamban at positions 10 and 16. This

induces an increase in the activity of the SERCA, which pumps Ca^{2+} back into its intracellular storage and is reflected in an unchanged diastolic Ca^{2+} concentration and an increased relaxation speed of the cells [81]. As outlined above, CaSR signalling requires translocation of the receptor from the ER/GA to the plasma membrane. This process critically depends on the participation of RAMPs. As shown for cardiomyocytes, depletion of cells with RAMP-1 attenuates the responsiveness of cardiomyocytes to agonists of CaSR [82].

2.3.2. Electrophysiological aspects of CaSR expression in the heart

The action potential (AP) of the individual cardiomyocytes is initiated by opening of fast Na^+ channels ($Na_v1.5$), which enables Na^+ to move into the cell along their chemical and electrostatic gradients (I_{Na}). After a brief delay, voltage-dependent K^+ channels ($K_v4.3$ and $K_v1.4$) open, thus already partly initiating repolarisation via the efflux of K^+ ions ($I_{to.fast}$, $I_{to.slow}$). These ion flows are superimposed by a prolonged, depolarising Ca^{2+} influx through voltage-gated L-type Ca^{2+} channels ($Ca_v1.2$) that protects the membrane against progressive repolarisation and is responsible for the characteristic plateau phase (lasting up of 400 ms) of the action potential in the working myocardium. The repolarisation is accomplished by a massive efflux of K^+ (I_{Kr}, I_{Ks}; I_{K1}) through K^+ channels (hERG, K_vLQT1, and Kir). Recent studies suggest that the activity of CaSR in cardiomyocytes modifies the electromechanical coupling.

Liu et al. were able to show that the expression of the Kir channels can be induced by activation of CaSR. In this way, CaSR can exert membrane-stabilising effects on cardiomyocytes because I_{K1} plays the most important role in the maintenance of a stable resting membrane potential [83].

In line with these findings Tagliavini et al. reported anti-arrhythmic properties of putrescine, a natural ligand of CaSR, which could be attributed to its membrane-stabilising and antioxidant properties [84]. Acute changes in the polyamine metabolism are also observed during a myocardial infarction. Zhao et al. showed that myocardial ischaemia led firstly to an accumulation of putrescine, while in the subsequent reperfusion the level of polyamines dropped. They suggested that this further limits the survival and functionality of the myocytes. However, direct stimulation of CaSR during reperfusion induced a pro-apoptotic phenotype, whereas inhibition of polyamine metabolism protected post-ischaemic hearts against apoptosis [85]. Again, a definitive answer about possible protective or maladaptive effects by CaSR activation during reperfusion cannot be given at the present state.

With respect to cardiac protection it was shown that an exogenous supply of spermine, another strong ligand of CaSR, can be protective and mimicked the effect of ischaemic pre-conditioning [86]. From these results it seemed to be clear that activation of CaSR prior to an extensive index ischaemia is protective, whereas it is less clear whether post-ischaemic activation of CaSR is also protective. There are only very few data available whether in subsequent post-infarction remodelling, CaSR itself is subject to selective regulation. At least in one case CaSR expression in the left ventricle decreased significantly seven days after LAD occlusion but right ventricular expression of CaSR was enhanced by a factor of 4 [87]. A direct correlation between these changes in the expression and functional aspects is still missing.

Because both putrescine and spermine are potent CaSR agonists, by implication the membrane-stabilising properties of CaSR stimulation must be taken into account for all cardioprotective effects that are induced by polyamines. On the downside, however, consideration must be given to the fact that in post-ischaemic hearts CaSR activation induced apoptosis. Therefore, clarification how agonists of CaSR can modify post-ischaemic remodelling and function requires more specific work.

2.4. CaSR and cardiac pathophysiology

2.4.1. Myocardial hypertrophy

Tfelt-Hansen et al. first described using a neonatal cardiomyocyte model that activation of CaSR led to a reduction in the DNA synthesis and concluded from this that there are potential anti-hypertrophic effects [88]. Other studies were subsequently carried out, however, that confirmed predominantly pro-hypertrophic properties for CaSR activation. In a model of angiotensin-II-induced hypertrophy, Wang et al. described an induction of CaSR that is in turn thought to activate calcineurin-dependent hypertrophic signalling pathways [89]. Liu et al. used a model of ISO-induced hypertrophy and used a CaSR inhibitor in vivo and in vitro. They found that suppression of CaSR ameliorates cardiac hypertrophy through inhibition of autophagy [90]. The use of neonatal cardiomyocytes in all three studies is a strong methodological limitation, however, because the hypertrophic signalling mechanisms in this cellular stage can only be transferred to a limited degree to the adult cardiomyocyte. Dyukova et al. found that endothelin-1-induced hypertrophy in adult rat cardiomyocytes causes an upregulation of CaSR. Because CaSR activation contributes to a functional preservation of cardiomyocytes in these experiments, CaSR activation exerts predominantly cardioprotective effects in this model that may contributed to adaptive rather than mal-adaptive hypertrophy [82].

2.4.2. Cardiac apoptosis

The effects of CaSR on apoptosis-associated signalling pathways have been investigated in recent years in different rat models both in vitro and in vivo. In all studies activation of the CaSR in the myocardium leads to the induction of pro-apoptotic signalling pathways or alternatively inhibition of CaSR activation triggers anti-apoptotic protection. In models of heart failure, diabetes and ischaemia/reperfusion (I/R), the intracellular Ca^{2+} concentration increases mediated by CaSR, which contributes to the activation of pro-apoptotic signalling pathways with the involvement of the mitochondria [85,91,92].

During I/R, CaSR activation induces the C-Jun NH_2 terminal protein kinase signalling pathway and the translocation of PKCδ. Both pathways were considered to be responsible for the pro-apoptotic effects [93,94]. Accordingly, cardioprotective effects achieved by ischaemic post-conditioning were explained by down-regulation or desensitization of CaSR. Desensitization of CaSR, however, seems to be dependent on PKCε activation [95].

In the latter studies, the authors used Gd^{3+} as a ligand of CaSR rather than the physiological agonists such as polyamines to analyze the role of CaSR. Furthermore, the detailed analysis of signalling events are again limited by the fact that neonatal cardiomyocytes were used [96]. Collectively, all these data have therefore a strong limitation as they are exclusively based on agonist-dependent effects and believe that the observed effects are specific for the ligand.

2.4.3. Pro-fibrotic effects

Expression of CaSR was also shown in cardiac fibroblasts suggesting a role for CaSR in cardiac fibrosis [97]. Activation of CaSR expressed in neonatal rat fibroblasts led to proliferation, migration and increased secretion of extracellular matrix proteins. All these effects required an increase in intracellular Ca^{2+}. Selective inhibition of CaSR in an in vivo model of ISO-induced hypertrophy reduced the development of cardiac fibrosis [98]. Cultured cardiac fibroblasts loose the expression of CaSRs [96]. Therefore, mechanistic studies about the role of CaSR activation for cardiac fibroblasts are limited to in vivo studies.

2.4.4. Cardioprotection

Due to the important role of Ca^{2+} as a first and second messenger and the myocardial expression of CaSR, it was further investigated whether the CaSR participates in cardiac protection caused by ischaemic pre-conditioning (IPC). During the application of IPC, the hearts were perfused with NPS-2143, a selective CaSR antagonist. IPC-

mediated induction of cardioprotective kinases (ERK1/2, AKT and GSK3) were attenuated under CaSR inhibition; positive changes in the size of the infarction and the post-ischaemic functional recovery were likewise absent [99].

In diabetic rats with dilated cardiomyopathy (DCM) reduced myocardial expression of CaSR was observed and linked to the disease [100]. These data are in assumption with the in vitro studies showing that CaSR are required for normal function of cardiomyocytes at physiological levels of Ca^{2+} [82].

Along with its importance for the blood pressure and vascular remodelling, the renin-angiotensin-aldosterone system (RAAS) also plays a major role in cardiac remodelling processes. Important protective properties are attributed to CaSR in this context because renin secretion from juxtaglomerular cells can be inhibited by activation of CaSR. The mechanism is again most likely based on IP_3-mediated inhibition of adenylate cyclase [47]. Furthermore, Qu et al. observed a reduced CaSR expression in the vascular bed during the progression of arterial hypertension in spontaneously hypertensive rats and linked this finding mechanistically to the activation of local RAAS and stimulation of proliferation of VSMCs [101].

3. CaSR – Therapeutic target for cardiovascular diseases

Because of its broad range of functions and its involvement in numerous physiological and pathophysiological signalling mechanisms, both selective activation and inhibition of CaSR are considered to be promising therapeutic options depending on the function.

Calcimimetics (cinacalcet, etetcalcetide) are allosteric modulators of CaSR that increase the sensitivity of the receptor by changing the conformation of the tertiary structure. On the other hand, calcilytics act as antagonists of CaSR [38,102–104].

The only two CaSR agonists that are currently approved, cinacalcet and etelcalcetide, are indicated for treating secondary hyperparathyroidism in cases of chronic kidney failure or chronic kidney disease on dialysis and hypercalcaemia with parathyroid carcinoma. For etelcalcetide, which was approved by the US Food and Drug Administration in February 2017, nausea, vomiting, diarrhea and muscle spasms are listed as some of the very common adverse reactions. Also common, the medication leads to hypotension, prolongation of the QT interval and worsening of heart failure. Unlike the adverse reactions in the gastrointestinal tract, the effects in the cardiovascular system are classified as ‘serious’ [105,106].

With a structure very similar to that of the calcimimetics, negative allosteric modulators (calcilytics) of CaSR have recently been developed that are predominantly intended for treating autosomal dominant hypocalcaemia and osteoporosis in menopausal women. NPS2143 and its further modification SB423557, ronacaleret and JTT-305/MK-5442 as well as NPSP795 were not superior to the current standard therapy in any of the phase II and phase III studies carried out to date – approval has not yet been issued. In general, however, the clinical data for the calcilytics confirm that they are well tolerated and have a favourable safety profile [107,108].

More recent studies suggest that the indications for calcilytic therapy will be expanded in future to include treatment of bronchial asthma and PAH [78,109].

Many studies that were cited in this review ultimately recommend pharmaceutical activation or inhibition of CaSR to prevent or treat vascular or cardiac diseases respectively. For cell culture studies, these recommendations are entirely valid and reasonable. However, both blood vessels and the myocardium are made up of various cells that are closely bound in a functional cellular network.

In vivo, the choice of therapeutic strategy (calcimimetics vs. calcilytics) is more difficult because organ functions are sometimes contrarily regulated (vasorelaxation by the endothelial derived effects of CaSR activation vs. vasoconstriction by VSMC-derived effects). In addition, CaSR expression in adjacent cells may be protective or mal-adaptive (i.e.: improved Ca^{2+} transients in myocytes vs. proliferation of cardiac fibroblasts).

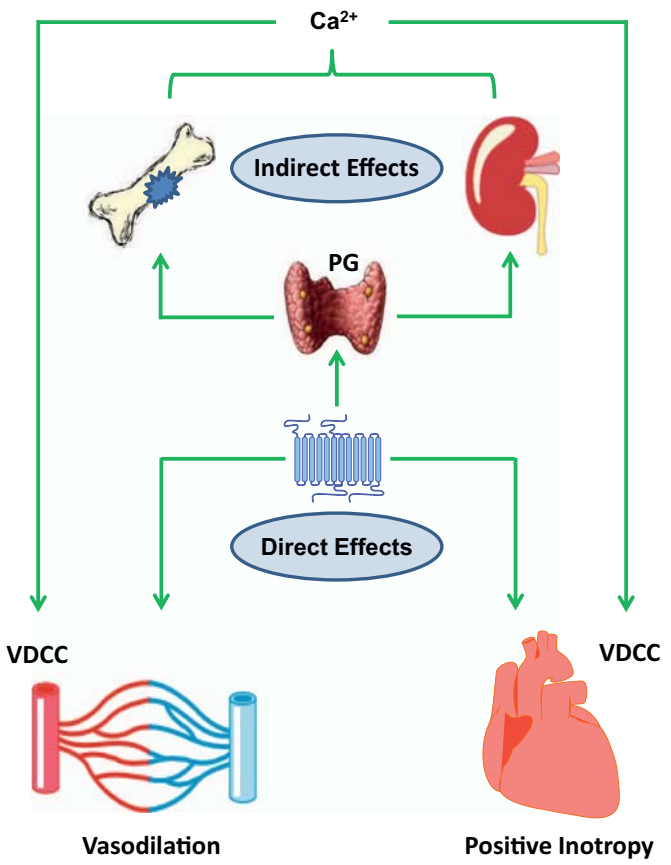

Fig. 4. CaSR activity affects cardiovascular cells via direct stimulation of receptors expressed on vascular cells and cardiomyocytes as well as indirectly via regulation of plasma calcium homeostasis (PG, parathyroid glands) and thereby influencing the activity of voltage-dependent calcium channels (VDCC).

With the exception of PAH, the current body of data still does not allow any concrete conclusions to be drawn about generally valid therapeutic strategies within the cardiovascular system.

4. Conclusion

To maintain the required perfusion of the entire periphery, both the vascular system and cardiac function are continuously adapted to the specific situation. Ca^{2+} ions and Ca^{2+} sensing play a major role in this process throughout the entire cardiovascular system (Fig. 4). All the data obtained in recent years suggest that CaSR plays a significant role in physiological adaptation of adequate tissue perfusion and that dysregulation of CaSR signalling participates in cardiovascular diseases. However, our current understanding does not yet allow to use these findings for effective pharmacotherapy because of highly specific cell type specificity of CaSR regulation and signalling.

References

[1] E.M. Brown, Extracellular Ca^{2+} sensing, regulation of parathyroid cell function, and role of Ca^{2+} and other ions as extracellular (first) messengers, Physiol. Rev. 71 (1991) 371–411.
[2] E.M. Brown, G. Gamba, D. Riccardi, M. Lombardi, R. Butters, O. Kifor, A. Sun, M.A. Hediger, J. Lytton, S.C. Hebert, Cloning and characterization of an extracellular Ca(2+)-sensing receptor from bovine parathyroid, Nature 366 (1993) 575–580.
[3] J. Tfelt-Hansen, E.M. Brown, The calcium-sensing receptor in normal physiology and pathophysiology: a review, Crit. Rev. Clin. Lab. Sci. 42 (2005) 35–70.
[4] S. Smajilovic, J. Tfelt-Hansen, Calcium acts as a first messenger through the calcium-sensing receptor in the cardiovascular system, Cardiovasc. Res. 75 (2007)

457–467.
[5] J.E. Garrett, I.V. Capuano, L.G. Hammerland, B.C. Hung, E.M. Brown, S.C. Hebert, E.F. Nemeth, F. Fuller, Molecular cloning and functional expression of human parathyroid calcium receptor cDNAs, J. Biol. Chem. 270 (1995) 12919–12925.
[6] N. Janicic, E. Soliman, Z. Pausova, M.F. Seldin, M. Riviere, J. Szpirer, C. Szpirer, G.N. Hendy, Mapping of the calcium-sensing receptor gene (CASR) to human chromosome 3q13.3-21 by fluorescence in situ hybridization, and localization to rat chromosome 11 and mouse chromosome 16, Mamm. Genome 6 (1995) 798–801.
[7] G.N. Hendy, V. Guarnieri, L. Canaff, Calcium-sensing receptor and associated diseases, Prog. Mol. Biol. Transl. Sci. 89 (2009) 31–95.
[8] J. Hu, A.M. Spiegel, Naturally occurring mutations of the extracellular Ca^{2+}-sensing receptor: implications for its structure and function, Trends Endocrinol. Metab. 14 (2003) 282–288.
[9] H. Brauner-Osborne, P. Wellendorph, A.A. Jensen, Structure, pharmacology and therapeutic prospects of family C G-protein coupled receptors, Curr. Drug Targets 8 (2007) 169–184.
[10] K. Ray, P. Clapp, P.K. Goldsmith, A.M. Spiegel, Identification of the sites of N-linked glycosylation on the human calcium receptor and assessment of their role in cell surface expression and signal transduction, J. Biol. Chem. 273 (1998) 34558–34567.
[11] M. Bai, S. Trivedi, O. Kifor, S.J. Quinn, E.M. Brown, Intermolecular interactions between dimeric calcium-sensing receptor monomers are important for its normal function, Proc. Natl. Acad. Sci. U. S. A. 96 (1999) 2834–2839.
[12] S. Pidasheva, M. Grant, L. Canaff, O. Ercan, U. Kumar, G.N. Hendy, Calcium-sensing receptor dimerizes in the endoplasmic reticulum: biochemical and biophysical characterization of CASR mutants retained intracellularly, Hum. Mol. Genet. 15 (2006) 2200–2209.
[13] M.P. Grant, A. Stepanchick, A. Cavanaugh, G.E. Breitwieser, Agonist-driven maturation and plasma membrane insertion of calcium-sensing receptors dynamically control signal amplitude, Sci. Signal. 4 (2011) ra78, http://dx.doi.org/10.1126/scisignal.2002208.
[14] M. Pi, R.H. Oakley, D. Gesty-Palmer, R.D. Cruickshank, R.F. Spurney, L.M. Luttrell, L.D. Quarles, Beta-arrestin- and G protein receptor kinase-mediated calcium-sensing receptor desensitization, Mol. Endocrinol. 19 (2005) 1078–1087.
[15] E.M. Brown, R.J. MacLeod, Extracellular calcium sensing and extracellular calcium signaling, Physiol. Rev. 81 (2001) 239–297.
[16] E.F. Nemeth, M.E. Steffey, L.G. Hammerland, B.C. Hung, B.C. van Wagenen, E.G. DelMar, M.F. Balandrin, Calcimimetics with potent and selective activity on the parathyroid calcium receptor, Proc. Natl. Acad. Sci. U. S. A. 95 (1998) 4040–4045.
[17] A.D. Conigrave, S.J. Quinn, E.M. Brown, L-amino acid sensing by the extracellular Ca^{2+}-sensing receptor, Proc. Natl. Acad. Sci. U. S. A. 97 (2000) 4814–4819.
[18] H.J. Lee, H.C. Mun, N.C. Lewis, M.F. Crouch, E.L. Culverston, R.S. Mason, A.D. Conigrave, Allosteric activation of the extracellular Ca^{2+}-sensing receptor by L-amino acids enhances ERK1/2 phosphorylation, Biochem. J. 404 (2007) 141–149.
[19] G.E. Breitwieser, The calcium sensing receptor life cycle: trafficking, cell surface expression, and degradation, Best Pract. Res. Clin. Endocrinol. Metab. 27 (2013) 303–313.
[20] K. Ray, Calcium-sensing receptor: trafficking, endocytosis, recycling, and importance of interacting proteins, Prog. Mol. Biol. Transl. Sci. 132 (2015) 127–150.
[21] J. Bosel, M. John, M. Freichel, E. Blind, Signaling of the human calcium-sensing receptor expressed in HEK293-cells is modulated by protein kinases A and C, Exp. Clin. Endocrinol. Diabetes 111 (2003) 21–26.
[22] T. Bouschet, S. Martin, J.M. Henley, Regulation of calcium sensing receptor trafficking by RAMPs, Adv. Exp. Med. Biol. 744 (2012) 39–48.
[23] T. Bouschet, S. Martin, J.M. Henley, Regulation of calcium-sensing-receptor trafficking and cell-surface expression by GPCRs and RAMPs, Trends Pharmacol. Sci. 29 (2008) 633–639.
[24] D. Riccardi, P.J. Kemp, The calcium-sensing receptor beyond extracellular calcium homeostasis: conception, development, adult physiology, and disease, Annu. Rev. Physiol. 74 (2012) 271–297.
[25] S.C. Brennan, A.D. Conigrave, Regulation of cellular signal transduction pathways by the extracellular calcium-sensing receptor, Curr. Pharm. Biotechnol. 10 (2009) 270–281.
[26] A.L. Magno, B.K. Ward, T. Ratajczak, The calcium-sensing receptor: a molecular perspective, Endocr. Rev. 32 (2011) 3–30.
[27] S. Siehler, Regulation of RhoGEF proteins by G12/13-coupled receptors, Br. J. Pharmacol. 158 (2009) 41–49.
[28] R. Mamillapalli, J. Wysolmerski, The calcium-sensing receptor couples to Galpha (s) and regulates PTHrP and ACTH secretion in pituitary cells, J. Endocrinol. 204 (2010) 287–297.
[29] C. Huang, R.T. Miller, The calcium-sensing receptor and its interacting proteins, J. Cell. Mol. Med. 11 (2007) 923–934.
[30] M.E. Rodríguez-Ortiz, A. Canalejo, C. Herencia, J.M. Martínez-Moreno, A. Peralta-Ramírez, P. Perez-Martinez, J.F. Navarro-González, M. Rodríguez, M. Peter, K. Gundlach, S. Steppan, J. Passlick-Deetjen, J.R. Muñoz-Castañeda, Y. Almaden, Magnesium modulates parathyroid hormone secretion and upregulates parathyroid receptor expression at moderately low calcium concentration, Nephrol. Dial. Transplant. 29 (2014) 282–289.
[31] M. Stenovec, P.P. Gonçalves, R. Zorec, Peptide hormone release monitored from single vesicles in “membrane lawns” of differentiated male pituitary cells: SNAREs and fusion pore widening, Endocrinology 154 (2013) 1235–1246.
[32] C.S. Ritter, S. Pande, I. Krits, E. Slatopolsky, A.J. Brown, Destabilization of parathyroid hormone mRNA by extracellular Ca^{2+} and the calcimimetic R-568 in parathyroid cells: role of cytosolic Ca and requirement for gene transcription, J. Mol. Endocrinol. 40 (2008) 13–21.
[33] P. Houillier, Calcium-sensing in the kidney, Curr. Opin. Nephrol. Hypertens. 22 (2013) 566–571.
[34] O. Egbuna, S. Quinn, L. Kantham, R. Butters, J. Pang, M. Pollak, D. Goltzman, E. Brown, The full-length calcium-sensing receptor dampens the calcemic response to 1alpha,25(OH)2 vitamin D3 in vivo independently of parathyroid hormone, Am. J. Physiol. Ren. Physiol. 297 (2009) 720–728.
[35] D.M. Richard, M.A. Dawes, C.W. Mathias, A. Acheson, N. Hill-Kapturczak, D.M. Dougherty, L-tryptophan: basic metabolic functions, behavioral research and therapeutic indications, Int. J. Tryptophan Res. 23 (2009) 45–60.
[36] S.E. Lakhan, K.F. Vieira, Nutritional therapies for mental disorders, Nutr. J. 7 (2008) 2.
[37] Z. Saidak, M. Brazier, S. Kamel, R. Mentaverri, Agonists and allosteric modulators of the calcium-sensing receptor and their therapeutic applications, Mol. Pharmacol. 76 (2009) 1131–1144.
[38] M. Filopanti, S. Corbetta, A.M. Barbieri, A. Spada, Pharmacology of the calcium sensing receptor, Clin. Cases Miner. Bone Metab. 10 (2013) 162–165.
[39] L. Tang, C.Y. Cheng, X. Sun, A.J. Pedicone, M. Mohamadzadeh, S.X. Cheng, The extracellular calcium-sensing receptor in the intestine: evidence for regulation of colonic absorption, secretion, motility, and immunity, Front. Physiol. 7 (2016) 245, , http://dx.doi.org/10.3389/fphys.2016.00245.
[40] S.X. Cheng, Calcium-sensing receptor: a new target for therapy of diarrhea, World J. Gastroenterol. 22 (2016) 2711–2724.
[41] A.D. Conigrave, E.M. Brown, Taste receptors in the gastrointestinal tract. II. L-amino acid sensing by calcium-sensing receptors: implications for GI physiology, Am. J. Physiol. Gastrointest. Liver Physiol. 291 (2006) 753–761.
[42] J.P. Geibel, S.C. Hebert, The functions and roles of the extracellular Ca^{2+}-sensing receptor along the gastrointestinal tract, Annu. Rev. Physiol. 71 (2009) 205–217.
[43] G.Z. Racz, A. Kittel, D. Riccardi, R.M. Case, A.C. Elliott, G. Varga, Extracellular calcium sensing receptor in human pancreatic cells, Gut 51 (2002) 705–711.
[44] S.X. Cheng, Calcium-sensing receptor inhibits secretagogue-induced electrolyte secretion by intestine via the enteric nervous system, Am. J. Physiol. Gastrointest. Liver Physiol. 303 (2012) 60–70.
[45] D. Riccardi, G. Valenti, Localization and function of the renal calcium-sensing receptor, Nat. Rev. Nephrol. 12 (2016) 414–425.
[46] D. Riccardi, E.M. Brown, Physiology and pathophysiology of the calcium-sensing receptor in the kidney, Am. J. Physiol. Ren. Physiol. 298 (2010) 485–499.
[47] D.K. Atchison, M.C. Ortiz-Capisano, W.H. Beierwaltes, Acute activation of the calcium-sensing receptor inhibits plasma renin activity in vivo, Am. J. Physiol. Regul. Integr. Comp. Physiol. 299 (2010) 1020–1026.
[48] T. Yamaguchi, The calcium-sensing receptor in bone, J. Bone Miner. Metab. 26 (2008) 301–311.
[49] M.M. Dvorak-Ewell, T.H. Chen, N. Liang, C. Garvey, B. Liu, C. Tu, W. Chang, D.D. Bikle, D.M. Shoback, Osteoblast extracellular Ca^{2+}-sensing receptor regulates bone development, mineralization, and turnover, J. Bone Miner. Res. 26 (2011) 2935–2947.
[50] W. Chang, C. Tu, T.H. Chen, D. Bikle, D. Shoback, The extracellular calcium-sensing receptor (CaSR) is a critical modulator of skeletal development, Sci. Signal. 1 (2008) ra1, http://dx.doi.org/10.1126/scisignal.1159945.
[51] D.L. Washburn, J.W. Anderson, A.V. Ferguson, The calcium receptor modulates the hyperpolarization-activated current in subfornical organ neurons, Neuroreport 11 (2000) 3231–3235.
[52] S. Yano, E.M. Brown, N. Chattopadhyay, Calcium-sensing receptor in the brain, Cell Calcium 35 (2004) 257–264.
[53] B. Lu, Q. Zhang, H. Wang, Y. Wang, M. Nakayama, D. Ren, Extracellular calcium controls background current and neuronal excitability via an UNC79-UNC80-NALCN cation channel complex, Neuron 68 (2010) 488–499.
[54] N. Chattopadhyay, A. Espinosa-Jeffrey, J. Tfelt-Hansen, S. Yano, S. Bandyopadhyay, E.M. Brown, J. de Vellis, Calcium receptor expression and function in oligodendrocyte commitment and lineage progression: potential impact on reduced myelin basic protein in CaR-null mice, J. Neurosci. Res. 86 (2008) 2159–2167.
[55] M. Ruat, E. Traiffort, Roles of the calcium sensing receptor in the central nervous system, Best Pract. Res. Clin. Endocrinol. Metab. 27 (2013) 429–442.
[56] T.I. Alfadda, A.M. Saleh, P. Houillier, J.P. Geibel, Calcium-sensing receptor 20 years later, Am. J. Physiol. Cell Physiol. 307 (2014) 221–231.
[57] S. Smajilovic, J. Tfelt-Hansen, Novel role of the calcium-sensing receptor in blood pressure modulation, Hypertension 52 (2008) 994–1000.
[58] R.D. Bukoski, K. Bian, Y. Wang, M. Mupanomunda, Perivascular sensory nerve Ca^{2+} receptor and Ca^{2+}-induced relaxation of isolated arteries, Hypertension 30 (1997) 1431–1439.
[59] N. Ishioka, R.D. Bukoski, A role for N-arachidonylethanolamine (anandamide) as the mediator of sensory nerve-dependent Ca^{2+}-induced relaxation, J. Pharmacol. Exp. Ther. 289 (1999) 245–250.
[60] A.H. Weston, M. Absi, D.T. Ward, J. Ohanian, R.H. Dodd, P. Dauban, C. Petrel, M. Ruat, G. Edwards, Evidence in favor of a calcium-sensing receptor in arterial endothelial cells: studies with calindol and Calhex 231, Circ. Res. 97 (2005) 391–398.
[61] A.H. Weston, M. Absi, E. Harno, A.R. Geraghty, D.T. Ward, M. Ruat, R.H. Dodd, P. Dauban, G. Edwards, The expression and function of Ca^{2+}-sensing receptors in rat mesenteric artery; comparative studies using a model of type II diabetes, Br. J. Pharmacol. 154 (2008) 652–662.
[62] R.C. Ziegelstein, Y. Xiong, C. He, Q. Hu, Expression of a functional extracellular calcium-sensing receptor in human aortic endothelial cells, Biochem. Biophys. Res. Commun. 342 (2006) 153–163.

[63] H.Z. Greenberg, J. Shi, K.S. Jahan, M.C. Martinucci, S.J. Gilbert, W.S. Vanessa Ho, A.P. Albert, Stimulation of calcium-sensing receptors induces endothelium-dependent vasorelaxations via nitric oxide production and activation of IKCa channels, Vasc. Pharmacol. 80 (2016) 75–84.
[64] K. Wonneberger, M.A. Scofield, P. Wangemann, Evidence for a calcium-sensing receptor in the vascular smooth muscle cells of the spiral modiolar artery, J. Membr. Biol. 175 (2000) 203–212.
[65] M. Schepelmann, P.L. Yarova, I. Lopez-Fernandez, T.S. Davies, S.C. Brennan, P.J. Edwards, A. Aggarwal, J. Graça, K. Rietdorf, V. Matchkov, R.A. Fenton, W. Chang, M. Krssak, A. Stewart, K.J. Broadley, D.T. Ward, S.A. Price, D.H. Edwards, P.J. Kemp, D. Riccardi, The vascular Ca^{2+}-sensing receptor regulates blood vessel tone and blood pressure, Am. J. Physiol. Cell Physiol. 310 (2016) 193–204.
[66] S. Smajilovic, J.L. Hansen, T.E. Christoffersen, E. Lewin, S.P. Sheikh, E.F. Terwilliger, E.M. Brown, S. Haunso, J. Tfelt-Hansen, Extracellular calcium sensing in rat aortic vascular smooth muscle cells, Biochem. Biophys. Res. Commun. 348 (2006) 1215–1223.
[67] A. Farzaneh-Far, D. Proudfoot, P.L. Weissberg, C.M. Shanahan, Matrix gla protein is regulated by a mechanism functionally related to the calcium-sensing receptor, Biochem. Biophys. Res. Commun. 277 (2000) 736–740.
[68] M.U. Alam, J.P. Kirton, F.L. Wilkinson, E. Towers, S. Sinha, M. Rouhi, T.N. Vizard, A.P. Sage, D. Martin, D.T. Ward, M.Y. Alexander, D. Riccardi, A.E. Canfield, Calcification is associated with loss of functional calcium-sensing receptor in vascular smooth muscle cells, Cardiovasc. Res. 81 (2009) 260–268.
[69] A. Mary, L. Hénaut, C. Boudot, I. Six, M. Brazier, Z.A. Massy, T.B. Drüeke, S. Kamel, R. Mentaverri, Calcitriol prevents in vitro vascular smooth muscle cell mineralization by regulating calcium-sensing receptor expression, Endocrinology 156 (2015) 1965–1974.
[70] G. Molostvov, T.F. Hiemstra, S. Fletcher, R. Bland, D. Zehnder, Arterial expression of the calcium-sensing receptor is maintained by physiological pulsation and protects against calcification, PLoS One 10 (2015) e0138833, , http://dx.doi.org/10.1371/journal.pone. 0138833.
[71] X. Zhong, Y. Wang, J. Wu, A. Sun, F. Yang, D. Zheng, T. Li, S. Dong, Y. Zhao, G. Yang, C. Xu, D. Sun, F. Lu, W. Zhang, Calcium sensing receptor regulating smooth muscle cells proliferation through initiating cystathionine-gamma-lyase/hydrogen sulfide pathway in diabetic rat, Cell. Physiol. Biochem. 35 (2015) 1582–1598.
[72] Y. Wang, X. Wang, X. Liang, J. Wu, S. Dong, H. Li, M. Jin, D. Sun, W. Zhang, X. Zhong, Inhibition of hydrogen sulfide on the proliferation of vascular smooth muscle cells involved in the modulation of calcium sensing receptor in high homocysteine, Exp. Cell Res. 347 (2016) 184–191.
[73] M.L. Handoko, F.S. de Man, C.P. Allaart, W.J. Paulus, N. Westerhof, A. Vonk-Noordegraaf, Perspectives on novel therapeutic strategies for right heart failure in pulmonary arterial hypertension: lessons from the left heart, Eur. Respir. Rev. 19 (2010) 72–82.
[74] H. Tang, A. Yamamura, H. Yamamura, S. Song, D.R. Fraidenburg, J. Chen, Y. Gu, N.M. Pohl, T. Zhou, L. Jiménez-Pérez, R.J. Ayon, A.A. Desai, D. Goltzman, F. Rischard, Z. Khalpey, S.M. Black, J.G. Garcia, A. Makino, J.X. Yuan, Pathogenic role of calcium-sensing receptors in the development and progression of pulmonary hypertension, Am. J. Physiol. Lung Cell Mol. Physiol. 310 (2016) 846–859.
[75] X. Peng, H.X. Li, H.J. Shao, G.W. Li, J. Sun, Y.H. Xi, H.Z. Li, X.Y. Wang, L.N. Wang, S.Z. Bai, W.H. Zhang, L. Zhang, G.D. Yang, L.Y. Wu, R. Wang, C.Q. Xu, Involvement of calcium-sensing receptors in hypoxia-induced vascular remodeling and pulmonary hypertension by promoting phenotypic modulation of small pulmonary arteries, Mol. Cell. Biochem. 396 (2014) 87–98.
[76] J. Zhang, J. Zhou, L. Cai, Y. Lu, T. Wang, L. Zhu, Q. Hu, Extracellular calcium-sensing receptor is critical in hypoxic pulmonary vasoconstriction, Antioxid. Redox Signal. 17 (2012) 471–484.
[77] A. Yamamura, N. Ohara, K. Tsukamoto, Inhibition of excessive cell proliferation by calcilytics in idiopathic pulmonary arterial hypertension, PLoS One 10 (2015) e0138384, , http://dx.doi.org/10.1371/journal.pone.0138384.
[78] A. Yamamura, S. Yagi, N. Ohara, K. Tsukamoto, Calcilytics enhance sildenafil-induced antiproliferation in idiopathic pulmonary arterial hypertension, Eur. J. Pharmacol. 784 (2016) 15–21.
[79] O.M. Sejersted, Calcium controls cardiac function—by all means!, J. Physiol. 589 (2011) 2919–2920.
[80] R. Wang, C. Xu, W. Zhao, J. Zhang, K. Cao, B. Yang, L. Wu, Calcium and polyamine regulated calcium-sensing receptors in cardiac tissues, Eur. J. Biochem. 270 (2003) 2680–2688.
[81] R. Schreckenberg, E. Dyukova, G. Sitdikova, Y. Abdallah, K.D. Schlüter, Mechanisms by which calcium receptor stimulation modifies electromechanical coupling in isolated ventricular cardiomyocytes, Pflugers Arch. 467 (2015) 379–388.
[82] E. Dyukova, R. Schreckenberg, C. Arens, G. Sitdikova, K.D. Schlüter, The role of calcium-sensing receptors in endothelin-1-dependent effects on adult rat ventricular cardiomyocytes: possible contribution to adaptive myocardial hypertrophy, J. Cell. Physiol. 232 (2017) 2508–2518.
[83] C.H. Liu, H.K. Chang, S.P. Lee, R.C. Shieh, Activation of the Ca^{2+}-sensing receptors increases currents through inward rectifier K^+ channels via activation of phosphatidylinositol 4-kinase, Pflugers Arch. 468 (2016) 1931–1943.
[84] S. Tagliavini, S. Genedani, A. Bertolini, C. Bazzani, Ischemia- and reperfusion-induced arrhythmias are prevented by putrescine, Eur. J. Pharmacol. 194 (1991) 7–10.
[85] C. Mörlein, R. Schreckenberg, K.D. Schlüter, Basal ornithine decarboxylase activity modifies apoptotic and hypertrophic marker expression in post-ischemic hearts, Open Heart Failure J. 3 (2010) 31–36.
[86] Y.J. Zhao, C.Q. Xu, W.H. Zhang, L. Zhang, S.L. Bian, Q. Huang, H.L. Sun, Q.F. Li, Y.Q. Zhang, Y. Tian, R. Wang, B.F. Yang, W.M. Li, Role of polyamines in myocardial ischemia/reperfusion injury and their interactions with nitric oxide, Eur. J. Pharmacol. 562 (2007) 236–246.
[87] E. Dyukova, R. Schreckenberg, G. Sitdikova, K.D. Schlüter, Influence of ischemic pre- and post-conditioning on cardiac expression of calcium-sensing receptor, BioNanoSci. DOI https://doi.org/10.1007/s12668-016-0316-8.
[88] J. Tfelt-Hansen, J.L. Hansen, S. Smajilovic, E.F. Terwilliger, S. Haunso, S.P. Sheikh, Calcium receptor is functionally expressed in rat neonatal ventricular cardiomyocytes, Am. J. Physiol. Heart Circ. Physiol. 290 (2006) 1165–1171.
[89] L.N. Wang, C. Wang, Y. Lin, Y.H. Xi, W.H. Zhang, Y.J. Zhao, H.Z. Li, Y. Tian, Y.J. Lv, B.F. Yang, C.Q. Xu, Involvement of calcium-sensing receptor in cardiac hypertrophy-induced by angiotensinII through calcineurin pathway in cultured neonatal rat cardiomyocytes, Biochem. Biophys. Res. Commun. 369 (2008) 584–589.
[90] L. Liu, C. Wang, Y. Lin, Y. Xi, H. Li, S. Shi, H. Li, W. Zhang, Y. Zhao, Y. Tian, C. Xu, L. Wang, Suppression of calcium-sensing receptor ameliorates cardiac hypertrophy through inhibition of autophagy, Mol. Med. Rep. 14 (2016) 111–120.
[91] F.H. Lu, S.B. Fu, X. Leng, X. Zhang, S. Dong, Y.J. Zhao, H. Ren, H. Li, X. Zhong, C.Q. Xu, W.H. Zhang, Role of the calcium-sensing receptor in cardiomyocyte apoptosis via the sarcoplasmic reticulum and mitochondrial death pathway in cardiac hypertrophy and heart failure, Cell. Physiol. Biochem. 31 (2013) 728–743.
[92] H. Qi, Y. Cao, W. Huang, Y. Liu, Y. Wang, L. Li, L. Liu, Z. Ji, H. Sun, Crucial role of calcium-sensing receptor activation in cardiac injury of diabetic rats, PLoS One 8 (2013) e65147, , http://dx.doi.org/10.1371/journal.pone.0065147.
[93] C.M. Jiang, C.Q. Xu, Y. Mi, H.Z. Li, R. Wang, W.M. Li, Calcium-sensing receptor induced myocardial ischemia/reperfusion injury via the C-Jun NH2-terminal protein kinase pathway, Mol. Cardiol. Acta Cardiol. Sin. 26 (2010) 102–110.
[94] H. Zheng, J. Liu, C. Liu, F. Lu, Y. Zhao, Z. Jin, H. Ren, X. Leng, J. Jia, G. Hu, S. Dong, X. Zhong, H. Li, B. Yang, C. Xu, W. Zhang, Calcium-sensing receptor activating phosphorylation of PKCδ translocation on mitochondria to induce cardiomyocyte apoptosis during ischemia/reperfusion, Mol. Cell. Biochem. 358 (2011) 335–343.
[95] S. Dong, Z. Teng, F.H. Lu, Y.J. Zhao, H. Li, H. Ren, H. Chen, Z.W. Pan, Y.J. Lv, B.F. Yang, Y. Tian, C.Q. Xu, W.H. Zhang, Post-conditioning protects cardiomyocytes from apoptosis via PKC(epsilon)-interacting with calcium-sensing receptors to inhibit endo(sarco)plasmic reticulum-mitochondria crosstalk, Mol. Cell. Biochem. 341 (2010) 195–206.
[96] S. Smajilovic, N. Chattopadhyay, J. Tfelt-Hansen, Calcium-sensing receptor in cardiac physiology, Open Heart Failure J. 3 (2010) 11–15.
[97] G.L. Klein, P. Enkhbaatar, D.L. Traber, L.M. Buja, C.C. Jonkam, B.J. Poindexter, R.J. Bick, Cardiovascular distribution of the calcium sensing receptor before and after burns, Burns 34 (2008) 370–375.
[98] X. Zhang, T. Zhang, J. Wu, X. Yu, D. Zheng, F. Yang, T. Li, L. Wang, Y. Zhao, S. Dong, X. Zhong, S. Fu, C.Q. Xu, F. Lu, W.H. Zhang, Calcium sensing receptor promotes cardiac fibroblast proliferation and extracellular matrix secretion, Cell. Physiol. Biochem. 33 (2014) 557–568.
[99] J. Sun, E. Murphy, Calcium-sensing receptor: a sensor and mediator of ischemic preconditioning in the heart, Am. J. Physiol. Heart Circ. Physiol. 299 (2010) 1309–1317.
[100] S.Z. Bai, J. Sun, H. Wu, N. Zhang, H.X. Li, G.W. Li, H.Z. Li, W. He, W.H. Zhang, Y.J. Zhao, L.N. Wang, Y. Tian, B.F. Yang, G.D. Yang, L.Y. Wu, R. Wang, C.Q. Xu, Decrease in calcium-sensing receptor in the progress of diabetic cardiomyopathy, Diabetes Res. Clin. Pract. 95 (2012) 378–385.
[101] Y.Y. Qu, J. Hui, L.M. Wang, N. Tang, H. Zhong, Y.M. Liu, Z. Li, Q. Feng, F. He, Reduced expression of the extracellular calcium-sensing receptor (CaSR) is associated with activation of the renin-angiotensin system (RAS) to promote vascular remodeling in the pathogenesis of essential hypertension, PLoS One 11 (2016) e0157456, , http://dx.doi.org/10.1371/journal.pone.0157456.
[102] P.E. Harrington, C. Fotsch, Calcium sensing receptor activators: calcimimetics, Curr. Med. Chem. 14 (2007) 3027–3034.
[103] D.T. Ward, D. Riccardi, New concepts in calcium-sensing receptor pharmacology and signaling, Br. J. Pharmacol. 165 (2012) 35–48.
[104] S. Letz, C. Haag, E. Schulze, K. Frank-Raue, F. Raue, B. Hofner, B. Mayr, C. Schöfl, Amino alcohol- (NPS-2143) and quinazolinone-derived calcilytics (ATF936 and AXT914) differentially mitigate excessive signalling of calcium-sensing receptor mutants causing Bartter syndrome Type 5 and autosomal dominant hypocalcemia, PLoS One 9 (2014) e115178, , http://dx.doi.org/10.1371/journal.pone.0115178.
[105] Parsabiv New FDA Drug Approval, CenterWatch, www.centerwatch.com (Retrieved 2017-10-30).
[106] "Parsabiv - Incidence of adverse reactions from controlled clinical studies", www.medicines.org.uk/emc/medicine/32575#UNDESIRABLE_EFFECTS.
[107] F.M. Hannan, V.N. Babinsky, R.V. Thakker, Disorders of the calcium-sensing receptor and partner proteins: insights into the molecular basis of calcium homeostasis, J. Mol. Endocrinol. 57 (2016) 127–142.
[108] M. Filopanti, S. Corbetta, A. Maria Barbieri, A. Spada, Pharmacology of the calcium sensing receptor, Clin. Cases Miner. Bone Metab. 10 (2013) 162–165.
[109] R.B. Penn, Calcilytics for asthma relief - a promiscuous calcium receptor holds promise as a therapeutic target for asthma, Science 348 (2015) 398–399.

Journal of Cellular Physiology

The Role of Calcium-Sensing Receptors in Endothelin-1-Dependent Effects on Adult Rat Ventricular Cardiomyocytes: Possible Contribution to Adaptive Myocardial Hypertrophy

ELENA DYUKOVA,[1,2]* ROLF SCHRECKENBERG,[1] CHRISTOPH ARENS,[1] GUZEL SITDIKOVA,[2] AND KLAUS-DIETER SCHLÜTER[1]

[1]*Physiologisches Institut, Justus-Liebig-Universität Gießen, Giessen, Germany*

[2]*Institute of Fundamental Medicine and Biology, Kazan Federal University, Kazan, Russia*

Nitric oxide (NO)-deficiency as it occurs during endothelial dysfunction activates the endothelin-1 (ET-1) system and increases the expression of receptor activity modifying protein (RAMP)-1 that acts as a chaperon for calcium-sensing receptors (CaR) that have recently been identified to improve cardiac function. Here, we hypothesized that ET-1 increases the cardiac expression of CaR and thereby induces an adaptive type of hypertrophy. Expressions of RAMP-1, endothelin receptors, and CaR were analyzed by RT-PCR in left ventricular tissues of L-NAME-treated rats. Effects of ET-1 on CaR expression and cell function (load free cell shortening) were analyzed in adult rat ventricular cardiomyocytes. siRNA directed against CaR and RAMP-1 was used to investigate a causal relationship. PD142893 and BQ788 were used to dissect the contribution of ET_{B1}, ET_{B2}, and ET_A receptors. Non-specific NO synthase inhibition with L-Nitro arginine methyl ester (L-NAME) caused a cardiac upregulation of ET_B receptors and CaR suggesting a paracrine effect of ET-1 on cardiomyocytes. Indeed, ET-1 induced the expression of CaR in cultured cardiomyocytes. Under these conditions, cardiomyocytes increased cell size (hypertrophy) but maintained normal function. Inhibition of ET_A and ET_{B1} receptors led to ET-1-dependent reduction in cell shortening and attenuated up-regulation of CaR. Down-regulation of RAMP-1 reduced CaR responsiveness. In conclusion, ET-1 causes an adaptive type of hypertrophy by up-regulation of CaR in cardiomyocytes via ET_A and/or ET_{B1} receptors.

J. Cell. Physiol. 232: 2508–2518, 2017.

Cardiomyocytes are very sensitive to changes in intracellular and extracellular calcium. Calcium enters the cell during electro-mechanical coupling via voltage-dependent calcium channels leading to additional release of calcium from intracellular stores, such as the sarcoplamatic reticulum, via ryanodine receptors type 2. This process is known as calcium-induced calcium-release and it results in increase of intracellular calcium concentration by approximately 100–1,000-fold. Furthermore, cardiomyocytes are sensitive to extracellular calcium (Hofer and Brown, 2003). They express calcium-sensing receptors (CaR) that are classical seven transmembrane domain G-proteins coupled receptors (Tfelt-Hansen et al., 2003). Activation of CaR activates IP_3 receptors on the sarcoplasmatic reticulum and thereby they modify calcium transients and contractility (Tfelt-Hansen et al., 2006). We have recently shown that approximately 10% of load-free cell shortening of isolated cardiomyocytes depends on activation of CaR at physiological extracellular calcium concentrations (Schreckenberg et al., 2015a). CaR are not selective for calcium. They respond to positive charged molecules such as polyamines, like putrescine, that can be released by cells. Polyamines are products of the polyamine metabolism that is required for growth and differentiation of cells. An activation of the polyamine metabolism is also part of the hypertrophic reprogramming of cardiomyocytes and it potentially affects cardiac function in hypertrophic tissue (Caldarera et al., 1971; Bartolome et al., 1980; Pegg and Hibasami, 1980).

There is upcoming evidence that activation of CaR participates in post-ischemic recovery of hearts and progression of heart failure (Gan et al., 2012). In contrast, the cardiac role of CaR activation in systemic hypertension remains elusive. CaR require the chaperon activity of receptor activity modifying protein (RAMP)-1 to be regularly exposed to the sarcolemmal membrane (Bouschet et al., 2005). Interestingly, RAMP-1 is up-regulated in cardiomyocytes in vivo under NO-deficiency in a blood pressure independent way (Zhao et al., 2006) giving raise to the hypothesis that CaR signalling is also induced under this condition. As NO-deficiency is a common finding in hypertensive heart disease, it is important to define the precise role of RAMP-1 and CaR under such conditions in order to understand their role in cardiac hypertrophy.

NO-deficiency leads also to an increased release of endothelin-1 (ET-1) from endothelial cells (Thakali et al., 2006;

Conflicts of interest: Authors have nothing to declare.

Contract grant sponsor: von-Behring-Röntgen-Stiftung.

*Correspondence to: Elena Dyukova, Physiologisches Institut, Justus-Liebig-Universität Gießen, Aulweg 129, 35392 Gießen, Germany. E-mail: elena.dyukova@med.uni-giessen.de

Manuscript Received: 10 August 2016
Manuscript Accepted: 20 September 2016

Accepted manuscript online in Wiley Online Library (wileyonlinelibrary.com): 23 September 2016.
DOI: 10.1002/jcp.25612

TABLE 1. List of primers

Gene	Forward	Reverse
Calcium-sensing receptor	AAGTGCCCGGATGACTTCTG	GGTTGGTGGCCTTGACGATA
ET_A receptor	ATTTGGCCCTGCCTAGCAAT	CCCACCATTCCCACGATGAA
ET_B receptor	GCTAGCCATCACTGCGATCT	TGTCTTGGCCACTTCTCGTC
ECE-1	TCTGGCCAACATCACCATCC	TAGACCACGATGGGCTCAGA
RAMP-1	AGCATCCTCTGCCCTTTCATT	GACCACCAGGGCAGTCATG
B2M	GCCGTCGTGCTTGCCATTC	CTGAGGTGGGTGGAACTGAGAC
HPRT	CCAGCGTCGTGATTAGTGAT	CAAGTCTTTCAGTCCTGTCC

Hsu et al., 2008). This is a direct effect of NO-deficiency rather than a cGMP-dependent effect (Brunner et al., 1995). ET-1 is a potent vasoconstrictor but in the myocardium ET-1 targets preferentially cardiomyocytes due to the dense endothelium–myocardium interaction. Therefore, we hypothesized that chronic NO-deficiency triggers an ET-1-dependent effect on cardiac tissue. Furthermore, the study was aimed to identify endothelin receptor subtypes involved in this process. Finally, as NO-deficiency increases the expression of RAMP-1 (Zhao et al., 2006) we analyzed the interaction between ET-1, RAMP-1, and CaR.

Materials and Methods

The investigation conforms the *Guide for the Care and Use of Laboratory Animals* published by the US National Institute of Health

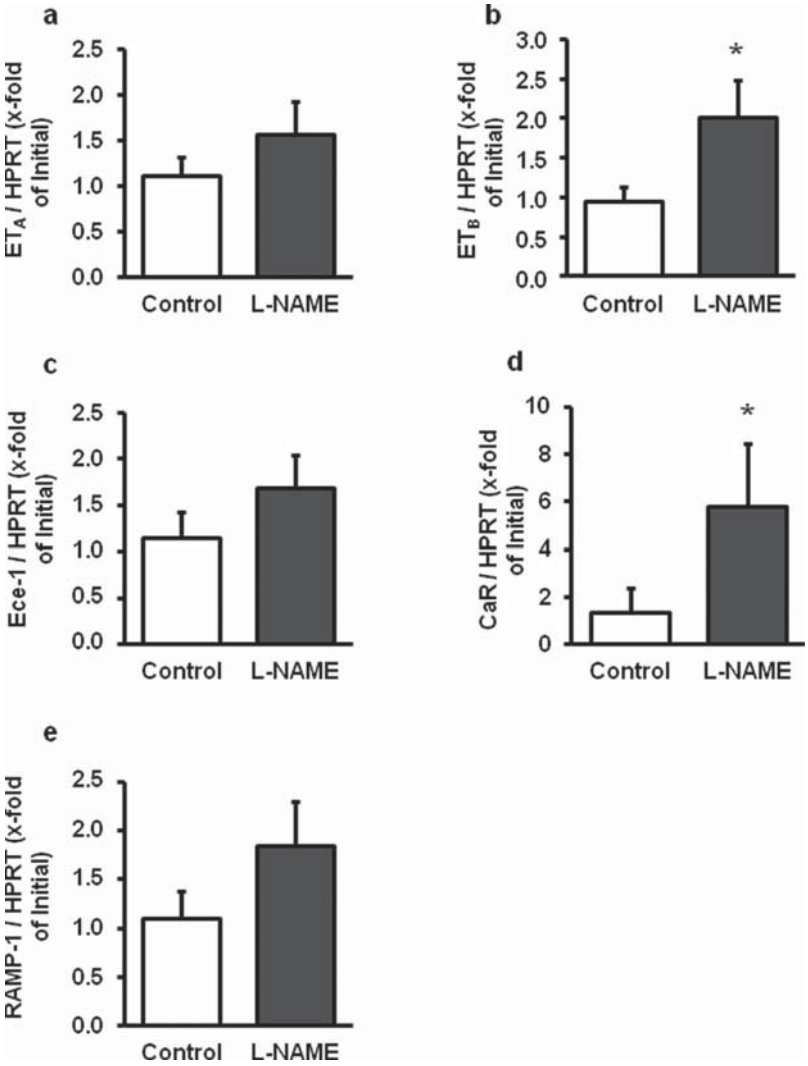

Fig. 1. Left ventricular expression of CaR and endothelin receptors under NO-deficiency in vivo. mRNA levels are shown for (a) Endothelin type A receptors (ET_A); (b) Endothelin type B receptors (ET_B); (c) Endothelin converting enzyme (Ece-1); (d) CaR; and (e) RAMP-1 at 0 (control) and 1 month time points of L-NAME (NO-synthase inhibitor, see Material and Methods section for details) treatment. Data are normalized to HPRT. Data are means ± SD from n = 8 rats, $^*P < 0.05$ versus control ($t = 0$).

(NIH Publication no. 85-23, revised 1996). L-Nitro arginine methyl ester (L-NAME) treatment of rats was approved by the local authorities (V 54–19 c 20-15 (1) GI 20/1–Nr. 58/2005). The permission to scarifice rats is registered as 560_M at the Justus-Liebig University.

Materials

ET-1 was purchased from Merck Chemicals Ltd. (Nottingham, UK). PD142893 and BQ788 were obtained from Sigma-RBI (Taufkirchen, Germany). CaR protein was detected by Anti-Calcium Sensing Receptor antibody produced in rabbit (Sigma–Aldrich Cat# SAB4503369, RRID:AB_10747268, Steinheim, Germany). RAMP1 was detected by RAMP1 antibody produced in rabbit (Santa Cruz Biotechnology Cat# sc-11379, RRID:AB_2269273, Heidelberg, Germany). CaR and RAMP-1 levels were normalized to β-actin (Rabbit Anti-Actin antibody, Sigma–Aldrich Cat# A2668, RRID: AB_258014) or GAPDH (Mouse Anti-GAPDH antibody, Millipore Cat# CB1001, RRID:AB_2107426, Darmstadt, Germany). Secondary antibodies directed against rabbit IgG (Affinity Biologicals Cat# SAR-APHRP, RRID: AB_2619658, Ancaster, Canada) and mouse IgG (Affinity Biologicals Cat# GAM-APHRP, RRID: AB_2619657) were used. Specificity of the antibody directed against CaR was proven previously by down-regulation of CaR with siRNA in cardiomyocytes (Schreckenberg et al., 2015a). CaR agonist putrescine was also purchased from Sigma–Aldrich (Germany). NPS 2143, a CaR antagonist, was purchased from Sigma–Aldrich. The non-selective NO synthase inhibitor L-NAME was provided by Sigma–Aldrich.

Isolation and cultivation of cardiomyocytes

Four months old Wistar rats were used. Ventricular heart muscle cells were isolated from rats as described previously (Schlüter and Schreiber, 2005). Briefly, hearts were excised under deep anesthesia, transferred rapidly to ice-cold saline, and mounted on the cannula of a Langendorff perfusion system. Hearts were perfused in a non-circulating mode with a calcium-free perfusion buffer and then in recirculating mode adding collagenase (Type 2 CLS 2 270 u/mg, Worthington Biochemical Corporation, Lakewood, NJ) with $CaCl_2$ (25 μM) for 25 min. Thereafter, ventricular tissue was minced and incubated for another 5 min in recirculating buffer. The remaining cell solution was filtered through a 200 μm nylon mesh. The filtered material was resuspended in buffer with a stepwise increase in calcium and finally transferred to culture medium (Medium 199, supplemented with creatine, carnitine, taurine, and 2% penicillin–streptomycin, Biochrom Merck Millipore, Darmstadt, Germany). Cells were plated to Petri dishes which were precoated with 4% (v/v) FCS (PAA, BioPharm, Pasching, Austria) and penicillin–streptomycin (Gibco, Thermo Fisher Scientific, Grand Island, NY) in culture medium for 1 h. Thereafter, cell culture medium was refreshed and cells were used for subsequent analysis or futher incubated for 24–48 h at 37°C. In experiments in which cardiomyocytes were compared to non-myocytes from the same heart, non-myocytes were also collected and the remaining cell pellet was frozen into fluid nitrogen until further analysis.

Cell shortening

Cells were stimulated via two AgCl electrodes with biphasic electrical stimuli composed of two equal but opposite rectangular 50–V stimuli of 5 ms duration as described before (Wenzel et al., 2010). Cells were stimulated with 2 Hz frequency. Four signals were registered from each cell. The mean of these four measurements was used to define the contractile responsiveness of a given cell. Cell lengths were measured at a rate of 500 Hz via a line camera. Cells were used in M199 with an extracellular calcium concentration of 1.25 mM. Data are expressed as ΔL/L (%) in which the shortening amplitude (ΔL) is expressed as percent of the diastolic cell length (L). Furthermore, maximal contraction and relaxation velocity was analyzed.

Western blots

Isolated cardiomyocytes were incubated with lysis buffer as described before (Schreckenberg et al., 2015b). Samples (≈100 μg protein dissolved with 10 μl of bromphenol blue) were loaded on a 10% SDS–PAGE and blotted onto membranes. Anti-CaR, C-terminal, antibody produced in rabbit was used to detect the expression of CaR protein (see Materials section). Glyceraldehyde 3-phosphate dehydrogenase (GAPDH) and β-actin were used as loading control. Detection of GAPDH was performed using

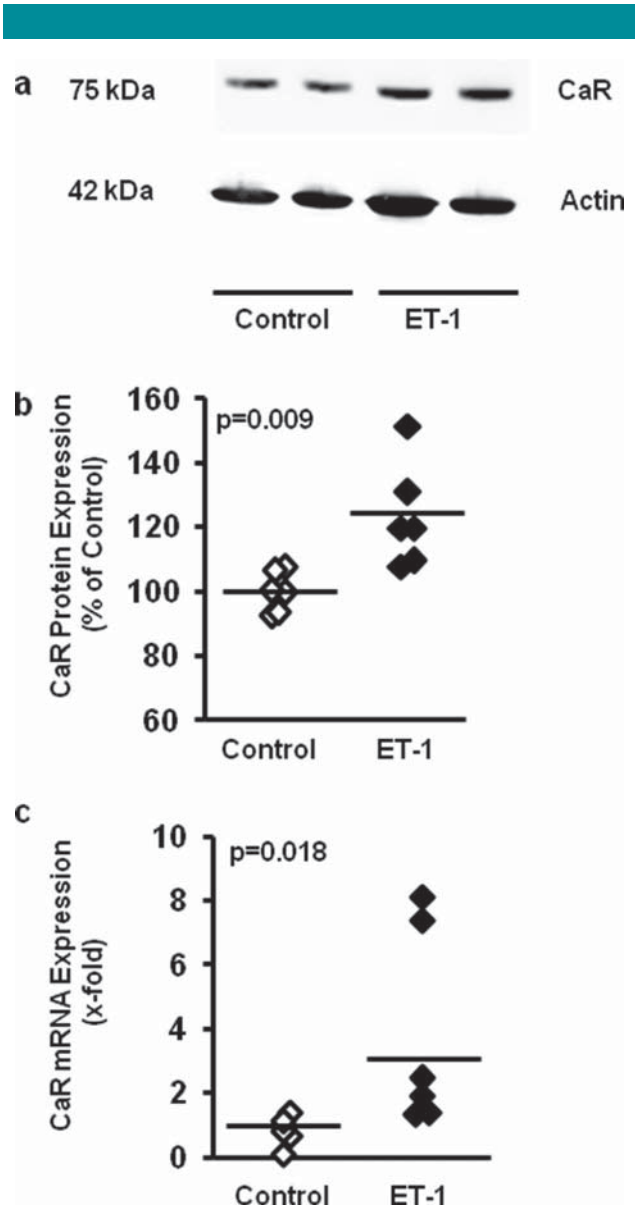

Fig. 2. ET-1 effects on the calcium sensing receptor (CaR) expression in vitro (a) representative western blot of CaR protein after incubation with ET-1 at 100 nM for 24 h; (b) Quantitative analysis of the expression of CaR protein expression; and (c) mRNA level of CaR expression after incubation with ET-1 (100 nM, 6 h). Data are means ± SD from n = 6 preparations, *$P < 0.05$ versus non-stimulated controls.

anti-GAPDH monoclonal antibody produced in mouse (see Materials section). Detection of β-actin was achieved using anti-β-actin antibodies developed in rabbit (see Materials section). To detect levels of RAMP1 protein expression anti-RAMP-1 antibody produced in rabbit (see Materials section) was used. Results are displayed as the ratio of CaR and RAMP-1 to GAPDH and β-actin as loading controls.

qRT-PCR

Isolated cells were collected for PCR analysis using PBS cold solution. RNA isolation and PCR was performed as described before (Anwar et al., 2008). Briefly, total RNA from cardiomyocytes was extracted with Trizol (Invitrogen, Erlangen, Germany) as described by the manufacturer. After conversion of RNA into complementary DNA (cDNA) with reverse transcriptase, PCR was performed. Primers for CaR, endothelin A and B receptors (ET_A, ET_B), endothelin converting enzyme (ECE-1), RAMP-1, hypoxanthine-guanine phosphoribosyltransferase (HPRT), and β-2-microglobulin (B2M) were used (Table 1). All primers are provided by Invitrogen.

L-NAME treatment

The experimental model of L-NAME treatment to investigate the left ventricular expression of CaR and endothelin receptors has been described before in greater detail (Schreckenberg et al., 2015b). The cDNA used to quantify the mRNA expression was depicted from these samples. Please see the previous manuscript for details about treatment, blood pressure control, and RNA isolation from tissues (Schreckenberg et al., 2015b).

Statistics

Data are expressed as raw data points or means ± SD as indicated in the legend to the figures. ANOVA and the Student–Newman–Keuls test for post hoc analysis were used to analyze experiments in which more than one group was compared. In cases in which only two groups were compared, Student's *t*-test or Mann–Whitney test was employed, depending on a normal distribution of samples (Levene test). *P* levels are indicated as expressed in the legend to the figures.

Results

The effect of NO-deficiency on left ventricular expression of CaR and endothelin receptors

Left ventricular mRNA expression of ET_A, ET_B, ECE-1, CaR, and RAMP-1 were analyzed 1 month after the administration of L-NAME to healthy, normotensive Wistar rats. Data were normalized to two different house-keeping genes (hprt, b2m) to minimize the ability that false positive results are obtained by normalization to house-keeping genes. Data normalized to hprt are shown here and data normalized to b2m are given in the supplement. The ET_B expression was transiently up-regulated

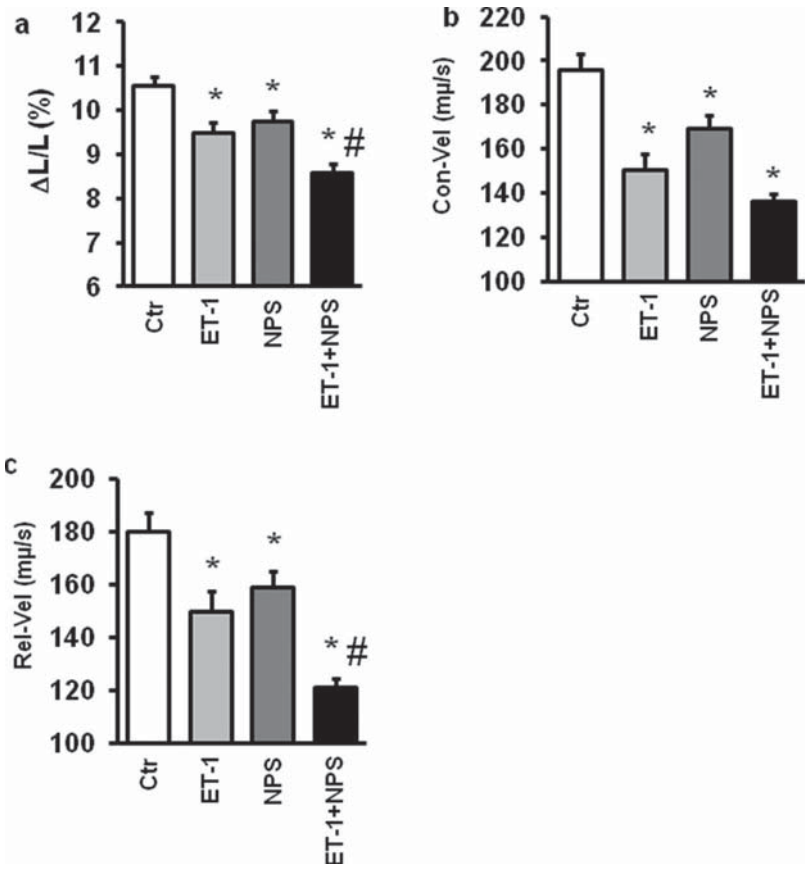

Fig. 3. ET-1 effects on cell shortening with pharmacological inhibition of CaR. (a) Load free cell shortening expressed as shortening amplitude normalized to diastolic cell lengths (dL/L%); (b) contraction velocity of cardiomyocytes; and (c) relaxation velocity of cardiomyocytes. Cells were exposed to ET-1 at 100 nM and/or NPS2390 (NPS) at 10 μM for 24 h. Data are means ± SD from n = 72 cells, *$P < 0.05$ versus non-stimulated controls, #$P < 0.05$ versus ET-1.

after one month L-NAME treatment (Fig. 1b and Suppl. Fig. S1b). Similarly, CaR were up-regulated (Fig. 1d and Suppl. Fig. S1d). The expression of RAMP-1 showed a tendency to increase, but it was not significant (Fig. 1e and Suppl. Fig. S1e). In contrast, the expression of ET_A and ECE-1 did not change (Fig. 1a and c and Suppl. Fig. S1a and c). Collectively, the data suggest slight up-regulation of RAMP-1 in L-NAME treated rats and a co-activation of the local endothelin- and CaR-dependent signaling. It is assumed that up-regulation of CaR may stabilize cardiac function during ET-1-dependent effects on cardiac tissue. As up-regulation of CaR under NO-deficiency might be important for cardiac function, we analyzed CaR expression on the protein level and confirmed increased CaR protein levels (Suppl. Fig. S2). Collectively, these data raise the possibility that ET-1 affects CaR expression and function. This was analyzed in depth in the subsequent in vitro experiments.

The effect of ET-1 on the expression of calcium receptors in adult rat ventricular cardiomyocytes

To investigate whether ET-1 can indeed induce the cardiac expression of CaR, ET-1 was administered to cultures of cardiomyocytes. The protein and mRNA expression of CaR were analyzed 24 h later and 6 h later, respectively. ET-1 caused a significant up-regulation of CaR on the protein level (Fig. 2a and b). Moreover, CaR mRNA (determined after 6 h) was induced (Fig. 2c). Collectively, the data suggest an ET-1-dependent up-regulation of CaR in cardiomyocytes via induction of transcription.

Functional relevance of ET-1 dependent up-regulation of CaR

To investigate the functional significance of the up-regulated CaR in adult ventricular cardiomyocytes, load free cell shortening was monitored. ET-1 caused a small decrease in load free cell shortening, as indicated by lower shortening amplitude (Fig. 3a), lower contraction velocity (Fig. 3b), and lower relaxation velocity (Fig. 3c). NPS2390, used to antagonize the activity of CaR, also caused a significant cardio-depressive effect, confirming our previous findings that CaR activation contributes to basal cell shortening (Schreckenberg et al., 2015a). However, ET-1 in the co-presence of NPS2390 caused a much stronger decreasing effect on load free cell shortening as found for each of the two factors alone (Fig. 3a–c). A similar effect was observed when CaR was silenced by small inhibitory RNA (siRNA). We have recently documented that siRNA directed against CaR significantly reduces receptor protein expression (Schreckenberg et al., 2015a). As shown also before, siRNA

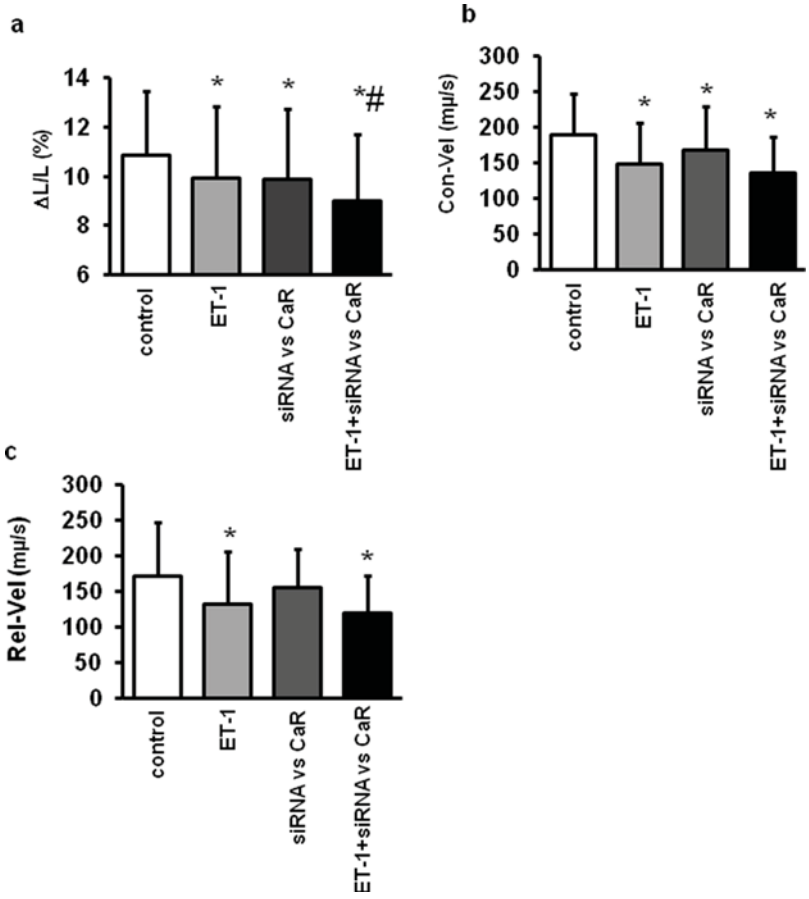

Fig. 4. ET-1 effects on cell shortening with silencing of CaR expression. (a) Load free cell shortening expressed as shortening amplitude normalized to diastolic cell lengths (dL/L%); (b) contraction velocity of cardiomyocytes; and (c) relaxation velocity of cardiomyocytes. Cells were pretreated with siRNA (0.05 μM) directed against CaR (6 h) and subsequently stimulated with ET-1 (100 nM). Data are means ± SD from n = 72 cells, $^*P < 0.05$ versus non-stimulated controls, $\#P < 0.05$ versus ET-1.

directed against CaR slightly decreased load-free cell shortening as well as relaxation and contraction velocities (Fig. 4a–c). The new finding of these experiments is, however, that silencing or pharmacologically inhibition of CaR expression potentiate the effect of ET-1 on cell shortening (Figs. 3a–c and 4a–c). Collectively, the data suggest that ET-1-dependent up-regulation of CaR partly compensates for ET-1-dependent loss of function.

ET-1 acts also as a pro-hypertrophic agonist in cardiomyocytes (Hinrichs et al., 2011). Therefore, we extended our analysis and evaluated the relationship between ET-1, cardiac hypertrophy and CaR function. As expected and previously reported (Hinrichs et al., 2011), ET-1 did not affect cell length (Fig. 5a) but caused an increase in cell thickness (Fig. 5b) and volume (Fig. 5c). Inhibition of CaR by NPS2390 had no effect on cell size. Similarly, NPS2390 did not modify the

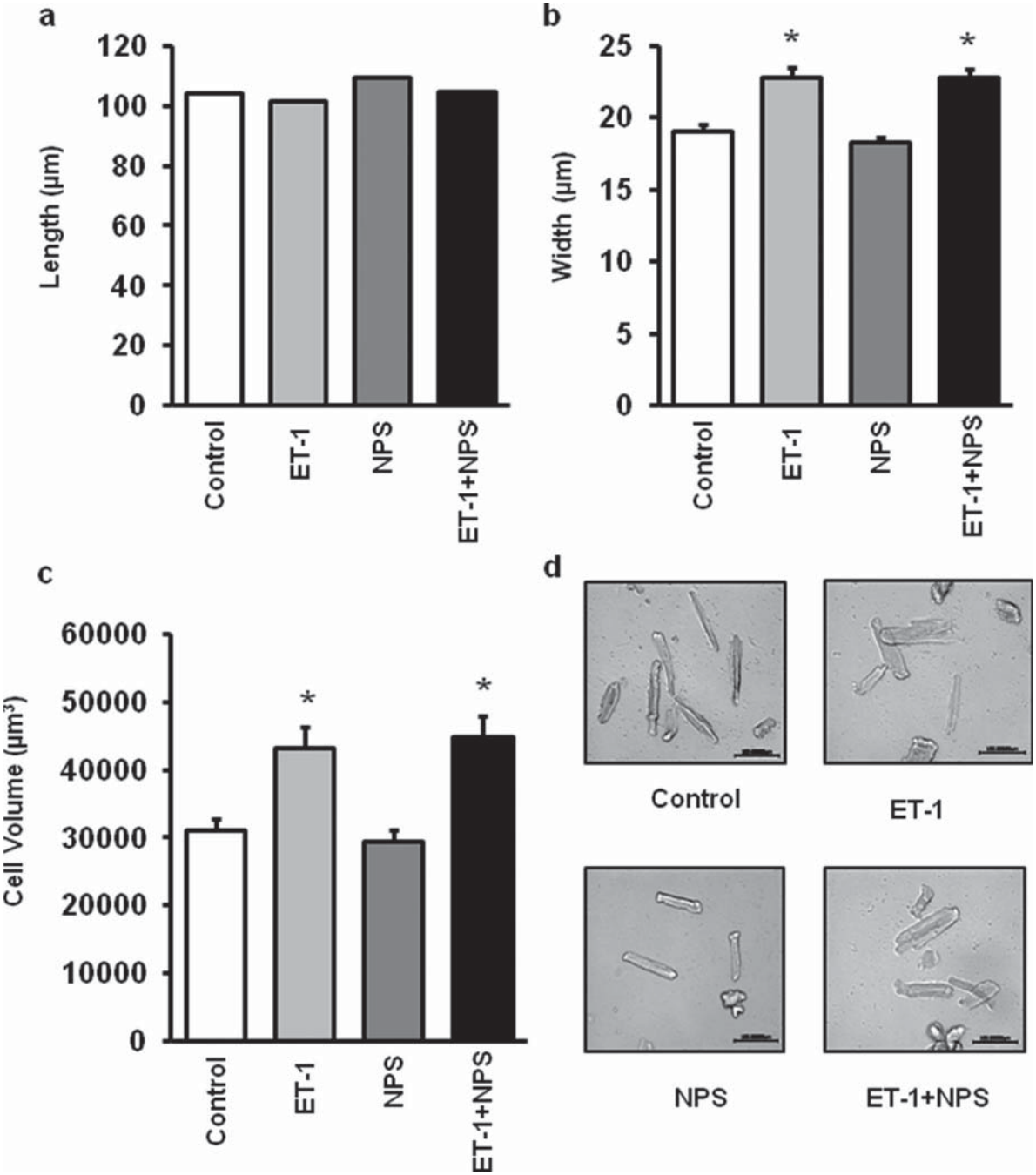

Fig. 5. Effects of ET-1 on hypertrophy with pharmacological inhibition of CaR. (a) Cell length (µm); (b) cell width (µm); (c) cell volume (µm³); and (d) representative pictures. Cells were incubated as described in Figure 3. Data are means ± SD from at least 108 cells per condition, *$P < 0.05$ versus non-stimulated controls; bars on pictures indicate 100 µm.

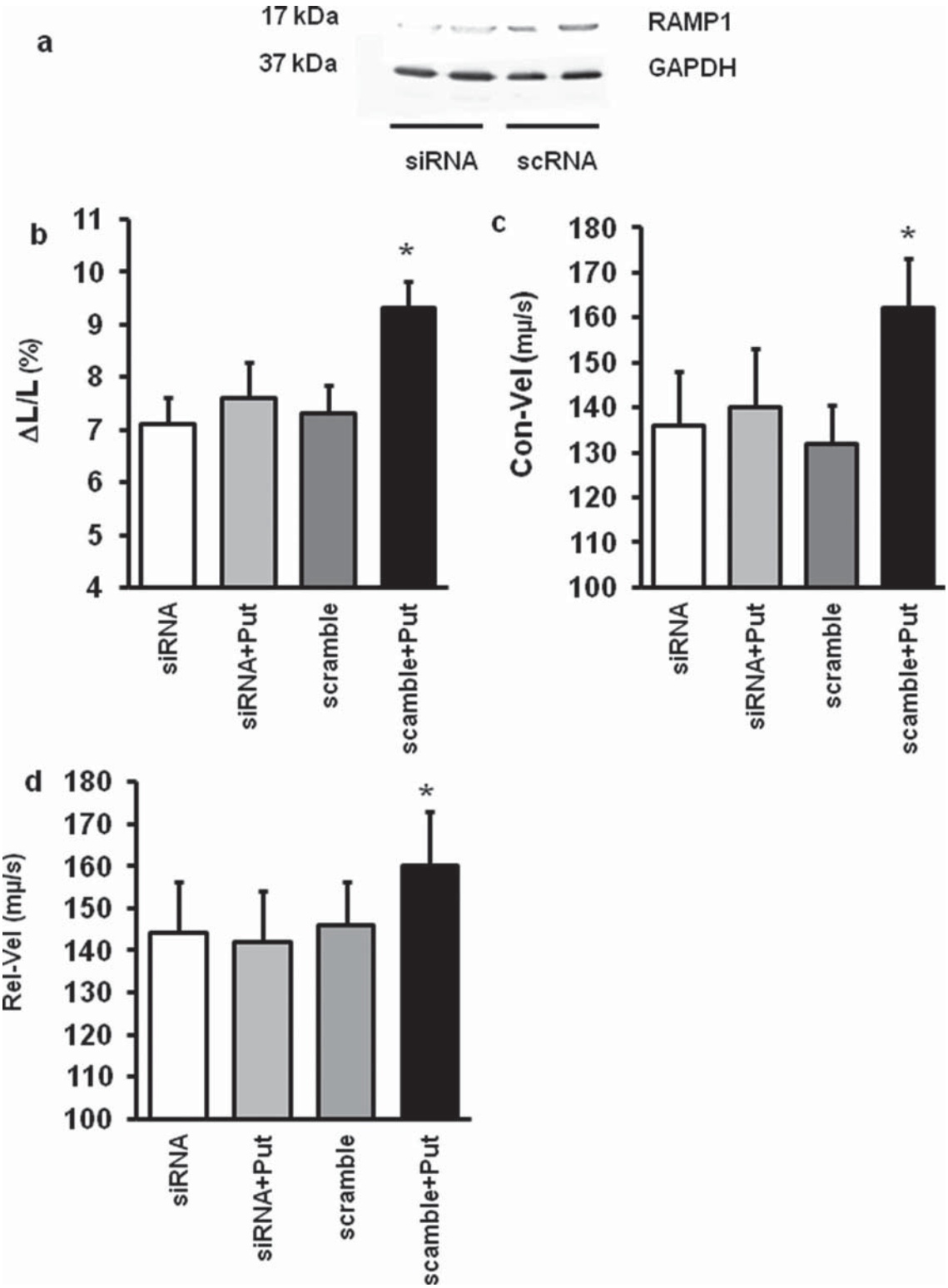

Fig. 6. Influence of silencing of RAMP-1 on CaR function. (a) Representative immunoblot indicating the effect of siRNA directed against RAMP-1 (siRNA) on protein expression of RAMP-1; (b–d) effect of putrescine (CaR agonist, 3 mM) on cardiomyocytes exposed to siRNA directed against RAMP-1 (siRNA), (b) load free cell shortening, (c) contraction velocity of cardiomyocytes, (d) relaxation velocity of cardiomyocytes; Scramble RNA (scRNA) was used in comparison. Data are means ± SD from n = 36 cells, $^{*}P < 0.05$ versus non-stimulated controls.

response of cardiomyocytes to ET-1 with respect to cell sizes. Collectively, the data suggest that ET-1-dependent up-regulation of CaR helps cardiomyocytes to maintain function under conditions of ET-1-induced hypertrophy.

Association between RAMP-1 and CaR

RAMP-1 is required for proper function and sarcolemmal expression of CaR. We hypothesized that RAMP-1 stabilizes CaR function in cardiac tissues. To prove this hypothesis, adult rat ventricular cardiomyocytes were incubated with siRNA directed against RAMP-1 and CaR responsiveness was analyzed thereafter. As expected, siRNA directed against RAMP-1 reduced its cellular expression (Fig. 6a). Administration of siRNA directed against RAMP-1 significantly reduced the expression of RAMP-1 by 37.0 ± 4.8% ($P = 0.022$). Putrescine was used as a specific agonist of CaR to investigate CaR responsiveness. Load-free cell shortening was used as a read-out. Scramble RNA (scRNA) was used as a control (Fig. 6). A CaR agonist, putrescine, did not increase load-free cell shortening in cells pre-treated with siRNA directed against RAMP-1 but it successfully increased load-free cell shortening, relaxation, and contraction velocities in cells exposed to scRNA (Fig. 6b–d). Collectively, the data suggest that RAMP-1 is required for proper function of CaR in cardiomyocytes as reported before. However, cells treated with siRNA directed against RAMP-1 showed no differences in CaR protein expression (Fig. 7a and b). It is supposed that RAMP-1 proteins are required for CaR trafficking to the cell surface but not for the expression itself.

Role of ET_B receptors

The initial analysis of left ventricular expression of endothelin receptors in cardiac tissue from L-NAME treated rats suggested a causative role for ET_B receptors in cardiac adaptation. ET_B receptors are expressed in two different isotypes derived from one gene and both isoforms can only be distinguished by pharmacological approaches (Bras-Silva et al., 2006). The functional importance of the two variants was investigated by pharmacological approaches using PD142893 and BQ788. PD142893 selectively inhibits ET_A and ET_{B1} receptors (Warner et al., 1993). All remaining effects of ET-1 are directed by ET_{B2} receptors. BQ788 selectively inhibits both isoforms of ET_B receptors (Drimal et al., 2003; Sato and Ebina, 2013). All remaining effects of endothelin-1 are therefore triggered by ET_A receptors. PD142893 significantly attenuated the effect of ET-1 on cardiac expression of CaR (Fig. 8a and b). ET-1 in the co-presence of PD142893 caused a similar cardiac decrease in cell shortening as seen before in experiments using either the CaR inhibitor NPS2390 or silencing CaR expression (Fig. 9). This effect of PD142893 on ET-1-dependent decreased load-free cell shortening was attenuated in the co-presence of BQ788 (Suppl. Fig. S3). Finally, we investigated the effect of PD142893 on cardiac hypertrophy. Inhibition of ET_A/ET_{B1} with PD142893 completely attenuated the concentration-dependent increase in cell width and volume (Fig. 10). Collectively, the data suggest that ET-1 exerts a compensatory type of cardiac hypertrophy by stimulation of ET_A and/or ET_{B1} receptors, while it reduces cell function via activation of ET_{B2} receptors. We finally confirmed that ET_A and ET_B mRNA transcripts analyzed in ventricular tissue material derived from non-myocytes and myocytes (Suppl. Fig. S4).

Discussion

The regulation of the expression of CaR in chronic hypertension has not yet been investigated. The in vivo model used here is a pharmacological model of hypertension that

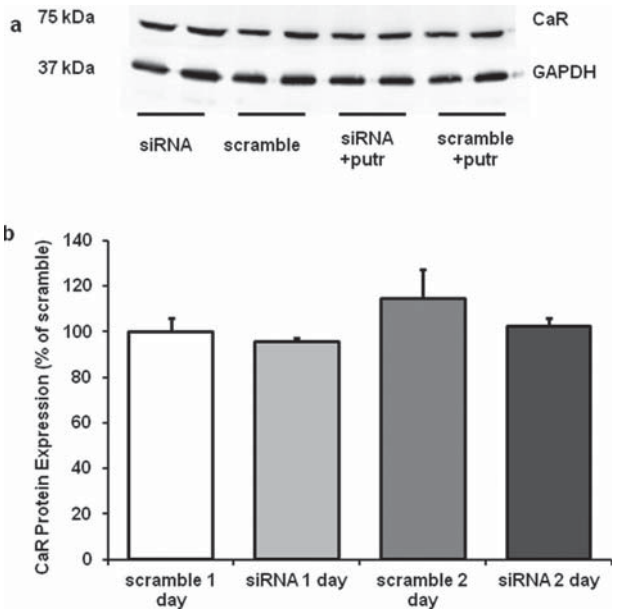

Fig. 7. Influence of RAMP-1 on CaR expression. (a) Representative immunoblot; (b) quantitative analysis of the expression. Cells were incubated as described in Figure 6. Data are means ± SD from n = 4 cultures.

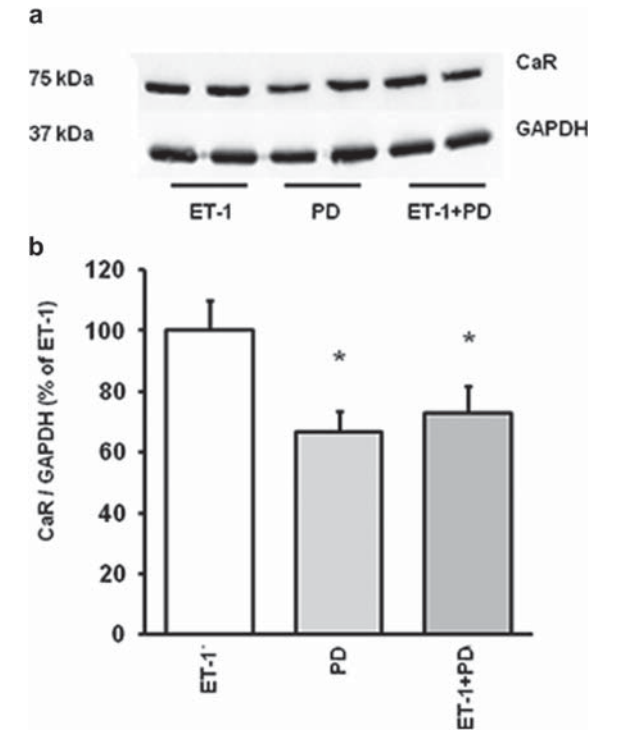

Fig. 8. Role of ET_B receptors subtypes in ET-1-dependent up-regulation of CaR (a) representative immunoblot; (b) quantitative analysis of the expression. Cells were incubated with ET-1 (100 nM) and/or PD142893 (PD, 100 nM) for 24 h. Data are means ± SD from n = 4 cultures and normalized to ET-1 induced values, $^*P < 0.05$ versus ET-1.

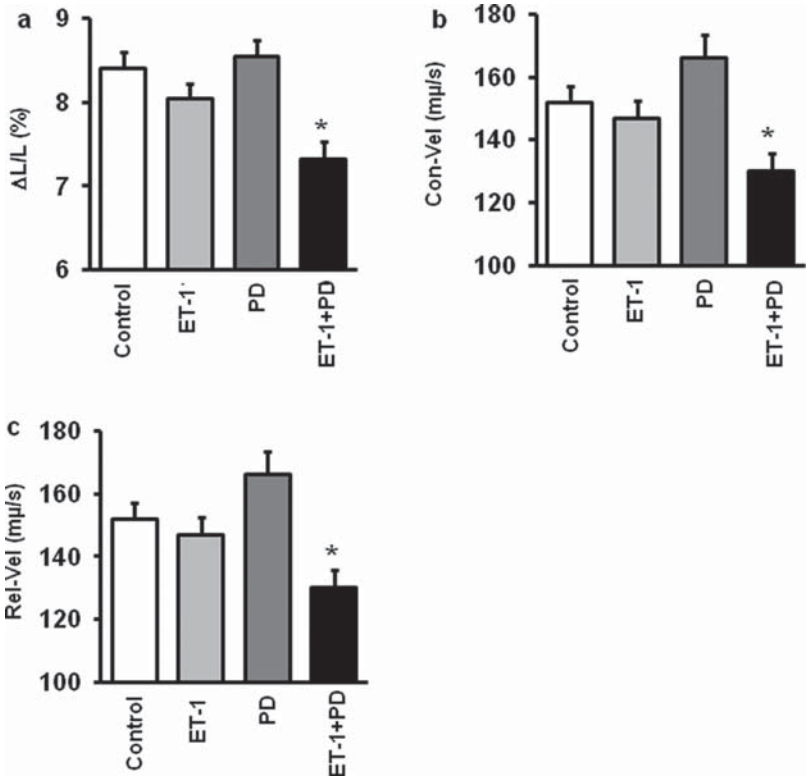

Fig. 9. Role of ET_B receptor subtypes in ET-1 –dependent modification of cell shortening. (a) Load free cell shortening expressed as shortening amplitude normalized to diastolic cell lengths (dL/L%); (b) contraction velocity of cardiomyocytes; and (c) relaxation velocity of cardiomyocytes. Cells were exposed to ET-1 (100 nM) and/or PD142893 (PD, 100 nM) for 24 h. Data are means ± SD from at least 21 cells. *$P < 0.05$ versus non-stimulated controls.

combines NO-deficiency with hypertension. mRNA and protein expression levels of CaR in left ventricles of these rats were up-regulated and associated with acute induction of ET_B expression and slight increase of RAMP-1 expression, a chaperon required for CaR function. Therefore, the initial analysis suggested a coupling between ET-1, RAMP-1, and CaR. The aim of this study was to confirm such a coupling in cardiomyocytes with in depth with in vitro experiments. Up to now, this is the first report indicating that ET-1 increases the expression of CaR in cardiomyocytes and it shows that this allows cardiomyocytes to maintain proper function (adaptive hypertrophy). The second new finding of this study is the linkage of two types of ET-1 receptors in cardiomyocytes to either adaptive hypertrophy (triggered by ET_A and/or ET_{B1}) or mal-adaptive effects (ET_{B2}). Furthermore, this is the first report showing CaR responsiveness in cardiomyocytes requires sufficient RAMP-1 expression in adult terminally differentiated cardiomyocytes.

NO deficiency associated with endothelial dysfunction is a common finding under various cardiovascular stress conditions (Cai and Harrison, 2000). Experimentally, this can be induced by administration of NOS inhibitors to rats. ET-1 is released mainly from endothelial cells. As a strong vasoconstrictor, it antagonizes the activity of NO on smooth muscle cells and, at least in the ventricle, on cardiomyocytes as well. Moreover, NO has an antagonistic effect on ET-1 release as NO reduces ET-1 secretion while NO-deficiency favors ET-1 release (Brunner et al., 1995). Independent of these known effects we found further arguments for an activation of ET-1 pathways in L-NAME treated rats, as the left ventricular expression of ET_B receptors was transiently increased. Interestingly, although ET_A receptors are quantitative dominant in cardiac tissue, the ET_B receptors underlie a regulated expression in cardiomyocytes (Lee et al., 2004). The expression of ET_B receptors was analyzed in left ventricular tissue and in cardiomyocytes in this study. The general picture from previous reports and this study suggest that ET_A and ET_B receptors are constitutively expressed while ET_B receptors are differentially regulated in cardiac tissue. ET_A receptors have previously been linked to induction of cardiac hypertrophy (Penna et al., 2006). Our finding that PD142893 attenuated the hypertrophic effect ET-1 is in line with this assumption as PD142893 inhibits ET_A receptor coupling (Warner et al., 1993). The role of ET_B receptors in cardiac adaptation to pressure overload is less clear. The functional role of the two variants, known as ET_{B1} and ET_{B2}, can be dissected by PD142893 (Warner et al., 1993). In the in vitro experiments described here we found that PD142893 insensitive receptors, ET_{B2}, are responsible for ET-1-dependent cardiac depressive effects but not for the hypertrophic response. This conclusion is also supported by the finding that BQ788 could attenuate this effect of PD142893-insensitive receptors because BQ788 is an ET_B receptor antagonist (Drimal et al., 2003; Sato and Ebina, 2013). The in vitro part of our work links ET_A/ET_{B1} receptors to the up-regulation of CaR, stabilization of cardiac function, and cardiac hypertrophy. Our work cannot distinguish between ET_{B1} and ET_{B2} receptor subtypes because it remains elusive whether BQ788 is specific for ET_{B2} as suggested before, and whether cardiomyocytes display pharmacological responsiveness linked to ET_{B1} and ET_{B2} receptor subtypes. However, it is clear from the current study that ET_{B2} triggers the negative effect on cell shortening (PD142893-non-sensitive

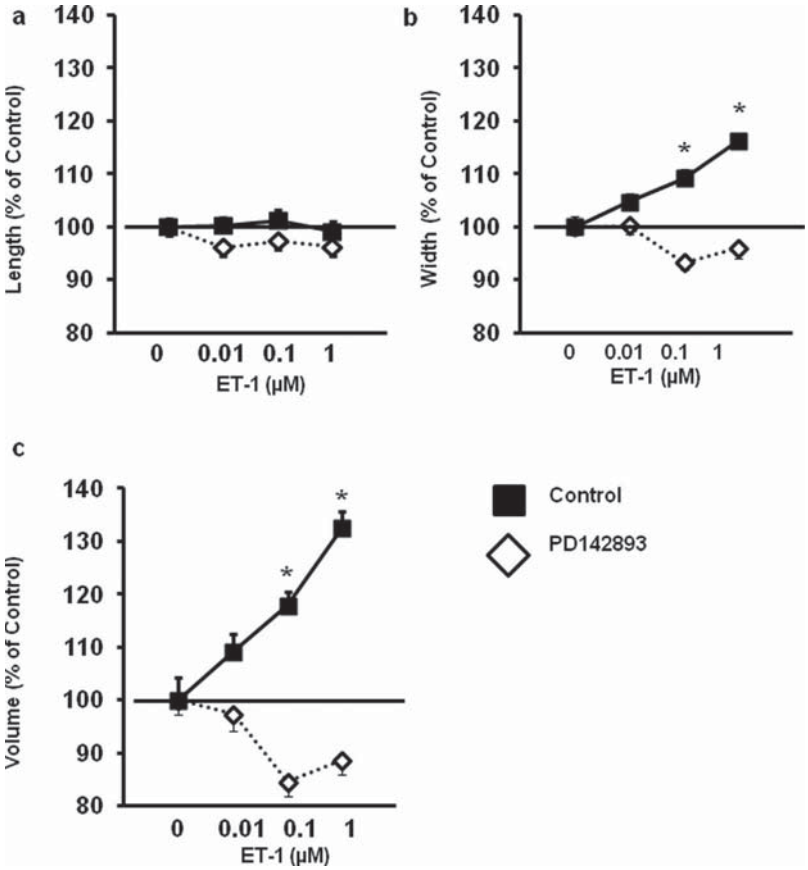

Fig. 10. Role of ET_B receptor subtypes in ET-1-dependent hypertrophy. (a–c) Length, width, and volume of cardiomyocytes cultured with ET-1 (10 nM–1 μM) and PD142893 (PD, 100 nM) as described in Figure 8. Data are means from at least 59 cells, $^*P < 0.05$ versus non-stimulated controls.

receptors). Collectively, these data would argue for the use of ET_{B2}-specific antagonists in chronic hypertension associated with NO-deficiency.

RAMPs are important molecules in cardiac cells although there are only rare data investigating the expression and function of RAMPs in hypertrophy and pressure overload. In this study, the interest was focused on RAMP-1 that plays a dual role in cardiomyocytes. It is required for signaling of calcitonin receptor-like receptor (CLR) where it defines ligand selectivity (McLatchie et al., 1998). Recently, another important role for RAMP-1 was found in cells: RAMP-1 acts as a chaperon directing CaR to the plasma membrane and thereby defining its activity (Bouschet et al., 2005). NO-deficiency increases the expression of RAMP-1 (Zhao et al., 2006). The in vivo part of our study confirmed this finding. The next question was of course whether RAMP-1 is required for the physiological function of CaR in cardiomyocytes. siRNA directed against RAMP-1 successfully down-regulated RAMP-1 protein expression and it attenuated the responsiveness of cardiomyocytes towards CaR by putrescine. However, the protein expression of CaR did not change under these conditions. The data strongly suggest that lack of RAMP-1 attenuates translocation of preformed CaR to the plasma membrane. Putrescine is the natural product of the polyamine metabolism. NO-deficiency directly activates ornithine decarbocxylase (ODC) the rate limiting enzyme of the polyamine metabolism (Zhao et al., 2007). Overall, activation of ODC, subsequent accumulation of putrescine, and increased expression of RAMP-1 and CaR all together suggest that this pathway stabilizes cardiac function under conditions of NO deficiency.

ET-1 and CaR have also been linked to cardiac hypertrophy (Jones et al., 1992; Wang et al., 2008). However, the data from this study do not support a role for CaR in ET-1-dependent cardiac hypertrophy. Although ET-1 clearly increased the expression of CaR in cardiomyocytes and cell sizes in parallel, inhibition of CaR activity by NPS2390 did not attenuate the hypertrophic effect of ET-1. In post-ischemic hearts CaR activation has been also linked to apoptosis (Dong et al., 2010). A possible mechanism is that activation of CaR affects intracellular calcium handling in which CaR activation increases calcium concentration in mitochondria thereby favoring an activation of cell death pathways (Dong et al., 2010). However, the data of the current study support a different role for CaR activation. Previously, we described that CaR in cardiomyocytes contribute to electromechanical coupling. Here, we show that up-regulation of CaR expression by ET-1 stabilizes cardiac function that otherwise would be depressed by co-activation of ET_{B2} receptors. Endothelin receptor antagonists have been used in antihypertensive treatments but they failed in clinical trials due to liver toxicity (Hoeper, 2009).

In conclusion, this study is the first report about an ET-1-dependent regulation of CaR in cardiomyocytes and may

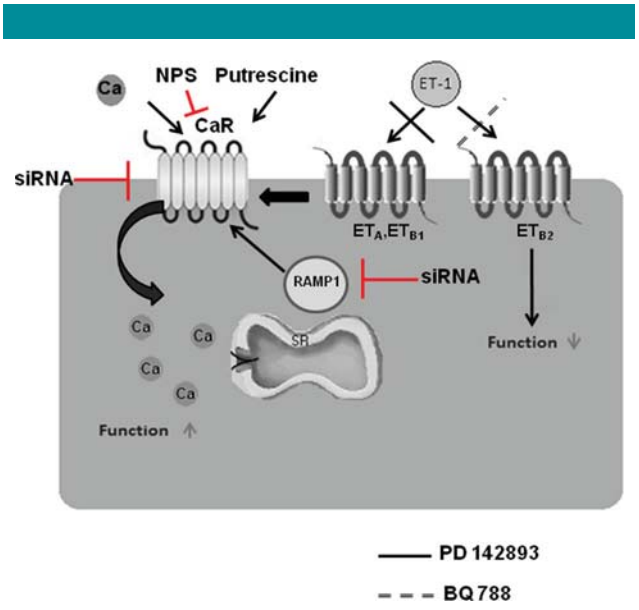

Fig. 11. Schematic summary of the data obtained in this study. ET-1 acts on different populations of endothelin receptors (ET_A, ET_{B1}) and ET_{B2}. Although selective ET_{B2} receptor activation (ET-1 in presence of PD142893) induces a loss of cell function (reduced load-free cell shortening), activation of ET_A and/or ET_{B1} receptors up-regulates CaR that stabilizes cell function. Functional coupling of CaR requires RAMP-1. Participation of CaR in cell shortening was analyzed by administration of CaR antagonists (NPS), agonists (putrescine), or silencing of CaR (siRNA).

describe adaptation to chronic pressure overload. A schematic overview about the conclusion of this report is given in Figure 11.

Acknowledgments

The study was supported by a grant from the von-Behring-Röntgen-Stiftung given to E. Dyukova. The study is part of the thesis submitted by E. Dyukova and C. Arens.

Literature Cited

Anwar A, Schlüter KD, Heger J, Piper HM, Euler G. 2008. Enhanced SERCA2A expression improves contractile performance of ventricular cardiomyocytes of rat under adrenergic stimulation. Eur J Physiol 457:485–491.

Bartolome JV, Guguenard J, Slotkin TA. 1980. Role of ornithine decarboxylase in cardiac growth and hypertrophy. Science 210:793–794.

Bouschet T, Martin S, Henley JM. 2005. Receptor-activity-modifying proteins are required for forward trafficking of the calcium-sensing receptor to the plasma membrane. J Cell Sci 118:4709–4720.

Bras-Silva C, Fontes-Sousa AP, Moura C, Areias JC, Leite-Moreira AF. 2006. Impaired response to ET(B) receptor stimulation in heart failure: Functional evidence of endocardial endothelial dysfunction? Exp Biol Med (Maywood) 231:893–898.

Brunner F, Stessel H, Kukovetz WR. 1995. Novel guanylyl cyclase inhibitor, ODQ reveals role of nitric oxide, but not of cyclic GMP in endothelin-1 secretion. FEBS Lett 376:262–266.

Cai H, Harrison DG. 2000. Endothelial dysfunction in cardiovascular diseases: The role of oxidant stress. Circ Res 87:840–844.

Caldarera CM, Casti A, Rossoni C, Visioli O. 1971. Polyamines and noradrenaline following myocardialhypertrophy. J Mol Cell Cardiol 3:121–126.

Dong S, Teng Z, Lu FH, Zhao YJ, Li H, Ren H, Chen H, Pan ZW, Lv YJ, Yang BF, Tian Y, Xu CQ, Zhang WH. 2010. Post-conditioning protects cardiomyocytes from apoptosis via PKC(epsilon)-interacting with calcium-sensing receptors to inhibit endo(sarco)plasmatic reticulum-mitochondria crosstalk. Mol Cell Biochem 341:195–206.

Drimal J, Knezl V, Drimal J, Jr., Drímal D, Bauerova K, Kettmann V, Doherty AM, Stefek M. 2003. Cardiac effects of endothelin-1 (ET-1) and related C-terminal peptide fragment: Increased inotropy or contribution to heart failure? Physiol Res 52:701–708.

Gan R, Hu G, Zhao Y, Li H, Jin Z, Ren H, Dong S, Zhong X, Li H, Yang B, Xu C, Lu F, Zhang W. 2012. Post-conditioning protecting rat cardiomyocytes from apoptosis via attenuated calcium-sensing receptor-induced endo(sarco)plasmic reticulum stress. Mol Cell Biochem 361:123–134.

Hinrichs S, Heger J, Schreckenberg R, Wenzel S, Euler G, Arens C, Bader M, Rosenkranz S, Caglayan E, Schlüter KD. 2011. Controlling cardiomyocyte length: Role of renin and PPAR-gamma. Cardiovasc Res 89:344–352.

Hoeper MM. 2009. Liver toxicity: The Achilles' heel of endothelin receptor antagonist therapy? Eur Respir J 34:529–530.

Hofer AM, Brown EM. 2003. Extracellular calcium sensing and signalling. Nat Rev Mol Cell Biol 4:530–538.

Hsu YH, Hsu BG, Chen HI. 2008. Malignant alterations following early blockade of nitric oxide synthase in hypertensive rats. Chin J Physiol 50:283–293.

Jones LG, Rozich JD, Tsutsui H, Cooper G, 4th. 1992. Endothelin stimulates multiple responses is isolated adult ventricular cardiac myocytes. Am J Physiol 263:H1447–H1454.

Lee GR, Bell D, Kelso EJ, Argent CC, McDermott BJ. 2004. Evidence for altered ETB receptor characteristics during development and progression of ventricular cardiomyocyte hypertrophy. Am J Physiol Heart Circ Physiol 287:H425–H432.

McLatchie LM, Fraser NJ, Main MJ, Wise A, Brown J, Thompson N, Solari R, Lee MG, Foord SM. 1998. RAMPs regulate the transport and ligand specificity of the calcitonin-receptor-like receptor. Nature 393:333–339.

Pegg AE, Hibasami H. 1980. Polyamine metabolism during cardiac hypertrophy. Am J Physiol 239:E372–E378.

Penna C, Rastaldo R, Mancardi D, Cappello S, Pagliaro P, Westerhof N, Losano G. 2006. Effect of endothelins on the cardiovascular system. J Cardiovasc Med (Hagerstown) 7:645–652.

Sato A, Ebina K. 2013. Endothelin-3 at low concentrations attenuates inflammatory responses via the endothelin B2 receptor. Inflamm Res 62:417–424.

Schreckenberg R, Dyukova E, Sitdikova G, Abdallah Y, Schlüter KD. 2015a. Mechanisms by which calcium receptor stimulation modifies electromechanical coupling in isolated ventricular cardiomyocytes. Pflugers Arch 467:379–388.

Schreckenberg R, Rebelo M, Deten A, Weber M, Rohrbach S, Pipicz M, Csonka C, Ferdinandy P, Schulz R, Schlüter KD. 2015b. Specific mechanisms underlying right heart failure: The missing upregulation of superoxide dismutase-2 and its decisive role in antioxidative defense. Antioxid Redox Signal 23:1220–1232.

Schlüter KD, Schreiber D. 2005. Adult ventricular cardiomyocytes: Isolation and culture. Methods Mol Biol 290:305–314.

Thakali KM, Lau Y, Fink GD, Galligan JJ, Chen AF, Watts SW. 2006. Mechanisms of hypertension induced by nitric oxide (NO) deficiency: Focus on venous function. J Cardiovasc Pharmacol 47:742–750.

Tfelt-Hansen J, Hansen JL, Smajilovic S, Terwilliger EF, Haunso S, Sheikh SP. 2006. Calcium receptor is functionally expressed in rat neonatal ventricular cardiomyocytes. Am J Physiol Heart Circ Physiol 290:H1165–H1171.

Tfelt-Hansen J, Schwarz P, Brown EM, Chattopadhyay N. 2003. The calcium-sensing receptor in human disease. Front Biosci 8:s377–s390.

Wang LN, Wang C, Lin Y, Xi YH, Zhang WH, Zhao YJ, Li HZ, Tian Y, Lv YJ, Yang BF, Xu CQ. 2008. Involvement of calcium-sensing receptor in cardiac hypertrophy-induced by angiotensin II through calcineurin pathway in cultured neonatal rat cardiomyocytes. Biochem Biophys Res Commun 369:584–589.

Warner TD, Allcock DH, Corder R, Vane JR. 1993. Use of the endothelin antagonists BQ-123 and PD142893 to reveal three different endothelin receptors mediating smooth muscle contraction and the release of EDRF. Br J Pharmacol 117:777–782.

Wenzel S, Tastan I, Abdallah Y, Schreckenberg R, Schlüter KD. 2010. Aldosterone improves contractile function of adult rat ventricular cardiomyocytes in a non-acute way: Potential relationship to the calcium paradox of aldosteronism. Basic Res Cardiol 105:247–256.

Zhao Y, Bell D, Smith LR, Zhao L, Devine AB, McHenry EM, Nicholls DP, McDermott BJ. 2006. Differential expression of components of the cardiomyocytes adrenomedullin/intermedin receptor system following blood pressure reduction in nitric oxide-deficient hypertension. J Pharmacol Exp Ther 316:1269–1281.

Zhao YJ, Xu CQ, Zhang WH, Zhang L, Bian SL, Huang Q, Sun HL, Li QF, Zhang YQ, Tian Y, Wang R, Yang BF, Li WM. 2007. Role of polyamines in myocardial ischemia/reperfusion injury and their interactions with nitric oxide. Eur J Pharmacol 562:236–246.

Supporting Information

Additional supporting information may be found in the online version of this article at the publisher's web-site.

BioNanoSci. (2017) 7:112–114
DOI 10.1007/s12668-016-0316-8

Influence of Ischemic Pre- and Post-Conditioning on Cardiac Expression of Calcium-Sensing Receptor

Elena Dyukova[1] · **Rolf Schreckenberg**[1] · **Guzel Sitdikova**[2] · **Klaus-Dieter Schlüter**[1]

Published online: 11 October 2016

Abstract Ischemic heart disease is a common cause of patients' death worldwide. Recently, cardiac pre- and post-conditioning (IPC, IPoC) were indentified to reduce infarct size. Nevertheless, not only infarct size but also post-infarct remodelling is critical for the long-term enhancing effect. Calcium-sensing receptors (CaSRs) signalling was shown to be involved in IPC and IPoC in the heart. This study aims to clarify CaSRs expression after ischemia-reperfusion injury (I/R), IPC and IPoC. Experiments were performed on adult Wistar rats with left anterior descending coronary artery (LAD) occlusion. Troponin I (TnI) levels were measured in plasma of all animals to quantify the infarct size. Sham-operated animals, rats with I/R, IPC, and IPoC were compared. Left and right ventricular tissue samples from these groups were collected for qRT-PCR analysis. CaSR expression was enhanced in rats with I/R and IPC. Its increase after IPoC was not pronounced. In contrast, left ventricles (LV) showed decreased CaSR expression in rat hearts after I/R, IPC, and IPoC. Data suggest differences in CaSR regulation between LV and RV. Enhanced CaSR expression in RV was observed in tissue with small infarct size.

Keywords Calcium-sensing receptor · Ischemia-reperfusion injury · Pre-conditioning · Post-conditioning

1 Introduction

Myocardial ischemia-reperfusion injury (I/R) is a serious life-threatening event worldwide. Blood-flow limitations occurring during ischemia are not able to cover myocardial tissue requirements in oxygen resulting in cellular damage in the heart. Moreover, reperfusion of the heart after ischemic events also causes the huge disruptions in cardiac tissue [1]. Recently, ischemic pre-conditioning (IPC) and post-conditioning (IPoC) were described to reduce infarct size [2, 3]. Cardiac post-conditioning is also considered as possible clinical therapy [3]. However, not only reduction of infarct size is responsible for the long-term improvement, but also post-infarct remodelling is crucial for the future enhancement. Signalling cascades activated after post-infarct remodelling are of high interest. Recently, calcium-sensing receptor (CaSR) signalling has been identified to trigger changes in post-ischemic receptor coupling [4]. CaSRs are G-protein coupled receptors (GPCRs) and expressed throughout the cardiovascular system [5–7]. Its involvement in cardiomyocytes contractility and apoptosis was demonstrated [6, 8]. Endogenous activation of CaSRs was reported to be involved in IPC [4] but its activation during IPoC seems to be damaging [9]. Thus, the aim of our study was to investigate the expression of CaSRs in ischemic hearts after IPC and IPoC.

2 Material and Methods

The investigation conforms with the *Guide for the Care and Use of Laboratory Animals* published by the US National Institute of Health (NIH Publication no. 85–23, revised 1996).

Rats with left anterior descending coronary artery (LAD) occlusion, induced by a left thoracotomy, were used [10, 11]. Occlusion of LAD was performed for 30 min. The presence of ischemia was confirmed by ST segment elevation and

✉ Elena Dyukova
elena.dyukova@med.uni-giessen.de

[1] Physiologisches Institut, Justus-Liebig-Universität Gießen, Aulweg 129, 35392 Gießen, Germany

[2] Department of Human and Animal Physiology, Kazan Federal University, Kremlevskaya 18, 42008 Kazan, Russia

ventricular arrhythmias. Reperfusion was confirmed by the arrhythmias during the first min after blood-flow restoration. Animals were divided into four groups: (1) Sham-operated animals which were treated the same procedure except occlusion of the coronary artery; (2) Animals with I/R; (3) Animals with IPC which were subjected to 3 cycles of 3 min ischemia followed by 5 min reperfusion preceding 30 min ischemia; (4) Animals with IPoC which were exposed to ischemia and 3 - cycles of 30 s reperfusion/30 s ischemia thereafter. Plasma samples were collected from animals 30 min after reperfusion. Infarct size was estimated by cardiac troponin I (TnI) levels in plasma by conventional ELISA kit (Life Diagnostics, Inc, West Chester, PA) according to the recommendations of the manufacturer. Rats had 7 days to recover and tissue material was taken for subsequent analysis. CaSR expression was analyzed by qRT-PCR. CaSR primer sequence: forward—AAGTGCCC GGATGACTTCTG; reverse—GGTTGGTGGCCTTG ACGATA (Invitrogen, USA). Amplification of cDNA is normalized to well established housekeeping gene B2M (β2 microglobulin). CaSR expression was compared according to different conditioning protocol or infarct size within the same animal sampling. Data are expressed as means ± SD. ANOVA and the Student-Newman-Keuls test for post hoc analysis were used to analyze experiments in which more than two groups were compared. Student's *t* test or Mann-Whitney test was used in cases of only two groups comparison. Normal distribution was checked by Levene's test.

3 Results and Discussion

CaSR expression in left ventricles (LV) decreased after I/R, IPC, and IPoC compared to the expression in Sham-operated animals (Fig. 1a). Interestingly, right ventricles (RV) showed enhanced CaSR after LAD and LAD plus IPC. However, its expression after IPoC was not pronounced (Fig. 1c). CaSR mRNA level was also increased after ischemia in RV tissue with small infarct size, whereas big infarct size did not lead to an increased expression (Fig. 1d). CaSR expression in LV tissue with both small and large infarct sizes showed a slight decrease compared to the Sham-operated animals' tissue (Fig. 1b). CaSR is known to trigger PLC-dependent Ca^{2+}-release from sarcoplasmic reticulum (SR) in cardiomyocytes [8]. These events lead to SR stress during I/R and suggest that suppression of CaSR signalling cascades may protect cardiac cells [4]. In the same time, activation of CaSRs during IPC improved heart recovery [9]. Mechanisms by which CaSR influences ischemic heart remodelling are crucial to be investigated. As a first step, CaSR expression during ischemic events in the heart was investigated in this study, suggesting that there are some differences in CaSR regulation between LV and RV tissues. This regulation is probably also infarct size dependent.

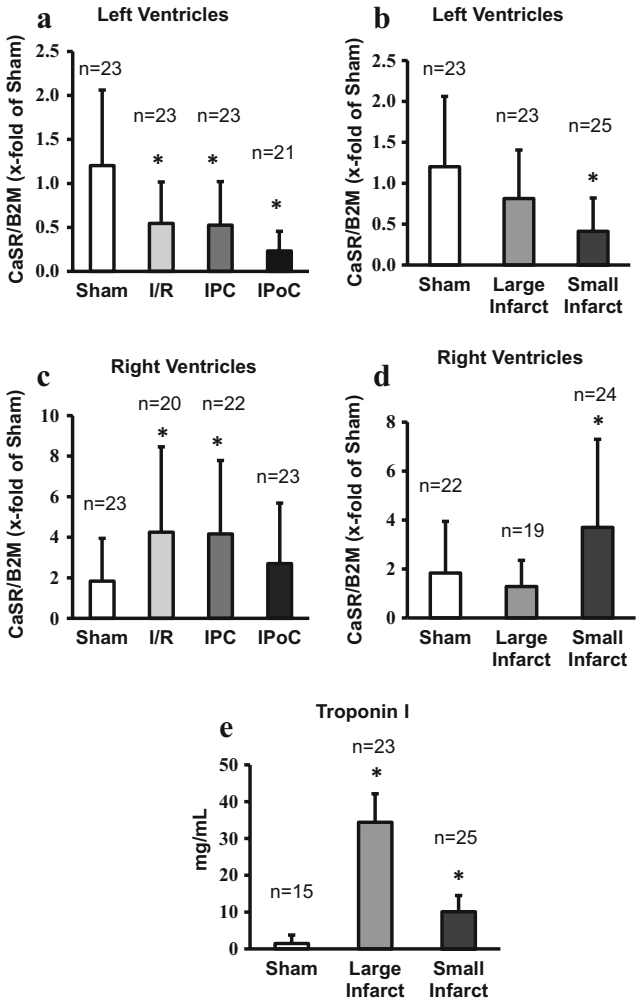

Fig. 1 Expression of CaSR under different ischemic conditions and infarct size estimation. **a** mRNA levels of CaSR in LV of Sham-operated rats, rats exposed to I/R, IPC, and IPoC. **b** mRNA levels of CaSR in LV under small and large infarct size. **c** mRNA levels of CaSR in RV of Sham-operated rats, rats exposed to I/R, IPC, and IPoC. **d** mRNA levels of CaSR in RV under small and large infarct size. **e** Determination of infarct size by quantification of troponin I levels. Data are means ± SD; $*p < 0.05$ vs Sham

4 Conclusion

In conclusion, this work suggests different regulation patterns of CaSR during I/R, IPC, or IPoC in LV and RV. Infarct size can be also crucial for these effects. These data is just the preliminary result about the regulation of CaSR during ischemic events in the heart. In future, functional analysis and protein levels will be investigated.

Acknowledgments The study was supported by a grant from the von-Behring-Röntgen-Stiftung given to E. Dukova. Tissue samples were kindly provided by R. Schreckenberg.

References

1. Frank, A., Bonney, M., Bonney, S., Weitzel, L., Koeppen, M., Eckle, T. (2012). Myocardial ischemia reperfusion injury: from basic science to clinical bedside. *Seminars in Cardiothoracic and Vascular Anesthesia, 16*, 123–132. doi:10.1177/1089253211436350.
2. Kapur, N. K., Qiao, X., Paruchuri, V., Morine, K. J., Syed, W., Dow, S., et al. (2015). Mechanical pre-conditioning with acute circulatory support before reperfusion limits infarct size in acute myocardial infarction. *JACC Heart Failure, 3*, 873–882. doi:10.1016/j.jchf.2015.06.010.
3. Thuny, F., Lairez, O., Roubille, F., Mewton, N., Rioufol, G., Sportouch, C., et al. (2012). Post-conditioning reduces infarct size and edema in patients with ST-segment elevation myocardial infarction. *Journal of the American College of Cardiology, 59*, 2175–2181. doi:10.1016/j.jacc.2012.03.026.
4. Gan, R., Hu, G., Zhao, Y., Li, H., Jin, Z., Ren, H., et al. (2012). Post-conditioning protecting rat cardiomyocytes from apoptosis via attenuating calcium-sensing receptor-induced endo(sarco)plasmic reticulum stress. *Molecular and Cellular Biochemistry, 361*, 123–134. doi:10.1007/s11010-011-1096-7.
5. Wang, R., Xu, C., Zhao, W., Zhang, J., Cao, K., Yang, B., et al. (2003). Calcium and polyamine regulated calcium-sensing receptor in cardiac tissues. *European Journal of Biochemistry, 270*, 2680–2688.
6. Tfelt-Hansen, J., Hansen, J. L., Smajilovic, S., Terwilliger, E. F., Haunso, S., Sheikh, S. P. (2006). Calcium receptor is functionally expressed in rat neonatal ventricular cardiomyocytes. *American Journal of Physiology. Heart and Circulatory Physiology, 290*, 1165–1171. doi:10.1152/ajpheart.00821.2005.
7. Smajilovic, S., Hansen, J. L., Christoffersen, T. E., Lewin, E., Sheikh, S. P., Terwilliger, E. F., et al. (2006). Extracellular calcium sensing in rat aortic vascular smooth muscle cells. *Biochemical and Biophysical Research Communications, 348*, 1215–1223. doi:10.1016/j.bbrc.2006.07.192.
8. Schreckenberg, R., Dyukova, E., Sitdikova, G., Abdallah, Y., Schlüter, K. D. (2015). Mechanisms by which calcium receptor stimulation modifies electromechanical coupling in isolated ventricular cardiomyocytes. *Pflügers Archiv - European Journal of Physiology, 467*, 379–388. doi:10.1007/s00424-014-1498-y.
9. Sun, J., & Murphy, E. (2010). Calcium-sensing receptor: a sensor and mediator of ischemic preconditioning in the heart. *American Journal of Physiology Heart and Circulatory Physiology, 209*, H1309–H1317. doi:10.1152/ajpheart.00373.2010.
10. Bencsik, P., Kupai, K., Giricz, Z., Görbe, A., Pipis, J., Murlasits, Z., et al. (2010). Role of iNOS and peroxynitrite-matrix metalloproteinase-2 signaling in myocardial late preconditioning in rats. *American Journal of Physiology Heart and Circulatory Physiology, 299*, 512–518.
11. Bencsik, P., Pálóczi, J., Kocsis, G. F., Pipis, J., Belecz, I., Varga, Z. V., et al. (2014). Moderate inhibition of myocardial matrix metalloproteinases2 by ilomastat is cardioprotective. *Pharmacological Research, 80*, 36–42.

Pflugers Arch - Eur J Physiol (2015) 467:379–388
DOI 10.1007/s00424-014-1498-y

MUSCLE PHYSIOLOGY

Mechanisms by which calcium receptor stimulation modifies electromechanical coupling in isolated ventricular cardiomyocytes

Rolf Schreckenberg · Elena Dyukova · Guzel Sitdikova · Yaser Abdallah · Klaus-Dieter Schlüter

Received: 4 February 2014 / Revised: 3 March 2014 / Accepted: 7 March 2014 / Published online: 1 April 2014

Abstract The calcium-sensing receptor (CaR) is widely expressed throughout the entire cardiovascular system and is capable of activating signaling pathways in different cells. Alongside calcium, the CaR also responds to physiological polycations such as putrescine underlining a participation in physiological and pathophysiological processes. Here, we aimed to determine mechanisms as to how CaR activation affects the contractile responsiveness of ventricular cardiomyocytes under basal and stimulated conditions. For that purpose, cardiac myocytes from 3-month-old male Wistar rats were isolated, and the acute effects of an antagonist (NPS2390), agonists (putrescine and gadolinium), or of downregulation of the CaR by siRNA on cell shortening were recorded in a cell-edge-detection system. In addition, experiments were performed on muscle stripes and Langendorff preparations. Mechanistic insights were taken from calcium transients of beating fura-2 AM-loaded cardiomyocytes and western blots. Isolated ventricular cardiomyocytes constitutively express CaR. The expression in the atria is less pronounced. Acute inhibition of CaR reduced basal cell shortening of ventricular myocytes at nearly physiological levels of extracellular calcium. Inhibition of CaR strongly reduced contractility of ventricular muscle stripes but not of atria. Activation of CaR by putrescine and gadolinium influences the contractile responsiveness of isolated cardiomyocytes. Increased calcium mobilization from the sarcoplasmic reticulum via an IP_3-dependent mechanism was responsible for amplified systolic calcium transients and a subsequent improvement in cell shortening. Alongside with these effects, activation of CaR increased relaxation velocity of the cells. In conclusion, ventricular CaR expression affects contractile parameters of ventricular heart muscle cells and modifies electromechanical coupling of cardiomyocytes.

Keywords Calcium-sensing receptor · Cardiomyocytes · Polyamines · Gadolinium · Contraction · Calcium transients · IP_3 receptor · Sarcoplasmic reticulum · Protein kinase C

Introduction

As a classical second messenger, calcium plays an important role in many intracellular signaling steps. Through its interaction with calcium-binding proteins such as troponin C and calmodulin, calcium is not only involved in muscle contraction. It also helps to regulate many metabolic processes such as growth, differentiation, and apoptosis [14, 32, 33]. Via its interaction with the calcium-sensing receptor (CaR), calcium can also act as a first messenger, enabling it to regulate cell functions in tissues that directly affect calcium homeostasis. Initially identified as a sensor on the parathyroid gland and C cells, CaR regulates the secretion of parathyroid hormone and calcitonin relative to the extracellular calcium concentration [4, 7]. In the kidneys, bones and intestines, CaR is also involved in important regulatory processes in the calcium balance [8, 18, 30].

Recently, however, it was possible to demonstrate the expression of CaR in many organs and tissues that do not

Electronic supplementary material The online version of this article (doi:10.1007/s00424-014-1498-y) contains supplementary material, which is available to authorized users.

R. Schreckenberg (✉) · E. Dyukova · Y. Abdallah · K.-D. Schlüter
Physiologisches Institut, Justus-Liebig-Universität Gießen, Aulweg 129, 35392 Gießen, Germany
e-mail: Rolf.Schreckenberg@physiologie.med.uni-giessen.de

E. Dyukova · G. Sitdikova
Institute of Fundamental Medicine and Biology, Federal University Kazan, Kazan, Russia

Y. Abdallah
Department of Cardiology, Justus-Liebig-Universität Gießen, Gießen, Germany

primarily serve to maintain calcium homeostasis. In the cardiovascular system, CaR has been found in cardiomyocytes, endothelial cells, and smooth muscle cells [15, 27, 37]. It has also been shown that, alongside calcium, there are a number of direct, type 1 agonists whose potency is directly correlated with the number of positive charges they carry. Among these agonists are the substances used in this study, gadolinium (Gd^{3+}) and polyamine putrescine, the latter of which carries two positive charges [19, 27].

In cardiomyocytes CaR, a G-protein coupled receptor, is able to increase the concentration of IP_3 via the activation of phospholipase C [26, 27]. It has also been demonstrated that CaR is involved in the activation of ERK1/2 (=p42/p44 MAP kinase), and, presumably, protects against cardiac hypertrophy [24]. It has already been shown that during a myocardial infarction there is upregulation of CaR in the heart as a result of ischaemia and reperfusion [34]. Zhao et al. were able to demonstrate that acute cardiac ischaemia disrupts polyamine metabolism, leading to an accumulation of putrescine and thus increased concentrations of a potential CaR agonist [35]. During subsequent reperfusion, the polyamine pool was exhausted. It was therefore postulated that the intracardial pool is filled through the exogenous addition of spermine, thus resulting in cardioprotective effects [35]. Unlike putrescine, spermine has four positive charges and is a much more potent agonist of CaR. As early as 1990 Tagliavini et al. reported about the antiarrhythmic properties of putrescine that could be attributed to its membrane-stabilizing and antioxidative properties [23].

All these hypotheses and findings have disregarded the functional consequences for cardiomyocytes arising from simultaneous stimulation of the CaR. In the current study, we examine to what extent the activation of the CaR affects the contractile responsiveness of ventricular cardiomyocytes. To this end, cardiomyocytes were isolated from the hearts of adult male rats and the acute effects of putrescine and gadolinium were recorded using a cell-edge-detection system. The simultaneous measurement of calcium transients should shed light on any changes in cytoplasmic calcium homeostasis. Furthermore, using muscle stripe preparations and Langendorff perfusion systems the impact of CaR stimulation on cardiac performance was investigated. The results of our study will show that adult rat ventricular cardiomyocytes constitutively express CaRs that contribute to basal cell shortening at physiological concentrations of extracellular calcium and that further activation of CaRs accelerate the relaxation of cardiomyocytes and further enhance cell shortening via a PLC-dependent mechanism.

Materials and methods

The investigation conforms the Guide for the Care and Use of Laboratory Animals published by the US National Institute of Health (NIH Publication no. 85-23, revised 1996).

Cell preparations and cultivation

Ventricular heart muscle cells were isolated from 4-month-old male Wistar rats as described previously in greater detail [20]. Hearts were excised under deep ether anesthesia, transferred rapidly to ice-cold saline and mounted on the cannula of a Langendorff perfusion system. Heart perfusion and subsequent steps were all performed at 37 °C. First, hearts were perfused in the noncirculating mode for 5 min at 10 mL/min (perfusate in mmol/L: NaCl, 110; KH_2PO_4, 1.2; KCl, 1.2; $MgSO_4$, 1.2; $NaHCO_3$, 25; and glucose, 11; gassed with 5 % CO_2–95 % O_2). Thereafter, perfusion was continued with recirculation of 50 mL of the above perfusate supplemented with 0.06 % (*w*/*v*) crude collagenase and 25 μM $CaCl_2$ at 5 mL/min. After 25 min, ventricular tissue was minced and incubated for 20 min in recirculating medium with 1 % (*w*/*v*) bovine serum albumin under 5 % CO_2–95 % O_2. Gentle trituration through a pipette released cells from the tissue chunks. The resulting cell suspension was filtered through a 200-μm nylon mesh. The filtered material was washed twice by centrifugation (3 min, 25×*g*) and resuspended in the above perfusate, in which the concentration of $CaCl_2$ was increased stepwise to 0.2 and 0.5 mmol/L. After further centrifugation (3 min, 25×*g*), the cell pellet was resuspended in serum-free culture medium (medium 199 with Earle's salts, 5 mmol/L creatine, 2 mmol/L L-carnitine, 5 mmol/L taurine, 100 IU/mL penicillin, and 100 μg/mL streptomycin) and cells were plated at a density of 7×10^4 elongated cells per 35 mm culture dish (Falcon, type 3001). The culture dishes had been pre-incubated overnight with 4 % (*v*/*v*) fetal calf serum in medium 199. Two hours after plating, cultures were washed with the serum-free medium 199 to remove round and nonattached cells. Cells were used either within the next 2 h or cultured overnight together with siRNA (Rn_Casr_5; Quiagen, Germany), scramble RNA (AllStars Negative Control siRNA; Quiagen, Germany), or NPS 2390.

Determination of cell contraction

Cells were allowed to contract at room temperature and analyzed using a cell-edge-detection system as previously described [13]. Cells were stimulated via two AgCl electrodes with biphasic electrical stimuli composed of two equal but opposite rectangular 50-V stimuli of 5 ms duration. Each cell was stimulated at 1 and 2 Hz for 1 min. Every 15 s contractions were recorded. The mean of these four measurements at a given frequency was used to define the cell shortening of a given cell. Cell lengths were measured via a line camera (data recording at 500 Hz). Cells were used in M199 with an extracellular calcium concentration of 1.25 mM. In an additional series of experiments the effect of extracellular calcium concentration was analyzed. In this set of experiments, cells were incubated in a cell culture buffer as described before [17]. Calcium concentration was set to 0.5, 1.0, 1.25, 2.0, and

4.0 mM in this part of the study. Data are expressed as cell shortening normalized to diastolic cell length (dL/L (%)).

Quantification of calcium transients

To explain the potential effects of a calcium receptor stimulation on cell shortening, cytosolic calcium transients were measured with the fluorescent dye fura-2 AM as described [12]. Briefly, isolated cardiomyocytes were placed on FCS-coated glass cover-slips and were loaded at 37 °C for 30 min with the acetoxymethyl ester of fura-2 (2.5 μmol/L). After loading, cells were washed twice with medium 199 for 30 min to allow hydrolysis of the acetoxymethyl esters within the cells. Cover-slips with loaded cells were introduced into a gas-tight, temperature-controlled (37 °C), transparent perfusion chamber positioned in the light path of an inverted microscope. Alternating excitation of the fluorescence dye at wavelengths of 340/380 nm was performed with an AR-Cation system adapted to the microscope. Light emitted (500–520 nm) from an area of 10×10 μm within a single fluorescent cell was collected by an ION Optix Corp. imaging system. The data are analyzed as the ratio of light emitted at 340-to-380-nm wavelength. The fluorescense from dye-loaded cells was 10–20 times higher than background fluorescense. When calcium transient of beating cells were determined, cells were submitted to field stimulation at 1 Hz.

Determination of contractility of heart muscle strips and Langendorff preparations

Experiments were performed on isolated hearts from Wistar rats as previously described [9]. Hearts were rapidly excised and the aorta was cannulated for retrograde perfusion with a 16-gauge needle connected to a Langendorff perfusion system. A polyvinyl chloride balloon was inserted into the left ventricle through mitral valve and held in place by a suture tied around the left atrium. The other end of the tubing was connected to a pressure transducer for continuous measurements of left ventricular pressure. The intraventricular balloon was inflated to give a diastolic pressure of 10 mmHg and balloon volume was held constant thereafter.

For registration of contractile activity the stripes of working myocardium of 4–6 mm length and 1 mm diameter were excised from the right atrium or left ventricle preparations and mounted in a special perfusion chamber (Biopac systems, Inc, USA). During the experiment tissue strips were perfused (perfusate in mmol/L: NaCl, 137.0; NaH_2PO_4, 1.0; KCl, 5.0; $MgSO_4$, 1.0; $NaHCO_3$, 11.0; glucose, 11; and ascorbic acid, 0.3; pH 7.2–7.4; gassed with 95 % O_2 and 5 % CO_2) and stimulated with a frequency of 0.1 Hz via pair of silver electrodes. The calcium concentration of the buffer was 1.0 mM in this part of the study. The force of contractions was registered using a isometric transducer TDS 125C (Biopac systems, Inc, USA). The *c*ontraction force was measured in gr. The effect of the drug was analyzed in percents compare to basal level.

Determination of protein kinase C activation

In order to quantify protein kinase C activity the nonradioactive activity assay from Assay Designs, Inc. (Ann Arbor, USA) was used. The concept is based on a solid phase enzyme-linked immuno-absorbent assay that utilizes a specific substrate for PKC and a specific antibody raised against the phosphorylated form of the substrate. However, isolated cardiomyocytes were exposed to one of the calcium receptor agonists, putrescine or gadolinium for 20 min. Then media were removed from plates, the plates were washed with ice-cold PBS and 1 mL of lysis buffer (composition in mM: MOPS, 20; ß-glycerolphosphate, 50; sodium fluoride, 50; sodium vanadate, 1; EGTA, 5; EDTA, 2; NP40, 1 %; dithiothreitol, 1; benzamidine, 1; phenylmethanesulphonylfluoride, 1; leupeptin, 10 μg/mL; and aprotinin, 10 μg/mL) was added. Cells were scraped into the lysis buffer using a rubber policeman, transferred to pre-chilled conical tubes and centrifuged. The clear supernatant was used to measure the entire protein concentration and the protein kinase C activity exactly according to the manufacturer's suggestions.

Western blots

Isolated cardiomyocytes were incubated with lysis buffer as described before [21]. Samples (100 μg protein) were loaded on a 15.0 % SDS-PAGE and blotted onto membranes as described before. The phosphorylation status of phospholamban was detected using an anti Ser 16 polyclonal antibody (antibody ab15000, Abcam plc, UK) and second an anti-rabbit IgG antibody coupled to alkaline phosphatase. Total phospholamban was probed with a nonphosphorylation specific polyclonal antibody (FL-52: sc-30142, Santa Cruz Biotechnology, Inc.). The expression of the calcium-sensing receptor was detected using an anti-calcium-sensing receptor, C-terminal, antibody produced in rabbit (SAB 4503369M; Sigma-Aldrich Chemie, Taufkirchen, Germany). Results are displayed as the ratio of phosphorylated phospholamban to total phospholamban.

PCR

RNA isolation and PCR was performed as described before [1]. Briefly, total RNA from cardiomyocytes was extracted with Trizol (Invitrogen) as described by the manufacturer. After conversion of RNA into complementary DNA (cDNA) with reverse transcriptase, PCR was performed. The forward primer had the following sequence: AAGTGCCCGG

ATGACTTCTG. The reverse primer had the following sequence: GGTTGGTGGCCTTGACGATA. The product length was 193 bp.

Materials and solutions

1,4-diaminobutane dihydrochlorid (putrescine), gadolinium (III) chloride hexahydrate, and caffeine were obtained from Sigma/RBI (Sigma-Aldrich Chemie, Taufkirchen, Germany) and dissolved as stock solutions of 10 mM in sterile water and stored at −20 °C. The calcium receptor blocker NPS2390 (working solution, 10 μM; ref. [16]) and the IP_3 receptor blocker xestospongin D (working solution, 5 μM;, ref. [29]) were obtained from Sigma/RBI (Sigma-Aldrich Chemie, Taufkirchen, Germany) and dissolved as stock solutions of 1 mM in dimethylsulfoxide (DMSO). Working solutions were prepared by dilution with sterile water. Chelerythrine Chloride (working solution, 10 μM; ref. [25]) was obtained from Calbiochem (Merck Bioscience Ltd., USA) and dissolved in dimethylsulfoxide (DMSO) as a 1 mM stock solution.

Statistics

Data are expressed as indicated in the legends. ANOVA and the Student–Newman–Keuls test for post hoc analysis were used to analyze experiments in which more than one group was compared. In cases in which two groups were compared, Student's *t* test for paired samples was employed. $P<0.05$ was regarded as significant.

Results

Expression of CaR in cardiomyocytes and ventricular tissue

Constitutive expression of CaR in neonatal rat heart cells and cardiac tissue derived from Sprague–Dawley rats has been reported [24, 30]. Here, we confirmed these findings in isolated ventricular cardiomyocytes derived from adult Wistar rats. In three different preparations, we found stable mRNA expression of the CaR (Fig. 1a). Furthermore, CaR was stably expressed on protein level, too. Specificity of the protein band was confirmed by downregulation of the receptor with siRNA (Fig. 1b). In tissue samples from ventricle and atria, it was found that the expression of the CaR is stronger in ventricles than in atria (Fig. 1c).

Effect of inhibition and downregulation of CaR on cardiac performance

In order to address the question whether the CaR contributes to basal cell shortening and contractility, we blocked the receptor by administration of NPS2390. This reduced the contractile force produced in muscle stripes derived from the left ventricle but did not significantly affect muscle stripes from atria (Fig. 2). These data suggest that basal CaR

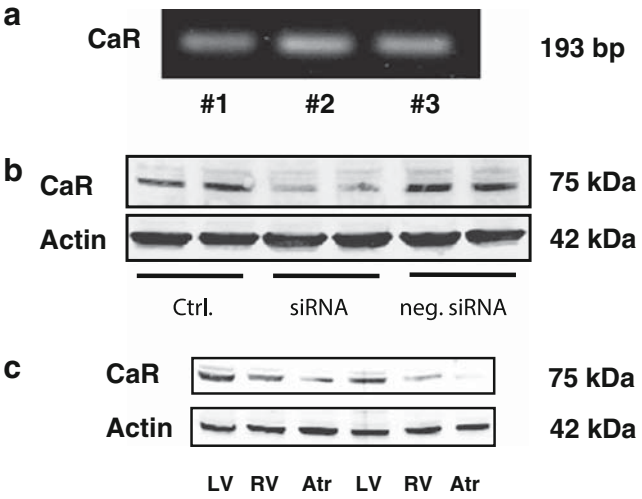

Fig. 1 Ventricular expression of CaR in ventricular cardiomyocytes and tissues. **a** Detection of CaR mRNA by RT-PCR in isolated ventricular cardiomyocytes from adult rats in three different preparations (no. 1–3). **b** Detection of CaR proteins by Western blot in cardiomyocytes cultured for 24 h in presence of siRNA or scramble siRNA (neg. siRNA) or control cells. **c** Detection of CaR proteins by Western blots in tissue samples from left or right ventricles and atria

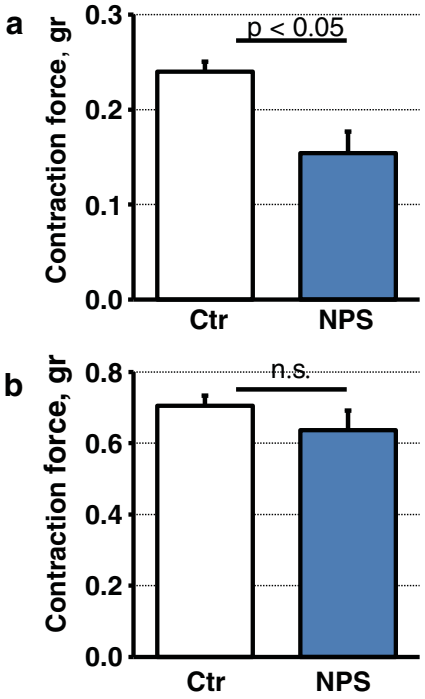

Fig. 2 Effect of acute inhibition of CaR on the contractility of muscle stripes. Inhibition was performed by administration of NPS2390 (100 μM). **a** Inhibition of contractile force of ventricular muscle stripes; **b** inhibition of contractile force of atrial muscle stripes. Data are means± SE from $n=8$ experiments

expression contributes to basal function in ventricles but not in atria in which the expression of CaR is low. In Langendorff perfused rat hearts, left ventricular developed pressure (LVDP) declined from basal 111.9±13.8 mmHg in the presence of NPS2390 by 9.6±7.9 % (n=11, p<0.05). On the level of the isolated adult rat ventricular cardiomyocyte, NPS2390 significantly attenuated basal cell shortening by 9.2 % (control: dL/L 10.43±1.70 %, n=37 cells; NPS2390: 9.51±1.47 %, n=48 cells; p=0.012). A representative original tracing is given in Supplementary Fig. 1A. In addition, calcium transients measured in fura-2 AM-loaded adult rat ventricular cardiomyocytes were significantly attenuated in the presence of NPS2390. In control cells the fura signal (340 nm/380 nm) remained constant about a 20-min observation period (0.40±0.04 vs. 0.38±0.08, n=8 cells), whereas it constitutively declined in the presence of NPS2390 (0.40±0.03 vs. 0.21±0.03, n=10 cells, p<0.05). Moreover, administration of either NPS2390 or siRNA to cardiomyocytes for 24 h downregulates CaR expression (Fig. 3a). Under such conditions NPS and siRNA directed against CaR significantly reduced cell shortening (Fig. 3b, c). Representative single cell recordings are given in Supplementary Fig. 1B. Collectively, these data suggest that CaR plays an important role in maintaining a steady state of cell shortening and subsequent contractility in the ventricle.

Effects of CaR stimulation on load-free cell shortening and cardiac contractility

First, the effect of extracellular calcium concentration on NPS-sensitive cell shortening was determined. As calcium is a natural agonist of the receptor that, however, can also impact cell shortening by calcium up-take distinct from receptor activation the extracellular calcium concentration significantly affected basal cell shortening (Fig. 4a). At near physiological concentrations of extracellular calcium (1.00–1.25 mM) NPS significantly reduced load-free cell shortening. At higher extracellular concentration the NPS-sensitive part of the effect of extracellular calcium was smaller (Fig. 4a). The question whether selective stimulation of CaR can additionally increase cell shortening was investigated by administration of two CaR agonists, putrescine and gadolinium, at physiological calcium concentration. Using a beating frequency of 2 Hz, isolated cardiomyocytes were stimulated and incubated for 20 min with putrescine or gadolinium. Preliminary experiments were performed with three different concentrations of putrescine (1.0, 3.0 and 5.0 mM) and their effect on relative cell shortening was analyzed (data not shown). For putrescine, maximal cell shortening was achieved with concentrations at or above 3.0 mM, and for gadolinium, at or above 1.0 mM. In all subsequent experiments, the agonists were therefore used at these particular concentrations.

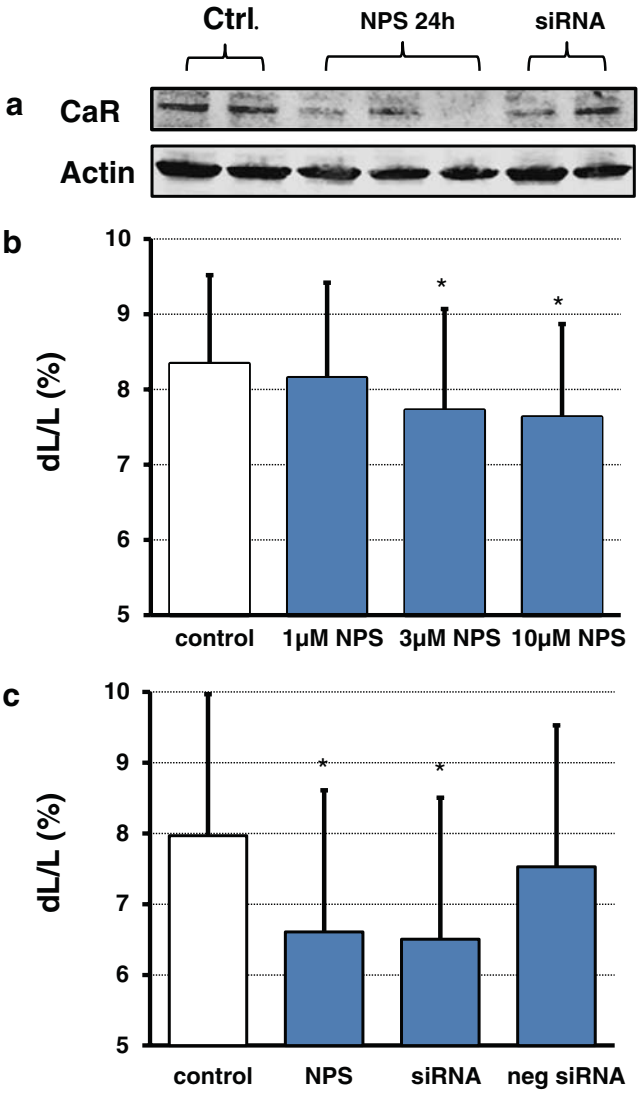

Fig. 3 Effect of downregulation of CaR on basal cell shortening of cardiomyocytes. **a** Detection of CaR proteins by Western blot in cardiomyocytes cultured for 24 h in presence of siRNA or NPS (10 μM) or control cells. **b** Mean load-free cell shortening of cardiomyocytes normalized to diastolic cell lengths after overnight incubation with different concentrations of NPS. **c** Effect of NPS in comparison to siRNA and scramble RNA (neg. siRNA) on load-free cell shortening. Data are means±SD from n=100 to 120 cells

Putrescine improved load-free cell shortening of isolated myocytes from 9.43±1.13 (ΔL/dL(%), n=43) to 10.55±1.21 (ΔL/dL(%), n=42) by 11.8±1.4 % (p<0.05). For myocytes previously incubated with gadolinium, there was an increase in the relative cell shortening from 9.43±1.13 (ΔL/dL(%), n=43) to 11.50±1.53 (ΔL/dL(%), n=34) by 22.0±1.8 % (p<0.05) (Fig. 4b). Representative single cell recordings are shown in Supplementary Fig. 2.

Similar to the experiments performed with isolated adult rat ventricular cardiomyocytes, putrescine increased contractility of muscle stripes from the left ventricle (Fig. 4c). As expected from the expression analysis (see Fig. 1c), putrescine exerted

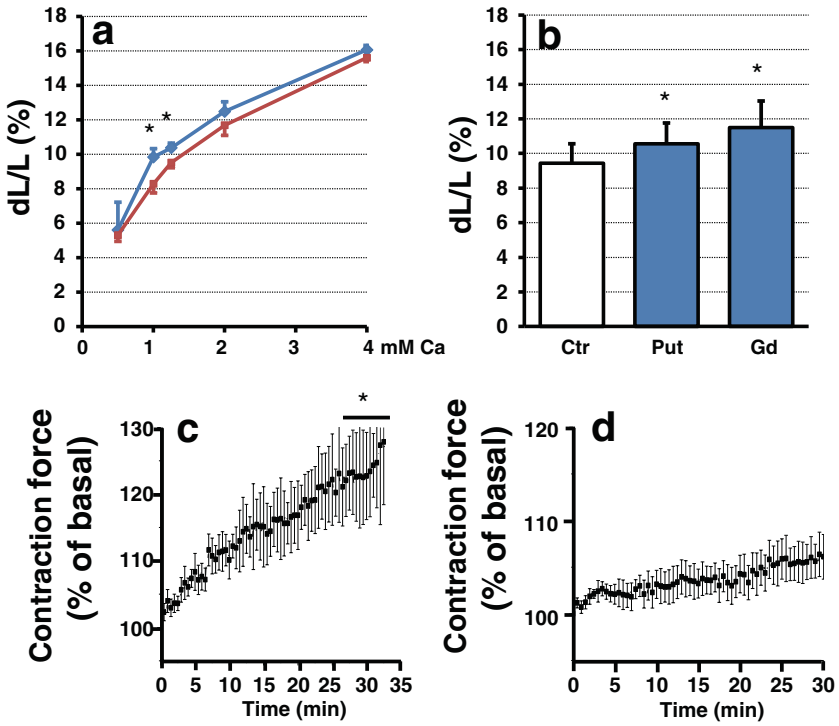

Fig. 4 Effect of a CaR stimulation on cell shortening and contractility of muscle stripes. **a** Extracellular calcium concentration was set to 0.5–4.0 mM and cell shortening was recorded from cells cultured with and without NPS2390. Data are means±SEM from n=25 to 27 cells; *p<0.05 between control and NPS-treated cells. **b** Isolated cardiomyocytes were exposed to putrescine (*PUT*; 3.0 mM) or gadolinium (*Gd*; 1.0 mM) for 20 min and cell shortening was measured thereafter at 2 Hz. Data are expressed as relative cell shortening normalized to the diastolic cell lengths; *p<0.05 vs. control cells. **c** Contractility of ventricular muscle stripes in the presence of putrescine (300 μM). **d** Contractility of atrial muscle stripes in the presence of putrescine

only a minor effect on muscle stripes from atria (Fig. 4d). The data were also confirmed by Langendorff preparations in which putrescine increased LVDP from 102.6±13.3 mmHg by 7.4±5.3 % (n=9 hearts) within 15 min.

Acute effects of putrescine and gadolinium on the calcium transients of isolated cardiomyocytes

In order to get a stronger mechanistic insight into effects of putrescine and gadolinium, fura-2 AM-loaded, isolated cardiomyocytes were constitutively stimulated and then incubated for 10 min with putrescine or gadolinium. This method enables changes in the previously described functional parameters as well as any variation in the underlying calcium transients to be recorded simultaneously. Analogous to the improved cell shortening, both agonists produced a slow but progressive increase in systolic calcium that peaked after 10 min and then went into a stable plateau phase (Fig. 5a, g). A representative single cell recording for a cell incubated with putrescine is given in the Supplementary Fig. 3. There were no significant changes in diastolic calcium in the presence of either of the two agonists over the entire observation period. As a correlate of the previously described increase in the relaxation velocity (Fig. 5b) a significant reduction in the time to basal at 50 % can be taken. The time required for the transport of calcium from the cytosol to its intracellular pools decreased by 8.0±0.8 % after incubation with putrescine and by 7.2±0.6 % after incubation with gadolinium (Fig. 5d, j).

Whether the observed effects can be ascribed to activation of the CaR was examined in a further series of experiments using the receptor blocker NPS2390. Fura-2 AM-loaded cells were pre-incubated for 30 min with the inhibitor and then treated in the same manner as previously described. Under these conditions, putrescine and gadolinium did not affect either the calcium transients or the time to basal at 50 % (Fig. 5b, e, h, k).

CaR is able to generate inositol 1.4.5-triphosphate (IP_3) from phosphatidylinositol 4.5-biphosphate (PIP_2) via activation of phospholipase C, and this IP_3 releases additional calcium from the sarcoplasmic reticulum via the IP_3 receptor. In a further experimental series, the IP_3 receptor was blocked using 30-min pre-incubation with xestospongin D and then treated in an identical way to that described above. Neither putrescine nor gadolinium affected the amplitude of calcium transients under these conditions (Fig. 5c, i). However, both agonists still improved calcium sequestration under these conditions, which was reflected in a shorter time to basal at 50 % of 8.9±0.8 % and 7.3±0.7 %, respectively (Fig. 5f, l). Finally, we investigated whether the accelerated refilling of the SR by CaR-stimulation increases SR Ca load. To that purpose, quiescent fura-2-loaded cells were incubated for 10 min with gadolinium and subsequently exposed to caffeine (10 mM) to release all calcium stored in the SR. Gadolinium alone did not increase the SR Ca load probably because IP3-receptor activation release calcium from the SR. When the IP3-receptor was blocked mean SR Ca load was normalized to control values. However, a significant increase of SR Ca load was not achieved by increasing the velocity of calcium refilling into the SR (Supplementary Fig. 4).

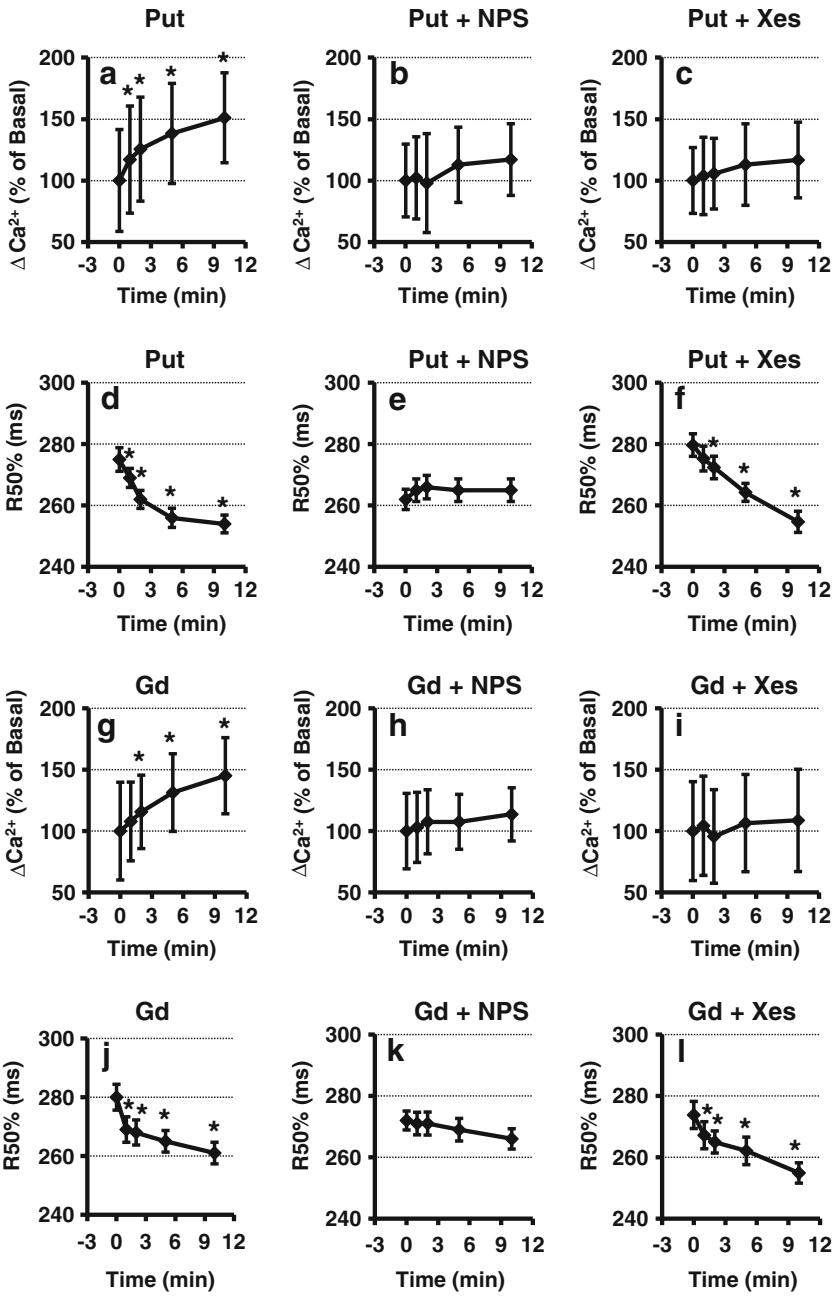

Fig. 5 Acute effects of putrescine and gadolinium on the calcium transients. Intracellular calcium was measured in fura-2 AM-loaded myocytes and indicated as the ratio of the fluorescence at 340–380 nm (Δ Ca^{2+}). The velocity for the calcium sequestration is expressed as time to basal, 50 % (R50%, ms). Effect of 10-min PUT (*top*) or Gd (*bottom*) stimulation on the calcium transients and time to basal, 50 %. Where indicated cells were co-incubated with the CaR receptor blocker NPS2390 (NPS; 10 μM) or the IP_3 receptor blocker xestospongin D (*Xes*; 5 μM). Data are means±SEM of n=25 to 31 cells. *p<0.05 vs. t_0

Effect of putrescine and gadolinium on protein kinase C activity

Along with the increased availability of IP_3, there is parallel formation of diacylglycerol, which is required for the activation of protein kinase C (PKC). PKC phosphorylates phospholamban at positions 10 and 16. In an ELISA-based activity assay the total PKC activity was determined in isolated cardiomyocytes after 20 min incubation with putrescine or gadolinium and compared with untreated control cells. Putrescine increased PKC activity by 26.2±1.3 % and gadolinium by 35.7±2.2 % (Fig. 6a). A Western blot confirmed PKC activation by determining an increased phosphorylation of phospholamban by putrescine. The fraction of phosphorylated phospholamban to total phospholamban increased after 20 min incubation by 26.0±2.5 %. The PKC inhibitor chelerythrine chloride had no effect on basal phosphorylation but was, however, able to completely inhibit the putrescine-induced increase (Fig. 6b, c).

Effect of protein kinase C on putrescine-induced functional improvement

The functional consequences arising from the Western blot results on the contractile responsiveness of isolated cardiomyocytes were investigated using the previously

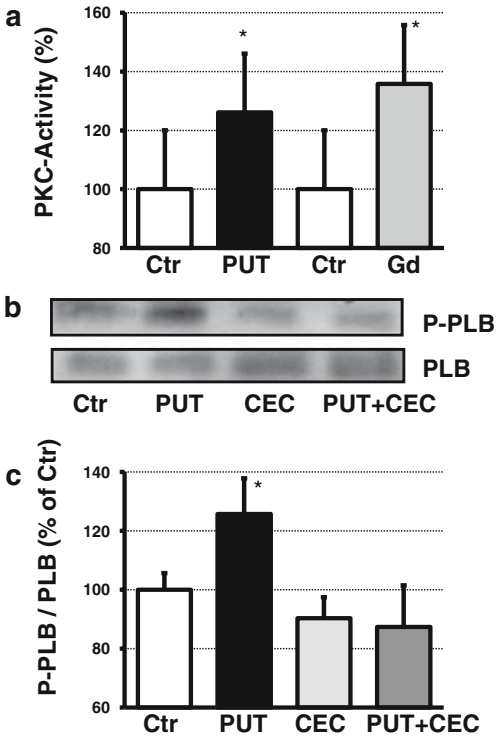

Fig. 6 **a** Determination of protein kinase C (*PKC*) activity and PKC-dependent phosphorylation of phospholamban. Cells were exposed to putrescine (*PUT*; 3.0 mM) or gadolinium (*Gd*; 1.0 mM) for 20 min and protein kinase C activity was measured thereafter. Data are means±SEM of $n=4$ cell preparations. *$p<0.05$ vs. control. **b** Representative immunoblot indicating p-phospholamban immunoreactivity in isolated heart muscle cells after 20-min PUT stimulation. p-phospholamban values were normalized to total phospholamban levels. **c** Densitometric analysis of immunoblots. The fraction of p-phospholamban to total phospholamban was significantly increased after 20 min incubation. The PKC inhibitor chelerythrine chloride (*CEC*; 10 μM) completely inhibits the PUT-induced increase. Data are means±SEM of $n=4$ cell preparations. *$p<0.05$ vs. untreated controls

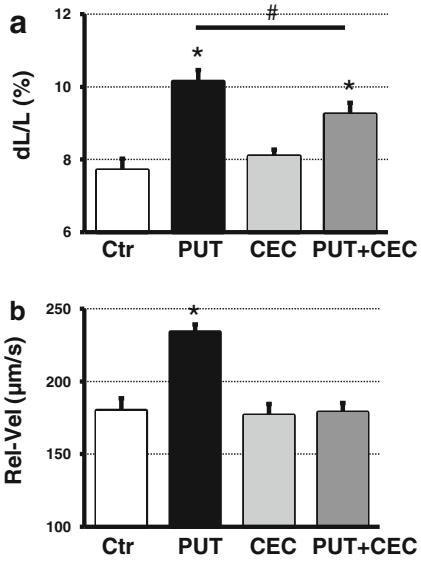

Fig. 7 Effect of PKC inhibition on putrescine-induced functional improvement. **a** Isolated cardiomyocytes were pre-incubated for 30 min with CEC and stimulated for further 20 min with putrescine. Cell shortening was measured thereafter at 2 Hz. **b** Relaxation velocity was quantified from single-cell recordings simultaneously. Data are means±SEM of $n=34$ cells. *$p<0.05$ vs. untreated controls

described cell-edge-detection system. At a frequency of 2 Hz the cardiomyocytes were initially pre-incubated for 30 min with the PKC inhibitor CEC and then stimulated for a further 20 min with putrescine. Putrescine alone led to a significant increase in cell shortening and the relaxation velocity, as previously shown. CEC did not affect either basal cell shortening or the relaxation of the cells. The effect of putrescine on the relative cell shortening was, however, significantly reduced in the presence of the PKC inhibitor by 34.1±1.2 % compared with stimulation with putrescine alone (Fig. 7a). Representative single cell recordings are given at Supplementary Fig. 5. The increased relaxation velocity was completely inhibited to control levels (Fig. 7b).

Discussion

Various studies have shown that the CaR is widely distributed throughout the entire cardiovascular system and is capable of specifically activating various signaling pathways in different cells. Furthermore, it has become apparent in recent years in the light of newly identified agonists that the name 'calcium receptor' inadequately reflects its physiological and pathophysiological significance. In addition to the polyamines—which, for instance, play a significant role during a myocardial infarction or the development of cardiac hypertrophy—gadolinium, a component of the contrast agent in magnetic resonance imaging, is a potential agonist of CaR. The aim of the current study was to more accurately characterize the results of CaR activation on the contractile function of isolated cardiomyocytes.

The most important experimental findings in this study show that in the presence of nearly physiological levels of calcium the basal expression of CaR significantly contribute to cardiac performance. Moreover, further activation of CaR by agonists such as putrescine or gadolinium leads to a progressive increase in the calcium transients in isolated ventricular cardiomyocytes from adult rats. Calcium is released from the sarcoplasmic reticulum via an IP_3-dependent mechanism, which is then responsible for improving cell shortening via an increase in systolic calcium. Activation of CaR improved cell shortening and restored calcium more quickly into its intracellular pool, which is reflected accelerated normlaiozation of intracellular calcium and an increased relaxation speed of the cells. As expected SR Ca load was higher in cells in which IP3-receptors were blocked by xestospongin in the presence of CaR activation.

Not only has the expression of CaR in various cell types of the cardiovascular system been demonstrated in previous

years. There is also increasingly more evidence suggesting CaR is directly involved in many metabolic and functional processes. Its activation by spermine in endothelial cells of the aorta leads to an increase in the intracellular calcium concentration with a subsequent increase in nitric oxide production [37]. Weston et al. have shown that CaR participates in the opening of the calcium-sensitive potassium channel (IK_{Ca}) in endothelial cells [31]. Wang et al. have found indications that calcium-induced vasorelaxation in isolated arteries is mediated by activation of CaR in perivascular nerves [28]. Although the expression of CaR in smooth muscle cells is currently considered controversial, it is clear that the regulation of vessel tone and thus the modulation of blood pressure proceeds under direct involvement of CaR [22].

In both neonatal and adult cardiomyocytes, a CaR subtype is present that provides both the messengers IP_3 and DAG via a subsequent activation of phospholipase C [19, 24]. Alongside its participation in the signaling pathways of MAP kinases, CaR also appears to play a role as an antihypertrophic component in the development of cardiac hypertrophy. It has been shown that activation of CaR in rat neonatal cardiomyocytes induces a downregulation in DNA synthesis, without any effects on the cell number [24].

Calcium release from IP_3-sensitive pools has also been previously demonstrated in HEK-293 cells and hepatocytes [5, 11]. In the current study, the use of beating isolated myocytes enabled a connection to be established between this mechanism and improved contractile function in cardiomyocytes. Furthermore, simultaneous activation of PKC via an increase in the phospholamban phosphorylation at Ser10 and Ser16 leads to increased SERCA activity, which also contributes to improved contraction [6]. The data of the current study suggest that basal extracellular calcium via stimulation of CaR contributes to the basal phosphorylation of phospholamban. Although NPS did not significantly decrease phospholamban phosphorylation in our study this might be because the study is underpowered to solve this question. It should be mentioned that the mean phosphorylation of phospholamban was reduced by NPS and NPS plus putrescine. For the model used here, activation of the CaR represents a positive inotropic intervention that only gradually and moderately elevates the systolic calcium concentration to a new level. Simultaneous activation of SERCA ensures that the diastolic relaxation is not negatively affected. The contractile parameters recorded in this model do not show the typical drawbacks of other substances with positive inotropic effects. As an example, the impaired relaxation caused by some calcium sensitisers or the proarrhythmogenic effect of catecholamines must be mentioned.

In 1997, Quinn et al. showed that polyamines, as small polycationic molecules, are effective agonists of CaR [19]. The development of cardiac hypertrophy is associated with an upregulation of polyamine metabolism and an increase in the polyamines putrescine, spermidine and spermine [10]. To what extent the subsequent polyamine levels contribute to a paracrine effect via stimulation of the CaR cannot be answered at the moment. Changes in polyamine metabolism are also observed during a myocardial infarction. Zhao et al. showed that acute ischaemia initially involves an accumulation of putrescine, and that there is a shortage of polyamines during the subsequent reperfusion that further reduces the survival and functionality of myocytes [35]. They postulated that exogenous addition of spermine could achieve cardioprotective effects [36]. Parallel stimulation of the CaR in this case must also be considered, such as in other studies, in which the antiarrhythmic properties of polyamines or gadolinium were examined [2, 3, 23].

In summary, the results of this study show for the first time that acute activation of CaR by physiological and nonphysiological agonists influences the contractile function of isolated cardiomyocytes. Improved cell shortening can be attributed to an increase in the systolic calcium transients. An increased relaxation velocity and a stable diastolic calcium transient can be explained by an increase in the activity of SERCA. Further studies are required to understand more precisely the metabolic and functional consequences of cardiac CaR activation.

Acknowledgments The authors thank Nadine Woitasky, Peter Volk, and Daniela Schreiber for excellent technical support. The data of this study are in part results of the thesis of Elena Dyukova.

Funding This study was supported by the DAAD (cooperation program of the universities of Giessen, Germany and Kazan, Russia).

References

1. Anwar A, Schluter KD, Heger J, Piper HM, Euler G (2008) Enhanced SERCA2a expression improves contractile performance of ventricular cardiomyocytes of rat under adrenergic stimulation. Pflugers Arch – Eur J Physiol 457:485–491
2. Barrabés JA, Garcia-Dorado D, Agulló L, Rodríguez-Sinovas A, Padilla F, Trobo L, Soler-Soler J (2006) Intracoronary infusion of Gd^{3+} into ischemic region does not suppress phase Ib ventricular arrhythmias after coronary occlusion in swine. Am J Physiol Heart Circ Physiol 290:H2344–H2350
3. Bergeron RJ, Wiegand J, Weimar WR, Snyder PS (1998) Polyamine analogue antiarrhythmics. Pharmacol Res 38:367–380
4. Brown EM, Gamba G, Riccardi D, Lombardi M, Butters R, Kifor O, Sun A, Hediger MA, Lytton J, Herbert SC (1993) Cloning and characterization of an extracellular $Ca^{(2+)}$-sensing receptor from bovine parathyroid. Nature 366(6455):575–580
5. Canaff L, Petit JL, Kisiel M, Watson PH, Gascon-Barré M, Hendy GN (2001) Extracellular calcium-sensing receptor is expressed in rat hepatocytes: coupling to intracellular calcium mobilization and stimulation of bile flow. J Biol Chem 276:4070–4079
6. Colyer J (1998) Phosphorylation states of phospholamban. Ann N Y Acad Sci 853:79–91
7. Garrett JE, Tamir H, Kifor O, Simin RT, Rogers KV, Mithal A, Gagel RF, Brown EM (1995) Calcitonin-secreting cells of the thyroid

express an extracellular calcium receptor gene. Endocrinology 136: 5202–5211
8. Geibel J, Sritharan K, Geibel R, Geibel P, Persing JS, Seeger A, Roepke TK, Deichstetter M, Prinz C, Cheng SX, Martin D, Herbert SC (2006) Calcium-sensing receptor abrogates secretagogue- induced increases in intestinal net fluid secretion by enhancing cyclic nucleotide destruction. Proc Natl Acad Sci U S A 103:9390–9397
9. Grohè C, van Eickels M, Wenzel S, Meyer R, Degenhardt H, Doevendans PA, Heinemann MP, Ross G, Schlüter K-D (2004) Sex-specific differences in ventricular expression and function of parathyroid hormone-related peptide. Cardiovasc Res 61:307–316
10. Harris P (1982) Polyamine metabolism in myocardial hypertrophy. Eur Heart J Suppl A 3:73–74
11. Huang C, Handlogten ME, Miller RT (2002) Parallel activation of phosphatidylinositol 4-kinase and phospholipase C by the extracellular calcium-sensing receptor. J Biol Chem 277:20293–20300
12. Ladilov Y, Efe O, Schäfer C, Rother B, Kasseckert S, Abdallah Y, Meuter K, Schlüter K-D, Piper HM (2003) Reoxygenation-induced rigor-type contracture. J Mol Cell Cardiol 35:1481–1490
13. Langer M, Luttecke D, Schluter KD (2003) Mechanism of the positive contractile effect of nitric oxide on rat ventricular cardiomyocytes with positive force/frequency relationship. Pflugers Arch-Eur J Physiol 447:289–297
14. McConkey DJ, Orrenius S (1997) The role of calcium in the regulation of apoptosis. Biochem Biophys Res Commun 239:357–366
15. Molostvov G, James S, Fletcher S, Bennett J, Lehnert H, Bland R, Zehnder D (2007) Extracellular calcium-sensing receptor is functionally expressed in human artery. Am J Physiol Ren Physiol 293:F946–F955
16. Nemeth EF, Delmar EG, Heaton WL, Miller MA, Lambert LD, Conklin RL, Gowen M, Gleason JG, Bhatnagar PK, Fox J (2001) Calcilytic compounds: potent and selective Ca^{2+} receptor antagonists that stimulate secretion of parathyroid hormone. J Pharmacol Exp Ther 299:323–331
17. Piper HM, Millar BC, McDermott BJ (1989) The negative inotropic effect of neuropeptide Y on the ventricular cardiomyocyte. Naunyn-Schmiedeberg's Arch Pharmacol 340:333–337
18. Purroy J, Spurr NK (2002) Molecular genetics of calcium sensing in bone cells. Hum Mol Genet 11:2377–2384
19. Quinn SJ, Ye CP, Diaz R, Kifor O, Bai M, Vassilev P, Brown E (1997) The Ca^{2+}-sensing receptor: a target for polyamines. Am J Physiol 273:C1315–C1323
20. Schlüter K-D, Piper HM (2005) Isolation and culture of adult ventricular cardiomyocytes. In: Dhein S et al (eds) Practical methods in cardiovascular research. Springer, Berlin-Heidelberg, pp 557–567
21. Schlüter K, Katzer C, Frischkopf K, Wenzel S, Taimor G, Piper HM (2000) Expression, release, and biological activity of parathyroid hormone-related peptide from coronary endothelial cells. Circ Res 86:946–951
22. Smajilovic S, Tfelt-Hansen J (2008) Novel role of the calcium-sensing receptor in blood pressure modulation. Hypertension 52: 994–1000
23. Tagliavini S, Genedani S, Bertolini A, Bazzani C (1991) Ischemia- and reperfusion-induced arrhythmias are prevented by putrescine. Eur J Pharmacol 194:7–10
24. Tfelt-Hansen J, Hansen JL, Smajilovic S, Terwilliger EF, Haunso S, Sheikh SP (2006) Calcium receptor is functionally expressed in rat neonatal ventricular cardiomyocytes. Am J Physiol Heart Circ Physiol 290:H1165–H1171
25. Wang JW, Yazawa K, Hao LY, Onoue Y, Kameyama M (2007) Verrucotoxin inhibits KATP channels in cardiac myocytes through a muscarinic M3 receptor-PKC pathway. Eur J Pharmacol 563:172–179
26. Wang M, Yao Y, Kuang D, Hampson DR (2006) Activation of family C G-protein-coupled receptors by the tripeptide glutathione. J Biol Chem 281:8864–8870
27. Wang R, Xu C, Zhao W, Zhang J, Cao K, Yang B, Wu L (2003) Calcium and polyamine regulated calcium-sensing receptors in cardiac tissues. Eur J Biochem 270:2680–2688
28. Wang Y, Bukoski RD (1998) Distribution of the perivascular nerve Ca^{2+} receptor in rat arteries. Br J Pharmacol 125:1397–1404
29. Wang YG, Dedkova EN, Ji X, Blatter LA, Lipsius SL (2005) Phenylephrine acts via IP_3-dependent intracellular NO release to stimulate L-type Ca^{2+} current in cat atrial myocytes. J Physiol 567(Pt 1):143–157
30. Ward DT, Riccardi D (2002) Renal physiology of the extracellular calcium-sensing receptor. Pflugers Arch 445:169–176
31. Weston AH, Absi M, Ward DT, Ohanian J, Dodd RH, Dauban P, Petrel C, Ruat M, Edwards G (2005) Evidence in favor of a calcium-sensing receptor in arterial endothelial cells: studies with calindol and Calhex 231. Circ Res 97:391–398
32. Wilkins BJ, Molkentin JD (2004) Calcium-calcineurin signaling in the regulation of cardiac hypertrophy. Biochem Biophys Res Commun 322:1178–1191
33. Zayzafoon M (2006) Calcium/calmodulin signaling controls osteoblast growth and differentiation. J Cell Biochem 97:56–70
34. Zhang WH, Fu SB, Lu FH, Wu B, Gong DM, Pan ZW, Lv YJ, Zhao YJ, Li QF, Wang R, Yang BF, Xu CQ (2006) Involvement of calcium-sensing receptor in ischemia/reperfusion-induced apoptosis in rat cardiomyocytes. Biochem Biophys Res Commun 347:872–881
35. Zhao YJ, Xu CQ, Zhang WH, Zhang L, Bian SL, Huang Q, Sun HL, Li QF, Zhang YQ, Tian Y, Wang R, Yang BF, Li WM (2007) Role of polyamines in myocardial ischemia/reperfusion injury and their interactions with nitric oxide. Eur J Pharmacol 562:236–246
36. Zhao YJ, Zhang WH, Xu CQ, Li HZ, Wang LN, Li H, Sun YH, Lin Y, Han LP, Zhang L, Tian Y, Wang R, Yang BF, Li WM (2009) Involvement of the ornithine decarboxylase/polyamine system in precondition-induced cardioprotection through an interaction with PKC in rat hearts. Mol Cell Biochem 332:135–144
37. Ziegelstein RC, Xiong Y, He C, Hu Q (2006) Expression of a functional extracellular calcium-sensing receptor in human aortic endothelial cells. Biochem Biophys Res Commun 342:153–163

Open Access

Role of Extracellular Calcium Control, Calcium Sensing, and Regulation of Calcium Regulating Hormones in Heart Failure

R. Schreckenberg, S. Wenzel and K.-D. Schlüter*

Justus-Liebig-Universität Giessen, Germany, Physiologisches Institut, Aulweg 129, 35392 Giessen, Germany

Abstract: Calcium plays a pivotal role in excitation-contraction coupling of cardiomyocytes and many other cellular responses observed in cardiovascular cells. Thus maintaining a healthy status requires very strict regulation of cytoplasmatic but also plasma ionized calcium concentration. Plasma ionized calcium is regulated by calcium sensing and the regulation of calcium uptake and secretion. Under conditions of heart failure, however, electrolyte deregulation occurs due to an activation of the sympathetic nervous system and the renin-angiotensin-aldosterone system because both systems are coupled calcium regulation and thereby also to the regulation of hormones controlling calcium homeostasis such as parathyroid hormone, parathyroid hormone-related protein, and vitamin D that are activated in a calcium-dependent way. Of note, these hormones and receptors have also direct cardiac effects that modulate cardiac and renal function. Therefore, they play not only a role in end-stage heart failure but also in essential hypertension and reno-cardiovascular complications. In this review we summarize our current understanding about the role of calcium deregulation in heart failure and discuss the consequences from these observations. In conclusion, controlling plasma ionized calcium, plasma parathyroid hormone, and vitamin D status are pivotal in successful pharmacotreatment of patients with heart failure.

Keywords: Parathyroid hormone, PTH receptors, calcium sensing receptor, vitamin D, aldosterone, kidney.

1. CALCIUM CONTROL IN HEART FAILURE

Systemic calcium control is crucial for the maintenance of a normal and healthy status. Therefore, plasma calcium levels are strongly controlled by various mechanisms including the control of calcium uptake, calcium release, and calcium mobilization from the bone. In these processes hormones like parathyroid hormone (PTH) and vitamin D are involved. As a result of these control mechanisms plasma calcium concentrations are strictly controlled and show little variations. However, the above mentioned control mechanisms are embedded in a complex network of regulator circuits that play also a role in cardiovascular regulation. The most prominent example is that of the renin-angiontensin-aldosteron system (RAAS). The RAAS is activated as a compensatory mechanism that counterbalances reduced pump activity of the heart and it is one key pathway that is deregulated in heart failure. As the release of renin is regulated by the sympathetic nervous system, RAAS is also connected to sympathetic hyperactivation, another key event in heart failure. As a consequence, renin is released from the kidney and promotes the formation of angiotensin I from angiotensinogen. Angiotensin I is subsequently converted to angiotensin II (Ang II) *via* the angiotensin-converting-enzyme (ACE). The formation of Ang II by ACEs is a complex system, including different isoforms of ACE, different peptidases, and finally different angiotensin I-derived peptides that act on various receptor subtypes again. This will not be discussed in this review but has recently been summarized [1]. In the context of calcium regulation, Ang II seems to be the most important peptide among the different angiotensin I-derived peptides. It induces the release of aldosterone from the adrenal cortex and therefore it indirectly favours urinary and faecal calcium extrusion. Thus, patients with heart failure are at an increased risk of hypocalcaemia. This fall of calcium levels is detected by the calcium(-sensing) receptor (CaSR) of the parathyroidea that results in an increased release of PTH (Fig. **1**). But what is the evident that patients with heart failure develop indeed hypocalcaemia? In blood samples from patients with chronic heart failure a linear correlation exists between the concentration of ionized calcium and the NYHA classification of the patients [2]. This indicates that hypocalcaemia is indeed present in severely ill patients with chronic heart failure (Fig. **2**). Ionized calcium directly modifies pacemaker activity in the heart and it is a key player in excitation-contraction coupling in cardiomyocytes [3-5]. We could recently show that reducing extracellular calcium to values depicted in the plasma of patients with chronic heart failure in the NYHA classification IV directly reduced the contractile performance of cardiomyocytes underlining the relevance of small changes in extracellular calcium for heart function [6]. Lower ionized calcium levels in patients with heart failure seem to be a common finding. In African-Amercian patients hospitalized with chronic heart failure lower ionized calcium levels were measured [7]. Noteworthy, Carlstedt *et al*. [8] found a significant difference in ionized calcium between patients in the emergency department that survived and those that did not survive. Patients that did not survive had again lower ionized plasma levels. Although hypocalcaemia is not restricted to patients with heart failure in an emergency department, patients with acute myocardial infarct and heart failure represented the most remarkable subgroup. Again, severity of illness and survival were related to less ionized calcium. Of

*Address correspondence to this author at the Justus-Liebig-Universität Giessen, Germany, Physiologisches Institut, Aulweg 129, 35392 Giessen, Germany; Tel: +49 641 99 47 212; Fax: +49 641 99 47 219;
E-mail: Klaus-Dieter.Schlueter@physiologie.med.uni-giessen.de

1876-5351/10

note is the observation that the use of loop diuretics further improves the excretion of calcium and thereby will intensify the problem. The importance of lost minerals in heart failure has recently been reviewed [9].

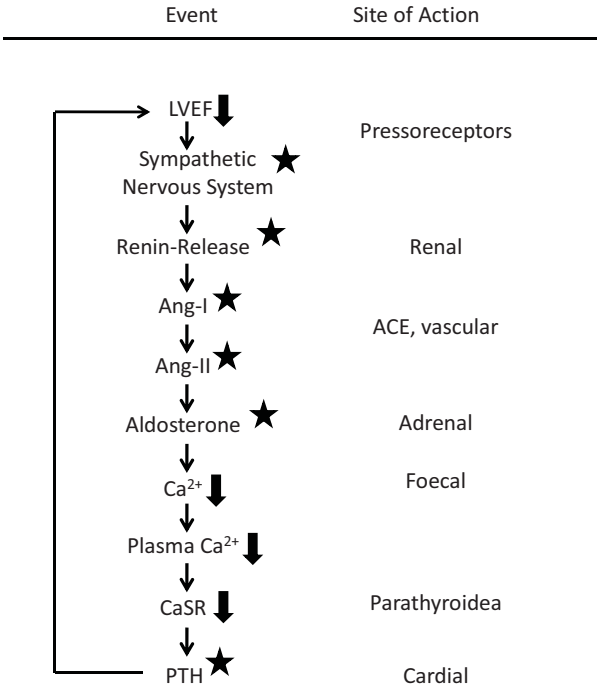

Fig. (1). Event sequence and localization of events involved in neurohumoral changes that influence systemic calcium handling. LVEF = left ventricular ejection fraction; *, indicates activation or induction; arrows indicate release or fall of the corresponding parameter.

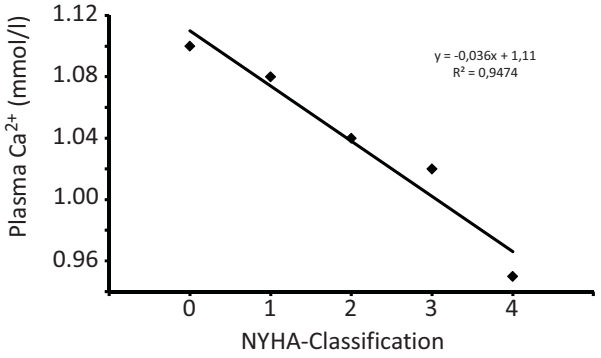

Fig. (2). Association between plasma ionized calcium and NYHA classification in patients with heart disease (data depicted from Aralkelyan *et al*., 2007).

Similar to the above mentioned relationship between NYHA classification and loss of ionized plasma calcium, plasma ionized calcium levels also fall in aldosterone treated rats [10]. These rats seem to represent a reasonable model to study the effect of plasma calcium deregulation on heart failure. The data on aldosterone treated rats suggest that the loss of ionized plasma calcium in heart failure is indeed initiated by the alterations of the RAAS. However, direct evidence that plasma ionized calcium levels will be normalized again by the administration of aldosterone antagonists in patients with heart failure is still lacking. Unfortunately, many studies dealing with the relationship between calcium homeostasis and heart failure investigated total calcium but not ionized calcium levels and cannot address this question.

In summary, there is compelling evidence that reduced ionized calcium is common in patients with heart failure resulting in compensatory elevation of PTH. This has strong implications in cardiac function due to the interaction of calcium with the CaSR expressed in the parathyroidea but also in cardiomyocytes in which the CaSR contributes to calcium load of cardiomyocytes [11].

2. PTH LEVELS IN HYPERTENSION AND HEART FAILURE

Following the assumptions outlined in the previous chapter one must predict that patients with heart failure and lower levels of plasma ionized calcium develop an increased release of PTH from the parathyroidea. There are many studies that have addressed the question whether heart failure is associated with increased plasma PTH in clinical settings. In example, in the above mentioned study [7] serum PTH was elevated in all patients with chronic heart failure of four weeks or longer duration. In a small number of patients with chronic left ventricular dysfunction (EF <35%) PTH levels were above the normal range [12]. Surprisingly, patients with a combined treatment consistent of ACE inhibitors, loop diuretics (furosemide) and small-dose aldosterone antagonist spironolacton still had PTH levels above the normal range. Arakelyan *et al*. [2] reported about a correlation between plasma PTH and NYHA classification. Elevated PTH was also found in patients with end stage heart failure awaiting cardiac transplantation [13]. Of note, in heart failure patients PTH levels are not only elevated under basal conditions but PTH release under stress conditions is also depressed [14]. As PTH release is linked to the CaSR, a receptor directly contributing to cardiac performance, one must predict a defect in calcium handling in myocytes as well. The increase in PTH may be caused by aldosterone-dependent sodium retention, use of loop diuretics in such patients, or hypovitaminosis D as outlined later and reviewed in more detail before [15]. A very recently published analysis based on nearly 1,000 patients revealed that plasma PTH predicts cardiovascular mortality, even in individuals with PTH within the normal range [16]. Noteworthy, this holds after adjustment for established cardiovascular risk factors, indicating that PTH plays an independent role in cardiovascular disease.

Preliminary, PTH seems to play a major role in hypertension. A fall in plasma ionized calcium levels leads to more PTH release from the parathyroidea. In spontaneously hypertensive rats, the best investigated hypertensive model in respect to calcium deregulation, hypertension can be reduced by high-calcium diet or parathyroidectomy [17-19]. Moreover, administration of PTH is sufficient to reverse the effect of high calcium diet or parathyroidectomy [20]. Even administration of calcimimetics, acting on CaSRs of the parathyroidea, seems to attenuate high blood pressure *via* decreased PTH release [21]. It is nevertheless questionable whether dietary calcium uptake is sufficient to improve patients' outcome. In spontaneously hypertensive rats high

calcium diet normalized plasma ionized calcium levels and PTH levels, but did not alter the progression of hypertensive heart disease [22] or even did not normalize plasma ionized calcium levels [23]. High calcium intake may stimulate renin production in the kidney which in turn raises Ang II levels, another factor leading to heart failure [24-26]. In contrast to the association between PTH and hypertension, PTH acts as a vasodilator even in chronic hypertensive vessels [27]. It is well known that the expression of PTH receptors is regulated in a tissue-specific way. In spontaneously hypertensive rats, angiotensin II destabilizes PTH receptor transcripts and thereby down-regulates renal PTH receptors independent of the blood pressure in the kidney [28]. *Via* this mechanism, kidney perfusion is reduced and renin release increases as well as that of other renal hormones. Similarly, PTH receptor expression is dramatically decreased in folic-acid induced acute renal failure in rats [29]. However, in twenty patients with proven primary hyperparathyroidism only a weak correlation between PTH and plasma renin activity was found [30]. On the other hand, patients with primary hyperparathyroidism display higher plasma renin activity at least in those subgroups that developed hypertension [31]. It has been assumed that the effect on renin release overrides the potential blood pressure lowering effect of PTH observed in peripheral vessels.

In summary, the data on spontaneously hypertensive rats and on patients with primary hyperparathyroidism suggest a possible relationship between PTH, kidney-derived down-regulated PTH receptors, and increased plasma renin activity. Another mechanism by which PTH acts on kidneys and influences electrolyte balance and thereby indirectly blood pressure and favours heart failure is by induction of glomerular hyperfiltration. Down-regulation of PTH receptors in the kidney will produce vasoconstriction.

3. DIRECT CARDIAC EFFECTS OF PTH

Cardiovascular effects of PTH have been recognized as early as the early 80ths of the last century [32]. Since that the role of excessive PTH on cardiac cells under conditions such as secondary hyperparathyroidism has been addressed. In general it has been accepted from such studies that excessive PTH has a direct deleterious effect on cardiomyocytes. As cardiovascular complications are the main secondary effect of secondary hyperparathyroidism it seems reasonable to assume that PTH acts directly on cardiomyocytes thereby influencing hypertrophic growth control, contractile responsiveness, and energy metabolism [33-35]. As a main finding of these studies, PTH was identified as a factor that increases calcium load and activates phospolipase C-dependent pathways. However, an unsolved problem was still to explain why these cells should express a PTH receptor. The identification of sister-peptides such as parathyroid hormone-related peptide (PTHrP), and moreover the observation that PTHrP is synthesised and released from microvascular coronary cells in the heart, suggests that PTHrP acts in a paracrine matter on cardiomyocytes. The observed cardiac effects of PTH on cardiomyocytes are then attributed to the structural homology between PTH and PTHrP allowing both peptides to act on the same receptor. This explains the responsiveness of cardiomyocytes to PTH. However, a correlation between PTH and cardiovascular events as described above requires PTH effects at concentrations much below the levels found in patients with secondary hyperparathyroidism. Therefore, the question about the role for PTH in heart failure in patients without secondary hyperparathyroidism was still obscure. Only recently two distinct ways of receptor-ligand interaction were described for PTH on cardiomyocytes. PTH displays two functional domains in its N-terminal part that is represented by the amino acids 1-34. *Via* the first six amino acids PTH binds to a Gαs-coupled PTH receptor of cardiomyocytes and activates adenylyl cyclase. In principle this should result in an increase of calcium influx that promotes cardiac function. However, at physiological or high-physiological extracellular calcium concentrations extracellular ionized calcium does not only move into the cell but also binds to cardiac CaSRs and activates them. CaSRs have been shown to adversely affect the activation of PTH receptors [36]. Therefore, as higher the extracellular calcium concentration is as less effective are PTH-dependent effects on cell shortening. A drop in ionized calcium results in less calcium influx and less activation of CaSRs. Therefore, PTH can now compensate for the loss of calcium influx by lower calcium concentrations (Fig. **3**). Moreover, PTH down-regulates CaSRs and therefore further potentiates its effect on cardiac performance at low extracellular ionized calcium [6]. As a consequence, PTH compensates for the lower plasma ionized calcium levels. Noteworthy, this occurs at very low concentrations of PTH that are not sufficient to improve cell function in a direct way comparable to other Gαs-activating agonists such as norepinephrine [37].

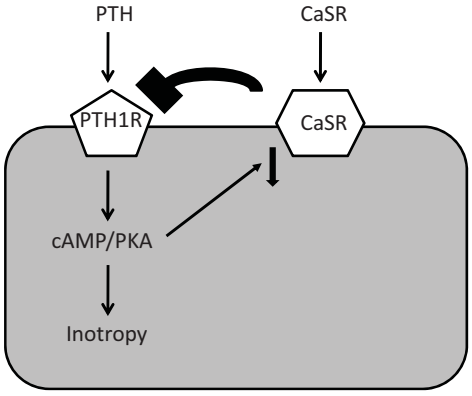

Fig. (3). Interaction of PTH receptors and CaSRs on cardiomyocytes. Normal plasma calcium leads to a CaSR-dependent inhibition of PTH signalling, while activation of PTH receptors will down-regulate CaSR and thereby intensify its action on inotropy.

PTH displays another functional domain in its first 34 amino acids, namely that covered by amino acids 28-32. *Via* these amino acids PTH activates Gαq-coupled PTH receptors that trigger activation of phospholipase C and subsequently that of protein kinase C [38]. This activation requires higher concentrations of PTH than that responsible for the effects on cell shortening *via* cAMP/PKA. It is linked to induction of protein synthesis thereby inducing cardiac hypertrophy. It is most likely that this mechanism contributes to cardiac side effects seen in patients with primary hyperparathyroidism which is associated with increased prevalence of left ventricular hypertrophy independent of blood pressure [39]. PTH also plays an important role in secondary hyperparathyroidism. This is a clinical relevant problem as patients with

heart failure and renal failure display a poor prognosis compared to patients with heart failure alone (reviewed by [40]). Renal failure requiring hemodialysis is associated with an increased risk of secondary hyperpararthroidism. The severity of secondary hyperparathyroidism in chronic renal insufficiency is associated with cardiovascular disease. PTH was associated with myocardial infarction and congestive heart failure in these patients [41]. A case report on 52-year-old women with secondary hyperparathyroidism and left ventricular dysfunction showed a marked improvement of left ventricular function after parathyroidectomy indicating the contribution of PTH in left ventricular dysfunction [42]. Similarly, in a cohort study on patients with primary hyperparathyroidism patients who underwent surgery had a lower prevalence of acute myocardial infarction and stroke and mortality was lower [43]. On the other hand, regression of left ventricular hypertrophy in patients on high-flux haemodialysis did not occur when PTH levels remained above 300 pg/ml [44]. All these data argue for a main role of PTH in left ventricular hypertrophy and dysfunction in patients with hyperparathyroidism.

But how can we explain the difference between cAMP/PKA- and PKC-dependent effects in a mechanistic way? PTH-receptors are G-protein coupled receptors belonging to the same receptor family as calcitonin gene related peptides. This receptor superfamily is characterized by an interaction between receptors and so-called receptor associated modifying proteins (RAMPs). Calcitonin gene-related peptide (CGRP) receptors are prominent members of this superfamily. In those receptors, RAMPs decide about the affinity to CGRP, adrenomedullin, and intermedin (=adrenomedullin 2). It may be that the coupling of PTH receptors to either Gαs or Gαq depends on the interaction between PTH receptor molecules and different RAMPs. For CGRP it has been shown that this results in a concentration-dependent increase or decrease of cell shortening on cardiomyocytes [45]. Of note, expression of RAMP isoforms is changed in rats with chronic heart failure thereby changing ligand-dependent receptor activation under these conditions [46].

Stimulation of PTH receptors results in a different inotropic responsiveness in adult versus young rats [47]. Interestingly, in most of the aforementioned studies patients were rather old and in these patients a close relationship between PTH and heart failure was found. One may speculate that PTH compensates for variations in ionized calcium concentrations in young individuals but that the same mechanism contributes to heart failure in elder individuals. It may also be that this different behaviour depends on alterations in RAMP proteins. However, this hypothesis requires future studies to be verified and is a pure speculation drawn from present studies at the moment.

The regulation of PTH receptors in cardiomyocytes has not been analyzed so far in deep. Given the known role of PTH and PTH signalling in heart failure it is of emerging interest to understand the regulation of receptor expression and coupling. Most recently, it was found that the regulation of cardiac rather than vascular PTH receptors is of particular relevance in postmenopausal females. Nitric oxide (NO) deficiency leads to a down-regulation of PTH receptors [48]. Oestrogen contributes significantly to the local generation of NO. Consequently, ovariectomized rats had a nearly 40% lower left ventricular steady state mRNA level of PTH receptors and this deficit could be nearly normalized by oestrogen supplementation. Keeping in mind that PTH receptors act different in hearts from old or young rats these data can be seen again as a compensatory down-regulation of PTH receptors in elder individuals. Noteworthy, hormone-replacement-therapy in post-menopausal women has unexpectedly been combined with increased cardiovascular events although oestrogen should be cardioprotective [49]. A possible explanation may be that down-regulation of PTH receptors in elder hearts is a compensatory mechanism and that replenished oestrogen pools increase its expression again.

4. INDIRECT CARDIAC EFFECTS OF PTH

Despite the effect of PTH on cardiomyocytes that has been addressed above, non-direct effects of PTH on cardiac performance must also be taken into consideration due to the strong correlation between PTH and heart failure. PTH acts on its classical targets such as kidney and bone. Special interest has been drawn to the effect of PTH on bone turnover with respect to cardiovascular function. PTH mobilizes the release of stem cells from the bone niche. In an infarct model, cardiac expression of SDF-1 is increased and this recruits more stem cells to the heart [50] (Zaruba *et al.*, 2008). In the presence of PTH in which more stem cells are mobilized from the bone niche, stem cell recruitment is optimized by a more intensive release of such cells from the bone marrow and a direction of such cells to the heart by SDF-1 (reviewed by [51]). It is still an open question at the moment to what extent such cells contribute to post-infarct remodelling and by which mechanisms. However, there is compelling evidence that PTH directly improves stem cell mobilization. Whether the moderate high PTH plasma levels in patients with heart failure are already sufficient to increase stem cell mobilization is nevertheless unclear.

Finally, PTH has vasodilatory properties that are independent of its effect on cardiomyocytes. PTH hyperpolarizes vessels and therefore reduces vascular resistances [52]. Whether a cAMP-dependent or NO-dependent effect contributes to its vasodilatory effect is not completely understood at present. By hyperpolarization of endothelial cells PTH can act even on cells with endothelial dysfunction due to a reduction of endothelial NO synthase activity. Although all experimental data on direct effects of PTH on peripheral resistances indicate a vasorelaxant effect of PTH the hormone is associated with high blood pressure. It is still unclear why PTH acting as a vasodilatory hormone contributes to high blood pressure. From the clinical point of view, however, it is important to note that PTH cannot compensate for the induction of high blood pressure under chronic conditions. Thus it remains unclear at the moment to what extent and under which conditions PTH modifies the peripheral resistances.

5. PTHrP IN HEART FAILURE

The identification of the formerly named hypercalcemia factor of malignancy as PTHrP and the discovery of a high structural similarity to PTH has greatly improved our understanding why cardiovascular cells express a receptor that responds to PTH and PTHrP. Cardiac PTHrP is synthesized

and released by endothelial cells [53]. This suggests that PTHrP acts as a paracrine factor in cardiac physiology. Indeed, the role of locally produced PTHrP in the vascular system has been established in transgenic mice that constitutively overexpress PTH receptors in smooth muscle cells and develop lower blood pressure [54, 55]. Furthermore, a decrease in blood pressure has been observed in adult rats with overexpression of PTH receptors in the vessels after i.v. delivery of PTH receptor cDNA [56]. It was found that PTHrP is locally up-regulated in a pressure-dependent manner and released by mechanical stress consistent with the role as a negative feedback mechanism to oppose the myogenic contractile response [57]. There are less studies dealing with plasma PTHrP levels and heart failure than those analyzing plasma PTH and heart failure. A direct comparison gave a strong increase of PTH and PTHrP in correlation to NYHA classification [2]. This can be explained in part related to a pressure-dependent release of PTHrP from endothelial cells. Of note, plasma PTHrP in females exceeded the values depicted in males. As one may assume from this observation, PTHrP expression is regulated at least in part in an oestrogen-dependent way [58]. Vascular PTHrP expression is down-regulated by TGF-β1 but left ventricular expression of PTH receptors seems to be up-regulated [59-61]. Therefore, in heart failure PTHrP is predominantly down-regulated by an increased expression of corresponding PTH receptors that is just the opposite of what is known from the kidney (Fig. **4**). Noteworthy, in contrast to the study mentioned above, in which an association between plasma PTHrP and NYHA classification was found, an inverse correlation between plasma PTHrP and NYHA classification was found as well [62]. The latter represents more closely the down-regulation of microvascular PTHrP in the heart although completely opposite results in two different studies do not allow any strong judgement at the moment. A problem with the different studies may be that PTHrP undergoes a strong posttranslational modification. Therefore, antibody-driven analysis might display different isoforms of PTHrP that lead to different results. It is nevertheless quite clear that increased myocardial PTHrP expression leads to a local release of PTHrP from the myocardium [57, 63]. Interestingly, TGF-β1 is induced in pressure-overloaded hearts at the transition from adaptive to mal-adaptive hypertrophy. Therefore in the chronic hypertensive heart a decrease in PTHrP expression is expected to be accompanied by an increased cardiac expression of PTH receptors and an increase in plasma PTH. This shifts the contribution of locally delivered PTHrP to PTH. If these alterations have any prediction in the scenario leading to heart failure than PTH and PTHrP must exert different effects on cardiac tissues. Indeed, despite a structural similarity between both peptides a detailed analysis of the structure-function relationship reveals strong differences.

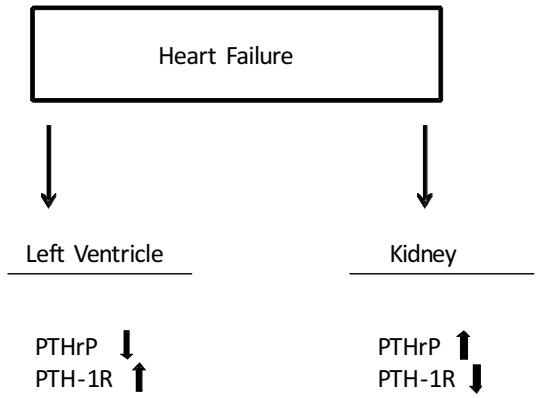

Fig. (4). Differential regulation of PTHrP and the corresponding receptor in the left ventricle and the kidney in patients with heart failure.

PTHrP also affects blood pressure control *via* renal mechanisms. In the kidney any increase in blood pressure increases PTHrP expression. However, renal PTHrP-dependent vasodilation is blunted in spontaneously hypertensive rats due to a down-regulation of the corresponding receptors. Furthermore, PTHrP is a potent stimulator of renin release by direct interaction with juxtaglomerular cells [64]. Modulation of renal PTHrP receptor expression in these rats increased renovascular responsiveness to PTHrP but did not modify blood pressure due to a corresponding 60% increase in plasma renin activity [65].

6. CARDIOVASCULAR EFFECTS OF PTHrP

As mentioned above PTHrP and PTH share structural similarities in their N-terminal part leading to a similar binding to a common receptor and activation of similar pathways. However, PTHrP is a peptide formed in three different lengths in humans (1-139, 1-141, and 1-173) and is target of proteolytic cleavage and glycosylation. This high amount of post-translational modification leads to the formation of various locally produced peptide variants. Therefore, PTHrP and PTH display significant different physiological effects. In respect to their interaction with cardiomyocytes this means they have a different impact on inotropy and hypertrophic growth regulation. While PTH improves contractile performance of cardiomyocytes preferentially *via* its N-terminal part (amino acids 1-6) at picomolar concentrations in a non-acute way, PTHrP improves cardiomyocytes performance *via* a cAMP/PKA-dependent pathway involving amino acids 6-11 in a more acute way at higher concentrations [6, 66]. Further, PTH exerts a positive hypertrophic effect *via* its PKC-activating domain covering amino acids 28-32, while a PKC-activating domain of PTHrP is located at amino acid 107-111 and therefore be represented by a C-terminal degradation peptide, known as osteostatin [66]. It is still an open field to identify those *in vitro* effects that are the most relevant *in vivo*. In terms of acute regulation of inotropy, cardiomyocytes seem to be more sensitive to PTHrP than to PTH. However, long-term effects might be more effectively evoked by PTH than by PTHrP.

In respect to vascular effects of either PTH or PTHrP, PTHrP differs from PTH because it exerts paracrine and intracrine effects whereas PTH acts as an endocrine factor. The intracrine effect of PTHrP depends on an active nuclear location site (NLS) represented by amino acids 87-107. Therefore, PTHrP unlike PTH can influence smooth muscle cell proliferation *via* receptor-dependent and receptor-independent effects. Interestingly, the effect of PTHrP on smooth muscle cell proliferation evoked by receptor-dependent processes is opposed by its intracrine effects [67]. Therefore, PTHrP plays a complex role in the progression of atherosclerotic plaques, yet not fully understood. Similarly, PTHrP acts on endothelial cells which represent the main

source of the peptide in the heart [52, 60, 68]. There is some evidence that PTHrP can enter the nucleus of endothelial cells as well, however, a precise role for this intracrine activity on endothelial growth and apoptotic signalling has not been described. Further, PTH unlike PTHrP can bind to and activate at least two different receptor subtypes (PTH-1 receptor and PTH-2 receptor) that influence agonist-dependent signalling in a contradictory matter [69]. Therefore, the question whether PTHrP controls basal blood pressure is at least dependent on the ratio between expressions of both receptor subtypes.

Finally, it should be mentioned that another member of this peptide family acts on PTH receptor subtypes, namely tuberoinfundibular peptide of 39 amino acids (TIP39). The latter one is known to influence inotropy of the heart *via* PTH-2 receptors and seems to be the physiological agonist of this receptor rather than PTH [70]. Whether this represents a redundant system to maintain normal pump function or whether it plays a genuine role in heart failure is not clear at present and requires additional research.

7. VITAMIN D, SYSTEMIC CALCIUM REGULATION, AND HEART FAILURE

The aforementioned increase in plasma PTH is initiated by a fall in plasma ionized calcium. Reduced levels of vitamin D, specifically of the most active vitamin D metabolite, 1,25-dihydroxyvitamin D3 or calcitriol, are common in patients with heart failure [71-73]. It is reasonable to assume that low vitamin D status contributes to low levels of plasma ionized calcium. In spontaneously hypertensive rats, vitamin D3 normalized plasma ionized calcium levels [74]. Furthermore, as vitamin D3 is a negative regulator of renin production its lower availability is associated with an activation of the RAAS [24]. However, vitamin D-receptor ablation in knockout mice (VDRKO mice) was not accompanied by elevated plasma renin levels, possibly because mice and rats display a different regulation of renin formation [75]. Alternatively, vitamin D3 may exert cardiac effects *via* an inhibition of leptin synthesis. The latter observation might be of cardiovascular relevance because cardiovascular cells express leptin receptors. Noteworthy, vitamin D treatment reduced cardiac hypertrophy in SHHF (cp/+) rats [76]. It has been proposed that low vitamin D status is caused by lower outdoor activity of patients with heart failure [77]. This hypothesis is supported by studies such as those that observed seasonality in heart failure deaths and total cardiovascular deaths in Australia [78]. However, vitamin D is added to many nutrients and it is questionable whether low outdoor activity is indeed responsible for low vitamin D levels in patients with heart failure. As mentioned above, renal expression of PTH receptors is lower in chronic hypertensive patients. Therefore, PTH-mediated renal formation of 1,25-dihydroxyvitamin D3 might also be impaired. Alternatively, a genetic abnormality of the hepatic 25-hydroxylase activity has been described as a reason for hypovitaminosis D [79]. Nevertheless, lower vitamin D impairs calcium uptake and contributes to the fall in plasma ionized calcium. Therefore, low vitamin D is associated with already mentioned effects of lower calcium and higher PTH on cardiovascular cells. Despite these effects, vitamin D deficiency is associated with altered cardiac function and hypertension in rat models that are independent of any effects on calcium homeostasis [80]. Furthermore, cardiac myocytes express functionally coupled vitamin D receptors [81]. Vitamin D affects directly contractile performance of cardiomyocytes in a PKC-dependent mechanism that leads to a phosphorylation of phospholamban and troponin I [82]. Although a direct comparison between effects of vitamin D on cardiovascular cells and effects linked to lower calcium uptake has not been worked out, it is reasonable to assume that vitamin D modifies cardiovascular physiology at different levels. Based on the aforementioned physiological activities of vitamin D3 it has been suggested that vitamin D deficiency is an underestimated non-classical risk factor for cardiovascular disease, specifically in patients with chronic kidney disease [83]. There is also some clinical evidence that vitamin D and calcium diet decreases inflammatory markers in patients with heart failure although a subsequent follow-up of this study did not further indicate an additive effect of vitamin D on calcium diet [84, 85].

8. ALDOSTERONE AND SYSTEMIC CALCIUM REGULATION IN HEART FAILURE

Aldosterone is part of the endocrine deregulation that is associated with left ventricular dysfunction because it is linked to the renin-angiotensin system. Classical endocrine effects of aldosterone are focussed on the kidney where the mineralocorticoid hormone aldosterone improves sodium retention and thereby volume regulation. The additional effect on calcium and magnesium secretion has been mentioned before [10]. Of note, loop diuretics exaggerate the losses of calcium and magnesium evoked by aldosterone and therefore increase electrolyte deregulation independent of direct cardiovascular effects evoked by aldosterone [86]. Aldosteronism is coupled to secondary hyperparathyroidism as the loss of ionized calcium increases PTH release, that favours cell uptake of calcium associated with altered function of target cells such as cardiomyocytes [34] and peripheral blood mononuclear cells [87]. As a consequence aldosteronism leads to cardiac oxi/nitrosative stress and a proinflammatory phenotype [15]. Despite this, aldosterone has direct effects on cardiomyocytes. In an acute way aldosterone modifies contractile responsiveness but also as a long-term effect [88]. *In vivo* the endocrine and cardiovascular effects lead to an improvement of fibrosis in hearts adding another risk factor to the long-term prognosis. In the light of these experimental data, aldosterone antagonism has been introduced into clinical practice and is now part of advanced pharmacotherapy in patients with heart failure. Of note, the concentration of aldosterone used during *in vitro* studies is far above the levels found *in vivo*. However, conclusions drawn from such experiments have lead to the introduction of aldosterone antagonism in clinical practice and lead to a significant reduction in total mortality and mortality linked to cardiovascular events. Therefore, the non-physiological high concentration of aldosterone used in these *in vitro* studies is properly linked to the experimental system but does not exclude these studies from (patho)physiological relevance per se.

CONCLUSIVE REMARKS

Calcium deregulation is commonly found in patients with heart failure. This is associated with deregulation of calcium homeostatic controlling hormones, such as PTH and vitamin

D, a deregulation of the corresponding receptor expression and signalling, and direct and indirect effects of such hormones on cardiovascular cells. Although deregulation can be observed at different levels, PTH and plasma ionized calcium concentration seem to have an outstanding role specifically in the elderly. As these mechanisms are linked to classical neurohumoral regulatory circuits that control cardiovascular physiology, a better understanding of the molecular and cellular effects under physiological and pathophysiological conditions seems to be a key to improve our current pharmacotherapy of patients with heart failure that have still a poor prognosis.

REFERENCES

[1] Schlüter KD, Wenzel S. Angiotensin II: A hormone involved in and contributing to pro-hypertrophic networks and target of anti-hypertrophic cross-talks. Pharmacol Ther 2008; 119: 311-25.

[2] Aralkelyan KP, Sahakyan YA, Hayrapetyan LR, *et al*. Calcium-regulating peptide hormones and blood electrolyte balance in chronic heart failure. Regul Pept 2007; 142: 95-100.

[3] Cleemann L, Morad M. Role of Ca^{2+} channel in cardiac excitation-contraction coupling in the rat: evidence from Ca^{2+} transients and contraction. J Physiol 1991; 432: 283-312.

[4] Levi AJ, Brooksby P, Hancox JC. One hump or two? The triggering of calcium release from the sarcoplasmatic reticulum and the voltage dependence of contraction in mammalian cardiac muscle. Cardiovasc Res 1993; 27: 1743-57.

[5] Wang SQ, Song LS, Lakatta EG, Cheng H. Ca^{2+} signalling between single L-type Ca^{2+} channels and ryanodine receptors in heart cells. Nature 2001; 410: 592-6.

[6] Tastan I, Schreckenberg R, Mufti S, Abdallah Y, Piper HM, Schlüter KD. Parathyroid hormone improves contractile performance of adult rat ventricular cardiomyocytes at low concentrations in a non-acute way. Cardiovasc Res 2009; 82: 77-83.

[7] Laguardia SP, Dockery BK, Bhattacharya SK, Nelson MD, Carbone LD, Weber KT. Secondary hyperparathyroidism and hypovitaminosis D in African-Americans with decompensated heart failure. Am J Med Sci 2006; 332: 112-8.

[8] Carlstedt F, Lind L, Wide L, *et al*. Serum levels of parathyroid hormone are related to the mortality and sensitivity of illness in patients in the emergency department. Eur J Clin Invest 1997; 27: 977-81.

[9] Newman KP, Neal MT, Roberts M, Goodwin KD, Hatcher EA, Bhattacharya SK. The importance of lost minerals in heart failure. Cardiovasc Hematol Agents Med Chem 2007; 5: 295-9.

[10] Chhokar VS, Sun Y, Bhattacharya SK, *et al*. Hyperparathyroidism and the calcium paradox of aldosteronism. Circulation 2005; 111: 871-8.

[11] Tfelt-Hansen J, Hansen JL, Smajilovic S, Terwilliger EF, Hanso S, Seikh SP. Calcium receptor is functionally expresses in rat neonatal ventricular cardiomyocytes. Am J Physiol 2006; 290: H1165-71.

[12] Khouzam RN, Dishmon DA, Farah V, Flax SD, Carbone LD, Weber KT. Secondary hyperparathyroidism in patients with untreated and treated congestive heart failure. Am J Med Sci 2006; 331: 30-4.

[13] Lee AH, Mull RL, Keenan GF, *et al*. Osteoporosis and bone morbidity in cardiac transplant recipients. Am J Med 1994; 96: 35-41.

[14] Stefanelli T, Pacher R, Woloszczuk R, Glogar D, Kaindl F. Parathyroid hormone and calcium behavior in advanced congestive heart failure. Zts Kardiol 1992; 81: 121-5.

[15] Sun Y, Ahokas RA, Bhattacharya SK, Gerling IC, Carbone LD, Weber KT. Oxidative stress in aldosteronism. Cardiovasc Res 2006; 71: 300-9.

[16] Hagström E, Hellman P, Larsson TE, *et al*. Plasma parathyroid hormone and the risk of cardiovascular mortality in the community. Circulation 2009; 119: 2765-71.

[17] Rao RM, Yan Y, Wu Y. Dietary calcium reduces blood pressure, parathyroid hormone, and platelet cytosolic calcium responses in spontaneously hypertensive rats. Am J Hypertension 1994; 7: 1052-7.

[18] Uchimoto S, Tsumura K, Kishimoto H, Yamashita N, Morii H. Implication of parathyroid hormone for the development of hypertension in young spontaneously hypertensive rats. Miner Electrolyte Metabol 1995; 21: 82-6.

[19] Mann JF, Wiecek, A, Bommer J, Ganten U, Ritz E. Effects of parathyroidectomy on blood pressure in spontaneously hypertensive rats. Nephron 1987; 45: 46-52.

[20] Kishimoto H, Tsuzmura K, Fujioka S, Uchimoto S, Morii H. Chronic parathyroid hormone administration reverses the anti-hypertensive effect of calcium loading in young spontaneously hypertensive rats. Am J Hypertension 1993; 6: 234-40.

[21] Rybczynska A, Boblewski K, Lehmann A, *et al*. Calcimimetic NPS R-568 induces hypotensive effect in spontaneously hypertensive rats. AMJ Hypertension 2005; 18: 364-71.

[22] Stern N, Lee DB, Silis V, *et al*. Effects of high calcium intake on blood pressure and calcium metabolism in young SHR. Hypertension 1984; 6: 639-46.

[23] McCarron DA, Yung NN, Ugoretz BA, Krutzik S. Distrubances of calcium metabolism in the spontaneously hypertensive rat. Hypertension 1981; 3: 1162-7.

[24] Li YC, Kong J, Wei M, Chen ZF, Liu SQ, Cao LP. 1,25-Dihydroxyvitamin D3 is a negative endocrine regulator of the renin-angiotensin system. J Clin Invest 2002; 110: 229-38.

[25] Sigmund CD. Regulation of renin expression and blood pressure by vitamin D3. J Clin Invest 2002; 110: 155-6.

[26] Petrov V, Lijnen P. Modification of intracellular calcium and plasma rennin by dietary calcium in men. Am J Hypertension 1999; 12: 1217-24.

[27] DiPette DJ, Christenson W, Nickols MA, Nickols GA. Cardiovascular responsiveness to parathyroid hormone (PTH) and PTH-related protein in genetic hypertension. Endocrinology 1992; 130: 2045-51.

[28] Welsch S, Schordan E, Coquard C, *et al*. Abnormal renovascular parathyroid hormone-1 receptor in hypertension: Primary defect or secondary to angiotensin II type 1 receptor actuivation? Endocrinology 2006; 147: 4384-91.

[29] Santos S, Bosch RJ, Ortega A, *et al*. Up-regulation of parathyroid hormone-related protein in folic acid-induced acute renal failure. Kidney Int 2001; 60: 982-95..

[30] Bernini G, Moretti A, Lonzi S, Bendinelli C, Miccoli P, Salvetti A. Renin-angiotensin-aldosterone system in primary hyperparathyroidism before and after surgery. Metabolism 1999; 48: 298-300.

[31] Gennari C, Nami R, Gonelli S. Hypertension and primary hyperprarthyroidsm: the role of adrenergic and renin-angiotensin-aldosterone systems. Miner Electrolyte Metab 1995; 21: 77-81.

[32] Bogin E, Massry SG, Harary I. Effect of parathyroid hormone on rat heart cells. J Clin Invest 1981; 67: 1215-27.

[33] Schlüter KD, Piper HM. Trophic effects of catecholamines and parathyroid hormone on adult ventricular cardiomyocytes. Am J Physiol 1992; 263: H1739-46.

[34] Smogorzewski M, Zayed M, Zhang Y-B, Roe J, Massry SG. Parathyroid hormone increases cytosolic calcium concentration in adult rat cardiac myocytes. Am J Physiol 1993; 264: H1998-2006.

[35] Baczynski R, Massry SG, Kohan R, Magott M, Saglikes Y, Brautbar N. Effect of parathyroid hormone on myocardial energy metabolism in the rat. Kidney Int 1985; 27: 718-25.

[36] Motoyama HI, Friedman PA. Calcium-sensing receptor regulation of PTH-dependent calcium absorption by mouse cortical ascending limbs. Am J Physiol 2002; 283: F399-406.

[37] Schlüter KD, Weber M, Piper HM. Parathyroid hormone induce protein kinase C but not adenylate cyclase in adult cardiomyocytes and regulates cyclic AMP levels *via* protein kinase C-dependent phosphosdiesterase activity. Biochem J 1995; 310: 439-44.

[38] Schlüter KD, Wingender E, Tegge W, Piper HM. Parathyroid hormone-related protein antagonizes the action of parathyroid hormone on adult cardiomyocytes. J Biol Chem 1996; 271: 3074-8.

[39] Andersson P, Rydberg E, Willenheimer R. Primary hyperparathyroidism and heart disease –a review. Eur Heart J 2004; 25: 1776-87.

[40] Rostand SG, Drüecke TB. Parathyroid hormone, vitamin D, and cardiovascular disease in chronic renal failure. Kidney Int 1999; 56: 383-92.

[41] De Boer IH, Gorodetskaya I, Young B, Hsu C-Y, Chertow GM. The severity of secondary hyperparathyroidms in chronic renal insuffiency is GFR-dependent, race-dependent, and associated with cardiovascular disease. J Am Soc Nephrol 2002; 13: 2762-9.

[42] Nagashima M, Hashimoto K, Shinsato T, *et al*. Marked improvement of left ventricular function after parathyroidectomy in a he-

madialysis patient with secondary hyperparathyroidism and left ventricular dysfunction. Circ J 2003; 67: 269-72.

[43] Vestergaard P, Mosekilde L. Cohort study on effects of parathyroid surgery on multiple outcomes in primary hyperparathyroidism. Br Med J 2003; 327: 530-5.

[44] Kong CH, Farrington K. Determinants of left ventricular hypertrophy and its progression in high-flux haemodialysis. Blood Purif 2003; 21: 163-9.

[45] Schlier A, Schreckenberg R, Abdallah Y, *et al*. CGRP-α responsiveness of adult rat ventricular cardiomyocytes from normotensive and spontaneously hypertensive rats. Eur J Cell Biol 2009; 88: 227-41.

[46] Cueille C, Pidoux E, de Vernejoul M-C, Ventura-Clapier R, Garel J-M. Increased myocardial expression of RAMP1 and RAMP3 in rats with chronic heart failure. Biochem Biophys Res Commun 2002; 2945: 340-6.

[47] Ross G, Schlüter KD. Cardiac-specific effects of parathyroid hormone-related peptide: Modification by aging and hypertension. Cardiovasc Res 2005; 66: 334-44.

[48] Schreckenberg R, Wenzel S, da Costa Rebelo RM, Röthig A, Meyer R, Schlüter KD. Cell-specific effects of nitric oxide deficiency on parathyroid hormone-related peptide (PTHrP) responsiveness and PTH1 receptor expression in cardiovascular cells. Endocrinology 2009; 150: 3735-41.

[49] Rossouw JE, Anderson GL, Prentice RL, *et al*. Risks and benefits of estrogen plus progestin in healthy postmenopausal women: principle results from the Women's Health Initiative randomized controlled trial. JAMA 2002; 288: 321-33.

[50] Zaruba MM, Huber BC, Brunner S, *et al*. Parathyroid hormone treatment after myocardial infarction promotes cardiac repair by enhanced neovascularization and cell survival. Cardiovasc Res 2008; 77: 722-31.

[51] Schlüter KD, Maxeiner H, Wenzel S. Mechanisms that regulate homing function of progenitor cells in myocardial infarction. Minerva Cardiol 2009; 57: 203-17.

[52] Abdallah Y, Ross G, Dolf A, Heinemann MP, Schlüter KD. N-terminal parathyroid hormone-related peptide hyperpolarizes endothelial cells and causes a reduction of the coronary resistance of the rat heart *via* endothelial hyperpolarization. Peptides 2006; 27: 2927-34.

[53] Schlüter KD, Katzer C, Frischkopf K, Wenzel S, Taimor G, Piper HM. Expression, release, and biological activity of parathyroid hormone-related peptide from coronary endothelial cells. Circ Res 2000; 86: 946-51.

[54] Maeda S, Sutliff RL, Qian J, *et al*. Targeted overexpression of parathyroid hormone-related protein (PTHrP) to vascular smooth muscle in transgenic mice lowers blood pressure and alters vascular contractility. Endocrinology 1999; 140: 1815-25.

[55] Qian J, Lorenz NJ, Maeda S, *et al*. Reduced blood pressure and increased sensitivity of the vasculature to parathyroid hormone-related protein (PTHrP) in transgenic mice overexpressing the PTH/PTHrP receptor in vascular smooth muscle cells. Endocrinology 1999; 140: 1826-33.

[56] Fritsch S, Lindner V, Welsch S, *et al*. Intravenous delivery of PTH/PTHrP type 1 receptor cDNA to rats decreases heart rate, blood pressure, renal tone, renin angiotensin system, and stress-induced cardiovascular response. Am J Soc Nephrol 2004; 15: 2588-600.

[57] Degenhardt H, Jansen J, Schulz R, Sedding D, Braun-Dulläus R, Schlüter KD. Mechanosensitive release of parathyroid hormone-related peptide from cornary endothelial cells. Am J Physiol 2002; 283: H1489-96.

[58] Grohé C, van Eickels M, Wenzel S, *et al*. Sex-specific differences in ventricular expression and function of parathyroid hormone-related peptide. Cardiovasc Res 2004; 61: 307-16.

[59] Wenzel S, Schorr K, Degenhardt H, *et al*. TGF-β1 downregulates PTHrP in coronary endothelial cells. J Mol Cell Cardiol 2001; 33: 1181-90.

[60] Conzelmann C, Krasteva G, Weber K, Kummer W, Schlüter KD. Parathyroid hormone-related protein (PTHrP)-dependent regulation of bcl-2 and tissue inhibitor of metalloproteinase (TIMP)-1 in coronary endothelial cells. Cell Physiol Biochem 2009; 24: 493-502.

[61] Monego G, Arena V, Pasquini S, *et al*. Ischemic injury activates PTHrP and PTH1R expression in human ventricular cardiomyocytes. Basic Res Cardiol 2009; 104: 427-34.

[62] Giannakoulas G, Karvounis H, Koliakos G, *et al*. Parathyroid hormone-related protein is reduced in severe chronic heart failure. Peptides 2006; 27: 1894-7.

[63] Ogino K, Omura K, Kinugasa Y, *et al*. Parathyroid hormone-related protein is produced in the myocardium and increased in patients with congestive heart failure. J Clin Endocrinol Metab 2002; 87: 4722-7.

[64] Saussine C, Massfelder T, Parnin F, Judes C, Simeoni U, Helwig JJ. Renin stimulating properties of parathyroid hormone-related peptide in the isolated perfused rat kidney. Kidney Int 1993; 44: 764-73.

[65] Massfelder T, Taesch N, Fritsch S, *et al*. Type 1 parathyroid hormone receptor expression level modulates renal tone and plasma renin activity in spontaneously hypertensive rats. J Am Soc Nephrol 2002; 13: 639-48.

[66] Schlüter KD, Weber M, Piper HM. Effects of PTH-rP(107-111) and PTH-rP(7-34) on adult cardiomyocytes. J Mol Cell Cardiol 1997; 29: 3057-65.

[67] Massfelder T, Dann P, Wu TL, Vasavada R, Helwig JJ, Stewart AF. Opposing mitogenic and anti-mitogenic actions of parathyroid hormone-related protein in vascular smooth muscle cells: a critical role for nuclear targeting. Proc Natl Acad Sci USA 1997; 94: 13630-5.

[68] Schorr K, Taimor G, Degenhardt H, Weber K, Schlüter KD. Parathyroid hormone-related peptide is induced by stimulation of α1A-adrenoceptors and improves resistance against apoptosis in coronary endothelial cells. Mol Pharmacol 2003; 63: 111-8.

[69] Ross G, Heinemann MP, Schlüter KD. Vasodilatory effect of tuberoinfundibular peptide (TIP39): Requirement of receptor desensitization and its beneficial effect in the post-ischemic heart. Peptides 2007; 28: 878-86.

[70] Ross G, Engel P, Abdallah Y, Kummer W, Schlüter KD. Tuberoinfundibular peptide of 39 residues: A new mediator of cardiac function *via* nitric oxide production in the rat heart. Endocrinology 2005; 146: 2221-8.

[71] Shane E, Mancini D, Aaronson K, *et al*. Bone mass, vitamin D deficiency, and hyperparathyroidism in congestive heart failure. Am J Med 1997; 103: 197-207.

[72] Zittermann A, Schleithoff SS, Tenderich G, Berthold HK, Korfer R, Stehle P. Low vitamin D status: a contributing factor in the pathogenesis of congestive heart failure. J Am Coll Cardiol 2003; 41: 105-12.

[73] Kim DH, Sabour S, Sagar UN, Adams S, Whellan DJ. Prevalence of hypovitaminosis D in cardiovascular diseases. Am J Cardiol 2008; 102: 1540-4.

[74] Hsu CH, Patel S, Young EW. Calcemic response to parathyroid hormone in spontaneously hypertensive rats: role of calcitriol. J Lab Clin Med 1987; 110: 682-9.

[75] Simpson RU, Hershey SH, Nibbelink KA. Characterization of heart size and blood pressure in the vitamin D receptor knockout mouse. J Steroid Biochem Mol Biol 2007; 103: 521-4.

[76] Mancouso P, Rahman A, Hershley SD, Dandu L, Nibbelink KA, Simpson RU. 1,25-Dihydroxyvitamin-D3 treatment reduces cardiac hypertrophy and left ventricular diameter in spontaneously hypertensive heart failure-prone (cp/+) rats independent of changes in serum leptin. J Cardiocvasc Pharmacol 2008; 51: 559-64.

[77] McCarty MF. Nutritional modulation of parathyroid hormone secretion may influence risk for left ventricular hypertrophy. Med Hypothesis 2005; 64: 1015-21.

[78] Barnett AG, De Looper M, Fraser JF. The seasonality in heart failure and total cardiovascular deaths. Aust NZ J Public Health 2008; 32: 408-13.

[79] Zittermann A, Schleithoff SS, Koerfer R. Vitamin D insufficiency in congestive heart failure: Why and what to do about? Heart Fail Rev 2006; 11: 25-33.

[80] Weishaar RE, Simpson RU. Vitamin D3 and cardiovascular function in rats. J Clin Invest 1987; 79: 1706-12.

[81] Walters MR, Ilenchuk TT, Claycomb WC. 1,25-Dihydroxyvitamin D3 stimulates 45Ca2+ uptake by cultured adult rat ventricular cardiac muscle cells. J Biol Chem 1987; 262: 2536-41.

[82] Green JJ, Robinson DA, Wilson GE, Simpson RU, Westfall MV. Calcitriol modulation of cardiac performance *via* protein kinase C. J Mol Cell Cardiol 2006; 41: 350-9.

[83] Levin A, Li YC. Vitamin D and its analogues: do they protect against cardiovascular disease in patients with kidney disease? Kidney Int 2005; 68: 1973-81.

[84] Schleithoff SS, Zittermann A, Tenderich G, Berthold HK, Stehle P, Koerfer R. Vitamin D supplementation improves cytokine profiles in patients with congestive heart failure: a double-blind, randomized, placebo-controlled trial. Am J Clin Nutr 2006; 83: 754-9.

[85] Schleithoff SS, Tittermann A, Tenderich G, Berthold HK, Stehle P, Koerfer R. Combining calcium and vitamin D supllementation is not superior to calcium supplementation alone in improving disturbed bone metabolism in patients with congestive heart failure. Eur J Clin Nutr 2008; 62: 1388-94.

[86] Law PH, Sun Y, Bhattacharya SK, Chhokar VS, Weber KT. Diuretics and bone loss in rats with aldosteronism. J Am Coll Cardiol 2005; 46: 142-6.

[87] Goodwin KD, Ahokas RA, Bhattacharya SK, Sun Y, Gerling IC, Webter KT. Preventing oxidative stress in rats with aldosteronism by calcitriol and dietary calcium and magnesium supplements. Am J Med Sci 2006; 332: 73-8.

[88] Wenzel S, Tastan I, Abdallah Y, Schreckenberg R, Schlüter KD. Aldosterone improves contractile function of adult rat ventricular cardiomyocytes in a non-acute way: potential relationship to the calcium paradox of aldostzeronism. Basic Res Cardiol 2010; 105(2): 247-56.

Received: September 29, 2009 Revised: October 30, 2009 Accepted: November 30, 2009

frontiers in Physiology

ORIGINAL RESEARCH
published: 03 August 2017
doi: 10.3389/fphys.2017.00556

Effects of 6-months' Exercise on Cardiac Function, Structure and Metabolism in Female Hypertensive Rats–The Decisive Role of Lysyl Oxidase and Collagen III

Rolf Schreckenberg[1], Anja-Maria Horn[1], Rui M. da Costa Rebelo[1], Sakine Simsekyilmaz[2], Bernd Niemann[3], Ling Li[1], Susanne Rohrbach[1] and Klaus-Dieter Schlüter[1]*

[1] Physiologisches Institut, Justus-Liebig-Universität Giessen, Giessen, Germany, [2] Institut für Pharmakologie und Klinische Pharmakologie, Universitätsklinikum Düsseldorf, Düsseldorf, Germany, [3] Klinik für Herz-, Kinderherz- und Gefäßchirurgie, Universitätsklinikum Giessen, Giessen, Germany

OPEN ACCESS

Edited by:
Jun Sugawara, National Institute of Advanced Industrial Science and Technology, Japan

Reviewed by:
Masaki Mizuno, University of Texas Southwestern Medical Center, United States
Risto Kerkela, University of Oulu, Finland

***Correspondence:**
Rolf Schreckenberg
rolf.schreckenberg@physiologie.med.uni-giessen.de

Specialty section:
This article was submitted to Exercise Physiology, a section of the journal Frontiers in Physiology

Received: *18 April 2017*
Accepted: *17 July 2017*
Published: *03 August 2017*

Citation:
Schreckenberg R, Horn A-M, da Costa Rebelo RM, Simsekyilmaz S, Niemann B, Li L, Rohrbach S and Schlüter K-D (2017) Effects of 6-months' Exercise on Cardiac Function, Structure and Metabolism in Female Hypertensive Rats–The Decisive Role of Lysyl Oxidase and Collagen III. Front. Physiol. 8:556. doi: 10.3389/fphys.2017.00556

Purpose: According to the current therapeutic guidelines of the WHO physical activity and exercise are recommended as first-line therapy of arterial hypertension. Previous results lead to the conclusion, however, that hearts of spontaneously hypertensive rats (SHR) with established hypertension cannot compensate for the haemodynamic stresses caused by long-term exercise. The current study was initiated to investigate the effects of aerobic exercise on the cardiac remodeling as the sole therapeutic measure before and during hypertension became established.

Methods: Beginning at their 6th week of life, six SHR were provided with a running wheel over a period of 6 months. Normotensive Wistar rats served as non-hypertensive controls.

Results: In Wistar rats and SHR, voluntary exercise led to cardioprotective adaptation reactions that were reflected in increased mitochondrial respiration, reduced heart rate and improved systolic function. Exercise also had antioxidant effects and reduced the expression of maladaptive genes (TGF-β1, CTGF, and FGF2). However, at the end of the 6-months' training, the echocardiograms revealed that SHR runners developed a restrictive cardiomyopathy. The induction of lysyl oxidase (LOX), which led to an increased network of matrix proteins and a massive elevation in collagen III expression, was identified as the underlying cause.

Conclusions: Running-induced adaptive mechanisms effectively counteract the classic remodeling of hearts subject to chronic pressure loads. However, with sustained running stress, signaling pathways are activated that have a negative effect on left ventricular relaxation. Our data suggest that the induction of LOX may play a causative role in the diagnosed filling disorder in trained SHR.

Keywords: arterial hypertension, aerobic exercise, cardiac function, lysyl oxidase, osteopontin, cardiac fibrosis, cardiac hypertrophy

INTRODUCTION

Arterial hypertension is of central importance as a direct risk factor for the development of numerous cardiovascular diseases. A number of primary and secondary risk factors are also indirectly responsible for a deterioration in the cardiovascular risk profile due to an increase in blood pressure (BP). Accordingly, there is a clear need for systematic antihypertensive therapy for the prevention of cardiovascular events and sequelae.

The current therapy guidelines from the WHO and the German Hypertension League recommend physical activity and sport as the first-line therapy—without, however, specifying individual therapy plans (Chobanian et al., 2003; WHO, 2003; Deutsche Hochdruckligae, 2008). Unlike drug intervention, there is little information available regarding the effects of physical activity and sport on the cardiovascular system in cases of existing hypertension (Schlüter et al., 2010).

The results of a number of studies based on animal experiments suggest that senescent rats with established hypertension do not compensate for additional running-induced hemodynamic stresses and therefore cannot benefit from the associated cellular adaptation mechanisms (Schultz et al., 2007; da Costa Rebelo et al., 2012). Prominent among the clinical and pathomorphological results of these studies is significant cardiac fibrosis, which primarily affects relaxation and thus diastolic function. Massive performance-induced myocardial hypertrophy and reduced calcium handling also lead to a detrimental functional and structural remodeling of the hearts. The stimulation of the sympathetic nervous system with subsequent activation of the renin-angiotensin system (RAAS) as well as induction of pro-fibrotic mediators such as transforming growth factor-β (TGF-β) and biglycan are largely responsible for these effects (O'Keefe et al., 2012; van de Schoor et al., 2016).

On the other hand, there are results that can be viewed as desirable adaptation reactions to aerobic endurance training: past studies have described the induction of antiapoptotic genes (Lajoie et al., 2004), improved mitochondrial respiration (Chicco et al., 2008), a reduction in free radicals (Bertagnolli et al., 2006), as well as a significant reduction in resting heart rate (HR) (Lee et al., 2006).

The precise circumstances and causes that have led to these heterogeneous results in the various hypertensive animal models are the subject of our research. Consequently, it is not yet possible to make concrete statements about the factors or mechanisms that determine the therapeutic success of endurance training and sport in patients with hypertension (Thompson et al., 2007).

Abbreviations: Ang-II, Angiotensin II; ANP, atrial natriuretic peptide; BP, blood pressure; BW, body weight; Col-I, collagen I; Col-III, collagen III; CTGF, connective tissue growth factor; DHE, dihydroethidium; EF, ejection fraction; FGF2, fibroblast growth factor-2; FS, fractional shortening; HR, heart rate; IHD, ischaemic heart disease; LOX, lysyl oxidase; LV, left ventricle; NAC, N-acetyl-L-cystein; Nrf-1, nuclear respiratory factor-1; OPN, osteopontin; $O_2^{-\bullet}$, superoxide; PGC-1α, peroxisome proliferator activated receptor gamma coactivator-1α; RAAS, renin-angiotensin system; SHR, spontaneously hypertensive rat; TGF-β1, transforming growth factor-β1; TL, tibia length.

To what extent physical training alone contributes to a fall in BP or prevents the development of arterial hypertension is still largely unknown (Pagan et al., 2015; Sharman et al., 2015).

In a prospective study, Allesøe et al. determined the risk of 12,093 female volunteers developing ischaemic heart disease (IHD) under the combined influence of physical activity and arterial hypertension. Hypertensive patients who completed a high level of daily physical activity had a three-fold higher risk of developing IHD but the underlying pathological mechanisms are unclear (Allesøe et al., 2016).

Our current project is primarily aimed at investigating the effects of a 6-months' running wheel training program on the cardiac remodeling of young, 1½-month-old spontaneously hypertensive rats (SHR) before and during hypertension became established.

Accordingly, the following hypothesis was formulated: Starting the physical training at a time when no hypertension-induced structural and metabolic dysfunctions are yet observed in the cardiovascular system should counteract the development of hypertension as a result of intact adaptation mechanisms and should thus have a long-term positive effect on the functional and structural remodeling of the hearts.

In addition to hypertrophy, the characteristic findings for the left ventricular myocardium that is subject to chronic pressure loads in SHR include excess production of radicals and remodeling of the extracellular matrix with the involvement of TGF-β, lysyl oxidase (LOX) and structure-forming proteins (Rysä et al., 2005; Brooks et al., 2010).

Training data such as the distance and time run and the speed were recorded continuously throughout the experiment; any changes in the systolic and diastolic BP and the HR were also recorded.

We have been able to show for the first time that endurance training has a positive effect on the classic remodeling of a heart that has been subject to a chronic pressure load but over the long term this adaptive response causes a massive induction of LOX through alternative signaling pathways, which results in a clinically relevant filling disorder of the left ventricular myocardium.

MATERIALS AND METHODS

The investigation conforms the Guide for the Care and Use of Laboratory Animals published by the US National Institute of Health (NIH Publication No. 85–23, revised 1996). The study was approved by the local authorities for animal experiments (V54–19c 2015h 01 GI 20/1 No. 77/2014).

Animals and Exercise Model

At the start of the 6th week of life, 6 female SHR were provided with a running wheel over a period of 6-months'. Normotensive female Wistar rats were used as non-hypertensive controls and were also allocated to 6 cages with running wheels. Both groups were supplemented by corresponding "non-running" control groups that were kept under identical conditions without access to running wheels.

The health status of the experimental animals was determined weekly using a "distress score" (Lloyd and Wolfensohn, 1999). Over the entire experimental period no animals had to be eliminated from the experiment based on the exclusion criteria of the score.

Determination of the BP and HR

The systolic and diastolic BP and the HR were initially measured weekly and then subsequently every 2 or 4 weeks using non-invasive tail-cuff BP measurement. Prior to the start of the experiment the animals were adjusted to the experimental procedure over a week. The median of 10 consecutive measurements was calculated for each parameter described.

Preparation of the Heart

At the end of the experimental period rats were anesthetized by isoflurane inhalation. After cervical dislocation hearts were isolated and perfused in Langendorff technique to remove blood contamination.

RNA Isolation and Real Time RT-PCR

Total RNA was isolated from left ventricular tissue using peqGold TriFast (peqlab, Biotechnologie GmbH, Germany) according to the manufacturer's protocol. To remove genomic DNA contamination, isolated RNA samples were treated with 1 U DNase/µg RNA (Invitrogen, Karlsruhe, Germany) for 15 min at 37°C. One µg of total RNA was used in a 10 µl reaction to synthesize cDNA using Superscript RNaseH Reverse Transcriptase (200 U/µg RNA, Invitrogen, Karlsruhe, Germany) and oligo dTs as primers. RT reactions were performed for 50 min at 37°C. Real-time quantitative PCR was performed using MyiQ® detection system (Bio-Rad, Munich, Germany) in combination with the iTaq Universal SYBR Green Real-Time PCR Supermix (Bio-Rad, Munich, Germany). Quantification was performed as described before (Livak and Schmittgen, 2001). Primer sequences are listed in Supplementary Table 1.

Picrosirius Red Staining

Samples were embedded with Tissue-Tek® (Sakura, Alphen, Netherlands) and sectioned in 10 µm slices. Histological sections were fixed in Bouin solution and subsequently stained in 0.1% (wt/vol) Sirius red solution (Sigma-Aldrich Chemie, Steinheim, Germany). Sections were washed by 0.01 N HCl, Aqua dest. and counterstained for nuclei by Mayers hemalaun solution, washed with Aqua dest. for 5 min and dehydrated with ethanol. Finally, histological slices were visualized under light microscopy. Total collagen content was quantified by digital image analysis using Leica Confocal Software Lite Version (LCS Lite). The mean of $n = 6$ preparations was used to quantify the extent of interstitial fibrosis.

Microrespirometry

Immediately before oxygraphic measurements muscle fibers were permeabilized 30 min with saponin. After permeabilization the fibers were washed to remove saponin and adenine nucleotides. We used the high-resolution OROBOROS® oxygraph, a two chamber respirometer with a Peltier thermostat and integrated electromagnetic stirrers. The measurements were performed at 30°C in 1.42 ml incubation medium using different substrates: 10 mM pyruvate + 2 mM malate and 10 mM succinate + 5 µM rotenone. The weight specific oxygen consumption was calculated as the time derivative of the oxygen concentration (DATGRAPH Analysis software, OROBOROS®). The rate of state 3 respiration was determined following the addition of 5 mM ADP. State 4 respiration was measured after the addition of 1.8 mM atractyloside. The respiratory control index was calculated as ratio between state 3 to state 4 respiratory rates for each addition of ADP. For the analysis of uncoupled respiration, 2,4-dinitrophenol was added in a two-step titration up to 60 µM. The difference between atractylate-and antimycin A respiration (45 µM antimycin A) indicates the leak respiration (Niemann et al., 2010).

Measurement of Superoxide ($O_2^{-\bullet}$)

To perform DHE staining, cryosections of the left ventricle (LV) were incubated with DHE (dissolved in 1 X PBS) for 10 min at 37°C in a light-protected humidity chamber, then fixed with Dako Fluorescent Mounting Medium (Dako, North America Inc., USA). Slides were imaged by fluorescence microscopy (LSM 510 META; Carl Zeiss, Jena, Germany) using an excitation wavelength of 488 nm; emission was recorded at 540 nm (Nazarewicz et al., 2013). Analysis was performed by digital image analysis using Leica Confocal Software Lite Version (LCS Lite). The mean fluorescence intensity of $n = 4$ ventricles was used to quantify the extent of $O_2^{-\bullet}$.

Western Blot

Total protein was extracted from LV using RIPA Buffer (Cell Signaling, Danvers, MA, USA) according to the manufacturer's protocol. Briefly, the homogenate was centrifuged at 14,000 g at 4°C for 10 min and supernatant was treated with Laemmli buffer (Sigma-Aldrich, Taufkirchen, Germany). Protein samples were loaded on NuPAGE Bis-Tris Precast gels (10%; Life Technology, Darmstadt, Germany) and subsequently transferred onto nitrocellulose membranes. Blots were then incubated with a rabbit polyclonal LOX antibody purchased from Merck Millipore (Darmstadt, Germany; product ABT112) or rabbit polyclonal Col-III antibody purchased from Novus Biologicals (Littleton, USA; product NB600-594). Secondary antibody (HRP-conjugated) directed against rabbit IgG was purchased from Affinity Biologicals (Ancaster, ON; Canada).

Rat Cardiac Fibroblasts

For isolation of adult cardiac fibroblasts, the non-myocytes fraction obtained from the isolation of cardiomyocytes by the Langendorff method was utilized. Cardiac fibroblasts are enriched by a period of brief attachment (2 h) and subsequent removal of less adherent cells such as endothelial cells. Cardiac fibroblasts were maintained in DMEM supplemented with 10% FCS and 1% penicillin and streptomycin under an atmosphere of 5% CO_2 in air at 37°C. After reaching 60–70% confluency, cardiac fibroblasts were trypsinized and transferred to 6-well plates (1×10^5 cells / well). 24 h later LOX siRNA, OPN siRNA or control siRNA (FlexiTube siRNA, Qiagen) oligonucleotides

were transfected to the cells at a concentration of 0.5 nmol/l with Lipofectamine® RNAiMAX (Invitrogen) according to the protocol of the manufacturer. 48 h after siRNA transfection, medium was replaced by serum-free medium and 2 h later cell treatment was initiated as indicated. These primary cultures are >95% fibroblasts at the time of confluency as judged by positive staining for vimentin and lack of staining for von Willebrand factor.

Echocardiography

Rats were anesthetized by isoflurane inhalation (2% isoflurane, 98% O_2) and left ventricular function was assessed by two-dimensional echocardiography using a 12.5-MHz probe (Vivid i, GE Health Care). All measurements were performed in accordance with the conventions of the American Society of Echocardiography and were conducted by the same trained, blinded sonographer. Left ventricular function was visually scanned by B-mode imaging in short and long parasternal axis. Measurement of left systolic and diastolic ventricular wall thicknesses and diameters as well as measurement of aortal and left atrial diameters was performed in long parasternal axis by M-Mode imaging. Fractional shortening (FS) was calculated as FS = (LVEDD-LVESD/LVEDD) × 100, where LVEDD and LVESD are LV internal diameters in end-diastole and end-systole, respectively. Fractional shortening (% FS) and left ventricular ejection fraction (% EF) were calculated from mean-values of 6 independently performed measurements per setting. Pulsed wave (PW) doppler was used to assess transmitral valve flow velocities during early (E) and atrial (A) filling periods.

Statistics

Data are expressed as indicated in the legends. ANOVA and the Student-Newman-Keuls test for *post hoc* analysis were used to analyze experiments in which more than one group was compared. In cases in which two groups were compared, Student's *t*-test or Mann-Whitney-test was employed, depending of a normal distribution of samples (Levene-test). $P < 0.05$ was regarded as significant.

RESULTS

Running Performance and Training-Induced Adaptations in Cardiac and Skeletal Muscles

Over the entire training period the mean weekly running performance was 30.2 km for the Wistar and 51.9 km for the SHR. However, with an average speed of 3.2 km/h the Wistar significantly surpassed the speed of the SHR (2.5 km/h). The profile of the running performance is shown in Supplemental Figure 1.

At the end of the experimental period the functional status of the mitochondria was analyzed using microrespiratory measurements on permeabilized heart and skeletal muscle fibers. The efficiency of the pyruvate respiration increased in the running Wistar by 25 ± 4% (LV) or 61 ± 10% (soleus muscle) compared to the non-running controls. In the trained SHR a comparable increase of 28 ± 9% (LV) and 59 ± 13% (soleus muscle) was observed. Succinate respiration, on the other hand, did not change in the cardiac muscle in either the Wistar or SHR. In the soleus muscle there was a training-induced increase of 30 ± 3% identified in Wistar and of +32 ± 11% in SHR (**Figure 1**).

The weight of the skeletal musculature was also determined, indicating comparable individual training efficiency of Wistar and SHR. The weights of the gastrocnemius muscles (red and white fraction, normalized to the tibia length (TL)), representative of the muscle groups in the extremities, are shown in **Figure 2A**. The mean body weights of all treatment groups at the beginning and the end of the experimental period are shown in **Figure 2B**.

Effects of Running Training on the Development of BP and HR

Compared to the results for the corresponding non-running control groups, the running training did not affect either the temporal development or the level of the systolic or diastolic BP (**Figures 3A,B**). Only the resting pulse was lowered over the course of the training in the running animals compared to the non-running controls (Wistar −100 bpm, SHR −106 bpm, $p < 0.05$); see **Figure 3C**.

Effects of Training on the Cardiac Remodeling

The wet weight of the LV was normalized to the TL of the particular animal. In normotensive Wistar the running wheel training did not have any effect on the LV/TL ratios. The corresponding expression of the atrial natriuretic peptide (ANP) also showed no differences (**Figure 4A**). The hypertension-induced myocardial hypertrophy of the LV in the non-running SHR compared to the Wistar was additionally increased by the running. This was apparent in both a significant increase in the LV/TL ratios and a significantly increased expression of ANP (**Figure 4B**).

Moreover, in SHR the running training induced a change in cardiac geometry which is characterized by an incipient dilatation of the LV in diastole (LVIDd) measured using echocardiography (**Table 1**).

Regulation of Reactive Oxygen Species in the Left Ventricular Myocardium

In the fluorescence microscopy images of the dihydroethidium (DHE) staining, the hypertensive LV of non-running SHR had an elevated radical load compared to normotensive Wistar rats. The 6-months' of running training led to a significant reduction in the concentration of $O_2^{-\bullet}$ in the myocardium of the LV in both the SHR and the Wistar rats (**Figure 5**).

Effects of Running Training on the Remodeling of the Extracellular Matrix

The left ventricular expression of the extracellular matrix proteins collagen I (Col-I) and collagen III (Col-III) and the fibrosis-associated proteins TGF-β1, connective tissue growth factor (CTGF) and fibroblast growth factor-2 (FGF2) was

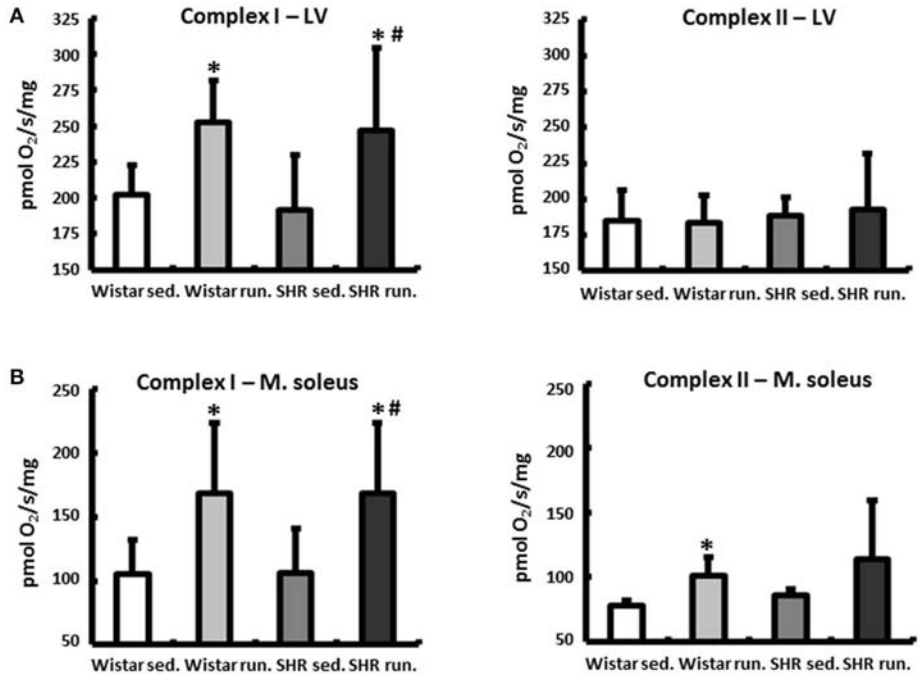

FIGURE 1 | Microrespiratory measurements on permeabilized heart and skeletal muscle fibers. **(A)** Running training improved complex I respiration and did not influence complex II activity in the LV. **(B)** The efficiency of complex I as well as complex II respiration was increased in the soleus muscle of both running groups. Data are means ± S.D. of $n = 6$ animals. $^{*}p < 0.05$ vs. Wistar sed., $^{\#}p < 0.05$ vs. SHR sed.

quantified using real-time RT-PCR. The running training did not have any effect on the relative expression of Col-I in either the Wistar or the SHR. For Col-III, on the other hand, a 4.5-fold induction in the LV of trained Wistar was detected compared to their non-running controls. The SHR showed per se a 37-fold higher expression of Col-III that was increased by the running training to 326-fold (**Figure 6A**).

The massive upregulation of Col-III in the SHR runners could subsequently be confirmed using Sirius Red staining and western blotting (**Figures 6B,C**). TGF-β1, CTGF and FGF2 play a critical role in the induction of extracellular matrix proteins and thus for the development and progression of cardiac fibrosis. However, in contrast to the results for increased Col-III deposition, the running wheel training led to a significant reduction in the pro-fibrotic factors examined in runners compared to non-running controls (**Figure 6D**).

The observed expression pattern, and especially the selective induction of Col-III, raised the question of what mechanisms are responsible for this kind of cardiac remodeling.

Induction of LOX and Its Effect on Cardiac Remodeling

The primary function of LOX, a copper-dependent amine oxidase, is extracellular polymerisation of monomeric matrix proteins. Intracellularly, LOX affects cell adhesion and migration as well as specifically modifying the gene expression of the Col-III isoform (Rodríguez et al., 2008).

The left ventricular mRNA expression of LOX is increased by the running training only by a moderate 12 ± 4% in the hearts of trained Wistar rats compared to their controls and does not reach the significance level. The LOX expression in the non-running SHR was already significantly above the level of the normotensive controls at 68 ± 24% and was increased by a further 132 ± 48% as a result of the running training (**Figure 7A**).

In parallel to the mRNA, in the SHR running group a 69 ± 22% increase in the pre-LOX detected at 50 kDa was also identified in the Western blot. For the Wistar running group again only a very moderate increase of 12 ± 2% was measured (**Figure 7B**).

The band of catalytically active mature LOX was detected with a molecular weight of about 30 kDa. In the Wistar runners the concentration of this fragment only increased by 29 ± 3% while in the SHR runners we observed an increase of 478 ± 72% (**Figure 7C**).

In both the SHR groups there is a significant correlation between LOX expression and the expression of the Col-III isoform as well as the LV/TL ratio. LOX does not correlate with the mRNA expression of Col-I, however (**Figures 7D–F**).

Regulatory Mechanisms for LOX in Cardiac Fibroblasts

During the induction and progression of cardiac fibrosis involving LOX, the glycoprotein SPP1 (also known as osteopontin or OPN) is considered to play an important role in the regulation of LOX (López et al., 2013).

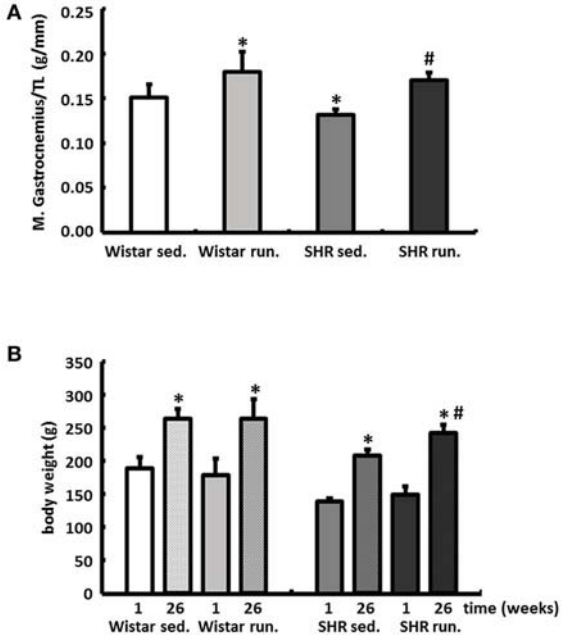

FIGURE 2 | Effects of running training on muscle growth. **(A)** A comparable increase in muscle weight (red and white fraction of the gastrocnemius muscle) was found in both running groups. Data are means ± S.D. of $n = 6$ animals. $^{*}p < 0.05$ vs. Wistar sed., $^{\#}p < 0.05$ vs. SHR sed. **(B)** Gains in BW could be observed in all groups over the study period, however, the largest increase could be determined in running SHR. Data are means ± S.D. of $n = 6$ animals. $^{*}p < 0.05$ vs. first week, $^{\#}p < 0.05$ vs. 26th week SHR sed.

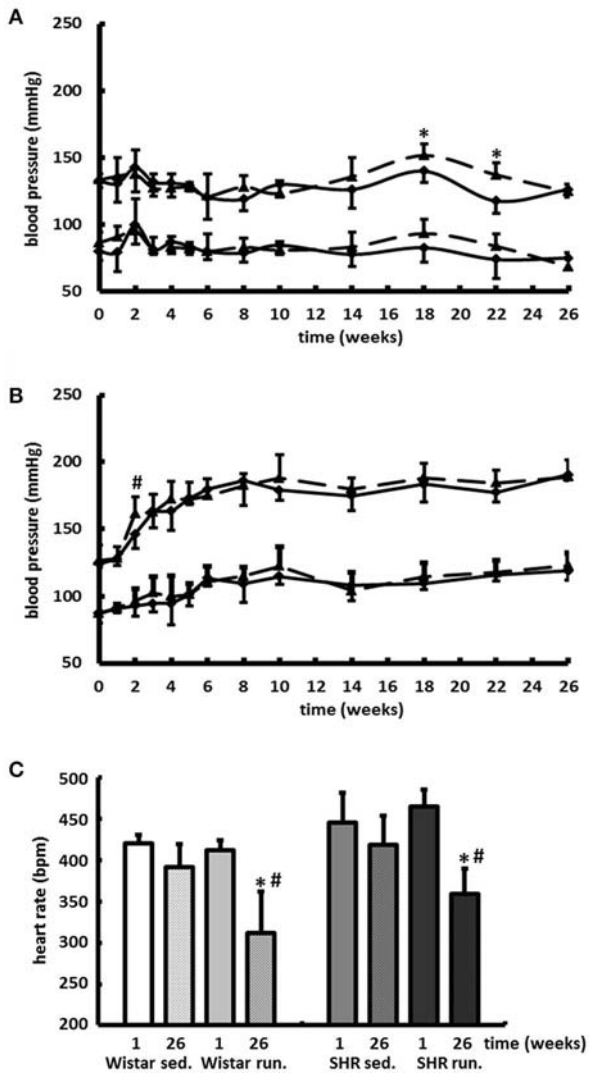

FIGURE 3 | Development of the BP and the resting HR. Neither the temporal development nor the level of the systolic or diastolic BP were affected by 6-months' voluntary aerobic training in **(A)** Wistar rats and **(B)** pre-hypertensive SHR. Blood pressure values of non-runners are represented by a solid line, values of runners are represented by a broken line. Data are means ± S.D. of $n = 6$ animals. $^{*}p < 0.05$ vs. Wistar sed., $^{\#}p < 0.05$ vs. SHR sed. **(C)** HR was lowered over the entire course of the training in the running animals compared to the non-running controls. Data are means ± S.D. of $n = 6$ animals. $^{*}p < 0.05$ vs. first week, $^{\#}p < 0.05$ vs. 26th week sed.

By incubating rat cardiac fibroblasts with OPN, the expression of LOX initially increased significantly after 24 h followed by an increase in the expression of Col-III after a further 24 h (**Figure 8A**).

The expression of OPN could in turn be induced by stimulating the fibroblasts with angiotensin II (Ang-II). If the antioxidant effects of running training that have been described previously were simulated in fibroblast cultures by N-acetyl-L-cysteine (NAC), not only is the Ang-II effect potentiated depending on the NAC concentration but at a higher concentration (2 mM), NAC itself exerted a stimulating effect on the OPN expression (**Figure 8B**).

Ang-II directly induced (via OPN) the expression of LOX after 48 h (**Figure 8C**). By pre-incubating the fibroblasts with siRNA against LOX, the expression of LOX both at an mRNA and protein level was reduced by more than 90% (**Figures 8C,D**). This means that the expression of Col-III, which was already reduced at the basal level, could no longer be induced by Ang-II either (**Figure 8E**). However, knocking down OPN reduced the expression of LOX both at basal conditions and under Ang-II stimulation (**Figure 8F**).

The left ventricular express of OPN was elevated in both running groups compared to their controls (Wistar: +37.5%, n.s. or SHR +302.4%, $p = 0.04$) and thus conformed to the expression pattern for LOX (**Figure 8G**).

Functional Consequences of the Structural Remodeling Process

Cardiac morphology and function were assessed using echocardiography as check-ups after 3 months and at the end of the experiment. The systolic left ventricular function was characterized using fractional shortening (FS) determined along the long parasternal axis in M mode. For the Wistar there was a significant improvement in the FS only in the second part (3rd to 6th month) of the training period while there was an improvement in the FS in the SHR after just 3 months (**Table 1**).

As a surrogate of diastolic function the ratio of the early diastolic filling and the late atrial filling (E/A ratio) was used. For the Wistar no change was observed in either the running or the non-running animals over the entire training period. While the non-running SHR also maintained a ratio at the level of the Wistar, in the trained SHR the E/A ratio—along with a significant reduction in A max velocity—increased above the value of 2 in the second half of the training period, resembling a pseudonormalization and thus may indicate a functionally relevant restrictive filling disorder (**Table 1**). The significant correlation between the E/A ratio and the Col-III expression indicates a causal involvement of the Col-III isoform in the diagnosed relaxation disorder in the trained SHR (**Figure 7G**).

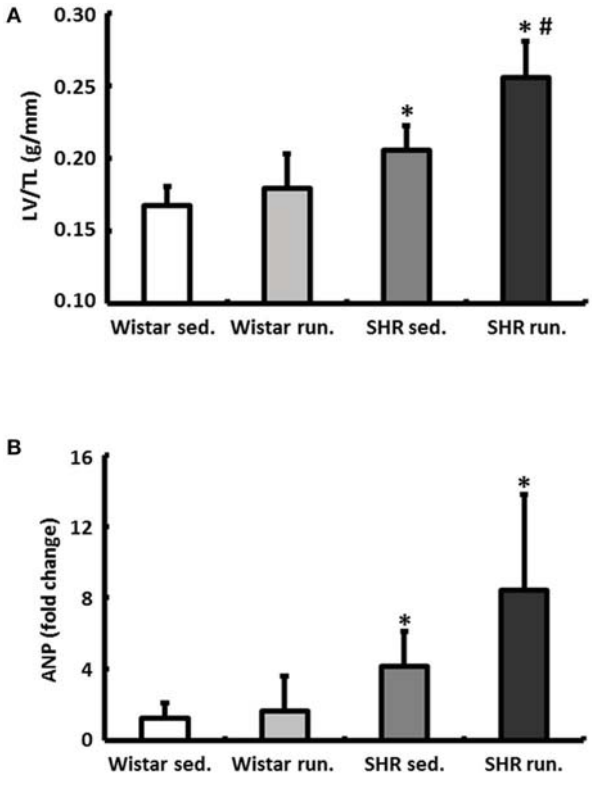

FIGURE 4 | Effects of running training on cardiac hypertrophy. **(A)** The wet weight of the LV was normalized to the TL. **(B)** Left ventricular hypertrophy is also marked by the corresponding expression of ANP. Data are means ± S.D. of $n = 6$ animals. $^{*}p < 0.05$ vs. Wistar sed., $^{\#}p < 0.05$ vs. SHR sed.

DISCUSSION

Following 6-months' voluntary training on a running wheel young Wistar and pre-hypertensive SHR were analyzed for various markers of cardiac remodeling. A rise in the mitochondrial respiration was observed in the animals in both running groups in the cardiac muscle and the skeletal musculature. The running training also reduced not only the left ventricular concentration of $O_2^{-\bullet}$ in the Wistar rats and SHR but also the expression of genes that are involved in the induction and progression of heart failure. The training led to a continuous reduction in the HR in both running groups and improved the systolic function of Wistar and SHR.

On the downside, however, the running training induced a myocardial hypertrophy in the SHR runners as well as a marked Col-III specific fibrosis that was reflected in a functionally relevant filling disorder in the echocardiograms. A massive upregulation of OPN and LOX has been identified as the underlying cause of the subsequent remodeling of the left ventricular myocardium in hypertensive runners. The findings also show that a 6-months' voluntary endurance training does not have any effect on the changes over time or on the absolute systolic or diastolic BP throughout the entire observation period in Wistar rats or SHR.

The key experimental finding of this study that is described here for the first time is the identification of LOX as a critical risk factor for cardiac remodeling during a 6-months' aerobic endurance training.

TABLE 1 | Functional and morphological data assessed by echocardiography.

	Wistar sed.		Wistar running		SHR sed.		SHR running	
	3 mo.	6 mo.	3 mo.	6 mo.	3 mo.	6 mo.	3 mo.	6 mo.
FS (%)	0.36 ± 0.01	0.35 ± 0.04	0.35 ± 0.01	0.39 ± 0.02$^{\#}$	0.32 ± 0.02	0.28 ± 0.01*	0.36 ± 0.03*	0.36 ± 0.05*
EF (Teich,%)	0.71 ± 0.01	0.70 ± 0.06	0.71 ± 0.01	0.76 ± 0.03$^{\#}$	0.65 ± 0.03	0.61 ± 0.02*	0.71 ± 0.04	0.72 ± 0.02*
MV E/A	1.55 ± 0.10	1.58 ± 0.14	1.63 ± 0.04	1.65 ± 0.15	1.63 ± 0.18	1.63 ± 0.12	1.66 ± 0.12	2.10 ± 0.14$^{*\#}$
IVSd (mm)	0.88 ± 0.13	0.91 ± 0.14	0.99 ± 0.20	0.90 ± 0.20	0.75 ± 0.08	0.74 ± 0.03	0.78 ± 0.07	0.88 ± 0.06$^{*\#}$
LVPWd(mm)	1.00 ± 0.10	0.94 ± 0.09	1.09 ± 0.08	0.94 ± 0.08$^{\#}$	0.95 ± 0.09	0.92 ± 0.07	1.05 ± 0.14	1.10 ± 0.18*
LVPWs(mm)	1.43 ± 0.18	1.52 ± 0.24	1.47 ± 0.14	1.64 ± 0.15	1.25 ± 0.11	1.16 ± 0.14	1.64 ± 0.25*	1.82 ± 0.31*
LVIDd (mm)	6.51 ± 0.50	6.23 ± 0.51	6.47 ± 0.24	6.14 ± 0.27	6.61 ± 0.20	6.78 ± 0.16	7.47 ± 0.33*	7.66 ± 0.23*
LVIDs (mm)	4.16 ± 0.35	4.08 ± 0.50	4.13 ± 0.09	3.79 ± 0.31	4.58 ± 0.22	4.85 ± 0.18	4.82 ± 0.33	4.98 ± 0.47

FS (%): fractional shortening, EF (Teich,%): ejection fraction, MV E/A ratio: relationship between the E and A waves, IVSd (mm): end-diastolic interventricular septum thickness, LVPWd (mm): left ventricular posterior wall thickness in diastole, LVPWs (mm): left ventricular posterior wall thickness in systole, LVIDd (mm): left ventricular internal diameter in diastole, LVIDs (mm): left ventricular internal diameter in systole. Data are means ± S.D. of n = 6 animals. Wistar/SHR sed.: $^{*}p < 0.05$ vs. 3 mo. sed., Wistar/SHR running: $^{*}p < 0.05$ vs. sed., $^{\#}p < 0.05$ vs. 3 mo. running.

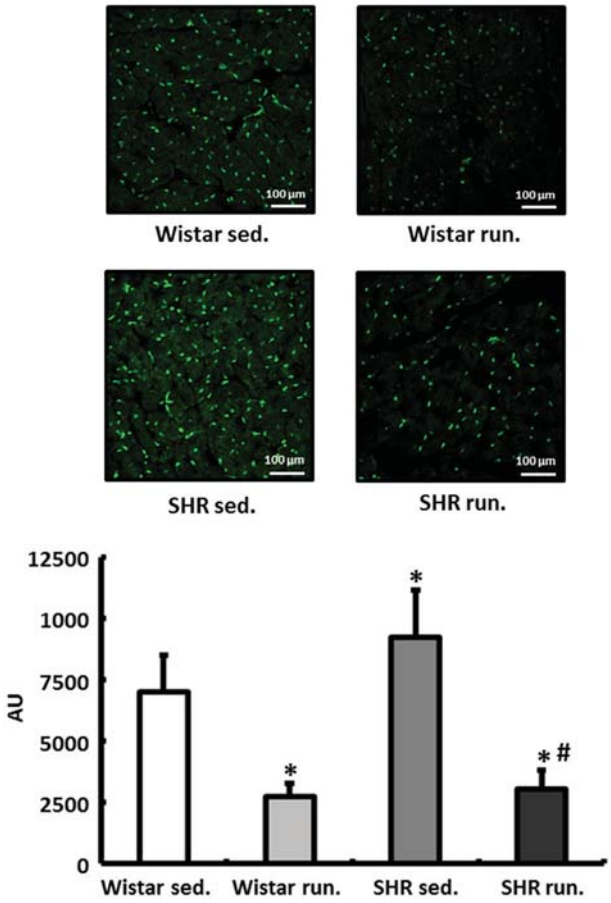

FIGURE 5 | Regulation of reactive oxygen species in the LV. DHE staining was performed to measure the formation of $O_2^{-\bullet}$ in heart tissue from the LV of all treatment groups. Slides were imaged by fluorescence microscopy using an excitation wavelength of 488 nm and an emission wavelength of 540 nm. Data are means ± S.D. of $n = 4$ hearts. $^{*}p < 0.05$ vs. Wistar sed., $^{\#}p < 0.05$ vs. SHR sed.

Collagen isoforms are first secreted as monomers into the extracellular space and only form stable polymers as a result of post-translational modification. The initial step to form these aggregates, oxidative deamination of epsilon amino groups, is carried out by the catalytically active form of LOX (Rodríguez et al., 2008). An elevated expression of cardiac LOX subsequently results in an increased network of collagen (and elastin) isoforms and has already been described as the reason for the increase in ventricular stiffness with the resultant symptoms of heart failure (López et al., 2010). Intracellularly, pre-LOX also affects the gene expression of the Col-III isoform by specifically activating the COL3A1 promoter (Giampuzzi et al., 2000). Cardiac fibrosis in the SHR was not yet functionally relevant after 3 months of the experimental setup but after 6 months the E/A ratio increased to a value ≥2, corresponding to stage 3 of a restrictive filling disorder (Oh et al., 2011). Both properties of LOX, the increased network of matrix proteins and the elevated Col-III expression, must be considered responsible for the diastolic functional disorder. Even the moderate increase in the LOX expression in the Wistar runners increased Col-III production by 4.5 times but did not have any functional consequences.

OPN, an acidic, highly phosphorylated glycoprotein for which clinically relevant pleiotropic effects within the cardiovascular system have previously been described, is considered a direct stimulus for increasing LOX expression (Collins et al., 2004; López et al., 2013). Combined with the *in vitro* experiments carried out here, the situation in the heart of runners can be described as follows: adaptive, predominantly antioxidative, mechanisms prevent "classic" remodeling based on oxidative stress and TGF-β in the myocardium of the runners. Instead, activation of the sympathetic nervous system or RAAS that is caused by running and hypertension induces via Ang-II the expression of OPN and subsequently of LOX which specifically activates the Col-III promoter and increases the rigidity of the ventricle due to cross-linking (Matsui et al., 2004; Nakayama et al., 2011; Lorenzen et al., 2015).

The pathomechanism described above was also reflected in the training performance of the animals: While normotensive running animals completed a consistently steady training workload, the weekly distance ran by the SHR declined continuously and at the end of the experiment the distance was about 45% below the baseline values in the first month of training.

In contrast to the described antihypertrophic effects or delayed re-expression of fetal genes, the SHR in this study developed a cardiac hypertrophy during their 6-months' training period, which was accompanied by an accelerated upregulation of the ANP. This development corresponds to the cardiac changes previously observed to an even greater degree in older hypertensive animals (Schultz et al., 2007; da Costa Rebelo et al., 2012). However, it has already been demonstrated for OPN that it is causally involved in the development of cardiac hypertrophy, meaning that the development of left ventricular hypertrophy in the SHR runners must also be taken into account as a consequence of the above-described "non-classic" remodeling (Graf et al., 1997; Xie et al., 2004). The normotensive Wistar did not differ from their non-running controls in terms of heart weight or ANP expression, however. The systolic pump function measured using echocardiography also improved during the training period in the animals in both running groups. These results indicate that the additional running-induced hypertrophy in the SHR up to this point can be attributed to the stage of adaptation. Moreover, incipient left ventricular dilatation, a well-recognized precursor of congestive heart failure, could be almost completely compensated in view of the improved EF. To what extent physical training contributes to an improved EF or prevents the development of systolic heart failure is still largely unknown. Important factors of influence are the animal model used, the age of the experimental animals, and the duration and intensity of the training. In this context, beneficial effects are predominantly described in young experimental animals combined with a "moderate" training workload (Garciarena et al., 2009). On the other hand, Schultz et al. (2007) reported a deterioration of systolic function in older hypertensive animals after a training program of high physical intensity.

Arterial hypertension is a primary risk factor that is directly associated with the pathogenesis of coronary heart

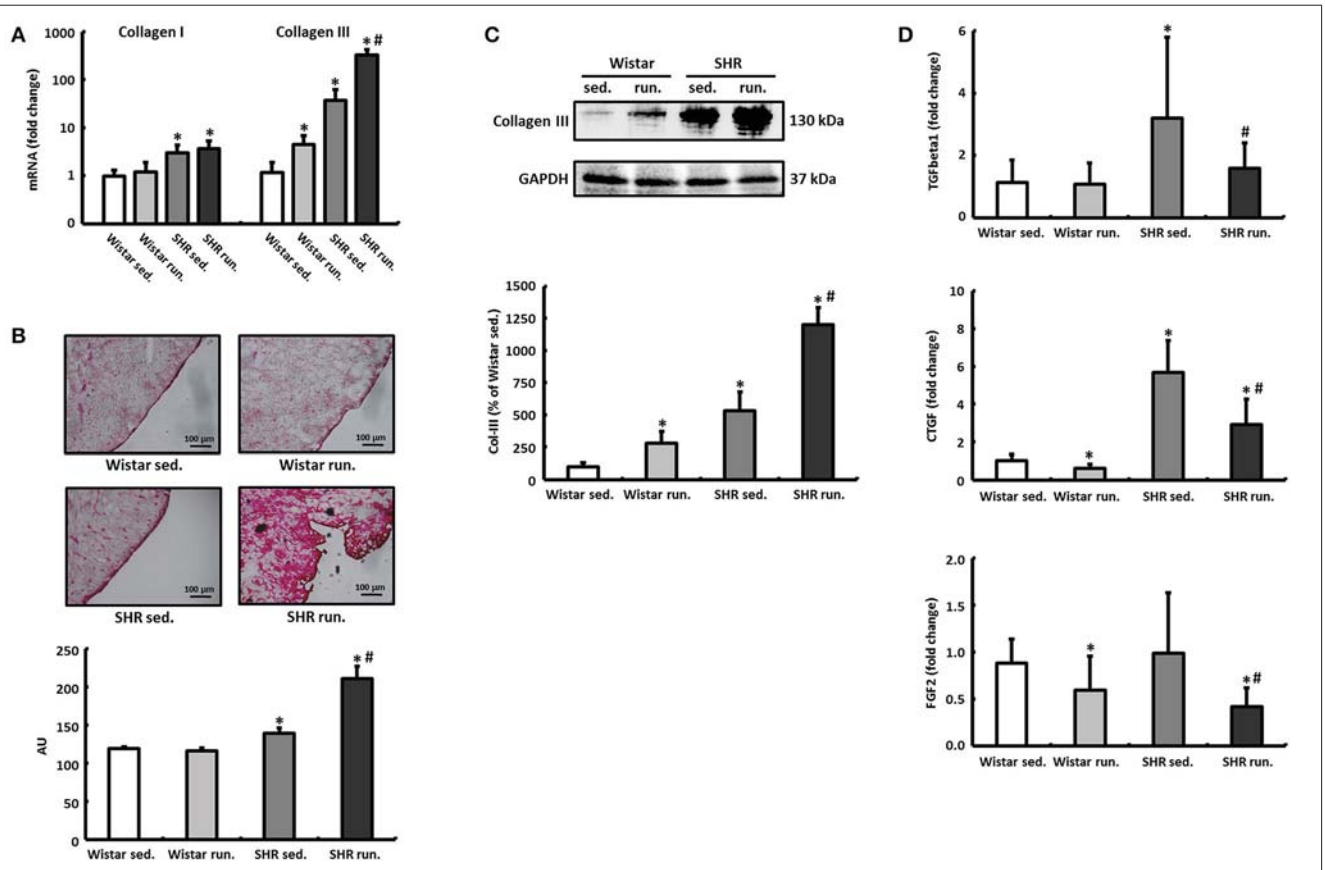

FIGURE 6 | Remodeling of the extracellular collagen matrix. **(A)** The running training did not affect the expression of Col-I but markedly increased the expression of Col-III notably in SHR. **(B,C)** PCR results for collagen could be verified subsequently using both Sirius Red staining of histological sections and western blot. **(D)** The expression of pro-fibrotic factors (TGF-β1, CTGF, and FGF2) was reduced in both exercise groups. Data are means ± S.D. of $n = 6$ animals. $^{*}p < 0.05$ vs. Wistar sed., $^{\#}p < 0.05$ vs. SHR sed.

disease, myocardial infarction, and heart failure. Systematic antihypertensive therapy enables a critical reduction in the morbidity and mortality of patients. In addition to a drug intervention, a fundamental component of systematic antihypertensive therapy in general is the recommendation for patients to appropriately adjust their lifestyle: This includes adopting a low-fat and low-sodium diet, stopping smoking, and incorporating more physical activity (Hagberg et al., 2000).

However, the extent to which physical training alone contributes to lowering BP can only be estimated with difficulty because a number of factors change along with the change in lifestyle. In an animal model it is possible to specifically control these factors. The current study therefore takes the approach of defining physical training alone as the test condition.

Compared to "moderate" swimming or treadmill training, the weekly running performances achieved by the Wistar rats and the SHR in this study are indicative of a high training performance or intensity. However, voluntary training of rats is performed as an intermittend, noctural running pattern which consists of 100–150 individual running bouts per 24 h. Typically, each revolution/bout takes a maximum of 3 min (Overton et al., 1986; Rodnick et al., 1989). This means that the average running distance of ∼6 km per day is distributed over many hours in intervals with longer recovery phases. Thus, voluntary wheel-running in rodents is thought to be an appropriate model of aerobic exercise in humans (Yasumoto et al., 2015). In light of these factors, voluntary training with a running wheel allows the rat a largely natural running behavior, and thus represents the most physiological model. However, the significant increase in BW in running SHR can be mainly attributed to higher food consumption during exercise and have already been identified as a characteristic specific to SHR (Gordon et al., 2016).

The running wheel as a training device enables the individual animal to complete an individual training workload according to its willingness to run. The naturally higher physical activity of the SHR compared to the Wistar is thus reflected in a significantly higher weekly running distance and time (Sagvolden et al., 1993). Nevertheless, the individual desired functional and metabolic adaptation reactions of the training on SHR and Wistar are highly comparable despite the varying running performances as described in the following sections.

At the end of the experimental period, the function of the complexes I and II were examined using microrespiratory tests on permeabilized muscle fibers from the LV and the soleus

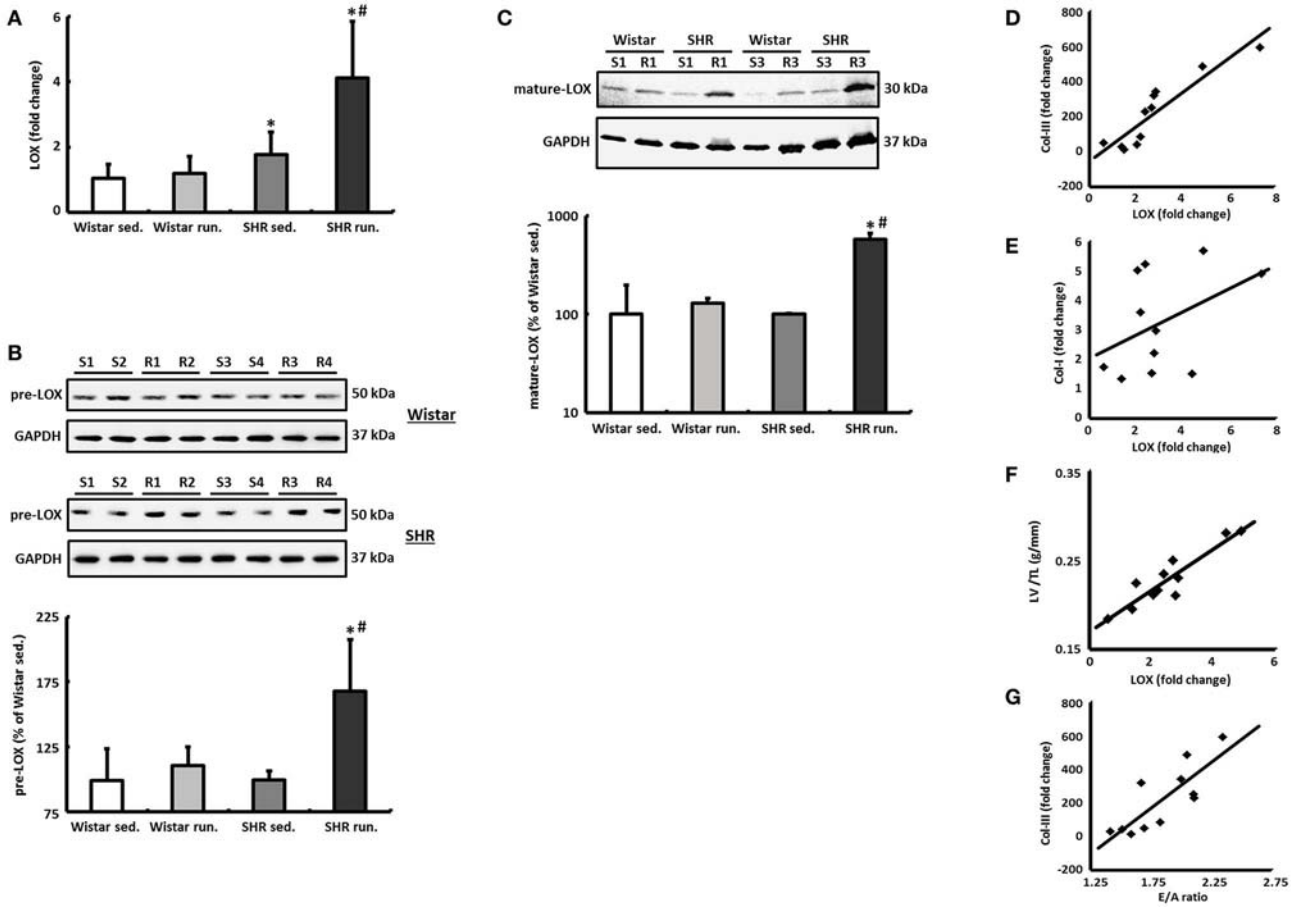

FIGURE 7 | LOX as a critical risk factor for cardiac remodeling during a 6-months' aerobic running training. **(A)** The mRNA expression of LOX was analyzed in tissue from the LV using real-time RT PCR. The expression of HPRT was used for normalization. **(B,C)** Representative immunoblots and densitometric analysis of the pre-LOX (50 kDa) and the catalytically active mature LOX (30 kDa). Immunoblot bands were all normalized to GAPDH (S, sed.; R, run.). **(D–F)** A significant correlation was found between LOX expression and the expression of Col-III ($R^2 = 0.83$) as well as the LV/TL ratio ($R^2 = 0.84$) in SHR. However, LOX does not correlate with the mRNA expression of the Col-I isoform ($R^2 = 0.18$). **(G)** There is also a significant correlation between the E/A ratio and the Col-III expression in SHR ($R^2 = 0.66$). Data are means ± S.D. of $n = 6$ animals. $^*p < 0.05$ vs. Wistar sed., $^{\#}p < 0.05$ vs. SHR sed.

muscle. In the LV the activity of the pyruvate-dependent complex I respiration increased in the animals in both running groups while no change was detected in the succinate respiration of complex II. The resulting large increase in the succinate-related pyruvate respiration (SRPR) together with unchanged expression of PGC-1 α and NRF1 (mRNA, measured by real time PCR), which are involved directly in the biogenesis of mitochondria as transcriptional cofactors, is indicative mainly of an increase in the activity of complex I and less of an increase in the number of mitochondria (Ventura-Clapier et al., 2008).

A clear increase in the complex I activity was also verified in the skeletal musculature for both running groups. Unlike the LV, the succinate respiration also increased in the soleus muscle in Wistar and SHR. The resulting increase in the SRPR resulting from these values corresponds to the qualitative changes in individual respiratory chain complexes in the skeletal musculature described by Daussin et al. as a result of a two-year defined training program of moderate to high training intensities (Daussin et al., 2008).

The lowering of the resting HR in both running groups also contributes to an improvement of the cardiac energy metabolism due to a reduction in both ventricular work and myocardial oxygen consumption.

The causal involvement of the cytokine TGF-β1 in the induction and progression of heart failure has already been well documented. It is also critically involved in the development and maintenance of cardiac fibrosis (Rosenkranz, 2004). The training program used in this study did not have any effect on the left ventricular expression of TGF-β1 in the normotensive Wistar but did lead to a significant reduction in the SHR. The expression of Col-III was induced in both running groups while that of Col-I was not affected by the running training. Thus, the Col-III specific fibrosis developed independently of TGF-β1 as well as CTGF or FGF2 which were also expressed less in both running groups. CTGF, however, is causally involved in pathological fibrosis and also contributes to heart failure development (Koshman et al., 2013; Szabó et al., 2014). FGF2 mainly promotes cardiac hypertrophy and cardiac fibrosis (Nusayr et al., 2013).

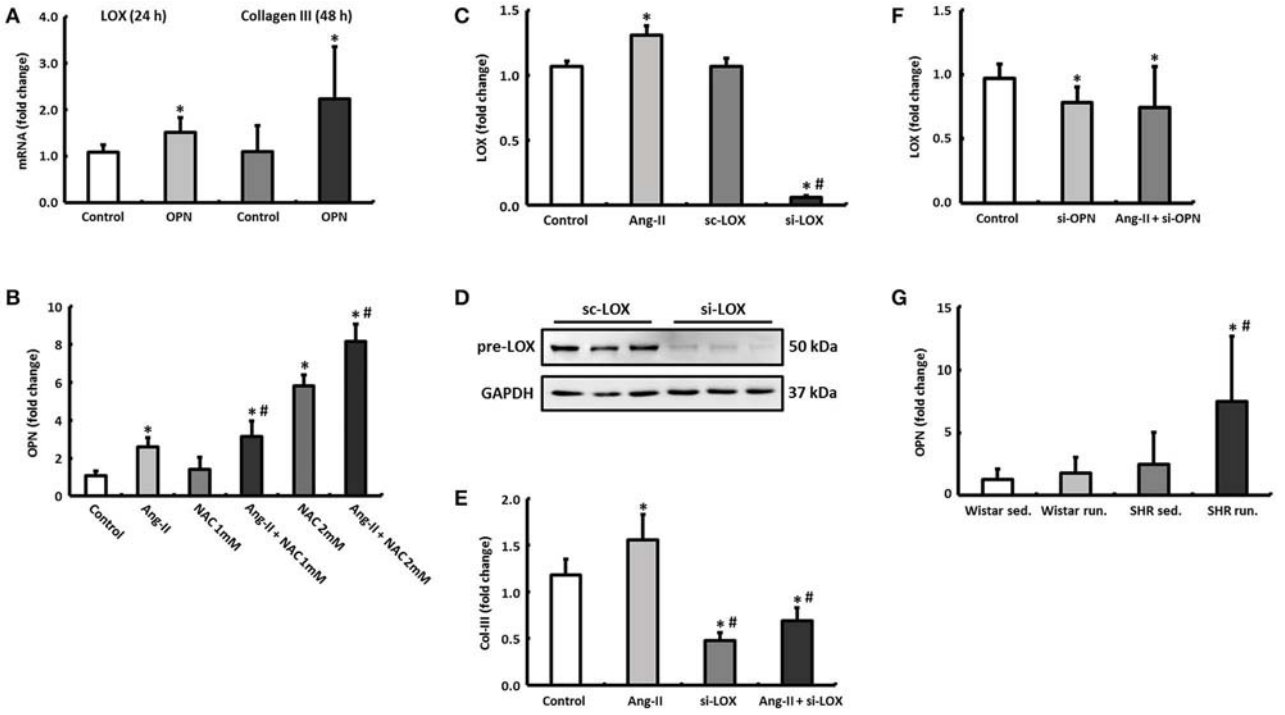

FIGURE 8 | Regulatory mechanisms in cardiac fibroblasts. **(A)** By incubating cardiac fibroblasts with OPN, the mRNA expression of LOX and Col-III increased after 24 and 48 h, respectively. **(B)** OPN expression in cardiac fibroblasts could be induced by Ang-II and NAC. **(C–E)** Ang-II increased the expression of LOX and Col-III, however, Col-III expression depends on the presence of LOX (si-LOX, siRNA against LOX; sc-LOX, control siRNA). Data are means ± S.D. of $n = 6$ hearts. $^{*}p < 0.05$ vs. control, $^{\#}p < 0.05$ vs. Ang-II. **(F)** Downregulation of OPN reduced the expression of LOX in both unstimulated and Ang-II stimulated cells after 48 h (si-OPN, siRNA against OPN). Data are means ± S.D. of $n = 6$ hearts. $^{*}p < 0.05$ vs. control. **(G)** OPN mRNA was primarily elevated in left ventricular tissue of trained SHR. The expression of HPRT was used for normalization. Data are means ± S.D. of $n = 6$ animals. $^{*}p < 0.05$ vs. Wistar sed., $^{\#}p < 0.05$ vs. SHR sed.

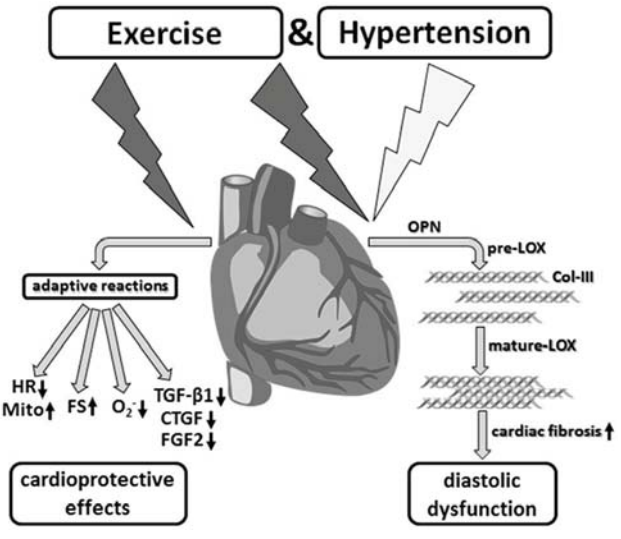

FIGURE 9 | Aerobic endurance training in the concomitant presence of hypertension. Despite desired functional and metabolic adaptation reactions, running training in combination with arterial hypertension induced a myocardial hypertrophy as well as significant fibrosis, and thus, a diastolic functional disorder, which critically affects the prognosis in the medium to long term.

The downregulation of these three genes, the expression of which is fundamentally affected by radical metabolism, can also be explained by the antioxidant effects of the running training that are revealed by a reduction in the production of $O_2^{-\bullet}$ in the left ventricular tissue (Dekleva et al., 2017).

CONCLUSION

Adaptive responses in both normotensive Wistar rats and pre-hypertensive SHR that improved the metabolic and functional remodeling of the myocardium were induced by 6 months' running training but with no effect on either the temporal development or the absolute value of the BP.

At the same time, however, during sustained running stress these cardioprotective adaptive mechanisms contribute to the development of non-classic remodeling of the left ventricular myocardium that is characterized by induction of LOX, Col-III specific fibrosis and diastolic dysfunction (**Figure 9**).

PROSPECTS

Analogous to the indication, dosage and duration of pharmacotherapy administered in accordance with the

guidelines, developing and monitoring an individual training program are essential to reduce cardiovascular risk factors for existing hypertension. The results of this study show that aerobic endurance training with existing high BP can be of therapeutic benefit but is also associated with corresponding risks. Consistent with the conclusions drawn by Allesøe et al., further studies are essential to establish sports and physical activity as a safe preventive and therapeutic option for cardiovascular diseases (Allesøe et al., 2016; Williamson et al., 2016).

STUDY LIMITATIONS

This study investigates the impact of voluntary wheel-running as a sole intervention on the cardiac remodeling in terms of functional, structural, and metabolic adaptation reactions using female Wistar rats and SHR. Both male and female rats have been used frequently in studies examining the effects of exercise on the cardiovascular system. However, the estrous cycle and the ovarian hormones are likely to be responsible for well-reported differences in voluntary running performance in female compared to male rats. Thus, it could be shown that running wheel activity increased significantly during the night of proestrus. Although the influence of stage of estrous cycle are likely to be averaged out during 6 months' experimental period within the four treatment groups, we cannot rule out that male Wistar rats and SHR differ by the type of cardiac remodeling in response to 6-months' voluntary training on a running wheel.

Furthermore, the strong correlation between LOX expression and the expression of the Col-III isoform as well as Col-III expression and the E/A ratio indicates a causal involvement of LOX in the diagnosed relaxation disorder in the trained SHR. However, the extent of collagen cross-linking has not been determined directly in cardiac tissue.

AUTHOR CONTRIBUTIONS

RS and KS: Conceptualization, Supervision, Methodology, Formal analysis, Writing–Original Draft, Funding acquisition; AH, Rd, SS, and LL: Methodology, Investigation; BN and SR: Methodology, Investigation, Formal analysis.

FUNDING

The study was supported by the research funding program of the Justus-Liebig-University Giessen (project number: 60080179) and the von-Behring-Röntgen-Stiftung (Graduate School ERAGON, project number: TP 5).

SUPPLEMENTARY MATERIAL

The Supplementary Material for this article can be found online at: http://journal.frontiersin.org/article/10.3389/fphys.2017.00556/full#supplementary-material

REFERENCES

Allesøe, K., Søgaard, K., Aadahl, M., Boyle, E., and Holtermann, A. (2016). Are hypertensive women at additional risk of ischaemic heart disease from physically demanding work? *Eur. J. Prev. Cardiol.* 23, 1054–1061. doi: 10.1177/2047487316631681

Bertagnolli, M., Campos, C., Schenkel, P. C., de Oliveira, V. L. L., de Angelis, K., Bello'-Klein, A., et al. (2006). Baroreflex sensitivity improvement is associated with decreased oxidative stress in trained spontaneously hypertensive rats. *J. Hypertension* 24, 2437–2443. doi: 10.1097/01.hjh.0000251905.08547.17

Brooks, W. W., Shen, S. S., Conrad, C. H., Goldstein, R. H., and Bing, O. H. (2010). Transition from compensated hypertrophy to systolic heart failure in the spontaneously hypertensive rat: Structure, function, and transcript analysis. *Genomics.* 95, 84–92. doi: 10.1016/j.ygeno.2009.12.002

Chicco, A. J., McCune, S. A., Emter, C. A., Sparagna, G. C., Rees, M. L., Bolden, D. A., et al. (2008). Low-intensity exercise training delays heart failure and improves survival in female hypertensive heart failure rats. *Hypertension* 51, 1096–1102. doi: 10.1161/HYPERTENSIONAHA.107.107078

Chobanian, A. V., Bakris, G. L., Black, H. R., Cushman, W. C., Green, L. A., Izzo, J. L. Jr., et al. (2003). The seventh report of the Joint National Committee on Prevention, Detection, Evaluation, and Treatment of High Blood Pressure: the JNC 7 report. *JAMA* 289, 2560–2572. doi: 10.1001/jama.289.19.2560

Collins, A. R., Schnee, J., Wang, W., Kim, S., Fishbein, M. C., Bruemmer, D., et al. (2004). Osteopontin modulates angiotensin II-induced fibrosis in the intact murine heart. *J. Am. Coll. Cardiol.* 43, 1698–1705. doi: 10.1016/j.jacc.2003.11.058

da Costa Rebelo, R. M., Schreckenberg, R., and Schlüter, K. D. (2012). Adverse cardiac remodelling in spontaneously hypertensive rats: acceleration by high aerobic exercise intensity. *J. Physiol. (Lond).* 590, 5389–5400. doi: 10.1113/jphysiol.2012.241141

Daussin, F. N., Zoll, J., Ponsot, E., Dufour, S. P., Doutreleau, S., Lonsdorfer, E., et al. (2008). Training at high exercise intensity promotes qualitative adaptations of mitochondrial function in human skeletal muscle. *J Appl Physiol.* 104, 1436–1441. doi: 10.1152/japplphysiol.01135.2007

Dekleva, M., Lazic, J. S., Arandjelovic, A., and Mazic, S. (2017). Beneficial and harmful effects of exercise in hypertensive patients: the role of oxidative stress. *Hypertens. Res.* 40, 15–20. doi: 10.1038/hr.2016.90

Deutsche Hochdruckligae, V. (2008). *eitlinien zur Behandlung der arteriellen Hypertonie.* Heidelberg: Deutsche Hochdruckliga e.V. DHL- Deutsche Hypertonie Gesellschaft.

Garciarena, C. D., Pinilla, O. A., Nolly, M. B., Laguens, R. P., Escudero, E. M., Cingolani, H. E., et al. (2009). Endurance training in the spontaneously hypertensive rat: conversion of pathological into physiological cardiac hypertrophy. *Hypertension* 53, 708–714. doi: 10.1161/HYPERTENSIONAHA.108.126805

Giampuzzi, M., Botti, G., Di Duca, M., Arata, L., Ghiggeri, G., Gusmano, R., et al. (2000). Lysyl oxidase activates the transcription activity of human collagene III promoter. Possible involvement of Ku antigen. *J. Biol. Chem.* 275, 36341–36349. doi: 10.1074/jbc.M003362200

Gordon, C. J., Phillips, P. M., and Johnstone, A. F. (2016). Impact of genetic strain on body fat loss, food consumption, metabolism, ventilation, and motor activity in free running female rats. *Physiol. Behav.* 153, 56–63. doi: 10.1016/j.physbeh.2015.10.025

Graf, K., Do, Y. S., Ashizawa, N., Meehan, W. P., Giachelli, C. M., Marboe, C. C., et al. (1997). Myocardial osteopontin expression is associated with left ventricular hypertrophy. *Circulation* 96, 3063–3071. doi: 10.1161/01.CIR.96.9.3063

Hagberg, J. M., Park, J. J., and Brown, M. D. (2000). The role of exercise training in the treatment of hypertension: an update. *Sports Med.* 30, 193–206. doi: 10.2165/00007256-200030030-00004

Koshman, Y. E., Patel, N., Chu, M., Iyengar, R., Kim, T., Ersahin, C., et al. (2013). Regulation of connective tissue growth factor gene expression and fibrosis in human heart failure. *J. Card. Fail.* 19, 283–294. doi: 10.1016/j.cardfail.2013.01.013

Lajoie, C., Calderone, A., and Be' liveau, L. (2004). Exercise training enhanced the expression of myocardial proteins related to cell protection in spontaneously hypertensive rats. *Pflug. Arch. Eur. J. Physiol.* 449, 26–32. doi: 10.1007/s00424-004-1307-0

Lee, Y. I., Cho, J. Y., Kim, M. H., Kim, K. B., Lee, D. J., and Lee, K. S. (2006). Effects of exercise on pathological cardiac hypertrophy related gene expression and apoptosis. *Eur. J. Appl. Physiol.* 97, 216–224. doi: 10.1007/s00421-006-0161-5

Livak, K. J., and Schmittgen, T. D. (2001). Analysis of relative gene expression data using real-time quantitative PCR and the $2^{-\Delta\Delta C_T}$). *Methods* 25, 402–408. doi: 10.1006/meth.2001.1262

Lloyd, M. H., and Wolfensohn, S. E. (1999). "Practical use of distress scoring systems in the application of humane endpoints," in *Humane Endpoints in Animal Experiments for Biomedical Research* (Oxford: Royal Society of Medicine Press), 48–53.

López, B., González, A., Hermida, N., Valencia, F., de Teresa, E., and Díez, J. (2010). Role of lysyl oxidase in myocardial fibrosis: from basic science to clinical aspects. *Am. J. Physiol. Heart Circ. Physiol.* 299, 1–9. doi: 10.1152/ajpheart.00335.2010

López, B., González, A., Lindner, D., Westermann, D., Ravassa, S., Beaumont, J., et al. (2013). Osteopontin-mediated myocardial fibrosis in heart failure: a role for lysyl oxidase? *Cardiovasc. Res.* 99, 111–120. doi: 10.1093/cvr/cvt100

Lorenzen, J. M., Schauerte, C., Hübner, A., Kölling, M., Martino, F., Scherf, K., et al. (2015). Osteopontin is indispensible for AP1-mediated angiotensin II-related miR-21 transcription during cardiac fibrosis. *Eur. Heart J.* 36, 2184–2196. doi: 10.1093/eurheartj/ehv109

Matsui, Y., Jia, N., Okamoto, H., Kon, S., Onozuka, H., Akino, M., et al. (2004). Role of osteopontin in cardiac fibrosis and remodeling in angiotensin II-induced cardiac hypertrophy. *Hypertension* 43, 1195–1201. doi: 10.1161/01.HYP.0000128621.68160.dd

Nakayama, H., Nagai, H., Matsumoto, K., Oguro, R., Sugimoto, K., Kamide, K., et al. (2011). Association between osteopontin promoter variants and diastolic dysfunction in hypertensive heart in the Japanese population. *Hypertens. Res.* 34, 1141–1146. doi: 10.1038/hr.2011.102

Nazarewicz, R. R., Bikineyeva, A., and Dikalov, S. I. (2013). Rapid and specific measurements of superoxide using fluorescence spectroscopy. *J. Biomol. Screen.* 18, 498–503. doi: 10.1177/1087057112468765

Niemann, B., Chen, Y., Issa, H., Silber, R. E., and Rohrbach, S. (2010). Caloric restriction delays cardiac ageing in rats: role of mitochondria. *Cardiovasc. Res.* 88, 267–276. doi: 10.1093/cvr/cvq273

Nusayr, E., Sadideen, D. T., and Doetschman, T. (2013). FGF2 modulates cardiac remodeling in an isoform- and sex-specific manner. *Physiol. Rep.* 1:e00088. doi: 10.1002/phy2.88

Oh, J. K., Park, S. J., and Nagueh, S. F. (2011). Established and novel clinical applications of diastolic function assessment by echocardiography. *Circ. Cardiovasc. Imaging* 4, 444–455. doi: 10.1161/CIRCIMAGING.110.961623

O'Keefe, J. H., Patil, H. R., Lavie, C. J., Magalski, A., Vogel, R. A., and McCullough, P. A. (2012). Potential adverse cardiovascular effects from excessive endurance exercise. *Mayo Clin. Proc.* 87, 587–595. doi: 10.1016/j.mayocp.2012.04.005

Overton, J. M., Tipton, C. M., Matthes, R. D., and Leininger, J. R. (1986). Voluntary exercise and its effects on young SHR and stroke-prone hypertensive rats. *J. Appl. Physiol.* 61, 318–324.

Pagan, L. U., Damatto, R. L., Cezar, M. D., Lima, A. R., Bonomo, C., Campos, D. H., et al. (2015). Long-term low intensity physical exercise attenuates heart failure development in aging spontaneously hypertensive rats. *Cell. Physiol. Biochem.* 36, 61–74. doi: 10.1159/000374053

Rodnick, K. J., Reaven, G. M., Haskell, W. L., Sims, C. R., and Mondon, C. E. (1989). Variations in running activity and enzymatic adaptations in voluntary running rats. *J. Appl. Physiol.* 66, 1250–1257.

Rodríguez, C., Martínez-González, J., Raposo, B., Alcudia, J. F., Guadall, A., and Badimon, L. (2008). Regulation of lysyl oxidase in vascular cells: lysyl oxidase as a new player in cardiovascular diseases. *Cardiovasc. Res.* 79, 7–13. doi: 10.1093/cvr/cvn102

Rosenkranz, S. (2004). TGF-beta1 and angiotensin networking in cardiac remodeling. *Cardiovasc. Res.* 63, 423–432. doi: 10.1016/j.cardiores.2004.04.030

Rysä, J., Leskinen, H., Ilves, M., and Ruskoaho, H. (2005). Distinct upregulation of extracellular matrix genes in transition from hypertrophy to hypertensive heart failure. *Hypertension* 45, 927–933. doi: 10.1161/01.HYP.0000161873.27088.4c

Sagvolden, T., Petterson, M., and Larsen, M. (1993). Spontaneously Hypertensive Rats (SHR) as a putative animal-model of childhood hyperkinesia – SHR behavior compared to 4 other rat strains. *Phsiol. Behav.* 54, 1047–1055. doi: 10.1016/0031-9384(93)90323-8

Schlüter, K. D., Schreckenberg, R., and da Costa Rebelo, R. M. (2010). Interaction between exercise and hypertension in spontaneously hypertensive rats: a meta-analysis of experimental studies. *Hypertens. Res.* 33, 1155–1161. doi: 10.1038/hr.2010.155

Schultz, R. L., Swallow, J. G., Waters, R. P., Kuzman, J. A., Redetzke, R. A., Said, S., et al. (2007). Effects of excessive long-term exercise on cardiac function and myocyte remodeling in hypertensive heart failure rats. *Hypertension* 50, 410–416. doi: 10.1161/HYPERTENSIONAHA.106.086371

Sharman, J. E., La Gerche, A., and Coombes, J. S. (2015). Exercise and cardiovascular risk in patients with hypertension. *Am. J. Hypertens.* 28, 147–158. doi: 10.1093/ajh/hpu191

Szabó, Z., Magga, J., Alakoski, T., Ulvila, J., Piuhola, J., Vainio, L., et al. (2014). Connective tissue growth factor inhibition attenuates left ventricular remodeling and dysfunction in pressure overload-induced heart failure. *Hypertension* 63, 1235–1240. doi: 10.1161/HYPERTENSIONAHA.114.03279

Thompson, P. D., Franklin, B. A., Balady, G. J., Blair, S. N., Corrado, D., Estes, N. A. III., et al. (2007). Exercise and acute cardiovascular events placing the risks into perspective: a scientific statement from the American Heart Association Council on Nutrition, Physical Activity, and Metabolism and the Council on Clinical Cardiology. *Circulation* 115, 2358–2368. doi: 10.1161/CIRCULATIONAHA.107.181485

van de Schoor, F. R., Aengevaeren, V. L., Hopman, M. T., Oxborough, D. L., George, K. P., Thompson, P. D., et al. (2016). Myocardial fibrosis in athletes. *Mayo Clin. Proc.* 91, 1617–1631. doi: 10.1016/j.mayocp.2016.07.012

Ventura-Clapier, R., Garnier, A., and Veksler, V. (2008). Transcriptional control of mitochondrial biogenesis: the central role of PGC-1alpha. *Cardiovasc. Res.* 79, 208–217. doi: 10.1093/cvr/cvn098

Williamson, W., Boardman, H., Lewandowski, A. J., and Leeson, P. (2016). Time to rethink physical activity advice and blood pressure: a role for occupation-based interventions? *Eur. J. Prev. Cardiol.* 23, 1051–1053. doi: 10.1177/2047487316645008

WHO (2003). World Health Organisation (WHO)/International Society of Hypertension (ISH) statement on management of hypertension. *J. Hypertens.* 21, 1983–1992. doi: 10.1097/00004872-200311000-00002

Xie, Z., Singh, M., and Singh, K. (2004). Osteopontin modulates myocardial hypertrophy in response to chronic pressure overload in mice. *Hypertension* 44, 826–831. doi: 10.1161/01.HYP.0000148458.03202.48

Yasumoto, Y., Nakao, R., and Oishi, K. (2015). Free access to a running-wheel advances the phase of behavioral and physiological circadian rhythms and peripheral molecular clocks in mice. *PLoS ONE* 10:e0116476. doi: 10.1371/journal.pone.0116476

Conflict of Interest Statement: The authors declare that the research was conducted in the absence of any commercial or financial relationships that could be construed as a potential conflict of interest.

Am J Physiol Heart Circ Physiol 311: H927–H943, 2016.
First published August 12, 2016; doi:10.1152/ajpheart.00049.2016.

CALL FOR PAPERS | *Cardiovascular Mitochondria and Redox Control in Health and Disease*

Diastolic dysfunction in prediabetic male rats: Role of mitochondrial oxidative stress

Gábor Koncsos,[1]* Zoltán V. Varga,[1,13]* Tamás Baranyai,[1] Kerstin Boengler,[2] Susanne Rohrbach,[2] Ling Li,[2] Klaus-Dieter Schlüter,[2] Rolf Schreckenberg,[2] Tamás Radovits,[3] Attila Oláh,[3] Csaba Mátyás,[3] Árpád Lux,[3] Mahmoud Al-Khrasani,[1] Tímea Komlódi,[4] Nóra Bukosza,[5] Domokos Máthé,[6,7] László Deres,[8] Monika Barteková,[9,10] Tomáš Rajtík,[11] Adriana Adameová,[11] Krisztián Szigeti,[6] Péter Hamar,[5] Zsuzsanna Helyes,[12] László Tretter,[4] Pál Pacher,[1,13] Béla Merkely,[3] Zoltán Giricz,[1]* Rainer Schulz,[2]* and Péter Ferdinandy[1]*

[1]*Department of Pharmacology and Pharmacotherapy, Faculty of Medicine, Semmelweis University, Budapest, Hungary;* [2]*Institute of Physiology, Faculty of Medicine, Justus-Liebig University, Giessen, Germany;* [3]*Heart and Vascular Center, Semmelweis University, Budapest, Hungary;* [4]*Department of Medical Biochemistry, Faculty of Medicine, Semmelweis University, Budapest, Hungary;* [5]*Institute of Pathophysiology, Faculty of Medicine, Semmelweis University, Budapest, Hungary;* [6]*Department of Biophysics and Radiation Biology, Faculty of Medicine, Semmelweis University, Budapest, Hungary;* [7]*CROmed Translational Research Centers, Budapest, Hungary;* [8]*1st Department of Internal Medicine, Faculty of Medicine, University of Pécs, Pécs, Hungary;* [9]*Institute of Physiology, Faculty of Medicine, Comenius University in Bratislava, Slovakia;* [10]*Institute for Heart Research, Slovak Academy of Sciences, Bratislava, Slovakia;* [11]*Department of Pharmacology and Toxicology, Faculty of Pharmacy, Comenius University in Bratislava, Slovakia;* [12]*Department of Pharmacology and Pharmacotherapy, Faculty of Medicine and Szentágothai Research Centre & MTA-PTE NAP B Chronic Pain Research Group, University of Pécs, Pécs, Hungary; and* [13]*Laboratory of Cardiovascular Physiology and Tissue Injury, National Institute on Alcohol Abuse and Alcoholism, National Institutes of Health, Bethesda, Maryland*

Submitted 15 January 2016; accepted in final form 25 July 2016

Koncsos G, Varga ZV, Baranyai T, Boengler K, Rohrbach S, Li L, Schlüter KD, Schreckenberg R, Radovits T, Oláh A, Mátyás C, Lux A, Al-Khrasani M, Komlódi T, Bukosza N, Máthé D, Deres L, Barteková M, Rajtík T, Adameová A, Szigeti K, Hamar P, Helyes Z, Tretter L, Pacher P, Merkely B, Giricz Z, Schulz R, Ferdinandy P. Diastolic dysfunction in prediabetic male rats: Role of mitochondrial oxidative stress. *Am J Physiol Heart Circ Physiol* 311: H927–H943, 2016. First published August 12, 2016; doi:10.1152/ajpheart.00049.2016.—Although incidence and prevalence of prediabetes are increasing, little is known about its cardiac effects. Therefore, our aim was to investigate the effect of prediabetes on cardiac function and to characterize parameters and pathways associated with deteriorated cardiac performance. Long-Evans rats were fed with either control or high-fat chow for 21 wk and treated with a single low dose (20 mg/kg) of streptozotocin at *week 4*. High-fat and streptozotocin treatment induced prediabetes as characterized by slightly elevated fasting blood glucose, impaired glucose and insulin tolerance, increased visceral adipose tissue and plasma leptin levels, as well as sensory neuropathy. In prediabetic animals, a mild diastolic dysfunction was observed, the number of myocardial lipid droplets increased, and left ventricular mass and wall thickness were elevated; however, no molecular sign of fibrosis or cardiac hypertrophy was shown. In prediabetes, production of reactive oxygen species was elevated in subsarcolemmal mitochondria. Expression of mitofusin-2 was increased, while the phosphorylation of phospholamban and expression of Bcl-2/adenovirus E1B 19-kDa protein-interacting protein 3 (BNIP3, a marker of mitophagy) decreased. However, expression of other markers of cardiac auto- and mitophagy, mitochondrial dynamics, inflammation, heat shock proteins, Ca^{2+}/calmodulin-dependent protein kinase II, mammalian target of rapamycin, or apoptotic pathways were unchanged in prediabetes. This is the first comprehensive analysis of cardiac effects of prediabetes indicating that mild diastolic dysfunction and cardiac hypertrophy are multifactorial phenomena that are associated with early changes in mitophagy, cardiac lipid accumulation, and elevated oxidative stress and that prediabetes-induced oxidative stress originates from the subsarcolemmal mitochondria.

Listen to this article's corresponding podcast http://ajpheart.podbean.com/e/myocardial-dysfunction-in-prediabetes/.

obesity; type 2 diabetes; high-fat diet; reactive oxygen species; diabetic cardiomyopathy

NEW & NOTEWORTHY

In prediabetes induced by chronic high-fat diet and a low single dose of streptozotocin in rats, mild diastolic dysfunction and ventricular hypertrophy are observed. Elevated cardiac lipid accumulation, subsarcolemmal mitochondrial reactive oxygen species production, and early changes in cardiac mitophagy may be responsible for cardiac effects of prediabetes.

TYPE 2 DIABETES MELLITUS is a common civilization disease with a growing prevalence worldwide (2, 68, 81). It is well established that type 2 diabetes mellitus is a risk factor of cardiovascular diseases, such as heart failure and myocardial infarc-

* G. Koncsos and Z. Varga contributed equally to this work, and Z. Giricz and R. Schulz contributed equally to this work.

Address for reprint requests and other correspondence: Z. Giricz, H-1089 Budapest, Nagyvárad tér 4. Hungary (e-mail: giricz.zoltan@med.semmelweis-univ.hu).

tion, contributing to their increased morbidity and mortality (6, 68). However, before the development of overt diabetes, a period of prediabetic state (i.e., impaired glucose and insulin tolerance, insulin and leptin resistance, oscillations of normo- and hyperglycemic states, mild to moderate obesity) occurs (54), which may also promote cardiovascular complications (21, 30, 45). Although cardiac pathophysiological alterations are relatively well characterized in fully developed diabetes (i.e., diabetic cardiomyopathy), information about prediabetes is quite limited. It has been reported that prediabetes induces mild diastolic dysfunction in OLETF rats, which is a genetic model for spontaneous long-term hyperglycemia (51); however, cardiac consequences of prediabetes and their molecular mechanism are unknown in nongenetic prediabetic settings.

Contractile dysfunction in diabetic cardiomyopathy has been attributed to numerous factors and pathways [i.e., increased oxidative stress or activated apoptosis (13, 78), which could be connected to an impaired mitochondrial function (24), autophagy (41, 78), or to an imbalance in the calcium homeostasis (60)]. Although these pathways are well studied in diabetes, their role in prediabetes has not been uncovered. Furthermore, because mitochondrial function is heavily influenced by mitochondrial dynamics including mitochondrial biogenesis, fusion, fission, and autophagy-mitophagy and because these processes have been linked to the development of diabetic cardiomyopathy (13, 32, 41, 78), we hypothesized that altered mitochondrial dynamics might be involved in the mechanism of deteriorated cardiac functions in prediabetes. Moreover, development of diabetes leads to systemic sensory neuropathy that has been shown to result in diastolic dysfunction in the rat heart (7, 86).

Therefore, here we aimed to systematically characterize the cardiac effect of prediabetes on functional, morphological, and molecular levels in a nongenetic rodent model.

MATERIALS AND METHODS

This investigation conforms to the *Guide for the Care and Use of Laboratory Animals* published by the US National Institutes of Health (NIH publication No. 85-23, revised 1996) and was approved by the animal ethics committee of the Semmelweis University, Budapest, Hungary (registration numbers: XIV-I-001/450-6/2012). Chemicals were purchased from Sigma (St. Louis, MO) unless otherwise noted.

Animal model and experimental design. Male Long-Evans rats of 5–7 wk of age were purchased from Charles River Laboratories (Wilmington, MA). Animals were housed in a room maintained in a 12-h:12-h light/dark cycle and constant temperature of 21°C. Animals were allowed access to food and water ad libitum. After 1 wk of acclimatization, rats were divided into two groups: control (CON; $n = 20$) and prediabetic group (PRED; $n = 20$) (Fig. 1). The control group was fed control chow, whereas the prediabetic group was fed a chow supplemented with 40% lard as a high-fat diet. Body weights were measured weekly. Blood was taken, and fasting blood glucose levels were measured from the saphenous vein every second week with a blood glucose monitoring system (Accu-Check; Roche, Basel, Switzerland). To facilitate the development of prediabetes and to avoid hypoinsulinemia, animals on high-fat diet received 20 mg/kg streptozotocin (STZ; Santa Cruz Biotechnology, Dallas, TX) intraperitoneally (i.p.) at the fourth week of the diet according to Mansor et al. (50), whereas the control group was treated with the same volume of ice-cold citrate buffer as vehicle. At the 20th wk, oral glucose tolerance test (OGTT) was performed in overnight fasted rats with per os administration of 1.5 g/kg glucose and measurements of plasma glucose levels at 15, 30, 60, and 120 min. Insulin tolerance test (ITT) was also performed at the 20th wk in overnight fasted rats. Insulin (0.5 IU/kg, Humulin R; Ely Lilly, Utrecht, The Netherlands) was injected i.p., and plasma glucose levels were checked at 15, 30, 45, 60, 90, and 120 min. At *week 21* of the diet, animals were anesthetized with pentobarbital (60 mg/kg, i.p.; Euthasol; Produlab Pharma, Raamsdonksveer, The Netherlands). Echocardiography and cardiac catheterization were performed, and then hearts were excised, shortly perfused with oxygenated Krebs-Henseleit buffer in Langendorff mode as described earlier, and weighed. Epididymal and interscapular brown fat tissue, which are the markers of adiposity (9, 34), were isolated, and their weights were measured. Blood and tissue samples were collected and stored at −80°C.

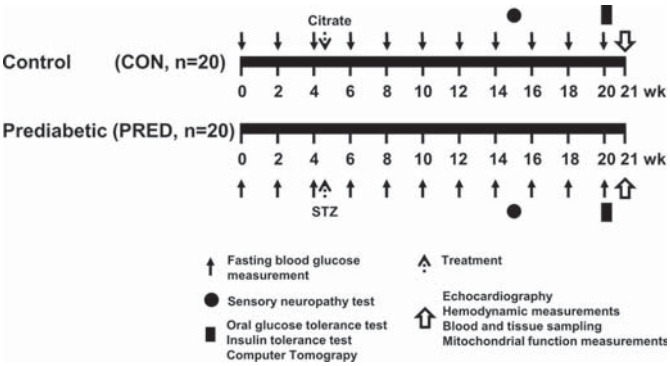

Fig. 1. Experimental protocol. Long-Evans rats were fed with either control (CON) diet for 21 wk, or with high-fat diet and treated with 20 mg/kg streptozotocin (STZ) at *week 4* (PRED) to induce prediabetes. Body weights were measured weekly, and blood samples were taken from the saphenous vein every second week. Sensory neuropathy was measured at *week 15*. Oral glucose tolerance test (OGTT), insulin tolerance test (ITT), and computer tomography (CT) were performed at *week 20*. Echocardiography, hemodynamic analysis, and parameters of mitochondrial function were measured at *week 21* of diet. Tissue sampling was performed after terminal procedures.

Assessment of sensory neuropathy. To test whether sensory neuropathy develops in prediabetes, plantar Von Frey test was performed. At *week 15* of the diet, rats were placed in a plastic cage with a wire mesh bottom to allow full access to the paws. After 5–10-min acclimation time, mechanical hind paw withdrawal thresholds were measured by a dynamic plantar aesthesiometer (UGO-Basile, Monvalle, Italy) as previously described (56).

Evaluation of body fat content. At *week 20* of the diet, computed tomography (CT) measurements were performed on NanoSPECT/CT PLUS (Mediso, Budapest, Hungary). The semicircular CT scanning was acquired with a 55-kV tube voltage, 500-ms exposure time, 1:4 binning, and 360 projections in 18 min, 7 s. During the acquisitions, rats were placed in a prone position in a dedicated rat bed and were anesthetized with 2% isoflurane in oxygen. Temperature of the animals was kept at 37.2 ± 0.3°C during imaging. In the reconstruction, 0.24-mm in-plane resolution and slice thickness were set, and Butterworth filter was applied (volume size: 76.8 × 76.8 × 190 mm). Images were further analyzed with VivoQuant (inviCRO, Boston, MA) dedicated image analysis software products by placing appropriate volumes of interest (VOI) on the whole body fat of animals. The aim of segmentation was to separate the fat from other tissues. The connected threshold method helped to choose the adequate attenuated pixels for fat tissue analysis, and then the isolated points were detected by erode 4 voxel and dilate 4 voxel steps. After the measurements, animals recovered from anesthesia.

Cardiac function by echocardiography. Before euthanasia, to measure cardiac function, echocardiography was performed as previously described (42, 64). Briefly, anesthetized animals were placed on a controlled heating pad, and the core temperature, measured via rectal probe, was maintained at 37°C. Transthoracic echocardiography was performed with animals in the supine position by one investigator

blinded to the experimental groups. Two-dimensional and M-mode echocardiographic images of long and short (midpapillary muscle level) axis were recorded, using a 13-MHz linear transducer (GE 12L-RS; GE Healthcare, Little Chalfont, Buckinghamshire, United Kingdom), connected to an echocardiographic imaging unit (Vivid i, GE Healthcare). The digital images were analyzed by a blinded investigator using an image analysis software (EchoPac, GE Healthcare). On two-dimensional recordings of the short axis at the midpapillary level, left ventricular (LV) anterior (LVAWT) and posterior wall thickness (LVPWT) in diastole (index: d) and systole (index: s) as well as LV end-diastolic (LVEDD) and end-systolic diameter (LVESD) were measured. In addition, end-diastolic and end-systolic LV areas were planimetered from two-dimensional recordings of short and long axis. End-systole was defined as the time point of minimal LV dimensions and end-diastole as the time point of maximal dimensions. All values were averaged over three consecutive cycles. The following parameters were derived from these measurements (65). Fractional shortening (FS) was calculated as [(LVEDD − LVESD)/LVEDD] × 100. LV mass was calculated according to the following formula: [LVmass = (LVEDD + AWTd + PWTd)3 − LVEDD × 3]1.04 × 0.8 + 0.14.

Hemodynamic measurements, LV pressure-volume analysis. After echocardiographic measurements, hemodynamic measurement was performed as previously described (62, 63). Briefly, rats were tracheotomized, intubated, and ventilated, while core temperature was maintained at 37°C. A median laparotomy was performed. A polyethylene catheter was inserted into the left external jugular vein. A 2-Fr microtip pressure-conductance catheter (SPR-838; Millar Instruments, Houston, TX) was inserted into the right carotid artery and advanced into the ascending aorta. After stabilization for 5 min, mean arterial blood pressure (MAP) was recorded. After that, the catheter was advanced into the LV under pressure control. After stabilization for 5 min, signals were continuously recorded at a sampling rate of 1,000/s using a pressure-volume (P-V) conductance system (MPVS-Ultra, Millar Instruments) connected to the PowerLab 16/30 data acquisition system (AD Instruments, Colorado Springs, CO), stored, and displayed on a personal computer by the LabChart5 Software System (AD Instruments). After positioning the catheter, we registered baseline P-V loops. With the use of a special P-V analysis program (PVAN, Millar Instruments), LV end-systolic pressure, LV end-diastolic pressure, the maximal slope of LV systolic pressure increment (dP/d*t*max) and diastolic pressure decrement, time constant of LV pressure decay (τ; according to the Glantz method), ejection fraction (EF), stroke work (SW), and LV maximal power were computed and calculated. Stroke volume and cardiac output (CO) were calculated and corrected according to in vitro and in vivo volume calibrations using the PVAN software. Total peripheral resistance (TPR) was calculated by the following equation: TPR = MAP/CO. In addition to the above parameters, P-V loops recorded at different preloads can be used to derive other useful systolic function indexes that are less influenced by loading conditions and cardiac mass (37, 58). Therefore, LV P-V relations were measured by transiently compressing the inferior vena cava (reducing preload) under the diaphragm with a cotton-tipped applicator. The slope of the LV end-systolic P-V relationship (according to the parabolic curvilinear model), preload recruitable stroke work, and the slope of the dP/dtmax-end-diastolic volume (EDV) relationship (dP/d*t*max-EDV) were calculated as load-independent indexes of LV contractility. The slope of the LV end-diastolic P-V relationship (EDPVR) was calculated as a reliable index of LV stiffness (37). At the end of each experiment, 100 μl of hypertonic saline was injected intravenously, and, from the shift of P-V relations, parallel conductance volume was calculated by the software and used for the correction of the cardiac mass volume. The volume calibration of the conductance system was performed as previously described (37).

Adipokine array from rat plasma. Adipokine array was performed from 1 ml rat plasma according to manufacturer's instructions (Proteome Profiler Rat Adipokine Array Kit; R&D Systems, Abingdon, United Kingdom).

Biochemical measurements. Serum cholesterol, high-density lipoprotein (HDL), and triglyceride levels were measured by colorimetric assays (Diagnosticum, Budapest, Hungary) as previously described (19). Plasma leptin (Invitrogen, Camarillo, CA), tissue inhibitor of matrix metalloprotease (TIMP) metallopeptidase inhibitor 1 (TIMP-1; R&D System, Minneapolis, MN), and angiotensin-II (Phoenix Pharmaceuticals, Karlsruhe, Germany) were measured by ELISA according to manufacturer's instructions. Urea, glutamate oxaloacetate transaminase, glutamate pyruvate transaminase, low-density lipoprotein, C-reactive protein (CRP), cholesterol, uric acid, and creatinine were measured by automated clinical laboratory assays (Diagnosticum).

Histology. Heart, liver, and pancreas samples were fixed in 4% neutral-buffered formalin. After 24 h, samples were washed with PBS and stored in 70% ethanol in PBS until embedded in paraffin. Samples were stained with hematoxylin-eosin (HE) and Masson's trichrome (MA) staining. LV samples were analyzed to examine histopathological differences and evaluate cardiomyocyte hypertrophy and fibrosis. The level of fibrosis was measured on MA-stained LV sections, and transverse transnuclear width (cardiomyocyte diameter) was assessed on longitudinally oriented cardiomyocytes on HE-stained LV sections by a Zeiss microscope (Carl Zeiss, Jena, Germany). Digital images were acquired using an imaging software (QCapture Pro 6.0; QImaging, Surrey, British Columbia, Canada) at ×200 magnification. Quantification of cardiomyocyte diameter and fibrosis was performed with ImageJ Software (v1.48; NIH, Bethesda, MD). Liver samples were evaluated for hepatic steatosis/fibrosis and scored as previously described (40).

Nitrotyrosine immunostaining of LV samples. After embedding and cutting 5-μm-thick sections, heat-induced antigen epitope retrieval was performed (95°C, 10 min, in citrate buffer with a pH of 6.0). Sections were stained with rabbit polyclonal anti-nitrotyrosine antibody (5 μg/ml; Cayman Chemical, Ann Arbor, MI) by using the ABC kit of Vector Laboratories (Burlingame, CA) according to the manufacturer's protocol. Nitrotyrosine-stained sections were counterstained with hematoxylin. Specific staining was visualized, and images were acquired using a BX-41 microscope (Olympus, Tokyo, Japan).

Quantitative RT-PCR. Total RNA was isolated from LV tissue with Reliaprep RNA Tissue Miniprep kit (Promega, Madison, WI) according to the manufacturer's instructions. cDNA was synthesized using Tetro cDNA Synthesis Kit (Bioline, London, UK) according to the manufacturer's protocol. PCR reaction was performed with iQ SYBR Green Supermix (Bio-Rad, Hercules, CA) or TaqMan Universal PCR MasterMix (Thermo Fisher Scientific, Waltham, MA) and 3 nM forward and reverse primers for collagen type 1 and 3 (COL1 and COL3), atrial natriuretic peptide (ANP), brain natriuretic peptide (BNP) (Integrated DNA Technologies, Leuven, Belgium), assay mixes for α-myosin heavy chain (α-MHC, assay ID: Rn00691721_g1), β-MHC (assay ID: Rn00568328_m1), TNF-α (assay ID: Rn99999017_m1), and IL-6 (assay ID: Rn01410330_m1, Thermo Fisher Scientific) were used. β2-Microglobulin or *GAPDH* (assay ID: Rn01775763_g1) were used as reference genes. Quantitative real-time PCR was performed with the StepOnePlus Real-Time PCR System (Thermo Fisher Scientific). Expression levels were calculated using the CT comparative method ($2^{-\Delta CT}$).

Measurement of pancreatic insulin. Freeze-clamped and pulverized pancreas samples were used to determine pancreatic insulin content. Analysis was performed with insulin (I-125) IRMA Kit (Izotop Kft, Budapest, Hungary) according to the manufacturer's instructions.

Electron microscopy. LV tissue samples (1 × 1 mm) were placed in modified Kranovsky fixative (2% paraformaldehyde, 2.5% glutaraldehyde, 0.1 M Na-cacodylate buffer, pH 7.4, and 3 mM $CaCl_2$). After being washed in cacodylate buffer, samples were incubated in 1% osmium tetroxide in 0.1 M PBS for 35 min. Samples were then washed in buffer several times for 10 min and dehydrated in an

ascending ethanol series, including a step of uranyl acetate (1%) solution in 70% ethanol to increase contrast. Dehydrated blocks were transferred to propylene oxide before being placed into Durcupan resin. Blocks were placed in a thermostat for 48 h at 56°C. From the embedded blocks, 1-μm-thick semithin and serial ultrathin sections (70 nm) were cut with a Leica ultramicrotome and mounted either on mesh or on Collodion-coated (Parlodion; Electron Microscopy Sciences, Fort Washington, PA) single-slot copper grids. Additional contrast was provided to these sections with uranyl acetate and lead citrate solutions, and they were examined with a JEOL1200EX-II electron microscope. Areas of subsarcolemmal (SSM), interfibrillar mitochondria (IFM), and lipid droplets were measured by freehand polygon selection in iTEM Imaging Platform.

Mitochondrial enzyme activity measurements. Fresh myocardial samples were homogenized in 1/30 weight per volume Chappel-Perry buffer (100 mM KCl, 5 mM $MgCl_2$, 1 mM EDTA, 50 mM Tris, pH 7.5) supplemented with 15 mg/l trypsin inhibitor, 15.5 mg/l benzamidine, 5 mg/l leupeptin, and 7 mg/l pepstatin A. All enzyme activities were measured as duplicates with a photometer (Cary 50 Scan UV-Visible Spectrophotometer; Agilent Technologies, Palo Alto, CA). Before we added substrate or cofactor, the reaction mix was incubated at 30°C for 10 min (except for cytochrome *c* oxidase). Enzyme activities were expressed relative to citrate synthase activity or total protein levels (measured with bicinchoninic acid assay). The activity of rotenone-sensitive NADH:ubiquinone-oxidoreductase (Complex I) was measured at 340 nm in the presence of 1 mM EDTA, 2.5 mM KCN, 1 μM antimycin A, and 20 μM rotenone after the addition of coenzyme Q and NADH to a final concentration of 60 μM. The activity of NADH:cytochrome *c*-oxidoreductase (Complex I+III) was measured at 550 nm as the antimycin A- and rotenone-sensitive fraction of total NADH-cytochrome *c* oxidoreductase in the presence of 0.1 mM EDTA, 3 mM KCN, and 0.1% cytochrome *c* after adding NADH to a final concentration of 0.2 mM. The activity of succinate: cytochrome *c*-oxidoreductase (Complex II+III) was measured at 550 nm in the presence of 0.1 mM EDTA, 2.5 mM KCN, 0.1% bovine serum albumin, and 4 mM succinate after the addition of cytochrome *c* to a final concentration of 0.1%. The activity of succinate-dehydrogenase was measured at 600 nm in the presence of 0.1 mM EDTA, 2.5 mM KCN, 0.1% bovine serum albumin, and 2 mM succinate after the addition of 2,6-dichloroindophenol and phenazine-methosulfate to a final concentration of 34.900 μM and 1.625 mM, respectively. The activity of cytochrome *c*-oxidase was measured at 550 nm in the presence of 0.08% reduced cytochrome *c*. The activity of citrate synthase was measured at 412 nm in the presence of 0.1% Triton X-100, 0.1 mM 5,5′-dithiobis (2-nitrobenzoic acid), and 0.1 mM acetyl-coenzyme A after the addition of oxaloacetate to a final concentration of 0.5 mM.

Preparation of isolated mitochondria. SSM and IFM fractions were isolated according to a protocol described previously (74) with the use of homogenization buffer (buffer A) containing the following (in mM): 100 KCl, 50 MOPS, 5 $MgSO_4$, 1 EGTA, and pH 7.4 Tris·HCl. Isolation buffer (buffer B) contained the following (in mM): 250 sucrose, 10 HEPES, 1 EGTA, and pH 7.4 Tris·HCl. Before the isolation, 1 mM ATP was added freshly to the homogenization buffer. All steps were carried out on ice. After Langendorff perfusion of the heart, LV samples were cut to small species with scissors and washed in buffer A, then homogenized with five strokes of Teflon pistils in a glass potter. The homogenate was centrifuged for 10 min at 800 *g*, 4°C. For isolation of SSM, the supernatant was centrifuged for 10 min at 8,000 *g*. This pellet was suspended in buffer A and centrifuged for 10 min at 8,000 *g*, and the resulting sediment was resuspended in a small volume of buffer A. The pellet of the first centrifugation was used for isolation of IFM fraction and resuspended in buffer B (10 ml/g tissue) and after addition of 8 U/g of bacterial protease incubated for 1 min on ice and then homogenized with five strokes of Teflon pistil in a glass potter and centrifuged for 10 min at 800 *g*. The supernatant was centrifuged for 10 min at 8,000 *g*, and the resulting mitochondrial pellet was finally resuspended in buffer A and used for mitochondrial respiration, membrane potential, H_2O_2 production, and Ca^{2+} uptake measurements. For Western blots, the resulting SSM and IFM pellets were finally resuspended in a 200 μl volume of Buffer B, which were layered on 30% Percoll solution and ultracentrifuged (Rotor type: Beckman Type 70.1 Ti) for 30 min at 18,700 *g* at 4°C. After ultracentrifugation, lower rings were collected (100 μl/tube) and filled with 1 ml Buffer B and centrifuged for 10 min at 12,200 *g*, 4°C. After being washed, pellets were stored at −80°C.

Measurement of mitochondrial respiration. Protein concentration of SSM and IFM samples was determined by the Biuret method (11). Mitochondrial oxygen consumption was measured by high-resolution respirometry with Oxygraph-2K (Oroboros Instruments, Innsbruck, Austria), a Clark-type O_2 electrode, for 40 min. The mitochondrial protein content was 0.1 mg/ml in the measurements. Measuring mitochondrial respiration followed the substrate-uncoupler-inhibitor titration protocol. Mitochondria were energized with 5 mM glutamate and 5 mM malate. Mitochondrial respiration was initiated with 2 mM adenosine diphosphate. Cytochrome *c* (4 μM), succinate (5 mM), rotenone (1 μM), and carboxyatractyloside (2 μM) were used as indicated. Measurements were performed in an assay medium containing 125 mM KCl, 20 mM HEPES, 100 μM EGTA, 2 mM K_2HPO_4, 1 mM $MgCl_2$, and 0.025% BSA. Data were digitally recorded using DatLab4 software.

Measurement of mitochondrial membrane potential. To detect mitochondrial membrane potential, we used the fluorescent, cationic dye, safranine *O* (2 μM), which can bind to the protein possessing negative charge in the inner mitochondrial membrane depending on the mitochondrial membrane potential. The excitation/emission wavelengths were 495/585 nm, respectively. Fluorescence was recorded at 37°C by Hitachi F-4500 spectrofluorometer (Hitachi High Technologies, Maidenhead, UK). The reaction medium was the following: 125 mM KCl, 20 mM HEPES, 100 μM EGTA, 2 mM K_2HPO_4, 1 mM $MgCl_2$, and 0.025% BSA.

Detection of H_2O_2 formation in mitochondria. H_2O_2 production of SSM and IFM was assessed by Amplex UltraRed fluorescent dye method (52). Horseradish peroxidase (2.5 U/ml) and Amplex UltraRed reagent (1 μM) and then 0.05 mg/ml mitochondria were added to the incubation medium. H_2O_2 formation was initiated by the addition of 5 mM glutamate and 5 mM malate or 5 mM succinate, and fluorescence was detected at 37°C with Deltascan fluorescence spectrophotometer (Photon Technology International, Lawrenceville, NJ). The excitation wavelength was 550 nm, and the fluorescence emission was detected at 585 nm. A calibration signal was generated with known quantities of H_2O_2 at the end of each experiment.

Measurement of Ca^{2+} uptake in mitochondria. The free Ca^{2+} concentration at each added concentration of Ca^{2+} was calculated and measured. Ca^{2+} uptake by mitochondria was followed by measuring calcium-green-5N (100 nM) fluorescence at 505 nm excitation and 535 emission wavelengths at 37°C using a Hitachi F-4500 spectrofluorometer (Hitachi High Technologies). The reaction medium was the following: 125 mM KCl, 20 mM HEPES, 100 μM EGTA, 2 mM K_2HPO_4, 1 mM $MgCl_2$, and 0.025% BSA.

Western blot of LV lysates and isolated mitochondria fractions. Freeze-clamped LVs were pulverized under liquid nitrogen and homogenized in homogenization buffer containing (in mmol/l) 20 Tris·HCl, 250 sucrose, 1.0 EGTA, and 1.0 dithiothreitol or in radioimmunoprecipitation assay buffer (Cell Signaling Technology, Danvers, MA), supplemented with 1 mM PMSF (Roche, Basel, Switzerland), 0.1 mM sodium fluoride, 200 mM sodium orthovanadate, and complete protease inhibitor cocktail (Roche) with TissueLyser LT (Qiagen, Venlo, The Netherlands) to obtain LV soluble protein fraction or LV whole cell lysate. Previously isolated mitochondrial samples were resuspended in ice-cold 1× cell lysis buffer (Cell Signaling Technology). Concentration of proteins was assessed with Lowry's assay or bicinchoninic acid assay kit (Thermo Fisher Scientific).

For tropomyosin oxidation analysis, tissue samples were homogenized in ice-cold PBS, pH 7.2, containing an antiprotease mixture (Complete, Roche) and 5 mM EDTA. Just before use, the protein samples were stirred under vacuum and bubbled with argon to maximally reduce the oxygen tension. The protein suspension was centrifuged at 12,000 *g* for 10 min at 4°C. The resulting pellet was resuspended in sample buffer (2% SDS, 5% glycerol, 1% β-mercaptoethanol, 125 mM Tris·HCl, pH 6.8) and denatured by 10 min of boiling. This procedure referred to as reducing condition was compared with the nonreducing condition obtained without the addition of β-mercaptoethanol. To avoid artifacts attributable to the oxidation of thiol groups in vitro, nonreducing conditions were performed in the presence of 1 mM *N*-ethylmaleimide.

Protein samples were resolved on precast 4–20% Criterion TGX gels (Bio-Rad) or Bis-Tris gels depending on the protein of interest and transferred to nitrocellulose or Immun-Blot PVDF membranes (Bio-Rad). Quality of transfer was verified with Ponceau *S* staining. Membranes were blocked with 5% nonfat milk (Bio-Rad) or 2–5% BSA (Santa Cruz Biotechnology) in Tris-buffered saline with 0.05% Tween 20 (TBS-T) for 0.5–2.0 h. Membranes were incubated with primary antibodies in 1–5% nonfat milk or BSA in TBS-T: anti-tropomyosin (Tm; 1:250), anti-phospho-phospholamban (PLB-Ser^{16}; 1:5,000), p-PLB (Thr^{17}; 1:5,000), anti-sarco/endoplasmic reticulum Ca^{2+}-ATPase II (SERCA2A; 1:5,000; Badrilla, Leeds, United Kingdom), anti-heat shock protein-60 (HSP-60; 1:500), anti-HSP-70 (1:500), anti-HSP-90 (1:500), anti-B-cell lymphoma 2 (Bcl-2; 1:500), anti-caspase-3 (1:500), anti-Ca^{2+}/calmodulin-dependent protein kinase II (CaMKIIδ; 1:2,000), anti-Parkin (1:5,000, Santa Cruz Biotechnology), anti-Shc (1:1,000), anti-dynamin-related/like protein 1 (DRP1/DLP1; 1:5,000), anti-optic atrophy 1 protein (OPA1; 1:2,500, BD Biosciences, Franklin Lakes, NJ), anti-mitofusin-2 (MFN2; 1:2,500, Abcam, Cambridge, UK), anti-phospho-CaMKIIδ (Thr^{287}; 1:2,000), anti-phospho-HSP-27 (Ser^{82}; 1:1,000), anti-HSP-27 (1:1,000), anti-Bax (1:1,000), anti-sequestosome 1 (SQSTM1/p62; 1:1,000), anti-microtubule-associated protein 1 light chain 3 A/B (LC3 A/B; 1:5,000), anti-Beclin-1 (1:1,000), anti-Bcl-2/adenovirus E1B 19-kDa protein-interacting protein 3 (BNIP3; 1:5,000), anti-phospho-Akt (Ser^{473}; 1:1,000), anti-Akt (1:1,000), anti-phospho-AMP-activated protein kinase α (AMPKα-Thr^{172}; 1:1,000), anti-AMPKα (1:1,000), anti-phospho-ribosomal S6 (Ser$^{235/236}$; 1:1,000), anti-ribosomal S6 (1:1,000), anti-phospho-glycogen synthase kinase-3β (GSK3β-Ser^{9}; 1:1,000), anti-GSK3β (1:1,000), and anti-GAPDH (1:5,000) as loading control (Cell Signaling Technology). For isolated mitochondria, the following primary antibodies were used in 5% nonfat milk in TBS-T: anti-OPA1 (1:2,500) from BD Bioscience, anti-SQSTM1/p62 (1:1,000), anti-LC3 A/B (1:1,000), and anti-cytochrome *c* oxidase subunit 4 (COX4; 1:5,000) as loading control from Cell Signaling Technology. After three washes with TBS-T, horseradish peroxidase-conjugated secondary antibody was added for 2 h at room temperature (1:5,000 in 5% nonfat milk in TBS-T). Signals were detected with an enhanced chemiluminescence kit (Bio-Rad) by Chemidoc XRS+ (Bio-Rad). For the analysis of tropomyosin oxidation, the density of the additional band with higher molecular weight reflecting the formation of disulfide cross bridges was normalized to densitometric values of the respective tropomyosin monomer. Antibodies against phosphorylated epitopes were removed with Pierce Stripping Buffer (Thermo Fisher Scientific) before incubation with antibodies detecting the total protein.

Statistical analysis. Values are expressed as means ± SE. Statistical analysis was performed between groups by unpaired two-tailed *t*-test or by Mann-Whitney *U*-test by using GraphPad Prism 6 software. A $P < 0.05$ value was considered significant.

RESULTS

Moderately increased adiposity in prediabetic animals. To determine the effect of high-fat diet and the single, low-dose STZ injection, we measured body weight, fat tissue volumes, and plasma lipid parameters. We found that body weights of the prediabetic animals were moderately but statistically significantly elevated from *week 9* compared with the control group and that this difference reached 18% at the end of the diet period (Fig. 2, *A* and *B*). At *week 20*, plasma leptin level was significantly increased in prediabetes; however, CRP level was decreased, and plasma cholesterol, HDL cholesterol, triglyceride levels, and parameters of liver and kidney function were unchanged (Table 1). To characterize prediabetes-induced changes in further obesity-related molecules, we performed an adipokine array measurement, which revealed that the circulating level of TIMP-1 might be influenced by prediabetes; however, we could not confirm these results by ELISA (data not shown). CT scan showed that body fat volume of prediabetic rats was substantially increased at the end of the diet (Fig. 2, *C* and *D*). Epididymal fat tissue weight, which is an indicator of total body adiposity, was increased in the prediabetic group; however, the weight of interscapular brown adipose tissue was not changed (Fig. 2, *G–I*). Histological score analysis of HE- and MA-stained liver samples showed the development of hepatic steatosis in the prediabetic group (CON: 0.5 ± 0.3 vs. PRED: 2.25 ± 0.5; $P < 0.05$); however, no signs of hepatic fibrosis were detected (Fig. 2*H*). Furthermore, electron microscopy showed an increased number of lipid droplets in the myocardium of prediabetic animals compared with controls (Fig. 2, *E* and *F*). These results demonstrated a moderately increased adiposity and hepatic and cardiac fat deposits without signs of hyperlipidemia in the prediabetic group.

Impaired glucose tolerance, insulin resistance, and sensory neuropathy evidence disturbed carbohydrate metabolism in prediabetes. We aimed to characterize the glucose homeostasis in our rat model of prediabetes. At *week 20* of the diet, fasting blood glucose levels were slightly elevated in prediabetes from *week 10*; however, they remained in the normoglycemic range (Fig. 3, *A* and *B*). OGTT and ITT demonstrated impaired glucose tolerance and insulin resistance in the prediabetic group (Fig. 3, *C–F*); however, there was no difference in pancreatic insulin content (Fig. 3*G*) or in pancreatic islet morphology (data not shown) between groups. These results demonstrate prediabetic conditions in the present model and reveal that type 1 diabetes did not develop due to the STZ treatment. Sensory neuropathy is a well-accepted accompanying symptom of diabetes (80). Accordingly, here we have found a decrease in the mechanical hind limb withdrawal threshold at *week 15* (CON: 48 ± 1 g vs. PRED: 42 ± 2 g; $P < 0.05$) of diet in the prediabetic group, which indicates a moderate sensory neuropathy in this model of prediabetes.

Diastolic dysfunction and hypertrophy in prediabetes with no sign of fibrosis. To determine the cardiac effect of prediabetes, we measured morphological and functional parameters of the hearts. Heart weights were significantly increased (Fig. 4*A*); however, heart weight/body weight ratio was decreased in prediabetes (CON: 0.27 ± 0.01% vs. PRED: 0.24 ± 0.01%; $P < 0.05$), plausibly attributable to obesity. LV mass, LVAWTs, LVPWTs, and LVPWTd were increased in the prediabetic group as assessed with echocardiography; however, other cardiac dimensional parameters were unchanged (Table 2). The slope of EDPVR, which is a very early and sensitive marker of diastolic dysfunction, was significantly

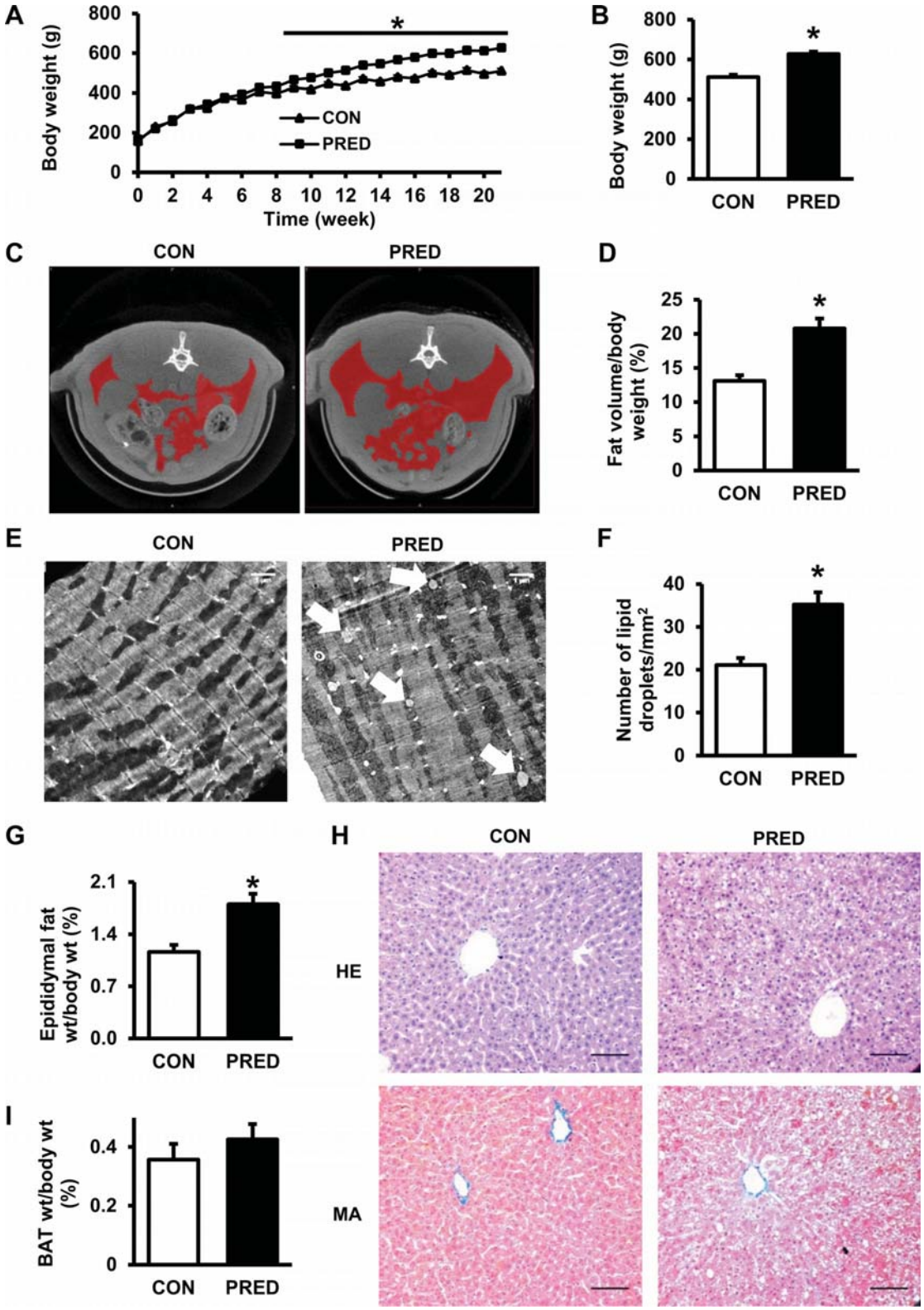

Fig. 2. High-fat feeding with a single low-dose STZ treatment increased adiposity. Changes in body weight during the experiment (*A*) and body weight data after 21 wk (*B*) are shown. Axial representative CT slice shows the middle of the 4th lumbar spine. *C*: red color indicates the segmented volumes of interest (VOIs) showing the volume of fat in the control (CON) and prediabetic (PRED) rats. *D*: whole body fat volume:body weight ratio at *week 20*. Representative transmission electron micrographs of myocardial lipid droplets (*E*; white arrows) and the number of lipid droplets in CON and PRED cardiomyocytes (*F*) are shown; magnification ×7,500; scale bar = 1 μm. Epididymal fat tissue (*G*) and interscapular brown adipose tissue (BAT) (*I*) weight:body weight ratios are shown. Hematoxylin-Eosin (HE) and Masson's trichrome (MA) staining of liver sections (*H*) are shown; magnification ×200; scale bar = 100 μm. Data are means ± SE, n = 3–19 per group (*$P < 0.05$).

Table 1. *Plasma parameters at week 20*

	CON	PRED
Plasma leptin, ng/ml	2.51 ± 0.33	5.91 ± 0.60*
Plasma cholesterol, mmol/l	1.88 ± 0.06	1.72 ± 0.08
HDL cholesterol, mmol/l	2.75 ± 0.14	2.75 ± 0.10
Plasma triglyceride, mmol/l	1.20 ± 0.10	1.31 ± 0.09
LDL cholesterol, mmol/l	0.44 ± 0.02	0.47 ± 0.03
Total cholesterol, mmol/l	1.61 ± 0.05	1.51 ± 0.08
GOT, U/l	82.00 ± 15.00	58.00 ± 4.00
GPT, U/l	50.00 ± 14.00	49.00 ± 5.00
Uric acid, mmol/l	24.00 ± 4.00	16.00 ± 1.00
Creatinine, μmol/l	46.00 ± 3.00	40.00 ± 3.00
CRP, mg/l	109.56 ± 1.24	94.96 ± 3.87*

Data are means ± SE for 12 rat per group (*$P < 0.05$). HDL, high-density lipoprotein; LDL, low-density lipoprotein; GOT glutamate oxaloacetate transaminase; GPT, glutamate pyruvate transaminase; CRP, C-reactive protein; CON, control; PRED, prediabetes group.

elevated in prediabetes although other hemodynamic parameters, including blood pressure, were unchanged, demonstrating the lack of systolic dysfunction or hypertension (Table 3, Fig. 4*B*). To uncover the molecular background of the observed mild diastolic dysfunction, we performed measurements on the common mechanistic contributors of heart failure (38). On HE-stained LV sections, increased cardiomyocyte diameter was detected in prediabetes (Fig. 4, *C* and *D*). To characterize components affecting diastolic function, we analyzed MHC expression. Interestingly, the gene expression of *β-MHC* was decreased, and *α-MHC* also showed a tendency to decrease ($P = 0.17$), the ratio of which resulted in a strong tendency to decrease in prediabetes. No increase in *ANP* or *BNP* gene expressions (Fig. 4, *G* and *H*) or in angiotensin-II level (data not shown) was detected in prediabetes. To evaluate the extent of fibrosis, MA-stained LV sections were analyzed, which revealed no difference between groups (Fig. 4*E*). Similarly, we found that gene expression of type I (*COL1*) and III (*COL3*) collagen isoforms were unchanged in the LV (Fig. 4*F*). These results indicate that mild diastolic dysfunction developed in prediabetic animals, which was associated with a mild hypertrophy (increased LV mass, LVAWT, LVPWT, and cardiomyocyte diameter) without signs of fibrosis.

Elevated reactive oxygen species formation in cardiac subsarcolemmal mitochondria in prediabetic rats. To investigate whether cardiac mitochondrial disturbances contribute to the observed diastolic dysfunction, mitochondrial morphology and enzyme activity were analyzed from LVs of prediabetic rats. Our electron microscopy results showed that there is no major difference in the number of IFM between the groups (Fig. 5, *A* and *B*). However, area (CON: 0.43 ± 0.01 vs. PRED: 0.39 ± 0.01 μm^2; $P < 0.05$), perimeter (CON: 2.69 ± 0.02 vs. PRED: 2.63 ± 0.03 μm; $P < 0.05$), and sphericity (CON: 0.35 ± 0.01 vs. PRED: 0.31 ± 0.01; $P < 0.05$) of IFM are decreased in the prediabetes group. Previous studies indicated that IFM and SSM are affected by diabetes differentially (35, 82). Therefore, we analyzed our electron microscopy imagery containing SSM and found no difference in SSM size, perimeter, or sphericity (data not shown) although the statistical power of these analyses was not high enough ($n = 2$ for CON and $n = 4$ for PRED). Furthermore, we have not seen any major difference in mitochondrial oxygen consumption, enzyme activities (Tables 4 and 5), Ca uptake, or membrane potential (data not shown). However, we have found that hydrogen peroxide production was increased in the cardiac SSM fraction with glutamate-malate as a substrate (Fig. 5*C*) although there was no difference when succinate was used as substrate. Interestingly, there was no increase in reactive oxygen species (ROS) production of the IFM isolated from LV supported either with glutamate-malate or with succinate (Fig. 5, *D–F*). As leukocytes are one of the main sources of ROS, inflammatory mediators were measured. We could find no significant difference in TNF-α (CON: 1 ± 0.27 vs. PRED: 0.59 ± 0.07; ratio normalized to

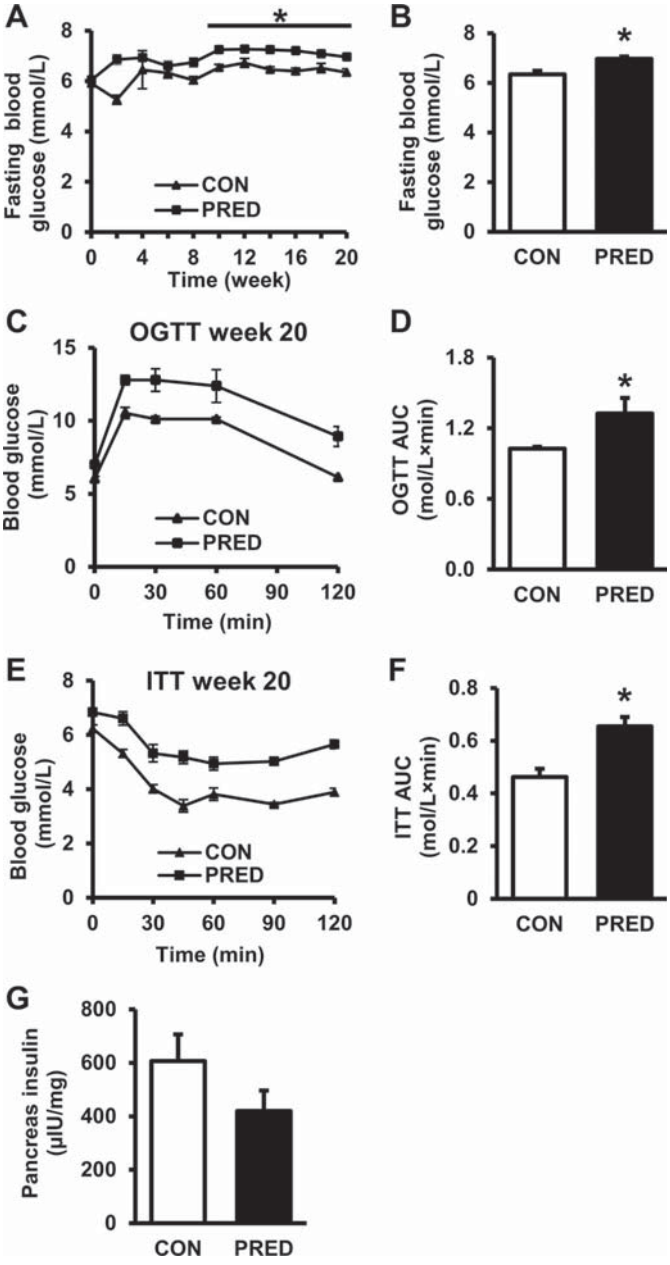

Fig. 3. Alterations in glucose homeostasis indicate the development of prediabetes in STZ-treated and high-fat-fed rats at *week 21*. Fasting blood glucose levels during the experiment (*A*) and at *week 20* (*B*) are shown. OGTT (*C* and *D*) and ITT (*E* and *F*) results at *week 20* of the diet are shown. Insulin content of pancreas at *week 21* (*G*) is shown. Data are means ± SE, $n = 6–19$ per group (*$P < 0.05$).

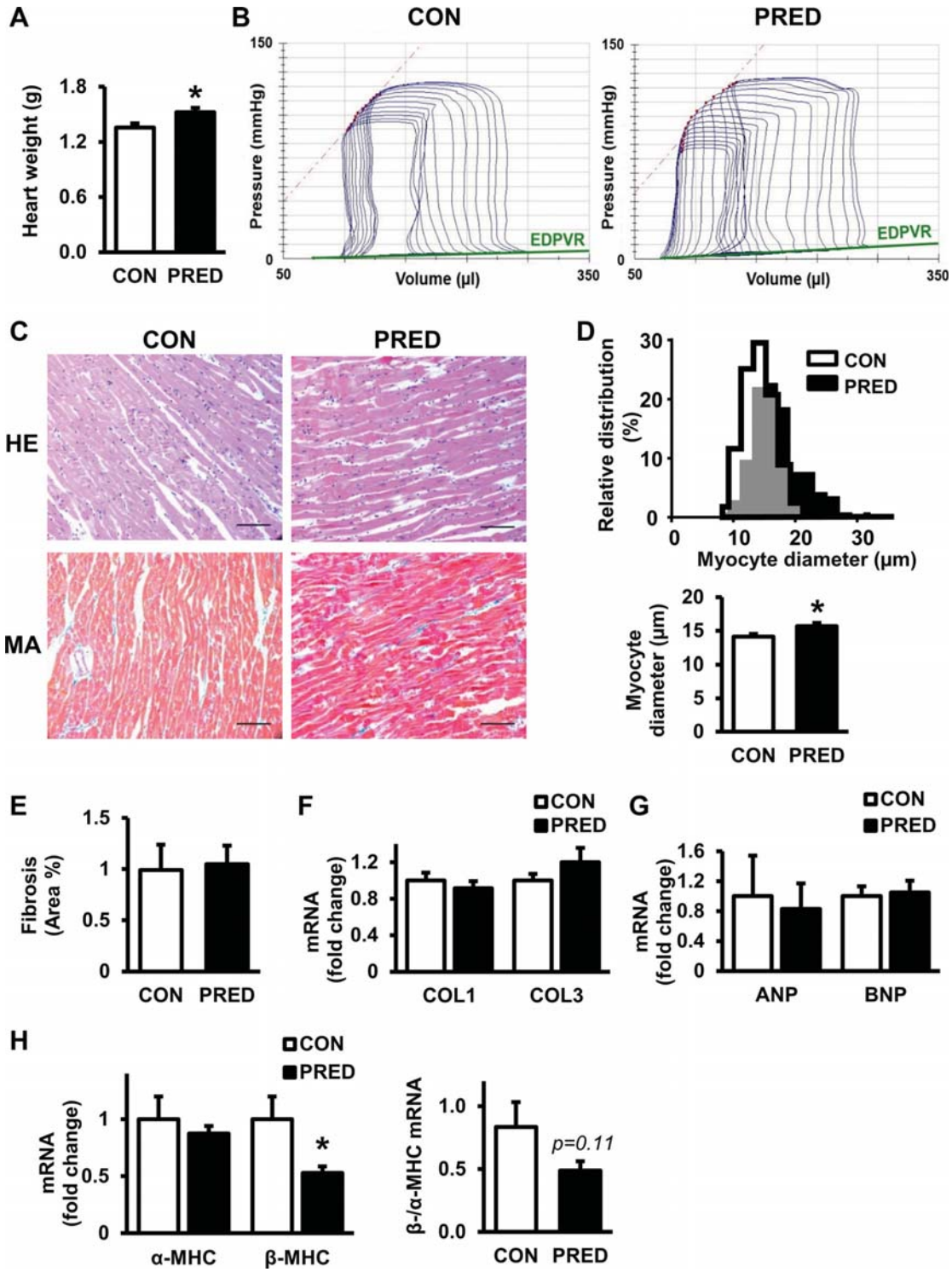

Fig. 4. Characterization of cardiac function, myocardial morphology, and fibrosis in prediabetic rats. *A*: quantification of heart weights after 21 wk. *B*: representative pressure-volume loops and slope of end diastolic pressure-volume relationship (EDPVR) in CON and PRED group. HE and MA staining of myocardial sections (*C*), quantification of cardiomyocyte diameter (*D*), and level of fibrosis (*E*) in control (CON) and prediabetic (PRED) rats are shown; magnification ×200; scale bar = 100 μm. Quantifications of collagen type I (COL1), COL3 (*F*), atrial natriuretic peptide (ANP), brain natriuretic peptide (BNP) (*G*), α-myosin heavy chain (α-MHC), β-MHC, and α-:β-MHC ratio (*H*) in CON and PRED group are shown. Data are means ± SE, n = 5–19 per group (*$P < 0.05$).

Table 2. *Characterization of cardiac morphology and function in prediabetes by means of echocardiography*

	CON	PRED
LV mass, g	1.01 ± 0.04	1.22 ± 0.07*
LVAWTd, mm	1.89 ± 0.12	2.07 ± 0.12
LVAWTs, mm	2.86 ± 0.17	3.42 ± 0.11*
LVPWTd, mm	1.86 ± 0.07	2.05 ± 0.04*
LVPWTs, mm	2.72 ± 0.12	3.25 ± 0.15*
LVEDD, mm	7.71 ± 0.22	7.75 ± 0.17
LVESD, mm	4.93 ± 0.22	4.96 ± 0.31
FS, %	36.00 ± 2.20	37.40 ± 3.80
HR, 1/min	335.00 ± 13.00	348.00 ± 10.00

Data are means ± SE for 10 rat per group (*$P < 0.05$). LV, left ventricular; LVAWTs, LV anterior wall thickness, diastolic; LVAWTs, LV anterior wall thickness, systolic; LVPWTs, LV posterior wall thickness, systolic; LVPWTd, LV posterior wall thickness, diastolic; FS%, fractional shortening %; HR, heart rate.

GAPDH; $P > 0.05$) and IL-6 (CON: 1 ± 0.27 vs. PRED: 0.69 ± 0.14; ratio normalized to GAPDH; $P > 0.05$) mRNA expressions between groups, which shows that, in our model, prediabetes does not elicit cardiac or systemic inflammation. Furthermore, we have not seen any difference in other markers of oxidative stress, namely the expression of p66Shc and tropomyosin oxidation between groups (Fig. 6, *B–E*). It is known that reactive nitrogen species have an important role in deteriorated contractile and endothelial function in diabetes (16, 59); therefore, we analyzed whether nitrative stress is influenced in prediabetes. Nitrotyrosine immunohistology indicated that protein nitrosylation is increased in prediabetes (Fig. 6*A*). As CaMKIIδ has been proposed to be activated in oxidative stress-associated conditions (46), we measured the levels of the active forms of the kinase that might affect the contractility and relaxation capacity of the heart (49). The phosphorylation of CaMKIIδ and of its target PLB on Thr^{17} was not changed by prediabetes (Fig. 6, *F–H*). Similarly, there was no change in the protein expression of SERCA2A in our model of prediabetes compared with control animals (Fig. 6*J*). On the other hand, the level of p-Ser^{16}-PLB showed a tendency for downregulation in prediabetes ($P = 0.08$; Fig. 6*I*).

Alterations in cardiac MFN2 expression and mitophagy in prediabetes. To investigate the effect of cardiac mitochondrial dynamics, autophagy, and mitophagy in prediabetes, we analyzed protein expression changes. Cardiac expression of the mitophagy-related protein, BNIP3, was decreased in the prediabetic group in LV lysates; however, other autophagy- and mitophagy-related proteins such as Beclin-1, LC3-II, SQSTM1/p62, and Parkin were unchanged (Fig. 7*A*; Table 6). Upstream modulators of autophagy such as Akt, AMPKα, GSK3β, and ribosomal S6 protein (a surrogate marker of mammalian target of rapamycin complex activity) were also measured; however, expression or phosphorylation of these proteins were not different between groups (Fig. 7*A*; Table 6). Furthermore, the expression of a mitochondrial fusion-related protein, MFN2, was elevated; however, expression of DRP1/DLP1 and OPA1 proteins was unchanged in whole LV lysates in the prediabetic group (Fig. 7*B*; Table 6). Nonetheless, we measured the expression of mitochondrial dynamics- and mitophagy-related proteins from SSM and IFM isolated from LVs. No difference was found in the expression of OPA1, LC3-II, and SQSTM1/p62 in isolated cardiac SSM and IFM between groups (Fig. 7, *C* and *D*; Table 6). Our results indicate that mitochondrial dynamics and autophagy/mitophagy were not modulated substantially by prediabetes; however, the upregulation of MFN2 (increased mitochondrial fusion, tethering to endoplasmic reticulum) and the downregulation of BNIP3 (decreased mitophagy) may implicate early changes in mitochondrial homeostasis, which might lead to the accumulation of dysfunctional mitochondria.

Expression of cardiac Bcl-2 decreases in prediabetes. Our study also aimed to explore the effect of prediabetes on apoptosis in the heart. Prediabetes did not affect the expression of proapoptotic caspase-3 and Bax in LVs. On the other hand, the antiapoptotic Bcl-2 was downregulated in prediabetic animals. However, the Bcl-2/Bax ratio was unchanged (Fig. 7*F*; Table 6).

No changes in cardiac HSPs in prediabetes. We also characterized the effect of prediabetes on the expression and/or phosphorylation of HSPs in the LV. Our results showed no differences in the expression of HSP-60, HSP-70, and HSP-90 or in either phosphorylation or expression of HSP-27 (Fig. 7*E*; Table 6).

DISCUSSION

This is the first comprehensive analysis of the cardiac effects of prediabetes in a nongenetic rodent model in which we assessed cardiac functions, parameters of hypertrophy, fibrosis, oxidative and nitrative stress, inflammation, mitochondrial dynamics, autophagy, mitophagy, markers of myocardial calcium handling, apoptosis, and expression of HSPs. In this model of prediabetes, we demonstrated an impaired glucose and insulin tolerance, increased adiposity and myocardial lipid accumula-

Table 3. *Characterization of LV hemodynamics in vivo in prediabetes by means of pressure-volume analysis*

	CON	PRED
MAP, mmHg	110.100 ± 7.300	113.600 ± 6.100
LVESP, mmHg	116.600 ± 5.600	120.000 ± 6.800
LVEDP, mmHg	4.400 ± 0.400	4.000 ± 0.200
LVEDV, μl	292.800 ± 14.500	280.200 ± 9.600
LVESV, μl	130.700 ± 6.900	127.500 ± 4.500
SV, μl	162.100 ± 9.100	152.800 ± 7.700
CO, ml/min	59.500 ± 3.200	56.600 ± 2.300
EF, %	55.300 ± 1.300	54.400 ± 1.300
SW, mmHg·ml	14.500 ± 0.500	13.600 ± 0.600
dP/d*t*max, mmHg/s	7226.000 ± 487.000	7387.000 ± 401.000
dP/d*t*min, mmHg/s	−8198.000 ± 680.000	−8551.000 ± 545.000
τ (Glantz), ms	12.600 ± 0.300	12.100 ± 0.400
TPR, (mmHg·min)/ml	1.900 ± 0.190	2.000 ± 0.120
Slope of ESPVR, mmHg/μl	2.680 ± 0.120	2.710 ± 0.060
Slope of EDPVR, mmHg/μl	0.026 ± 0.001	0.037 ± 0.004*
PRSW, mmHg	100.500 ± 5.200	98.900 ± 4.100
Slope of dP/d*t*max-EDV, (mmHg/s)/μl	34.300 ± 2.300	35.200 ± 2.200
Maximal power, mW	91.800 ± 8.200	98.200 ± 12.500

Data are means ± SE for 10 rat per group (*$P < 0.05$). MAP, mean arterial pressure; LVESP, LV end-systolic pressure; LVEDP, LV end-diastolic pressure; LVESV, LV end-systolic volume; LVEDV, LV end-diastolic volume; SV, stroke volume; CO, cardiac output; EF, ejection fraction; SW, stroke work; dP/d*t*max, maximal slope of LV systolic pressure increment; dP/d*t*min, maximal slope of LV diastolic pressure decrement; τ, time constant of LV pressure decay; TPR, total peripheral resistance; ESPVR, end-systolic pressure-volume relationship; EDPVR, end-diastolic pressure-volume relationship; PRSW, preload recruitable SW; dP/d*t*max-EDV, slope of the dP/d*t*max-end-diastolic volume relationship.

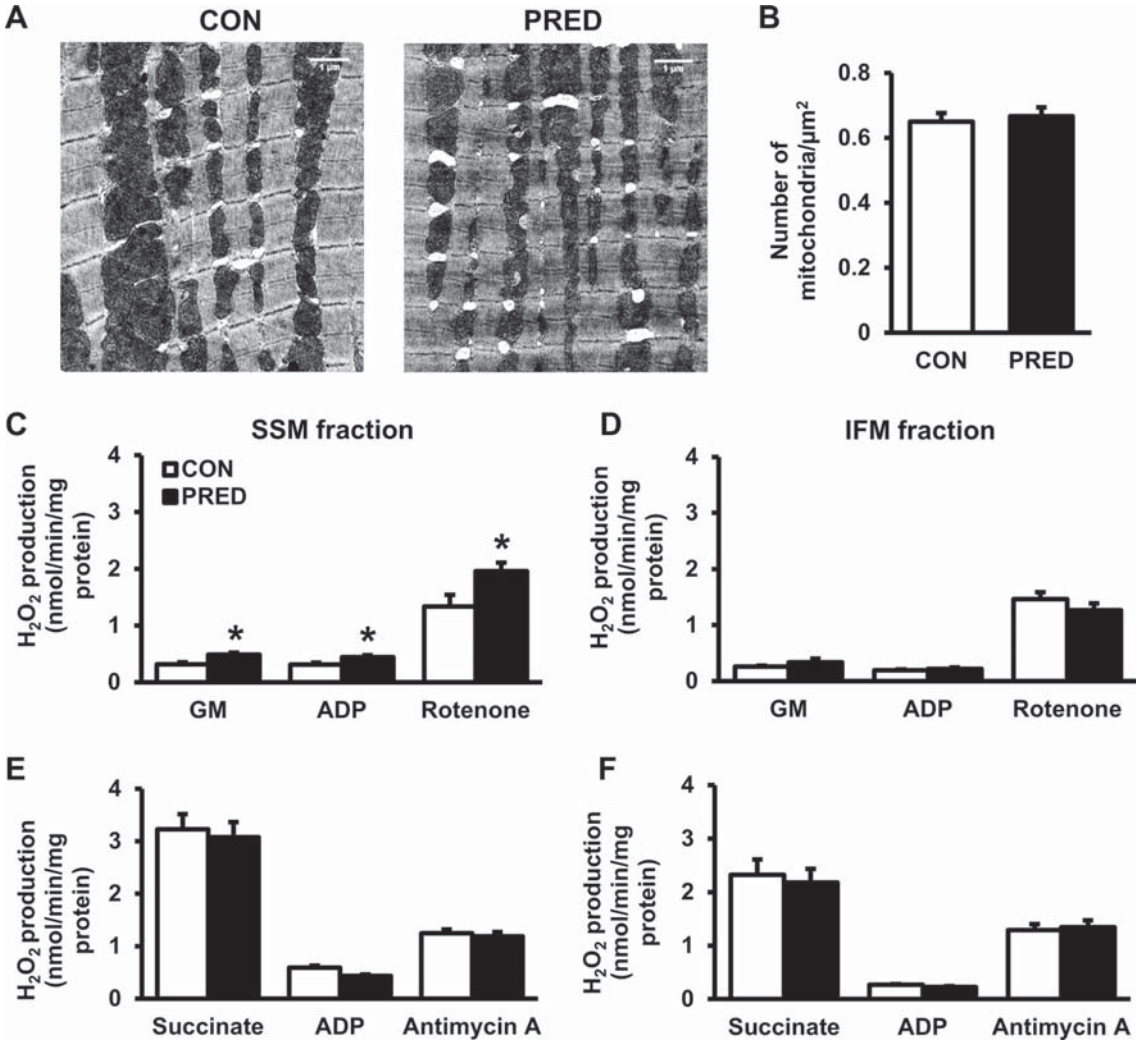

Fig. 5. Mitochondrial morphology and function in prediabetes at *week 21*. Representative transmission electron micrographs (*A*) and number of interfibrillar mitochondria (IFM) (*B*) in the left ventricle are shown; magnification ×12,000, scale bar = 1 μm. Quantifications of H_2O_2 production in subsarcolemmal mitochondria (SSM) (*C*) and IFM (*D*) with glutamate-malate as substrate (GM) are shown. Quantification of H_2O_2 production in SSM (*E*) and IFM (*F*) with succinate as substrate is shown. Data are means ± SE, n = 5–9 per group (*$P < 0.05$).

tion, a mild diastolic dysfunction, and sensory neuropathy despite normal fasting plasma glucose and lipid levels. We also observed elevated ROS production in the SSM, nitrative stress, elevated expression of MFN2, decreased expression of β-MHC, and phosphorylation of PLB. Furthermore, here we found early signs of dysregulated mitophagy and decreased mitochondrial size in prediabetes; however, other major markers of mitochondrial dynamics, autophagy, mitophagy, inflammation, or myocardial expression of apoptotic proteins or HSPs, were not modulated by prediabetes.

Table 4. *Quantification of cardiac mitochondria enzyme activity in LV*

	CON	PRED
Citrate-synthase activity, U/mg protein	223.12 ± 9.98	220.44 ± 8.32
NADH:ubiquinone-oxidoreductase activity, U/mg protein	40.52 ± 2.55	36.48 ± 2.99
NADH:cytochrome *c*-oxidoreductase activity, U/mg protein	7.85 ± 1.18	8.47 ± 1.31
Succinate:cytochrome *c*-oxidoreductase activity, U/mg protein	21.09 ± 1.49	23.57 ± 1.61
Succinate-dehydrogenase activity, U/mg protein	84.06 ± 5.83	80.09 ± 3.42
Cytochrome-*c*-oxidase activity, U/mg protein	38.74 ± 3.15	40.36 ± 2.33

Data are means ± SE for 5–9 rat per group.

In this study, we used high-fat chow-fed Long-Evans rats treated with a single, low-dose STZ. This setting allowed us to investigate cardiac consequences of a moderate metabolic derangement, prediabetes, rather than of a severely disturbed glucose and lipid homeostasis, such as seen in genetically modified models of diabetes, e.g., in *db/db* or *ob/ob* mice (36, 67). Because it has been reported that LV hypertrophy had a higher prevalence in patients with diabetes and that 40–75% of patients with type 1 or type 2 diabetes mellitus presented with diastolic dysfunction (12, 73), we aimed to investigate whether cardiac function is affected by prediabetes. Previously, it has been shown that diastolic dysfunction was developed in several pathological conditions; however, the underlying mechanisms are still not clearly understood (38). Here, we demonstrated that the deterioration of diastolic function and sensory neurop-

Table 5. *Quantification of mitochondrial oxygen consumption*

	CON	PRED	CON	PRED
	Subsarcolemmal, (pmol/ml)s	Subsarcolemmal, (pmol/ml)s	Interfibrillar, (pmol/ml)s	Interfibrillar, (pmol/ml)s
Glutamate-malate	25.08 ± 3.60	21.06 ± 3.53	58.60 ± 19.31	61.78 ± 21.41
ADP	203.31 ± 32.57	194.03 ± 42.16	304.23 ± 25.75	287.90 ± 22.35
Cytochrome *c*	260.80 ± 28.27	287.06 ± 54.91	335.96 ± 25.79	345.41 ± 28.17
Succinate	306.20 ± 25.19	289.74 ± 23.23	367.76 ± 15.74	393.56 ± 18.82
Rotenone	143.12 ± 18.19	139.70 ± 23.64	238.40 ± 18.44	220.73 ± 16.19
CAT	105.95 ± 8.89	106.50 ± 12.22	159.78 ± 6.86	156.60 ± 8.03

Data are means ± SE for 9 rat per group. CAT, carboxyatractyloside.

athy occurs well before overt diabetes develops, which is accompanied by early signs of cardiac hypertrophy. These findings are in agreement with previous reports showing that neuropathy might precede the development of full-fledged diabetes (48) and that high-fat diet-induced prediabetes increased heart weights and decreased contractile function, as assessed by a diminished aortic output (23, 29). However, in contrast to our report, plasma triglycerides and insulin levels

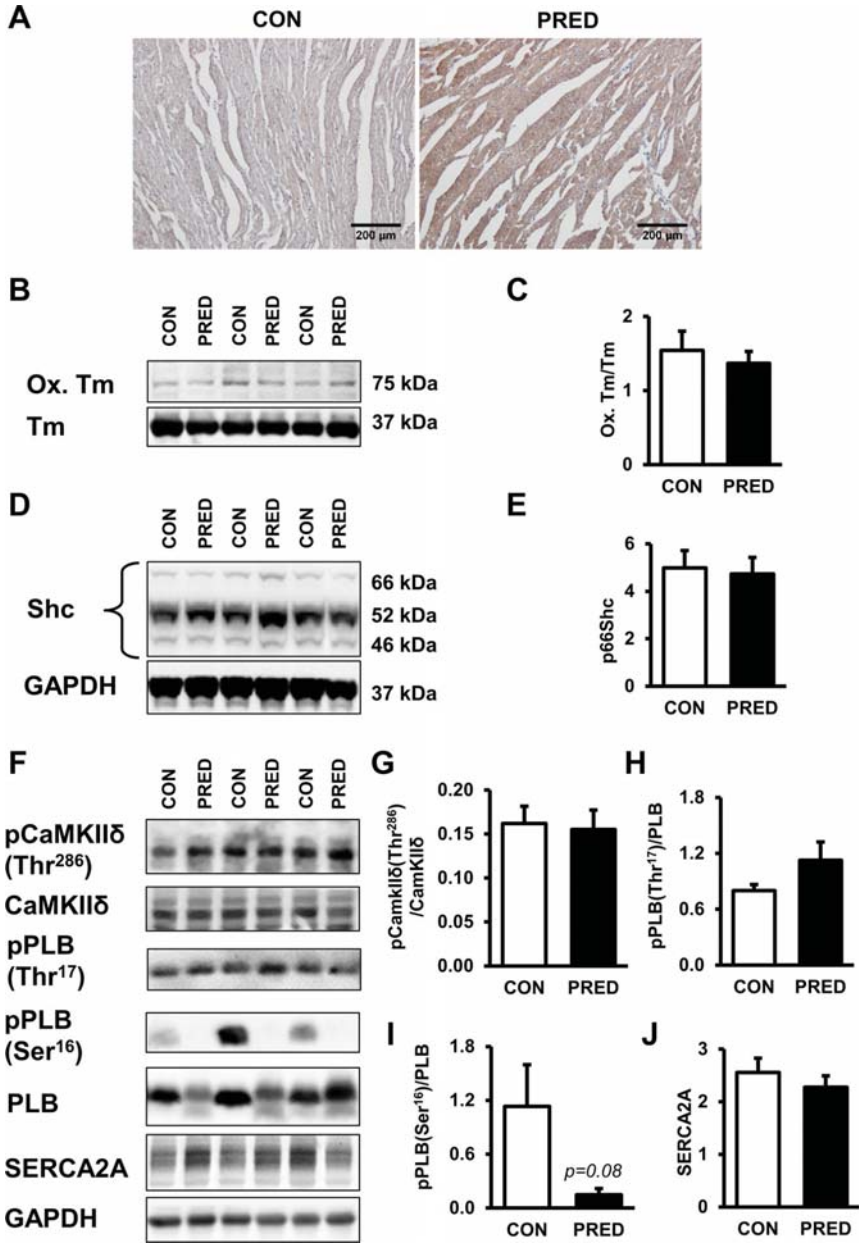

Fig. 6. Characterization of oxidative and nitrative stress in prediabetes. Representative immunostaining of nitrotyrosine in the left ventricle (*A*) is shown; magnification ×200; scale bar = 200 μm. Representative Western blots (*B*) and quantification (*C*) of tropomyosin oxidation are shown. Representative Western blots (*D*) and quantification (*E*) of cardiac p66Shc expression are shown. Representative Western blots (*F*), quantification of Ca^{2+}/calmodulin-dependent protein kinase II (CaMKIIδ) (*G*), phospholamban (PLB) phosphorylation on Thr^{17} (*H*) and Ser^{16} (*I*), and sarco/endoplasmic reticulum Ca^{2+} ATPase II (SERCA2A) (*J*) expression are shown. Tm, tropomyosin; Ox. Tm, oxidized tropomyosin. Data are means ± SE, n = 6–8 per group.

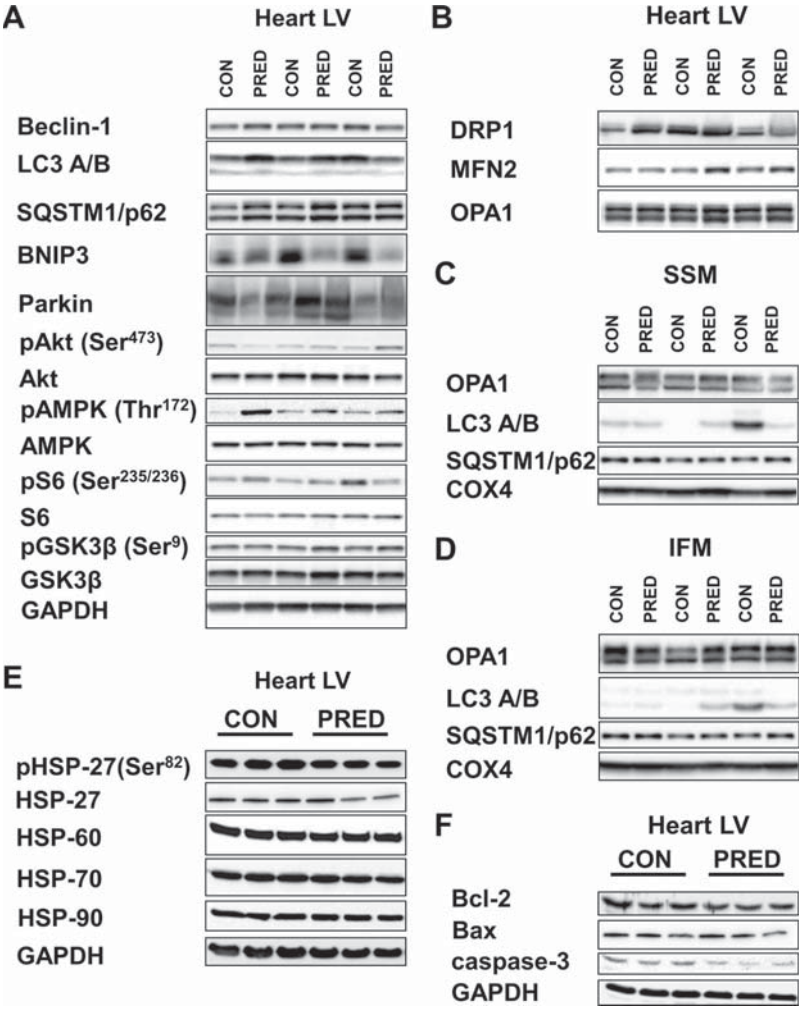

Fig. 7. Cardiac expression of mitochondrial dynamics, autophagy/mitophagy, heat shock proteins (HSPs), and apoptosis-related proteins in prediabetes. Representative Western blots of autophagy/mitophagy-related proteins and upstream modulators of autophagy (*A*) and mitochondrial fission- and fusion-related protein (*B*) in whole left ventricles are shown. Representative Western blots of mitochondrial dynamics- and mitophagy-related proteins in isolated SSM (*C*) and IFM (*D*) are shown. Representative Western blots of HSP-related (*E*) and apoptosis-related (*F*) proteins in whole left ventricle are shown. DRP1/DLP1, dynamin-related/like protein 1; MFN2, mitofusin-2; OPA1, optic atrophy 1; COX4, cytochrome *c* oxidase subunit 4, mitochondrial; LC3, 1 microtubule-associated protein 1 light chain 3; SQSTM1/p62, sequestosome 1; BNIP3, Bcl-2/adenovirus E1B 19-kDa protein-interacting protein 3; AMPKα, AMP-activated protein kinase α; GSK3β, glycogen synthase kinase-3β.

were elevated in these studies, highlighting that a substantial difference can be observed between different diet-induced models and stages of prediabetes (29). Furthermore, it has been described that obesity promoted the hypertrophy-inducing effect of diabetes regardless of hypertension (26), which could be attributed to adipokines, such as leptin and resistin (5, 39). Similarly, here we showed that even mild obesity (only 18% increase in body weight was observed in the present study) with an elevated leptin level is sufficient to induce hypertrophy even without impairment of fasting plasma glucose and lipid levels or hypertension, which is in agreement with previous reports (23, 29). However, clinical data seem to contradict these findings because no increase in the prevalence of LV hypertrophy was observed in overweight prediabetic patients with impaired fasting glucose and impaired glucose tolerance (66). Mechanistic studies on how obesity abrogates cardiac function are scarce. Increased myocardial triglyceride content is associated with diastolic dysfunction in *ob/ob* mice (18), which is well in line with our findings that the number of lipid particles increased in the myocardium in prediabetes. Although microRNA-451 has been demonstrated to promote cardiac hypertrophy and diminished contractile reserves in mice on high-fat diet (44), further studies are warranted to describe the relationship between cardiac dysfunction and the disturbed cardiac lipid metabolism in prediabetes. Interestingly, unlike in genetic models of prediabetes (20), diet-induced prediabetes did not result in an elevation in classical molecular markers of hypertrophy or conventional signs of fibrosis in the heart, as expected in the case of hypertrophy. Moreover, this is the first evidence on decreased β-MHC in prediabetes. Although the vast majority of publications demonstrate an increase in β-MHC in diabetes (4, 83), a small number of studies indicate a downregulation of MHC expression in animals with diverse cardiac or metabolic challenges. For instance, in cardiomyocytes from STZ-treated rats, total MHC expression was significantly decreased (25). These results indicate that, although in most cardiometabolic derangements expression of the slow MHC isoform increases, in certain conditions, such as in prediabetes, a general suppression of MHC expression might be present. The reduction in MHC expression might also contribute to the observed cardiac dysfunction in prediabetes; however, to uncover its significance and mechanism, further experiments are warranted.

Oxidative stress has a major role in the development of diabetic cardiomyopathy (10, 31); however, it has not been well described whether it is responsible for the decreased cardiac function in prediabetes. Here we found elevated hydrogen peroxide production in SSM, increased nitrotyrosine

Table 6. *Quantification of HSPs, apoptosis, mitochondrial dynamics-related, and mitophagy-related protein expressions in isolated mitochondrial fractions and whole LVs*

Total LV	CON	PRED
BNIP3/GAPDH ratio	0.590 ± 0.030	0.440 ± 0.020*
MFN2/GAPDH ratio	0.270 ± 0.010	0.360 ± 0.020*
OPA1/GAPDH ratio	1.470 ± 0.110	1.630 ± 0.100
DRP1/GAPDH ratio	1.160 ± 0.080	1.340 ± 0.140
LC3-II/GAPDH ratio	0.560 ± 0.070	0.560 ± 0.050
p62/GAPDH ratio	3.050 ± 0.180	3.450 ± 0.230
Parkin/GAPDH ratio	2.250 ± 0.140	2.430 ± 0.170
Beclin1/GAPDH ratio	0.810 ± 0.070	0.820 ± 0.070
Phospho AKT(Ser^{473})/AKT ratio	0.320 ± 0.040	0.290 ± 0.020
Phospho AMPK(Thr^{172})/AMPK ratio	0.120 ± 0.020	0.210 ± 0.060
Phospho S6($Ser^{235/236}$)/S6 ratio	2.620 ± 1.080	2.160 ± 0.610
Phospho GSK3β(Ser^{9})/GSK3β ratio	0.800 ± 0.090	0.720 ± 0.100
Bcl-2/GAPDH ratio	0.230 ± 0.010	0.200 ± 0.003*
Bcl-2/Bax ratio	0.150 ± 0.020	0.150 ± 0.020
Caspase-3/GAPDH ratio	0.050 ± 0.001	0.040 ± 0.003
P-HSP-27(Ser^{82})/T-HSP-27 ratio	0.340 ± 0.050	0.280 ± 0.020
HSP-60/GAPDH ratio	0.850 ± 0.020	0.840 ± 0.020
HSP-70/GAPDH ratio	0.530 ± 0.010	0.510 ± 0.010
HSP-90/GAPDH ratio	0.460 ± 0.010	0.500 ± 0.020
Subsarcolemmal mitochondria		
OPA1/COX4 ratio	1.340 ± 0.070	1.320 ± 0.060
LC3-II/COX4 ratio	0.220 ± 0.100	0.250 ± 0.040
p62/COX4 ratio	0.130 ± 0.020	0.120 ± 0.030
Interfibrillar mitochondria		
OPA1/COX4 ratio	1.440 ± 0.150	1.520 ± 0.140
LC3-II/COX4 ratio	0.220 ± 0.090	0.290 ± 0.070
p62/COX4 ratio	0.350 ± 0.060	0.360 ± 0.040

Data are means ± SE for 8 rat per group (*$P < 0.05$). HSP, heat shock protein; BNIP3, Bcl-2/adenovirus E1B 19-kDa protein-interacting protein 3; MFN2, mitofusin-2; OPA1, optic atrophy 1; DRP1, dynamin-related protein 1; LC3, 1 microtubule-associated protein 1 light chain 3; AMPK, AMP-activated protein kinase; GSK3β, glycogen synthase kinase-3β; COX4, cytochrome *c* oxidase subunit 4, mitochondrial.

formation, and elevated cardiac expression of MFN2. These findings are in agreement with previous reports in which elevated oxidative stress, such as seen in our model of prediabetes, leads to an increase in MFN2 in rat vascular smooth muscle cells (33), and its robust overexpression induced apoptotic cell death in neonatal rat cardiomyocytes (72). Similarly, in another study, high-fat diet induced oxidative stress and MFN2 overexpression in the liver of C57BL/6 mice after 16 wk (27). However, in a previous study on diet-induced prediabetes, no sign of cardiac mitochondrial oxidative stress was shown in male Wistar rats after 16 wk (29), which may suggest that mitochondrial oxidative stress might not be present in all models and stages of prediabetes and that it might not be the primary driving force of prediabetes-induced cardiac functional alterations.

It is well established that mitochondria, especially the mitochondrial electron transport chain, is one of the main sources of ROS; however, several other intracellular components can produce ROS in mitochondria (17). For instance, it is known that p66Shc translocation to mitochondria can increase the formation of ROS (22), and NADPH oxidase 4 and monoamine oxidase also have important roles in mitochondrial ROS production (8, 43). Although here we observed a moderately increased ROS production in SSM, no difference can be seen in mitochondrial oxygen consumption between normal and prediabetic mitochondria (see Table 5), showing no impairment in mitochondrial redox chains. It is presently unknown what mechanism leads to the increased ROS production exclusively in SSM in prediabetes. In mice on a high-fat diet, cardiac mitochondrial ROS production was elevated, and, similar to our results, mitochondrial oxygen consumption did not change substantially, whereas a significant amount of cardiac lipid accumulation was observed (1). However, the source of ROS has not been identified in this study either. Thus, to reveal the direct connection between elevated ROS production and mitochondrial and cardiac dysfunction, further studies are warranted.

Molecular mechanisms that contribute to hypertrophy and cardiac dysfunction in prediabetes have not been investigated in detail. In our previous studies on diet-induced hypercholesterolemia or metabolic syndrome in ZDF rats, we have shown by DNA and miRNA microarrays that a multitude of cardiac cellular processes is modulated by these conditions (69, 79). Similarly, in this study, we showed changes in several cellular processes, suggesting that hypertrophy and deteriorated diastolic function in prediabetes may be consequences of numerous concurrent alterations in the cardiac homeostasis (see Fig. 8). Characterizing active components of the contractile apparatus and Ca^{2+} homeostasis, here we observed a tendency for a decrease in the Ser^{16} phosphorylation of PLB in prediabetes. In previous studies, decreased phosphorylation of PLB on Ser^{16} was demonstrated to be associated with abnormalities in contraction and relaxation in the diabetic heart (57, 85). This notion is further supported by the findings of Abdurrachim et al. (1), who demonstrated that phosphorylation of PLB was reduced in the heart of mice with diastolic dysfunction induced by a high-fat diet. Therefore, decreased phosphorylation of PLB may also contribute to the development of early diastolic dysfunction that we uncovered in prediabetes. Increased activity and expression of CaMKIIδ and reduced phosphorylation of PLB by CaMKIIδ have been found to be associated with contractile dysfunction, diabetes (47, 49), and fructose-rich diet-induced prediabetes (75). In our model, expression and phosphorylation of CaMKIIδ and phosphorylation of PLB on Thr^{17} were unchanged. This is in contrast with previous findings that have reported the phosphorylation of CaMKIIδ being increased in the heart of STZ-treated diabetic rats (71, 76) although, in these reports, a significant hyperglycemia was present, which was shown to facilitate the activation of CaMKIIδ (28). Apoptosis is considered to be one of the hallmarks of diabetic cardiomyopathy, and it is induced by oxidative stress in diabetes (10, 78). It has been described that experimental diabetes induces upregulation of proapoptotic and downregulation of antiapoptotic proteins (3, 84); however, no data have been available on the cardiac apoptosis in prediabetes. In the present study, we show a modest downregulation of Bcl-2; however, no change in Bcl-2/Bax ratio and caspase-3 expression was detected in prediabetic animals. Thus our data suggest an early dysregulation of pro- and antiapoptotic proteins in prediabetes; however, they do not show a gross induction of apoptosis in prediabetes. Tropomyosin is prone to loss of function by oxidative modifications that are associated with the severity of heart failure in humans (14, 15). In this study, oxidized tropomyosin content of the heart was not modulated by prediabetes. These data suggest that neither the CaMKIIδ pathway, apoptosis induction, nor tropomyosin oxi-

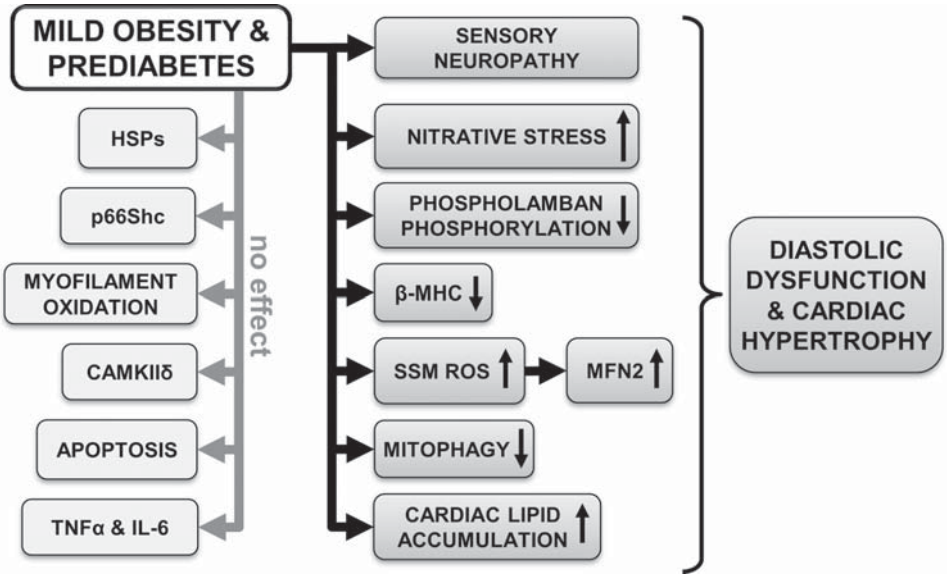

Fig. 8. Schematic representation of the cardiac effects of prediabetes. ROS, reactive oxygen species.

dation are responsible for the diastolic dysfunction observed in prediabetes.

Here we also demonstrate an early dysregulation of mitochondrial fusion and mitophagy first in the literature, as shown by elevated MFN2 and attenuated BNIP3 expression in prediabetes; however, other canonical markers of autophagy, mitophagy, and apoptosis were unaffected. Similarly, right atrial myocardial samples of type-2 diabetic patients presenting no signs of overt cardiomyopathy, the expression of the majority of mitochondrial dynamics, and autophagy-related proteins were not elevated, except for that of ATG5 and MFN1 (53). Therefore, we can assume that only major disturbances in glucose and lipid homeostasis, such as seen in untreated patients or in genetic models of diabetes, might be a powerful enough signal to extensively modulate cardiac autophagy, mitophagy, or mitochondrial dynamics, which might result in grossly deteriorated cardiac function. Moreover, experimental systemic sensory neuropathy by itself has been previously shown to cause diastolic dysfunction and global gene expression changes in the rat heart (7, 86). Therefore, prediabetes-induced sensory neuropathy observed in the present study might also contribute to the diabetic cardiomyopathy.

Furthermore, this is the first report to show that prediabetes does not modulate cardiac expression of HSP-60, HSP-70, HSP-90, and phosphorylation or expression of HSP-27. In contrast, in STZ-induced diabetes, increased levels of HSP-70 have been detected in the rat heart (77), and increased levels of circulating HSP-60 were found in diabetic patients (70), suggesting that, in advanced stages of diabetes, HSPs might be involved in the development of cardiac dysfunction. However, our data suggest no role of HSPs in prediabetes in the heart.

A limitation of this study is that the prediabetic condition was not analyzed in female rats. Because pathophysiological processes might substantially differ between sexes (see NIH notice NOT-OD-15-102), it cannot be excluded that performing the study with the inclusion of both sexes might allow different conclusions to be drawn. Furthermore, because other studies showed that MHC protein expression is influenced by certain factors such as Foxo1 (61) or miR-27a (55), assessing α- and β-MHC protein levels might have helped to understand the molecular background of the mild diastolic dysfunction and hypertrophy observed in prediabetes better.

Taken together, this study emphasizes that parallel occurrence of several abnormalities of metabolic, oxidative, and contractile functions might trigger cardiac pathological changes characteristic of prediabetes well before hyperglycemia or major metabolic derangements occur and that preventing these abnormalities might be of importance for future therapies of cardiac pathologies observed in early metabolic diseases such as prediabetes.

ACKNOWLEDGMENTS

We thank Melinda Károlyi-Szabó, Jenőné Benkes, Henriett Biró, Ildikó Horváth, Teréz Bagoly, Sebestyén Tuza, and Anikó Perkecz for technical assistance.

GRANTS

This work was supported by the European Foundation for the Study of Diabetes (EFSD) New Horizons Collaborative Research Initiative from the European Association for the Study of Diabetes (EASD) and Hungarian Scientific Research Fund (OTKA K 109737, PD100245 to T. Radovits) and Slovak Scientific Grant Agency (VEGA1/0638/12). Z. Giricz, T. Radovits, and K. Szigeti hold a "János Bolyai Research Scholarship" from the Hungarian Academy of Sciences, and Z. Varga was supported by the Rosztoczy Foundation. P. Ferdinandy is a Szentágothai Fellow of the National Program of Excellence (TAMOP 4.2.4. A/2-11-1-2012-0001). T. Baranyai is supported by the European Cooperation in Science and Technology (COST-BM1203-STSM 090515-058721). K. Boengler and R. Schreckenberg are supported by the German Research Foundation (BO-2955/2-1 and SCHU 843/9-1).

DISCLOSURES

No conflicts of interest, financial or otherwise, are declared by the authors.

AUTHOR CONTRIBUTIONS

G.K., Z.V.V., T.B., K.B., S.R., L.L., T. Radovits, A.O., C.M., Á.L., M.A.-K., T.K., N.B., D.M., L.D., M.B., T. Rajtík, A.A., K.S., and R. Schulz performed experiments; G.K., Z.V.V., T.B., K.B., L.L., T. Radovits, A.O., C.M., Á.L., M.A.-K., T.K., N.B., L.D., M.B., T. Rajtík, and K.S. analyzed data; G.K., T.B., T. Radovits, D.M., and Z.G. interpreted results of experiments; G.K. prepared figures; G.K., Z.V.V., T.B., M.B., A.A., and Z.G. drafted manuscript; G.K., Z.G., R. Schulz, and P.F. approved final version of manuscript; Z.V.V., K.-D.S., R. Schreckenberg, Z.G., R. Schulz, and P.F. concep-

tion and design of research; Z.V.V., T.B., S.R., L.L., K.-D.S., R. Schreckenberg, T. Radovits, A.O., C.M., x.L., T.K., N.B., L.D., M.B., T. Rajtík, A.A., K.S., P.H., Z.H., L.T., P.P., B.M., Z.G., R. Schulz, and P.F. edited and revised manuscript.

REFERENCES

1. **Abdurrachim D, Ciapaite J, Wessels B, Nabben M, Luiken JJ, Nicolay K, Prompers JJ.** Cardiac diastolic dysfunction in high-fat diet fed mice is associated with lipotoxicity without impairment of cardiac energetics in vivo. *Biochim Biophys Acta* 1842: 1525–1537, 2014.
2. **American Diabetes Association.** Diagnosis and classification of diabetes mellitus. *Diabetes Care*, 37 *Suppl* 1: S81–S90, 2014.
3. **Amin AH, El-Missiry MA, Othman AI.** Melatonin ameliorates metabolic risk factors, modulates apoptotic proteins, and protects the rat heart against diabetes-induced apoptosis. *Eur J Pharmacol* 747: 166–173, 2015.
4. **Aragno M, Mastrocola R, Medana C, Catalano MG, Vercellinatto I, Danni O, Boccuzzi G.** Oxidative stress-dependent impairment of cardiac-specific transcription factors in experimental diabetes. *Endocrinology* 147: 5967–5974, 2006.
5. **Barouch LA, Berkowitz DE, Harrison RW, O'Donnell CP, Hare JM.** Disruption of leptin signaling contributes to cardiac hypertrophy independently of body weight in mice. *Circulation* 108: 754–759, 2003.
6. **Barr EL, Zimmet PZ, Welborn TA, Jolley D, Magliano DJ, Dunstan DW, Cameron AJ, Dwyer T, Taylor HR, Tonkin AM, Wong TY, McNeil J, Shaw JE.** Risk of cardiovascular and all-cause mortality in individuals with diabetes mellitus, impaired fasting glucose, and impaired glucose tolerance: The Australian Diabetes, Obesity, and Lifestyle Study (AusDiab). *Circulation* 116: 151–157, 2007.
7. **Bencsik P, Kupai K, Giricz Z, Gorbe A, Huliak I, Furst S, Dux L, Csont T, Jancso G, Ferdinandy P.** Cardiac capsaicin-sensitive sensory nerves regulate myocardial relaxation via S-nitrosylation of SERCA: Role of peroxynitrite. *Br J Pharmacol* 153: 488–496, 2008.
8. **Bianchi P, Kunduzova O, Masini E, Cambon C, Bani D, Raimondi L, Seguelas MH, Nistri S, Colucci W, Leducq N, Parini A.** Oxidative stress by monoamine oxidase mediates receptor-independent cardiomyocyte apoptosis by serotonin and postischemic myocardial injury. *Circulation* 112: 3297–3305, 2005.
9. **Bjorndal B, Burri L, Staalesen V, Skorve J, Berge RK.** Different adipose depots: Their role in the development of metabolic syndrome and mitochondrial response to hypolipidemic agents. *J Obes* 2011: 490650, 2011.
10. **Boudina S, Abel ED.** Diabetic cardiomyopathy, causes and effects. *Rev Endocr Metab Disord* 11: 31–39, 2010.
11. **Bradford MM.** A rapid and sensitive method for the quantitation of microgram quantities of protein utilizing the principle of protein-dye binding. *Anal Biochem* 72: 248–254, 1976.
12. **Brooks BA, Franjic B, Ban CR, Swaraj K, Yue DK, Celermajer DS, Twigg SM.** Diastolic dysfunction and abnormalities of the microcirculation in type 2 diabetes. *Diabetes Obes Metab* 10: 739–746, 2008.
13. **Cai L, Kang YJ.** Cell death and diabetic cardiomyopathy. *Cardiovasc Toxicol* 3: 219–228, 2003.
14. **Canton M, Menazza S, Sheeran FL, Polverino de Laureto P, Di Lisa F, Pepe S.** Oxidation of myofibrillar proteins in human heart failure. *J Am Coll Cardiol* 57: 300–309, 2011.
15. **Canton M, Neverova I, Menabo R, Van Eyk J, Di Lisa F.** Evidence of myofibrillar protein oxidation induced by postischemic reperfusion in isolated rat hearts. *Am J Physiol Heart Circ Physiol* 286: H870–H877, 2004.
16. **Cassuto J, Dou H, Czikora I, Szabo A, Patel VS, Kamath V, Belin de Chantemele E, Feher A, Romero MJ, Bagi Z.** Peroxynitrite disrupts endothelial caveolae leading to eNOS uncoupling and diminished flow-mediated dilation in coronary arterioles of diabetic patients. *Diabetes* 63: 1381–1393, 2014.
17. **Chen YR, Zweier JL.** Cardiac mitochondria and reactive oxygen species generation. *Circ Res* 114: 524–537, 2014.
18. **Christoffersen C, Bollano E, Lindegaard ML, Bartels ED, Goetze JP, Andersen CB, Nielsen LB.** Cardiac lipid accumulation associated with diastolic dysfunction in obese mice. *Endocrinology* 144: 3483–3490, 2003.
19. **Csont T, Bereczki E, Bencsik P, Fodor G, Gorbe A, Zvara A, Csonka C, Puskas LG, Santha M, Ferdinandy P.** Hypercholesterolemia increases myocardial oxidative and nitrosative stress thereby leading to cardiac dysfunction in apoB-100 transgenic mice. *Cardiovasc Res* 76: 100–109, 2007.
20. **D'Souza A, Howarth FC, Yanni J, Dobryznski H, Boyett MR, Adeghate E, Bidasee KR, Singh J.** Left ventricle structural remodelling in the prediabetic Goto-Kakizaki rat. *Exp Physiol* 96: 875–888, 2011.
21. **DeFronzo RA and Abdul-Ghani M.** Assessment and treatment of cardiovascular risk in prediabetes: Impaired glucose tolerance and impaired fasting glucose. *Am J Cardiol* 108: 3b–24b, 2011.
22. **Di Lisa F, Giorgio M, Ferdinandy P, Schulz R.** New aspects of p66Shc in ischemia reperfusion injury and cardiovascular diseases. *Br J Pharmacol*. In press.
23. **du Toit EF, Smith W, Muller C, Strijdom H, Stouthammer B, Woodiwiss AJ, Norton GR, Lochner A.** Myocardial susceptibility to ischemic-reperfusion injury in a prediabetic model of dietary-induced obesity. *Am J Physiol Heart Circ Physiol* 294: H2336–H2343, 2008.
24. **Duncan JG.** Mitochondrial dysfunction in diabetic cardiomyopathy. *Biochim Biophys Acta* 1813: 1351–1359, 2011.
25. **Dyntar D, Sergeev P, Klisic J, Ambuhl P, Schaub MC, Donath MY.** High glucose alters cardiomyocyte contacts and inhibits myofibrillar formation. *J Clin Endocrinol Metab* 91: 1961–1967, 2006.
26. **Eguchi K, Boden-Albala B, Jin Z, Rundek T, Sacco RL, Homma S, Di Tullio MR.** Association between diabetes mellitus and left ventricular hypertrophy in a multiethnic population. *Am J Cardiol* 101: 1787–1791, 2008.
27. **Enos RT, Velazquez KT, Murphy EA.** Insight into the impact of dietary saturated fat on tissue-specific cellular processes underlying obesity-related diseases. *J Nutr Biochem* 25: 600–612, 2014.
28. **Erickson JR, Pereira L, Wang L, Han G, Ferguson A, Dao K, Copeland RJ, Despa F, Hart GW, Ripplinger CM, Bers DM.** Diabetic hyperglycaemia activates CaMKII and arrhythmias by O-linked glycosylation. *Nature* 502: 372–376, 2013.
29. **Essop MF, Anna Chan WY, Valle A, Garcia-Palmer FJ, Du Toit EF.** Impaired contractile function and mitochondrial respiratory capacity in response to oxygen deprivation in a rat model of pre-diabetes. *Acta Physiol (Oxf)* 197: 289–296, 2009.
30. **Fonseca VA.** Identification and treatment of prediabetes to prevent progression to type 2 diabetes. *Clin Cornerstone* 9: 51–59; discussion 60-51, 2008.
31. **Frustaci A, Kajstura J, Chimenti C, Jakoniuk I, Leri A, Maseri A, Nadal-Ginard B, Anversa P.** Myocardial cell death in human diabetes. *Circ Res* 87: 1123–1132, 2000.
32. **Galloway CA, Yoon Y.** Mitochondrial dynamics in diabetic cardiomyopathy. *Antioxid Redox Signal* 22: 1545–1562, 2015.
33. **Guo X, Chen KH, Guo Y, Liao H, Tang J, Xiao RP.** Mitofusin 2 triggers vascular smooth muscle cell apoptosis via mitochondrial death pathway. *Circ Res* 101: 1113–1122, 2007.
34. **Harms M, Seale P.** Brown and beige fat: Development, function and therapeutic potential. *Nat Med* 19: 1252–1263, 2013.
35. **Holloway GP, Snook LA, Harris RJ, Glatz JF, Luiken JJ, Bonen A.** In obese Zucker rats, lipids accumulate in the heart despite normal mitochondrial content, morphology and long-chain fatty acid oxidation. *J Physiol* 589: 169–180, 2011.
36. **Hsueh W, Abel ED, Breslow JL, Maeda N, Davis RC, Fisher EA, Dansky H, McClain DA, McIndoe R, Wassef MK, Rabadan-Diehl C, Goldberg IJ.** Recipes for creating animal models of diabetic cardiovascular disease. *Circ Res* 100: 1415–1427, 2007.
37. **Kass D.** Clinical ventricular pathophysiology: a pressure-volume view. In: *Ventricular Function*, edited by Warltier DC. Baltimore, MD: Williams & Wilkins, 1995, pp. 131–151.
38. **Kass DA, Bronzwaer JG, Paulus WJ.** What mechanisms underlie diastolic dysfunction in heart failure? *Circ Res* 94: 1533–1542, 2004.
39. **Kim M, Oh JK, Sakata S, Liang I, Park W, Hajjar RJ, Lebeche D.** Role of resistin in cardiac contractility and hypertrophy. *J Mol Cell Cardiol* 45: 270–280, 2008.
40. **Kleiner DE, Brunt EM, Van Natta M, Behling C, Contos MJ, Cummings OW, Ferrell LD, Liu YC, Torbenson MS, Unalp-Arida A, Yeh M, McCullough AJ, Sanyal AJ.** Design and validation of a histological scoring system for nonalcoholic fatty liver disease. *Hepatology* 41: 1313–1321, 2005.
41. **Kobayashi S, Liang Q.** Autophagy and mitophagy in diabetic cardiomyopathy. *Biochim Biophys Acta* 1852: 252–261, 2015.
42. **Kovacs A, Olah A, Lux A, Matyas C, Nemeth BT, Kellermayer D, Ruppert M, Torok M, Szabo L, Meltzer A, Assabiny A, Birtalan E, Merkely B, Radovits T.** Strain and strain rate by speckle-tracking echocardiography correlate with pressure-volume loop-derived contractil-

ity indices in a rat model of athlete's heart. *Am J Physiol Heart Circ Physiol* 308: H743–H748, 2015.
43. **Kuroda J, Ago T, Matsushima S, Zhai P, Schneider MD, Sadoshima J.** NADPH oxidase 4 (Nox4) is a major source of oxidative stress in the failing heart. *Proc Natl Acad Sci USA* 107: 15565–15570, 2010.
44. **Kuwabara Y, Horie T, Baba O, Watanabe S, Nishiga M, Usami S, Izuhara M, Nakao T, Nishino T, Otsu K, Kita T, Kimura T, Ono K.** MicroRNA-451 exacerbates lipotoxicity in cardiac myocytes and high-fat diet-induced cardiac hypertrophy in mice through suppression of the LKB1/AMPK pathway. *Circ Res* 116: 279–288, 2015.
45. **Lewis CE, McTigue KM, Burke LE, Poirier P, Eckel RH, Howard BV, Allison DB, Kumanyika S, Pi-Sunyer FX.** Mortality, health outcomes, and body mass index in the overweight range: A science advisory from the American Heart Association. *Circulation* 119: 3263–3271, 2009.
46. **Luczak ED, Anderson ME.** CaMKII oxidative activation and the pathogenesis of cardiac disease. *J Mol Cell Cardiol* 73: 112–116, 2014.
47. **Luo M, Guan X, Luczak ED, Lang D, Kutschke W, Gao Z, Yang J, Glynn P, Sossalla S, Swaminathan PD, Weiss RM, Yang B, Rokita AG, Maier LS, Efimov IR, Hund TJ, Anderson ME.** Diabetes increases mortality after myocardial infarction by oxidizing CaMKII. *J Clin Invest* 123: 1262–1274, 2013.
48. **Lupachyk S, Watcho P, Obrosov AA, Stavniichuk R, Obrosova IG.** Endoplasmic reticulum stress contributes to prediabetic peripheral neuropathy. *Exp Neurol* 247: 342–348, 2013.
49. **Maier LS, Bers DM.** Role of Ca2+/calmodulin-dependent protein kinase (CaMK) in excitation-contraction coupling in the heart. *Cardiovasc Res* 73: 631–640, 2007.
50. **Mansor LS, Gonzalez ER, Cole MA, Tyler DJ, Beeson JH, Clarke K, Carr CA, Heather LC.** Cardiac metabolism in a new rat model of type 2 diabetes using high-fat diet with low dose streptozotocin. *Cardiovasc Diabetol* 12: 136, 2013.
51. **Mizushige K, Yao L, Noma T, Kiyomoto H, Yu Y, Hosomi N, Ohmori K, Matsuo H.** Alteration in left ventricular diastolic filling and accumulation of myocardial collagen at insulin-resistant prediabetic stage of a type II diabetic rat model. *Circulation* 101: 899–907, 2000.
52. **Mohanty JG, Jaffe JS, Schulman ES, Raible DG.** A highly sensitive fluorescent micro-assay of H2O2 release from activated human leukocytes using a dihydroxyphenoxazine derivative. *J Immunol Methods* 202: 133–141, 1997.
53. **Montaigne D, Marechal X, Coisne A, Debry N, Modine T, Fayad G, Potelle C, El Arid JM, Mouton S, Sebti Y, Duez H, Preau S, Remy-Jouet I, Zerimech F, Koussa M, Richard V, Neviere R, Edme JL, Lefebvre P, Staels B.** Myocardial contractile dysfunction is associated with impaired mitochondrial function and dynamics in type 2 diabetic but not in obese patients. *Circulation* 130: 554–564, 2014.
54. **Nathan DM, Davidson MB, DeFronzo RA, Heine RJ, Henry RR, Pratley R, Zinman B.** Impaired fasting glucose and impaired glucose tolerance: Implications for care. *Diabetes Care* 30: 753–759, 2007.
55. **Nishi H, Ono K, Horie T, Nagao K, Kinoshita M, Kuwabara Y, Watanabe S, Takaya T, Tamaki Y, Takanabe-Mori R, Wada H, Hasegawa K, Iwanaga Y, Kawamura T, Kita T, Kimura T.** MicroRNA-27a regulates beta cardiac myosin heavy chain gene expression by targeting thyroid hormone receptor beta1 in neonatal rat ventricular myocytes. *Mol Cell Biol* 31: 744–755, 2011.
56. **Orhan CE, Onal A, Uyanikgil Y, Ulker S.** Antihyperalgesic and antiallodynic effect of sirolimus in rat model of adjuvant arthritis. *Eur J Pharmacol* 705: 35–41, 2013.
57. **Ouwens DM, Boer C, Fodor M, de Galan P, Heine RJ, Maassen JA, Diamant M.** Cardiac dysfunction induced by high-fat diet is associated with altered myocardial insulin signalling in rats. *Diabetologia* 48: 1229–1237, 2005.
58. **Pacher P, Nagayama T, Mukhopadhyay P, Batkai S, Kass DA.** Measurement of cardiac function using pressure-volume conductance catheter technique in mice and rats. *Nat Protocol* 3: 1422–1434, 2008.
59. **Pechanova O, Varga ZV, Cebova M, Giricz Z, Pacher P, Ferdinandy P.** Cardiac NO signalling in the metabolic syndrome. *Br J Pharmacol* 172: 1415–1433, 2015.
60. **Pereira L, Ruiz-Hurtado G, Rueda A, Mercadier JJ, Benitah JP, Gomez AM.** Calcium signaling in diabetic cardiomyocytes. *Cell Calcium* 56: 372–380, 2014.
61. **Qi Y, Zhu Q, Zhang K, Thomas C, Wu Y, Kumar R, Baker KM, Xu Z, Chen S, Guo S.** Activation of Foxo1 by insulin resistance promotes cardiac dysfunction and beta-myosin heavy chain gene expression. *Circ Heart Fail* 8: 198–208, 2015.
62. **Radovits T, Korkmaz S, Loganathan S, Barnucz E, Bomicke T, Arif R, Karck M, Szabo G.** Comparative investigation of the left ventricular pressure-volume relationship in rat models of type 1 and type 2 diabetes mellitus. *Am J Physiol Heart Circ Physiol* 297: H125–H133, 2009.
63. **Radovits T, Korkmaz S, Matyas C, Olah A, Nemeth BT, Pali S, Hirschberg K, Zubarevich A, Gwanmesia PN, Li S, Loganathan S, Barnucz E, Merkely B, Szabo G.** An altered pattern of myocardial histopathological and molecular changes underlies the different characteristics of type-1 and type-2 diabetic cardiac dysfunction. *J Diabetes Res* 2015: 728741, 2015.
64. **Radovits T, Olah A, Lux A, Nemeth BT, Hidi L, Birtalan E, Kellermayer D, Matyas C, Szabo G, Merkely B.** Rat model of exercise-induced cardiac hypertrophy: hemodynamic characterization using left ventricular pressure-volume analysis. *Am J Physiol Heart Circ Physiol* 305: H124–H134, 2013.
65. **Reffelmann T, Kloner RA.** Transthoracic echocardiography in rats. Evaluation of commonly used indices of left ventricular dimensions, contractile performance, and hypertrophy in a genetic model of hypertrophic heart failure (SHHF-Mcc-facp-Rats) in comparison with Wistar rats during aging. *Basic Res Cardiol* 98: 275–284, 2003.
66. **Rerkpattanapipat P, D'Agostino RB Jr, Link KM, Shahar E, Lima JA, Bluemke DA, Sinha S, Herrington DM, Hundley WG.** Location of arterial stiffening differs in those with impaired fasting glucose versus diabetes: Implications for left ventricular hypertrophy from the Multi-Ethnic Study of Atherosclerosis. *Diabetes* 58: 946–953, 2009.
67. **Russell JC, Proctor SD.** Small animal models of cardiovascular disease: Tools for the study of the roles of metabolic syndrome, dyslipidemia, and atherosclerosis. *Cardiovasc Pathol* 15: 318–330, 2006.
68. **Ryden L, Grant PJ, Anker SD, Berne C, Cosentino F, Danchin N, Deaton C, Escaned J, Hammes HP, Huikuri H, Marre M, Marx N, Mellbin L, Ostergren J, Patrono C, Seferovic P, Uva MS, Taskinen MR, Tendera M, Tuomilehto J, Valensi P, Zamorano JL, Zamorano JL, Achenbach S, Baumgartner H, Bax JJ, Bueno H, Dean V, Deaton C, Erol C, Fagard R, Ferrari R, Hasdai D, Hoes AW, Kirchhof P, Knuuti J, Kolh P, Lancellotti P, Linhart A, Nihoyannopoulos P, Piepoli MF, Ponikowski P, Sirnes PA, Tamargo JL, Tendera M, Torbicki A, Wijns W, Windecker S, De Backer G, Sirnes PA, Ezquerra EA, Avogaro A, Badimon L, Baranova E, Baumgartner H, Betteridge J, Ceriello A, Fagard R, Funck-Brentano C, Gulba DC, Hasdai D, Hoes AW, Kjekshus JK, Knuuti J, Kolh P, Lev E, Mueller C, Neyses L, Nilsson PM, Perk J, Ponikowski P, Reiner Z, Sattar N, Schachinger V, Scheen A, Schirmer H, Stromberg A, Sudzhaeva S, Tamargo JL, Viigimaa M, Vlachopoulos C, Xuereb RG.** ESC guidelines on diabetes, prediabetes, and cardiovascular diseases developed in collaboration with the EASD: the Task Force on Diabetes, Prediabetes, and Cardiovascular Diseases of the European Society of Cardiology (ESC) and developed in collaboration with the European Association for the Study of Diabetes (EASD). *Eur Heart J* 34: 3035–3087, 2013.
69. **Sarkozy M, Zvara A, Gyemant N, Fekete V, Kocsis GF, Pipis J, Szucs G, Csonka C, Puskas LG, Ferdinandy P, Csont T.** Metabolic syndrome influences cardiac gene expression pattern at the transcript level in male ZDF rats. *Cardiovasc Diabetol* 12: 16, 2013.
70. **Shamaei-Tousi A, Stephens JW, Bin R, Cooper JA, Steptoe A, Coates AR, Henderson B, Humphries SE.** Association between plasma levels of heat shock protein 60 and cardiovascular disease in patients with diabetes mellitus. *Eur Heart J* 27: 1565–1570, 2006.
71. **Shao CH, Wehrens XH, Wyatt TA, Parbhu S, Rozanski GJ, Patel KP, Bidasee KR.** Exercise training during diabetes attenuates cardiac ryanodine receptor dysregulation. *J Appl Physiol* 106: 1280–1292, 2009.
72. **Shen T, Zheng M, Cao C, Chen C, Tang J, Zhang W, Cheng H, Chen KH, Xiao RP.** Mitofusin-2 is a major determinant of oxidative stress-mediated heart muscle cell apoptosis. *J Biol Chem* 282: 23354–23361, 2007.
73. **Shivalkar B, Dhondt D, Goovaerts I, Van Gaal L, Bartunek J, Van Crombrugge P, Vrints C.** Flow mediated dilatation and cardiac function in type 1 diabetes mellitus. *Am J Cardiol* 97: 77–82, 2006.
74. **Soetkamp D, Nguyen TT, Menazza S, Hirschhauser C, Hendgen-Cotta UB, Rassaf T, Schluter KD, Boengler K, Murphy E, Schulz R.** S-nitrosation of mitochondrial connexin 43 regulates mitochondrial function. *Basic Res Cardiol* 109: 433, 2014.
75. **Sommese L, Valverde CA, Blanco P, Castro MC, Rueda OV, Kaetzel M, Dedman J, Anderson ME, Mattiazzi A, Palomeque J.** Ryanodine receptor phosphorylation by CaMKII promotes spontaneous Ca(2+) re-

lease events in a rodent model of early stage diabetes: The arrhythmogenic substrate. *Int J Cardiol* 202: 394–406, 2016.

76. **Tuncay E, Zeydanli EN, Turan B.** Cardioprotective effect of propranolol on diabetes-induced altered intracellular Ca2+ signaling in rat. *J Bioenerg Biomembr* 43: 747–756, 2011.
77. **Ugurlucan M, Erer D, Karatepe O, Ziyade S, Haholu A, Gungor Ugurlucan F, Filizcan U, Tireli E, Dayioglu E, Alpagut U.** Glutamine enhances the heat shock protein 70 expression as a cardioprotective mechanism in left heart tissues in the presence of diabetes mellitus. *Expert Opin Ther Targets* 14: 1143–1156, 2010.
78. **Varga ZV, Giricz Z, Liaudet L, Hasko G, Ferdinandy P, Pacher P.** Interplay of oxidative, nitrosative/nitrative stress, inflammation, cell death and autophagy in diabetic cardiomyopathy. *Biochim Biophys Acta* 1852: 232–242, 2015.
79. **Varga ZV, Kupai K, Szucs G, Gaspar R, Paloczi J, Farago N, Zvara A, Puskas LG, Razga Z, Tiszlavicz L, Bencsik P, Gorbe A, Csonka C, Ferdinandy P, Csont T.** MicroRNA-25-dependent up-regulation of NADPH oxidase 4 (NOX4) mediates hypercholesterolemia-induced oxidative/nitrative stress and subsequent dysfunction in the heart. *J Mol Cell Cardiol* 62: 111–121, 2013.
80. **Verkhratsky A, Fernyhough P.** Mitochondrial malfunction and Ca2+ dyshomeostasis drive neuronal pathology in diabetes. *Cell Calcium* 44: 112–122, 2008.
81. **Wild S, Roglic G, Green A, Sicree R, King H.** Global prevalence of diabetes: Estimates for the year 2000 and projections for 2030. *Diabetes Care* 27: 1047–1053, 2004.
82. **Williamson CL, Dabkowski ER, Baseler WA, Croston TL, Alway SE, Hollander JM.** Enhanced apoptotic propensity in diabetic cardiac mitochondria: Influence of subcellular spatial location. *Am J Physiol Heart Circ Physiol* 298: H633–H642, 2010.
83. **Yagi K, Kim S, Wanibuchi H, Yamashita T, Yamamura Y, Iwao H.** Characteristics of diabetes, blood pressure, and cardiac and renal complications in Otsuka Long-Evans Tokushima Fatty rats. *Hypertension* 29: 728–735, 1997.
84. **Yu W, Zha W, Guo S, Cheng H, Wu J, Liu C.** Flos Puerariae extract prevents myocardial apoptosis via attenuation oxidative stress in streptozotocin-induced diabetic mice. *PLoS One* 9: e98044, 2014.
85. **Zhong Y, Ahmed S, Grupp IL, Matlib MA.** Altered SR protein expression associated with contractile dysfunction in diabetic rat hearts. *Am J Physiol Heart Circ Physiol* 281: H1137–H1147, 2001.
86. **Zvara A, Bencsik P, Fodor G, Csont T, Hackler L Jr, Dux M, Furst S, Jancso G, Puskas LG, Ferdinandy P.** Capsaicin-sensitive sensory neurons regulate myocardial function and gene expression pattern of rat hearts: A DNA microarray study. *FASEB J* 20: 160–162, 2006.

J Physiol 590.21 (2012) pp 5389–5400

The Journal of Physiology

Adverse cardiac remodelling in spontaneously hypertensive rats: acceleration by high aerobic exercise intensity

Rui Manuel da Costa Rebelo, Rolf Schreckenberg and Klaus-Dieter Schlüter

Justus-Liebig-Universität Gießen, Physiologisches Institut, Aulweg 129, 35392 Gießen, Germany

Key points

- Physical exercise is recommended as first line therapy for hypertensive patients. However, studies investigating long-term effects of high intensity exercise on the progression of hypertensive heart disease have revealed conflicting results.
- We show that high intensity aerobic exercise accelerates hypertensive heart disease and improves fibrosis.
- Surprisingly, high intensity aerobic exercise in the presence of an angiotensin converting enzyme inhibitor not only attenuated training induced mal-adaptation but exerts positive repair processes. These effects were independent of blood pressure effects.
- The results of this study provide evidence that high physical activity in hypertensives must be considered as an important risk factor rather than a therapeutic intervention.

Abstract In the present study it was hypothesized that voluntary aerobic exercise favours a pro-fibrotic phenotype and promotes adverse remodelling in hearts from spontaneously hypertensive rats (SHRs) in an angiotensin II-dependent manner. To test this, female SHRs at the age of 1 year were started to perform free running wheel exercise. Captopril was used to inhibit the renin–angiotensin system (RAS). Normotensive rats and SHRs kept in regular cages were used as sedentary controls. Training intensity, expressed as mean running velocity, was positively correlated with the left ventricular mRNA expression of TGF-β_1, collagen-III and biglycan but negatively correlated with the ratio of sarcoplasmic reticulum Ca^{2+}-ATPase (SERCA)2a to Na^{+}–Ca^{2+} exchanger (NCX). A pro-fibrotic phenotype was verified by Picrosirius red staining. Sixty-seven per cent of SHRs performing free running wheel exercise died either spontaneously or had to be killed during a 6 month follow-up. In the presence of captopril, aerobic exercise did not show a similar positive correlation between training intensity and the expression of fibrotic markers. Moreover, in SHRs receiving captopril and performing free running wheel exercise, a training intensity-dependent reverse remodelling of the SERCA2a-to-NCX ratio was observed. None of these rats died spontaneously or had to be killed. In captopril-treated SHRs performing exercise, expression of mRNA for decorin, a natural inhibitor of TGF-β_1, was up-regulated. Despite these differences between SHR-training groups with and without captopril, positive training effects (lower resting heart rate and no progression of hypertension) were found in both groups. In conclusion, high aerobic exercise induces an angiotensin II-dependent adverse

DOI: 10.1113/jphysiol.2012.241141

remodelling in chronic pressure overloaded hearts. However, high physical activity can potentially induce reverse remodelling in the presence of RAS inhibition.

(Resubmitted 18 July 2012; accepted after revision 24 August 2012; first published online 28 August 2012)
Corresponding author K.-D. Schlüter: Justus-Liebig Universität, Physiologisches Institut, Aulweg 129, 35392 Gießen, Germany. Email: klaus-dieter.schlueter@physiologie.med.uni-giessen.de

Abbreviations ACE, angiotensin converting enzyme; NCX, Na^+–Ca^{2+} exchanger; Nrf-1, nuclear respiratory factor-1; PGC-1α, peroxisome proliferator activated receptor γ coactivator 1α; RAS, renin–angiotensin system; SERCA, sarcoplasmatic reticulum Ca^{2+}-ATPase; SHR, spontaneously hypertensive rat; TGF-β1, transforming growth factor-β1.

Introduction

Cardiovascular disease is the leading cause of death in modern societies and is often associated with hypertension-dependent end organ damage. Advancing age is the major additional risk factor in particular in combination with hypertension. Aerobic exercise is a first-line therapeutic strategy to reduce the risk of cardiovascular disease with hypertension and ageing (Hagberg *et al.* 2000; Chobanian *et al.* 2003; Williams *et al.* 2004; Westhoff *et al.* 2007). However, the effect of aerobic exercise on heart remodelling and its potential mechanisms has not been examined. The limited available data in experimental animals do not support the idea of favourable effects of aerobic exercise on chronic pressure overloaded hearts (Schultz *et al.* 2007; van Deel *et al.* 2011). It remained unclear whether this maladaptive hypertrophy observed in such studies is indeed caused by over-stimulation of classical pro-hypertrophic stimuli such as the renin–angiotensin system.

Increased deposition of collagen I and III are believed to be important mechanisms mediating left ventricular stiffening concomitant with hypertension (Diez *et al.* 2002). Biglycan, a member of the small leucine rich proteoglycan family, is constitutively expressed in the heart; it triggers matrix assembly and activates TGF-β_1 (Latif *et al.* 2005; Ruoslahti & Yamaguchi, 1991; Bereczki *et al.* 2007). TGF-β_1, a cytokine locally produced in the heart, triggers the expression of collagens (Masague, 1990). Its activity can be attenuated by another small proteoglycan, decorin, which neutralizes TGF-β_1 by binding (Ruoslahti, 1988; Hildebrand *et al.* 1994). TGF-β_1 has been identified as a key molecule at the transition of adaptive cardiac hypertrophy to mal-adaptive cardiac hypertrophy (Villarreal & Dillmann, 1992; Boluyt *et al.* 1994). TGF-β_1 plays a critical role due to its pro-fibrotic effects and its influence on the expression of the calcium handling protein SERCA2a (Lijnen *et al.* 2000; Mufti *et al.* 2008). SERCA2a is responsible for refilling sarcoplasmatic reticulum during the diastolic phase of a heart cyclus (Bers, 2000). A low SERCA2a expression or activity requires an up-regulation of the Na^+–Ca^{2+} exchanger (NCX) to extrude calcium from the cytosol during the diastolic phase of a heart cycle (Schillinger *et al.* 2003). Therefore, a reduced SERCA/NCX ratio can be found in failing hearts and is a reliable marker of adverse remodelling.

The effect of aerobic exercise on pressure overloaded hearts is difficult to predict. On the one hand aerobic exercise lowers age-dependent arterial stiffening and thereby reduces afterload (Amaral *et al.* 2000; Fleenor *et al.* 2010). On the other hand aerobic exercise is associated with exercise-dependent activation of the sympathetic nervous system that then triggers a release of renin from cells of the juxtaglomerular apparatus and thereby activates the renin–angiotensin system (RAS). Angiotensin II, the main molecule of the RAS cascade, induces the cardiac expression of TGF-β_1 (Wenzel *et al.* 2001). As stated above, this scenario will accelerate fibrosis and malfunction of calcium handling in the left ventricle. In the current study the role of the RAS cascade on exercise-dependent effects of cardiac remodelling was investigated by administration of captopril, an inhibitor of angiotensin converting enzyme (ACE).

In the present study we hypothesized that inhibition of the RAS will attenuate possible mal-adaptive effects caused by aerobic exercise in hypertensives and will shift the response to exercise in a more favourable direction. We further hypothesized that a high training intensity will lead to more detrimental effects than moderate exercise. To test these hypotheses we used spontaneously hypertensive rats (SHRs) at the age of 1 year with established hypertension. SHRs represent a suitable model of long-term adaptation to hypertension and are extensively characterized. Voluntary wheel running was used as a model of voluntary aerobic exercise (Bradley *et al.* 2008; Fleenor *et al.* 2010). As voluntary exercise results in different exercise intensities between animals, this allows us to correlate exercise-dependent adaptations with exercise intensity.

Methods

Ethical approval

All rats used in this study were house strains obtained from the animal facility of our institute. The investigation conforms to the *Guide for the Care and Use of Laboratory Animals* published by the National Institutes of

Health (publication 85-23, revised 1996). The treatment protocols were approved by the local authorities.

Eleven normotensive female Wistar rats at the age of 12 months were used as normotensive control rats. Thirty-four female SHRs were used at the age of 12 months and randomly divided into one of the following four groups: SHR controls (SHR-sed; $n = 11$), SHR captopril (SHR-sed + Capto, $n = 11$), SHR exercise (SHR-train, $n = 6$), and SHR exercise with captopril (SHR-train + Capto; $n = 6$). Female rats were used because they have a higher spontaneous running activity (Eickelboom & Mills, 1988). Animals had free access to food and water. Rats in exercise groups had free access to running wheels that were connected to a computerized registration of running distances and running times. Where required, captopril was given with the drinking water at 30 mg kg^{-1} day^{-1}. All rats were monitored on a weekly basis and they were removed from the programme if they developed a constitutive loss of body weight and blood pressure for three consecutive weeks. These rats were killed at that time and analysed in the same way as all other rats as well. All experiments were terminated after 26 weeks if rats did not develop signs of decompensated heart failure. At the end of the experimental period all rats were killed by cervical dislocation, hearts were rapidly excised, and the aorta was cannulated for retrograde perfusion with a 16-gauge needle connected to a Langendorff perfusion system to remove any blood. From the blood free hearts, atria and right ventricles were separated and the remaining left ventricle was weighed and rapidly frozen in liquid nitrogen for later analysis. The tibia lengths were measured and the left ventricular plus septum weight was normalized to tibia lengths and taken as the left ventricular weight. To determine the length of tibia, bones were separated from the muscle tissue and measured with a calliper.

Determination of blood pressure *in vivo*

For weekly determination of blood pressure, rats were set in a separate chamber (TSE Systems GmbH, Bad Homburg, Germany) and blood pressure (peak systolic blood pressure, diastolic blood pressure and heart rate) was determined via the tail-cuff method. Briefly, the mean of 10 consecutive blood pressure readings was obtained for each animal at weekly intervals. Before starting, rats were conditioned for 1 week by daily measurements and handling before any data were recorded. All blood pressure measurements were performed by the same person to minimize any variations. Body weight was recorded weekly and water consumption daily.

qRT-PCR

Total RNA was isolated from left ventricles using peqGold TriFast (peqlab; Biotechnologie GmbH, Germany) according to the manufacturer's protocol. To remove genomic DNA contamination, isolated RNA samples were treated with 1 U DNase per μg RNA (Invitrogen, Karlsruhe, Germany) for 15 min at 37°C. One microgram of total RNA was used in 10 μl reaction to synthesize cDNA using Superscript RNaseH reverse transcriptase (200 U μg^{-1} RNA; Invitrogen) and oligo dTs (Roche, Mannheim, Germany) as primers. Reverse transcriptase reactions were performed for 60 min at 37°C. Real-time quantitative PCR was performed using the Icycler IQ detection system (Bio-Rad, Munich, Germany) in combination with the IQ SYBR Green real-time PCR supermix (Bio-Rad). The thermal cycling programme consisted of initial denaturation in one cycle of 3 min at 95°C, followed by 45 cycles of 30 s at 95°C (denaturation), 30 s at primer specific annealing temperature, and 30 s at 72°C (elongation). Primer sequences used for determination are given in Table 1. Data are normalized to Hypoxanthine phosphoribosyltransferase (HPRT) expression that was used as a house-keeping gene in this study. Preliminary experiments with actin and β_2 microglobulin, which were alternatively considered as house keeping genes, revealed the lowest variability in the HPRT group. Quantification was performed as described (Livak & Schmittgen, 2001).

Picrosirius red staining

Samples were fixed and pre-incubated with Tissue-Tek (Sakura, Alphen, Netherlands) and sliced in 10 μm pieces. Tissue slices were fixed in Bouin solution and subsequently stained in 0.1% (w/v) Sirius red solution (Sigma-Aldrich Chemie, Steinheim, Germany). Slices were washed by 0.01 N HCl, Aqua destillata and counterstained for nuclei by Mayer's hemalaun solution, washed with Aqua destillata for 5 min and dehydrated with ethanol. Finally, slices were visualized under light microscopy. The amount of stained tissue was quantified via Leica Confocal Software Lite Version 2.6.1 (LCS Lite). The mean of $n = 5$ preparations was used to quantify the extent of collagen labelling.

Immunoblotting

Protein was extracted from frozen left-ventricular heart tissue in extraction buffer, containing (mmol l^{-1}): Mops 5, sucrose 300, EGTA 1, bovine serum albumin 0.015, and 0.01% (v/v) protease inhibitor cocktail (Sigma, Taufkirchen, Germany). The homogenate was centrifuged at 1000 g at 4°C for 10 min and the supernatant was used for SERCA2a and NCX detection by Western blotting. Protein samples were loaded on NuPAGE Bis-Tris Precast gels (10%; Life Technology, Darmstadt, Germany) and subsequently transferred onto nitrocellulose membranes. Primary antibodies directed against SERCA2a, NCX and cardiac α-actin (loading control) were used as described before (Maxeiner *et al.* 2010).

Table 1. Description of all primers used in this study

Biglycan	Forward:	TGA TTG AGA ATG GGA GCC TGA G
	Reverse:	CCT TGG TGA TGT TGT TGG AGT G
	Product length:	144 bp
	NCBI:	NM_017087
Collagen-III	Forward:	TGG AGT CGG AGG AAT G
	Reverse:	GCC AGA TGG ACC AAT AG
	Product length:	184 bp
	NCBI:	NM_032085
Decorin	Forward:	GGC AGT CTG GCT AAT GTT C
	Reverse:	CTT CGG AGA TGT TGT TGT TAT G
	Product length:	133 bp
	NCBI:	NM_024129
HPRT	Forward:	CCA GCG TCG TGA TTA GTG AT
	Reverse:	CAA GTC TTT CAG TCC TGT CC
	Product length:	132 bp
	NCBI:	NM_ 012583
NCX	Forward:	CCG TAA TCA GCA TTT CAG AG
	Reverse:	GCC AGG TTC GTC TTC TTA AT
	Product length:	187 bp
	NCBI:	NM_019268
SERCA2a	Forward:	CGA GTT GAA CCT TCC CAC AA
	Reverse:	AGG AGA TGA GGT AGC GGA TGA A
	Product length:	268 bp
	NCBI:	NM_001110139
TGF-β_1	Forward:	ATT CCT GGC GTT ACC TTG
	Reverse:	CCT GTA TTC CGT CTC CTT GG
	Product length:	117 bp
	NCBI:	NM_021578
PGC-1α	Forward:	AGT GCT CAG CCG AGG ACA CGA
	Reverse:	TGC CCC TGC CAG TCA CAG GA
	Product length:	180 bp
	NCBI:	NM_031347
Nrf-1	Forward:	GGC ATC ACT GGC AGA GGC CG
	Reverse:	GCT GCT GCG GTT TCC CCA GA
	Product length:	168 bp
	NCBI:	NM_001100708

Heart function analysis

Left ventricular function was assessed by Langendorff technique *ex vivo* as described before. Briefly, hearts were quickly removed and connected to a Langendorff perfusion system and a balloon was inserted into the left ventricle. Left ventricular diastolic pressure was adjusted to 10 mmHg and kept constant thereafter. After 20 min of stabilization, hearts were paced at 240 bpm for 5 min and left ventricular developed pressure (systolic pressure – diastolic pressure) and +dp/dt were recorded.

Statistics

Data are given as means ± standard deviation. In all cases in which more than two groups were compared, two-side ANOVA was used to decide about differences among groups followed by the Student–Newman–Keuls test as a *post hoc* analysis to identify between group differences. In cases where only two groups were compared, Student's t test for unpaired samples was used. Correlation analysis was performed as a linear regression analysis. Exact P values are given for all experiments and differences between groups are indicated by appropriate symbols. The statistical analysis was performed using SPSS v. 17.0.

Results

Animal characteristics are shown in Table 2 for normotensive control rats, sedentary SHRs, and running SHRs. Left ventricular weights were greater in all SHRs compared to normotensive rats. Left ventricular weight was lower in SHR-sed + Capto compared to SHR-sed and SHR-train + Capto compared to SHR-train. SHR-train had greater left ventricular weight than SHR-sed. Among these animals one rat died spontaneously after 10 weeks and could not be used for further analysis, two rats had to be killed after 24 weeks and one rat after 25 weeks. All other rats survived for 26 weeks.

Absolute blood pressure values are also given in Table 2 as they were analysed 8 weeks after the onset of voluntary exercise or sedentary control period. Systolic blood pressures were greater in all SHRs compared to normotensive control rats. Systolic blood pressure in SHR-sed + Capto was lower than in SHR-sed. Systolic blood pressures were not different between SHR-train + Capto and SHR-train. Diastolic blood pressures were also greater in SHRs compared to normotensive rats but not significantly different between SHR groups.

Training performance and effect on blood pressure

Running distance, running time and mean running velocity did not differ between SHR-train and SHR-train + Capto (Table 3). Heart rates significantly dropped in SHR-train compared to SHR-sed and SHR-train + Capto compared to SHR-sed + Capto (Table 3). This was taken as an indicator of positive training effects. On a molecular level this positive training effect was further confirmed by increased Nrf-1 and PGC-1α expression (Fig. 1). Systolic blood pressure was further raised in SHR-sed and this was significantly different compared to all other SHR groups (Table 3). No significant difference occurred in the development of diastolic blood pressures (Table 3).

Effect of training intensity on left ventricular expression of fibrotic markers

In general, left ventricular TGF-β_1 expression was higher in SHR-sed compared to normotensive rats

Table 2. Animal characteristics

	LV/TL (mg mm^{-1})	P_{syst} (mmHg)	P_{diast} (mmHg)	HR (bpm)
ANOVA	$P \leq 0.000$	$P \leq 0.000$	$P \leq 0.000$	$P \leq 0.011$
Wistar ($n = 11$)	177 ± 22	136 ± 10	89 ± 9	398 ± 34
SHR-sed ($n = 11$)	259 ± 15*	183 ± 17*	119 ± 10	438 ± 24‡
SHR-sed + Capto ($n = 11$)	203 ± 16*#	158 ± 16*#	105 ± 11	422 ± 31
SHR-train ($n = 5/6$)	366 ± 55*#	169 ± 28*	107 ± 25	388 ± 49
SHR-train + Capto ($n = 6$)	286 ± 26*#§	179 ± 22*	119 ± 14	424 ± 20

Data are means ± SD. LV/TL, ratio of left ventricular weight to tibia length; P_{syst}, systolic blood pressure; P_{diast}, diastolic blood pressure; HR, heart rate. *$P < 0.05$ *vs.* Wistar; #$P < 0.05$ *vs.* SHR-sed; §$P < 0.05$ *vs.* SHR-train; ‡$P < 0.05$ *vs.* SHR-train.

Table 3. Training performance and training-induced changes in SHR

	SHR-sed	SHR-sed + Capto	SHR-train	SHR-train + Capto	*P* value
RD (km per week)	—	—	48.9 ± 19.8	47.3 ± 12.4	0.858
RT (h w^{-1})	—	—	19.6 ± 6.4	22.0 ± 4.0	0.460
RV (km per hour)	—	—	2.43 ± 0.56	2.47 ± 0.19	0.775
HR (bpm)	+1 ± 24	+12 ± 40	−60 ± 38*	−32 ± 27#	0.001
P_{syst} (mmHg)	+17 ± 16	−19 ± 13*	−8 ± 33*	−4 ± 19*	0.002
P_{diast} (mmHg)	+6 ± 14	−12 ± 10	−7 ± 27	−1 ± 14	0.084

Data are means ± SD; RD, running distance; RT, running time; RV, running velocity; HR, heart rate; P_{syst}, systolic blood pressure; P_{diast}, diastolic blood pressure. Two-side unpaired *t* test was used for RD, RT and RV. ANOVA and Student–Newman–Keuls *post hoc* analysis was used for HR, P_{syst} and P_{diast}. *$P < 0.05$ *vs.* SHR-sed.; #$P < 0.05$ *vs.* SHR-sed + Capto.

(2.01 ± 0.73 AU *vs.* 1.00 ± 0.40 AU; $n = 11$; $P = 0.001$) and this was attenuated by captopril (SHR-sed + Capto; 0.82 ± 0.34 AU). This pro-fibrotic effect was significantly increased in SHR-train rats (6.72 ± 3.72 AU; $P = 0.037$).

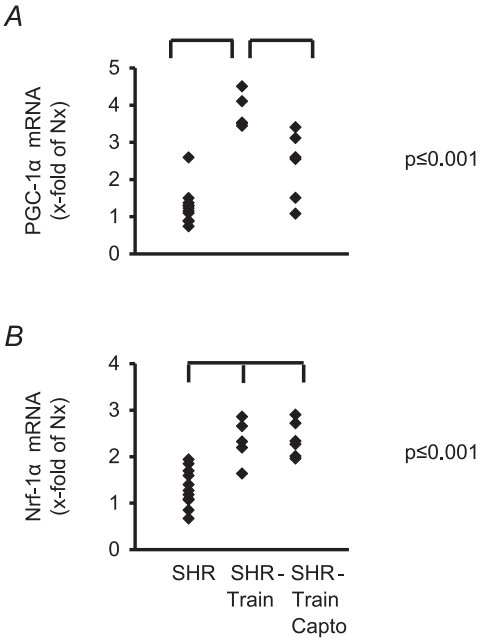

Figure 1. Induction of PGC-1α and Nrf-1 by exercise in the left ventricle of SHRs
Data points from all rats are normalized to the mean expression of normotensive rats (Nx).

Moreover, a significant positive correlation between total running distance and running velocity with left ventricular expression of TGF-β_1 was observed in SHR-train (Fig. 2). This positive correlation was converted into a negative correlation in SHR-train + Capto although this did not reach the level of significance. The strong correlation between tissue expression of TGF-β_1 and training intensity in SHR-train suggests a pro-fibrotic effect of high training intensities. This was confirmed by analysis of collagen III expression. Collagen III is a classical down-stream target of TGF-β_1. Again, left ventricular collagen III expression was higher in SHR-sed compared to normotensive rats and this effect was attenuated by captopril (Fig. 3). As assessed by Picrosirius red staining, total collagen was strongly increased in SHR-train and lower in SHR-train + Capto (Fig. 4). The pro-fibrotic influence of running in SHR-train was further stressed by a significant correlation of biglycan expression (Fig. 5). In contrast, decorin expression was not affected by wheel running but was more highly expressed in SHR-train + Capto compared to SHR-train (Fig. 6).

Effect of training intensity on left ventricular expression of SERCA2a and NCX

Finally, we evaluated the left ventricular expression of SERCA2a and NCX. Training intensity was negatively correlated with the SERCA2a-to-NCX ratio (Fig. 7). This

effect of training intensity was again converted into a significant accentuation of the SERCA2a-to-NCX ratio in SHR-train + Capto (Fig. 7). These data on SERCA2a and NCX mRNA expression were confirmed by Western blot. Protein expression of NCX significantly increased in the SHR-train group (Fig. 8). From the data on fibrosis and calcium handling proteins we expected a significant effect on cardiac function. As indicated in Fig. 9 left ventricular developed pressure (LVDP) and $+dp/dt_{max}$ were indeed significantly worsened in the SHR-train group and these detrimental effects were normalized by captopril.

Discussion

The present study assessed the effect of training intensity on left ventricular fibrosis and on the expression of calcium handling proteins. Both fibrosis and a low SERCA2a-to-NCX ratio favour diastolic heart failure (Diez *et al.* 2002; Schillinger *et al.* 2003). The results of the current study show that high training intensity of aerobic exercise in old SHRs with long-term established hypertension produces a pro-fibrotic phenotype with unfavourable expression patterns of calcium handling proteins. Inhibition of the angiotensin converting enzyme (ACE) attenuated any high intensity training-dependent effect on fibrotic markers. A complete new finding of this study is that under the tested conditions, high training intensity induces adverse remodelling as indicated by a correlation between training intensity and expression of pro-fibrotic markers and a highly significant inverse correlation between SERCA2a-to-NCX ratio and high intensity training. Of note, this effect was not accompanied by any significant differences in blood pressure. However, an age-dependent increase in blood pressure in SHRs was attenuated by free running wheel exercise independent of ACE inhibition.

In chronic pressure overload conditions the cytokine TGF-β_1 plays a key role at the transition of adaptive cardiac hypertrophy to mal-adaptive hypertrophy because TGF-β_1

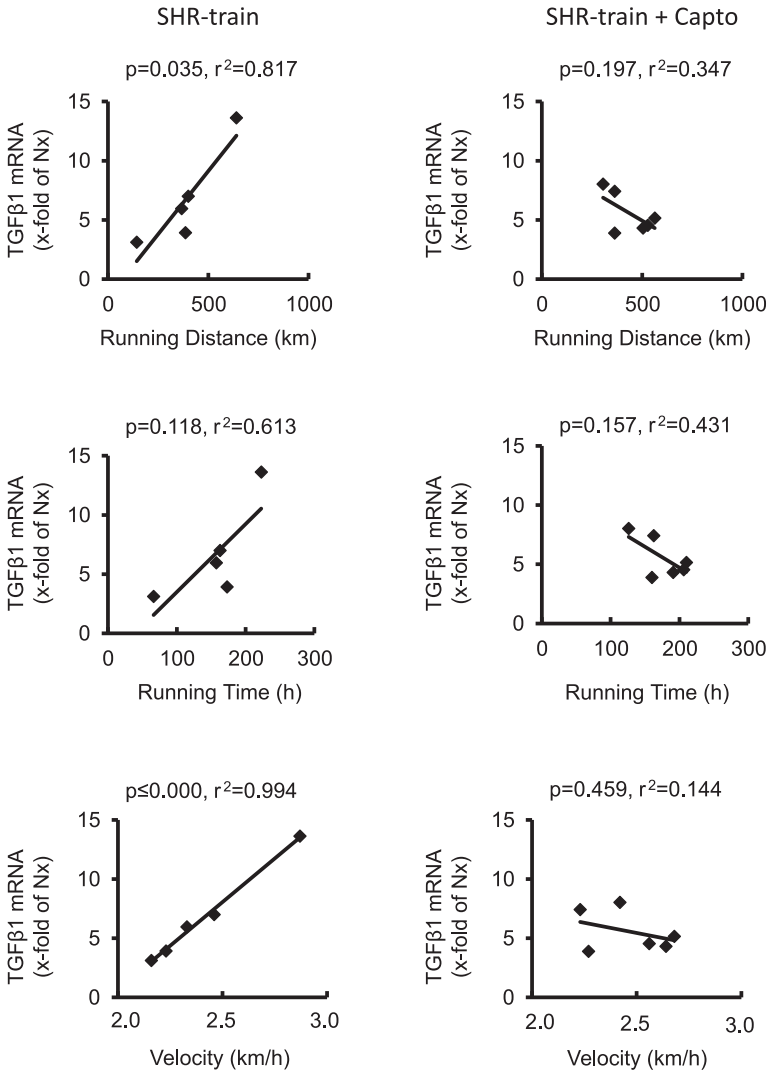

Figure 2. Correlation between training intensity and left ventricular TGF-β_1 expression in SHR-train and SHR-train + Capto
Expression is normalized to the mean expression of normotensive rats (Nx).

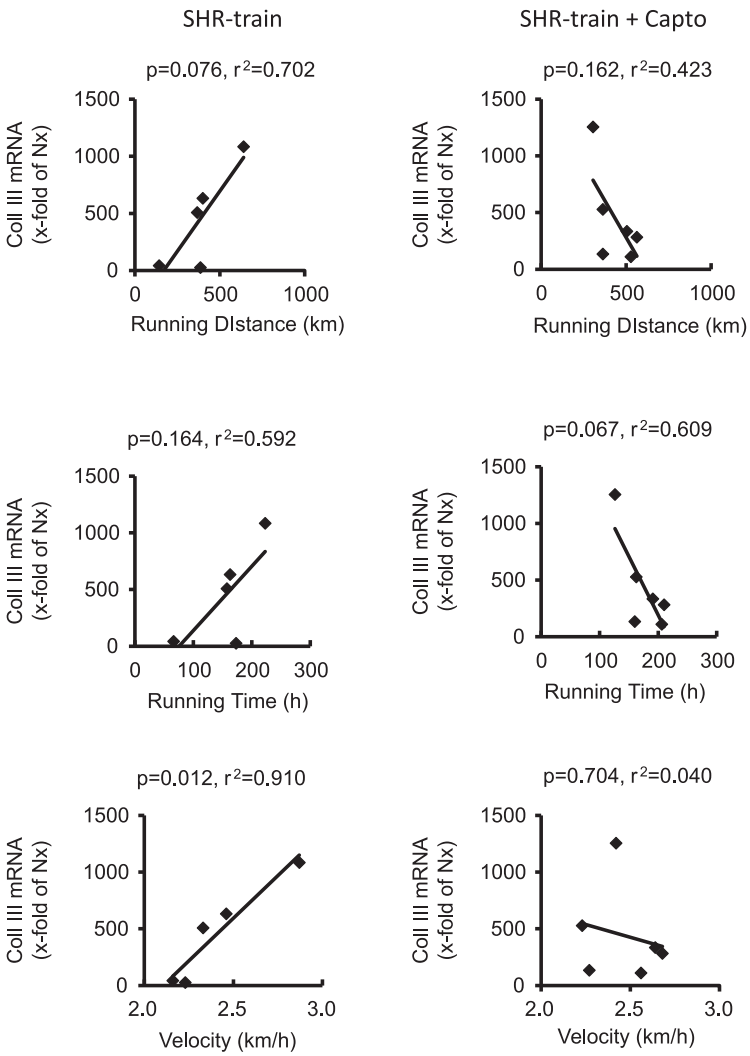

Figure 3. Correlation between training intensity and left ventricular collagen-III (Coll III) expression in SHR-train and SHR-train + Capto
Expression is normalized to the mean expression of normotensive rats (Nx).

expression is closely linked to this transition (Villarreal & Dillmann, 1992; Boluyt *et al.* 1994). Its cardiac expression is controlled by angiotensin II and depends on an activation of the RAS (Wenzel *et al.* 2001). Physical activity stimulates the sympathetic nervous system and thereby increases the release of renin from the cells of the juxtaglomerular apparatus. Therefore, it can be predicted that high physical activity is associated with strong activation of

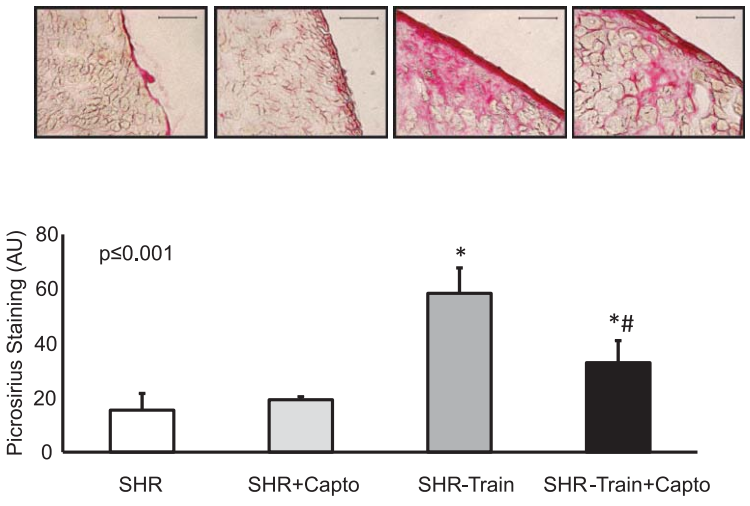

Figure 4. Left ventricular collagen expression
Tissue slices were stained for total collagen (Pircosirius red; top; scale bar 100 μm). Mean staining intensities ± SD are given as bar graphs. *Significant difference from SHRs; #significant difference from SHR-train.

RAS and this should stress the chronic pressure overloaded heart. In the current study we provide further evidence for this hypothesis. Old SHRs are already at the risk to develop mal-adaptive hypertrophy and heart failure. This process was accelerated in SHRs performing exercise in a training intensity-dependent way. Our study is in line with a previous finding in a two-kidney, one-clip model in which moderate exercise reduced neither blood pressure nor hypertrophy although moderate exercise did not worsen left ventricular remodelling (Boissiere *et al.* 2008).

It is proposed that myocardial fibrosis is responsible for an increase in myocardial stiffness that may alter left ventricular diastolic properties (Diez *et al.* 2002). In untreated SHRs performing free running wheel activity, we observed a high mortality during the subsequent 6 months of follow-up. Quantification of heart function indicated reduced cardiac function as monitored by left ventricular developed pressure. After a period of high physical activity with positive training effects, such as reduced resting heart rate and lack of progressive increase in hypertension compared to sedentary SHRs, they spontaneously lost body weight and developed a drop in blood pressure. This led to killing for ethical reasons (3 rats) or sudden death (1 rat). In total, 4 out of 6 rats did not reach the predicted end-point of follow-up. In contrast no such effect occurred in SHRs treated with captopril. Neither the absolute amount of physical activity nor the training effects on heart rate and blood pressure were different between both training groups. The only difference was the subsequent inhibition of the RAS. Among the fibrotic markers we found an attenuation of training intensity-dependent expression of TGF-β_1, of collagen III, a down-stream target of TGF-β_1 signalling, and biglycan in the captopril running group. TGF-β_1 and biglycan are known to be induced in a RAS-dependent manner (Zimmermann *et al.* 1999). High training intensity in captopril treated SHRs not only reveals a lack of progression of fibrosis but also shows a training intensity-dependent reverse remodelling. The effect of reverse remodelling was more stringent for the effect of SERCA2a-to-NCX ratio. This might be explained by earlier *in vitro* findings. In isolated and cultured adult

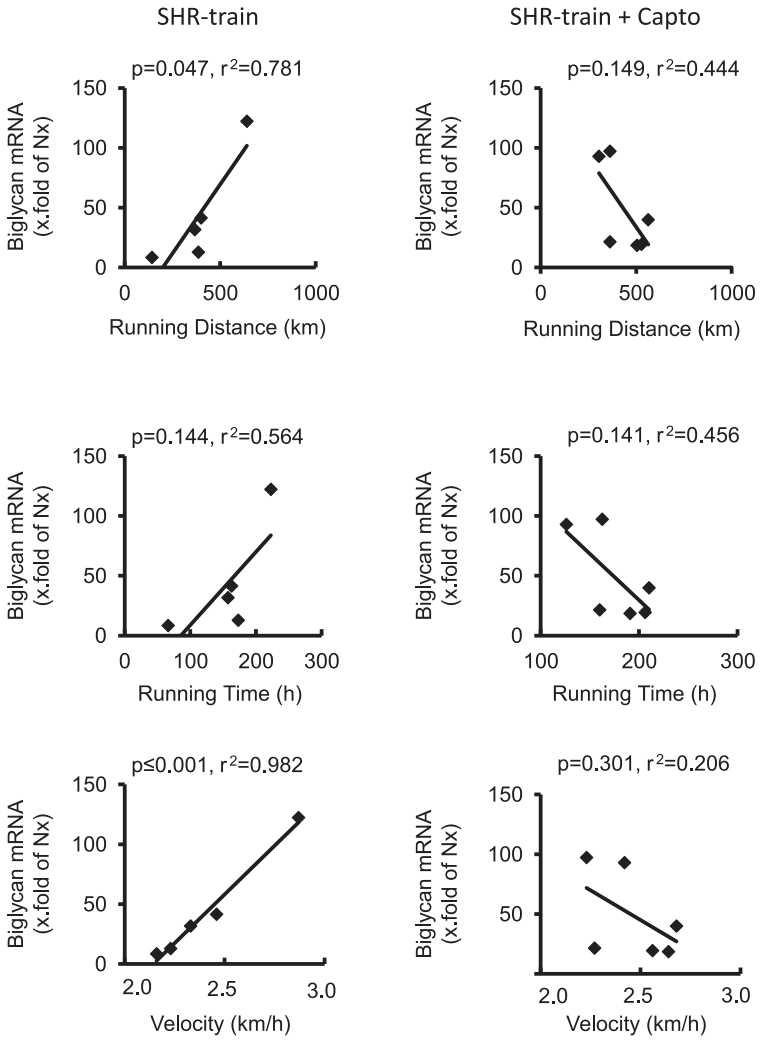

Figure 5. Correlation between training intensity and left ventricular biglycan expression in SHR-train and SHR-train + Capto
Expression is normalized to the mean expression of normotensive rats (Nx).

rat ventricular cardiomyocytes, angiotensin II reduces the expression of SERCA2a in a TGF-β_1-dependent way (Mufti *et al.* 2008). In contrast, stimulation of adrenergic receptors increases the expression of SERCA2a (Anwar *et al.* 2005, 2008). High training intensity activates the sympathetic nervous system leading to an activation of cardiac adrenoceptors. In the presence of ACE inhibition, angiotensin II does not repress SERCA2a expression and the remaining net effect of running activity is an improvement of the SERCA2a-to-NCX ratio. The effect of ACE inhibition in SHRs performing free running wheel exercise was less pronounced when fibrotic markers were analysed. However, the strong correlation between training intensity and expression of TGF-β_1, collagen III and biglycan was abrogated. TGF-β_1 activity is not strictly linked to TGF-β_1 expression and modified by small proteoglycans. Decorin normally binds TGF-β_1 and by such an immobilization it attenuates its binding to TGF-β_1 receptors (Ruoslahti, 1988; Hildebrand *et al.* 1994). Of note, in training performing SHRs with captopril the expression of decorin was higher than in all other groups. This might contribute to the positive effect of ACE inhibition in this case because decorin is known to ameliorate adverse remodelling by inhibiting TGF-β (Jahanyar *et al.* 2007). However, for decorin no association between training intensity and expression was found.

In the literature there is a controversy about differences between physiological and pathophysiological hypertrophy and the effect of exercise on these different types of hypertrophy. In general, pathophysiological hypertrophy is considered to be triggered by the calcineurin/NFAT pathway and this seems to be reduced by moderate cardiac hypertrophy (Oliveira *et al.* 2009; Libonati *et al.* 2011). In contrast, free running wheel models are known to induce excessive cardiac hypertrophy. Our study points out that activation of the renin–angiotensin system significantly contributed to this effect. We have previously demonstrated that angiotensin II reduces SERCA2a expression leading to reduced myocyte function and the data of this study are in agreement with this finding (Mufti *et al.* 2008).

It is still a matter of debate whether physical activity is protective against the progression of hypertension. To

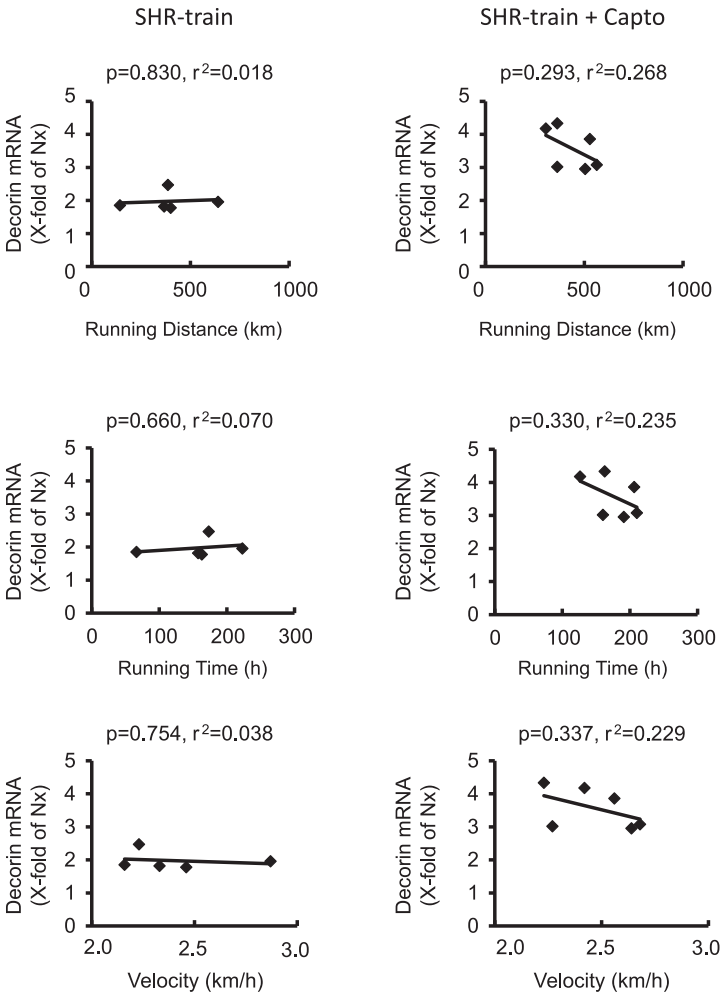

Figure 6. Correlation between training intensity and left ventricular decorin expression in SHR-train and SHR-train + Capto
Expression is normalized to the mean expression of normotensive rats (Nx).

date modest levels of regular voluntary aerobic exercise are recommended as first-line therapy for preventing cardiovascular disease. Physical activity does not only affect the heart but also age-dependent artery stiffening (Fleenor *et al.* 2010). Thus overall physical activity may affect more than the heart function only. However, animal experiments do not provide strong evidence that physical activity itself lowers blood pressure and improves the outcome (Schultz *et al.* 2007; van Deel *et al.* 2011). Our study is in line with previous animal studies showing detrimental effects of physical activity on chronic pressure overloaded hearts. Our study is also in line with proceeding animal studies that do not reveal a blood pressure lowering effect in SHRs (Schlüter *et al.* 2010; Coimbra *et al.* 2008). A main difference between animal studies and patient studies investigating the effect of exercise on blood pressure and heart function may be that the initiation of even moderate physical activity in humans lowers their body weight. The body mass index strongly correlates to blood pressure (Hedeyati *et al.* 2011). Furthermore, patients participating in life-style programmes have often additional changes in their diet which also influences the body mass index. Another difference between animal studies and clinical studies in this field is that the so-called sedentary rats are not really sedentary. They freely move around in their cages whereas sedentary patients often have very low and probably non-physiological low levels of physical activity. Despite these limitations the current study identifies the RAS as a potential risk in high training intensity and provides some evidence for a training-induced reverse remodelling in the presence of RAS inhibition. It has been reported that RAS inhibition may reverse myocardial fibrosis (Diez *et al.* 2002). Here we show that additional high aerobic exercise induces reverse remodelling in addition. The study may contribute to optimize treatment regimes of hypertensive patients performing aerobic exercise.

As a limitation of this study, the use of only one specific type of sex, female rats, must be considered. Of course, the data cannot predict the outcome if male rats are used. Female rats were used in this study because female rats have a higher spontaneous running activity (Eickelboom & Mills, 1988). This is a prerequisite of our study. However, in a recent meta-analysis of studies using SHR and exercise we could not find any major differences between male and female rats with respect to the influence of exercise on

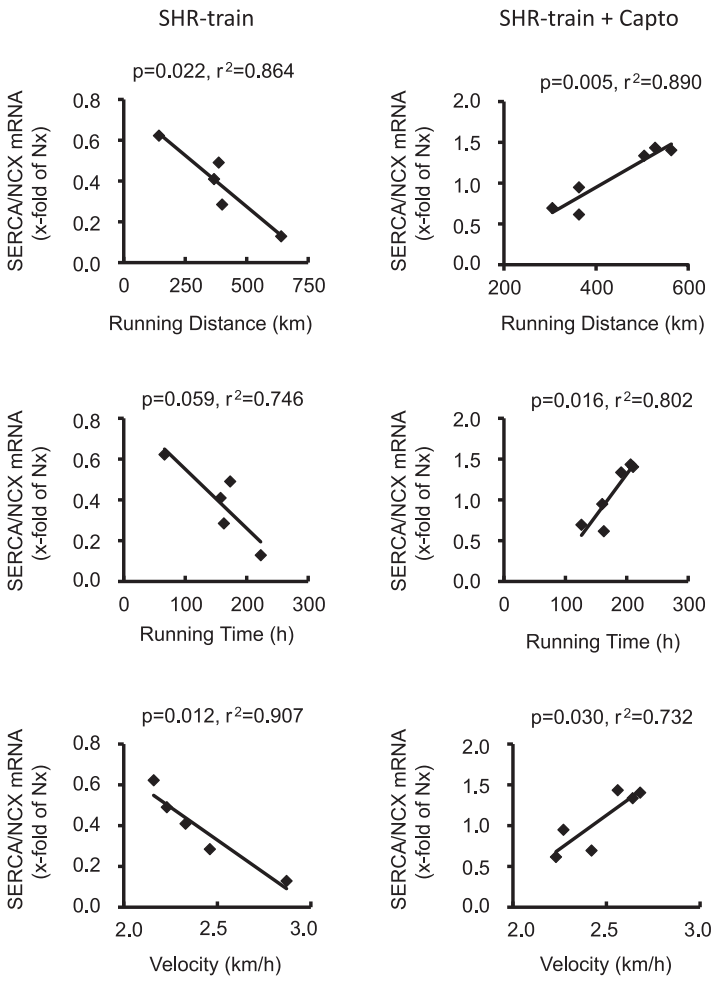

Figure 7. Correlation between training intensity and left ventricular SERCA2a-to-NCX ratio in SHR-train and SHR-train + Capto
Expression is normalized to the mean expression of normotensive rats (Nx).

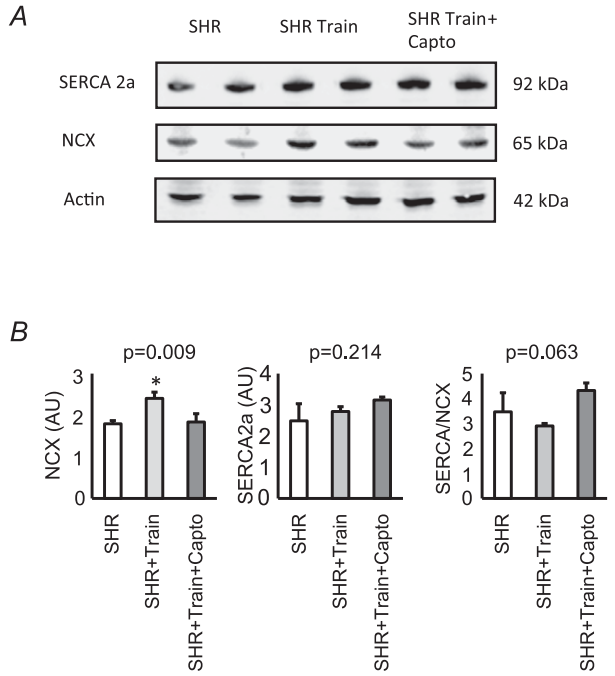

Figure 8. Left ventricular protein expression of sodium–calcium exchanger (NCX) and SERCA2a
A, original blots; *B*, mean data ± SD. *Significant difference from SHRs.

blood pressure and hypertrophy (Schlüter *et al.* 2010). Therefore, we do not expect such a difference. However, for the same reason than we used female rats, the majority of comparable studies were also performed with females rats (i.e. Schultz *et al.* 2007).

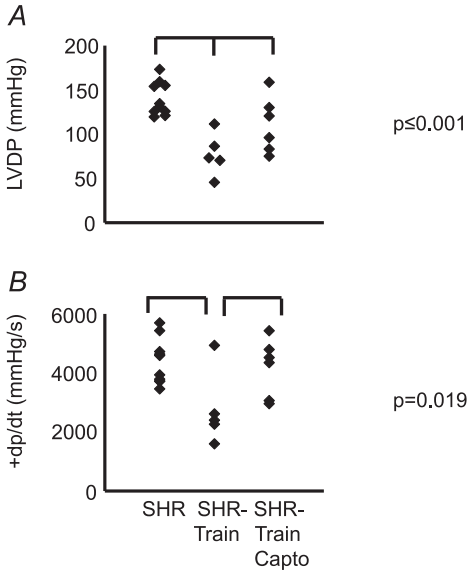

Figure 9. Left ventricular function of rat hearts from SHR, SHR-train, and SHR-train + Capto
Left ventricular developed pressure (LVDP) and the first derivative (+d*p*/d*t*) are given in *A* and *B*, respectively.

Conclusions

The results of this study provide evidence that high physical activity in hypertensives must be considered as an important risk factor rather than a therapeutic intervention. We identified the activation of RAS as a main trigger for adverse remodelling in hearts of SHRs with high training intensity. Moreover, in the presence of ACE inhibition there was a training intensity-dependent reverse remodelling not identified before. Therefore one may predict that in the presence of effective inhibition of RAS voluntary aerobic exercise significantly contributes to reverse remodelling.

References

Amaral SL, Zorn TMT & Michelini LC (2000). Exercise training normalizes wall-to-lumen ratio of the gracilis muscle arterioles and reduces pressure in spontaneously hypertensive rats. *J Hypertens* **18**, 1563–1572.

Anwar A, Taimor G, Korkusuz H, Schreckenberg R, Berndt T, Abdallah Y, Piper HM & Schlüter K-D (2005). PKC-dependent signal transduction pathways increase SERCA2a expression in adult rat cardiomyocytes. *J Mol Cell Cardiol* **39**, 911–919.

Anwar A, Schlüter K-D, Heger J, Piper HM & Euler G (2008). Enhanced SERCA2a expression improves contractile performance of ventricular cardiomyocytes of rat under adrenergic stimulation. *Pflugers Arch* **457**, 485–491.

Bereczki E, Gonda S, Csont T, Korpos E, Zvara A, Ferdinandy P & Santha M (2007). Overexpression of biglycan in the heart of transgenic mice: An antibody microarray study. *J Proteom Res* **6**, 854–861.

Bers DM (2000). Calcium flux involved in control of cardiac myocyte contraction. *Circ Res* **87**, 275–281.

Boissiere J, Eder V, Machet M-C, Courteix D & Bonnet P (2008). Moderate exercise training does not worsen left ventricle remodelling and function in untreated severe hypertensive rats. *J Appl Physiol* **104**, 321–327.

Boluyt MO, O'Neill L, Meredith AL, Bing OHL, Brooks WW, Conrad CH, Crow MT & Lakatta EG (1994). Alterations in cardiac gene expression during the transition from stable hypertrophy to heart failure. *Circ Res* **75**, 23–32.

Bradley RL, Jeon YL, Liu F-F & Maratos-Flier E (2008). Voluntary exercise improves insulin sensitivity and adipose tissue inflammation in diet-induced obese mice. *Am J Physiol Endocrinol Metab* **295**, E586–E594.

Chobanian AV, Bakris GL, Black HR, Cushman WC, Green LA, Izzo JL Jr, Jones DW, Materson BJ, Oparil S, Wright TJ Jr & Roccella EJ (2003). The seventh report of the Joint National Committee on Prevention, Detection, Evaluation, and Treatment of High Blood Pressure: the JNC 7 report. *JAMA* **289**, 2560–2572.

Coimbra R, Sanchez LS, Potenza JM, Rossoni LV, Amaral SL & Michelini LC (2008). Is gender crucial for cardiovascular adjustment induced by exercise training in female spontaneously hypertensive rats? *Hypertension* **52**, 514–521.

Diez J, Querejeta R, Lopez B, Gonzalez A, Larman M & Ubago JLM (2002). Losartan-dependent regression of myocardial fibrosis is associated with reduction of left ventricular chamber stiffness in hypertensive patients. *Circulation* **105**, 2512–2517.

Eickelboom R & Mills R (1988). A microanalysis of wheel running in male and female rats. *Physiol Behav* **43**, 625–630.

Fleenor BS, Marshall KD, Durrant JR, Lesniewski LA & Seals DR (2010). Arterial stiffening with ageing is associated with transforming growth factor-β1-related changes in adventitial collagen: reversal by aerobic exercise. *J Physiol* **588**, 3971–3982.

Hagberg JM, Park J-J & Brown MD (2000). The role of exercise training in the treatment of hypertension. *Sports Med* **30**, 193–206.

Hedeyati SS, Elsayed EF & Reilly RF (2011). Non-pharmacological aspects of blood pressure management: what are the data? *Kidney Int* **79**, 1061–1070.

Hildebrand A, Romaris M, Rasmussen LM, Heinegard D, Twardzik DR, Border WA & Ruoslahti E (1994). Interaction of the small interstitial proteoglycans biglycan, decorin and fibromodullin with transforming growth factor beta. *Biochem J* **302**, 527–534.

Jahanyar J, Joyce DL, Southard RE, Loebe M, Noon GP, Koerner MM, Torre-Amione G & Youker KA (2007). Decorin-mediated transforming growth factor-β inhibition ameliorates adverse cardiac remodelling. *J Heart Lung Transplan* **26**, 34–40.

Latif N, Sarathchandra P, Taylor PM, Antoniw J & Yacoub MH (2005). Localization and pattern of expression of extracellular matrix components in human heart valves. *J Heart Valve Dis* **14**, 542–548.

Libonati JR, Sabri A, Xiao C, MacDonnell SM & Renna BF (2011). Exercise training improves systolic function in hypertensive myocardium. *J Appl Physiol* **111**, 1637–1643.

Lijnen PJ, Petrov VV & Fagard FH (2000). Induction of cardiac fibrosis by transforming growth factor-β_1. *Mol Genet Metab* **71**, 418–435.

Livak KJ & Schmittgen TD (2001). Analysis of relative gene expression data using real-time quantitative PCR and the $2[-\Delta\Delta C_T]$. *Methods* **25**, 402–408.

Massagué J (1990). The transforming growth factor-β family. *Annu Rev Cell Biol* **6**, 597–641.

Maxeiner H, Krehbiel N, Müller A, Woitasky N, Akintürk H, Müller M, Weigand MA, Abdallah Y, Kasseckert S, Schreckenberg R, Schlüter K-D & Wenzel S (2010). New insights into paracrine mechanisms of human cardiac progenitor cells. *Eur J Heart Fail* **12**, 730–737.

Mufti S, Wenzel S, Euler G, Piper HM & Schlüter K-D (2008). Angiotensin II-dependent loss of cardiac function: Mechanisms and pharmacological targets attenuating this effect. *J Cell Physiol* **217**, 242–249.

Oliveira RSF, Ferreira JCB, Gomes ERM, Paixao NA, Rolim NPL, Medeiros A, Guatimosim S & Brum PC (2009) Cardiac anti-remodelling effect of aerobic training is associated with a reduction in the calcineurin/NFAT signalling pathway in heart failure mice. *J Physiol* **587**, 3899–3910.

Ruoslahti E (1988). Structure and biology of proteoglycans. *Annu Rev Cell Biol* **4**, 229–255.

Ruoslahti E & Yamaguchi Y (1991). Proteoglycans as modulators of growth factor activities. *Cell* **64**, 867–869.

Schillinger W, Fiolet JW, Schlotthauer K & Hasenfuss G (2003). Relevance of Na^+-Ca^{2+} exchange in heart failure. *Cardiovasc Res* **57**, 921–933.

Schlüter K-D, Schreckenberg R & da Costa Rebelo RM (2010). Interaction between exercise and hypertension in spontaneously hypertensive rats: a meta-analysis of exerpimental studies. *Hypertens Res* **33**, 1155–1161.

Schultz RL, Swallow JG, Waters RP, Kuzman JA, Redetzke RA, Said S, de Escobar GM & Gerdes AM (2007). Effects of excessive long-term exercise on cardiac function and myocyte remodeling in hypertensive heart failure rats. *Hypertension* **50**, 410–416.

Van Deel ED, de Boer M, Kuster DW, Boontje NM, Holemans P, Sipido KR, van der Velden J & Duncker DJ (2011). Exercise training does not improve cardiac function in compensated or decompensated left ventricular hypertrophy induced by aortic stenosis. *J Mol Cell Cardiol* **50**, 1017–1025.

Villarreal FK & Dillmann WH (1992). Cardiac hypertrophy-induced changes in mRNA levels of TGF-β1, fibronectin, and collagen. *Am J Physiol Heart Circ Physiol* **262**, H1861–H1866.

Wenzel S, Taimor G, Piper HM & Schlüter K-D (2001). Redox-sensitive intermediates mediate angiotensin II-induced p38 MAP kinase activation, AP-1 binding activity, and TGF-β expression in adult ventricular cardiomyocytes. *FASEB J* **15**, 2291–2293.

Westhoff TH, Franke N, Schmidt S, Vallbracht-Israng K, Meissner R, Yildirim H, Schlattmann P, Zidek W, Dimeo F & van der Giet M (2007). Too old to benefit from sports? The cardiovascular effects of exercise training in elderly subjects treated for isolated systolic hypertension. *Kidney Blood Press Res* **30**, 240–247.

Williams B, Poulter NR, Brown MJ, Davis M, McInnes GT, Potrter JF, Sever PS & McThom S (2004). Guidelines for management of hypertension: report of the fourth working party of the British Hypertension Society BHS IV. *J Hum Hypertens* **18**, 139–185.

Zimmermann R, Kastens J, Linz W, Wiemer G, Schölkens BA & Schaper J (1999). Effect of long-term ACE inhibition on myocardial tissue in hypertensive stroke-prone rats. *J Mol Cell Cardiol* **31**, 1447–1156.

Author contributions

The authors contributed to the study as follows: analysis and interpretation of data (R.M.); conception and design (R.S.); drafting the article and final approval of the revision to be published (K.D.S.). All experiments were done at the Physiologisches Institut, JLU Gießen, Germany.

Acknowledgements

Grant funding was performed by the Deutsche Forschungsgemeinschaft as a personal grant to KDS (SCHLU324/7-1) and PROMISE.

Hypertension Research (2010) 33, 1155–1161

www.nature.com/hr

ORIGINAL ARTICLE

Interaction between exercise and hypertension in spontaneously hypertensive rats: a meta-analysis of experimental studies

Klaus-Dieter Schlüter, Rolf Schreckenberg and Rui Manuel da Costa Rebelo

The effect of exercise on the progression of hypertension and development of heart failure has been extensively studied in spontaneously hypertensive rats (SHRs), but results published thus far have not revealed a clear picture. Studies differ with respect to the age and sex of rats, duration of exercise and exercise protocols. This study was aimed to examine the influence of age at the start of exercise and the effect of the duration of exercise on blood pressure and hypertrophy, which has not been previously investigated. We identified 18 reports in the literature (with a total of about 410 rats) that investigated the effect of exercise on SHR. A reduction in blood pressure was observed in rats that started exercise protocols in the pre-hypertensive or very early hypertensive state, but not in older rats. Exercise lowered the heart weight-to-body weight ratio in rats starting exercise at a very early age, but not in rats at an advanced age. A reduction in blood pressure was observed in animals that had a short period of training, but the effect was lost when the duration of exercise was prolonged. Exercise reduced resting heart rates in all groups and increased the heart weight-to-body weight ratio in groups that were exposed to free running wheels, but not in rats that performed treadmill exercise. In conclusion, exercise *per se* does not reduce blood pressure in SHR with established hypertension and may increase the incidence of myocardial hypertrophy, depending on the form of exercise.
Hypertension Research (2010) **33,** 1155–1161; doi:10.1038/hr.2010.155; published online 19 August 2010

Keywords: blood pressure; exercise; hypertrophy

INTRODUCTION

Treatment of hypertension is considered a successful intervention to reduce cardiovascular risk. Multiple blood pressure-reducing pharmaceutical approaches are in clinical use. However, recommendations for changes in lifestyle are used as the first and most promising steps leading to a reduction in blood pressure, use of blood pressure-lowering medication, delay of end-organ damage and increased insulin sensitivity. These recommendations include cessation of smoking, reduction in fat and salt intake and increased physical activity.[1–3] Furthermore, endurance training has become very popular over recent years, but due to the high prevalence of unrecognized hypertension in the population engaged in endurance training, it may be associated with cardiac risk. In contrast to blood pressure medication, which is a treatment that has been established after successful animal experiments and extensive basic research, the benefits of physical activity for controlling blood pressure have been less well studied and there are fewer data available. This is regrettable because it is difficult to determine whether any observed benefit in patients is related to physical activity or to other lifestyle changes that are recommended in combination with exercise.[3] Of note, exercise activities add hemodynamic stress to the cardiovascular system and increase the risk of ischemic episodes.[4] Endurance exercise is considered to trigger an adaptive type of myocardial hypertrophy that differs in various aspects from the well-known compensatory hypertrophy caused by chronic hypertension. However, it is largely unknown how the heart reacts to the onset of exercise in the context of established structural and functional adaptations to hypertension.

Spontaneously hypertensive rats (SHRs) are an established and widely used hypertension model, and SHRs have been used to investigate the effect of exercise on the progression of hypertension in numerous studies. Beneficial effects that have been described are a decrease in oxidative stress,[5,6] an increase of cytochrome oxidase activity in cardiac mitochondria,[7] a fall in blood pressure,[8,9] normalization of calcium-handling proteins,[10,11] delayed hypertrophy-associated fetal gene shifts,[12] improvement of endothelium-dependent vasorelaxation,[13,14] induction of antiapoptotic genes[15,16] and improved β-adrenoceptor coupling.[17] In contrast, a normalization of calcium-handling proteins was not observed by others,[7] nor was a fall in blood pressure,[18] a change in the function of cardiomyocytes,[19] or a change in heart function.[20] Moreover, exercise resulted in greater fibrosis and adverse remodeling in another study.[21] Therefore, although numerous studies have been performed on SHR, these studies involved small numbers of animals, different exercise protocols, different durations of exercise and rats of different ages and

Physiologisches Institut, Justus-Liebig-Universität, Giessen, Germany
Correspondence: Dr K-D Schlüter, Physiologisches Institut, Justus-Liebig-Universität Giessen, Aulweg 149, Giessen 35392, Germany.
E-mail: Klaus-Dieter.Schlueter@physiologie.med.uni-giessen.de
Received 8 January 2010; revised 7 June 2010; accepted 11 June 2010; published online 19 August 2010

groups of varying sex distribution. Therefore, key questions, such as the influence of age at the start of exercise and effects of the duration of exercise, have not been answered.

In order to address these questions, we performed a meta-analysis of animal studies dealing with the effect of exercise on hypertension. Using this approach, we were able to report on study results based on more than 400 rats. In this study, we describe the role of the animal's age at the start of exercise and the effect of the duration of exercise on blood pressure and hypertrophy in SHR. As pointed out above, these questions have not been addressed in individual studies.

METHODS

Literature

Studies were identified from the Medline database by a search with the keywords 'SHR' and 'exercise'. Studies were used for this analysis if they included a training group and a non-training group, which was usually denoted as sedentary (although this term might not be appropriate for animals that do not 'sit'). Studies selected for this analysis were only considered if they reported data about systolic blood pressure, heart rate and/or heart weight-to-body weight ratio. Furthermore, studies had to be published in English. The literature selected was published between 2002 and 2008.

Analysis

For further analysis of all studies, rats were grouped according to the age of the animals at the beginning of the experiments, at the start of the exercise program or according to the duration of the exercise protocol. Further details are given in the Results section.

Statistics

All data are expressed as means ± s.e. Comparisons between groups were performed by a *t*-test.

RESULTS

Study identification and description

A total of 17 studies published between 2002 and 2008 that fulfilled the criteria defined above were found (Table 1). In these studies, the age of rats at the beginning of the exercise treatment varied from 4 weeks (pre-hypertensive state) up to 16 weeks (established hypertension). Group sizes differed from $n=5$ to $n=30$ animals per study. Seven studies used female rats and 10 studies used male rats. In 16 studies, blood pressure was measured by a tail-cuff approach. Three studies compared blood pressure measurement by the tail-cuff method with direct measurement in anesthetized rats. In two of them, blood pressure was significantly higher when measured by the tail-cuff method (182 *vs.* 126 mm Hg and 189 *vs.* 126 mm Hg),[18,20] and no significant differences were found in the third study (179 *vs.* 188 mm Hg).[16] For that reason, only studies in which blood pressure was recorded by the tail-cuff method were included in the analysis of blood pressure. In 14 studies, a treadmill protocol was used. According to this protocol, rats were trained 5 days per week on average, at a mean rate of 19 m/min, accounting for a total running distance of 5.5 km per week. Two studies used a free running wheel model, in which the rats ran 41.1 km per week on average. Finally, one study used a swimming protocol (Table 1).

Table 1 Studies included in the meta-analysis and study details

Ref	*Age (months)*	*Sex*	n	*Training*
13	3	m	12	1.5 months, treadmill
14	1	m	30	2.5 months, free running
15	1.5	m	15	3 months, treadmill
16	1	m	6–8	2 months, treadmill
17	4	f	12	3 months, treadmill, low intensity
18	2–3	f	11	13 weeks, treadmill, low intensity
20	4	f	7–8	6 months, treadmill, low intensity
22	1	m	20–21	2.5 months, free running
23	1.5	m	6	2 months, swimming
24	1.5	m	5	5 months, treadmill
25	2	m	8	3 months, treadmill, low intensity
26	2	m	9	3 months, treadmill
27	2	f	12	3 months, treadmill
28	3	m	12	2.5 months, treadmill
29	4	f	9–10	4 months, treadmill low intensity
30	4	f	11–12	6 months, treadmill, low intensity
31	4	f	7–8	3 months, treadmill, low intensity
12[a]	9/15	m	9–10	6 months, treadmill
21[a]	6	f	11–12	16 months, free running

Abbreviations: f, females; m, males; n, number of animals per group; SHHF, spontaneously hypertensive heart failure.
[a]SHHF (only used for hypertrophy data).

Effect of exercise on blood pressure

Of the studies examined, 16 reported about the effect of exercise on systolic blood pressure. Animals used in these studies were between 1 and 4 months old. Rats in these studies were grouped according to their age at the beginning of exercise as follows: 1 month (3 studies),[14,16,22] 1.5 months (3 studies),[15,23,24] 2–2.5 months (4 studies)[18,25–27] and 3–4 months (6 studies).[17,20,28–31] The number of rats included in these groups is depicted in Figure 1a. Exercise duration varied in these groups. There was a trend toward higher exercise duration in studies using older rats (Figure 1a). On average, rats starting with exercise at the age of 4 months were exposed to longer exercise protocols than those beginning at 1 month (Figure 1a). Values for mean systolic blood pressure among rats were 133.1, 142.5, 172.0 and 167.7 mm Hg at the ages of 1.0, 1.5, 2.3 and 4.0 months, respectively. A blood pressure-lowering effect was observed in studies using rats at the pre-hypertensive or early hypertensive stage, independent of exercise duration and intensity (Figure 1b). On average, systolic blood pressure was 13.6 ± 1.0 and 17.2 ± 0.9 mm Hg lower than that of sedentary controls in animals starting exercise at the ages of 1.0 and 1.5 months, respectively. Similarly, when the age of rats at the end of the exercise protocol was considered, younger rats had lower blood pressure compared with their sedentary counterparts (Figure 1c). These data suggest that a blood pressure-lowering effect can be expected only in young and pre-hypertensive rats but not in older rats with established hypertension. Indeed, when the duration of exercise was analyzed separately for young (mean age 1.3 months) and older (mean age 4.0 months) rats, a blood pressure-lowering effect was seen only in young rats (Figure 2). Eleven studies provided additional information about blood pressure before the start of exercise. Of note, in none of these studies did exercise reduce blood pressure. The mean blood pressure at the start of the exercise was 162.6 ± 8.3 mm Hg; at the end it was 182.4 ± 8.0 mm Hg.

Effect of exercise on heart rate

Seven studies reported on the effect of exercise on heart rate.[15,18,20,25,29,30,32] Again, in all these studies, rats started with exercise at the age of 1–4 months, and those that were older at the beginning had a longer exercise period. Studies were grouped as before on the basis of the different ages of the animals at the beginning of the study. Group statistics are given in Figure 3a. In all studies, resting heart rate was lower in rats performing exercise, irrespective of the age of the rat at the beginning or end of the exercise periods (Figure 3b

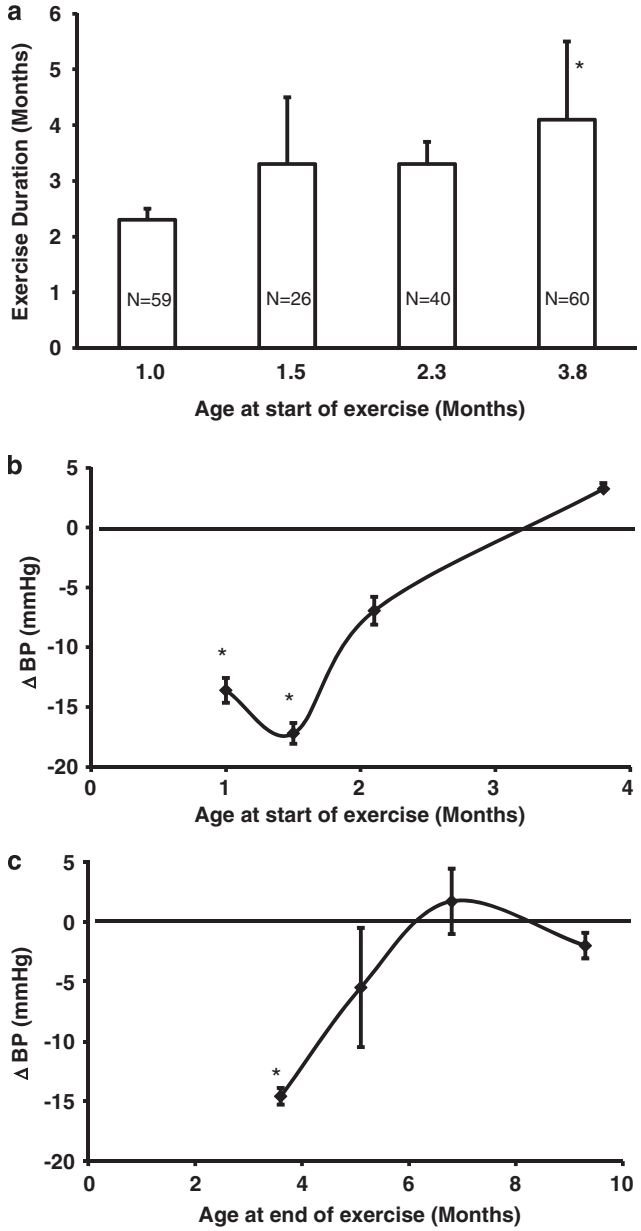

Figure 1 Effect of the age of animals on exercise-dependent changes in blood pressure. Animals were grouped according to their age at the beginning of the exercise training. (**a**) Bars represent the number of rats per group and indicate the mean exercise duration for each group. (**b**) Difference in blood pressure between rats performing exercise and their sedentary controls for the four groups defined above. (**c**) Difference in blood pressure between rats performing exercise and their sedentary controls for groups defined by similar age at the end of exercise. Data are means ± s.e.; $^*P<0.05$ *vs.* sedentary controls.

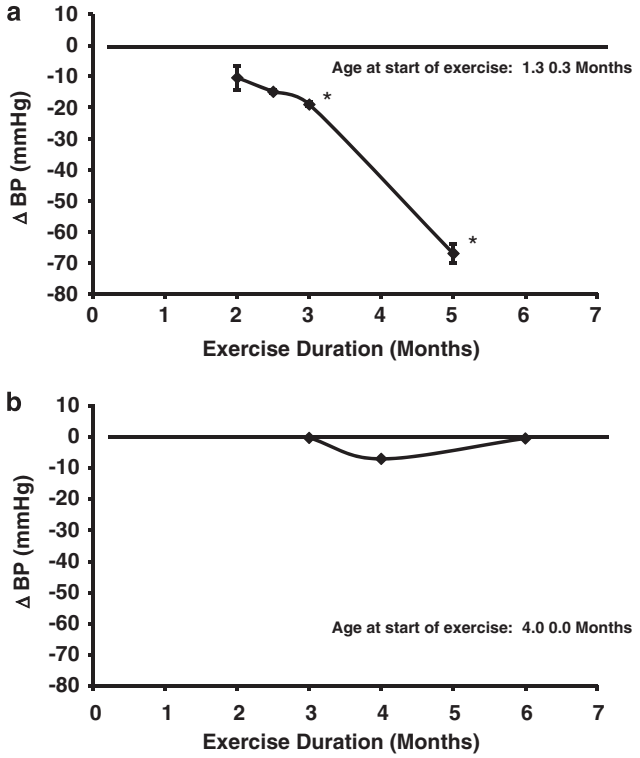

Figure 2 Effect of the age of spontaneously hypertensive rats (SHR) on changes in blood pressure during prolonged exercise. (**a**) Data are given for studies using rats at the age of 1.0–1.5 months. (**b**) Data are given for studies using rats at the age of 4 months. Data are means ± s.e.; $^*P<0.05$ *vs.* sedentary controls.

and c). There was a trend toward minor effects on heart rate if the animals were older, but whether this is a real physiological effect could not be discerned from these data.

Effect of exercise on heart weight-to-body weight ratio

Nine studies described the effect of moderate treadmill exercise or swimming on heart weight-to-body weight ratios. Two studies used young rats (1.5 months),[15,23] five studies used rats at an age between 3 and 4 months (mean of 3.8 months),[13,20,29–31] and two groups used rats at an age between 9 and 15 months (12 months).[12] The latter study was performed on spontaneously hypertensive heart failure rats. We included these data because no data on SHR are available. Unlike SHR, all spontaneously hypertensive heart failures develop heart failure that can be characterized as decompensated dilated heart failure. Although they differ from SHR in their genetic background, we decided to include this group because no major differences in blood pressure or heart weight-to-body weight ratio were seen in the sedentary group compared with SHR. Group statistics are given in Figure 4a. Again, older rats were exposed to exercise periods that were longer in duration. Lower heart weight-to-body weight ratios were only reported in studies with young rats (Figure 4b and c). In older animals, there is a clear trend toward higher values. When the changes in heart weight-to-body weight ratio are plotted against the duration of exercise, it becomes evident that the antihypertrophic effect of exercise in these hypertensive rats may be a transient phenomenon (Figure 5).

Effect of the type of exercise on blood pressure and heart weight-to-body weight ratio

The data reported above were based on treadmills (with the exception of one group that performed a swimming protocol). There were significant differences in training intensity between rats performing treadmill exercise and those exposed to a free running protocol. Rats performing treadmill exercise had a weekly running distance of 5–8 km per week, but those with free access to running wheels ran between 35 and 47 km per week. This leads to the question of whether there are significant differences between these types of exercise. Studies

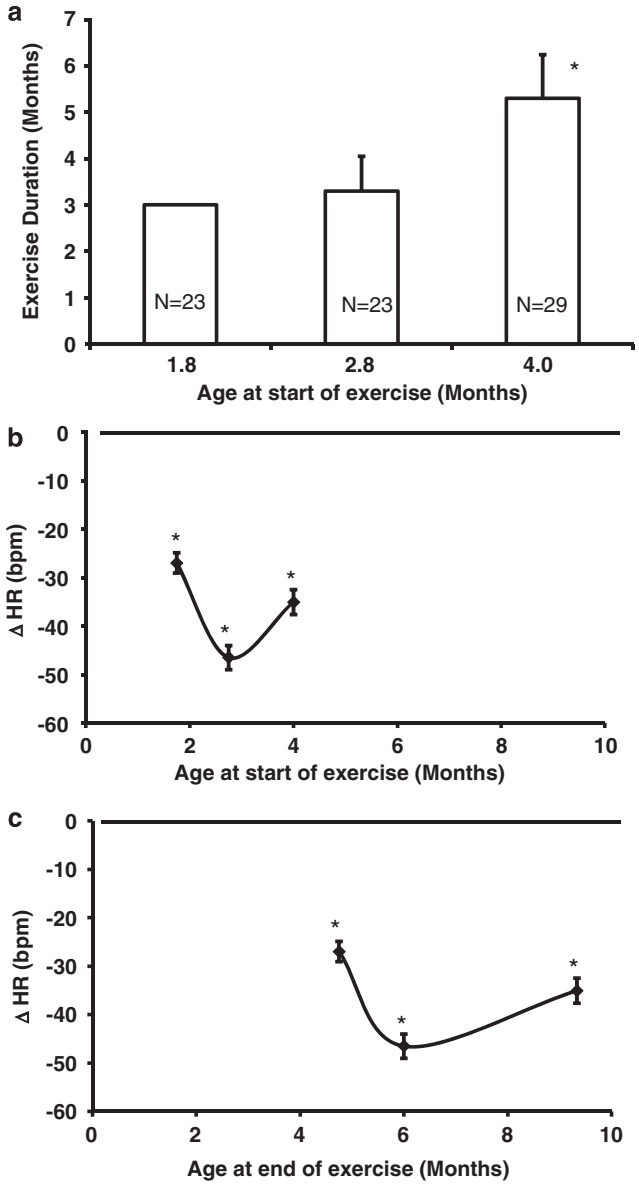

Figure 3 Effect of the age of animals on exercise-dependent changes in heart rates. Animals were grouped according to their age at the beginning of the exercise training. (**a**) Bars represent the number of rats per group and indicate the mean exercise duration of these groups. (**b**) Difference in heart rates between rats performing exercise and their sedentary controls for the three groups defined above. (**c**) Differences in heart rate between rats performing exercise and their sedentary controls for groups defined by similar age at the end of exercise. Data are means ± s.e.; $^*P<0.05$ *vs.* sedentary controls.

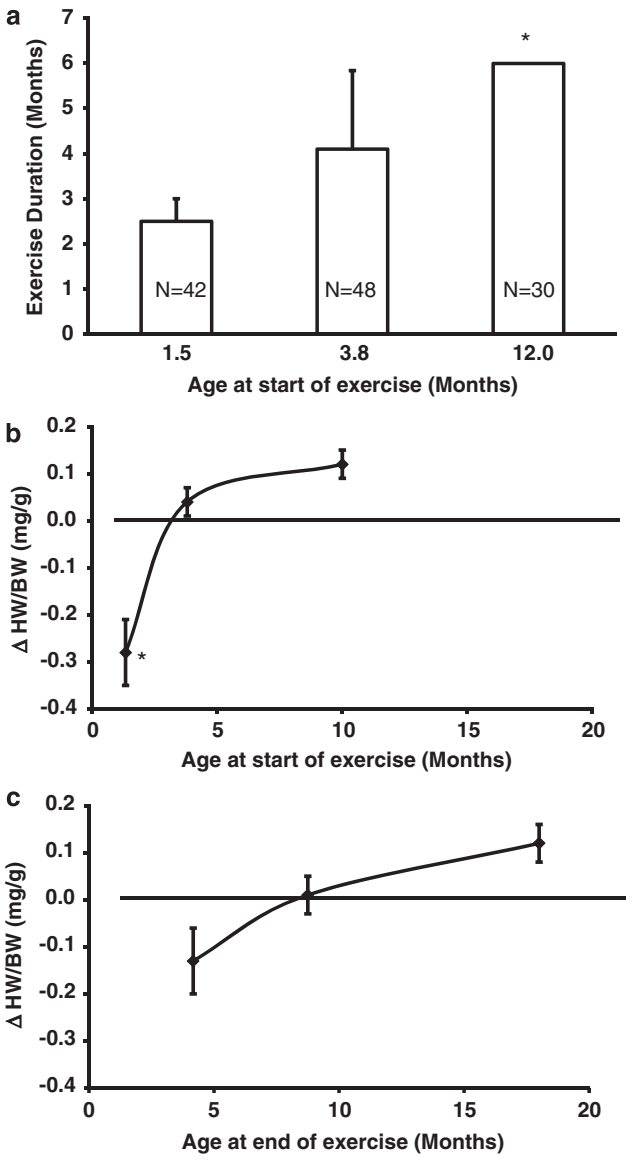

Figure 4 Effect of the age of animals on exercise-dependent changes in heart weight-to-body weight ratio (HW/BW). (**a**) Bars represent number of rats per group and indicate the mean exercise duration of these groups. (**b**) Difference in HW/BW between rats performing exercise and their sedentary controls for the three groups defined above. (**c**) Difference in HW/BW between rats performing exercise and their sedentary controls for groups defined by similar age at the end of exercise. Data are given as the difference between non-trained (sedentary) and trained SHR in mg g^{-1}. Data are means ± s.e.; $^*P<0.05$ *vs.* sedentary controls.

using young SHR at the age of 1.0–1.5 months and an exercise duration of 2–3 months were used to compare the effect of treadmill *vs.* free running wheel exercise protocols.[14–16,22] Systolic blood pressures were quite similar in these studies. Furthermore, a similar difference in blood pressure was observed in both groups, as expected for these young rats (Figure 6a). The effect of exercise on heart weight-to-body weight ratio was determined in two of these studies.[15,22] Although authors report a 15% increase in heart weight-to-body weight ratio in the free running group in the presence of a 6% decrease in blood pressure, they report about a 9% reduction in heart weight-to-body weight ratio in the treadmill group in the presence of a 5% decrease in blood pressure (Figure 6b). The data indicate that the form of training differentially modulates hypertrophy, irrespective of blood pressure.

Sex-specific difference in studies on effects of exercise

The data analysis presented above did not distinguish between male and female SHR. When considering the sex-specific differences, it is obvious that female rats were preferentially used in studies with older rats. As a consequence, female rats had longer exercise duration and weaker effects on blood pressure (Table 2). Therefore, sex-specific

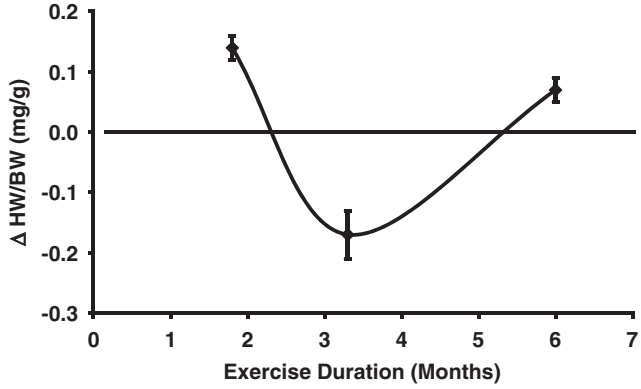

Figure 5 Effect of the duration of exercise on changes in heart weight-to-body weight ratio (HW/BW). Data are given as the difference between non-trained (sedentary) and trained SHR in mg g^{-1}. Data are means ± s.e.

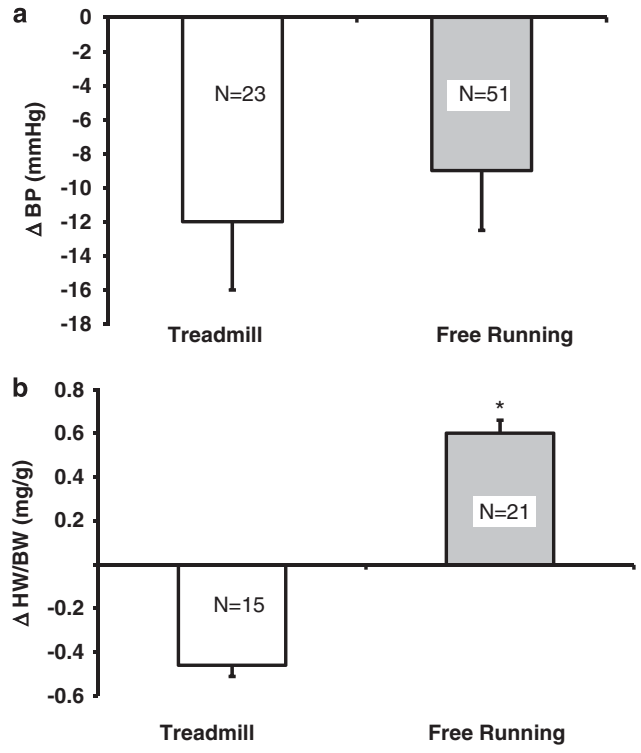

Figure 6 Effect of the type of exercise on blood pressure and heart weight-to-body weight ratio (HW/BW). Data are given for studies using rats at the age of 1.0–1.5 months, subjected to exercise protocols for 2–3 months. (**a**) Changes in blood pressure. (**b**) Changes in HW/BW. Data are given as the difference from sedentary controls. Data are means ± s.e.; *$P<0.05$ *vs.* treadmill.

differences can only be analyzed when comparing studies that use rats at the same age and with similar training intensity. Three studies used 2-month-old SHR with a 3-month treadmill protocol, but either male or female rats in order to compare the effects of sex.[25–27] Under these conditions, the difference in systolic blood pressure at the end of the exercise protocol was −7 mm Hg in the female group (n=12) and −14 mm Hg in the male group (n=14). This suggests that the observed effects of age and exercise duration on blood pressure are at least in part independent of sex. When considering the influence of sex on heart rate reductions, no significant differences were observed between female and male rats (Table 3). No comparison can be performed with regard to the effect of sex on heart weight-to-body weight ratio, because such studies are not available.

Table 2 Influence of sex on exercise-induced changes in BP

	Male	*Female*
N (sed/ex)	111/114	71/71
Age (months)	1.6 ± 0.6	3.5 ± 0.8, $P<0.05$
Exercise duration (months)	2.8 ± 0.8	4.1 ± 1.2, NS
BP (syst) sed (mm Hg)	207.6 ± 26.2	182.6 ± 5.6, $P<0.05$
BP (syst) ex (mm Hg)	194.0 ± 33.9	181.7 ± 7.4, NS
Δ BP (syst) (mm Hg)	−13.6	−0.9

Abbreviations: BP, blood pressure; ex, exercise-performing rats; NS, not significantly different; sed, sedentary rats; syst, systolic BP.

Table 3 Influence of sex on exercise-induced changes in blood pressure and heart rate when age-matched rats were considered

	Male	*Female*
N (sed/ex)	35/35	40/39
Age (months)	2.2 ± 0.6	3.6 ± 0.6, NS
Exercise duration (months)	2.8 ± 0.2	5.0 ± 1.0, $P<0.05$
HR sed (b.p.m.)	389 ± 31	481 ± 35, $P<0.05$
HR ex (b.p.m.)	350 ± 16	448 ± 38, $P<0.05$
Δ HR (b.p.m.)	−39	−33

Abbreviations: ex, exercise-performing rats; HR, heart rate; NS, not significant; sed, sedentary rats.

DISCUSSION

In this study, we investigated the effect of age and duration of exercise on blood pressure, heart rate and heart weight-to-body weight ratio in a large population of rats by performing a meta-analysis of 18 studies using the same genetic model of hypertension (SHR). It is noteworthy that the studies used different inbred strains, different sexes and different exercise protocols. So that the use of different methods to quantify the blood pressure did not present a confounding variable, this study is based exclusively on investigations using the tail-cuff method. Independent of these limitations, the published data allowed us to perform such an analysis on the basis of a large number of animals and to investigate the effects of age and duration of exercise, which were not addressed in any previous study. The main result of this study is that neither prolonged exercise nor exercise in rats with established hypertension reduces blood pressure or induces a favorable antihypertrophic effect. Moreover, depending on the type of exercise, the incidence of myocardial hypertrophy may be increased in rats with established hypertension. In contrast, exercise seems to reduce resting heart rate, irrespective of all other variables.

Exercise and physical activity are currently recommended for patients with high-normal blood pressure and hypertension without additional major risk factors.[2–4] These are recommendations that include other lifestyle modifications, such as cessation of smoking and lowering fat and salt intake. It is therefore difficult to determine whether there is a specific effect of exercise on blood pressure. A recent meta-analysis of randomized controlled trials reported a small but significant effect on blood pressure reduction at low or moderate intensity with no further effect at higher intensities, based on 29 studies with 1533 hypertensive and normotensive participants.[33]

There was nevertheless great heterogeneity among the different trials, and no information was given with regard to the age and weight of participants. Moreover, studies in patients normally lack adequate control groups.[34] It is therefore difficult to predict from clinical trials the advantage or risk of exercise in hypertensive individuals. To address this question, experimental studies that are based on a large number of animals and possess high reproducibility in different laboratories are required. Both requirements can be met with a meta-analysis, as we have performed here. Following this approach, blood pressure-lowering effects caused by physical activity cannot be predicted in individuals with established hypertension. On the other hand, exercise may prevent the onset of hypertension in subjects with a genetic predisposition to hypertension. Of note, blood pressure-lowering effects were obtained in pre-hypertensive SHR or in early hypertension.

Our conclusion is based on the collection of data published by different laboratories with similar but not identical methods. It should be noted that some limitations are still evident. As sex-specific differences cannot be ruled out completely, it should be kept in mind that nearly all studies using young SHR used males, whereas studies using SHR at an advanced age preferentially used females. This is due to the higher level of spontaneous running activity in female rats.[32] A sex-dependent effect has been suggested before.[18] However, no obvious difference was noted between males and females in the individual groups in terms of blood pressure reduction when compared on the basis of the same age and the same duration of exercise. In addition, the blood pressure difference between training and sedentary groups at the end of the study was +1 mm Hg in 16-month-old females and +4 mm Hg in 15-month-old males.[7,12] Therefore, we do not expect that sex-dependent differences are more important than the age at the start of the exercise protocol, although the latter data are given only for spontaneously hypertensive heart failures.

Furthermore, it is not clear whether treadmill protocols are more appropriate than free access to running wheels when blood pressure is used as a parameter. On one hand, rats on treadmill protocols often adjusted to their individual exercise capacity and trained thereafter at approximately 50% of maximal capacity. This resulted in significantly smaller running distances per week compared with rats with free access to running wheels. Furthermore, rats on treadmills had periodic running-free days. On the other hand, rats on treadmills performed one running bout for 45–75 min a day, whereas rats with free access to running wheels averaged 167 running bouts for 43 s each.[35] Therefore, the treadmill approach does not constitute a physiological type of running behavior. The same trends observed overall for the entire group of rats were observed when comparing rats that ran on running wheels to those that ran on treadmills. For example, 1-month-old rats on treadmills exhibited a 17 mm Hg reduction in blood pressure, but rats aged 6 months exhibited a reduction of only 7 mm Hg.[21,14] The only remarkable observation is that older rats on treadmills did not tolerate this well, although they are reported to achieve longer running distances on running wheels. The lower treadmill tolerance obviously indicates a limitation in age-dependent stress tolerance rather than exercise capacity.

Despite the lack of effect on resting blood pressure in these animals, there was also a clear trend toward a further increase in myocardial hypertrophy that exceeded that of non-trained SHR. Again, a favorable effect cannot be predicted from these findings based on exercise alone. In general, exercise has been reported to reverse adverse hypertrophy.[11,36,37] However, a clear molecular characterization of this type of hypertrophy or exercise-reversed hypertrophy in the absence of hypertension has not yet been performed. This topic requires specific attention, as hypertrophic cardiomyopathy is the major cardiovascular cause of sudden cardiac death in young competitive athletes.[38] Furthermore, the data published suggest that the type of exercise (running wheels *vs.* treadmills) affects the incidence of myocardial hypertrophy.

It is noteworthy that only a few studies that have been published on this topic combine exercise with the administration of a standard blood pressure-lowering medication, such as an angiotensin converting enzyme inhibitor. Angiotensin converting enzyme inhibitors have been shown to lower blood pressure, limit end-organ damage and increase survival in this model.[28] Indeed, the interaction between angiotensin converting enzyme inhibition and exercise requires more attention as it mimics the situation normally occurring in hypertensive patients, specifically in patients that display blood pressures as high as those seen in SHR at an advanced stage.

Finally, the data not only indicate that there is no beneficial effect of exercise on established high blood pressure, but also identify a potential risk of endurance exercise on the background of hypertension without efforts to control blood pressure. This might have specific implications for non-professional runners who commonly participate in city marathons.

CONFLICT OF INTEREST

The authors declare no conflict of interest.

1 Kokkinos PF, Papademetriou V. Exercise and hypertension. *Cornary Artery Dis* 2000; **11**: 99–102.
2 Joint National Committee on the prevention detection evaluation treatment of high blood pressure. Sixth report of the Joint National Committee. National Institute of Health: Washington, DC, 1997.
3 Hagberg JM, Park J-J, Brown MD. The role of exercise training in the treatment of hypertension. *Sports Med* 2000; **30**: 193–206.
4 Thompson PD, Franklin BA, Balady GJ, Blair SN, Corrado D, Estes NAM, Fulton JE, Gordon NF, Haskell WL, Link MS, Maron BJ, Mittleman MA, Pelliccia A, Wenger NK, Willich SN, Costa F. Exercise and acute cardiovascular events. *Circ* 2007; **115**: 2358–2368.
5 Bertagnolli M, Campos C, Schenkel PC, de Oliveira VLL, de Angelis K, Belló-Klein A, Rigatto K, Irigoyen C. Baroreflex sensitivity improvement is associated with decreased oxidative stress in trained spontaneously hypertensive rats. *J Hypertension* 2006; **24**: 2437–2443.
6 Hägg U, Gröndos J, Wikström J, Jonsdottir IH, Bergström G, Gan L-M. Voluntary physical exercise and coronary flow velocity reserve: a transthoracic colour Doppler echocardiography study in spontaneously hypertensive rats. *Clin Sci* 2005; **109**: 325–334.
7 Chicco AJ, McCune SA, Emter CA, Sparagna GC, Rees ML, Bolden DA, Marshall KD, Murphy RC, Moore RL. Low-intensity exercise training delays heart failure and improves survival in female hypertensive heart failure rats. *Hypertension* 2008; **51**: 1096–1102.
8 Felix JVC, Michelini LC. Training-induced pressure fall in spontaneously hypertensive rats is associated with reduced angiotensinogen mRNA expression within the nucleus tractus solitarii. *Hypertension* 2007; **50**: 780–785.
9 Amaral SL, Zorn TMT, Michelini LC. Exercise training normalizes wall-to-lumen ratio of the gracilis muscle and reduces pressure in spontaneously hypertensive rats. *J Hypertension* 2000; **18**: 1563–1572.
10 Collins HL, Loka AM, DiCarlo SE. Daily exercise-induced cardioprotection is associated with changes in calcium regulatory proteins in hypertensive rats. *Am J Physiol* 2005; **288**: H532–H540.
11 Garciarena CD, Pinilla OA, Nolly MB, Laguens RP, Escudero EM, Cingolani HE, Ennis IL. Endurance training in the spontaneously hypertensive rat. *Hypertension* 2009; **53**: 708–714.
12 Emter CA, McCune SA, Sparagna GC, Radin J, Moore RL. Low-intensity exercise training delays onset of decompensated heart failure in spontaneously hypertensive rats. *Am J Physiol* 2005; **289**: H2030–H2038.
13 Graham DA, Rush JWE. Exercise training improves aortic endothelium-dependent vasorelaxation and determinants of nitric oxide bioavailability in spontaneously hypertensive rats. *J Appl Physiol* 2004; **96**: 2088–2096.
14 Kohno H, Furukawa S, Naito H, Minamitani K, Ohmori D, Yamakura F. Contribution of nitric oxide, angiotensin II and superoxide dismutase to exercise-induced attenuation of blood pressure elevation in spontaneously hypertensive rats. *Jpn Heart J* 2002; **43**: 25–34.

15 Lee YI, Cho JY, Kim MH, Kim KB, Lee DJ, Lee KS. Effects of exercise on pathological cardiac hypertrophy related gene expression and apoptosis. *Eur J Appl Physiol* 2006; **97**: 216–224.
16 Lajoie C, Calderone A, Béliveau L. Exercise training enhanced the expression of myocardial proteins related to cell protection in spontaneously hypertensive rats. *Pflugers Arch – Eur J Physiol* 2004; **449**: 26–32.
17 MacDonnell SM, Kubo H, Crabbe DL, Renna BF, Reger PO, Mohara J, Smithwick LA, Koch WJ, Houser SR, Libonati JR. Improved myocardial β-adrenergic responsiveness and signalling with exercise training in hypertension. *Circulation* 2005; **111**: 3420–3428.
18 Coimbra R, Sanchez LS, Potenza JM, Rossoni LV, Amaral SM, Michelini LC. Is gender crucial for cardiovascular adjustments induced by exercise training in female spontaneously hypertensive rats? *Hypertension* 2008; **52**: 514–521.
19 Natali AJ, Turner DL, Harrison SM, White E. Regional effects of voluntary exercise on cell size and contraction-frequency responses in rat cardiac myocytes. *J ExptI Biol* 2001; **204**: 1191–1199.
20 Renna BF, MacDonnell SM, Reger PO, Crabbe DL, Houser SR, Libonati JR. Relative systolic dysfunction in female spontaneously hypertensive rat myocardium. *J Appl Physiol* 2007; **103**: 353–358.
21 Schultz RL, Swallow JG, Waters RP, Kuzman JA, Redetzke RA, Said S, de Escobar GM, Gerdes AM. Effects of excessive long-term exercise on cardiac function and myocyte remodeling in hypertensive heart failure rats. *Hypertension* 2007; **50**: 410–416.
22 Beatty JA, Kramer JM, Plowey ED, Waldrop TG. Physical exercise decreases neuronal activity in the posterior hypothalamic area of spontaneously hypertensive rats. *J ApII Physiol* 2005; **98**: 572–578.
23 Zhang J, Ren CX, Qi YF, Lou LX, Chen L, Zhang LK, Wang X, Tang C. Exercise training promotes expression of apelin and APJ of cardiovascular tissues in spontaneously hypertensive rats. *Life Sci* 2006; **79**: 1153–1159.
24 Horta PP, de Carvalho JJ, Mandarim-de-Lacerda CA. Exercise training attenuates blood pressure elevation and adverse remodelling in the aorta of spontaneously hypertensive rats. *Life Sci* 2005; **77**: 3336–3343.
25 Melo RM, Martinho Jr E, Michelini LC. Training-induced, pressure-lowering effect in SHR. *Hypertension* 2003; **42**: 851–857.
26 Martins AS, Crescenzi A, Stern JE, Bordin S, Michelini LC. Hypertension and exercise training differentially affect oxytocin and oxytocin receptor expression in the brain. *Hypertension* 2005; **46**: 1004–1009.
27 Amaral SL, Sanchez LS, Chang AJBA, Rossoni LV, Michelini LC. Time course of training-induced microcirculatory changes and of VEGF expression in skeletal muscles of spontaneously hypertensive female rats. *Braz J Med Biol Res* 2008; **41**: 424–431.
28 Zioada AM, Hassan MO, Tahlikar KI, Inuwa IM. Long-term exercise training and angiotensin-converting enzyme inhibition differentially enhance myocardial capillarization in the spontaneously hypertensive rat. *J Hypertension* 2005; **23**: 1233–1240.
29 Reger PO, Barbe MF, Amin M, Renna BF, Hewston LA, MacDonnell SM, Houser SR, Libonati JR. Myocardial hypoperfusion/reperfusion tolerance with exercise training in hypertension. *J Appl Physiol* 2006; **100**: 541–547.
30 Renna BF, Kubo H, MacDonnell SM, Crabbe DL, Reger PO, Houser SR, Libonati JR. Enhanced acidotic myocardial Ca2+ responsiveness with training in hypertension. *Med Sci Sports Exerc* 2006; **38**: 847–855.
31 Kolwicz SC, Kubo H, MacDonnell SM, Houser SR, Libonati JR. Effects of forskolin on inotropic performance and phospholamban phosphorylation in exercise-trained hypertensive maocardium. *J Appl Physiol* 2007; **102**: 628–633.
32 Eikelboom R, Mills R. A microanalysis of wheel running in male and female rats. *Physiol Behav* 1988; **43**: 625–630.
33 Halbert JA, Silagy CA, Finucane P, Withers RT, Hamdorf PA, Andrews GR. The effectiveness of exercise training in lowering blood pressure: a meta-analysis of randomised controlled trials of 4 weeks or longer. *J Hum Hypertenison* 1997; **11**: 641–649.
34 Petrella RJ. How effective is exercise training for the treatment of hypertension? *Clin J Sport Med* 1998; **8**: 224–231.
35 Ridnock KJ, Reaven GM, Haskell WL, Sims CR, Mondon CE. Variations in running activity and enzymatic adaptations in voluntary running rats. *J ApII Physiol* 1989; **66**: 1250–1257.
36 Konhilas JP, Watson PA, Maass A, Boucek DA, Horn T, Stauffer BL, Luckey SW, Rosenberg P, Leinwand LA. Exercise can prevent and reverse the severity of hypertrophic cardiomyopathy. *Circ Res* 2006; **98**: 540–548.
37 Miyachi M, Yazawa H, Furukawa M, Tsuboi K, Ohtake M, Nishizawa T, Hashimoto K, Yokoi T, Kojima T, Murate T, Yokota M, Murohara T, Koike Y, Nagata K. Exercise training alters left ventricular geometry and attenuates heart failure in Dahl Salt-Sensitive hypertensive rats. *Hypertension* 2009; **53**: 701–707.
38 Maron BJ, Thompson PD, Ackerman MJ, Balady G, Berger S, Cohen D, Dimeff R, Douglas PS, Glover DW, Hutter AM, Krauss MD, Maron MS, Mitten MJ, Roberts WO, Puffer JC. Recommendations and considerations related to preparticipation screening for cardiovascular abnormalities in competitive athletes: 2007 update. *Circ* 2007; **115**: 1643–1655.

ORIGINAL RESEARCH

Adverse Effects on β-Adrenergic Receptor Coupling: Ischemic Postconditioning Failed to Preserve Long-Term Cardiac Function

Rolf Schreckenberg, MD, PhD;* Péter Bencsik, MD, PhD;* Martin Weber, MD; Yaser Abdallah, MD, PhD; Csaba Csonka, MD, PhD; Kamilla Gömöri, MSc; Krisztina Kiss, MD; János Pálóczi, MSc, PhD; Judit Pipis, MSc; Márta Sárközy, MD, PhD; Péter Ferdinandy, MD, PhD, DSc, MBA; Rainer Schulz, MD, PhD; Klaus-Dieter Schlüter, PhD

***Background*—**Ischemic preconditioning (IPC) and ischemic postconditioning (IPoC) are currently among the most efficient strategies protecting the heart against ischemia/reperfusion injury. However, the effect of IPC and IPoC on functional recovery following ischemia/reperfusion is less clear, particularly with regard to the specific receptor-mediated signaling of the postischemic heart. The current article examines the effect of IPC or IPoC on the regulation and coupling of β-adrenergic receptors and their effects on postischemic left ventricular function.

***Methods and Results*—**The β-adrenergic signal transduction was analyzed in 3-month-old Wistar rats for each of the intervention strategies (Sham, ischemia/reperfusion, IPC, IPoC) immediately and 7 days after myocardial infarction. Directly after the infarction a cardioprotective potential was demonstrated for both IPC and IPoC: the infarct size was reduced, apoptosis and production of reactive oxygen species were lowered, and the myocardial tissue was preserved. Seven days after myocardial ischemia, only IPC hearts showed significant functional improvement. Along with a deterioration in fractional shortening, IPoC hearts no longer responded adequately to β-adrenergic stimulation. The stabilization of β-adrenergic receptor kinase-2 via increased phosphorylation of Mdm2 (an E3-ubiquitin ligase) was responsible for desensitization of β-adrenergic receptors and identified as a characteristic specific to IPoC hearts.

***Conclusions*—**Immediately after myocardial infarction, rapid and transient activation of β-adrenergic receptor kinase-2 may be an appropriate means to protect the injured heart from excessive stress. In the long term, however, induction and stabilization of β-adrenergic receptor kinase-2, with the resultant loss of positive inotropic function, leads to the functional picture of heart failure. **(*J Am Heart Assoc*. 2017;6:e006809. DOI: 10.1161/JAHA.117.006809.)**

Key Words: cardiac remodeling • ischemic postconditioning • ischemic preconditioning • myocardial infarction • β-adrenergic receptor • β-adrenergic receptor kinase-2

The long-term prognosis of an acute myocardial infarction is determined both by the extent of the resultant irreversible tissue damage and by the reconstruction processes that are immediately triggered, which are referred to as cardiac remodeling. Short series of repetitive ischemia/reperfusion cycles (IR), which are described as ischemic preconditioning (IPC) and ischemic postconditioning (IPoC), are currently among the most efficient strategies for myocardial protection.[1,2] Both interventions share some signaling pathways, although they are applied at opposing time points of the ischemic period.[3] To what extent this protective intervention also leads to a better prognosis over the long term depends fundamentally on its effect on the remodeling of the postischemic myocardium.

From the Physiologisches Institut, Justus-Liebig-Universität Gießen, Gießen, Germany (R. Schreckenberg, M.W., Y.A., R. Schulz, K.-D.S.); Pharmahungary Group, Szeged, Hungary (P.B., K.K., J. Pálóczi, J. Pipis, P.F.); Cardiovascular Research Group, Department of Biochemistry, University of Szeged, Hungary (P.B., C.C., K.G., K.K., J. Pálóczi, M.S.); Department of Pharmacology and Pharmacotherapy, Semmelweis University, Budapest, Hungary (P.F.).

Accompanying Table S1 and Figures S1 through S6 are available at http://jaha.ahajournals.org/content/6/12/e006809/DC1/embed/inline-supplementary-material-1.pdf

*Dr Schreckenberg and Dr Bencsik contributed equally to this work.

Correspondence to: Rolf Schreckenberg, MD, PhD, Physiologisches Institut, Aulweg 129, D-35392 Gießen, Germany. E-mail: rolf.schreckenberg@physiologie.med.uni-giessen.de

Received June 1, 2017; accepted November 2, 2017.

Clinical Perspective

What Is New?

- Ischemic preconditioning and ischemic postconditioning are very efficient clinically applied strategies that protect the heart against ischemia/reperfusion injury.
- What remains unknown, however, is their effect on the function of cardiac receptors, which are significantly involved in the functional and structural remodeling of the postischemic myocardium.
- Here, we have been able to demonstrate that, unlike ischemic preconditioning, the application of ischemic postconditioning by inducing β-adrenergic receptor kinase-2 leads to desensitization of β-adrenergic receptors, which in turn induces cardiac dysfunction with restricted inotropic functional reserve.

What Are the Clinical Implications?

- The findings of this study not only provide a possible explanation for the previously disappointing long-term clinical trials of ischemic postconditioning but also identify the postconditioned heart as another indication for the therapeutic use of prospective β-adrenergic receptor kinase-2 inhibitors.

In the classical in vivo IPC and IPoC models, a reduction in the size of the infarct is chosen as the relevant end point in most cases even though this was often not accompanied by a corresponding functional recovery.[4,5] However, no information can be gleaned about long-term functional improvements or positive remodeling using these short-term models.

Therapeutically, application at the time of reperfusion is an appropriate intervention option, meaning that in routine clinical practice IPoC is the preferred protective strategy.[6,7]

However, the results from longitudinal human studies have not provided a uniform picture of the efficacy and safety of IPoC.[8] In 2013 a single-center study by Freixa et al showed rather a significant deterioration in the myocardial salvage and the myocardial salvage index along with reduced pump function 6 months after myocardial ischemia.[9] These results correspond to data published by Hahn et al from a multicenter study of 700 patients (POST [Effects of Postconditioning On Myocardial Reperfusion] trial, https://clinicaltrials.gov/show/NCT00942500) that was conducted between 2009 and 2012, also showing no cardiprotective effect.[10] Moreover, recently published results of the DANAMI-3–iPOST (DANish Study of Optimal Acute Treatment of Patients With ST-elevation Myocardial Infarction, https://clinicaltrials.gov/show/NCT01435408) trial have also demonstrated that IPoC in addition to primary percutaneous coronary intervention failed to significantly reduce death from any cause or hospitalization during a median follow-up of 38 months.[11]

It has already been shown for both IPC and IPoC that both prior pharmacological interventions and preexisting diseases (diabetes mellitus, chronic heart failure) can contribute to a reduction in their cardioprotective potential.[12–14]

What is not currently known, however, is the effect of both intervention strategies on cardiac receptors, which, as important components of the functional and structural remodeling, are significantly involved in the functional preservation of the postischemic myocardium and thus play a critical role in the efficiency of IPC or IPoC.[15]

The β-adrenergic receptor (β-AR) is primarily involved in the maintenance and, where necessary, adaptation of cardiac function. The density and the signaling of the cardiac β-ARs change over the course of many cardiac diseases. In the postischemic failing myocardium these changes are often associated with significant downregulation of the β-ARs. The activation and intracellular coupling of the β_1-AR, on the other hand, can be inadequately elevated in the early postischemic phase.[16–18]

The primary aim of this research was to study the effect of IPC or IPoC on the remodeling of the β-adrenergic system and their effects on the function of the postischemic myocardium.

A new signaling mechanism for the IPoC has been identified that considerably reduces the coupling of β-ARs independently of a reduction in the size of the infarction. The resulting restriction in the positive inotropic functional reserve induced a persistent cardiac dysfunction in the postconditioned myocardium.

Methods

The investigation conforms to the Guide for the Care and Use of Laboratory Animals published by the US National Institutes of Health (NIH Publication No. 85-23, revised 1996). The data and analytic methods that support the findings of this study are available from the corresponding author on request.

Langendorff Perfusion

Using the Langendorff technique, Krebs-perfused hearts from 3-month-old female Wistar rats were subject to 45 minutes of global ischemia and then reperfused for 120 minutes (IR). The IR protocol was either supplemented by IPC (3×3 minutes of no flow—5 minutes of perfusion) or IPoC (3×30 seconds of perfusion—30 seconds of no flow), and the corresponding functional recovery and the extent of the resultant tissue damage were compared to the values for a normoxic control group (Figure 1A). For this purpose, rats were anesthetized by isoflurane and killed by cervical dislocation. Their hearts were rapidly excised, and the aortas were cannulated for retrograde perfusion with a 16-gauge needle connected to a Langendorff perfusion system. A polyvinyl chloride balloon was inserted

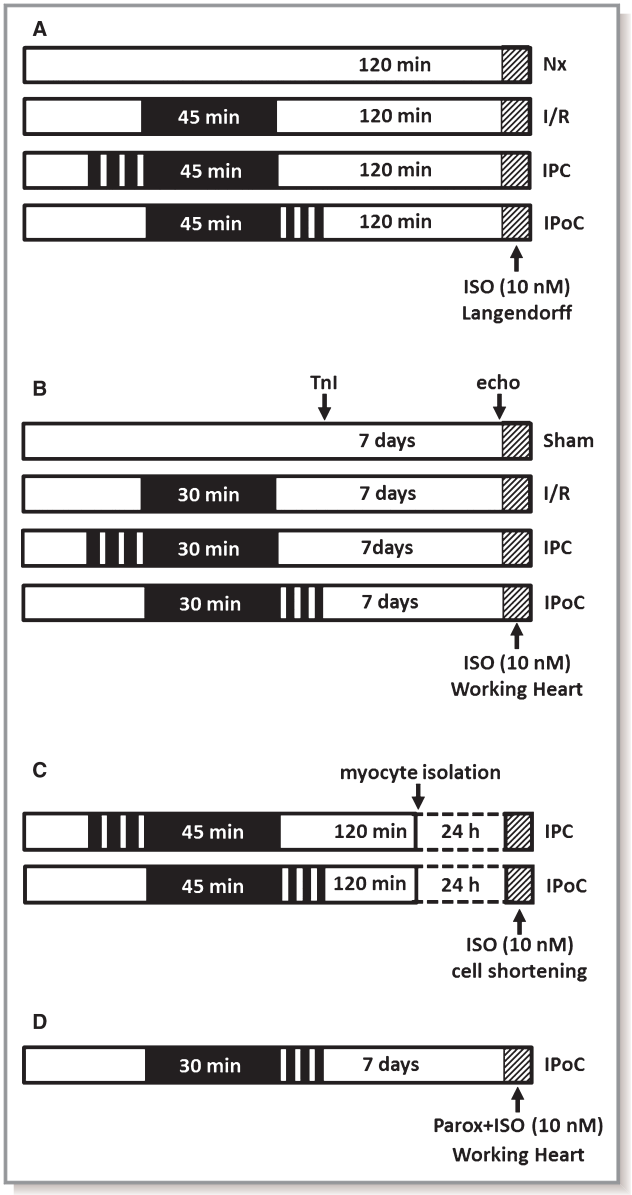

Figure 1. Study designs and treatment protocols. A, Stimulation of β-ARs at the end of a 2-hour reperfusion in the Langendorff model. B, Stimulation of β-ARs 7 days after infarction in the working heart model. C, Cardiomyocytes were isolated from IPC or IPoC hearts and cultured for 24 hours. Cell shortening was determined before and after stimulation with ISO using a cell-edge detection system. D, Perfusion of IPoC hearts 7 days after an infarction. After 10 minutes' infusion with paroxetine, the CO was measured continuously for 5 minutes with additional stimulation using ISO. β-AR indicates β-adrenergic receptor; CO, cardiac output; IPC, ischemic preconditioning; IPoC, ischemic postconditioning; ISO, isoproterenol.

into the left ventricle (LV) through the mitral valve and held in place by a suture tied around the left atrium. The other end of the tubing was connected to a pressure transducer for continuous measurement of LV pressure. A second transducer connected to the perfusion line just before the heart was used to measure coronary perfusion pressure. Hearts were perfused with an oxygenated saline medium containing (in mmol/L) 140 NaCl, 24 $NaHCO_3$, 2.7 KCl, 0.4 NaH_2PO_4, 1 $MgCl_2$, 1.8 $CaCl_2$ and 5 glucose, gassed with 95% O_2 and 5% CO_2, pH 7.4. After attachment to the Langendorff system, hearts were allowed to stabilize for at least 20 minutes. The intraventricular balloon was inflated to give a diastolic pressure of 10 mm Hg. The flow was adjusted to give a perfusion pressure of 50 mm Hg. To avoid differences in oxygen supply due to changes in the coronary resistance, hearts were perfused at a constant flow. The perfusion system was constantly kept at a temperature of 37°C throughout the whole experiment.[15] As a pharmacological inhibitor of protein kinase C (PKC), chelerythrine chloride (1 μmol/L, Merck Millipore, Darmstadt, Germany; product #220285) was applied from the onset of reperfusion.

Measurement of Lactate Dehydrogenase Activity

The lactate dehydrogenase (LDH) release of Langendorff hearts was measured in the perfusate, which was collected for 60 seconds after 5 minutes of reperfusion. LDH activity was determined using a colorimetric LDH assay kit (Abcam, Cambridge, UK). In brief, LDH reduces NAD to NADH, which then interacts with a specific probe to generate color at 450 nm. The intensity of the color is directly proportional to the LDH activity (U/L) in each sample. Fifty-microliter samples were incubated with LDH substrate mix and measured immediately at OD 450 nm on a microplate reader in a kinetic mode for 45 minutes at 37°C. LDH activity in each sample was calculated according to a standard curve.

Measurement of Superoxide

Fifteen minutes after the start of reperfusion, left ventricular tissue was prepared for cryosectioning by freezing in Tissue-Tek OCT Compound (Sakura Finetek Germany GmbH, Staufen, Germany). To perform dihydroethidium staining, cryoslices of the LV were incubated with the fluorescent probe dihydroethidium (dissolved in 1× PBS) for 10 minutes at 37°C in a light-protected humidity chamber, then fixed with Dako Fluorescent Mounting Medium (Dako North America Inc, Carpinteria, CA). Sections were imaged by fluorescence microscopy (LSM 510 META; Carl Zeiss, Jena, Germany) using an excitation wavelength of 488 nm; emission was recorded at 540 nm.[19]

Analysis was performed by digital image analysis using Leica Confocal Software Lite Version (LCS Lite; Leica, Wetzlar, Germany). The mean fluorescence intensity of n=6 ventricles was used to quantify the extent of superoxide.

Immunohistochemistry Analysis of Active Caspase-3 and Connexin 43

Subsequent to the particular reperfusion time, Langendorff-perfused hearts were fixed after snap-freezing and sectioned using a cryostat (section thickness 10 μm). Briefly, slides were rehydrated in PBS for 15 minutes and then blocked with bovine serum albumin (5%) for 1 hour. Primary antibodies against active caspase-3 or connexin 43 were diluted 1:100 in PBS/Tween containing 2.5% bovine serum albumin and incubated for 1 hour at room temperature. Slides were washed 20 minutes with PBS/Tween and incubated with an Alexa Fluor-488 coupled secondary antibody (Molecular Probes, Eugene, OR) for 1 hour. The visualization and quantification of the florescence were carried out using a florescence microscope (Till Photonics, Gräfelfing, Germany).

Rat Model of Ischemia and Reperfusion In Vivo

In brief, female Wistar-Hannover rats weighing 210 to 265 g were anesthetized by intraperitoneal injection of 60 mg/kg sodium pentobarbital (Euthasol, Produlab Pharma b.v., Raamsdonksveer, the Netherlands). Animals were intubated and mechanically ventilated (Model 683, Harvard Apparatus, Holliston, MA) with room air in a volume of 6.2 mL/kg and a frequency of 72±5 breaths/min according to body weight. Rats were placed in a supine position on a heating pad to maintain body core temperature in physiological range (37.0±1.0°C). Body surface ECG was monitored throughout the experiments (Haemosys, Experimetria Inc, Budapest, Hungary). Left anterior descending coronary artery occlusion was induced by a left thoracotomy. A 5-0 Prolene suture (Ethicon, Johnson & Johnson Kft Hungary, Budapest, Hungary) was placed around the left anterior descending artery and a small plastic knob, which was threaded through the ligature and placed in contact with the heart, was used for making occlusion for 30 minutes. Animals for the IPC group were subjected to 3 cycles of 3 minutes of ischemia followed by 5 minutes of reperfusion before a 30-minute test ischemia; IPoC was performed after test ischemia by using 3 cycles of 30 seconds of reperfusion/30 seconds of ischemia. The presence of ischemia was confirmed by the appearance of ST segment elevation and ventricular arrhythmias. After 30 minutes of ischemia or the postconditioning protocol, the occlusion was released, and the suture was removed from the heart. Restoration of blood flow was confirmed by the appearance of arrhythmias observed in the first minutes after the onset of reperfusion. Then the chest was closed in layers with a 4-0 Monocryl suture (Ethicon, Johnson & Johnson Kft Hungary, Budapest, Hungary), and 0.3 mg/kg nalbuphin (Nalbuphin Orpha, Torrex Chiesi Pharma GmbH, Vienna, Austria) was given subcutaneously to alleviate postoperative pain. Rats were allowed to recover for 7 days after coronary occlusion. Sham-operated animals were treated with the same procedure except occlusion of the coronary artery (Figure 1B). The surgical procedure was performed according to previous publications.[20,21]

Transthoracic Echocardiography

Cardiac morphology and function were also assessed by transthoracic echocardiography 7 days after the induction of ischemia/reperfusion injury or sham operation. Echocardiography was performed as described previously.[22] Briefly, rats were anesthetized with sodium pentobarbital (Euthasol, 40 mg/kg body weight, intraperitoneally), the chest was shaved, and the animal was placed in supine position onto a heating pad. Two-dimensional and M-mode echocardiographic examinations were performed in accordance with the criteria of the American Society of Echocardiography with a Vivid 7 Dimension ultrasound system (General Electric Medical Systems, Waukesha, WI) using a phased-array 5.5- to 12-MHz transducer (10S probe). Data of 3 consecutive heart cycles were analyzed (EchoPac Dimension Software, General Electric Medical Systems) and then the mean values of the 3 measurements were calculated and used for statistical evaluation. Systolic and diastolic wall thicknesses were obtained from parasternal short-axis view at the level of the papillary muscles. The left ventricular diameters were measured by means of M-mode echocardiography from short-axis views between the endocardial borders. Functional parameters including fractional shortening and ejection fraction were calculated on short-axis view images.

Measurement of Functional Parameters of Hearts: Working Heart Perfusion

After echocardiographic examinations, rat hearts were isolated and prepared for working heart perfusion according to Neely et al.[23-25] Hearts were perfused at 37°C with freshly prepared Krebs-Henseleit bicarbonate buffer containing (in mmol/L) NaCl 118, KCl 4.3, $CaCl_2$ 2.4, $NaHCO_3$ 25, KH_2PO_4 1.2, $MgSO_4$ 1.2 and glucose 11.1, gassed with 95% O_2 and 5% CO_2. Preload (17 cm H_2O) and afterload (100 cm H_2O) were kept constant throughout the experiments. Coronary flow was measured by collecting effluent from the right atrium by a measuring cylinder for 1 minute, aortic flow was measured by a calibrated rotameter (KDG Flowmeters, Sussex, England), and cardiac output (CO) was calculated as the sum of aortic flow and coronary flow. Ventricular pressure was measured by means of a pressure transducer (B. Braun, Melsungen, Germany) connected to a small polyethylene catheter inserted into the LV through the left atrial cannula. Left ventricular developed pressure (LVDP) was calculated as peak systolic pressure minus LV end-diastolic pressure, positive and

negative first derivatives of left ventricular pressure (±dp/dt), and LV end-diastolic pressure were also defined. Heart rate was derived from the LV pressure curve.

Measurement of Cardiac Troponin I Release in Plasma

Plasma samples were collected into heparinized tubes (Sarstedt, Nümbrecht, Germany) from the femoral vein at the 60th minute of reperfusion, and plasma was separated to determine cardiac troponin I (TnI) release after acute myocardial infarction. Plasma TnI concentration was determined by a conventional ELISA kit (Life Diagnostics, Inc, West Chester, PA) according to the recommendations of the manufacturer. Briefly, plasma samples were diluted 4 to 40 times according to the treatment protocol (ie, sham or ischemic) and to previous preanalyses to get absorbances in the range of standard absorbances. Diluted samples were allowed to react simultaneously with 2 antibodies against rat TnI (1 is immobilized on the microtiter wells, and the other is conjugated to horseradish peroxidase [HRP] in soluble phase), resulting in TnI being sandwiched between the solid phase and HRP-conjugated antibodies. After 1 hour of incubation at room temperature on a plate shaker, the wells were washed with wash solution to remove unbound HRP-conjugated antibodies. A solution of tetramethylbenzidine, a HRP substrate, was then added and incubated for 20 minutes, resulting in the development of a blue color. The color development was stopped by addition of 1N HCl, which changed the color to yellow. The concentration of TnI was proportional to the absorbance at 450 nm.

Determination of Infarct Size

After 120 minutes of reperfusion, hearts were isolated for infarct size measurements. Hearts were perfused in a Langendorff perfusion system with 37°C Krebs-Henseleit buffer to remove blood from the coronary vessels. After 5 minutes of perfusion, the risk area was reoccluded, and hearts were perfused with 4 mL of 0.1% Evans blue dye through the ascending aorta. Following Evans staining, hearts were cut into 5 transverse slices and incubated in 1% triphenyltetrazolium chloride for 10 minutes at 37°C followed by formalin fixation for 10 minutes. Digital images were taken from both surfaces of heart slices by a Nikon DSLR camera (Nikon Corporation, Tokyo, Japan). Planimetric evaluation was carried out to determine infarct size using InfarctSize™ software version 2.5, (Pharmahungary, Szeged, Hungary[26]).

Western Blot

Total protein was extracted from the LV using Cell Lysis Buffer (10×) (Cell Signaling, Danvers, MA) according to the manufacturer's protocol. Briefly, the homogenate was centrifuged at 14 000*g* at 4°C for 10 minutes, and supernatant was treated with Laemmli buffer. Protein samples were loaded on NuPAGE Bis-Tris Precast gels (8%, 10%; Life Technology, Darmstadt, Germany) and subsequently transferred onto nitrocellulose membranes. Blots were incubated with 1 of the following antibodies: anti-β1-AR (V-19) (Santa Cruz Biotechnology, Inc, Heidelberg, Germany; product sc-568), anti-β2-AR (H-73) (Santa Cruz Biotechnology, Inc, Heidelberg, Germany; product sc-9042), anti-β-adrenergic receptor kinase-2 (anti-GRK2; Sigma-Aldrich, Taufkirchen, Germany; product G0296), anti-GRK2 phospho S29 (Abcam plc, Cambridge, UK; product ab58520), anti-β-arrestin1/2 (New England Biolabs GmbH, Frankfurt am Main, Germany; product #4674), anti-MDM2/HDM2 (R&D Systems, Wiesbaden, Germany; AF1244), anti-MDM2 phospho Ser166 (New England Biolabs GmbH, Frankfurt am Main, Germany; product #3521), anti-PI3 kinase p110α (Becton Dickinson GmbH, Heidelberg, Germany; product #611398), and anti-GAPDH (Merck Millipore, Darmstadt, Germany; product CB1001). Secondary antibodies (HRP-conjugated) directed against rabbit IgG or mouse IgG were purchased from Affinity Biologicals (Ancaster, ON, Canada; product SAR-APHRP, GAM-APHRP). In order to detect β_1-AR dimers, samples were treated with nonreducing Laemmli buffer and loaded on a 10% NuPAGE Bis-Tris Precast gel.

Densitometry of immunoblot bands was carried out using Quantity One software from Bio-Rad Laboratories (Hercules, CA). The intensities of the target proteins were normalized to that of GAPDH of the same sample.

RNA Isolation and Real-Time Reverse-Transcriptase Polymerase Chain Reaction

Total RNA was isolated from the LV using peqGold TriFast (peqlab, Biotechnologie GmbH, Erlangen, Germany) according to the manufacturer's protocol. To remove genomic DNA contamination, RNA samples were treated with 1 U DNase/μg RNA (Invitrogen, Karlsruhe, Germany) for 15 minutes at 37°C. One microgram of total RNA was used in a 10-μL reaction to synthesize cDNA using Superscript RNaseH Reverse Transcriptase (200 U/μg RNA, Invitrogen, Karlsruhe, Germany) and oligo-dTs as primers. Reverse transcriptase reactions were performed for 50 minutes at 37°C. Real-time quantitative polymerase chain reaction was performed using MyiQ® detection system (Bio-Rad, Munich, Germany) in combination with the iTaq Universal SYBR Green Real-Time PCR Supermix (Bio-Rad, Munich, Germany). The thermal cycling program consisted of initial denaturation in 1 cycle of 3 minutes at 95°C, followed by 45 cycles of 30 seconds at 95°C, 30 seconds at the individual annealing temperature for each primer, and 30 seconds at 72°C. Primers used for

determination had the following sequences: HPRT forward CCA GCG TCG TGA TTA GTG AT, HPRT reverse CAA GTC TTT CAG TCC TGT CC, β_1-AR forward GGC GCT CAT CGT GCT GCT CA, β_1-AR reverse AGG CAC CAC CAG CAG TCC CA, β_2-AR forward GCT TCT GTG CCT TCG CCG GT, β_2-AR reverse AGC CTT CCA TGC CAG GG GCT, β_3-AR forward GGT TGG GCT ATG CCA ACT CT, β_3-AR reverse CCT GTT GAG CGG TGA GTT CT, GRK2 forward GCT CTT CAA GTT GTT GCG GG, GRK2 reverse AAA CCT TCC AGC AGG GAT CG. Quantification was performed as described before.[27]

Isolation and Culture of Cardiomyocytes From the LV

Heart muscle cells from the LV were isolated from 3-month-old Wistar rats. Briefly, hearts were excised and transferred rapidly to ice-cold saline and mounted on the cannula of a Langendorff perfusion system. Heart perfusion and subsequent steps were all performed at 37°C. First, hearts were perfused in a noncirculating manner for 5 minutes at 10 mL/min. Thereafter, perfusion was continued with recirculation using 50 mL perfusate supplemented with 0.06% (w/v) crude collagenase and 25 μmol/L $CaCl_2$ at 5 mL/min for 25 minutes. Then, the LV was dissected from the RV, minced, and incubated for 5 minutes in medium with 1% (w/v) bovine serum albumin under 5% CO_2 and 95% O_2. The resulting cell suspension was filtered through a 200-μm nylon mesh. Filtered cells were washed twice by centrifugation and resuspended in perfusate with a stepwise increase in $CaCl_2$ to 0.2 and 0.5 mmol/L. After further centrifugation, cells were resuspended in serum-free culture medium and plated in 35-mm culture dishes (Falcon, type 3001).[28]

Isolated cardiomyocytes were then incubated with siRNA against GRK2 (Qiagen GmbH, Hilden, Germany, product Rn_Adrbk1_1), siRNA against β-arrestin1 (Qiagen GmbH, Hilden, Germany, product Rn_Arrb1_2), or siRNA against β-arrestin2 (Qiagen GmbH, Hilden, Germany, product Rn_Arrb2_1) for 24 hours. Paroxetine (LKT Laboratories, St. Paul, MN) was used as a pharmacological inhibitor of GRK2.

Determination of Cell Contraction

Cell shortening was measured as described before in greater detail.[28] Briefly, isolated cardiomyocytes were allowed to contract at room temperature and analyzed using a cell-edge detection system. Cells were stimulated via 2 AgCl electrodes with biphasic electrical stimuli composed of 2 equal but opposite rectangular 50-V stimuli of 0.5 milliseconds duration. Each cell was stimulated for 1 minute at a frequency of 2.0 Hz. Every 15 seconds contractions were recorded. The mean of these 4 measurements was used to define the cell shortening of a given cell. Cell lengths were measured via a line camera (data recording at 500 Hz). Data are expressed as cell shortening normalized to diastolic cell length (dL/L [%]).

Statistical Analysis

Data are presented as mean±SD as indicated in the legends of the figures and tables. All data sets were initially analyzed by a Shapiro-Wilk test to analyze whether the data are normally distributed. If this was the case, data were analyzed either by paired or unpaired t-test depending on the study design. If the 2 groups had different variances (as analyzed by the Levene test), we calculated the *P*-value by a Welch test. In the case that the data were not normally distributed, we performed a Mann-Whitney test for unpaired samples or a Friedman test for paired samples. In those figures in which more than 2 groups were compared, we performed a 1-way ANOVA with a subsequent Student-Newman-Keuls test for post hoc analysis as long as the data were normally distributed. If data were not normally distributed, we used a Kruskal-Wallis test to decide whether differences between groups occurred. A *P*-value of $\leq$0.05 is always indicated by an asterisk to indicate that this was used as the threshold to reject the null hypothesis. Statistical analysis was performed by SPSS (IBM, Armonk, NY) version 22.0.

Results

Evidence of Cardiac Protection for IPC and IPoC Algorithms Used on the Ex Vivo Perfused Heart

The efficiency of IPC and IPoC was analyzed in Langendorff perfused hearts using the experimental protocol in Figure 1A. LDH release, the formation of superoxide, and the proportion of activated caspase-3 were significantly elevated in the hearts in the IR group compared with those in the normoxic group (Figure 2A through 2C). All parameters were improved by both IPC and IPoC. The cardioprotective potential of both protocols was also reflected in the structural preservation (connexin 43), whereas the short-term functional recovery within the 120-minute reperfusion period did not improve significantly (Figure 2D and 2E).

Stimulation of β-ARs 2 Hours After Infarction in the Langendorff Model

In another series of experiments the previously described perfusion protocols (normoxia, IR, IPC, IPoC) were supplemented by a final stimulation with isoproterenol (ISO, 10 nmol/L) for 5 minutes (Figure 1A). Both the ISO-induced increase in the heart rate and the reduction in the coronary resistance were equally pronounced in the 4 treatment groups. A significant increase in the LVDP was observed only

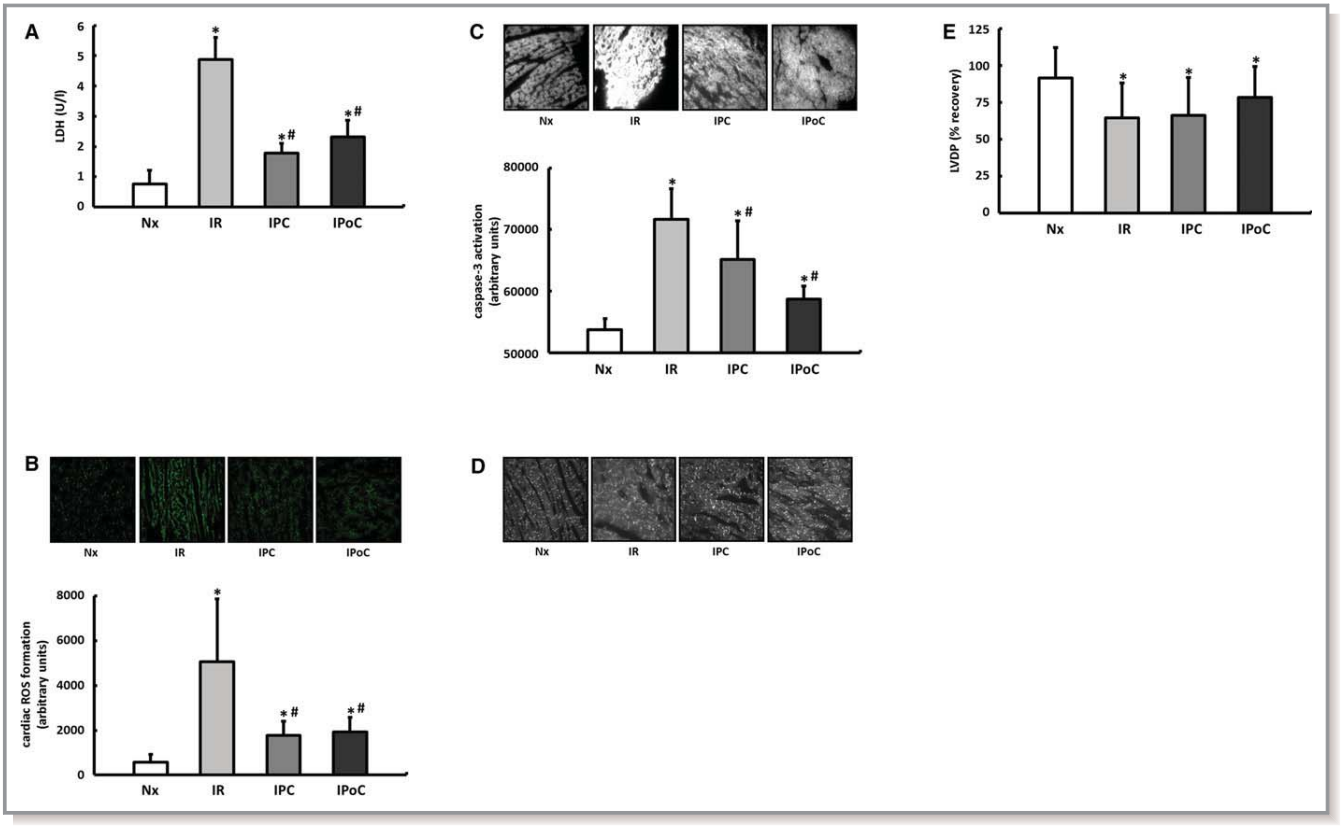

Figure 2. Proof of cardiac protection for IPC and IPoC algorithms in a Langendorff model of myocardial ischemia and reperfusion. A, Five minutes after the onset of reperfusion, the LDH level was determined in the perfusate as a surrogate parameter for tissue damage. B, After 15 minutes of reperfusion reactive oxygen species (ROS) were determined in the left ventricular myocardium using DHE staining. C, Activation of caspase-3 was determined by immunohistochemistry after 120 minutes of reperfusion. D, The structural preservation of the myocardium was qualitatively assessed using connexin 43 staining. E, Functional recovery was expressed as a percentage of the preischemic LVDP. Data are means±SD of n=6 to 8 hearts. *$P \leq 0.05$ vs Nx, #$P \leq 0.05$ vs IR. DHE indicates dihydroethidium; IPC, ischemic preconditioning; IPoC, ischemic postconditioning; IR, ischemia/reperfusion; LDH, lactate dehydrogenase; LVDP, left ventricular developed pressure; Nx, normoxia.

in the hearts in the normoxia, IR, and IPC groups but, unexpectedly, not in IPoC hearts (Table 1).

There were no differences observed in the LV expression of the β_1-AR in the Western blot among the comparator groups. However, compared with normoxic control hearts, the proportion of β_1-AR dimers was significantly reduced in the myocardium of reperfused hearts regardless of the particular protocol used (Figure 3A through 3C).

The β-adrenergic receptor kinases (GRKs), which mediate the accumulation of β-arrestin by phosphorylating serine and threonine residues on the intracellular domains of the receptor, are critically involved in the regulatory mechanisms for intracellular coupling of the β-ARs and, in turn, can prevent activation of the Gs subunit or induce internalization of the receptor.

The phosphorylation, and thus the activation, of GRK2 was significantly reduced in the hearts in the IR and IPC groups. Consequently, the ratio of receptor dimers to phosphorylated GRK2 did not differ from that of the hearts in the control group. In contrast, in postconditioned hearts, the increased proportion of phosphorylated GRK2 combined with the significant reduction in the β-AR dimers led to an imbalance, which may be the underlying cause of the missing increase in the LVDP following β-adrenergic stimulation (Figure 3A, 3D through 3F, Table 1).

Significance of PKC for GRK2 Phosphorylation in the Postconditioned Heart

It has already been shown for PKC that it can effectively contribute to the desensitization of G-protein-coupled receptors via phosphorylation of GRK2.[29] By inhibiting PKC using chelerythrine chloride, the IPoC-induced phosphorylation of GRK2 is significantly reduced, and consequently, the ISO-induced increase in the LVDP at the end of a 2-hour reperfusion can be reestablished (Figure 3G and 3H).

Table 1. Influence of IR, IPC, and IPoC on β-AR–Mediated Effects 2 Hours After Myocardial Infarction

	Heart Rate (beats/min)	
	Baseline	ISO
Nx	244±44	318±26*
IR	234±42	305±48*
IPC	246±24	314±52*
IPoC	230±60	303±36*
	Perfusion Pressure (mm Hg)	
	Baseline	ISO
Nx	57±8	46±3*
IR	64±8	55±7*
IPC	62±13	50±7*
IPoC	72±18	62±14*
	LVDP (mm Hg)	
	Baseline	ISO
Nx	109±18	126±7*
IR	85±13	98±12*
IPC	91±20	100±22*
IPoC	94±24	93±21

The heart rate increased and the perfusion pressure fell uniformly under ISO stimulation in all 4 treatment groups. A significant increase in the LVDP was observed only in hearts of the Nx, IR, and IPC groups. Data are means±SD of n=6 to 8 hearts.
IPC indicates ischemic preconditioning; IPoC, ischemic postconditioning; IR, ischemia/reperfusion; ISO, isoproterenol; LVDP, left ventricular developed pressure; Nx, normoxia.
*$P \leq 0.05$ vs baseline.

Effect of IR, IPC, and IPoC on the Size of the Infarct and the Cardiac Function In Vivo

IPoC has already induced a specific remodeling of the β-adrenergic signaling during the short-term reperfusion ex vivo. It is certainly an important question whether IPoC also affects the coupling of β-ARs over the long term in vivo (see experimental protocol in Figure 1B). One hour after the onset of reperfusion, the TnI plasma level was determined. Compared with the sham group (1.1±0.8 ng/mL), the plasma samples from the IR group had the highest concentrations of TnI at 104.3±33.6 ng/mL and were significantly reduced by IPC to 32.8±33.9 ng/mL or by IPoC to 41.9±41.1 ng/mL (Figure 4A). The validity of TnI as a marker to determine the size of the infarct in the IR model used here was demonstrated in a separate group of animals. Plasma TnI values measured 1 hour after infarction confirm a reduction in the size of the infarct in conditioned animals of the same magnitude as that determined using triphenyltetrazolium chloride staining in the corresponding hearts 2 hours after starting reperfusion (Figure S1).

After 7 days the left ventricular morphology and function were assessed using echocardiography. Fractional shortening was 59.8±12% in the sham group, which was significantly reduced (42.9±10%) in the IR group. The application of IPC improved the fractional shortening to 49.8±14%, whereas the hearts in the IPoC group only achieved a value of 32.2±12%, which did not differ statistically from the IR group (Figure 4B).

There were no significant differences in the ventricular geometry determined by echocardiography (Table S1) and the wet weight analyzed postmortem (data not shown) between the groups at the end of the experimental period.

Stimulation of β-ARs 7 Days After Infarction in the Working Heart Model

After the 7 days had elapsed, the pump function and hemodynamics of the hearts were recorded ex vivo in the working heart model, first at a basal level and again immediately after stimulation with ISO (10 nmol/L) (Figure 1B). The basal CO, respectively the LVDP and dP/dt_{max}, confirmed the values for the function previously determined by echocardiography and also identified the IPC as the only cardioprotective application in terms of a medium-term preservation of function. The 4 groups did not differ in terms of their heart rates or the coronary flow (Table 2).

After stimulation with ISO, a significant increase was recorded for the CO and the LVDP only for the sham-operated hearts and the hearts in the IR and the IPC groups. IPoC hearts were no longer able to adequately respond to the β-adrenergic stimulus in terms of all contraction parameters (Table 2).

On the other hand, the heart rate increased uniformly by 30±4% on average under ISO stimulation in all 4 treatment groups. The coronary flow also rose with the increase in the hearts of the sham group (63%) about one and a half times as high as that in the hearts of the IR, IPC, and IPoC groups, which had a mean rise in the flow of 42±3% and did not differ from each another (Table 2).

Effect of IR, IPC, and IPoC on the Remodeling and the Intracellular Coupling of Cardiac β-Receptors

The expression (mRNA and protein) of the β_1- and β_2-ARs was significantly reduced in the hearts in the IR, IPC, and IPoC groups compared with the sham group 7 days after the infarction with no differences seen among the groups. Receptor dimers can no longer be detected under these conditions. The expression of the β_3-AR is stable postischemia and was unaffected by either IPC or IPoC (Figure 5A through 5D, for mRNA data; please see Figure S2). A selective influence of IPoC on the expression of cardiac β-ARs can therefore be excluded. This result was also verified by measuring sodium-potassium-ATPase as a surrogate marker for membrane density, which in the

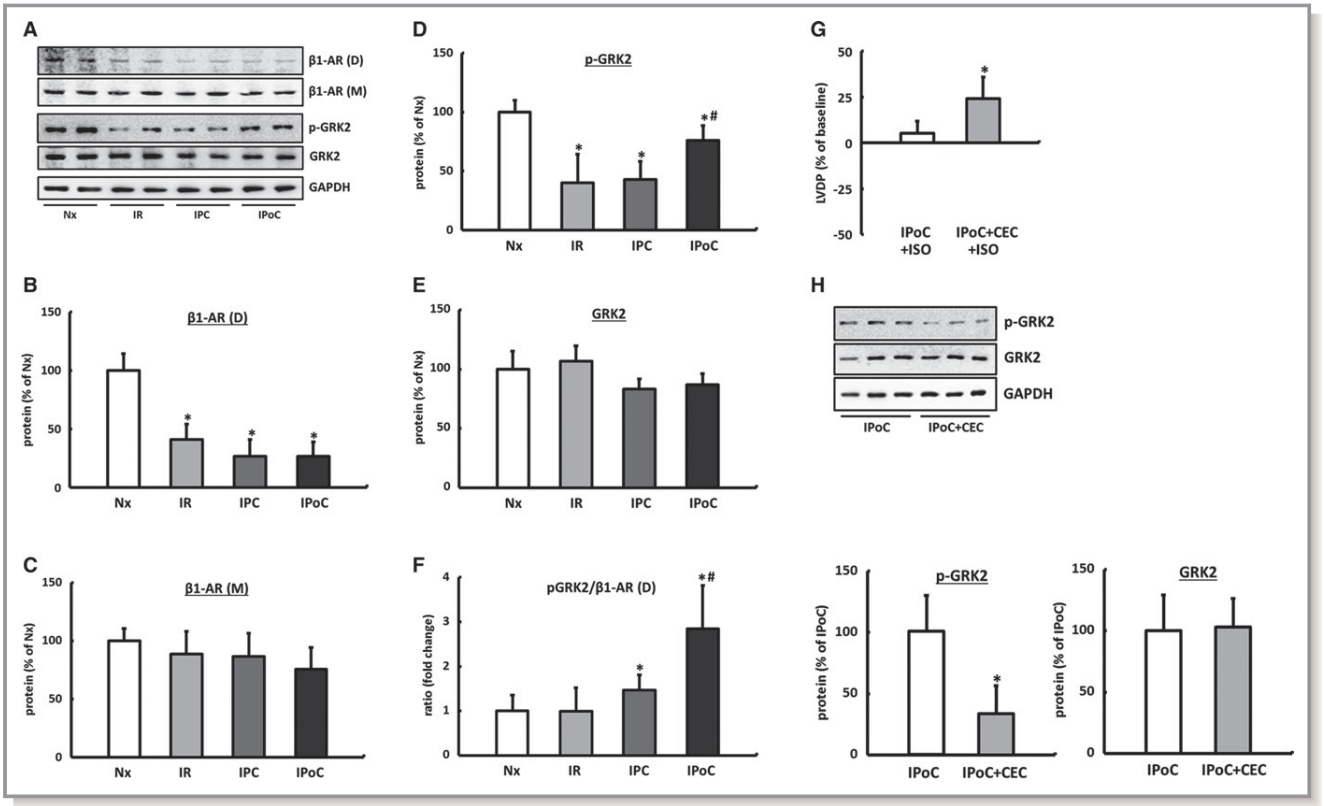

Figure 3. Influence of IR, IPC, and IPoC on β-adrenergic signaling 2 hours after starting reperfusion. A, Representative immunoblots and quantification by densitometric analysis of (B) β1-AR dimers (D, MW 95 kDa) and (C) β_1-AR monomers (M, MW 50 kDa). Quantification of the (D) phosphorylated (p-GRK2) and (E) total GRK2 protein. F, The p-GRK2 to β1-AR (D) ratio was calculated for each animal, and group means were expressed as fold change of Nx. Data are means±SD of n=6 hearts. *$P \leq 0.05$ vs Nx, #$P \leq 0.05$ vs IPC. The significance of PKC for GRK2 phosphorylation. G, ISO-induced inotropic response of IPoC hearts perfused with the PKC inhibitor CEC. H, The effect of PKC inhibition on GRK2 phosphorylation in IPoC hearts. Immunoblot bands were normalized to GAPDH and expressed as a percentage of Nx. Data are means±SD of n=6 hearts. *$P \leq 0.05$ vs IPoC. CEC indicates chelerythrine chloride; D, dimer; GAPDH, Glyceraldehyde 3-phosphate dehydrogenase; GRK2, G protein-coupled receptor kinase 2; IPC, ischemic preconditioning; IPoC, ischemic postconditioning; IR, ischemia/reperfusion; ISO, isoproterenol; M, monomer; Nx, normoxic; p-GRK2, phosphorylated GRK2; PKC, protein kinase C; β_1-AR, β_1-adrenergic receptor.

postconditioned myocardium does not differ from IR or IPC hearts (Figure 5K).

In hearts of the IR and IPC groups, GRK2 was significantly downregulated, meaning that the ratio of β-ARs to GRK2 was unchanged compared to the hearts of the control group. In IPoC hearts, on the other hand, significant increases in GRK2 as well as its phosphorylated fraction were recorded. The receptor/pGRK2 ratio was shifted 2.6 times toward GRK2, which thus explains the reduced response of IPoC hearts to β-adrenergic stimuli (Figure 5E through 5H).

The expression of GRK2 was positively correlated with β-arrestin1/2 in all groups, meaning that desensitization of the β-receptors in the IPoC hearts was synergistically amplified (Figure 5J).

The high levels of GRK2 in the IPoC hearts cannot be attributed to an increase in the mRNA expression but are instead due to stabilization of the protein (Figure 5I).

Cardiomyocyte as the Cause of Dysfunction in the IPoC Heart

Using the isolated cardiomyocyte model, the previously described molecular and functional remodeling of the postconditioned myocardium can be confirmed at a cellular level (Figure 1C). Cardiomyocytes isolated from postconditioned hearts showed no difference in basal cell shortening after 24-hour culture compared to IPC myocytes, but their responsivity to ISO was significantly reduced with a simultaneous induction of GRK2 (Figure 6A and 6B). This finding suggests that the limited inotropy of postconditioned hearts can be attributed exclusively to remodeling of the β-adrenergic signaling and not to structural remodeling processes of the cardiomyocytes or the myocardium. Consequently, postconditioned hearts with simultaneous inhibition of GRK2 should be able to achieve a positive inotropic response to ISO.

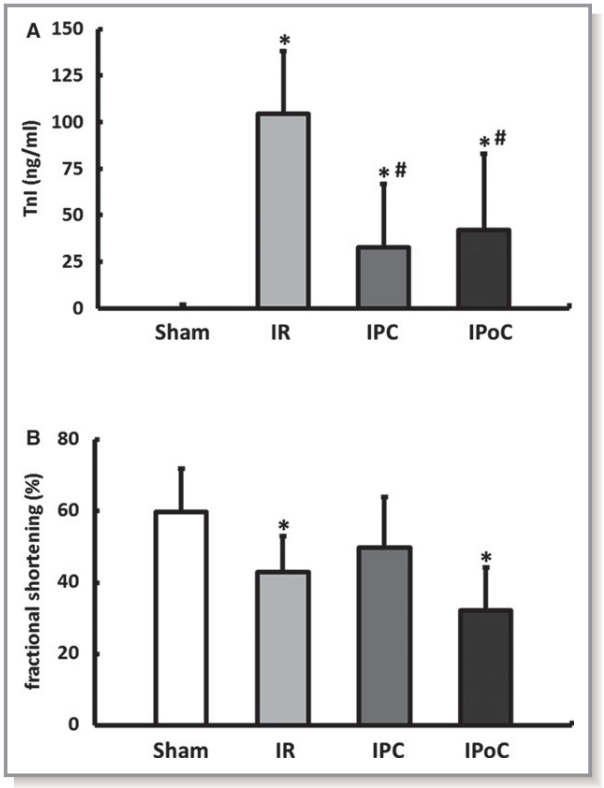

Figure 4. Influence of IR, IPC, and IPoC on infarct size and cardiac function in vivo. A, Plasma levels of cardiac troponin I (TnI) were determined 1 hour after the onset of reperfusion as an early index of myocardial infarct size. B, Left ventricular systolic function, represented as fractional shortening (%), was determined 7 days following the reperfusion. Data are means±SD of n=6 to 10 animals. *$P \leq 0.05$ vs Sham, #$P \leq 0.05$ vs IR. IPC indicates ischemic preconditioning; IPoC, ischemic postconditioning; IR, ischemia/reperfusion.

This hypothesis was tested experimentally using the working heart model by perfusing postconditioned hearts after 7 days' reperfusion first with the GRK2 inhibitor paroxetine for 10 minutes and then stimulating them with ISO (Figure 1D).

With inhibition of the GRK2, the CO of IPoC hearts rose by 55±30% on average during the β-adrenergic stimulation. In the direct comparison, ISO induced only a moderate increase of 14±4% in the CO of IPoC hearts, which were not perfused with paroxetine (Figure 6C).

The functional relevance of GRK2 (and β-arrestin) was confirmed in all experimental models (isolated cardiomyocytes, isolated perfused hearts) using selective knockdown with siRNA and/or pharmacological inhibition. The ISO concentration used is based on the dose-response curves determined on isolated normoxic cardiomyocytes (Figures S3 through S6).

Table 2. Functional Data Were Assessed Ex Vivo in a Working Heart Model

	Heart Rate (beats/min)	
	Baseline	ISO
Sham	272±29	341±34*
IR	276±48	364±32*
IPC	263±22	352±72*
IPoC	273±25	347±41*
	Coronary Flow (mL/min)	
	Baseline	ISO
Sham	18±6	30±11*
IR	15±5	22±7*
IPC	15±4	23±7*
IPoC	13±5	18±7*
	Cardiac Output (mL/min)	
	Baseline	ISO
Sham	48±7	66±6*
IR	36±8†	51±12*
IPC	42±9	54±11*
IPoC	33±10†	38±15
	LVDP (kPa)	
	Baseline	ISO
Sham	15±1	19±3*
IR	12±2†	17±2*
IPC	13±2†	16±3*
IPoC	12±2†	13±2
	dP/dt_{max} (kPa/s)	
	Baseline	ISO
Sham	612±58	986±251*
IR	468±148†	876±214*
IPC	515±134	872±207*
IPoC	445±114†	607±186*

Seven days after the myocardial infarction, cardiac function and hemodynamics were recorded first at a basal level and then 5 minutes after stimulation with ISO (10 nmol/L). dP/dt_{max} indicates rate of pressure rise; IPC, ischemic preconditioning; IPoC, ischemic postconditioning; IR, ischemia/reperfusion; ISO, isoproterenol; LVDP, left ventricular developed pressure. Data are means±SD of n=6 to 10 hearts.
*$P \leq 0.05$ vs baseline.
†$P \leq 0.05$ vs Sham.

Signaling Mechanisms Underlying GRK2 Induction

GRK2 is regulated both at the transcription level and to a considerable degree via its degradation, in which the E3-ubiquitin ligase Mdm2 is primarily involved.

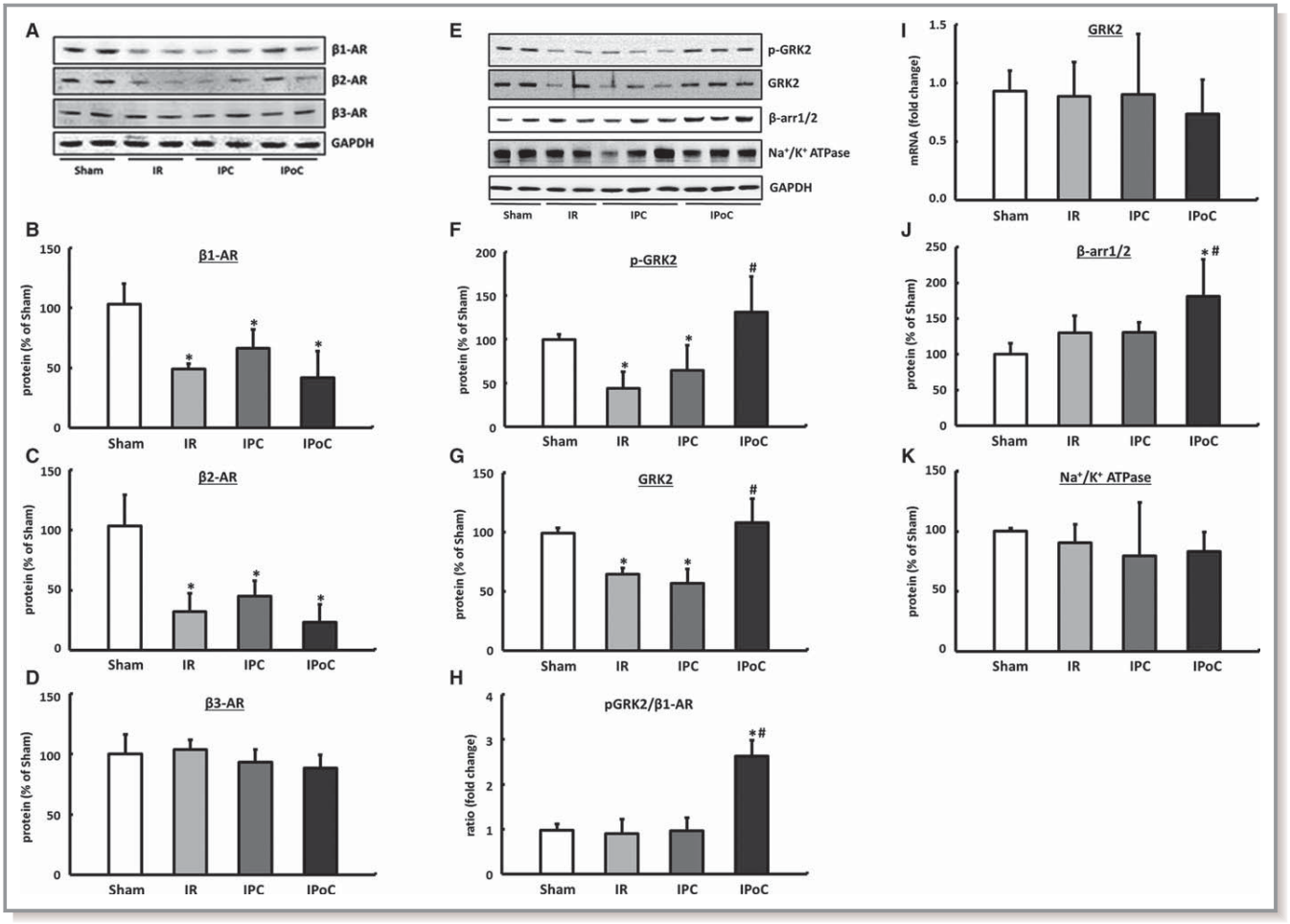

Figure 5. Expression pattern of β-ARs. A, Representative immunoblots and densitometric analysis of (B) the β_1-AR, (C) the β_2-AR and (D) the β_3-AR. Remodeling and intracellular coupling of cardiac β-ARs. E, Representative blots and densitometric data of the (F) phosphorylated and (G) total GRK2 protein. H, The pGRK2 to β_1-AR ratio was calculated for each animal, and group means were expressed as fold change of Sham. I, The mRNA expression of GRK2 was analyzed in left ventricular tissue and normalized to HPRT. J, β-Arrestin1/2, also critically involved in β-AR coupling, was exclusively upregulated in IPoC hearts. K, Na^+/K^+ ATPase was determined as a surrogate marker for the membrane density. Immunoblot bands were normalized to GAPDH and expressed as a percentage of Sham. Data are means±SD of n=6 hearts. *$P \leq 0.05$ vs Sham, $^{\#}P \leq 0.05$ vs IR. AR indicates adrenergic receptor; arr, arrestin; GAPDH, Glyceraldehyde 3-phosphate dehydrogenase; GRK2, G protein-coupled receptor kinase 2; HPRT, hypoxanthine-guanine phosphoribosyltransferase; IPC, ischemic preconditioning; IPoC, ischemic postconditioning; IR, ischemia/reperfusion; p-GRK2, phosphorylated GRK2.

The Mdm2 expression did not differ across the 4 treatment groups, but its phosphorylated fraction was significantly reduced in the IR and IPC groups compared with the sham group. In the IPoC hearts the phosphorylated fraction was significantly higher than that in the IR and IPC groups and did not differ from the hearts of the sham group (Figure 7A through 7C).

In the current study, induction or normalization of the phosphoinositide 3-kinase (PI3 kinase) (Figure 7D and 7E) was detected in IPoC hearts. Because PI3 kinase and Mdm2 have already been described as directly interacting partners, the PI3 kinase/Akt/Mdm2 signaling pathway should be primarily responsible for stabilizing the GRK2 in the hearts of the IPoC group.[30]

Discussion

The development of contractile dysfunction as a consequence of a myocardial infarction is often unavoidable, even after successful reperfusion. The reduction in the size of the infarct and metabolic disorder by applying IPC or IPoC should also enable positive functional and structural remodeling over the long term based on an improved initial short-term situation.

The key finding of this study is that, unlike ischemic preconditioning, ischemic postconditioning does not lead to functional preservation of the postischemic myocardium over the long term, despite having short-term cardioprotective potential.

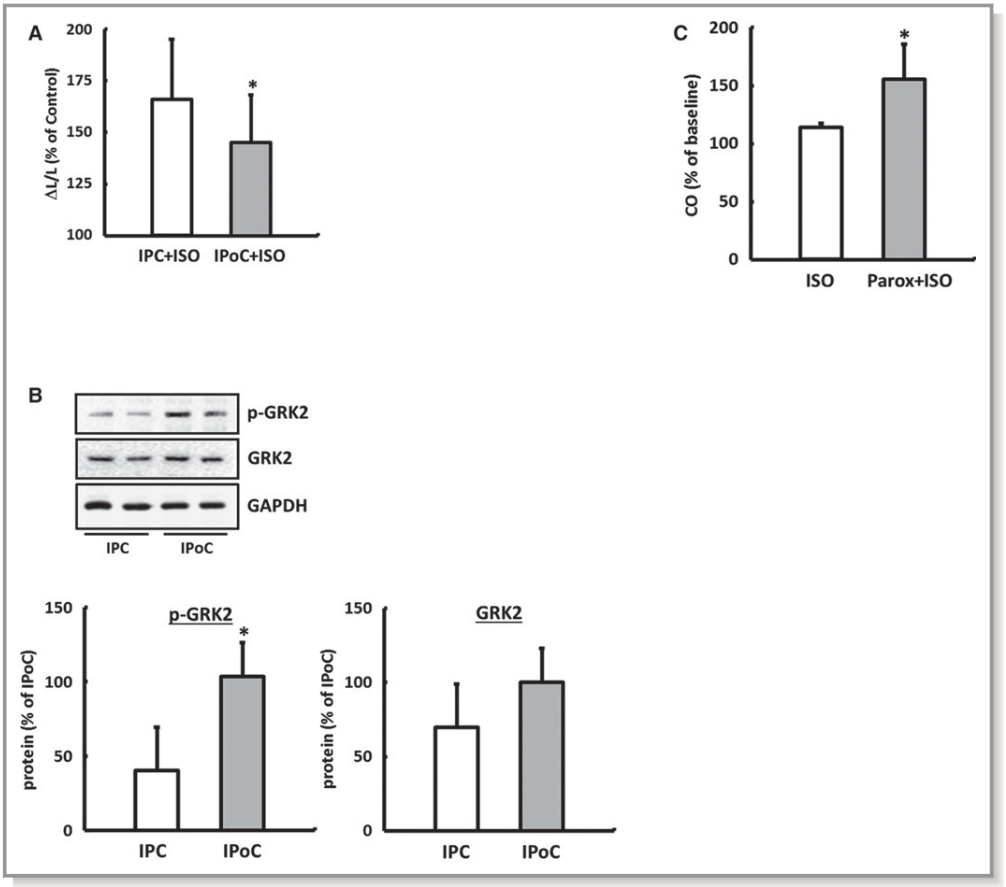

Figure 6. Remodeling of β-ARs as the main cause for the loss of the inotropic reserve in IPoC hearts. A, Responsivity of cardiomyocytes isolated from IPC or IPoC hearts to ISO was analyzed using a cell-edge detection system. B, Induction of GRK2 varied depending on whether IPC or IPoC was applied. Data are means±SD of n=4 hearts/216 cells. *$P \leq 0.05$ vs IPC. IPoC-induced loss of the β-adrenergic functional reserve. C, IPoC hearts 7 days after an infarction were perfused using the working heart technique. After 10 minutes' infusion with paroxetine, the CO was measured continuously for 5 minutes with additional stimulation using ISO. Data are means±SD of n=4 hearts. *$P \leq 0.05$ vs ISO. AR indicates adrenergic receptor; CO, cardiac output; GAPDH, Glyceraldehyde 3-phosphate dehydrogenase; GRK2, G protein-coupled receptor kinase 2; IPC, ischemic preconditioning; IPoC, ischemic postconditioning; ISO, isoprenaline; Parox, paroxetine; p-GRK2, phosphorylated GRK2.

Just 2 hours after the start of the reperfusion, the intracellular coupling of the β_1 receptor via amplified phosphorylation of GRK2 was weakened by application of IPoC. In the long term the specific induction/phosphorylation of GRK2 combined with the reduced expression of β-ARs caused molecular remodeling in the postconditioned heart, which, as a pathophysiological correlate of a contractile functional disorder, characterizes the start of systolic heart failure. IPoC-induced desensitization of the β-receptors only affected the myocardium, however, and thus only reduced the rate of pressure rise and the positive inotropic potential of the ventricle. The pacemaker cells were not affected by the application, meaning that a (desirable) frequency control was not observed. Apart from a desensitization, the coronary vessels were also able to continue ensuring myocardial perfusion as required thanks to the preservation of the β-adrenergic-receptor-mediated vasodilation.

At the moment it is largely unclear to what extent the conditioned heart also benefits over the long term from 1 of the 2 protective strategies and to what extent receptor-mediated signaling is affected by the 2 strategies. However, effective use of therapy/medication following IPC or IPoC assumes a well-founded understanding of the receptor status of the conditioned postischemic heart.[31]

The ratio of β_1 to β_2 receptors is about 70:30 in the heart. Functionally, their effect is primarily synergistic, but the β_1 receptor has a greater effect on the myocardium, whereas the β_2 receptor has a greater effect on the smooth muscle cells of the vessels. Quantitatively, the β_3-AR plays a subordinate role

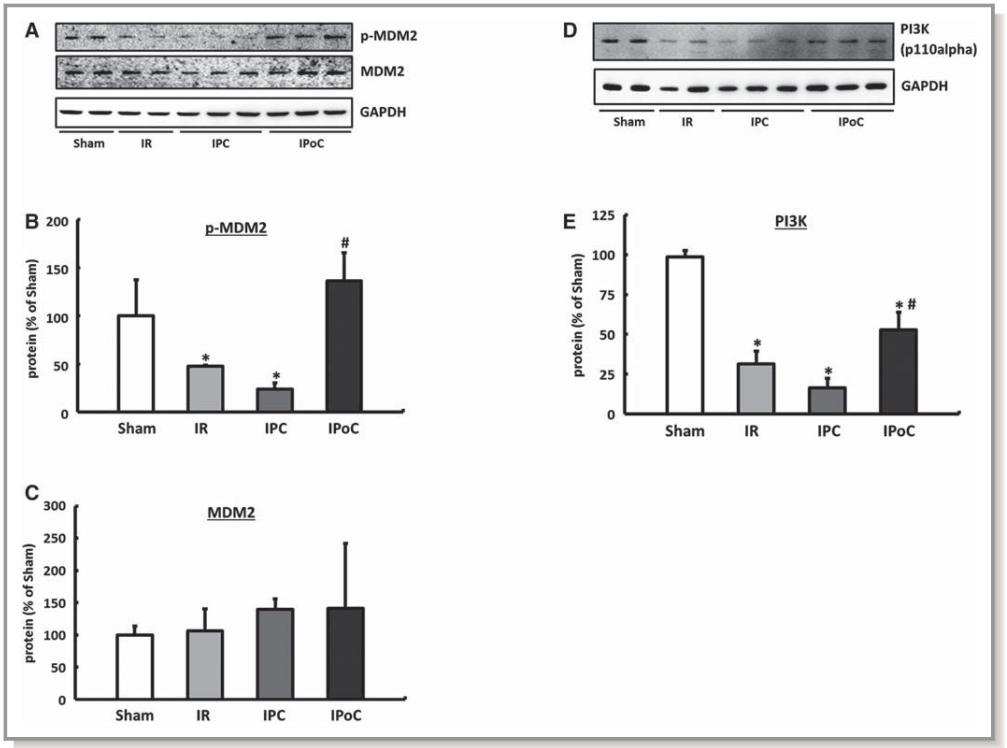

Figure 7. Regulatory mechanisms for GRK2. A, Representative immunoblots and densitometric data of the (B) phosphorylated and (C) total MDM2 protein. D, Western blot image and (E) analysis of PI3 kinase expression. Immunoblot bands were normalized to GAPDH and expressed as a percentage of Sham. Data are means±SD of n=6 hearts. **P*≤0.05 vs Sham, #*P*≤0.05 vs IR. GAPDH indicates Glyceraldehyde 3-phosphate dehydrogenase; GRK2, G protein–coupled receptor kinase 2; IPC, ischemic preconditioning; IPoC, ischemic postconditioning; IR, ischemia/reperfusion; MDM2, mouse double minute 2 homolog/E3 ubiquitin-protein ligase Mdm2; p-GRK2, phosphorylated GRK2; PI3K, phosphoinositide 3-kinase; p-MDM2, phosphorylated MDM2.

in the heart, but protective effects are attributed to it, particularly in the insufficient myocardium.[32]

No change in the protein concentration of the β_1 receptor was recorded during the 2-hour reperfusion ex vivo. The significantly reduced proportion of receptor dimers indicates, however, that remodeling of the β-adrenergic signaling has already occurred during this short period independent of the 2 intervention strategies. A reduction in the receptor dimers in turn leads to a lessening of the signal transduction and to accelerated receptor internalization.[33-36]

The in vivo protocol used led to a significant reduction in the β_1- and β_2-AR subtypes, with the expression of the β_3-AR remaining stable, in the left ventricular myocardium in the IR, IPC, and IPoC hearts 7 days after the infarction.

The effect on the intracellular coupling varied depending on whether IPC or IPoC was used. The response of the postconditioned left ventricular myocardium to a β-adrenergic stimulus was significantly reduced toward all comparator groups. Selective increases in the GRK2 protein and its phosphorylated fraction in the heart of the IPoC group were identified as the cause.

It was originally postulated that an elevation in the GRK2 level during the progression of heart failure may be a sensible protective mechanism that protects the heart against excessive exposure to catecholamines.[37] For the postinfarcted heart, rapid and transient elevation or activation of the GRK2 could reduce the reperfusion injury and protect the myocardium against hypercontractions. This mechanism may be causally involved in the initial trend toward improved recovery of postconditioned hearts compared with the IR and IPC groups in the Langendorff model. At the start of the reperfusion the IPoC-induced phosphorylation of GRK2 by CEC could be significantly reduced, and consequently the ISO-induced increase in the LVDP can be reestablished. Consequently, the activation of GRK2 should also be a PKC-dependent process in the reperfused myocardium as well.

A sustained and long-term upregulation of GRK2 with the resultant desensitization or uncoupling of cardiac receptors leads inevitably to impaired cardiac function and loss of the positive inotropic reserve.[38-40] In a transgenic mouse model, a cardiac-specific overexpression of the GRK2 inhibitor βARKct not only improved the basal and catecholamine-stimulated

heart function, it also led to a significant reduction in cardiac dysfunction and mortality in various models of heart failure.[41-43] These results were confirmed by using cardiac-specific heterozygous GRK2 knockout mice that also had a significantly better prognosis after induction of heart failure.[44]

Particularly when considering the early cardioprotective effects that can be achieved by the postconditioning protocol used here, the importance of desensitized or uncoupled β-ARs becomes clear because, along with the loss of their β-adrenergic contraction reserve, IPoC hearts have the worst heart function at rest measured using echocardiography after 7 days have elapsed.

At this point there are only a few verified findings for the precise regulatory mechanisms for GRK2 within the cardiovascular system. The expression is controlled both at the level of the transcription and by affecting the degradation and thus the stabilization of the protein.[45] The precise interplay between synthesis and degradation under physiological and pathophysiological conditions is largely unknown, but ubiquitination with subsequent proteasomal degradation is considered to play a significant role in the degradation of GRK2.[46] Both β-arrestin and the E3-ubiquitin ligase Mdm2 are also involved in this process, initiating the degradation of GRK2 by the proteasome by forming a complex.[47] Various functions are attributed to β-arrestin as part of the regulatory mechanisms that underlie the receptor coupling or desensitization. Together with GRK2, it is directly involved in the uncoupling and internalization of G-protein-coupled receptors. Furthermore, in the absence of receptor stimulation, it can inhibit GRK2-Mdm2 interaction and thus the degradation of GRK2, but if the receptor is stimulated, it can boost complex formation and thus the degradation of GRK2.[48]

Based on the present results, the significant increase in GRK2 levels in IPoC hearts can be ascribed to impaired degradation that is caused by increased phosphorylation of Mdm2. Phosphorylated Mdm2 translocates increasingly into the nucleus and is thus no longer available for ubiquitination of GRK2 in the cytosol. It is also postulated that the interaction between phosphorylated Mdm2 and GRK2 is impaired, and subsequently, the complex cannot be transported to the proteasome.[47]

PI3 kinase and Akt have already been identified as direct upstream elements of Mdm2 and are considered responsible for its phosphorylation.[30,49,50] The induction of both PI3 kinase and Akt plays a crucial role in cardioprotection during IPoC and is classified as a key element of the prosurvival RISK pathway.[51,52]

The functional effects of a pharmacological GRK2 inhibition could be demonstrated in both isolated cardiomyocytes and in the isolated, perfused heart. In the IPoC heart, the CO could only be significantly elevated by β-adrenergic stimulation with selective inhibition of GRK2. These findings emphasize not only the importance of GRK2 for cardiac function, they also identify GRK2 as the reason for the loss of inotropic functional reserve of the postconditioned myocardium. GRK2 is currently being considered as a therapeutic target for chronic heart failure.[53] Along with the cardioprotective potential immediately after the start of reperfusion, selective inhibition of GRK2 could also achieve significant functional improvement in the postconditioned myocardium over the long term (Figure 8).

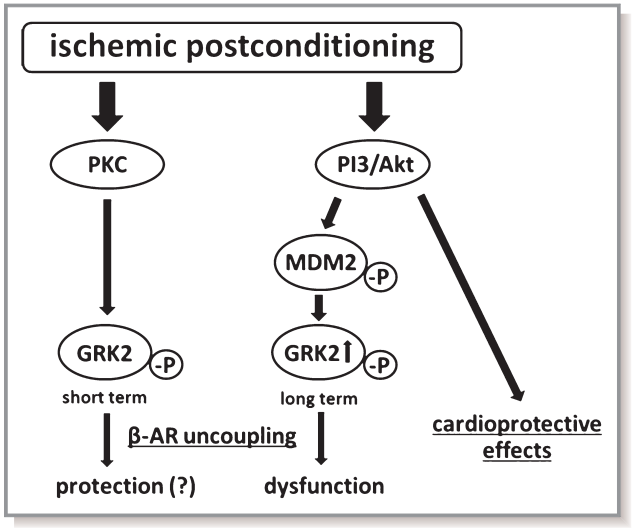

Figure 8. IPoC-induced desensitization of β-ARs. In the short term, rapid and transient activation of the GRK2 could reduce the reperfusion injury and protect the myocardium against hypercontractions. In the long term, however, stabilization of GRK2 and its phosphorylated fraction leads to a desensitization or decoupling of β-ARs with a resultant loss of the positive inotropic functional reserve. AR indicates adrenergic receptor; GRK2, G protein-coupled receptor kinase 2; MDM2, mouse double minute 2 homolog/E3 ubiquitin-protein ligase Mdm2; PI3, phosphoinositide 3-kinase; PKC, protein kinase C.

In summary, the results of this study demonstrate for the first time that the application of IPoC induces desensitization or uncoupling of β-ARs, which leads to induction of cardiac dysfunction with a restricted inotropic functional reserve. With comparable cardioprotective properties immediately after acute myocardial infarction, IPC also ensures that the function of the postischemic myocardium is preserved over the long term without exerting a negative effect on the β-adrenergic system. The present results must be considered a possible reason behind the disappointing results obtained in longitudinal clinical studies to date and should lead to a critical review of the clinical use of IPoC.

Sources of Funding

The study was supported by the Deutsche Stiftung für Herzforschung and by the "János Bolyai Scholarship" of the Hungarian Academy of Sciences (Bencsik, Csonka);

Ferdinandy was a Szentágothai Fellow of the National Program of Excellence (Grant TAMOP 4.2.4.A/2-11-1-2012-0001).

Disclosures

None.

References

1. Hausenloy DJ, Yellon DM. Survival kinases in ischemic preconditioning and postconditioning. *Cardiovasc Res*. 2006;70:240–253.
2. Zhao ZQ, Corvera JS, Halkos ME, Kerendi F, Wang NP, Guyton RA, Vinten-Johansen J. Inhibition of myocardial injury by ischemic postconditioning during reperfusion: comparison with ischemic preconditioning. *Am J Physiol Heart Circ Physiol*. 2003;285:H579–H588.
3. Heusch G. Molecular basis of cardioprotection: signal transduction in ischemic pre-, post-, and remote conditioning. *Circ Res*. 2015;116:674–699.
4. van Vuuren D, Genis A, Genade S, Lochner A. Postconditioning the isolated working rat heart. *Cardiovasc Drugs Ther*. 2008;22:391–397.
5. Couvreur N, Lucats L, Tissier R, Bize A, Berdeaux A, Ghaleb B. Differential effects of postconditioning on myocardial stunning and infarction: a study in conscious dogs and anesthetized rabbits. *Am J Physiol Heart Circ Physiol*. 2006;291:H1345–H1350.
6. Staat P, Rioufol G, Piot C, Cottin Y, Cung TT, L'Huillier I, Aupetit JF, Bonnefoy E, Finet G, André-Fouët X, Ovize M. Postconditioning the human heart. *Circulation*. 2005;112:2143–2148.
7. Granfeldt A, Lefer DJ, Vinten-Johansen J. Protective ischaemia in patients: preconditioning and postconditioning. *Cardiovasc Res*. 2009;83:234–246.
8. Hausenloy DJ, Erik Bøtker H, Condorelli G, Ferdinandy P, Garcia-Dorado D, Heusch G, Lecour S, van Laake LW, Madonna R, Ruiz-Meana M, Schulz R, Sluijter JP, Yellon DM, Ovize M. Translating cardioprotection for patient benefit: position paper from the Working Group of Cellular Biology of the Heart of the European Society of Cardiology. *Cardiovasc Res*. 2013;98:7–27.
9. Freixa X, Bellera N, Ortiz-Pérez JT, Jiménez M, Paré C, Bosch X, De Caralt TM, Betriu A, Masotti M. Ischaemic postconditioning revisited: lack of effects on infarct size following primary percutaneous coronary intervention. *Eur Heart J*. 2012;33:103–112.
10. Hahn JY, Yu CW, Park HS, Song YB, Kim EK, Lee HJ, Bae JW, Chung WY, Choi SH, Choi JH, Bae JH, An KJ, Park JS, Oh JH, Kim SW, Hwang JY, Ryu JK, Lim DS, Gwon HC. Long-term effects of ischemic postconditioning on clinical outcomes: 1-year follow-up of the POST randomized trial. *Am Heart J*. 2015;169:639–646.
11. Engstrøm T, Kelbæk H, Helqvist S, Høfsten DE, Kløvgaard L, Clemmensen P, Holmvang L, Jørgensen E, Pedersen F, Saunamaki K, Ravkilde J, Tilsted HH, Villadsen A, Aarøe J, Jensen SE, Raungaard B, Bøtker HE, Terkelsen CJ, Maeng M, Kaltoft A, Krusell LR, Jensen LO, Veien KT, Kofoed KF, Torp-Pedersen C, Kyhl K, Nepper-Christensen L, Treiman M, Vejlstrup N, Ahtarovski K, Lønborg J, Køber L; Third Danish Study of Optimal Acute Treatment of Patients With ST Elevation Myocardial Infarction–Ischemic Postconditioning (DANAMI-3–iPOST) Investigators. Effect of ischemic postconditioning during primary percutaneous coronary intervention for patients with ST-segment elevation myocardial infarction: a randomized clinical trial. *JAMA Cardiol*. 2017;2:490–497.
12. Ferdinandy P, Schulz R, Baxter GF. Interaction of cardiovascular risk factors with myocardial ischemia/reperfusion injury, preconditioning, and postconditioning. *Pharmacol Rev*. 2007;59:418–458.
13. Lecour S, Bøtker HE, Condorelli G, Davidson SM, Garcia-Dorado D, Engel FB, Ferdinandy P, Heusch G, Madonna R, Ovize M, Ruiz-Meana M, Schulz R, Sluijter JP, Van Laake LW, Yellon DM, Hausenloy DJ. ESC working group cellular biology of the heart: position paper: improving the preclinical assessment of novel cardioprotective therapies. *Cardiovasc Res*. 2014;104:399–411.
14. Ferdinandy P, Hausenloy DJ, Heusch G, Baxter GF, Schulz R. Interaction of risk factors, comorbidities, and comedications with ischemia/reperfusion injury and cardioprotection by preconditioning, postconditioning, and remote conditioning. *Pharmacol Rev*. 2014;66:1142–1174.
15. Schreckenberg R, Maier T, Schlüter KD. Post-conditioning restores pre-ischaemic receptor coupling in rat isolated hearts. *Br J Pharmacol*. 2009;156:901–908.
16. White DC, Hata JA, Shah AS, Glower DD, Lefkowitz RJ, Koch WJ. Preservation of myocardial β-adrenergic receptor signaling delays the development of heart failure after myocardial infarction. *Proc Natl Acad Sci USA*. 2000;97:5428–5433.
17. Anthonio RL, Brodde OE, van Veldhuisen DJ, Scholtens E, Crijns HJ, van Gilst WH. β-Adrenoceptor density in chronic infarcted myocardium: a subtype specific decrease of β_1-adrenoceptor density. *Int J Cardiol*. 2000;72:137–141.
18. Strasser RH, Marquetant R. Sensitization of the beta-adrenergic system in acute myocardial ischaemia by a protein kinase C-dependent mechanism. *Eur Heart J*. 1991;12:48–53.
19. Nazarewicz RR, Bikineyeva A, Dikalov SI. Rapid and specific measurements of superoxide using fluorescence spectroscopy. *J Biomol Screen*. 2013;18:498–503.
20. Bencsik P, Kupai K, Giricz Z, Görbe A, Pipis J, Murlasits Z, Kocsis GF, Varga-Orvos Z, Puskás LG, Csonka C, Csont T, Ferdinandy P. Role of iNOS and peroxynitrite-matrix metalloproteinase-2 signaling in myocardial late preconditioning in rats. *Am J Physiol Heart Circ Physiol*. 2010;299:H512–H518.
21. Bencsik P, Pálóczi J, Kocsis GF, Pipis J, Belecz I, Varga ZV, Csonka C, Görbe A, Csont T, Ferdinandy P. Moderate inhibition of myocardial matrix metalloproteinase-2 by ilomastat is cardioprotective. *Pharmacol Res*. 2014;80:36–42.
22. Kocsis GF, Sárközy M, Bencsik P, Pipicz M, Varga ZV, Pálóczi J, Csonka C, Ferdinandy P, Csont T. Preconditioning protects the heart in a prolonged uremic condition. *Am J Physiol Heart Circ Physiol*. 2012;303:H1229–H1236.
23. Neely JR, Liebermeister H, Battersby EJ, Morgan HE. Effect of pressure development on oxygen consumption by isolated rat heart. *Am J Physiol*. 1967;212:804–814.
24. Ferdinandy P, Szilvássy Z, Csont T, Csonka C, Nagy E, Koltai M, Dux L. Nitroglycerin-induced direct protection of the ischaemic myocardium in isolated working hearts of rats with vascular tolerance to nitroglycerin. *Br J Pharmacol*. 1995;115:1129–1131.
25. Ferdinandy P, Csonka C, Csont T, Szilvássy Z, Dux L. Rapid pacing-induced preconditioning is recaptured by farnesol treatment in hearts of cholesterol-fed rats: role of polyprenyl derivatives and nitric oxide. *Mol Cell Biochem*. 1998;186:27–34.
26. Csonka C, Kupai K, Kocsis GF, Novák G, Fekete V, Bencsik P, Csont T, Ferdinandy P. Measurement of myocardial infarct size in preclinical studies. *J Pharmacol Toxicol Methods*. 2010;61:163–170.
27. Livak KJ, Schmittgen TD. Analysis of relative gene expression data using real-time quantitative PCR and the $2(-\Delta\Delta C(T))$. *Methods*. 2001;25:402–408.
28. Tastan I, Schreckenberg R, Mufti S, Abdallah Y, Piper HM, Schlüter KD. Parathyroid hormone improves contractile performance of adult rat ventricular cardiomyocytes at low concentrations in a non-acute way. *Cardiovasc Res*. 2009;82:77–83.
29. Krasel C, Dammeier S, Winstel R, Brockmann J, Mischak H, Lohse MJ. Phosphorylation of GRK2 by protein kinase C abolishes its inhibition by calmodulin. *J Biol Chem*. 2001;276:1911–1915.
30. Mayo LD, Donner DB. A phosphatidylinositol 3-kinase/Akt pathway promotes translocation of Mdm2 from the cytoplasm to the nucleus. *Proc Natl Acad Sci USA*. 2001;98:11598–11603.
31. Ovize M, Baxter GF, Di Lisa F, Ferdinandy P, Garcia-Dorado D, Hausenloy DJ, Heusch G, Vinten-Johansen J, Yellon DM, Schulz R. Postconditioning and protection from reperfusion injury: where do we stand? *Cardiovasc Res*. 2010;87:406–423.
32. Niu X, Watts VL, Cingolani OH, Sivakumaran V, Leyton-Mange JS, Ellis CL, Miller KL, Vandegaer K, Bedja D, Gabrielson KL, Paolocci N, Kass DA, Barouch LA. Cardioprotective effect of beta-3 adrenergic receptor agonism: role of neuronal nitric oxide synthase. *J Am Coll Cardiol*. 2012;59:1979–1987.
33. Lan TH, Kuravi S, Lambert NA. Internalization dissociates β_2-adrenergic receptors. *PLoS One*. 2011;6:e17361.
34. He J, Xu J, Castleberry AM, Lau AG, Hall RA. Glycosylation of beta(1)-adrenergic receptors regulates receptor surface expression and dimerization. *Biochem Biophys Res Commun*. 2002;297:565–572.
35. Hebert TE, Moffett S, Morello JP, Loisel TP, Bichet DG, Barret C, Bouvier M. A peptide derived from a beta2-adrenergic receptor transmembrane domain inhibits both receptor dimerization and activation. *J Biol Chem*. 1996;271:16384–16392.
36. Kobayashi H, Ogawa K, Yao R, Lichtarge O, Bouvier M. Functional rescue of β_1-adrenoceptor dimerization and trafficking by pharmacological chaperones. *Traffic*. 2009;10:1019–1033.
37. Matkovich SJ, Diwan A, Klanke JL, Hammer DJ, Marreez Y, Odley AM, Brunskill EW, Koch WJ, Schwartz RJ, Dorn GW II. Cardiac-specific ablation of G-protein receptor kinase 2 redefines its roles in heart development and β-adrenergic signaling. *Circ Res*. 2006;99:996–1003.
38. Koch WJ, Rockman HA, Samama P, Hamilton RA, Bond RA, Milano CA, Lefkowitz RJ. Cardiac function in mice overexpressing the beta-adrenergic receptor kinase or a beta ARK inhibitor. *Science*. 1995;268:1350–1353.

39. Lymperopoulos A. GRK2 and β-arrestins in cardiovascular disease: something old, something new. *Am J Cardiovasc Dis*. 2011;1:126–237.
40. Raake PW, Zhang X, Vinge LE, Brinks H, Gao E, Jaleel N, Li Y, Tang M, Most P, Dorn GW II, Houser SR, Katus HA, Chen X, Koch WJ. Cardiac G-protein-coupled receptor kinase 2 ablation induces a novel Ca^{2+} handling phenotype resistant to adverse alterations and remodeling after myocardial infarction. *Circulation*. 2012;125:2108–2118.
41. Tevaearai HT, Walton GB, Keys JR, Koch WJ, Eckhart AD. Acute ischemic cardiac dysfunction is attenuated via gene transfer of a peptide inhibitor of the β-adrenergic receptor kinase (βARK1). *J Gene Med*. 2005;7:1172–1177.
42. Harding VB, Jones LR, Lefkowitz RJ, Koch WJ, Rockman HA. Cardiac βARK1 inhibition prolongs survival and augments β-blocker therapy in a mouse model of severe heart failure. *Proc Natl Acad Sci USA*. 2001;98:5809–5814.
43. Siryk-Bathgate A, Dabul S, Lymperopoulos A. Current and future G protein-coupled receptor signaling targets for heart failure therapy. *Drug Des Devel Ther*. 2013;7:1209–1222.
44. Rockman HA, Choi DJ, Akhter SA, Jaber M, Giros B, Lefkowitz RJ, Caron MG, Koch WJ. Control of myocardial contractile function by the level of beta-adrenergic receptor kinase 1 in gene-targeted mice. *J Biol Chem*. 1998;273:18180–18184.
45. Penela P, Murga C, Ribas C, Tutor AS, Peregrín S, Mayor F Jr. Mechanisms of regulation of G protein-coupled receptor kinases (GRKs) and cardiovascular disease. *Cardiovasc Res*. 2006;69:46–56.
46. Penela P, Ruiz-Gómez A, Castaño JG, Mayor F Jr. Degradation of the G protein-coupled receptor kinase 2 by the proteasome pathway. *J Biol Chem*. 1998;273:35238–35244.
47. Salcedo A, Mayor F Jr, Penela P. Mdm2 is involved in the ubiquitination and degradation of G-protein-coupled receptor kinase 2. *EMBO J*. 2006;25:4752–4762.
48. Nogués L, Salcedo A, Mayor F Jr, Penela P. Multiple scaffolding functions of {beta}-arrestins in the degradation of G protein-coupled receptor kinase 2. *J Biol Chem*. 2011;286:1165–1173.
49. Feng J, Tamaskovic R, Yang Z, Brazil DP, Merlo A, Hess D, Hemmings BA. Stabilization of Mdm2 via decreased ubiquitination is mediated by protein kinase B/Akt-dependent phosphorylation. *J Biol Chem*. 2004;279:35510–35517.
50. Ogawara Y, Kishishita S, Obata T, Isazawa Y, Suzuki T, Tanaka K, Masuyama N, Gotoh Y. Akt enhances Mdm2-mediated ubiquitination and degradation of p53. *J Biol Chem*. 2002;277:21843–21850.
51. Tsang A, Hausenloy DJ, Mocanu MM, Yellon DM. Postconditioning: a form of "modified reperfusion" protects the myocardium by activating the phosphatidylinositol 3-kinase-Akt pathway. *Circ Res*. 2004;95:230–232.
52. Zhu M, Feng J, Lucchinetti E, Fischer G, Xu L, Pedrazzini T, Schaub MC, Zaugg M. Ischemic postconditioning protects remodeled myocardium via the PI3K-PKB/Akt reperfusion injury salvage kinase pathway. *Cardiovasc Res*. 2006;72:152–162.
53. Schumacher-Bass SM, Traynham CJ, Koch WJ. G protein-coupled receptor kinase 2 as a therapeutic target for heart failure. *Drug Discov Today Ther Strateg*. 2012;9:155–162.

SUPPLEMENTAL MATERIAL

Table S1. Functional and morphological data assessed by echocardiography.

	Sham	IR	IPC	IPoC
FS (%)	59.8±11.9	42.9±10.3*	49.8±13.9	32.2±12.0*
IVSd (mm)	1.65±0.50	1.74±0.32	1.83±0.40	1,52±0.23
LVPWd (mm)	1.62±0.37	1.84±0.22	1.90±0.34	1.86±0.32
LVPWs (mm)	2.53±0.34	2.71±0.44	2.86±0.47	2.61±0.60
LVIDd (mm)	5.25±0.89	5.75±1.28	5.52±0.94	6.03±0.58
LVIDs (mm)	2.69±1.32	3.23±0.90	2.88±1.10	3.43±0.63

FS (%): fractional shortening, IVSd (mm): end-diastolic interventricular septum thickness, LVPWd (mm): left ventricular posterior wall thickness in diastole, LVPWs (mm): left ventricular posterior wall thickness in systole, LVIDd (mm): left ventricular internal diameter in diastole, LVIDs (mm): left ventricular internal diameter in systole. Data are means ± S.D. of n=6-10 animals. *, p≤0.05 vs. Sham.

Figure S1. The validity of TnI as a marker to determine the infarct size.

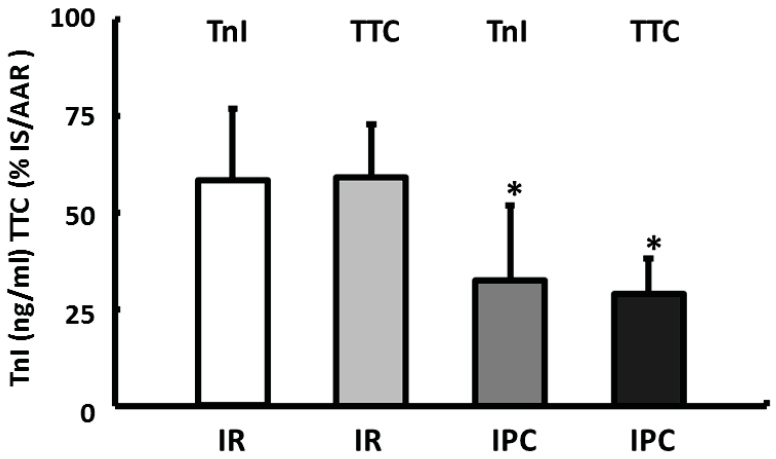

Plasma TnI values that were measured one hour after the start of the reperfusion confirm a reduction of the particular size of the infarct to the same magnitude as determined using TTC staining two hours after the start of the reperfusion. Data are means ± S.D. of n=6 hearts. *, p≤0.05 vs. IR.

Figure S2. Expression pattern of β-ARs in left ventricular tissue.

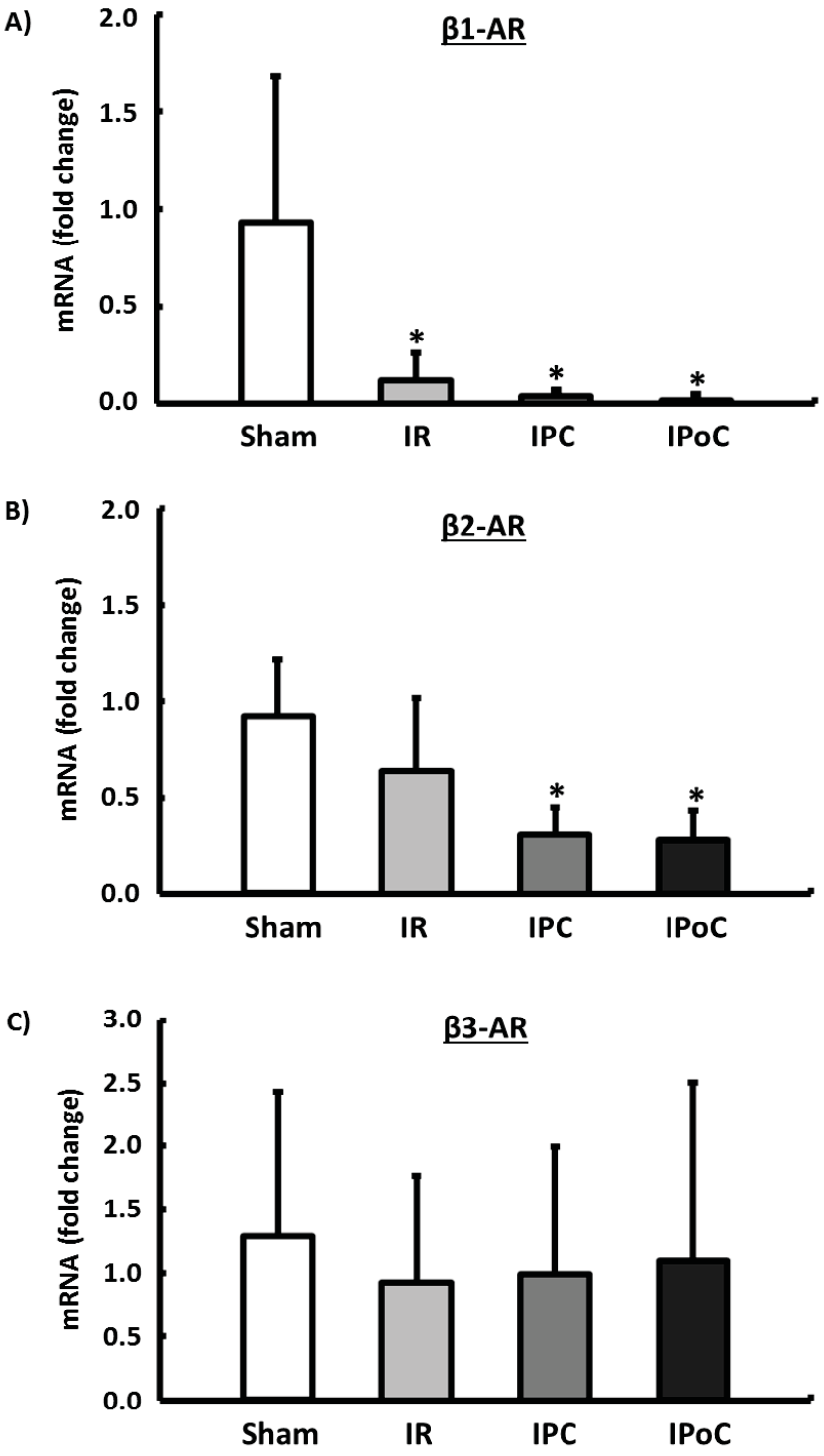

A-C) The mRNA expression of the β_1- and β_2-AR subtypes was reduced in the hearts in the IR, IPC and IPoC groups compared to the sham group seven days after the infarction. However, the expression of the β_3-AR remained stable and was unaffected by either IPC or IPoC. Data are means ± S.D. of n=6 hearts. *, $p \leq 0.05$ vs. Sham.

Figure S3. The effect of GRK2 and β-arrestin on the contraction of isolated ventricular cardiomyocytes.

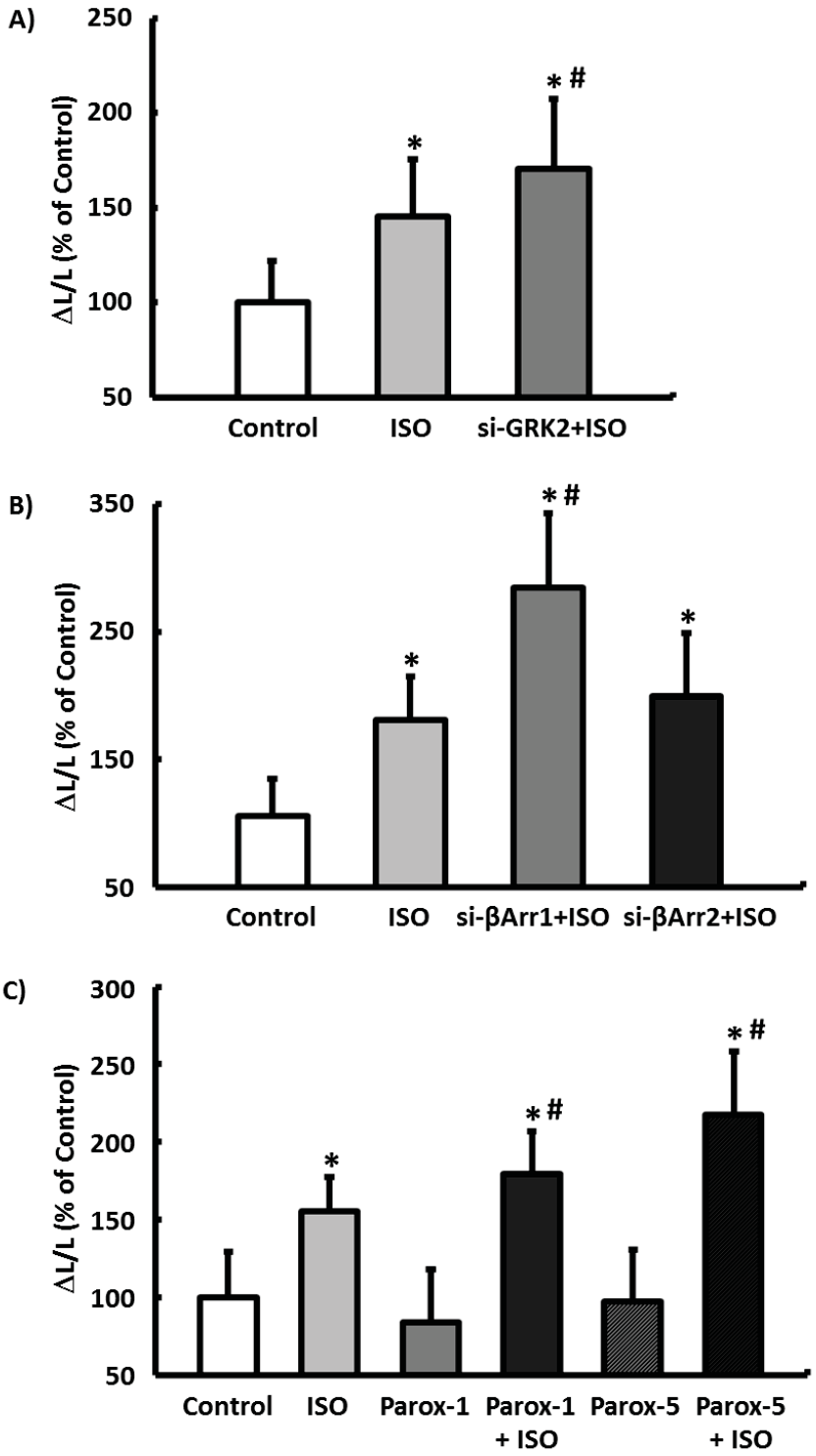

The importance of GRK2 and β-arrestin for the β-AR–mediated positive inotropic response of the myocardium was investigated using a model of left ventricular cardiomyocytes isolated from three-month-old Wistar rats. GRK2, β-arrestin 1

and β-arrestin 2 were selectively and effectively downregulated by transfection with siRNA over 24 hours (Figure S6A,B). The load free cell shortening before and after stimulation with ISO was then determined. **A)** In untreated cardiomyocytes ISO improved basal cell shortening by 45±9%. Cardiomyocytes in which the GRK2 was previously downregulated were sensitised to the β-adrenergic stimulus and showed an improvement in the cell shortening of about 70 ±15%. **B)** Specifically knocking down the β-arrestin 1 isoform improved the ISO-induced cell shortening by 57±12% while the β-adrenergic stimulation after successful knockdown of β-arrestin 2 did not differ significantly from ISO treated cells. Transfection of the cardiomyocytes with nonsense siRNA over 24 hours did not have any effect on cell shortening. **C)** The use of GRK2-specific siRNA was supplemented in the cell culture model described above by application of the selective GRK2 inhibitor paroxetine. After a 15-minute pre-incubation with paroxetine, the ISO-induced increase in cell shortening increased in a concentration-dependent manner from 55±8% to 79±12% (1 μM) and to 117 ±22% (5 μM). Data are means± S.D. of n=3 hearts. *, p≤0.05 vs. Control, #, p≤0.05 vs. ISO.

Figure S4. The functional relevance of GRK2 in ex-vivo perfused hearts.

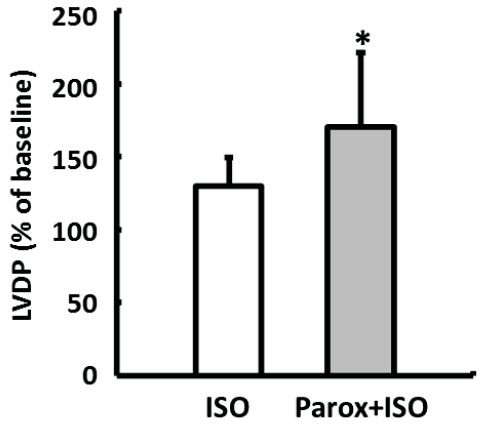

Using the Langendorff technique, rat hearts were initially perfused for 10 min with paroxetine and then stimulated for a further 5 min with ISO in the presence of paroxetine. Hearts that had not had their GRK2 inhibited responded to the β-adrenergic stimulation with an increase in the LVDP of 30±20% while the LVDP of hearts perfused with paroxetine increased by 71 ±51%. Data are means ± S.D. of n=4 hearts. *, p≤0.05 vs. ISO.

Figure S5. Concentration – response curves to isoprenaline (ISO) in isolated cardiomyocytes.

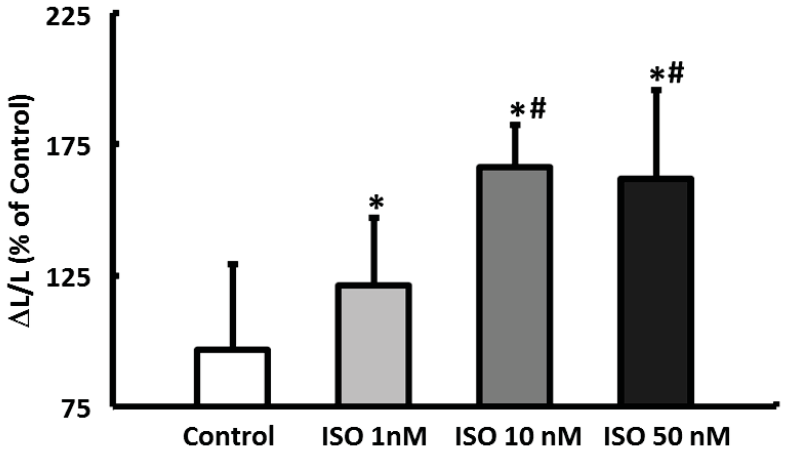

Left ventricular cardiomyocytes isolated from three-month-old Wistar rats were used to determine the ISO concentration used in all experiments to measure the β-AR–mediated positive inotropic response. The ISO-induced increase in cell shortening increased in a concentration-dependent, however, concentrations above 10 nM had no further effects. Data are means ± S.D. of n=3 hearts. *, p≤0.05 vs. Control, #, p≤0.05 vs. ISO 1 nM.

Figure S6. Western blot analysis to assess the efficiency of the siRNA-mediated knockdown.

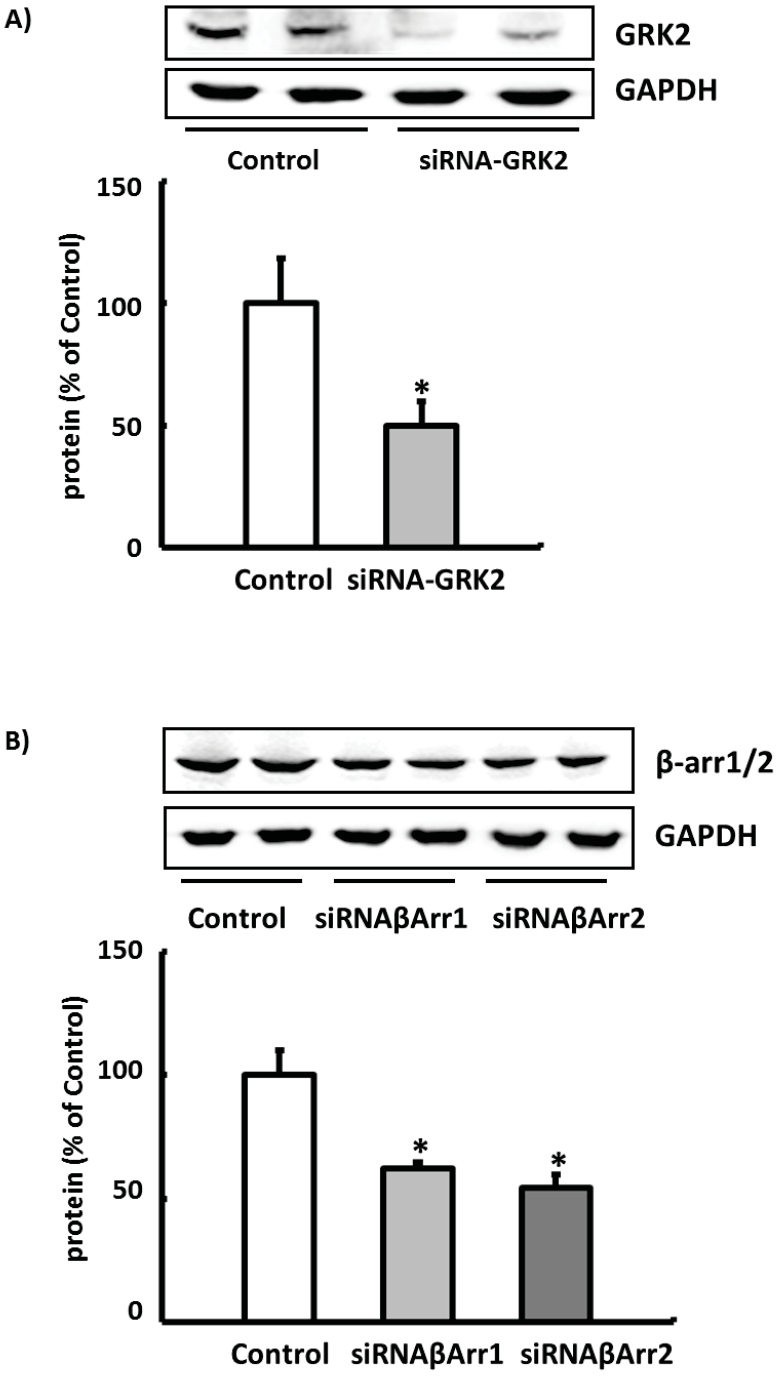

A-B) Representative immunoblots and densitometric analysis: the expression of GRK2 (A), β-arrestin1 and β-arrestin2 (B) was analysed 24 hours after transfection of isolated cardiomyocytes. Data are means ± S.D. of n=3 hearts. *, p≤0.05 vs. Control.

PLOS ONE

RESEARCH ARTICLE

The Effects of Swiprosin-1 on the Formation of Pseudopodia-Like Structures and β-Adrenoceptor Coupling in Cultured Adult Rat Ventricular Cardiomyocytes

Franziska Nippert*, Rolf Schreckenberg, Antonia Hess, Martin Weber, Klaus-Dieter Schlüter

Institute of Physiology, Justus-Liebig-University, Giessen, Germany

* Franziska.Nippert@physiologie.med.uni-giessen.de

OPEN ACCESS

Citation: Nippert F, Schreckenberg R, Hess A, Weber M, Schlüter K-D (2016) The Effects of Swiprosin-1 on the Formation of Pseudopodia-Like Structures and β-Adrenoceptor Coupling in Cultured Adult Rat Ventricular Cardiomyocytes. PLoS ONE 11(12): e0167655. doi:10.1371/journal.pone.0167655

Editor: Katherine Yutzey, Cincinnati Children's Hospital Medical Center, UNITED STATES

Received: August 12, 2016

Accepted: November 17, 2016

Published: December 16, 2016

Data Availability Statement: All relevant data are within the paper and its Supporting Information files.

Funding: The study was supported by the Deutsche Forschungsgemeinschaft (grant Schl 324/7-1; Klaus-Dieter Schlüter). The funders had no role in study design, data collection and analysis, decision to publish, or preparation of the manuscript.

Abstract

Background

Recent findings suggest that adult terminally differentiated cardiomyocytes adapt to stress by cellular de- and redifferentiation. In the present study we tested the hypothesis that swiprosin-1 is a key player in this process. Furthermore, the relationship between swiprosin-1 and β-adrenoceptor coupling was analyzed.

Methods

In order to study the function of swiprosin-1 in adult rat ventricular cardiomyocytes (ARVC) they were isolated and cultured in a medium containing 20% fetal calf serum (FCS). Changes in cell morphology of ARVC during cultivation were quantified by light and confocal laser scan microscopy. Small interfering RNA (siRNA) was used to reduce the expression of swiprosin-1. The impact of calcium on swiprosin-1 dependent processes was investigated with Bapta-AM. Immunoblot techniques and qRT-PCR were performed to measure mRNA and protein expression.

Results

In culture, ARVC first lost their contractile elements, which was followed by a formation of pseudopodia-like structures (spreading). Swiprosin-1 was detected in ARVC at all time points. However, swiprosin-1 expression was increased when ARVC started to spread. Reduction of swiprosin-1 expression with siRNA delayed ARVC spreading. Similarly, Bapta-AM attenuated swiprosin-1 expression and spreading of ARVC. Furthermore, swiprosin-1 expression correlated with the expression of G protein-coupled receptor kinase 2 (GRK2). Moreover, silencing of swiprosin-1 was associated with a down regulation of GRK2 and caused a sensitization of β-adrenergic receptors.

Competing Interests: The authors have declared that no competing interests exist.

Conclusion

Swiprosin-1 is required for ARVC to adapt to culture conditions. Additionally, it seems to be involved in the desensitization of β-adrenergic receptors. Assuming that ARVC adapt to cardiac stress in a similar way, swiprosin-1 may play a key role in cardiac remodeling.

Introduction

Neonatal cardiomyocytes have the ability to perform mitosis, however this capability vanishes within the first week post-partum. Terminally differentiated adult cardiomyocytes have lost the ability to proliferate [1]. However, cardiomyocytes are able to adapt to cardiac stress like hypertension, cell loss and aging. Recent findings suggest that adaptation is a complex process of cellular dedifferentiation and redifferentiation [2–6]. Adult rat ventricular cardiomyocytes (ARVC) in culture perform severe structural changes including sarcomere disassembly and reformation [7]. This is accompanied by a reexpression of fetal-type genes like β-myosin heavy chain (β-MHC) and α-smooth muscle actin (α-sm-actin) [8,9]. In culture ARVC form new sarcomeres alongside actin-driven stress fibers. This is preceded by the formation of pseudopodia-like structures, a process known as cell spreading. As a result, ARVC in culture transform into widespread, polymorphic cells [9]. The trigger that induces spreading is still unknown. We hypothesize that swiprosin-1, an actin-binding protein, plays a key role in this process. In a dimeric form Swiprosin-1, also known as EF-Hand Domain Family Member D2 (EFhd2), stabilizes F-actin filaments by blocking the binding site of cofilin. Cofilin is needed for the depolymerization of F-actin [10]. To date, swiprosin-1 has been only described in immune cells and in non-lymphatic brain tissue [10–12]. In immune cells it triggers the formation of lamellopodia which enable macrophages to migrate [10–12]. With the present study, we hypothesize that swiprosin-1 is required for the formation of pseudopodia-like structures (spreading) in ARVC.

The heart responds to pathological stress like hypertension or ischemia by hypertrophy, which eventually leads to maladaptive cardiac remodeling and finally heart failure. Some of these maladaptive processes are calcium-calcineurin-dependent [13–16]. However, not all changes linked to maladaptation may be explained by calcineurin activation, even though high diastolic calcium levels seem to be a trigger [13,15]. Notably, calcium is also required for swiprosin-1 activation by being involved in the formation of swiprosin-1 dimers which block the binding of cofilin [10,11]. Therefore, it may hamper cofilin activity. Activation of swiprosin-1 by calcium and its ability to stabilize actin stress fibers encouraged us to analyze whether ARVC express swiprosin-1, and whether swiprosin-1 is required for the formation of pseudopodia-like structures in these cells. The latter are necessary for the subsequent rearrangement of sarcomeres. Accordingly, we re-established the above described model of cultivation of ARVC. As a control molecule that has already been identified to be required in the process of spreading, oncostatin M was investigated [4]. Additionally, former studies have shown a reduction of β-adrenoceptor responsiveness under the same culture conditions that induce spreading of cardiomyocytes [17–19]. Therefore, we correlated swiprosin-1 expression with genes known to interfere with β-adrenoceptor-coupling.

Taken together, our study was done on the basis of recent discoveries that cardiac de- and redifferentiation as it occurs under culture conditions mimics features seen *in vivo* during cardiac remodeling [2,4]. We want to identify if swiprosin-1 plays a key role in the process of de- and redifferentiation and by that may be involved in the process of cardiac remodeling.

Materials, Animals and Protocols

The investigation was conducted according to the Guide for the Care and Use of Laboratory Animals published by the US National Institute of Health (NIH Publication No. 85–23, revised 1996). The protocol was approved by the Justus Liebig University Giessen (permission number: 507_M). Sacrifice was performed under isoflurane anesthesia, all efforts were made to minimize suffering of the animals.

Isolation and cultivation of adult rat ventricular cardiomyocytes

Ventricular cardiomyocytes of four month old male Wistar rats were isolated as described previously [20]. Briefly, the rat was sacrificed by cervical dislocation under deep anesthesia with isoflurane. The heart was immediately transferred into ice-cold saline solution. It was fixated on the cannula of a Langendorff perfusion system, followed by a 25 minute perfusion with Powell medium (80ml) containing collagenase (25mg) and $CaCl_2$ (25μM) at 37˚C. Subsequently, ventricular tissue was minced and incubated in 5ml of the re-circulated buffer for five minutes. The remaining cell solution was filtered through a nylon mesh (200μm). After centrifugation and stepwise addition of $CaCl_2$ (200μM, 400μM and 1000μM) cells were plated on petry dishes, coated with 4% (vol/vol) fetal calf serum (FCS). After one hour, the medium (medium 199) supplemented with carnitine (2mM), creatin (5mM), taurine (5mM), penicillin-streptomycin (2%) and 20% FCS was refreshed. Cytosine-β-arabinofuranoside (10mM) was supplemented to hamper the proliferation of any contaminating cells. The incubator was held at 37˚C.

Small interfering RNA (siRNA; FlexiTube siRNA Swiprosin, QIAGEN, Netherlands) at a concentration of 0.05μM was used to decease the expression of swiprosin-1. Scrambled siRNA ("scRNA", All Stars Negative Control siRNA, QIAGEN, Netherlands) served as negative control and was applied in the same concentration. This RNA interference took place once after washing the freshly plated ARVC.

Intracellular calcium was diminished by Bapta-AM (Molecular Probes ®invitrogen dectection technologies, USA). It was dissolved in DMSO (5μg/ml; Roth, Germany) and added to the plates in a concentration of 10μg/ml after the last washing step. Pure DMSO in a concentration of 5μg/ml was used as a control.

With each cell preparation 150 to 300 cardiomyocytes were evaluated per day and group by light microscopy. All counted cardiomyocytes were subdivided into four groups according to their appearance: "rod-shaped", "round down", "spreading" and "unusual appearance" (S1 Fig). The category "spreading" included all cardiomyocytes with pseudopodia-like structures. "Unusual appearance" included all ARVC with an irregular surface and no detectable intact cell membrane.

After five days in culture ARVC showed no expression of fibroblast markers (collagen-3), but of cardiac specific markers like ANP compared to isolated cardiac fibroblast after 24 hours in culture, which showed vice-versa results. Both, cardiac fibroblasts and ARVC expressed swiprosin-1 (Efhd2) on mRNA level (S2 Fig).

Immunofluorescence staining of cardiomyocytes

In order to analyze the morphological and structural conversion of cardiomyocytes in culture confocal laser scan microscopy was performed. Phalloidin TRITC (Santa Cruz Biotechnology, Germany) was used to stain F-actin according to the manufacturers protocol. The day of cell isolation, labeled as day zero, was used as control. Briefly, cells were fixated with paraformaldehyde (4%). After permeabilization with TritonX-100 (0.2%) cardiomyocytes were incubated

with Phalloidin-TRITC (10μMol). F-actin filaments appeared red in immunofluorescence microscopy.

Immunoblot technique

Isolated ARVC were incubated with lysis buffer as described previously [21]. SDS page gel electrophoresis was conducted with the system of NuPAGE, Novex® (Life Technologies, USA). The expression of swiprosin-1 was detected by using a swiprosin-1 antibody produced in goat (Biorbyt Ltd., USA). A GRK-2 antibody produced in rabbit (Sigma-Aldrich, Germany) was used to investigate GRK-2 expression in ARVC. All measurements were normalized to the expression of GAPDH using an antibody produced in mice (Calbiochem®, Germany). Protein expression was quantified with horseradish peroxidase and a chemiluminescence machine from Peqlab.

RT-PCR

Real-time quantitative RT-PCR in ARVC was performed as described before [22]. Total RNA was isolated using peqGOLD TriFast (Peqlab, Biotechnologie GmbH, Germany) according to the manufacturer‘s protocol. After conversion of RNA into complementary DNA (cDNA) with reverse transcriptase, PCR was performed with iQ™SYBR® Green Supermix (BIO Rad, Germany). In order to detect unspecific binding melting curve analysis or DNA gels were performed. For experiments with quantitative real time RT-PCR, ARVC of four petri dishes (2ml) were combined in one sample. Each group contained twelve to fourteen samples. For correlation analyses all samples were analyzed. The primers used are listed in supplementary materials (S1 Table).

Load free cell shortening

Determination of ARVC contraction was performed as described before [23,24]. ARVC were stimulated with two AgCl electrodes at 2Hz. Four measurements per cell were conducted and the mean of these measurements was used to define cell shortening. Isoprenaline (SERVA Feinbiochemica, Germany), a β-adrenoceptor agonist, was added five minutes before measurement in a concentration of 10μM. Additionally, ARVC were incubated for 24 hours with scRNA or siRNA directed against swiprosin-1 in a medium without FCS. All experiments were normalized to the control group of ARVC without any treatment.

Statistics

Statistical analysis was performed using two-way ANOVA followed by Student-Newman-Keuls post hoc analysis or one-side ANOVA with Tukey test. If required, Student´s T-Test was performed with Levene Test to test for normal distribution of samples within a group. Man-Whitney-U post hoc analysis was conducted for samples without normal distribution. For the statistical calculation of all data SPSS 22.0 was used. A value of $p < 0.05$ was considered to be significant. Results are presented as mean ± standard deviation (SD) or mean ± standard error of the mean (SEM), indicated in the legend to the figures.

Results

Adult cardiomyocytes in culture

Changes in the shape of ARVC adapting to the culture conditions were investigated daily over a time period of six days. Freshly isolated ARVC were typically rod shaped with a clearly visible cross striation (Fig 1A Day 0). Changes in cell morphology were observed during the following

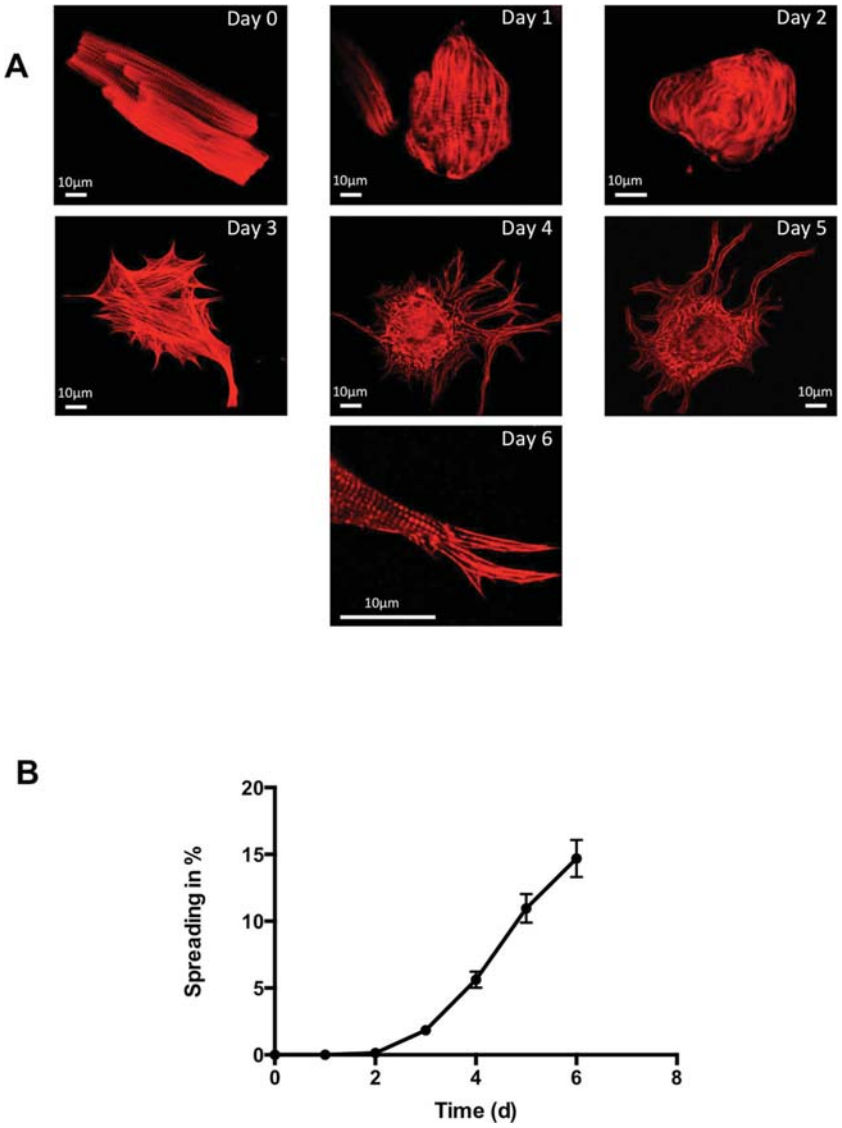

Fig 1. De- and redifferentiation of ARVC in culture with 20% FCS (A) Freshly isolated ARVC with their typical rod shape form (Day 0) completely rounded down by degrading sarcomeres starting in the periphery (Day 1) in the first days of culture. They lost all their contractile elements (Day 2) followed by formation of pseudopodia-like structures (spreading; Day 3–5) and subsequent reformation of their contractile elements indicating *de novo* sarcomerogenesis (Day 6). At day six in culture, cross striation was clearly detectable again. (B) Increase in cardiomyocytes with pseudopodia-like structures normalized to all counted cardiomyocytes (spreading in %) during cultivation time (n = 33 cell preparations). Data are presented as means ± SEM

doi:10.1371/journal.pone.0167655.g001

days in culture. First ARVC lost all their contractile elements beginning in the periphery (Fig 1A Day 1 and Day 2). This was followed by a reformation, implicating *de novo* sarcomerogenesis. This reformation was preceded by the typical formation of pseudopodia-like structures (spreading, Fig 1A Day 3 –Day 6). *De novo* sarcomerogenesis started with the appearance of actin stress fibers (Fig 1A Day 3). Actin bundles initially appeared in the perinuclear region and formed newly assembled sarcomeres (Fig 1A Day 4 and Day 5). Latter grew along the preformed actin stress fibers into the periphery (Fig 1A Day 6). At the end of the cultivation

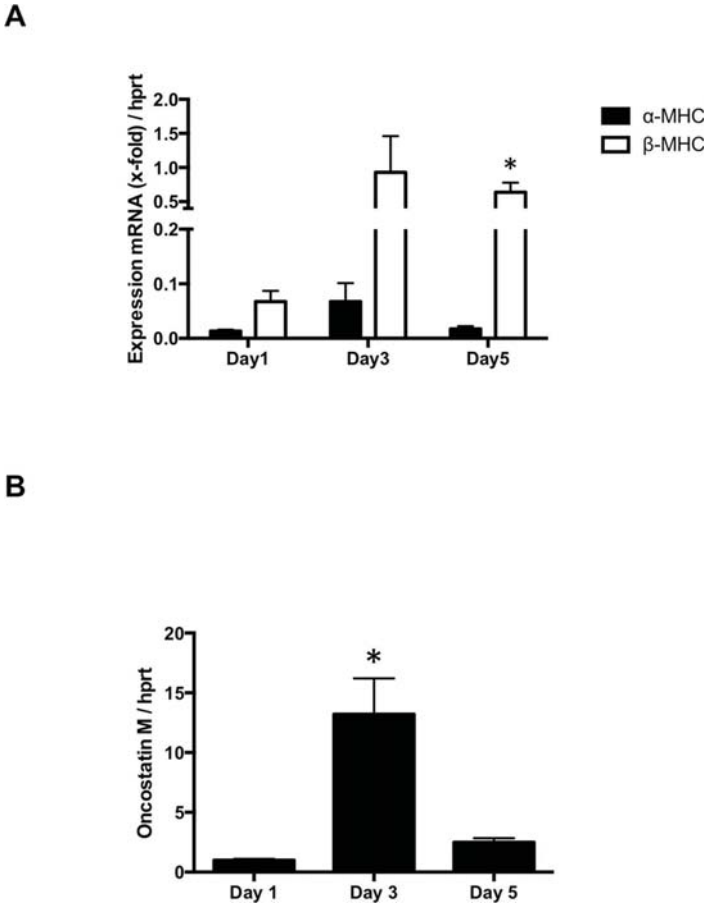

Fig 2. Expression of specific genes during cultivation (A) The expression of neonatal β-MHC mRNA increased whereas the expression of adult α-MHC stayed low at day one, three and five in culture (n = 12 samples; Man-Whitney-U-test). (B) The expression of oncostatin M increased during the first days in culture and decreased again at day five (n = 13 samples; one-side ANOVA with Tukey post hoc analysis). Data are presented as means ± SEM; *P ≤ 0.05

doi:10.1371/journal.pone.0167655.g002

period (Day 6), a typical cross striation from newly assembled sarcomeres in the spread ARVC was observed. Fig 1B displays the kinetic of the spreading process during cultivation. The fraction of ARVC showing pseudopodia-like structures at each time of examination are given as spreading in % (Fig 1B). Spreading started around day three and increased constantly during cultivation time, until 14.7% ± 1.39% ARVC showed pseudopodia-like structures at day six. This process was accompanied by reexpression of β-MHC, whereas the expression of α-MHC decreased during cultivation time (Fig 2A). Furthermore, oncostatin M was significantly increased, when the formation of pseudopodia-like structures started at day three (Fig 2B).

Expression of swiprosin-1 during cultivation

To our knowledge we are the first to provide evidence that swiprosin-1 is expressed in ARVC. Changes in the expression of swiprosin-1 in ARVC during cultivation are shown in Fig 3A and 3B. Swiprosin-1 mRNA levels increased during cultivation (day 1: 0.51-fold ± 0.13; day 3: 2.99-fold ± 0.55; day 5: 2.85-fold ± 0.72 compared to day 0) (Fig 3A). Protein expression of swiprosin-1 decreased throughout the first three days (data not shown) followed by a significant

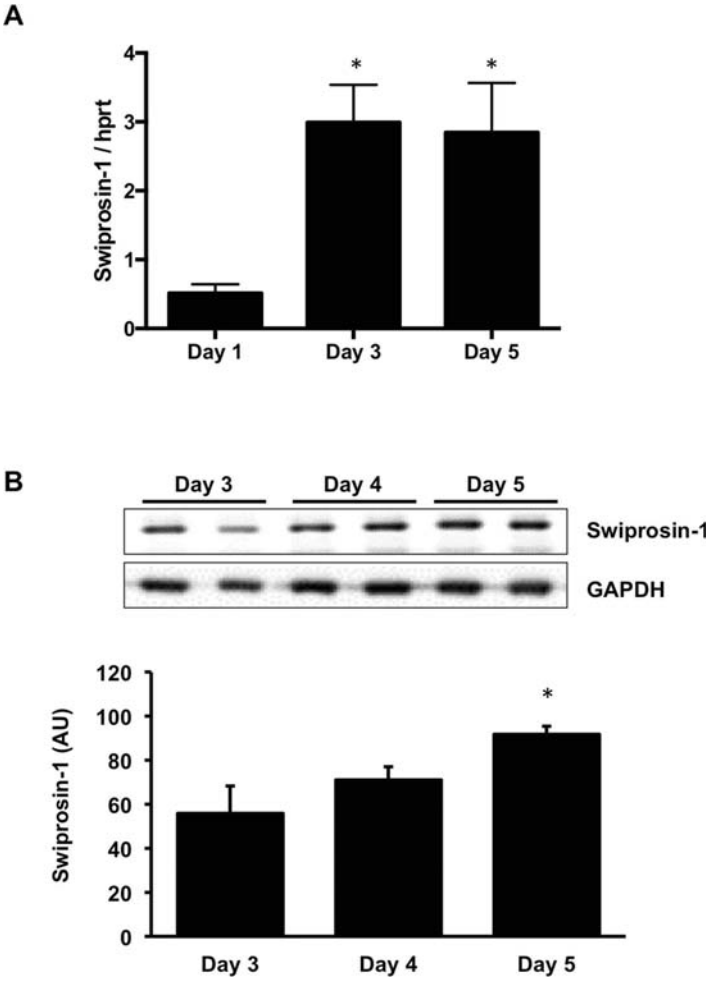

Fig 3. Expression of swiprosin-1 in ARVC (A) Expression of swiprosin-1 mRNA increased early during culture (n = 11–13 samples). (B) On protein level expression of swiprosin-1 decreased in the first days of culture (data not shown), followed by a significant increase in the last days of culture (n = 4 cell preparations). Data are presented as means ± SD; *P $\leq$ 0.05; one-side ANOVA with Tukey post hoc analysis, AU = arbitrary units

doi:10.1371/journal.pone.0167655.g003

increase when pseudopodia-like structures appeared (Fig 3B). Typically, mRNA expression of swiprosin-1 increased before protein expression. Thus, cell spreading is associated with increased swiprosin-1 expression during cultivation.

Swiprosin-1 is needed for *de novo* sarcomerogenesis in cultured ARVC

In order to investigate the role of swiprosin-1 in the spreading process more closely, experiments with siRNA directed against swiprosin-1 were performed. Immunoblot analysis confirmed a significant reduction to 74.77% ± 11.88% of swiprosin-1 at protein level with siRNA directed against swiprosin-1 compared to scramble RNA (scRNA) (Fig 4A). Addition of siRNA directed against swiprosin-1 delayed spreading of ARVC. At day six, siRNA against swiprosin-1 reduced spreading by 55.61% ± 14.34% compared to ARVC treated with scRNA (Fig 4B). Additionally, fewer cells performed spreading in the presence of siRNA against swiprosin-1 at day four (p = 0.052) and day five (p = 0.059). Although the number of ARVC

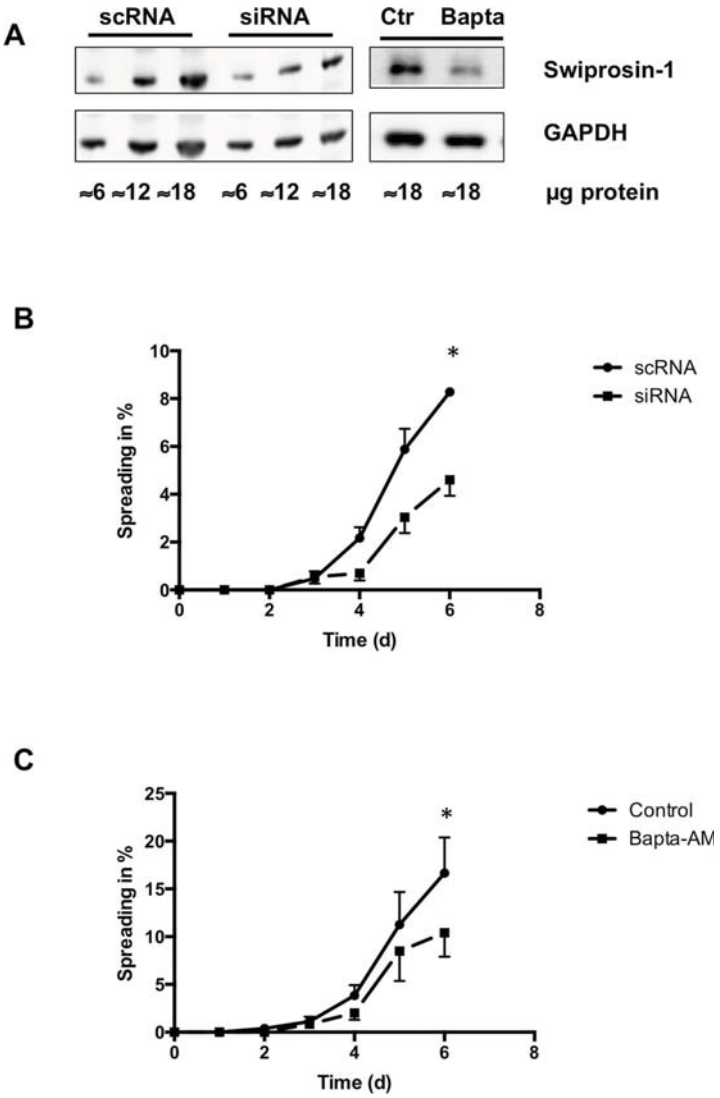

Fig 4. Blocking the translation of swiprosin-1 with siRNA and decreasing the intracellular calcium with Bapta-AM attenuated spreading in ARVC. (A) siRNA against swiprosin-1 (0.05µM) caused a down regulation in protein expression for swiprosin-1 compared to scRNA at day 2 in culture. Additionally, Bapta-AM (10µg/ml) decreased the expression of swiprosin-1 on protein level, too. (B) Through the whole cultivation a constant down regulation of spreading in ARVC treated with siRNA against swiprosin-1 was detectable. (C) Bapta-AM led to a constant decrease in spreading, too. Data are presented as means ± SEM; n = 3–4 cell preparations (n = 800–1000 cells); *P ≤ 0.05; unpaired T-Test or Man-Whitney-U-Test, Ctr = control group, Bapta = ARVC treated with Bapta-AM

doi:10.1371/journal.pone.0167655.g004

performing cell spreading was lower in cultures treated with siRNA, the ARVC that still showed pseudopodia-like structures, performed the same dedifferentiation and redifferentiation process as seen in control conditions. First they completely lost their contractile apparatus followed by a reformation of actin-stress fibers and *de novo* sarcomerogenesis (S3 Fig).

Effect of intracellular calcium modulation on cell spreading

Calcium is required to activate swiprosin-1 [10,11]. We hypothesize that an alteration in the intracellular calcium levels may influence the ability of adult cardiomyocytes to spread. Bapta-

AM, a known cell-permeable calcium chelator, caused a constant decrease in spreading of ARVC compared to the control group. At day six, Bapta-AM decreased spreading by 62.42% ± 24.10% compared to control (Fig 4C). On protein level a significant down regulation (49.89% ± 9.87%) of swiprosin-1 was found in Bapta-AM treated cardiomyocytes compared to control (Fig 4A).

Swiprosin-1 expression correlates with GRK2 expression and causes β-adrenoceptor desensitization

Experiments with ARVC in culture showed a change in the responsiveness of β_1- and β_2- adrenoceptors [17–19]. As swiprosin-1 significantly affected the adaptation to culture conditions during which also changes in β-adrenoceptor coupling were observed, we correlated the expression of swiprosin-1 *in vitro* with genes known to interfere with β-adrenoceptors. The following four proteins showed a distinct positive correlation with the expression of swiprosin-1: G protein-coupled receptor kinase 2 and 5 (GRK2 and GRK5), β1-arrestin and β2-arrestin (Fig 5). All of these proteins are proved to be involved in the desensitization of β-adrenoceptors. Additionally, a positive correlation between the expression of swiprosin-1 and β_1- and β_2-adrenoceptors was detected. The highest correlation with swiprosin-1 was found for GRK2 ($R^2 = 0.830$). Hence, swiprosin-1 may cause β-adrenoceptor desensitization via co-regulation of GRK2. To

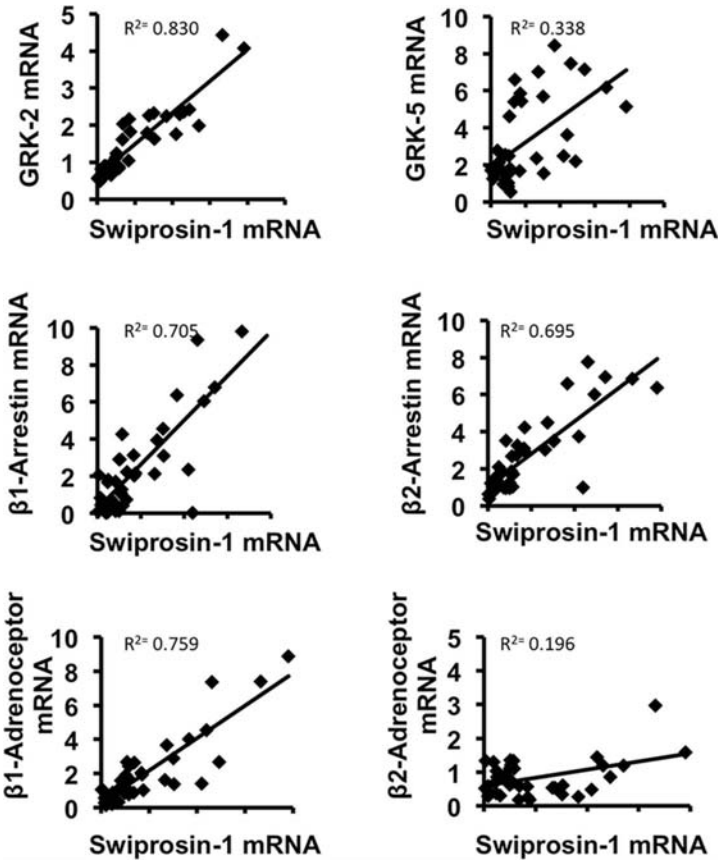

Fig 5. Linear correlation between swiprosin-1 and β_1- and β_2-adrenoceptor as well as with proteins known to interfere with β-adrenoceptors (n = 44 samples). ARVC were harvested at day 1,3 and 5 in culture. Changes in swiprosin-1 expression were correlated with genes of interest.

doi:10.1371/journal.pone.0167655.g005

investigate this assumption, the isoprenaline responsiveness of ARVC during electric stimulation was tested and immunoblot analyses of ARVC treated with siRNA against swiprosin-1 were performed. Western Blots showed a decrease in protein level of GRK2 in ARVC treated with siRNA against swiprosin-1 compared to ARVC treated with scRNA (Fig 6A). Load free cell shortening (2Hz) showed no difference in basal contractile responsiveness between ARVC treated with scRNA, siRNA or vehicle (Fig 6B). However, controls increased their contractile amplitude as a response to β-adrenergic stimulation with isoprenaline. Interestingly, this contractile responsiveness was further increased in ARVCs treated with siRNA directed against swiprosin-1 (Fig 6B). The same effect could be detected with siRNA against GRK2 (Rolf Schreckenberg, personal communication). Summarized, the data suggest a functional relevant GRK2 down regulation in swiprosin-1 depleted ARVC.

Discussion

This study reports three new findings. First, ARVC constitutively express swiprosin-1 as shown here in ARVC on mRNA and protein level. Second, swiprosin-1 is required to initiate the formation of pseudopodia-like structures (spreading), a process necessary to adapt to culture conditions. Third, the expression level of swiprosin-1 is associated to that of GRK2 and thereby to β-adrenoceptor responsiveness.

In the present study we successfully re-established the cultivation model of adult cardiomyocytes, which was described in the 1980s [8,9,25–27]. ARVC performed a severe remodeling during cultivation. First the cells lost their contractile elements accompanied by a transition from a rod-shaped morphology to a round form. Subsequently, ARVC formed pseudopodia-like structures (spreading) and finally emerged as polymorphic cells with an intracellular net of actin stress-fibers. Along these stress fibers new sarcomeres were formed. After six days in culture, the typical cross striation of sarcomeres reappeared in ARVC. This change was accompanied by replacing α-MHC by β-MHC. As expected, expression of oncostatin M, known to trigger the process of de- and redifferentiation was increased during cultivation [4]. Thus, within six days the process of de- and redifferentiation of ARVC, which is a well-known phenomenon, could be observed in our study. In this process ARVC showed a mixture between the fetal and embryonic cell-like cell type, but remained highly differentiated [25]. For example, they formed new sarcomeres alongside actin stress fibers like adult terminal differentiated cardiomyocytes do, whereas fetal cardiomyocytes start sarcomerogenesis at the sarcolemma [28]. The process of de- and redifferentiation enables ARVC to adapt to new environments and circumstances [2–6].

We showed with this study, swiprosin-1 is constitutively expressed in ARVC on mRNA and protein level. By hampering the translation of swiprosin-1 with siRNA, a significant reduction in spreading was detected in ARVC. Consequently, swiprosin-1 seems to be required for the adaptation of ARVC to culture conditions. According to the manufacturers' protocol, the intracellular level of siRNA is sufficient to maintain the gene silencing effect for five to six days. Although, this cannot be certain for the last days in culture an effect of siRNA directed against swiprosin-1 was detected on protein level in the first days of cultivation. The main effect of siRNA directed against swiprosin-1 is a delay in the induction of the spreading process. The ARVC treated with siRNA which showed spreading, performed a similar process of dedifferentiation and redifferentiation as seen in control conditions. According to the treatment protocol it is possible, that either not all the swiprosin-1 in the cardiomyocytes was blocked or that not all cardiomyocytes absorbed the small interfering RNA. Because we could only detect a 25% decrease of swiprosin-1 on protein level and no transfection medium was used to protect the sensitive cardiomyocytes, we suspect that ARVC exhibiting the typical spreading behavior as seen under control conditions did not absorb the siRNA against

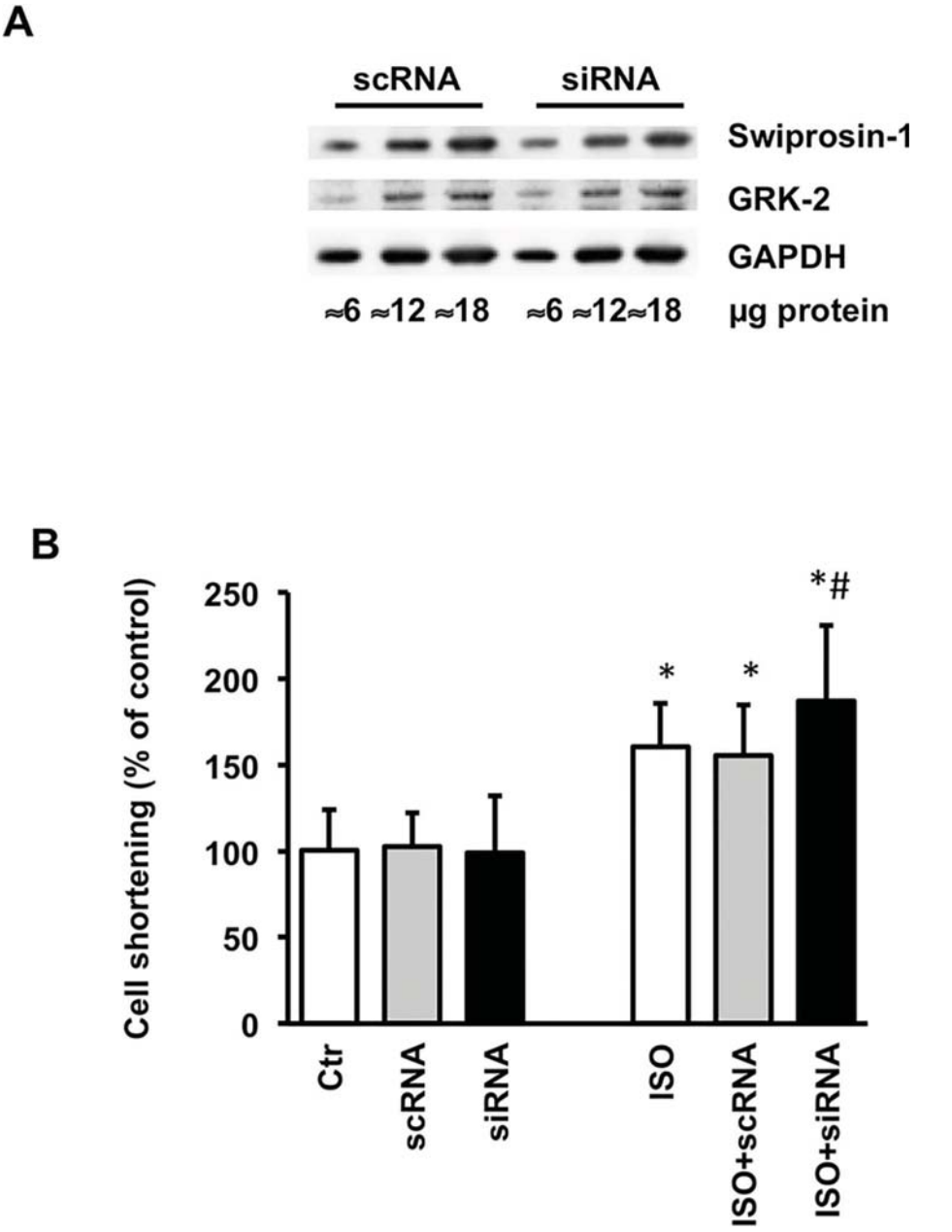

Fig 6. Swiprosin-1 caused β-adrenoceptor desensitization by interaction with GRK2. (A) GRK2 protein level was reduced in ARVC treated with siRNA against swiprosin-1 (0.05μM) compared to scRNA at day 1 in culture. (B) In cell shortening of ARVC after 24h in culture between control, scRNA and siRNA for swiprosin-1 no difference was detectable. Adding isoprenaline (ISO; 10μM) to control ARVC and ARVC treated with scRNA led to an increase in cell shortening ability. This effect was increased in ARVC treated with siRNA, thus down regulation of swiprosin-1 led to down regulation of GRK2 and therefore to an increased responsiveness to the β-adrenoceptor agonist isoprenaline. Data are means ± SD; n = 72 cells; *P $\leq$ 0.05 vs. control: #p $\leq$ 0.05 vs. ISO; two-side ANOVA and post-hoc test (Student-Newman-Keuls)

doi:10.1371/journal.pone.0167655.g006

swiprosin-1. Former researchers established that swiprosin-1 is required for the formation of lamellopodia in macrophages and by that for the formation of contractile elements enabling immune cells to migrate [10–12]. Taking our present results into consideration we proved that

swiprosin-1 plays a similar role in cardiomyocytes, in which the formation of pseudopodia-like structures is required for adaptation to culture conditions. Therefore, swiprosin-1 may be a key player in redifferentiation of adult cardiomyocytes.

Next, we investigated the role of calcium in swiprosin-1 dependent spreading. We decreased the intracellular calcium concentration using Bapta-AM. Bapta-AM is a well-known and often used cell-permanent calcium chelator [29]. Binding of free intracellular Ca^{2+} by Bapta-AM led to a decrease of pseudopodia-like structures in ARVC compared to the control group. Furthermore, western blot analysis revealed a reduction of swiprosin-1 on protein level in Bapta-AM treated ARVC. Hence, calcium seems to be required for swiprosin-1 expression and activity.

Finally, we found a strong correlation between swiprosin-1 expression and proteins, participating in β-adrenoceptor desensitization. Swiprosin-1 expression was positively correlated with the expression of GRK5, β1-arrestin, β2-arrestin, and especially GRK2. This relationship between swiprosin-1 and GRK2 was confirmed by Western blot analysis. Its functional relevance was implicated by load free cell shortening. This consequently leads to the assumption that an up-regulation of swiprosin-1, e.g. during cardiac stress, causes a decrease in ARVC responsiveness to β-adrenergic stimulation. β-adrenoceptor desensitization is a characteristic feature of heart failure. Here it is associated with cardiac remodeling and leads to an impaired cardiac function with a depression of heart rate and cardiac output [30]. However, the desensitization of β-adrenoceptors in an acute cardiac insult may have a protective effect [31]. Patients suffering from a myocardial infarction normally receive β-blockers [32–34]. Thus it is expedient for swiprosin-1, which seems to play a major role in the adaptation and regeneration process of ARVC via dedifferentiation and redifferentiation, to be coupled to GRK2 expression, which leads to β-adrenoceptor desensitization. This may protect dedifferentiating cardiomyocytes during the adaptation to stress.

Additionally, we detected a positive correlation of swiprosin-1 with β_1- and β_2-adrenoceptors, although the effect was stronger for β_1. Former studies revealed a shift from β_1- to β_2-adrenoceptors during cultivation, which caused an increased hypertrophic responsiveness [17,18].

The role of swiprosin-1 in chronic heart injuries was not part of the experiments shown here and needs to be investigated in the future. However, previous experiments have shown that chronic dedifferentiation in stressed adult cardiomyocytes leads to impaired cardiac function and survival rates. But, in acute states it had positive effects [4,6]. Therefore, we hypothesize that swiprosin-1 and the dedifferentiation process are needed for acute regeneration of adult cardiomyocytes under stress situations. Future investigations will have to focus on the relevance of cardiac swiprosin-1 expression *in vivo*.

Supporting Information

S1 Fig. Categorization of ARVC by light microscopy. Day 0: Freshly isolated cardiomyocytes are „rod-shaped". Day 2: In the first days of culture ARVC „round down"(1 and 2). Cardiomyocytes with „unusual appearance"(3) showed an irregular surface. Day 6: Cardiomyocytes with a round cell body and pseudopodia-like structures (1) as well as widespread cardiomyocytes (2) were counted as „spreading". „Unusual appearence"is shown in this picture as (3). Pseudopodia-like structures are shown exemplary.
(TIFF)

S2 Fig. DNA gel of qRT-PCR in ARVC. DNA gels showed a mRNA expression of the cardiac specific ANP in ARVC cultivated for five days, whereas an expression of the fibroblast marker collagen 3 could not be detected. Isolated cardiac fibroblasts (FB) served as control. Efhd2 and

our house-keeping gene hprt are expressed in both cell types.
(TIFF)

S3 Fig. Immunflourescent staining of ARVC treated with siRNA against swiprosin-1. Dedifferentiation and redifferentiation of ARVC treated with siRNA against swiprosin-1. Like controls ARVC lost their contractile apparatus and round down first. This was followed by spreading and reformation of the contractile apparatus with actin-stress fibers and *de novo* sarcomerogenesis.
(TIFF)

S1 Table. Sequences and annealing temperatures of all primers used. Shown are all primers used with specific annealing temperature and sequence.
(TIFF)

Acknowledgments

We thank Nadine Woitasky for technical assistance. We thank Mrs. Claudia Lorenz (medical writer, ACCEDIS) for her help in preparing the manuscript. This work is part of the doctoral thesis of Franziska Nippert.

Author Contributions

Conceptualization: FN RS KDS.

Data curation: FN.

Formal analysis: FN.

Funding acquisition: KDS.

Investigation: FN.

Methodology: FN AH MW.

Project administration: KDS RS.

Resources: KDS RS FN.

Software: FN.

Supervision: KDS.

Validation: FN.

Visualization: FN.

Writing – original draft: FN.

Writing – review & editing: KDS.

References

1. Li F, Wang X, Capasso JM, Gerdes AM, Rapid transition of cardiac myocytes from hyperplasia to hypertrophy during postnatal development. Journal of molecular and cellular cardiology 1996; 28: 1737–1746. doi: 10.1006/jmcc.1996.0163 PMID: 8877783
2. Leri A, Kajstura J, Anversa P, Mechanisms of myocardial regeneration. Trends in cardiovascular medicine 2011; 21: 52–58. doi: 10.1016/j.tcm.2012.02.006 PMID: 22578241

3. Szibor M, Pöling J, Warnecke H, Kubin T, Braun T, Remodeling and dedifferentiation of adult cardiomyocytes during disease and regeneration. Cellular and Molecular Life Sciences 2014; 71: 1907–1916. doi: 10.1007/s00018-013-1535-6 PMID: 24322910
4. Kubin T, Pöling J, Kostin S, Gajawada P, Hein S, Rees W et al., Oncostatin M Is a Major Mediator of Cardiomyocyte Dedifferentiation and Remodeling. Cell Stem Cell 2011; 9: 420–432. doi: 10.1016/j.stem.2011.08.013 PMID: 22056139
5. Pöling J, Gajawada P, Lörchner H, Polyakowa V, Szibor M, Böttger T et al., The Janus face of OSM-mediated cardiomyocyte dedifferentiation during cardiac repair and disease. Cell Cycle 2014; 11: 439–445.
6. Pöling J, Gajawada P, Richter M, Lörchner H, Polyakova V, Kostin S et al., Therapeutic targeting of the oncostatin M receptor-β prevents inflammatory heart failure. Basic Res Cardiol 2014; 109: 1–14.
7. Schwarzfeld T, Isolation and development in cell culture of myocardial cells of the adult rat. Journal of molecular and cellular cardiology 1981; 13: 563–575. PMID: 7277505
8. Eppenberger-Eberhardt M, Flamme I, Kurer V, Eppenberger HM, Reexpression of α-smooth muscle actin isoform in cultured adult rat cardiomyocytes. Developmental Biology 1990; 139: 269–278. PMID: 2186943
9. Eppenberger ME, Hauser I, Baechi T, Schaub MC, Brunner UT, Dechesne CA et al., Immunocytochemical analysis of the regeneration of myofibrils in long-term cultures of adult cardiomyocytes of the rat. Developmental Biology 1988; 130: 1–15. PMID: 2903104
10. Huh YH, Kim SH, Chung KH, Oh S, Kwon MS, Choi HW et al., Swiprosin-1 modulates actin dynamics by regulating the F-actin accessibility to cofilin. Cellular and Molecular Life Sciences 2013; 70: 4841–4854. doi: 10.1007/s00018-013-1447-5 PMID: 23959172
11. Dütting S, Brachs S, Mielenz D, Fraternal twins: Swiprosin-1/EFhd2 and Swiprosin-2/EFhd1, two homologous EF-hand containing calcium binding adaptor proteins with distinct functions. Cell communication and signaling 2011; 9: 2. doi: 10.1186/1478-811X-9-2 PMID: 21244694
12. Kwon MS, Park KR, Kim YD, Na BR, Kim HR, Choi HJ et al., Swiprosin-1 is a novel actin bundling protein that regulates cell spreading and migration. PLoS ONE 2013; 8 e71626. doi: 10.1371/journal.pone.0071626 PMID: 23977092
13. Fiedler B, Wollert KC, Interference of antihypertrophic molecules and signaling pathways with the Ca2+-calcineurin-NFAT cascade in cardiac myocytes. Cardiovascular Research 2004; 63: 450–457. doi: 10.1016/j.cardiores.2004.04.002 PMID: 15276470
14. Fiedler B, Wollert KC, Targeting calcineurin and associated pathways in cardiac hypertrophy and failure. Expert opinion on therapeutic targets 2005; 9: 963–973. doi: 10.1517/14728222.9.5.963 PMID: 16185152
15. Lim HW, Molkentin JD, Calcineurin and human heart failure. Nature medicine 1999; 5: 246–247. doi: 10.1038/6430 PMID: 10086361
16. Heineke J, Ruetten H, Willenbockel C, Gross SC, Naguib M, Schaefer A et al., Attenuation of cardiac remodeling after myocardial infarction by muscle LIM protein-calcineurin signaling at the sarcomeric Z-disc. Proceedings of the National Academy of Sciences of the United States of America 2005; 102: 1655–1660. doi: 10.1073/pnas.0405488102 PMID: 15665106
17. Schluter KD, Zhou XJ, Piper HM, Induction of hypertrophic responsiveness to isoproterenol by TGF-beta in adult rat cardiomyocytes. The American journal of physiology 1995; 269: 6.
18. Zhou XJ, Schluter KD, Piper HM, Hypertrophic responsiveness to beta 2-adrenoceptor stimulation on adult ventricular cardiomyocytes. Molecular and cellular biochemistry 1996; 163–164: 211–216. PMID: 8974059
19. Joshi-Mukherjee R, Dick IE, Liu T, O'Rourke B, Yue DT, Tung L et al., Structural and functional plasticity in long-term cultures of adult ventricular myocytes. Journal of molecular and cellular cardiology 2013; 65: 76–87. doi: 10.1016/j.yjmcc.2013.09.009 PMID: 24076394
20. Schlüter KD, Schreiber D, Adult Ventricular Cardiomyocytes: Isolation and Culture, in: Fabbro D., McCormick F. (Eds.), Protein Tyrosine Kinases: From Inhibitors to Useful Drugs. Humana Press Inc, Totowa, NJ, 2005; 305–314.
21. Schluter KD, Katzer C, Frischkopf K, Wenzel S, Taimor G, Piper HM, Expression, release, and biological activity of parathyroid hormone-related peptide from coronary endothelial cells. Circulation Research 2000; 86: 946–951. PMID: 10807866
22. Anwar A, Schluter KD, Heger J, Piper HM, Euler G, Enhanced SERCA2A expression improves contractile performance of ventricular cardiomyocytes of rat under adrenergic stimulation. Pflugers Archiv European journal of physiology 2008; 457: 485–491. doi: 10.1007/s00424-008-0520-7 PMID: 18581135
23. Schreckenberg R, Dyukova E, Sitdikova G, Abdallah Y, Schluter KD, Mechanisms by which calcium receptor stimulation modifies electromechanical coupling in isolated ventricular cardiomyocytes.

Pflugers Archiv European journal of physiology 2015; 467: 379–388. doi: 10.1007/s00424-014-1498-y PMID: 24687204

24. Fontana M, Olschewski H, Olschewski A, Schluter KD, Treprostinil potentiates the positive inotropic effect of catecholamines in adult rat ventricular cardiomyocytes. British journal of pharmacology 2007; 151: 779–786. doi: 10.1038/sj.bjp.0707300 PMID: 17533419

25. Bugaisky LB, Zak R, Differentiation of Adult Rat Cardiac Myocytes in Cell Culture, Circulation Research 1989; 64: 493–500. PMID: 2465096

26. Decker ML, Behnke-Barclay M, Cook MG, Lesch M, Decker RS, Morphometric evaluation of the contractile apparatus in primary cultures of rabbit cardiac myocytes. Circulation Research 1991; 69: 86–94. PMID: 2054944

27. Schlüter KD (Ed.), Cardiomyocytes–Active Players in Cardiac Disease, Springer International Publishing AG Switzerland, 2016, ISBN 978-3-319-31249-1

28. Hilenski LL, Terracio L, Borg TK, Myofibrillar and cytoskeletal assembly in neonatal rat cardiac myocytes cultured on laminin and collagen. Cell Tissue Research 1991; 264: 577–587. PMID: 1907887

29. Tsien RS, A non-disruptive technique for loading calcium buffers and indicators into cells. Nature 1981; 290: 527–528. PMID: 7219539

30. Mason RP, Giles TD, Sowers JR, Evolving mechanisms of action of beta blockers: focus on nebivolol. Journal of cardiovascular pharmacology 2009; 54: 123–128. doi: 10.1097/FJC.0b013e3181ad207b PMID: 19528811

31. Najafi A, Sequeira V, Kuster DW, van der Velden J, beta-adrenergic receptor signalling and its functional consequences in the diseased heart. European journal of clinical investigation 2016; 46: 362–374. doi: 10.1111/eci.12598 PMID: 26842371

32. Howard PA, Ellerbeck EF, Optimizing beta-blocker use after myocardial infarction. American family physician 2000; 62: 1853–60, 1865–6. PMID: 11057841

33. Kezerashvili A, Marzo K, de Leon J, Beta blocker use after acute myocardial infarction in the patient with normal systolic function: when is it "ok" to discontinue? Current cardiology reviews 2012; 8: 77–84. doi: 10.2174/157340312801215764 PMID: 22845818

34. Lange R, Kloner RA, Braunwald E, First ultra-short-acting beta-adrenergic blocking agent: its effect on size and segmental wall dynamics of reperfused myocardial infarcts in dogs. The American journal of cardiology 1983; 51: 1759–1767. PMID: 6134464

frontiers in Physiology

REVIEW
published: 11 March 2015
doi: 10.3389/fphys.2015.00065

Arginase induction and activation during ischemia and reperfusion and functional consequences for the heart

*Klaus-Dieter Schlüter *, Rainer Schulz and Rolf Schreckenberg*

Physiologisches Institut, Justus-Liebig-Univiersität Giessen, Giessen, Germany

Induction and activation of arginase is among the fastest responses of the heart to ischemic events. Induction of arginase expression and enzyme activation under ischemic conditions shifts arginine consumption from nitric oxide formation (NO) to the formation of ornithine and urea. In the heart such a switch in substrate utilization reduces the impact of the NO/cGMP-pathway on cardiac function that requires intact electromechanical coupling but at the same time it induces ornithine-dependent pathways such as the polyamine metabolism. Both effects significantly reduce the recovery of heart function during reperfusion and thereby limits the success of reperfusion strategies. In this context, changes in arginine consumption trigger cardiac remodeling in an unfavorable way and increases the risk of arrhythmia, specifically in the initial post-ischemic period in which arginase activity is dominating. However, during the entire ischemic period arginase activation might be a meaningful adaptation that is specifically relevant for reperfusion following prolonged ischemic periods. Therefore, a precise understanding about the underlying mechanism that leads to arginase induction as well as of it's mechanistic impact on post-ischemic hearts is required for optimizing reperfusion strategies. In this review we will summarize our current understanding of these processes and give an outlook about possible treatment options for the future.

Keywords: ornithine, nitric oxide, polyamines, reactive oxygen species, reperfusion injury

OPEN ACCESS

Edited by:
Gaetano Santulli,
Columbia University, USA

Reviewed by:
Amadou K. S. Camara,
Medical College of Wisconsin, USA
Sang-Bing Ong,
Universiti Teknologi Malaysia, Malaysia

****Correspondence:***
Klaus-Dieter Schlüter,
Physiologisches Institut,
Aulweg 129,
35392 Gießen, Germany
klaus-dieter.schlueter@
physiologie.med.uni-giessen.de

Specialty section:
This article was submitted to Striated Muscle Physiology, a section of the journal Frontiers in Physiology

Received: *15 December 2014*
Accepted: *07 February 2015*
Published: *11 March 2015*

Citation:
Schlüter K-D, Schulz R and Schreckenberg R (2015) Arginase induction and activation during ischemia and reperfusion and functional consequences for the heart. Front. Physiol. 6:65. doi: 10.3389/fphys.2015.00065

Arginase Isoforms and Biological Activity

Arginase is an enzyme that catalyzes the hydrolysis of L-arginine into urea and ornithine. It is expressed in two different isoforms. Arginase I is located in the cytosol and well-known from hepatic metabolism in which arginase is responsible for the elimination of metabolites from amino acid and nucleotide metabolism. The enzyme is expressed throughout the body in endothelial cells and muscle cells (Gonon et al., 2012). In contrast to arginase I, arginase II is predominantly located in the mitochondrial matrix and seems to be linked directly to polyamine metabolism, although its exact function is not known (Morris, 2005). The polyamine metabolism synthesizes polyamines such as spermine and spermidine that are required for cellular growth. The rate limiting step of this pathway is the induction of

Abbreviations: NOS, nitric oxide synthase; TNF, tumor necrosis factor; ODC, ornithine decarboxylase; ROS, reactive oxygen species; SOD, superoxide dismutase; Nor-NOHA, N^{ω}-hydroxy-nor-L-arginine.

ornithine decarboxylase (ODC) converting ornithine into putrescine. Polyamines, such as putrescine, spermine, and spermidine, may act within cells but they can also be released from cells. In the latter case they affect cell function as agonists of calcium-sensing receptors (Smajilovic et al., 2010). Arginase II may not be confined to the mitochondrial matrix when the expression level is elevated. Moreover, arginase can also be found in platelets where it plays a role in sickle cell disease not necessarily requiring mitochondrial participation (Raghavachari et al., 2007). When not specified within the text, the term arginase will be used as a synonym for both isoforms.

Arginine as the main substrate of both isoforms of arginase is also the substrate for the three isoforms of nitric oxide synthase (NOS). Therefore, excessive activity of either NOS or arginase reduces substrate availability for the other arginine consumer. In fact, most cells express arginase and NOS isoforms at the same time. In most cells enzymatic activity of each of these enzymes is tightly regulated by direct protein modification or by induction of enzyme expression. In case of arginase an increased activity of arginase has consequences for both pathways: a loss of NO/cGMP signaling and an improvement of polyamine metabolism. Examples for increased arginase activity and expression are found in artherosclerosis, hypertension, inflammation, aging, stroke, myocardial infarction, and heart failure to name just a few (Wu and Meininger, 2000; Ryoo et al., 2008; Bagnost et al., 2010; Heusch et al., 2010). It is commonly accepted that excessive activation of arginase is associated with disease progress. Whether the final effect of arginase activation depends on the activation of arginase-dependent pathways (polyamine pathways) or on the inhibitory effect on NO/cGMP-dependent pathways or on both pathways remains elusive. Furthermore, at least in case of atherosclerosis, arginase II may activate intracellular signaling independent of its enzymatic activity (Xiong et al., 2013). Regarding the role of arginase in endothelial dysfunction, arginine metabolism seems to play a relevant role by either reducing arginine uptake (Martens et al., 2014), activation of arginase II (Pandey et al., 2014), or activation of arginase I (Gao et al., 2007). A precise understanding of the regulation and function of arginase and a subsequent translation of these findings into medical therapies will certainly improve clinical outcomes. The current review will focus on the role of arginase during ischemia and in particular during reperfusion.

Arginase Activation in Ischemic and Post-Ischemic Hearts

Most, but not all investigators that studied the activity of arginase in ischemic and post-ischemic cardiac tissues found a significant increase in total arginase activity, arginase I expression, or both. In principle, expression of arginase II can also be induced by hypoxia as shown for human pulmonary artery smooth muscle cells (Chen et al., 2014; Jin et al., 2014). However, whether induction of arginase II contributes to the increased arginase activity in the heart during ischemia and reperfusion remains to be established. Most remarkable observations of increased arginase activity were made at a very early time-point after the onset of ischemia and reperfusion (Harpster et al., 2006; Grönros et al., 2013). The underlying mechanism by which arginase I expression is induced has been evaluated in detail as described now. Arginase I expression was identified as the strongest and fastest transcriptional adaptation during ischemia and reperfusion in the heart (Harpster et al., 2006). Several mechanisms seemed to be responsible for this effect: At first, hypoxia and reoxygenation damages cardiomyocytes because it leads to excessive calcium load during ischemia and subsequent reoxygenation generates energy that allows a very strong contraction disrupting the sarcolemmal membrane. This cell damage leads to a release of intracellular material into the extracellular compartment (Hearse et al., 1973). This hypercontraction-induced cell damage is the basis for diagnosis of infarct size by quantification of plasma levels of cardiac-specific enzymes, i.e., hs cTnI (= high sensitive cardiac-specific troponin I). Such molecules that are released by hypercontracture may have also a functional relevance in the subsequent activation of arginase expression. Extracellular RNA (eRNA), which is among intracellular materials released by hypercontracture, triggers the activation of a membrane-bound sheddase that, once activated, releases TNF-α (Cabrera-Fuentes et al., 2014; see **Figure 1**). TNF-α has been identified as a pro-inflammatory cytokine that activates arginase I (Schreckenberg et al., 2015b). This observation is further based on experiments with TNF-$\alpha^{-/-}$ mice in which ischemia and reperfusion does not lead to an induction of arginase I (Gao et al., 2007). TNF-α may trigger this process via activation of the transcription factor AP-1 (**Figure 1**). A potential AP-1 binding site has been identified in the promoter region of arginase and TNF-α activates the activity of the transcription factor AP-1 (Zhu et al., 2010). Hypoxia directly recruits c-jun to AP-1 binding sites of the arginase-1 promoter (Singh et al., 2014). c-Jun binds together with activating transcription factor-2 at the AP-1 site, which initiates the transactivation (Zhu et al., 2010). Acute myocardial infarction is sufficient to induce the expression of 15 different genes that are involved in assembly and activation of AP-1 within 15 min (Harpster et al., 2006). All these findings strongly support the assumption that AP-1 activation plays a major role in adaptation of arginine metabolism to hypoxia. Such a scenario would also explain the more general finding that arginase activation under ischemia and reperfusion is not specific for the heart but represents a more general pathway by which tissues respond to hypoxia because cell damage and loss of plasmalemmal integrity is a characteristic feature of anoxic cell damage. As outlined in the next section, hypoxic conditions trigger arginase I expression in nearly all tissues. As mentioned above, arginase II can also be induced by hypoxia. The mechanism has been worked out on pulmonary smooth muscle cells. Hypoxia induced the expression of miR-17-5p that then triggers the up-regulation of arginase II (Jin et al., 2014). Activation of PI3-kinase-Akt signaling pathways can attenuate this activation (Chen et al., 2014). However, it remains to be clarified whether similar concerns hold for arginase II in the heart during acute ischemia and reperfusion.

At least within cardiac tissue, induction of arginase I expression is a strong and early response of cells to hypoxic stress. This leads to the question whether this is exerts a protective effect? At first, during the hypoxic period the arginine-consuming counterpart of arginase, NOS, is functionally inactive, because formation

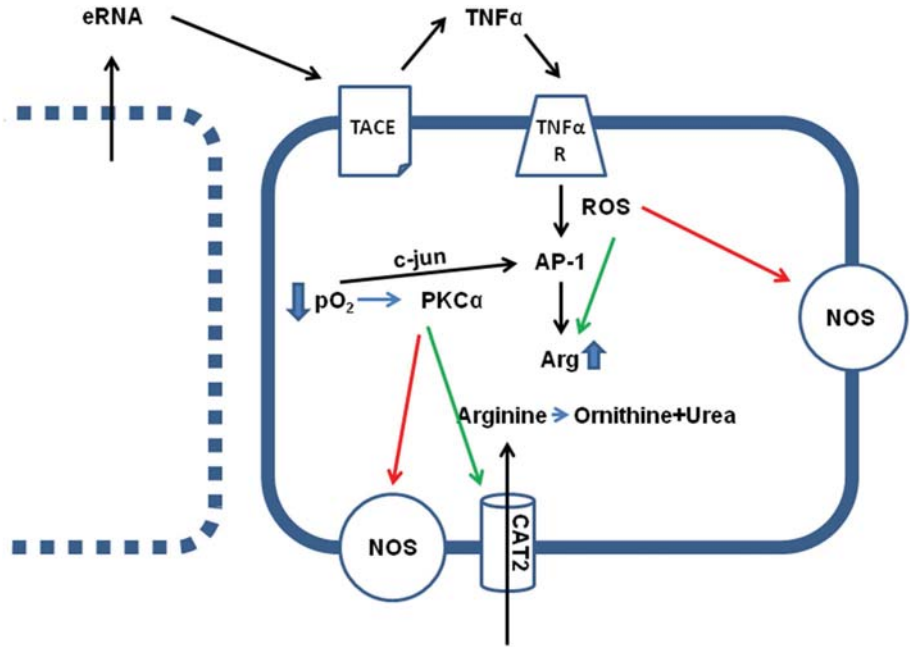

FIGURE 1 | Effect of hypoxia (ischemia) on arginine metabolism. Direct effects of low pO_2 are the translocation of c-jun in AP-1 dimers, thereby activating AP-1 transcriptional activity, an activation of PKCα and subsequent activation of arginine transporters (CAT2) and inhibition of constitutively expressed NOS isoforms (eNOS and nNOS). Indirect effects of low pO_2 are loss of sarcolemmal integrity in some cells (see left), leading to the release of intracellular particles, such as RNA (eRNA), that activates a sheddase (TACE) thereby releasing TNFα. TNFα augments the hypoxia-induced cell damage by activation of AP-1 and increasing arginase (Arg) expression, by activation of arginase activity via nitrosylation and reducing the K_M value for the enzymatic reaction, and ROS-dependent inhibition of NOS activity.

of NO from arginine requires molecular O_2. In the absence of O_2, NOS works in an uncoupled mode generating reactive oxygen species (ROS) that damages cells and this may be relevant at the onset of reperfusion. In this context it is also likely to understand that ROS stimulates arginase expression as well (**Figure 1**). Moreover, TNF-α activates ROS formation. In other words, ROS formation initiates a negative feedback loop by which arginine, the substrate of NOS, is removed in a condition in which uncoupled NOS forms damaging ROS.

Activation of arginase cannot reduce the level of overburden ROS formation alone. In transgenic mice with over-expression of TNF-α, it was found that the subsequent development of endothelial dysfunction can be reduced by administration of tempol, a superoxide dismutase (SOD) mimetic and radical scavenger (Zhang et al., 2010). In chronic ischemic injury, up-regulation of arginase I and SOD-2 are commonly found and it remains speculative whether the up-regulation of SOD-2 is not sufficient for ROS scavenging or whether arginase I activation and SOD-2 activation play divergent roles (Roy et al., 2009). Another piece of this puzzle is the finding that increased ROS formation favors S-nitrosylation of arginase thereby decreasing the K_m for L-arginine again favoring the reduction of arginine levels. Furthermore, activation of protein kinase C (PKC)-α in endothelial cells further decreases the activity of NOS by activation of the transcription factor AP-1 that induces not only the expression of arginase but also that of the up-take of arginine by induction of the expression of CAT-2 transporters (**Figure 1**). At the same time, PKC-α promotes eNOS phosphorylation at Thr 495 resulting in decreased NO production (Visigalli et al., 2010). Finally, in the ischemic/reperfused heart, arginase I induction is opposed by eNOS down-regulation (Hein et al., 2003). All these molecular responses to hypoxia shift arginine consumption from the NO pathway toward the arginase-dependent pathways and this may be a strategy of cells to withstand hypoxic stress. In conclusion, under conditions in which NOS cannot synthesize NO, reducing the intracellular arginine pool by arginase activation may protect cells. However, high concentrations of arginine can reduce the expression of NOS which is then lacking in the reperfused tissue. All these examples suggest that reducing arginine levels will protect hypoxic cells from irreversible damage (**Figure 2-I**).

This advantage of high arginase activity during ischemia may switch into a strong disadvantage as soon as the tissue is reperfused. Now, high arginase activity contributes to the reduced NOS activity in post-ischemic tissues resulting in low perfusion and prolongation of ischemic time. Moreover, low NO/cGMP levels contribute to reperfusion injury, loss of endothelial barrier function, and increase the susceptibility to cardiac arrhythmia (see Section Post-Ischemic Consequences of Reduced NO Formation and Contribution of Arginase for details). At the same time, the release of polyamines acts via activating of calcium-sensing receptors and this affects the rather sensitive intracellular calcium handling in cells during reperfusion (**Figure 2-II**).

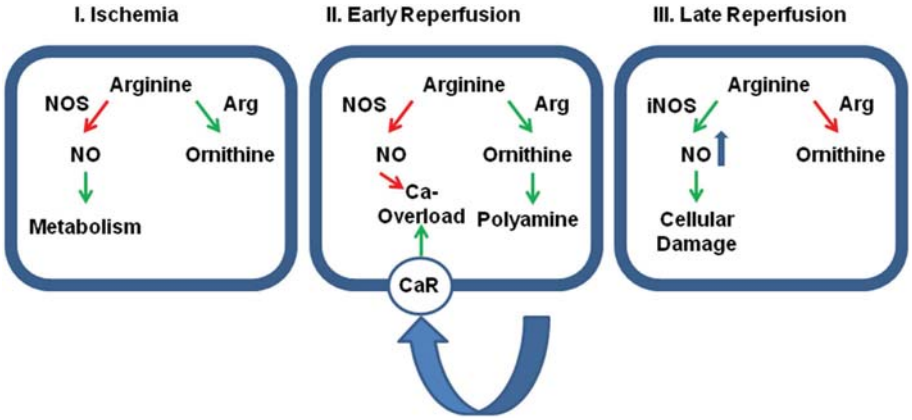

FIGURE 2 | Relative contribution of cellular protection vs. cellular damage of the two main arginine pathways. Panel (I): During ischemia the activation of arginase (Arg) activity reduces the effect of physiological levels of NO on cellular metabolism thereby and reduces otherwise accumulating arginine levels. At this time, inhibition of arginase would be detrimental for the outcome. **Panel (II)**: During early reperfusion, dominance of arginine pathway limits the protective role of NO, specifically on SR-calcium load that triggers fatal arrhythmic events. Moreover, the activated arginase/polyamine pathway potentially augments calcium overload by release polyamines that act on calcium receptors (CaR). Now, the further outcome will benefit from arginase inhibition. **Panel (III)**: At late reperfusion, inflammatory pathways have induced the expression of iNOS that generates detrimental amount of NO that are potentially damaging. In this phase, an inhibition of arginase will be again detrimental, because then more arginine can be converted into NO. Green arrows indicate activation and red arrows indicate inhibition.

Arginase Activation in Non-Cardiac Tissues

As mentioned above, arginase activation during hypoxia is not tissue specific. Like the heart, arginase activation occurs in the liver and some other tissues such as the detrusor (Kawano et al., 2006). Although this review is focussed on the heart, it seems to be important to compare the effect of ischemia on arginase activity in the heart with that in other organs to better understand the relevance of arginase activity in cells. Investigating the effect of ischemia on arginase activity was first performed in the liver. In the liver arginase is the most important enzyme that protects the organism from ammonia intoxication. Excessive release of arginase from liver transplants is a severe clinical problem that occurs in the reperfusion period. Arginase is able to metabolite plasma arginine and thereby reduce the substrate availability for NOS and arginase. Subsequently, a drop in plasma arginine and nitrite, a stable end product of NO, and an increase in plasma ornithine can be observed. Functionally, this leads to hemodynamic alterations specifically in the lung and liver (Roth et al., 1994; Längle et al., 1995; Silva et al., 2005). Supplementation of arginine could reduce liver transplant preservation injury in rats with orthotopic liver transplantation (Yagnik et al., 2002). Vice versa, inhibition of arginase by a specific inhibitor of arginase, Nor-NOHA, stabilized liver histology and function (Reid et al., 2007; Jeyabalan et al., 2008). A stabilization of arginase activity could be achieved by ischemic pre-conditioning of the liver (Ofluoglu et al., 2006). Moreover, administration of adrenomedullin, a multifunctional peptide with a putative beneficial role after ischemic insults, normalized arginase activity and NO formation. Interestingly, it reduced also the induction of the pro-inflammatory TNF-α pathway (Kerem et al., 2008). As outlined already, TNF-α is a likely candidate for arginase induction. Collectively, the data show a strong induction of arginase activity in ischemic/reperfused liver tissue that leads to a substrate deficit for NOS and thereby contributes to the post-ischemic tissue damage. Therefore, the situation in the liver is similar to that of the heart and supports translation of these findings to heart protection against ischemia and reperfusion injury.

On the other hand, reducing arginine pools by hyperactivation of arginase will also have beneficial effects as it limits the activity of iNOS in macrophages (**Figure 2-III**). Indeed pro-inflammatory macrophages (M1 cells) express large amounts of iNOS while anti-inflammatory macrophages that are involved in wound healing (M2 cells) express large amounts of arginase. Unfortunately, M2 macrophages are not only responsible for wound healing as for example in post-ischemic tissues but also for tumor growth. The relationship between M1 and M2 macrophages can be triggered by a specific tyrosine kinase, namely the Ron receptor tyrosine kinase, that upregulates Fos and enhances binding of Fos to the AP-1 binding site that has already been identified as a promoter element required for arginase I induction (Sharda et al., 2011). M2 macrophages play a distinctive role in reperfusion injury of the kidney. In the kidney M2 macrophages trigger the repair process days after the ischemic insult (Lee et al., 2011). Indeed, the role of arginase activation in post-ischemic tissue differs between the kidney on the one hand and the liver and heart on the other hand. Whereas, arginase is activated in liver and heart, arginase activity is reduced in post-ischemic kidneys. In the kidney increased NO production leads to augmented tubular injury. Hypoxia leads to an up-regulation of CAT-2 thereby providing arginine as a substrate for eNOS and iNOS (Schwartz et al., 2002). In addition, arginase I

and arginase II expression is reduced in post-ischemic kidney in contrast to the liver and heart. Erbas et al. showed that administration of N-acetylcysteine normalizes arginase activity in the kidney and improved the situation following ischemia and reperfusion (Erbas et al., 2004). Noteworthy, carefully measurements of renal arginase activity 2 weeks after the insult have revealed an up-regulation of the enzyme in the kidney that is required for the proliferative repair of the damaged kidney (Bogatzki, 1963). As in the kidney, ROS in the presence of high NOS activity trigger neurological disorders to hypoxia/anoxia in brain and improving arginase activity is again associated with protection (Swamy et al., 2010).

Collectively these data show different roles for arginase in hypoxic/reoxygenated tissues and indicate that a simple relationship between tissue damage and arginase activity is unlikely to be identified. Concerning the consequences of arginase activation in the heart, we may conclude from these studies on non-cardiac tissues that arginase activity affects different physiological activities in post-ischemic tissues that are linked to wound healing, tissue repair, and cell function. The data suggest that arginase activation may be necessary for some post-ischemic physiological adaptation but may also be detrimental for other ones. Like the kidney pharmacological options to affect the arginase activity will need to define the best time-window to either improve or inhibit activation. The consequences for arginase activity in the heart will be mentioned in the next section.

Post-Ischemic Consequences of Reduced NO Formation and Contribution of Arginase

As outlined above, arginase activation increases the formation of ornithine but also limits the substrate availability for NOS. Substrate limitation causes reduced NOS activity and NO has repeatedly shown before to be important for proper heart function (Rassaf et al., 2006). Reduced NOS activity may reduce ROS formation during ischemia but low NO levels are a common problem in post-ischemic hearts. NOS activity in endothelial cells is required for proper perfusion of the heart and as well as for the anti-thrombotic activity of NO. Impaired endothelial function in post-ischemic hearts could be restored by inhibition of arginase activity as repeatedly been shown (Hein et al., 2003; Gao et al., 2007; Grönros et al., 2013). Furthermore, NOS activity is also important within cardiomyocytes where NO/cGMP signaling contributes to calcium oscillation during the phase of reperfusion, although this may also be responsible for cell damage and arrhythmia. Indeed cardiac de-synchronization is a major problem in the early phase of reperfusion. NO/cGMP is required for normal cardiac function as it regulates calcium handling, ion channel open probability and thereby action potential duration and other aspects of cardiac function. Among them are effects on cellular cAMP levels by cGMP-dependent inhibition of phosphodiesterase (PDE) II, protein kinase G-dependent down-regulation of voltage-dependent L-type Ca^{2+} currents, desensitization of cardiac myofilaments by phosphorylation of troponin I, and metabolic effects. These consequences of reduced NO in cardiomyocytes are reviewed by Massion et al. (2005). Despite clear effects of cGMP on calcium currents, NO/cGMP also modulate ATP-sensitive K^+ channels, the hyperpolarization-activated pacemaker current I_f, and voltage-dependent fast Na^+ currents (Fischmeister et al., 2005). Furthermore, while NO/cGMP pathways inhibit cardiac hypertrophy, an activation of arginase-dependent polyamine metabolism is pro-hypertrophic (Schlüter et al., 2000; Booz, 2005). As expected some of these stressors could be minimized by improving NO/cGMP signaling in post-ischemic hearts. Moreover, uncoupling of NOS caused by hypoxia increases ROS formation and excessive ROS, due to oxidative stress, directly impairs cardiac function by formation of disulfides cross-bridges at tropomyosin (Canton et al., 2006). As a consequence arginase activation in post-ischemic hearts may have detrimental effects due to the substrate limitation of NOS and may contribute to NOS inefficiency at that time points.

Although increased substrate availability of arginine during reperfusion may allow NOS to generate NO/cGMP, the interaction between arginase and NOS is more complex than perceived. Indeed, a clinical trial that was aimed to increase substrate availability by administration of arginine to post-infarct patients had to be stopped due to lack of benefit and, even more important, risk of increased mortality (Schulman et al., 2006). These data indicate a detrimental effect of arginase-dependent pathways in the post-ischemic period. As the polyamine metabolism is one of the major pathways activated by arginase activity we will discuss the consequences of polyamine metabolism for the post-ischemic heart next.

Post-Ischemic Consequences of Increased Polyamine Metabolism and Contribution of Arginase

Arginase activation not only limits the activity of NOS isoforms but also generates the substrate for the polyamine metabolism of ornithine. An activation of the polyamine metabolism is normally associated with anabolism. In terms of cardiac tissue, activation of polyamine metabolism is required for cardiac hypertrophy. An activation of the polyamine metabolism critically depends on the induction of ODC, the rate limiting enzyme of the polyamine metabolism. Therefore, activation of arginase and ODC creates a situation in which synthesis of polyamines is most likely. The polyamine metabolism in general must be considered as a meaningful adaptive mechanism because it allows cardiac hypertrophy that means that survived cardiomyocytes can increase the number of their contractile units, the sarcomers. Furthermore, release of polyamines can initiate an autocrine loop that activates calcium-sensing receptors on cardiomyocytes that by itself increase cardiac power (Schreckenberg et al., 2015a). However, as often in physiology it is difficult to adapt the right power of activation. If the activation of the polyamine metabolism is excessive the same pathway favors the induction of apoptosis (Giordano et al., 2010; Mörlein et al., 2010). Moreover, as activation of calcium-sensing receptors activates a Gαq-dependent signaling in cardiomyocytes this involves the activation of IP_3 receptors that trigger again arrhythmic events (Schreckenberg et al.,

2015a). Collectively, activation of arginase in the post-ischemic myocardium has an increased risk of mal-adaption.

Experiences with Arginase Inhibition in Ischemic and Reperfused Hearts

As outlined above, a successful use of arginase inhibitors to improve post-ischemic recovery is limited at present by lack of knowledge about exact time, duration, and amount of inhibition. Nevertheless, recent studies have mostly shown beneficial effects if arginase inhibition was performed during the early phase of reperfusion. The majority of these studies have revealed that arginase inhibition significantly improves NO production in post-ischemic hearts (Jung et al., 2010; Gonon et al., 2012; Tratsiakovich et al., 2013). Moreover, inhibition of arginase before reperfusion reduced infarct sizes via preserved NO production (Grönros et al., 2013). Another potential mechanism by which inhibition of arginase during or immediately after reperfusion reduces reperfusion injury lies in the activation of PKC-ε and opening of mitochondrial ATP-dependent K^+ channels ($mitoK_{ATP}$). However, it remains unclear whether this already clarifies the role of arginase during reperfusion injury of the heart. Pharmacological activation of PKC-ε failed to improve strong end-points such as death and heart failure albeit reduction in infarct size (Mochly-Rosen et al., 2012). Furthermore, dietary supplementation of arginine in post-infarct patients to attenuate arginase-induced arginine depletion in target cells turned out to be not effective (Schulman et al., 2006). Even more disappointing, this trial had been stopped for increased mortality in the treatment group. Promising experimental data show a reduction in reperfusion injury by inhibition of arginase. However, up-regulation of arginase-2 in erythropoietin-treated rat hearts showed improvements in contractility and reduced myocardial (Lu et al., 2012). In a recent study on isolated rat hearts, Yang and colleagues provided evidence that inhibition of arginase I activity in red blood cells increases NO release from erythrocytes thereby improving post-ischemic recovery (Yang et al., 2013). While it is easily to understand that increased NO may improve post-ischemic recovery, it is difficult to explain why the inhibition of tissue-specific arginase activation does not play a role in these hearts unlike the inhibition of arginase in erythrocytes. Finally, in the setting of chronic ischemia, arginase activity is not related to coronary microvascular dysfunction (Sodha et al., 2008). Collectively, it remains unclear whether the hypothesis of substrate limitation is really cause of arginase-dependent malfunction in post-ischemic hearts and how post-ischemic hearts benefit mostly from arginase inhibition.

Possible Targets to Modify Arginase Activity and the Consequences of Arginase Activation in Post-Ischemic Hearts

Most studies published to date have used the arginase-specific inhibitor N^{ω}-hydroxy-nor-L-arginine (Nor-NOHA) to inhibit arginase during reperfusion. Nor-NOHA has the advantage not to interfere with NOS. Most but not all data published to date are promising (see above) but it remains unclear whether treatment with an arginase subtype unspecific inhibitor is optimal. Consequently, the development of other arginase inhibitors underway. Congeners of (R)-2-Amino-6-borono-2-(2-(piperidin-1-yl)ethyl)hexanoic acid have been shown to bind preferentially to arginase I, have antagonistic effects and are orally bioavailable (Van Zandt et al., 2013). Such compounds may be used to identify isoform specific effects of arginase in the future. Another problem might be the timing of inhibition. Arginase activation may be required during ischemic insults, detrimental during the early phase of reperfusion but again required at later time points to shift macrophage activity from pro-inflammatory M1 to anti-inflammatory M2 subpopulation. Long-time follow-ups are required to define electrophysiological remodeling and such data are not yet reported. As indicated in case of PKC-ε, reduction of infarct size alone is not sufficient. Another point that has to be clarified in the future is whether arginase inhibition is optimal or whether upstream elements of arginase induction are more effective. Alternatively to arginase inhibition an inhibition of TNF-α activation that attenuates arginase I activation might be more effective. TNF-α knock-out mice had no up-regulation of arginase. Subsequently, inhibition of a sheddase that releases bound TNF-α during hypoxia was sufficient to attenuate arginase induction (Schreckenberg et al., 2015b). Unlike the direct inhibition of arginase, such an approach does not block arginase activity in M2 macrophages. Therefore, a better understanding of the mechanism by which arginase is activated and contributes to reperfusion injury will lead to more specific targets to interfere with these pathways. If substrate competition between NOS and arginase is the main problem at the time of reperfusion, citrulline rather than arginine supplementation may be of specific advantage. Citrulline has less side effects, can be better administrated orally than arginine, because it is not metabolized in the liver, and can be converted into arginine at the site of action within the cell due to the close physical association between argininosuccinate lyase and eNOS (Romero et al., 2006; Smith et al., 2006).

Conclusive Remarks

Arginase activation is a common event in hypoxic tissues including the heart. Recent development of reperfusion therapies has led to a situation in which high arginase activity at the onset of reperfusion participates in reperfusion-induced damage. Therefore, there seems to be a therapeutic window by which either attenuation of arginase induction of inhibition of arginase activity attenuates reperfusion damage. The optimal timing of pharmacological interference has still to be defined as well as the optimal time point. **Figure 2** summarizes these assumptions.

Acknowledgments

The work was supported by the University of Giessen (grant to KS).

References

Bagnost, T., Ma, L., da Silva, R. F., Rezakhaniha, R., Houdayer, C., Stergiopulos, N., et al. (2010). Cardiovascular effects of arginase inhibition in spontaneously hypertensive rats with fully developed hypertension. *Cardiovasc. Res.* 87, 569–577. doi: 10.1093/cvr/cvq081

Bogatzki, M. (1963). Argininstoffwechsel im hypertrophischen und hyperplastischen nierengewebe und im myokard bei arbeitshypertrophie des herzens infolge renalen hochdrucks. *Zts. Ges. Exptl. Med.* 137, 256–262. doi: 10.1007/BF02045500

Booz, G. W. (2005). Putting the brakes on cardiac hypertrophy. *Hypertension* 45, 341–346. doi: 10.1161/01.HYP.0000156878.17006.02

Cabrera-Fuentes, H. A., Ruiz-Meana, M., Simsekyilmaz, S., Kostin, S., Inserte, J., Saffarzadeh, M., et al. (2014). RNAse 1 prevents the damaging interplay between extracellular RNA and tumor necrosis factor-α in cardiac ischemia/reperfusion injury. *Thromb. Haemost.* 112, 1110–1119. doi: 10.1160/TH14-08-0703

Canton, M., Skyschally, A., Menabo, R., Boengler, K., Gres, P., Schulz, R., et al. (2006). Oxidative modification of tropomyosin and myocardial dysfunction following coronary microembolization. *Eur. Heart J.* 27, 875–881. doi: 10.1093/eurheartj/ehi751

Chen, B., Xue, J., Meng, X., Slutzky, J. L., and Clavert, A. E. (2014). Resveratrol prevents hypoxia-induced arginase II expression and proliferation of human pulmonary artery smooth muscle cells via Akt-dependent signalling. *Am. J. Physiol. Lung Cell. Mol. Physiol.* 307, L317–L325. doi: 10.1152/ajplung.00285.2013

Erbas, H., Aydogdu, N., and Kaymak, K. (2004). Effects of N-aceytlcysteine on arginase, ornithine and nitric oxide in renal ischemia-reperfusion injury. *Pharmacol. Res.* 50, 523–527. doi: 10.1016/j.phrs.2004.04.005

Fischmeister, R., Castro, L., Abi-Gerges, A., Rochais, F., and Vandecasteele, G. (2005). Species- and tissue-dependent effects on NO and cyclic GMP on cardiav ion channels. *Comp. Biochem. Physiol. A Mol. Integr. Physiol.* 142, 136–143. doi: 10.1016/j.cbpb.2005.04.012

Gao, X., Xu, X., Belmadani, S., Park, Y., Tang, Z., Feldman, A. M., et al. (2007). TNF-α contributes to endothelial dysfunction by upregulating arginase in ischemic/reperfusion injury. *Arterioscler. Thromb. Vasc. Biol.* 27, 1269–1275. doi: 10.1161/ATVBAHA.107.142521

Giordano, E., Flamigni, F., Guarnieri, C., Muscari, C., Pignatti, C., Stefanelli, C., et al. (2010). Polyamine in cardiac physiology and disease. *Open Heart Fail. J.* 3, 25–30. doi: 10.2174/1876535101003020025

Gonon, A. T., Jung, C., Katz, A., Westerblad, H., Shemyakin, A., Sjoquist, P. O., et al. (2012). Local arginase inhibition during early reperfusion mediates cardioprotection via increased nitric oxide production. *PLoS ONE* 7:e42038. doi: 10.1371/journal.pone.0042038

Grönros, J., Kiss, A., Palmer, M., Jung, C., Berkowitz, D., and Pernow, J. (2013). Arginase inhibition improves corornary microvascular function and reduces infarct size following ischaemia-reperfusion in a rat model. *Acta Physiol.* 208, 172–179. doi: 10.1111/apha.12097

Harpster, M. H., Bandyopadhyay, S., Thomas, D. P., Ivanov, P. S., Keele, J. A., Pineguinea, N., et al. (2006). Earliest changes in the left ventricular transcriptome post-myocardialk infarction. *Mamm. Genome* 17, 701–715. doi: 10.1007/s00335-005-0120-1

Hearse, D. J., Humphrey, S. M., and Chain, E. B. (1973). Abrupt reoxygenation of the anoxic potassium-arrested perfused rat heart: a study of myocardial enzyme release. *J. Mol. Cell. Cardiol.* 5, 395–407. doi: 10.1016/0022-2828(73)90030-8

Hein, T. W., Zhang, C., Wang, W., Chang, C.-I., Thengchaisri, N., and Kuo, L. (2003). Ischemia-reperfusion selectively impairs nitric oxide-mediated dilation in coronary arterioles: counteracting role of arginase. *FASEB J.* 17, 2328–2330. doi: 10.1096/fj.03-0115fje

Heusch, P., Aker, S., Boengler, K., Deindl, E., van de Sand, A., Klein, K., et al. (2010). Increased inducible nitric oxide synthase and arginase II expression in heart failure: no net nitrite/nitrate production and protein S-nitrosylation. *Am. J. Physiol.* 299, H446–H553. doi: 10.1152/ajpheart.01034.2009

Jeyabalan, G., Klune, J. R., Nakao, A., Martik, N., Wu, G., Tsung, A., et al. (2008). Arginase blockade protects against hepatic damage in warm ischemia-reperfusion. *Nitric Oxide* 19, 29–35. doi: 10.1016/j.niox.2008.04.002

Jin, Y., Jin, Y., Chen, B., Tipple, T. E., and Nelin, L. D. (2014). Arginase II is a target of miR-17-5p and regulates miR17-5p expression in human pulmonary artery smooth muscle cells. *Am. J. Physiol. Lung Cell. Mol. Physiol.* 307, L197–L204. doi: 10.1152/ajplung.00266.2013

Jung, C., Gonon, A. T., Sjöquist, P.-O., Lundberg, J. O., and Pernow, J. (2010). Arginase inhibition mediates cardioprotection during ischemia-reperfusion. *Cardiovasc. Res.* 85, 147–154. doi: 10.1093/cvr/cvp303

Kawano, K., Masuda, H., Yano, M., Kihara, K., Sugimoto, A., and Azuma, H. (2006). Altered nitric oxide synthase, arginase and ornithine decarboxylase activities, and polyamine synthesis in response to ischemia of the rabbit detrusor. *J. Urol.* 176, 387–393. doi: 10.1016/S0022-5347(06)00515-5

Kerem, M., Bedirli, A., Pasaoglu, H., Ofluglu, E., Yilmazer, D., Salman, B., et al. (2008). Effects of adrenomedullin on hepatic damage in hepatic ischaemia/reperfusion injury in rats. *Liver Int.* 28, 972–981. doi: 10.1111/j.1478-3231.2008.01741.x

Längle, F., Roth, E., Steininger, R., Winkler, S., and Mühlbacher, F. (1995). Arginase release following liver reperfusion. *Transplantation* 59, 1542–1549. doi: 10.1097/00007890-199506000-00007

Lee, S., Huen, S., Nishio, S., Lee, H. K., Choi, B.-S., Ruhrberg, C., et al. (2011). Distinct macrophage phenotypes contribute to kidney injury and repair. *J. Am. Soc. Nephrol.* 22, 317–326. doi: 10.1681/ASN.2009060615

Lu, M.-J., Chen, Y.-S., Huang, H.-S., and Ma, M.-C. (2012). Erythropoietin alleviates post-ischemic injury of rat hearts by attenuating nitrosative stress. *Life Sci.* 90, 776–784. doi: 10.1016/j.lfs.2012.04.012

Martens, C. R., Kuczmarski, J. M., Lennon-Edwards, S., and Edwards, D. G. (2014). Impaired L-arginine uptake but not arginase contributes to endothelial dysfunction in rats with chronic kidney disease. *J. Cardiovasc. Pharmacol.* 63, 40–48. doi: 10.1097/FJC.0000000000000022

Massion, P. B., Pelat, M., Belge, C., and Balligand, J.-L. (2005). Regulation of the mammalian heart function by nitric oxide. *Comp. Biochem. Physiol. A Mol. Integr. Physiol.* 142, 144–150 doi: 10.1016/j.cbpb.2005.05.048

Mochly-Rosen, D., Das, K., and Grimes, K. V. (2012). Protein kinase C, an elusive therapeutic target? *Nat. Rev. Drug Discov.* 11, 937–957. doi: 10.1038/nrd3871

Mörlein, C., Schreckenberg, R., and Schlüter, K.-D. (2010). Basal ornithine decarboxylase activity modifies apoptotic and hypertrophic marker expression in post-ischemic hearts. *Open Heart Fail. J.* 3, 31–37. doi: 10.2174/1876535101003020031

Morris, S. M. Jr. (2005). Arginine metabolism in vascular biology and disease. *Vasc. Med.*10(Suppl 1), S83–S87. doi: 10.1177/1358836X0501000112

Ofluoglu, E., Kerem, M., Pasaoglu, H., Turkozkan, N., Seven, I., Bedirli, A., et al. (2006). Delayed energy protection of ischemic preconditioning on hepatic ischemia/reperfusion injury in rats. *Eur. Surg. Res.* 38, 114–121. doi: 10.1159/000093300

Pandey, D., Sikka, G., Bergman, Y., Kim, J. H., Ryoo, S., Romer, L., et al. (2014). Transcriptional regulation of endothelial arginase 2 by histone deacetylase 2. *Arterioscler. Thromb. Vasc. Biol.* 34, 1556–1566. doi: 10.1161/ATVBAHA.114.303685

Raghavachari, N., Xu, X., Harris, A., Villagra, J., Logun, C., Barb, J., et al. (2007). Amplified expression profiling of platelet transcriptome reveals changes in arginine metabolic pathways in patients with sickle cell disease. *Circulation* 115, 1551–1562. doi: 10.1161/CIRCULATIONAHA.106.658641

Rassaf, T., Poll, L. W., Brouzos, P., Lauer, T., Totzeck, M., Kleinbongard, P., et al. (2006). Positive effects of nitric oxide on left ventricular function in humans. *Eur. Heart J.* 27, 1699–1705. doi: 10.1093/eurheartj/ehl096

Reid, K. M., Tsung, A., Kaizu, T., Jeyabalan, G., Ikeda, A., Shao, L., et al. (2007). Liver I/R injury is improved by the arginase inhibitor, N^{ω}-hydroxy-nor-L-arginine (nor-NOHA). *Am. J. Physiol. Gastrointest. Liver Physiol.* 292, G512–G517. doi: 10.1152/ajpgi.00227.2006

Romero, M. J., Platt, D. H., Caldwell, R. B., and Caldwell, R. W. (2006). Therapeutic use of citrulline in cardiovascular disease. *Cardiovasc. Drug Rev.* 24, 275–290. doi: 10.1111/j.1527-3466.2006.00275.x

Roth, E., Steininger, R., Winkler, S., Längle, F., Grünberger, T., Függer, R., et al. (1994). L-Arginine deficiency after liver transplantation as an effect of arginase efflux from the graft. *Transplantation* 57, 665–669. doi: 10.1097/00007890-199403150-00006

Roy, S., Biswas, S., Khanna, S., Gordillo, G., Bergdall, V., Green, J., et al. (2009). Characterization of a preclinical model of chronic ischemic wound. *Physiol. Genomics* 37, 211–224. doi: 10.1152/physiolgenomics.90362.2008

Ryoo, S., Gupta, G., Benjo, A., Lim, H. K., Camara, A., Sikka, G., et al. (2008). Endothelial arginase II: a novel target for the treatment of atherosclerosis. *Circ. Res.* 102, 923–932. doi: 10.1161/CIRCRESAHA.107.169573

Schlüter, K.-D., Frischkopf, K., Flesch, M., Rosenkranz, S., Taimor, G., and Piper, H. M. (2000). Central role for ornithine decarboxylase in β-adrenoceptor mediated hypertrophy. *Cardiovasc. Res.* 45, 410–417. doi: 10.1016/S0008-6363(99)00351-X

Schreckenberg, R., Dyukova, E., Sitdikova, G., Abdallah, Y., and Schlüter, K.-D. (2015a). Mechanisms by which calcium receptor stimulation modifies electromechanical coupling in isolated ventricular cardiomyocytes. *Pflugers Arch.* 467, 379–388. doi: 10.1007/s00424-014-1498-y

Schreckenberg, R., Weber, P., Cabrera-Fuentes, H. A., Steinert, I., Preissner, K. T., Bencsik, P., et al. (2015b). Mechanism and consequences of the shift in cardiac arginine metabolism following ischemia and reperfusion in rats. *Thromb. Haemost.* 113, 482–493. doi: 10.1160/TH14-05-0477

Schulman, S. P., Becker, L. C., Kass, D. A., Champion, H. C., Terrin, M. L., Forman, S., et al. (2006). L-Arginine therapy in acute myocardial infarction. *JAMA* 295, 58–64. doi: 10.1001/jama.295.1.58

Schwartz, I. F., Schwartz, D., Traskonov, M., Chernikovsky, T., Wollman, Y., Gnessin, E., et al. (2002). L-Arginine transport is augmented through up-regulation of tubular CAT-2 mRNA in ischemic acute renal failure in rats. *Kidney Int.* 62, 1700–1706. doi: 10.1046/j.1523-1755.2002.t01-1-00622.x

Sharda, D. R., Yu, S., Ray, M., Squadrito, M. L., de Palma, M., Wynn, T. A., et al. (2011). Regulation of macrophage arginase expression and tumor growth by the ron receptor tyrosine kinase. *J. Immunol.* 187, 2181–2192. doi: 10.4049/jimmunol.1003460

Silva, M. A., Richards, D. A., Bramhall, S. R., Adams, D. H., Mirza, D. F., and Murphy, N. (2005). A study of the metabolites of ischemia-reperfusion injury and selected amino acids in the liver using microdialysis during transplantation. *Transplantation* 79, 828–835. doi: 10.1097/01.TP.0000153156.38617.97

Singh, M., Padhy, G., Vats, P., Bhargava, K., and Sethy, N. K. (2014). Hypobaric hypoxia induced arginase expression limits nitric oxide availability and signaling in rodent heart. *Biochem. Biophys. Acta* 1840, 1817–1824. doi: 10.1016/j.bbagen.2014.01.015

Smajilovic, S., Chattopadhyay, N., and Tfelt-Hansen, J. (2010). Calcium-sensing receptor in cardiac physiology. *Open Heart Fail. J.* 3, 11–15. doi: 10.2174/1876535101003020011

Smith, H. A. B., Canter, J. A., Christian, K. G., Drinkwater, D. C., Scholl, F. G., Christman, B. W., et al. (2006). Nitric oxide precursors and congenital heart surgery: a randomized controlled trial of oral citrulline. *J. Thorac. Cardiovasc. Surg.* 132, 58–65. doi: 10.1016/j.jtcvs.2006.02.012

Sodha, N. R., Boodhwani, M., Clements, R. T., Feng, J., Xu, S. H., and Sellke, F. W. (2008). Coronary microvascular dysfunction in the setting of chronic ischemia is independent of arginase activity. *Microvasc. Res.* 75, 238–246. doi: 10.1016/j.mvr.2007.06.008

Swamy, M., Salleh, M. J. M., Sirajudeen, K. N. S., Yusof, W. R. W., and Chandra, G. (2010). Nitric oxide (NO), citrulline – NO cycle enzymes, glutamine synthetase and oxidative stress in anoxia (hypobaric hypoxia) and reperfusion in rat brain. *Int. J. Med. Sci.* 7, 147–154. doi: 10.7150/ijms.7.147

Tratsiakovich, Y., Gonon, A. T., Krook, A., Yang, J., Shemyakin, A., Sjöquist, P.-O., et al. (2013). Arginase inhibition reduces infarct size via nitric oxide, protein kinase C epsilon and mitochondrial ATP-dependent K^+ channels. *Eur. J. Pharmacol.* 712, 16–21. doi: 10.1016/j.ejphar.2013.04.044

Van Zandt, M. C., Whitehouse, D. L., Golebiowski, A., Ji, M. K., Thang, M., Beckett, R. P., et al. (2013). Discovery of (R)-2-Amino-6-borono-2-(2-(piperidin-1-1yl)ethyl)hexanoic acid and congeners as highly potent inhibitors of human arginase I and II for treatment of myocardial reperfusion injury. *J. Med. Chem.* 56, 2568–2580. doi: 10.1021/jm400014c

Visigalli, R., Barilli, A., Parolari, A., Sala, R., Rotoli, B. M., Bussolati, O., et al. (2010). Regulation of arginine transport and metabolism by protein kinase Cα in endothelial cells: stimulation of CAT2 transporters and arginase activity. *J. Mol. Cell. Cardiol.* 49, 260–270. doi: 10.1016/j.yjmcc.2010.04.007

Wu, G., and Meininger, C. J. (2000). Arginine nutrition and cardiovascular function. *J. Nutr.* 130, 2626–2629.

Xiong, Y., Yu, Y., Montani, J. P., Yang, Z., and Ming, X. F. (2013). Arginase-II induces vascular smooth muscle cell senescence and apoptosis through p66Shc and p53 independently of its L-arginine ureahydrolase activity: implication for atherosclerotic plaque vulnerability. *J. Am. Heart Assoc.* 2:e000096 doi: 10.1161/JAHA.113.000096

Yagnik, G. P., Takahashi, Y., Tsoulfas, G., Reid, K., Murase, N., and Geller, D. A. (2002). Blockade of the L-arginine/NO synthase pathway worsens hepatic apoptosis and liver transplant preservation injury. *Hepatology* 36, 573–581. doi: 10.1053/jhep.2002.35058

Yang, J., Gonon, A. T., Sjöquist, P.-O., Lundberg, J. O., and Pernow, J. (2013). Arginase regulates red blood cell nitric oxide synthase and export of cardioprotective nitric oxide bioactivity. *Proc. Natl. Acad. Sci. U.S.A.* 110, 15049–15054. doi: 10.1073/pnas.1307058110

Zhang, C., Wu, J., Xu, X., Potter, B. J., and Gao, X. (2010). Direct relationship between levels of TNF-α expression and endothelial dysfunction in reperfusion injury. *Basic Res. Cardiol.* 105, 453–464. doi: 10.1007/s00395-010-0083-6

Zhu, W., Chandrasekharan, U. M., Bandyopadhyay, S., Morris, S. M. Jr., di Corleto, P. E., and Kashyap, V. S. (2010). Thrombin induces endothelial arginase through AP-1 activation. *Am. J. Physiol.* 298, C952–C960. doi: 10.1152/ajpcell.00466.2009

Conflict of Interest Statement: The authors declare that the research was conducted in the absence of any commercial or financial relationships that could be construed as a potential conflict of interest.

Mechanism and consequences of the shift in cardiac arginine metabolism following ischaemia and reperfusion in rats

Rolf Schreckenberg[1*]; Pia Weber[1*]; Hector A. Cabrera-Fuentes[2,6]; Isabel Steinert[1]; Klaus T. Preissner[2]; Péter Bencsik[3]; Márta Sárközy[4]; Csaba Csonka[3,4]; Péter Ferdinandy[3,5]; Rainer Schulz[1]; Klaus-Dieter Schlüter[1]

[1]Physiologisches Institut, Justus-Liebig University Giessen, Germany; [2]Biochemisches Institut, Justus-Liebig University Giessen, Germany; [3]Pharmahungary Group, Szeged, Hungary; [4]Cardiovascular Research Group, Department of Biochemistry, University of Szeged, Hungary; [5]Department of Pharmacology and Pharmacotherapy, Semmelweis University, Budapest, Hungary; [6]Kazan Federal University, Department of Microbiology, Kazan, Russia

Summary

Cardiac ischaemia and reperfusion leads to irreversible injury and subsequent tissue remodelling. Initial reperfusion seems to shift arginine metabolism from nitric oxide (NO) to polyamine formation. This may limit functional recovery at reperfusion. The hypothesis was tested whether ischaemia/reperfusion translates such a shift in arginine metabolism in a tumour necrosis factor (TNF)-α-dependent way and renin-angiotensin system (RAS)-dependent way into a sustained effect. Both, the early post-ischaemic recovery and molecular adaptation to ischaemia/reperfusion were analysed in saline perfused rat hearts undergoing global no-flow ischaemia and reperfusion. Local TNF-α activation was blocked by inhibition of TNF-α sheddase ADAM17. To interfere with RAS captopril was administered. Arginase was inhibited by administration of Nor-NOHA. Long-term effects of ischemia/reperfusion on arginine metabolism were analysed *in vivo* in rats receiving an established ischaemia/reperfusion protocol in the closed chest mode. mRNA expression analysis indicated a shift in the arginine metabolism from NO formation to polyamine metabolism starting within 2 hours (h) of reperfusion and translated into protein expression within 24 h. Inhibition of the TNF-α pathway and captopril attenuated these delayed effects on post-ischaemic recovery. This shift in arginine metabolism was associated with functional impairment of hearts within 24 h. Inhibition of arginase but not that of TNF-α and RAS pathways improved functional recovery immediately. However, no benefit was observed after four months. In conclusion, this study identified TNF-α and RAS to be responsible for depressed cardiac function that occurred a few hours after reperfusion.

Correspondence to:
Prof. Dr. Klaus-Dieter Schlüter
Physiologisches Institut, Justus-Liebig-University Giessen
Aulweg 129, 35392 Giessen, Germany
Tel.: +49 641 99 47 212, Fax:+49 641 99 47 219
E-mail: Klaus-Dieter.Schlueter@physiologie.med.uni-giessen.de

* These authors contributed equally to the study.

Financial support:
This study was supported by the Deutsche Forschungsgemeinschaft (grants to K. Preißner, R. Schulz and K.-D. Schlüter within the graduate school "PROMISE" [IRTG1566]) and a grant to K.-D. Schlüter (SCHL 324/7–1).

Received: May 29, 2014
Accepted after major revision: October 28, 2014
Epub ahead of print: December 11, 2014

http://dx.doi.org/10.1160/TH14-05-0477
Thromb Haemost 2015; 113: 482–493

Introduction

The acute coronary syndrome is one of the leading causes for the development and progression to heart failure (1, 2). It can be successfully treated by reperfusion strategies thereby limiting myocardial damage but yet leading to new onset of heart failure. Therefore, a better understanding of the molecular processes in the reperfused post-ischaemic heart is required to improve pharmacological options that prevent the progression of cardiac remodelling to heart failure under such conditions.

Inhibition of the angiotensin converting enzyme (ACE) can positively affect post infarct remodelling specifically if treatment is started after a successful revascularisation. Delayed but not immediate captopril therapy improved cardiac function and increased survival (3–7). This suggests that the renin-angiotensin system (RAS) contributes to early post-infarct remodelling leading to progression to heart failure but not to direct reperfusion-linked injury. The molecular mechanisms that may explain such a behaviour of ACE inhibition in this specific setting are not clear. In an experimental study, captopril improved the bioavailability of nitric oxide (NO) after ischaemia/reperfusion if administered together with arginine (8). This suggests that in the post-ischaemic heart arginine may not be used by nitric oxide synthases (NOS) but by alternative pathways.

In general, an activation of NO-dependent cGMP-linked pathways is considered to improve the early post-ischaemic recovery (9). However, the post-ischaemic myocardium has a characteristic loss of NO-dependent signalling (10, 11). This is mainly due to an increased oxidative stress and diminished NO formation rather than the impaired downstream signalling of NO, because administration of NO donors restores a normal NO-dependent signalling (12). Interestingly, chronic ischaemia leads to endothelial dysfunction in the heart that is independent of arginase activity (13). Therefore, the observed shift in arginine metabolism is specific for

ischaemia/reperfusion injury. Possible reasons for such a lack of responsiveness are either a down-regulation of NO forming pathways or an activation of pathways that compete with NO formation for the same substrates.

Arginine is also the substrate for the polyamine metabolism, a major pathway used for cell growth and differentiation (14, 15). In the polyamine metabolism, arginine is converted by arginases into urea and ornithine that is further decarboxylated by ornithine decarboxylase (ODC), the rate limiting enzyme of the polyamine metabolism. The polyamine metabolism has been shown to play a crucial role in myocardial adaptation and transition to heart failure in the chronic pressure overloaded heart (16). Furthermore, the induction of the polyamine metabolism is linked to the activation of the RAS (17). An activation of arginase-1 in post-ischaemic hearts seems to indicate an activation of the polyamine metabolism (18).

The current study tested the hypothesis that events related to ischaemia/reperfusion may trigger a shift of the arginine metabolism from NO formation to polyamine metabolism and was aimed to identify potential mechanisms that trigger this event. A likely candidate may be a rapid release of local TNF-α by ischaemia-dependent activation of the sheddase" TNF-α converting enzyme" (TACE, also known as ADAM17) because TNF-α has been shown to induce the expression of arginase-1 and an activation of arginase-1 was shown in post-ischaemic rat hearts (19–22). If this hypothesis holds, inhibition of TNF-α release during ischaemia should avoid an activation of the arginine/polyamine pathway. In order to address these questions we performed *in vitro* experiments on isolated perfused rat hearts that were exposed to global no-flow ischaemia and reperfusion and added TAPI, an inhibitor of TNF-α release, during ischaemia. However, as pre-ischaemic TACE inhibition cannot be used in clinical practice we tested next, whether captopril can restore the pre-ischaemic balance between NO and polyamine metabolism by induction of the NO pathway.

In order to test this hypothesis captopril, an ACE inhibitor, was added to the perfusate of saline perfused rat hearts 30 minutes (min) after the onset of reperfusion. It has previously been shown that administration of sulfhydryl group containing ACE inhibitors can reduce infarct size if administered prior to ischaemia (i.e. [23]). Once again, as pre-ischaemic administration of therapeutics is not practicable in ischaemia/reperfusion in the clinical setting, captopril was given during late reperfusion in the subsequent experiments. Hearts were reperfused for 2 hours (h) and molecular markers of remodelling as well as the functional recovery were determined. Finally, we tested the effect of arginase inhibition during the onset of reperfusion. Unlike the above mentioned effects on transcription, a shift in arginine / eNOS activity may also be caused by uncoupling of NOS. In this case, inhibition of arginase should directly normalize the relationship between both arginine consumers.

Material and methods

Animal models and animal handling

The investigation conforms to the directive 2010/63/EU of the European Parliament. Use of animals was registered at the Justus-Liebig-University (registration-no.: 417-M). The experimental protocols were approved by the ethics committee for animal experimentation of the local authorities in Giessen, Germany and Szeged, Hungary.

Myocardial infarction and reperfusion was performed in the closed-chest model. To achieve this, rats were anaesthetised by inhalation of isoflurane (induction: 5%, maintenance: 2–3%), intubated and placed on a respirator during surgery to maintain ventilation. Before surgery, 0.03 mg/kg nalbuphin (Nalbuphin Orpha, AOP Orpha Pharmaceuticals, Vienna, Austria) was injected (i.p.). The adequacy of anaesthesia was monitored by electrocardiography and pulse rate. A suture was placed around the left anterior descending coronary artery and remained subcutaneously (24). At 2 h after the wound closing, 0.03 mg/kg nalbuphin was repeated to alleviate postoperative pain. Seven days later, rats were anaesthetised as before and the suture was mobilised, and the LAD was occluded for 30 min. The occlusion was monitored by electrocardiography (ST elevation). Thereafter, the occluder was opened again and the suture was cut and the skin was closed in one layer. Sham rats received the same protocol but the occluder was not mobilised after seven days. Rats that received captopril after ischaemia/reperfusion received the ACE inhibitor captopril (300 mg/l) in tap water (accumulating to approximately 30 mg/kg*day).

Ex vivo analysis of cardiac function

In order to analyse the cardiac function *ex vivo*, rats were anaesthetised again by isoflurane and killed by cervical dislocation. Thereafter hearts were rapidly excised and the aorta was cannulated for retrograde perfusion with a 16-gauge needle connected to a Langendorff perfusion system. Left ventricular function was determined by insertion of a water filled balloon into the left ventricle as described before (25). Hearts were paced during measurements.

In vivo analysis of cardiac function

Transthoracic echocardiography was performed as described previously (26) under isoflurane anaesthesia (1.5%) at 120 days after ischaemia/reperfusion. Briefly, two-dimensional and M-mode echocardiographic examinations were performed in accordance with the criteria of the American Society of Echocardiography with a Vivid 7 Dimension ultrasound system (General Electric Medical Systems) using a phased array 5.5–12 MHz transducer (10S probe). Data of three consecutive heart cycles were analysed (EchoPac Dimension software; General Electric Medical Systems) by an experienced investigator in a blinded manner. The mean values of three measurements were calculated and used for statistical evaluation. Functional parameters including left ventricular

ejection fraction (EF) and fractional shortening (FS) were calculated on four-chamber view images.

qRT-PCR

After removing the hearts from the Langendorff apparatus, the left ventricular tissue was carefully isolated and quickly frozen in fluid nitrogen. Tissue samples were prepared to analyse the steady-state mRNA levels of proteins of interest according to the previously described method (25). Briefly, total RNA was isolated from the left ventricles using peqGoldTriFast (peqlab, Biotechnology GmbH, Erlangen, Germany) according to the manufacturer's protocol. To remove genomic DNA contamination, isolated RNA samples were treated with 1 U DNase per mg RNA (Invitrogen, Karlsruhe, Germany) for 15 min at 37°C. On µg of total RNA was used in 10 µl reaction to synthesise cDNA using superscript RNaseH reverse transcriptase (200 U/µg; Invitrogen) and oligo dTs (Roche, Mannheim, Germany) as primers. Reverse transcriptase reactions were performed for 60 min at 37°C. Real-time PCR was performed using the Icycler IQ detection system (Bio-Rad, Munich, Germany) in combination with IQ SYBR Green real-time supermix (Bio-Rad). A complete list of all primers used in this study is given in ▶Table 1. Data are normalised to hypoxanthine phosphoribosyltransferase (HPRT) expression that was used as a housekeeping gene in this study. Preliminary experiments with β_2 microglobulin, which was alternatively considered as housekeeping gene, revealed similar results but higher variability. The relative change in expression was quantified by the ΔΔCT method (27).

Western blots

Tissue samples from hearts stored at -80°C were used as described previously and prepared for standard SDS gel electrophoresis. Protein was extracted as described before (25). The lysis buffer contained (mmol/l): Tris-HCl (pH 7.5) 20, NaCl 150, EGTA 1, EDTA 2, Triton (1% v/v), sodium pyrophosphate (2.5), β-glycerophosphate 1, Na_3VO_4 1, leupeptin (1 µg/ml) (Cell Signalling Technology, Leiden, Netherland). The homogenate was centrifuged at 1,000 g at 4°C for 10 min and the supernatant was used for protein detection by Western blotting. Supernatants were treated with Laemmli buffer (reducing conditions with β-mercaptoethanol; non-reducing conditions without β-mercaptoethanol). Samples were subsequently heated for 5 min at 95°C (reducing conditions) or incubated for 30 min at room temperature (non-reducing conditions). Protein samples were loaded on NuPAGE Bis-Tris Precast gels (10%; Life Technology, Darmstadt, Germany) and subsequently transferred onto nitrocellulose membranes. Primary antibodies directed against eNOS , ODC, and cardiac α-actin (loading control) were used as described before (27). Tropomyosin blots were incubated with an anti-tropomyosin antibody purchased from Sigma-Aldrich (Taufkirchen, Germany; product T9283). The antibody was previously used to establish tropomyosin disulphide cross-bridging (29).

Measurement of superoxide

To perform DHE staining, cryosections of left ventricles were incubated with DHE (dissolved in 1 X PBS) for 10 min at 37°C in a light-protected humidity chamber, then fixed with Dako Fluorescent Mounting Medium (Dako, Glostrup, Denmark). Slides were then imaged by confocal microscopy (LSM 510 META; Carl Zeiss, Jena, Germany) using an excitation wavelength of 488 nm; emission was recorded at 540 nm. Assessment was performed by digital image analysis using Leica Confocal Software Lite Version (LCS Lite). The mean fluorescence intensity of n=8 per group was used to quantify the extent of superoxide.

Quantification of TNF-α concentrations

Langendorff heart-perfusates were collected prior to ischaemia and one minute after reperfusion and filtered through 0.2 µm filter to remove any residual debris. To quantify the TNF-α production, an enzyme-linked immunosorbent assay (ELISA) (Quantikine®, R&D Systems, Minneapolis, MN, USA) was used. Absorbance values for individual reactions were determined using VersaMax™ Microplate Reader with SoftmaxPro 3.0 data processing software.

Statistics

The results are expressed as means ± S.E.M. or box plots as indicated in the legend to the figures. Statistical comparisons were performed by two-side ANOVA and Student-Newman-Keuls post-hoc analysis. Levene test was used to check the normal distribution

	Forward	Reverse
HPRT	CCA GCG TCG TGA TTA GTG AT	CAA GTC TTT CAG TCC TGT CC
eNOS	AGC CCG GGA CTT CAT CAA TCA	GCC CCA AAC ACC AGC TCA CTC TC
ODC	GAA GAT GAG TCA AAC GAG CA	AGT AGA TGT TTG GCC TCT GG
Arginase-1	GGA AGC ATC TCT GGC CAC GCC	CAC CGG TTG CCC GTG CAG
Arginase-2	TGA GGA GCA GCG TCT CCC GT	GCT TCT CGG ATG GCG GCT GG
ANP	ATG GGC TCC TCC TCC ATC AC	TCT TCG GTA CCG GAA GCT
SERCA2a	CGA GTT GAA CCT TCC CAC AA	AGG AGA TGA GGT AGC GGA TGA A
Bax	ACT AAA GTG CCC GAG CTG ATC CAC	TGT CTG CCA TGT GGG G

Table 1: RNA primer sequences.

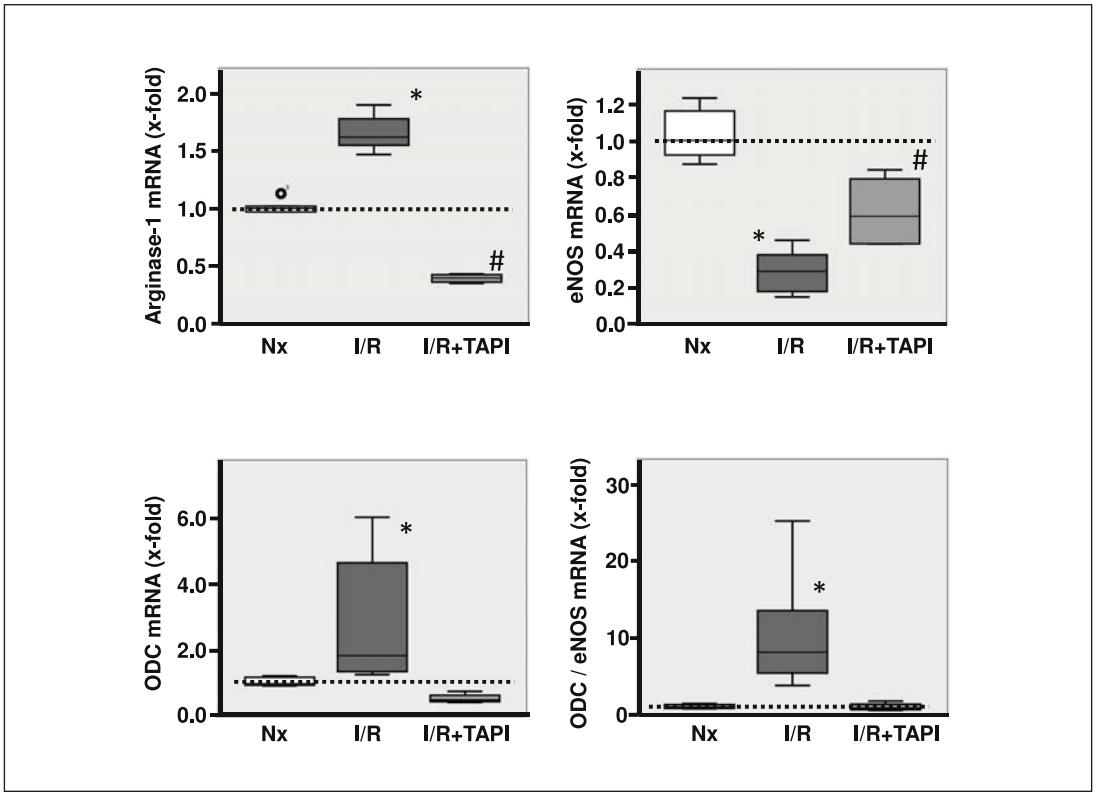

Figure 1: Left ventricular mRNA expression of arginase 1, eNOS, ODC and the ODC-to-eNOS ratio in hearts exposed to 45 min ischaemia and 120 min reperfusion. HPRT was used to normalise the data. Data are shown as box plots and individual data points outside the 5 % and 95 % are indicated separately. The dashed line indicates basal expression of control hearts (Nx) not undergoing 45 min of ischaemia and reperfusion (I/R). TAPI (1 µmol/l) was used to inhibit the activity of TACE. *, $p<0.05$ vs Nx (n=6–8 hearts).

of the samples. A p-value of 0.05 was considered as statistical significant.

Results

Influence of TAPI administration during ischaemia on the functional recovery of post-ischaemic hearts and the expression of genes linked to arginine metabolism

In the first set of experiments we tested the hypothesis that TNF-α released during ischaemia may trigger a molecular switch of arginine metabolism during reperfusion by an activation of the sheddase "TNF-α converting enzyme" (TACE). In order to address this question we administered the TACE inhibitor TAPI (1 µM) to hearts prior to the onset of ischaemia. ▶Figure 1 describes the subsequent changes in mRNA expression of arginase-1, eNOS, ornithine decarboxylase (ODC), and the ratio between eNOS and ODC. Ischaemia/reperfusion increased arginase-1 mRNA expression, whereas a decreased mRNA expression of eNOS and increased mRNA expression of ODC shifted the eNOS/ODC ratio into the direction of polyamine metabolism. Noteworthy, all these changes were completely attenuated if TAPI was administered prior to reperfusion. However, these molecular changes on mRNA expression had no effects on the functional heart recovery within 2 h. At 2 h after reperfusion, hearts developed a mean left ventricular pressure of 59.4 ± 8.9 mmHg in control hearts and 63.4 ± 5.8 mmHg in hearts treated with TAPI (p=0.717, n=6). Pre-ischaemic values had been 95.1 ± 2.6 mmHg and 96.2 ± 6.3 mmHg, respectively. As expected, TAPI significantly attenuated the release of TNF-α into the perfusate. This amount of TNF-α was 13.0 ± 4.3 pg/ml in the perfusate of normoxic control hearts and increased to 52.5 ± 10.9 pg/ml ($p<0.05$; n=6 hearts) in the perfusate of post-ischaemic hearts. TAPI reduced this increase to 19.6 ± 9.8 pg/ml. Collectively these data show that ischaemia/reperfusion shifts the arginine pathway into the direction of polyamine metabolism and identify TNF-α as a causative factor in this process. Whether this process can be reversed by inhibition of the local RAS was tested next.

Functional recovery of rat hearts after ischaemia/-reperfusion and influence of captopril

In order to address the question whether ACE inhibition can antagonise TNF-α-driven molecular changes of ischaemia/reperfusion, the ACE inhibitor captopril was added 30 min after the onset of reperfusion. Again, there were no functional differences between the treatment group and the captopril group. Pre-ischaemic values of left ventricular developed pressure (LVDP) were 115.3 ± 6.1 mmHg and 104.9 ± 6.6 mmHg. At 30 min after the onset of reperfusion and before starting captopril administration LVDP values were 85.9 ± 10.6 mmHg and 85.4 ± 5.3 mmHg, respectively. Finally, LVDP values amounted to 50.5 ± 5.2 mmHg and 48.0 ± 5.7 mmHg, respectively, 2 h after the start of reperfusion. Thus, captopril did not affect the functional recovery of hearts when administered 30 min after reperfusion and present for further 90 min.

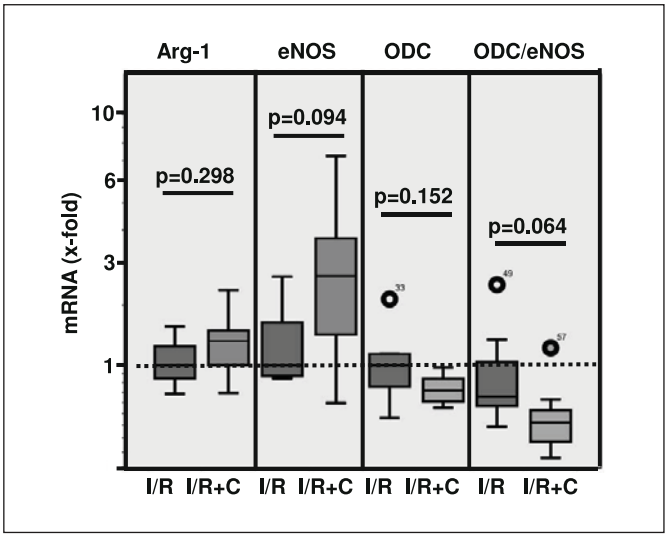

Figure 2: Left ventricular mRNA expression of arginase 1, eNOS, ODC and the ODC-to-eNOS ratio in hearts exposed to 45 min ischaemia and 120 min reperfusion. HPRT was used to normalise the data. Data are shown as box plots and individual data points outside the 5 % and 95 % are indicated separately. The dashed line indicates basal expression of control hearts (I/R) not receiving captopril (100 µmol/l) starting 30 min after the onset of reperfusion. Exact p-values are given (each n=8).

In contrast to the lack of effect on functional recovery, a clear trend to higher expression of eNOS following captopril was found. Moreover, the mRNA expression of arginase-1 and ODC was lower than in the non-treatment group (►Figure 2). Collectively, these data show that inhibition of the local ACE system potentially attenuates the shift of the arginine metabolism by up-regulation of eNOS. The data in the *in vitro* model show significant effects on the mRNA expression of enzymes involved in the arginine metabolism. However, these changes seem not to be functionally relevant within minutes because these changes have to be translated into proteins first. Whether this shift in arginine metabolism modifies the outcome at later time points was investigated next in an appropriate *in vivo* model.

Table 2: Effect of captopril on cardiac function *ex vivo* 24 and 72 hours after ischemia/reperfusion.

	LVDP (mmHg)	LVDP (%)
Day 1 (24 h)		
Sham	158 ± 7	100 ± 4
I/R	123 ± 7	78 ± 4
Δ	-35*	-22*
Sham / Capto	186 ± 11	100 ± 6
I/R / Capto	165 ± 5	89 ± 2
Δ	-21	-11
Day 3 (72 h)		
Sham	155 ± 8	100 ± 5
I/R	132 ± 10	85 ± 7
Δ	-23	-15
Sham / Capto	168 ± 8	100 ± 5
I/R / Capto	153 ± 8	91 ± 5
Δ	-15	-9

Data are means S.E.M. from n=8 hearts each.
*p<0.05 vs. Sham.

Functional recovery of rats after *in vivo* ischaemia/reperfusion and effect of administration of captopril

In order to address the functional relevance of eNOS up-regulation by captopril, rats underwent ischaemia and reperfusion in the so-called closed chest model. Rats received either captopril with their tap water directly after recovery from the surgery for one or three days (treatment group) or no drug (non-treatment group). Control rats underwent sham surgery without ligation of the left anterior descending artery. Cardiac function was analysed *ex vivo* in saline perfused rat hearts. Post-ischaemic rats developed a loss of cardiac function at day 1 after reperfusion that was less pronounced at day 3 after reperfusion (►Table 2). Of note, this early loss of function was largely attenuated in the captopril group. When the mRNA expression of eNOS, arginase-1 and ODC was analysed in post-ischaemic hearts from rats of the control group in comparison to the captopril group, they displayed significant differences. As indicated in ►Figure 3, the administration of the ACE inhibitor induced down-regulation of the mRNA expression of ODC and normalised the expression of eNOS. On the protein level, ODC mRNA expression was higher in post-ischaemic non-treated hearts, and the inhibitor attenuated the induction of ODC. It also normalised the expression of eNOS and the ODC-to-eNOS ratio.

The differences between treated and non-treated rats in left ventricular function were lower at day 3 (►Table 2) and at that time-point the molecular adaptations were also smaller compared to day 1 but all changes displayed a similar trend than at day 1 (►Figure 4). In addition, the induction of arginase-1 by ischaemia/reperfusion remained significant at day 1 after reperfusion but was again normalised by captopril administration (►Figure 5). This effect of ischaemia/reperfusion on arginase expression was lost within the subsequent days (►Figure 5). In summary, captopril shifted the arginine metabolism into the direction of NO metabolism. This effect was induced at a very early time point as seen in the saline perfused rat hearts (see above, although not functionally significant at this time point), strongest at day 1 after reperfusion, but already beginning to be lost within the next days in the presence of captopril.

Mechanistically the question occurred whether the attenuation of the shift in arginine metabolism may cause decreased oxidative stress. As expected, ischaemia/reperfusion caused an increase in superoxide formation as indicated by increased DHE staining (Suppl. Figure 1a, b, available online at www.thrombosis-online.com). As recently demonstrated, oxidative modification of tropomyosin leads to myocardial dysfunction by TNF-α-dependent in-

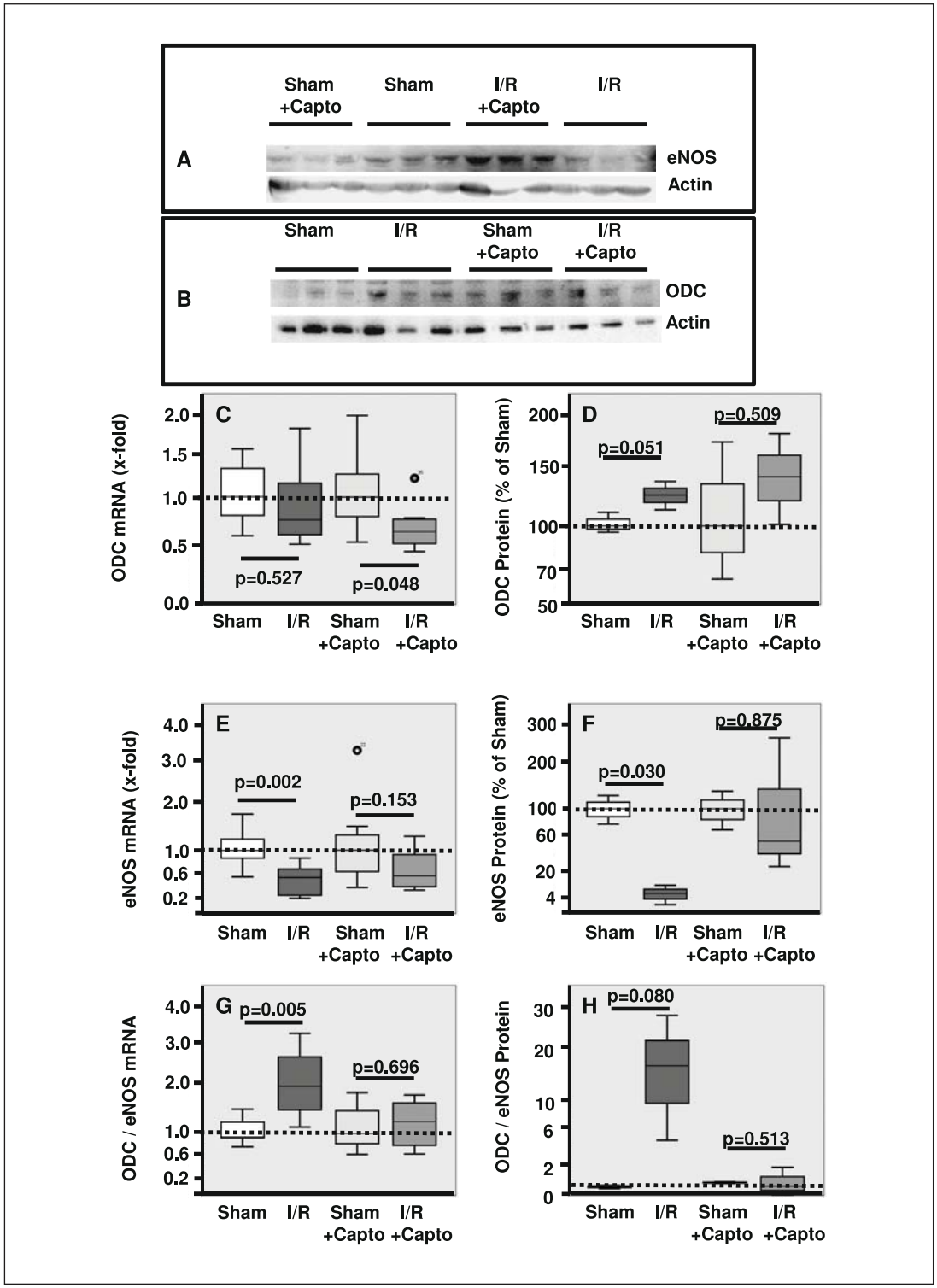

Figure 3: Protein and mRNA expression of eNOS and ODC in rat hearts from rats undergoing 30 min of ischaemia and 24 h of reperfusion *in vivo*. Where indicated, rats received captopril by tapwater after surgery. Data are shown as box plots and individual data points outside the 5 % and 95 % are indicated separately. The dashed line indicates basal expression of control hearts (Sham) not receiving captopril. Exact p-values are given (each n=8).

duced oxidative stress. As shown in Suppl. Figure 1c (available online at www.thrombosis-online.com), under non-reducing conditions the anti-tropomyosin antibody detected a band at approximately 45 kDa corresponding to a band detected under reducing conditions as well, and an additional band at a much higher molecular weight appeared (approximately at 80 kDa), which most likely was caused by disulphide cross-bridges (DCB; [29]). Ischaemia/reperfusion resulted in a higher degree of DCB amounts and this was no longer significantly enhanced if captopril was administered during the first day (Suppl. Figure 1c, available online at www.thrombosis-online.com).

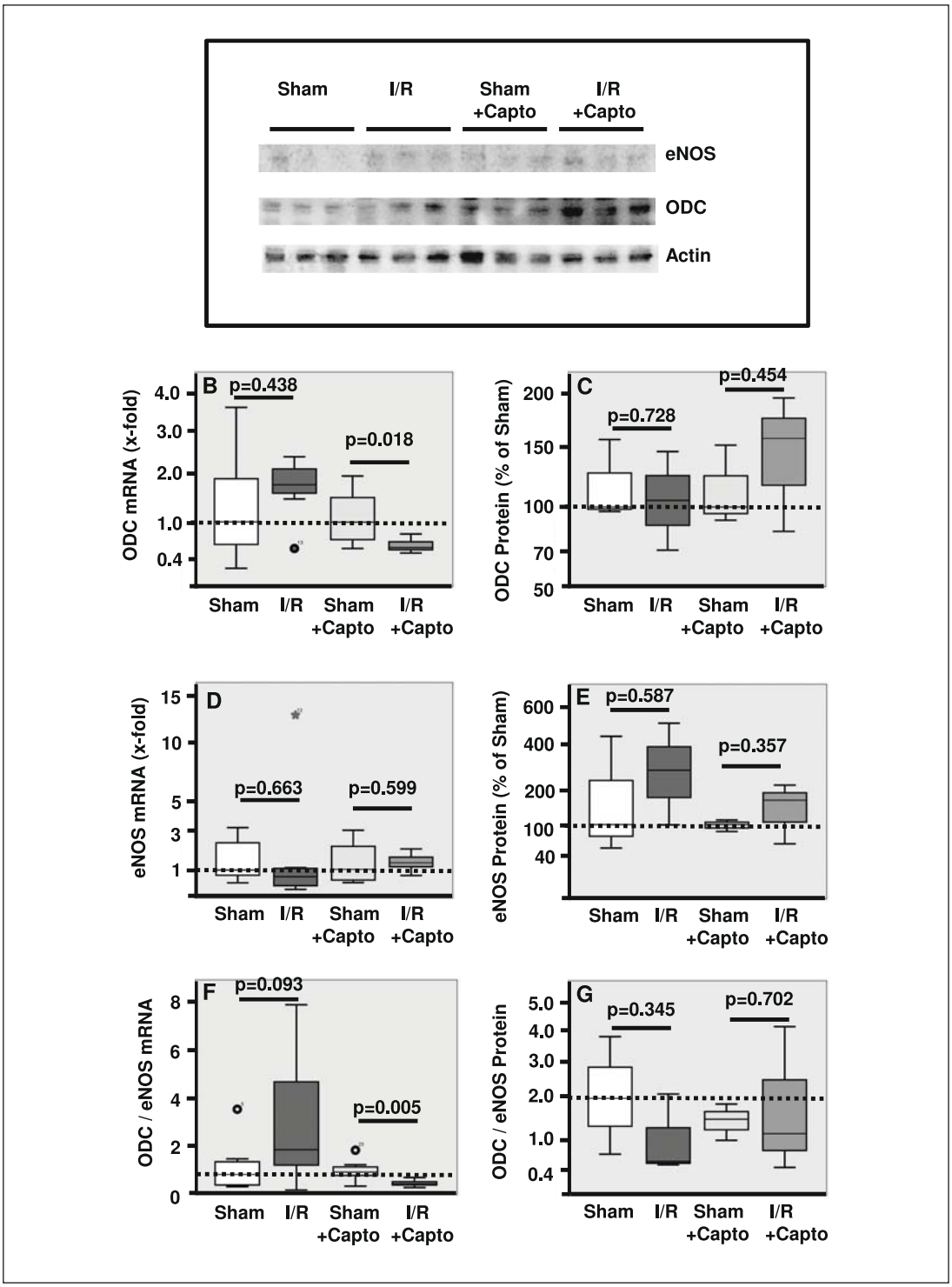

Figure 4: Protein and mRNA expression of eNOS and ODC in rat hearts from rats undergoing 30 min of ischaemia and 72 h of reperfusion *in vivo*. Where indicated, rats received captopril by tapwater after surgery. Data are shown as box plots and individual data points outside the 5 % and 95 % are indicated separately. The dashed line indicates basal expression of control hearts (Sham) not receiving captopril. Exact p-values are given (each n=8).

Functional recovery of rats after *in vitro* ischaemia/reperfusion and effect of administration of Nor-NOHA

The results shown above have clearly shown the impact of arginase/ODC and eNOS expression on post-ischaemic recovery within 24 h. Without changes in expression, a similar shift may occur at the onset of reperfusion due to eNOS uncoupling (see Introduction). Whether an increased activity of arginase relative to eNOS can contribute to oxidative stress, namely superoxide formation, and directly depress functional recovery was investigated next. To address this question, arginase activity was inhibited by Nor-NOHA, a specific inhibitor of arginase during rep-

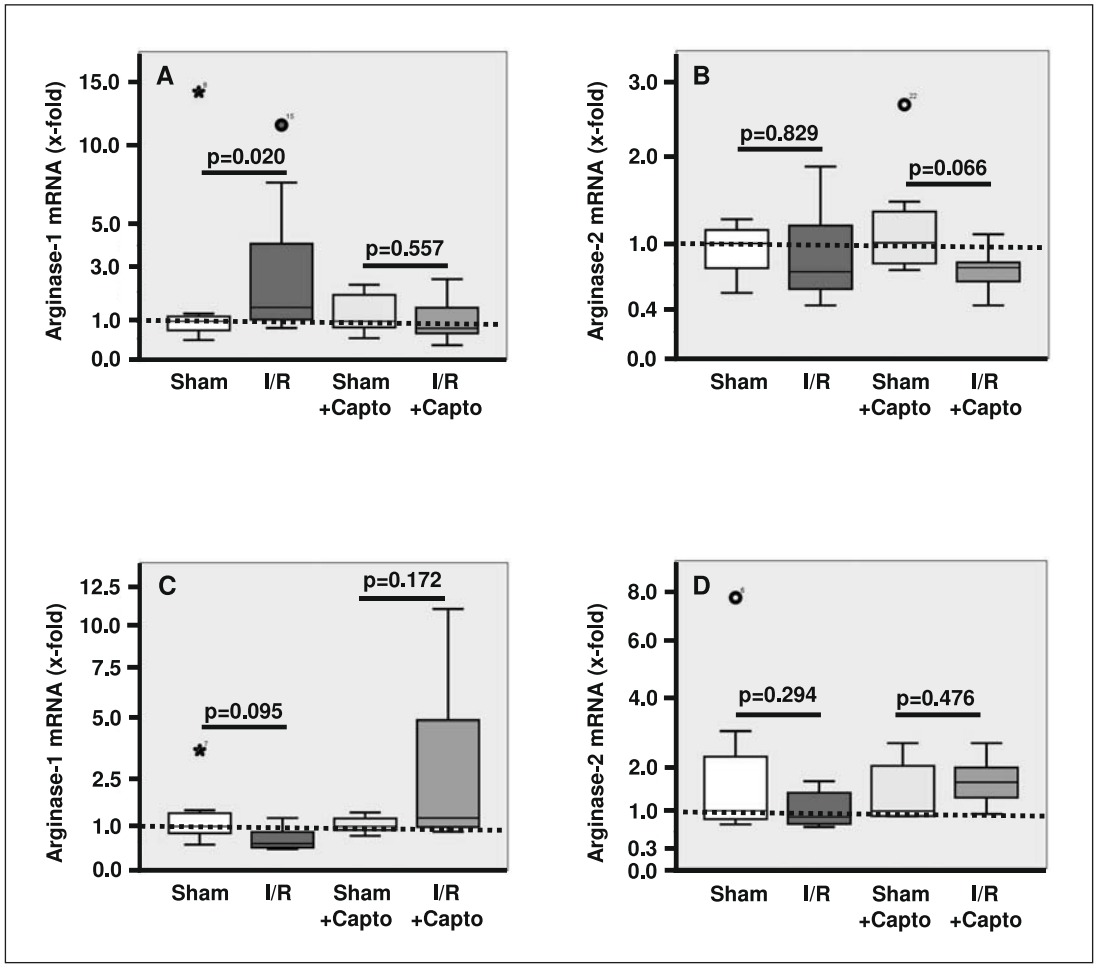

Figure 5: Left ventricular mRNA expression in rat hearts from rats undergoing 30 min of ischaemia and 24 h (A,B) or 72 h (C,D) of reperfusion *in vivo*. Data are shown as box plots and individual data points outside the 5 % and 95 % are indicated separately. The dashed line indicates basal expression of control hearts (Sham) not receiving captopril. Exact p-values are given (each n=8).

erfusion. As expected, ischaemia/reperfusion caused an increase in superoxide formartion as indicated by increased DHE staining (►Figure 6A, B). However, inhibition of arginase activity during reperfusion caused a significant reduction of oxidative stress and improved the functional recovery of these hearts (►Figure 6A, B). This increased oxidative stress went along with a clear shift in tropomyosin oxidation (►Figure 6C). In addition, the functional recovery (120 min reperfusion) was significantly improved in hearts that received Nor-NOHA at the onset of reperfusion [LVDP: 57.4 ± 9.2 mmHg (Nor-NOHA; n=8) vs 44.1 ± 9.2 mmHg (Control; n=11); $p<0.05$]. Pre-ischaemic values were 116.4 ± 20.5 and 121.1 ± 20.4 mmHg, respectively. These data suggest that the shift in arginine metabolism is associated with changes in the oxidative stress affecting directly the cardiac function. Collectively the data suggest that activation of the local TNF-α system convert the acute activation of arginase into sustained arginase activation by transcriptional activation and that this process can be attenuated by induction of the counter-regulatory eNOS by ACE inhibition.

Long-term effect of the captopril-driven attenuation of the shift in arginine metabolism in the early phase of reperfusion

Finally, we examined whether this early protection by captopril has any long-term consequences for the post-ischaemic recovery. At day 120, no differences in the mRNA expression of molecules linked to arginine metabolisms (eNOS, arginase-1, ODC) were found between both groups of ischaemia/reperfusion (Suppl. Figure 2, available online at www.thrombosis-online.com). Surprisingly, although captopril treatment had a significant better functional recovery of the heart during the first days after reperfusion *in vivo*, this did not end up in any functional improvements after four months. This was indicated *in vivo* by a similar reduction of EF compared to sham rats in treated and non-treated rats, and confirmed *in vitro* by a lower LVDP in saline reperfused rat hearts. However, although no functional effect was found in these rats three molecular markers of cardiac hypertrophy and remodelling showed significant difference in their mRNA expression between captopril-treated and non-treated rats. These were ANP, a marker of cardiac hypertrophy that was elevated in the captopril group, SERCA2a, a calcium transporter that improves cardiac function by

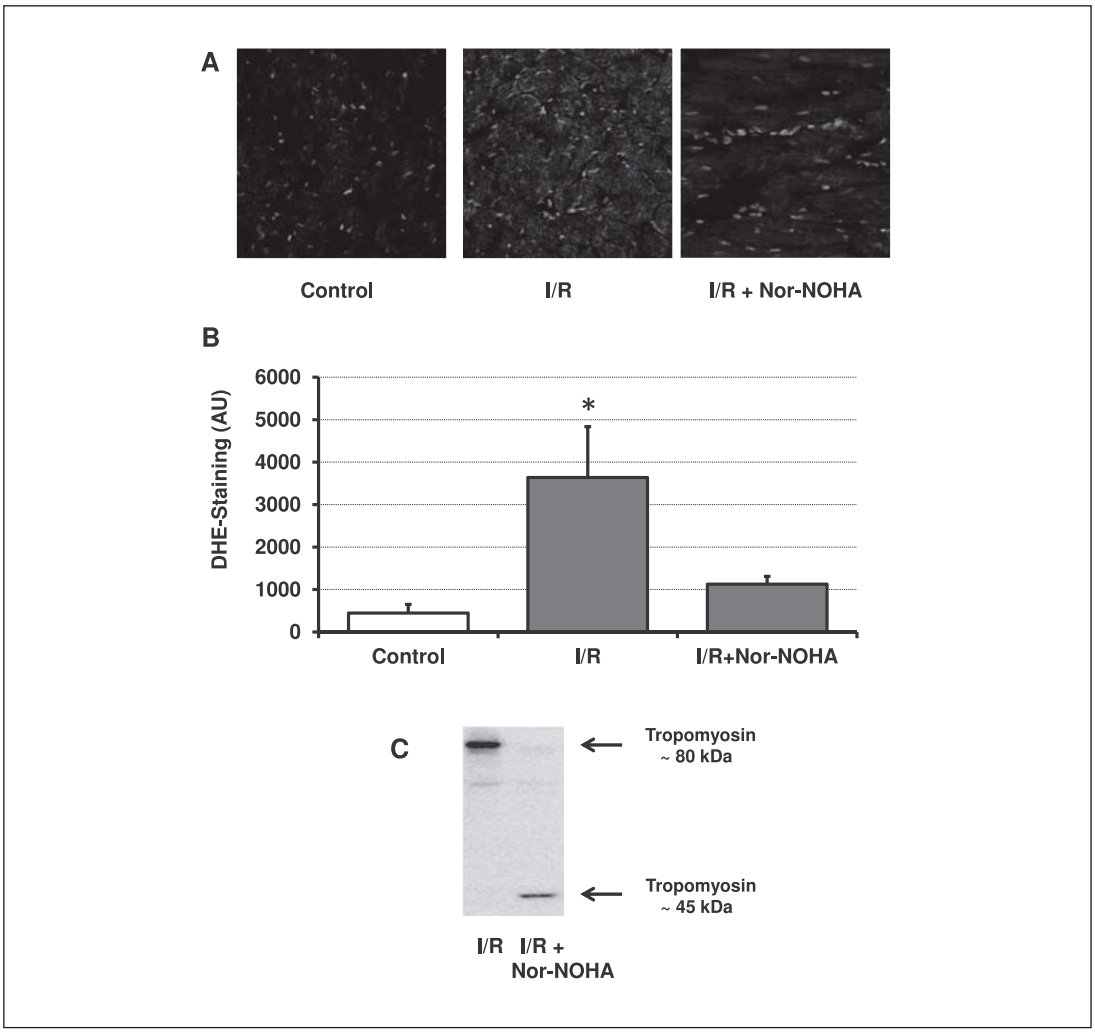

Figure 6: Superoxide formation in post-ischaemic hearts and its modification by arginase inhibition. Data are shown for control hearts (normoxic perfusion), post-ischaemic hearts (30 min after reperfusion; I/R), and hearts receiving the arginase inhibitor Nor-NOHA (100 µM) during reperfusion. A) Representative tissue slices with superoxide staining by DHE in green. B) Quantitative analysis of DHE staining for the three groups (each n=8). *, $p<0.000$ vs control and Nor-NOHA group. C) Representative immunoblots of tropomyosin under non-reducing conditions.

acceleration of calcium refilling of the sarcoplasmatic reticulum that was also higher expressed in the captopril group, and bax, a pro-apoptotic factor, which was less expressed in these rats (►Figure 7). These changes suggest a slightly different type of compensatory hypertrophy in captopril-treated rats.

Discussion

This study demonstrated that at the onset of reperfusion and several hours after reperfusion a shift within the arginine metabolism occurs that favours arginine consumption into the polyamine metabolism and reduces NO formation. Initially, this shift is triggered by eNOS uncoupling. Inhibition of arginase normalises the ratio between the activities of both arginine consumers and thereby reduces oxidative stress. This shift in arginine metabolism is maintained at later time points by an induction of arginase-1 and ODC mRNA and protein expression and a down-regulation of eNOS mRNA expression. As a potential mechanism that triggers this transcriptional activation, we identified ischaemia/reperfusion-dependent activation of TACE. As a new finding of this study we show for the first time that this shift in arginine metabolism can be normalised by inhibition of the cardiac RAS. This inhibition attenuates the down-regulation of eNOS. Under these conditions, cardiac function was maintained at day 1 after reperfusion. Mechanistically, it is suggested that NO as a radical acceptor binds ROS that would otherwise oxidise cysteine residues at tropomyosin and thereby reduce cardiac function. In this study we show that inhibition of arginase during reperfusion indeed reduces superoxide formation and improves the early functional recovery and that interference with arginase up-regulation and eNOS down-regulation improves the situation within hours. Despite these promising results the long-term cardioprotective effect is low in terms of functional aspects but is associated with moderate molecular adaptations on the mRNA expression level. A schematic overview about the proposed mechanism is given in ►Figure 8.

It has previously been shown that ischaemia leads to an induction of arginase-1 that converts arginine into ornithine so that arginine is no longer available as a substrate of eNOS. At least in the rat arginase-1 is the main isoform (18). Our study confirmed these findings and documented that within minutes after reperfusion argininase-1 mRNA expression increases in isolated saline perfused

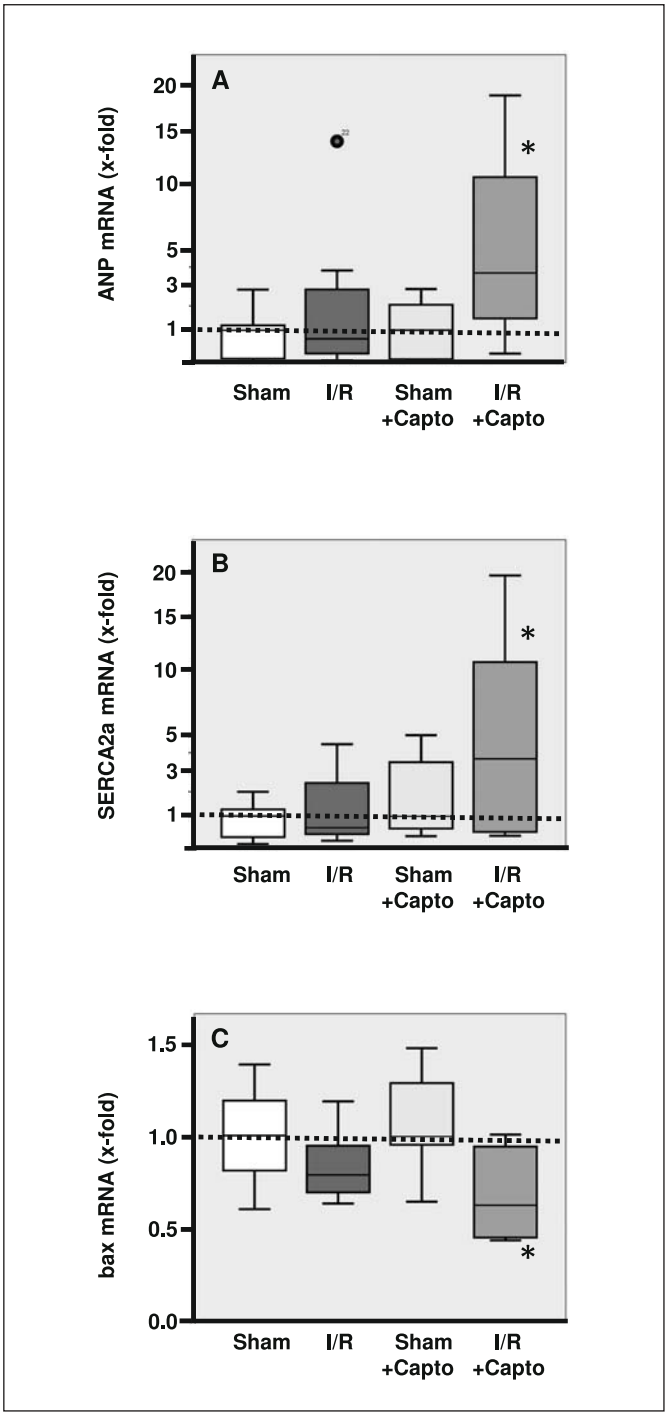

Figure 7: Left ventricular mRNA expression of ANP, SERCA2a, and bax in hearts exposed to 30 min ischaemia and 120 days of reperfusion. HPRT was used to normalise the data. Data are shown as box plots and individual data points outside the 5 % and 95 % are indicated separately. The dashed line indicates basal expression of control hearts (Sham) not receiving captopril. *, $p<0.05$ vs Sham (each n=8).

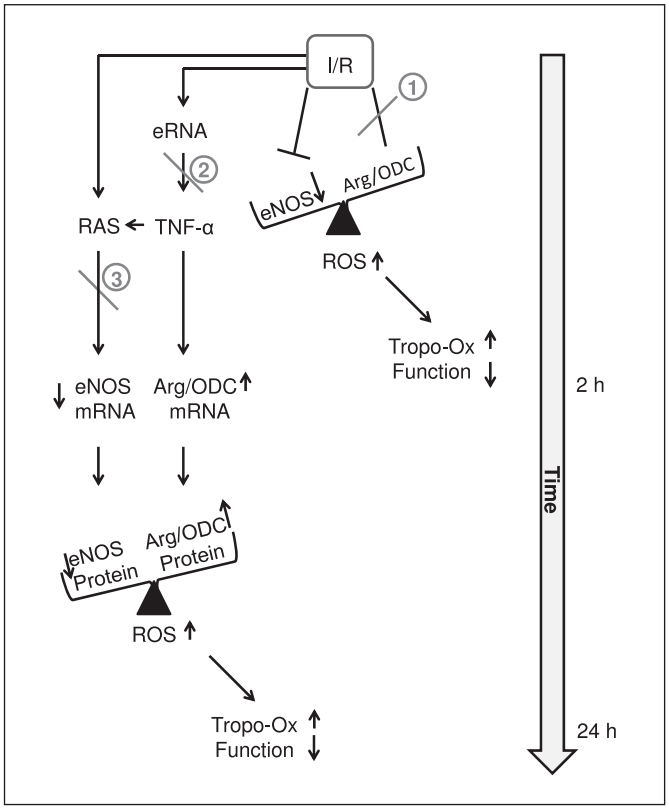

Figure 8: Summary figure - Ischaemia/Reperfusion (I/R) uncouples eNOS and thereby shifts the relationship between arginase / ODC and eNOS into the direction of arginase. This causes oxidative stress, oxidation of tropomyosin and loss of function. Inhibition of arginase (red labelled No. 1) normalised the relationship between arginase and eNOS. I/R also led to release of cell compounds due to loss of sarcolemmal integrity including RNA. Extracellular RNA (eRNA) activates TACE leading to liberation of bound TNF-α. TNF-α induces the expression of arginase and ODC and activates the renin-angiotensin-system (RAS) that down-regulated the expression of eNOS. The subsequent unbalance between arginase / ODC and eNOS causes again oxidative stress, oxidises tropomoysin, and reduces function. Please note the time scale. Liberation of TNF-α can be attenuated by inhibition of TACE (red labelled 2), RAS can be attenuated by captopril (red labelled 3). Inhibition of arginase has acute effects, inhibition of TACE or RAS delayed effects.

rat hearts its protein expression is increased 24 h after ischaemia/reperfusion *in vivo*. Furthermore, although it is unlikely that an induction of arginase expression leads to a functional active enzyme within minutes our data show that we can attenuate the formation of oxidiative stress by inhibition of arginase. The most likely explanation for these acute effects are eNOS uncoupling at the time of reperfusion (10, 11). Our finding that arginase-1 is strongly induced *in vitro* suggests that local mechanisms may trigger this increase. Arginase is known to be induced by TNF-α (22). In the context of ischaemia/reperfusion, local release of TNF-α triggered by TACE may induce this response. We hypothesised that TACE will be activated by ischaemic events and liberates TNF-α because it is reasonable to assume that necrotic cell death during ischaemia will lead to the release of cellular components like RNA that subsequently may activate TACE (19). Indeed, an inhibition of TACE blocked reduced TNF-α concentration in the perfusate and attenuated arginase-1 induction.

Although induction of arginase-1 may already indicate a shift of the arginine metabolism into the direction of the polyamine metabolism, the rate limiting enzyme of the polyamine metabolism is not arginase-1 but ODC. Of note, based on the analysis of arginase knockout mice, arginase expression and activity seems not to affect polyamine metabolism directly at least in healthy mice underlining the importance of ODC expression in the induction of polyamine metabolism (30). Interestingly, in the setting of cardiac ischaemia/reperfusion arginase-1 and ODC were co-induced *in vitro*. In the *in vivo* model protein expression of ODC was higher 24 h after the onset of reperfusion, although only at a borderline level of significance (p=0.051). Nevertheless, these data suggest that the induction of the polyamine metabolism in post-ischaemic hearts includes ODC.

From these experiments the question arises how TNF-α may trigger these changes with an adverse outcome. It is well known that an inhibition of the local RAS in post-infarct models improves the post-ischaemic heart recovery at least in a certain time window (see Introduction). Can it be that TNF-α activates a local RAS that then triggers the shift into the polyamine metabolism? Evidence for this hypothesis comes from experiments with transgenic mice with a restricted overexpression of TNF-α in the heart. These mice displayed an activation of the cardiac-specific RAS (31). Combining both findings, TNF-α may indeed activate a local RAS that then triggers the shift in the polyamine metabolism. Inhibition of the local RAS 30 min after the onset of reperfusion in the *in vitro* system induced eNOS expression and increased the eNOS-to-ODC ratio on the level of mRNA expression. This was not accompanied by a rapid functional improvement at that time. However, one cannot expect such an effect within 90 min after treatment because this may be too early for changes on the protein expression level. ACE inhibition significantly preserved the function compared to non-treated rats *in vivo,* although treatment was started late after reperfusion. The timing of the start of captopril treatment was based on previous findings that earlier treatment is not successful and excludes any effect on infarct size that is established within minutes after reperfusion (3). Of note, this treatment regime led to a normalisation of eNOS expression and moderate effects on arginase-1 and ODC expression as well. These promising effects were lost during the following days even in the presence of the ACE inhibitor. Collectively our data show a significant contribution of local RAS to the arginine switch that has functional consequences during the first days after reperfusion.

So far the data indicated that the post-ischaemic shift of the arginine metabolism is initiated by ischaemia-dependent activation of TNF-α, that then triggers an activation of the RAS. The final question to answer is, however, whether this leads to a long-term protection against the transition of the pre-ischaemic healthy heart into post-ischaemic heart failure. The closed chest model limits any inflammation linked to the experimental procedure and limits inflammation to the infarct healing-related aspects. This allowed to follow-up the animals for longer time periods up to four months. As expected, post-ischaemic rats developed a reduced cardiac function as shown by echocardiography. However, even rats that previously received the ACE inhibitor during the first seven days after reperfusion, in which wound healing and remodelling starts, still developed signs of heart failure. There was no functional difference between both groups after four months. Nevertheless, the left ventricular mRNA expression of ANP and SERCA2a were highest in these rats whereas the expression of the pro-apoptotic bax was lowest. Interestingly, we have previously shown that putrescine activates bax expression immediately after reperfusion, while inhibition of ODC activity reduced the bax expression (32). Collectively the data suggest that polyamines can affect bax mRNA expression and that ACE inhibition attenuates this effect. Any speculation about the contribution of altered bax mRNA expression on the rate of apoptosis, however, cannot be drawn from this study. Nevertheless, the data underline an effect of temporary ACE inhibition on post-infarct remodelling. The long-term functional consequences cannot be predicted at the present state and require further studies.

The aforementioned changes in cardiac expression of enzymes of the arginine metabolism *in vivo* are not due to changes in differences in infarct sizes as treatment stared at earliest 30 min after reperfusion, a time at which infarct size has already been established (see above). In the *in vitro* experiments performed here, infarct sizes can also not be impaired in the captopril experiments. In case of TACE and arginase inhibitors had to be given at earlier time points because their activity is critically involved at earlier time points. However, based on protein leakage from perfused rat hearts there was no difference in infarct sizes (data not shown). Collectively the data show that arginase metabolism can be modified independent of infarct sizes.

As mentioned above, timing of drug administration and type of linkage of ROS to tropomyosin oxidation suggest that the manipulation of arginine metabolism are direct consequences of ROS scavenging rather than consequences of cell death. The data are also consistent with the assumption that some of the cardiac depressive mechanisms at the early post-ischaemic period are transient effects as those shown in this study.

In summary, the current study describes new mechanisms how ischaemia/reperfusion leads to a shift in arginine metabolism during the early phase of reperfusion, how this can be attenuated and that this improves the early functional recovery. Importantly, the improved cardiac function observed during the initial phase after reperfusion indicates that this mechanism may significantly contribute to the early reduction of cardiac function after myocardial infarction and reperfusion. The study also shows that this mechanism is not part of the subsequent remodelling process leading to heart failure in post-ischaemic hearts and that a better initial recovery does not attenuate this process either. However, the early phase after reperfusion is a critical phase in general and any improvement of cardiac function at this time will probably reduce post-reperfusion complications.

Acknowledgement

We thank Nadine Woitasky and Peter Volk for excellent technical support. The data of this study are in part results of the thesis of Pia Weber. The work was supported in part by the German Research Council (DFG, Bonn, Germany) with the international

Graduate School PROMISE (IRTG-1566, Giessen-Barcelona), the excellent Cluster „Cardiopulmonary System“ (ECCPS) strat-up grant to HACF, and a university hospital-Giessen-Marburg grant. PB and CC hold Janos Bolyai Research Scholarship of the Hungarian Acedemy of Science.

Conflicts of interest
None declared.

References

1. Goel K, Pinto DS, Gibson M. Association of time to reperfusion with left ventricular function and heart failure in patients with acute myocardial infarction treated with primary percutaneous coronary intervention: A systematic review. Am Heart J 2013; 165: 451–467.
2. Brodie BR, Stone GW, Cox DA, et al.. Impact of treatment delays on outcomes of primary percutaneous coronary intervention for acute myocardial infarction: Analysis from the CADILLAC trial. Am Heart J 2006; 151: 1231–1238.
3. Schoemaker RG, Debets JJM, Struyker-Boudier HAJ, et al. Delayed but not immediate captopril therapy improves cardiac function in conscious rats, following myocardial infarction. J Mol Cell Cardiol 1991; 23: 187–197.
4. Litwin SE, Litwin CM, Raya TE, et al. Contractility and stiffness of noninfarcted myocardium after coronary ligation in rats. Effects of chronic angiotensin converting enzyme inhibition. Circulation 1991; 83: 1028–1037.
5. Pfeffer MA, Pfeffer JM, Steinberg C, et al. Survival after an experimental myocardial infarction: beneficial effects of long-term therapy with captopril. Circulation 1985; 72: 406–412.
6. Youn TJ, Kim HS, Oh BH. Ventricular remodelling and transforming growth factor-beta 1 mRNA expression after nontransmural myocardial infarction in rats: effects of angiotensin converting enzyme inhibition and angiotensin II type 1 receptor blockade. Basic Res Cardiol 1999; 94: 246–253.
7. Kingma JH, van Gilst WH, Peels CH, et al. Acute intervention with captopril during thrombolysis in patients with first anterior myocardial infarction. Eur Heart J 1994; 15: 898–907.
8. Divisova J, Vavrinkova H, Tutterova M, et al. Effect of ACE inhibitor captopril and L-arginine on the metabolism and on ischaemia-reperfusion injury of the isolated rat heart. Physiol Res 2001; 50: 143–152.
9. Jugdutt BI. Nitric oxide and cardioprotection during ischaemia-reperfusion. Heart Failure Reviews 2002; 7: 391–405.
10. Ferdinandy P, Schulz R. Nitric oxide, superoxide, and peroxynitrite in myocardial ischaemia-reperfusion injury and preconditioning. Br J Pharmacol 2003; 138: 532–543.
11. Csonka C, Szilvássy Z, Fülöp F, et al. Classic preconditioning decreases the harmful accumulation of nitric oxide during ischaemia and reperfusion in rat hearts. Circulation 1999; 100: 2260–2266.
12. Hein TW, Zhang C, Wang W, et al. Ischaemia-reperfusion selectively impairs nitric oxide-mediated dilation in coronary arterioles: counteracting role of arginase. FASEB J 2003; doi 10.1096/fj.03–0115fje.
13. Sodha, NR, Boodhwani M, Clements RT, et al. Coronary microvascular dysfunction in the setting of chronic ischaemia is independent of arginase activity. Microvascular Res 2008; 75: 238–146.
14. Tabor CW, Tabor H. 1, 4-Diaminobutane (putrescine), spermidine, spermine. Ann Rev Biochem 1976; 45: 285–306.
15. Giordano E, Flamigni F, Guarnieri C, et al. Poylamines in cardiac physiology and disease. Open Heart Failure Journal 2010; 3: 25–30.
16. Schlüter K–D, Frischkopf K, Flesch M, et al. Central role for ornithine decarboxylase in β-adrenoceptor mediated hypertrophy. Cardiovasc Res 2000; 45: 410–417.
17. Shimizu M, Irimajiri O, Nkano T, et al. Yamada H, Sasaki H, Isogai Y. Effect of captopril on isoproterenol-induced myocardial ornithine decarboxylase activity. J Mol Cell Cardiol 1991; 23: 665–670.
18. Jung C, Gonon AT, Sjoquist PO, et al. Arginase inhibition mediates cardiac protection during ischaemia-reperfusion. Cardiovasc Res 2010; 85: 147–154.
19. Fischer S, Grantzow T, Pagel JI, et al. Extracellular RNA promotes leukocyte recruitment in the vascular system by mobilising proinflammatory cytokines. Thromb Haemost11 2012; 108: 730–741.
20. Harpster MH, Bandyopadhyay S, Thomas P, et al. Earliest changes in the left ventricular transcriptosome post-myocardial infarction. Mammalian Genome 2006; 17: 701–715.
21. Gao X, Xu X, Belmadini S, et al. TNF-α contributes to endothelial dysfunction by upregulating arginase in ischaemia/reperfusion injury. Arterioscler Thromb Vasc Biol 2007; 27: 1269–1275.
22. Zhang C, Wu J, Xu X, et al. Potter BJ, Gao X. Direct relationship between levels of TNF-α expression and endothelial dysfunction in reperfusion injury. Basic Res Cardiol 2010; 105: 453–464.
23. Frascarelli S, Ghelardoni S, Ronca-Tzestoni S, et al. Cardioprotective effect of zofenopril in perfused rat hearts subjected to ischaemia and reperfusion. J Cardiovasc Pharmacol 2004; 43: 294–299.
24. Bencsik P, Kupai K, Giricz Z, et al. Role of iNOS and peroxynitrite-matrix metalloproteinase-2 signalling in myocardial late preconditioning in rats. Am J Physiol Heart Circ Physiol 2010; 299: H512-H518.
25. Da Costa Rebelo RM, Schreckenberg R, Schlüter K–D. Adverse cardiac remodelling in spontaneously hypertensive rats: acceleration by high aerobic exercise intensity. J Physiol 2012; 590: 5389–5400.
26. Kocsis GF, Sárközy M, Bencsik P, et al. Preconditioning protects the heart in a prolonged uremic condition. Am J Physiol Heart Circ Physiol 2012; 303: H1229–1236.
27. Livak KJ, Schmittgen TD. Analysis of relative gene expression data using real-time quantitative PCR and the 2(-ΔΔCT). Methods 2001; 25: 402–408.
28. Maxeiner H, Krehbiel N, Müller A, et al. New insights into paracrine mechanisms of human cardiac progenitor cells. Eur J Heart Fail 2010; 12: 730–737.
29. Canton M, Skyschally A, Menabo R, et al. Oxidative modification of tropomyosin and myocardial dysfunction following coronary microembolisation. Eur Heart J 2006; 27: 875–881.
30. Deignan JL, Livesay JC, Shantz LM, et al. Polyamine homeostasis in arginase knockout mice. Am J Physiol Cell Physiol 2007; 293: C1296-C1301.
31. Flesch M, Höper A, Dell'Italia L., et al. Activation and functional significance of the renin-angiotensin system in mice with cardiac restricted overexpression of tumor necrosis factor. Circulation 2003; 108: 598–604.
32. Mörlein C, Schreckenberg R, Schlüter K–D. Basal ornithine decarboxylase activity modifies apoptotic and hypertrophic marker expression in post-ischaemic hearts. Open Heart Failure J 2010; 3: 31–37.

Basal Ornithine Decarboxylase Activity Modifies Apoptotic and Hypertrophic Marker Expression in Post-Ischemic Hearts

Christian Mörlein, Rolf Schreckenberg and Klaus-Dieter Schlüter*

Justus-Liebig-Universität, Physiologisches Institut, Aulweg 129, 35392 Giessen, Germany

Abstract: Polyamines play a role in ischemia-reperfusion injury of brain, kidney and probably heart. Primary data on cardiac myoblasts suggested that the induction of polyamine metabolism induces a hypertrophy like effect in normoxic hearts but apoptosis in reperfused hearts. The aim of this study was to investigate the relevance of these findings for post-ischemic hearts. Rat hearts were exposed to 45 min global normothermic flow arrest followed by 120 min of reperfusion. Controls were constitutively perfused for 165 min under normoxic conditions. Ornithine decarboxylase (ODC) activity was inhibited by administration of difluoromethylornithine (DFMO, 100 μM) starting 30 min after the onset of reperfusion and lasting for 10 min. Calcium receptor activation was induced by administration of putrescine (100 μM) and its inhibition by administration of NPS (10 μM).Left ventricular mRNA expression of bcl-2, bax, and BNP were determined by real time RT-PCR. Results: BNP was induced by putrescine *via* activation of calcium receptors in normoxic and post-ischemic hearts. Inhibition of ODC had a strong effect on bcl-2 expression whereby putrescine induced bax in post-ischemic but not normoxic hearts. Inhibition of ODC increased the bcl-2/bax ratio but putrescine worsened it. In conclusion, induction of polyamine metabolism induced a pro-apoptotic profile in left ventricles *via* calcium receptor activation in post-ischemic hearts but not in normoxic hearts and induced BNP expression under both conditions.

Keywords: Calcium receptor, polyamines, putrescine.

1. INTRODUCTION

Acute coronary occlusion resulting in myocardial infarction is the main mechanism by which coronary artery disease reduces survival [1]. Restoration of blood flow is the most successful intervention that improves survival and functional recovery. It stops ischemia-induced cell damage and allows cells which are still alive to re-start contractile activity but it adds new stress to the heart at the same time. This phenomenon is known as reperfusion injury. At the time of reperfusion a couple of quite different processes are initiated such as recovery of pump activity and induction of a complex process of tissue regeneration termed remodelling. An induction of hypertrophic growth of survived myocytes may compensate for damaged myocytes as well as an induction of pro-apoptotic pathways [2]. The molecular mechanisms determining apoptotic cell death in the post-infarcted myocardium are still not fully understood but changes in the expression of pro- and anti-apoptotic genes like bax and bcl-2 are part of this process. The expression of pro- and anti-apoptotic genes starts to change during the first two hours of reperfusion as analyzed in Tyrode-perfused Langendorff hearts [3-5].

Ornithine decarboxylase (ODC) catalyzes the decarboxylation of ornithine to putrescine. Since ODC activation is part of pro-hypertrophic signalling in non-infarcted hearts, one may predict that an activation of the polyamine metabolism by ODC activation in reperfused hearts bridges the polyamine metabolism with key events of remodelling such as hypertrophy, apoptosis, and probably inotropy. Indeed administration of the polyamine spermidine prior to ischemia improved the functional recovery of the heart [6]. Spermidine also attenuates apoptosis in neonatal cardiomyocytes [7]. Most recently a study on H9c2 cells has challenged the hypothesis that ODC activation is protective in the post-ischemic heart [8]. H9c2 cells are embryonic rat-heart derived cardiomyoblasts. These cells were exposed to simulated ischemia resulting in an induction of ODC and of the expression of the pro-apoptotic molecule bax. Moreover, the authors supported direct evidence that both findings are causally related to each other. However, ODC activation is normally coupled to hypertrophy and most pro-hypertrophic signals have anti-apoptotic properties [9]. In contrast, ODC activation was linked to pro-apoptotic effects in other cases [10, 11]. Therefore, ODC activity may contribute to either pro- or anti-apoptotic pathways depending on cell types and environmental signals. This leads to the following question: Does ODC activity influence post-infarct recovery in functional aspects or in respect to the expression of either pro- or anti-apoptotic genes in the post ischemic heart?

To address these important questions a previously established ex vivo model of ischemia/reperfusion was used in this study. ODC was inhibited by administration of α-difluoromethylornithine (DFMO), an irreversible inhibitor of ODC, given during reperfusion. Putrescine, the product of the enzymatic activity of ODC, was used as a control to bypass ODC inhibition. In order to address the question whether putrescine acts in an autocrine fashion, NPS 2390 was used to antagonize calcium receptor stimulation. Noteworthy, all drugs were administered 30 min after the onset of reperfusion to exclude any influence on infarct sizes. As a matter of fact, this study is intended to describe the effect of

*Address correspondence to this author at the Justus-Liebig-Universität, Physiologisches Institut, Aulweg 129, 35392 Giessen, Germany; Tel: +49 641 99 47 212; Fax: +49 641 99 47 219;
E-mail: Klaus-Dieter.Schlueter@physiologie.med.uni-giessen.de

1876-5351/10

polyamines on post-ischemic hearts rather than on reperfusion injury.

2. MATERIALS AND METHODS

2.1. Isolated Rat Heart Preparation

Experiments were performed on isolated hearts from male Wistar rats as previously described [12]. Hearts were rapidly excised and the aorta was cannulated for retrograde perfusion with a 16-gauge needle connected to a Langendorff perfusion system. The perfusion system consisted of a warmed storage vat for perfusate solution, a speed rotary pump and a temperature controlled chamber in which hearts were mounted. Hearts were perfused with a modified Tyrode solution as described before [12]. After attachment to the Langendorff system, all hearts were allowed to stabilize for at least 20 min.

2.2. Experimental Protocols

In total 12 different groups were analyzed (each n=8 rat hearts). The following experiments were performed: Ischemia and Reperfusion (I/R): 45 min flow arrest and 120 min reperfusion; I/R + DFMO in which DFMO (100 μM) was given 30 min after the onset of reperfusion and washed out again after 10 min. I/R + putrescine in which putrescine (100 μM) was given 30 min after the onset of reperfusion and washed out again after 10 min; I/R + DFMO + putrescine in which DFMO and putrescine were given 30 min after the onset of reperfusion and washed out again after 10 min; I/R + NPS 2390 (NPS) in which NPS (10 μM) was given 30 min after the onset of reperfusion; I/R + NPS + putrescine in which NPS and putrescine were administered 30 min after the onset of reperfusion. All drugs were administered 30 min after the onset of reperfusion because at that time reperfusion-induced cell damage has been established and any drug administration does not interfere with reperfusion-induced damage any more. Therefore, any interventions performed in this study focus on the influence on the post-ischemic hearts and were not intended to reduce the reperfusion-induced cell damage. For all four groups normoxic controls were performed in which the 45 min flow arrest was replaced by normoxic perfusion. Perfusion flow was held constant and during the experiments hearts were allowed to beat free.

2.3. Real Time RT-PCR

At the end of all experiments left ventricles including the septum were separated from atria and right ventricles. Samples were immediately frozen with fluid nitrogen and stored at -80°C until use. Total RNA from left ventricles was extracted with Trizol (Invitrogen) as described by the manufacturer. RT reactions were performed for 1 h at 37°C in a final volume of 10 μl using 1 μg RNA, 100 ng of oligo$(dT)_{15}$, 1 mM dNTPs, 8 units of RNasin, and 60 units of Moloney murine leukemia virus reverse transcriptase. Aliquots were used for real-time PCR using the I-cycler (Biorad, Germany) and SYBR-green fluorescence for quantification. HPRT was used as a housekeeping gene to normalize sample contents. Primers used for determination had the following sequences: HPRT forward: CCA GCG TCG TGA TTA GTG AS, HPRT reverse: CAA GTC TTT CAG TCC TGT CC, bax forward: ACT AAA GTG CCC GAG CTG ATC, bax reverse: CAC TGT CTG CCA TGT GGG G, bcl-2 forward ATG GCG CAA GCC GGG AGA AC, bcl-2 reverse: CTT GTG GCC CAG GTA TGC AC, BNP forward: ATG ATT CTG CTC CTG CTT TTC CC, BNP reverse: TCT GCA TCG TGG ATT GTT CTG. The calculations of the results were carried out according to the $2^{-\Delta\Delta Ct}$ methods as described [13]. After amplification reaction, products were controlled and separated on 2 % agarose gels, stained with SYBR Safe, and photographed under UV illumination.

2.4. Materials

DFMO (Calbiochem; Merck Bioscience Ltd., USA) and putrescine (Sigma/RBI (Sigma-Aldrich Chemie, Taufkirchen, Germany) were dissolved as a stock solution of 100 mM dissolved in either dimethyl sulfoxide (DMSO) or sterile water (putrescine) and stored at -20°C. NPS 2390 (NPS) was obtained from Sigma/RBI and dissolved in DMSO as well. Working solutions were prepared by dilution with perfusion buffer. Control hearts received an equal volume of the vehicle solutions.

2.5. Statistics

Data are expressed as box and whiskers plots or means±s.e.m. as indicated in the legends of the figures. One-way ANOVA was used to compare different groups and if appreciable a Student-Newman-Keuls test was performed for *post hoc* analysis. In cases in which two groups were compared, Mann-Whitney-U-tests for paired samples were employed. $P<0.05$ was regarded as significant.

3. RESULTS

At first we investigated the effect of intracellular and extracellular polyamines on ODC expression. Neither inhibition of ODC nor stimulation of CaRs by putrescine caused any difference in ODC mRNA expression in normoxic hearts (Fig. **1A**). However, in post-ischemic hearts both experiments increased basal ODC expression (Fig. **1A**). In order to address the question whether a modification of polyamine metabolism in the normoxic or I/R heart causes an induction of molecular markers of hypertrophy mRNA expression levels of ANP were determined next. I/R increased ANP mRNA expression and this was not influenced by DFMO (Fig. **1B**). Putrescine decreased ischemia-induced ANF expression but not *via* stimulation of CaRs (Fig. **1B**). Finally, expression of BNP way determined. I/R alone did not influence BNP mRNA expression and DFMO did not modify this in any way although it increased BNP expression in normoxic hearts (Fig. **1C**). However, putrescine caused an increase of BNP mRNA expression in normoxic and I/R hearts that was attenuated by NPS in all cases (Fig. **1C**).

Next, mRNA expressions of the anti-apoptotic bcl-2, of the pro-apoptotic bax, and the ratio of bcl-2 to bax expression were determined. I/R did not modify the expression of bcl-2, but reduced the expression of bax resulting in a slight increase of the bcl-2/bax ratio (Fig. **2**). However, DFMO caused a significant increase in the expression of the anti-apoptotic bcl-2 without any effect on bax expression leading to a significant increase in the bcl-2/bax ratio (Fig. **2**). Putrescine induced the pro-apoptotic bax and normalized DFMO induced bcl-2/bax ratio (Fig. **2**). The effect of putrescine on bax expression was dependent on calcium receptor stimulation because NPS attenuated this effect (Fig. **2B**, **C**). In normoxic hearts putrescine caused a reduction of bax and thereby improved bcl2/bax ratios (Fig. **2**).

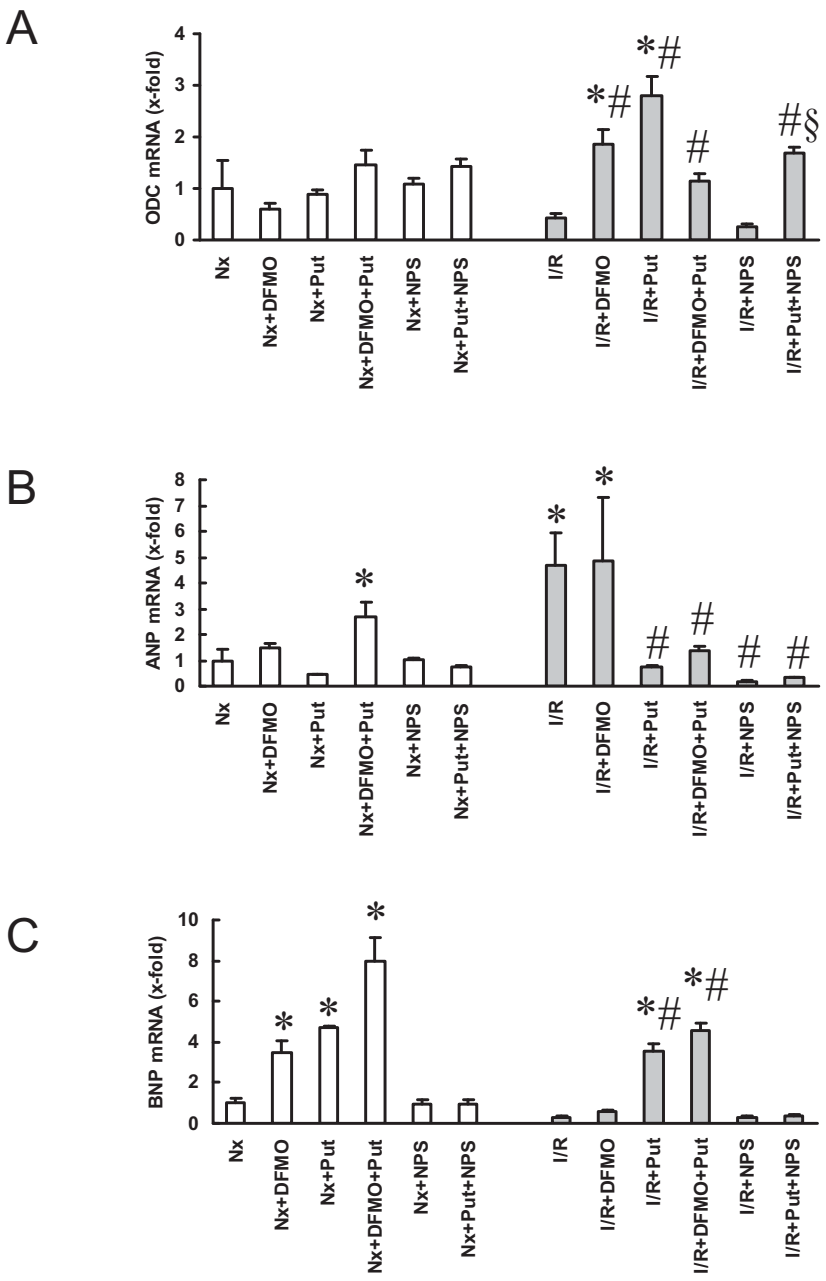

Fig. (1). Effect of ischemia/reperfusion (I/R) on the mRNA expression of brain natriuretic peptide (BNP) and the effect of polyamine metabolism on its expression. Each group n=8 hearts. Nx, normoxic controls; I/R, 45 min flow arrest and 2 h reperfusion; DFMO, difluoromethylornithine (100 μM) used as an irreversible inhibitor of ODC; Put, putrescine (100 μM); NPS 2390, NPS (10 μM) used as a specific antagonist of the calcium receptor. *, $p<0.05$ vs. Nx; #, $p<0.05$ vs. I/R; §, $p<0.05$ vs. I/R+putrescine.

DISCUSSION

In this study we investigated effects of ODC activity and putrescine on early regulation of mRNA expression levels of factors linked to hypertrophy or apoptosis. The main findings of this study are first that the product of ODC enzymatic activity, putrescine, increases the expression of the pro-apoptotic bax in post-ischemic hearts but not in normoxic hearts as predicted from studies on H9c2 cells and second that inhibition of ODC activity improves the bcl-2/bax ratio at least on the mRNA expression level. Furthermore, the data of this study that the effect of putrescine on left ventricular BNP expression is not modified at all by ischemia/reperfusion.

Upon reperfusion the heart is exposed to various pro-apoptotic events such as oxidative burst, mechanical load, excessive release of catecholamine and other factors [2]. As a result of this caspase 3 is getting activated, an enzyme closely linked to apoptosis. However, post-ischemic hearts

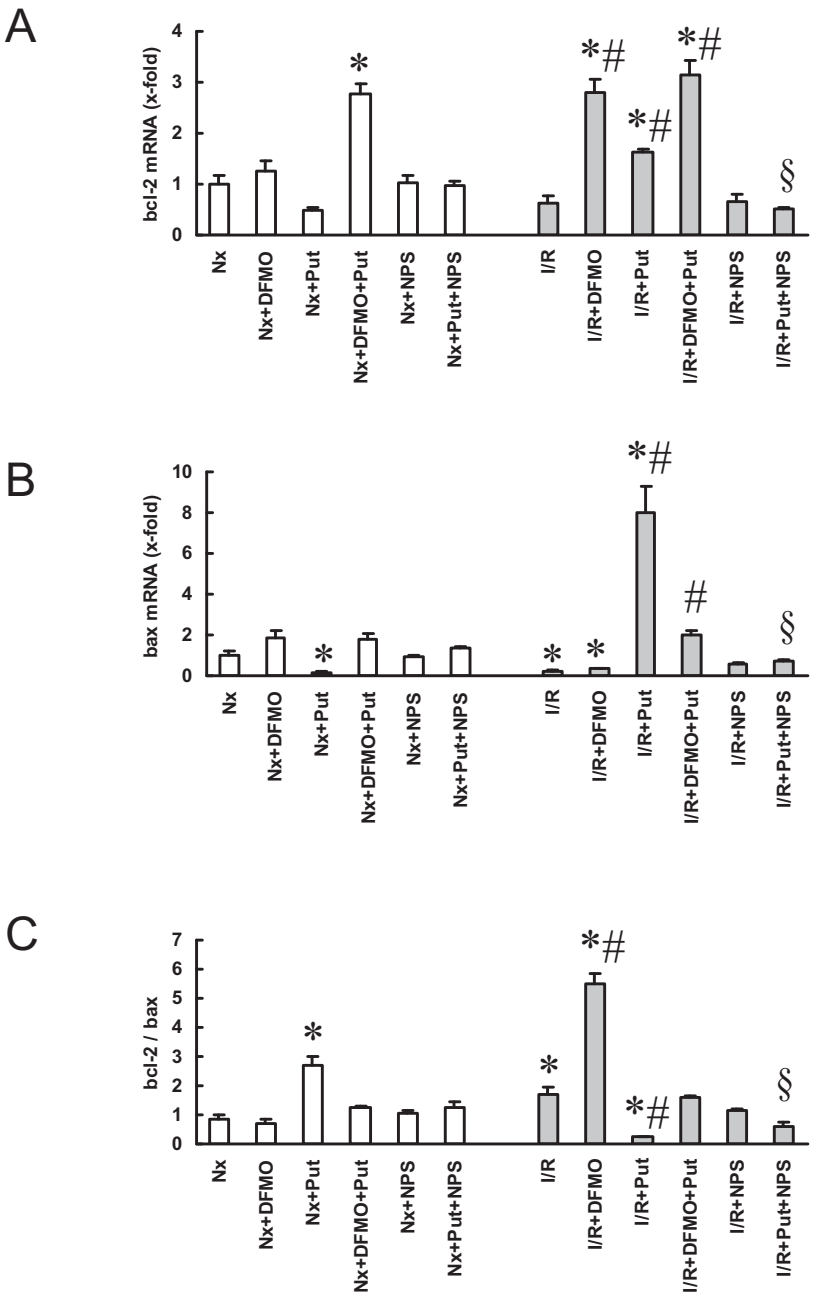

Fig. (2). Effect of ischemia/reperfusion (I/R) on the mRNA expression of the anti-apoptotic bcl-2 (**A**), the pro-apoptotic bax (**B**),and bcl-2 to bax ratio (**C**). Each group n=8 hearts. Nx, normoxic controls; I/R, 45 min flow arrest and 2 h reperfusion; DFMO, difluoromethylornithine (100 μM) used as an irreversible inhibitor of ODC; Put, putrescine (100 μM); NPS 2390, NPS (10 μM) used as an antagonist of the calcium receptor. *, $p<0.05$ vs. Nx; #, $p<0.05$ vs. I/R; §, $p<0.05$ vs. I/R+putrescine.

are quite resistant against pro-apoptotic events at the same time. It was shown before that an altered expression of bcl-2 and bax, controlling the release of cytochrome C from mitochondria, is involved in this protection [2, 14]. A previous study on cardiac-like cells suggested that an activation of the polyamine metabolism increases the expression of the pro-apoptotic gene bax and favours the susceptibility against apoptosis in post-ischemic heart cells but not in normoxic cells [8]. Basically, we confirmed this relationship in an established ischemia/reperfusion model because putrescine, the end product of ODC activity caused a marked increase in bax expression in post-ischemic hearts but not in non-ischemic hearts. As a result of this the bcl-2-to-bax ratio shifts into the direction of bax and an increased susceptibility to apoptosis must be predicted. Noteworthy, putrescine caused this effect *via* a stimulation of calcium receptors. An endogenous induction of polyamine metabolism by ischemia alone seems not be sufficient to induce bax expression. Ad-

ministration of putrescine was required to change bax expression. Indeed, we found no induction of ODC in post-ischemic hearts (data not shown). ODC activation is mediated by an increase in ODC mRNA expression within minutes when cardiomyocytes are exposed to isoprenaline as a pro-hypertrophic stimulus [9]. Polyamine metabolism itself is likely to be activated in post-ischemic hearts, because arginase, which metabolizes arginine to ornithine and urea, is up-regulated during myocardial ischemia [15]. However, if ischemia-dependent arginase activation requires a co-activation of ODC to shift arginine metabolism into the direction of polyamine metabolism, one would have seen this in these hearts because ODC activity is regulated on the transcriptional level. While putrescine, the natural product of ODC enzyme activity, induced bax and reduces bcl-2/bax ratio, inhibition of ODC increased bcl-2 expression and improved bcl-2/bax ratio.

On the other hand, polyamines as products of ODC enzymatic activity improve cardiac function [6]. This can be observed in these hearts in parallel to the induction of bax because as long as cells are not damaged by apoptosis they maintain functional activity [16]. Most likely, putrescine acts in a paracrine way to improve the functional recovery. In principle, polyamines are extruded from cells and act *via* binding to and activation of calcium sensing receptors [17]. It is in line with these suggestions that spermidine, another polycationic product of the polyamine metabolism, is also sufficient to improve post-ischemic function even if administered before ischemia [6].

Despite the effect of ODC activity on pro- and antiapoptotic genes, polyamine metabolism is normally considered as a pro-hypertrophic pathway [9]. Therefore, the expression of hypertrophy-associated gene like BNP was also analyzed. Endogenous ODC activity seems not to be involved in the regulation of BNP expression in post-ischemic hearts. Putrescine induced the expression of BNP. The effect was slightly more improved in co-presence of DFMO. The finding may indicate a difference between endogenous polyamines, required to stabilize nucleic acids, and exogenous polyamines, acting by binding to the calcium-sensing receptor. In post-ischemic hearts inhibition of ODC by DFMO was no more able to increase BNP mRNA expression indicating that BNP expression cannot influenced by intracellular polyamine effects under these conditions.

The expression of ODC was obviously not modified by ischemia/reperfusion itself. Furthermore, under normoxic conditions neither inhibition of ODC nor activation of calcium receptors influenced the basal expression of ODC mRNA. However, regulation of ODC steady state mRNA levels seems to be altered in post-ischemic hearts as both DFMO and putrescine increased ODC mRNA expression. The mechanism behind this altered regulation of ODC mRNA in post-ischemic hearts is less clear and requires further analysis. Putrescine increased ODC mRNA expression at least in part *via* interaction with calcium receptors as the effect of putrescine could be reduced by NPS. However, it was not completely normalized. Furthermore, DFMO also increased ODC mRNA expression indicating a feedback

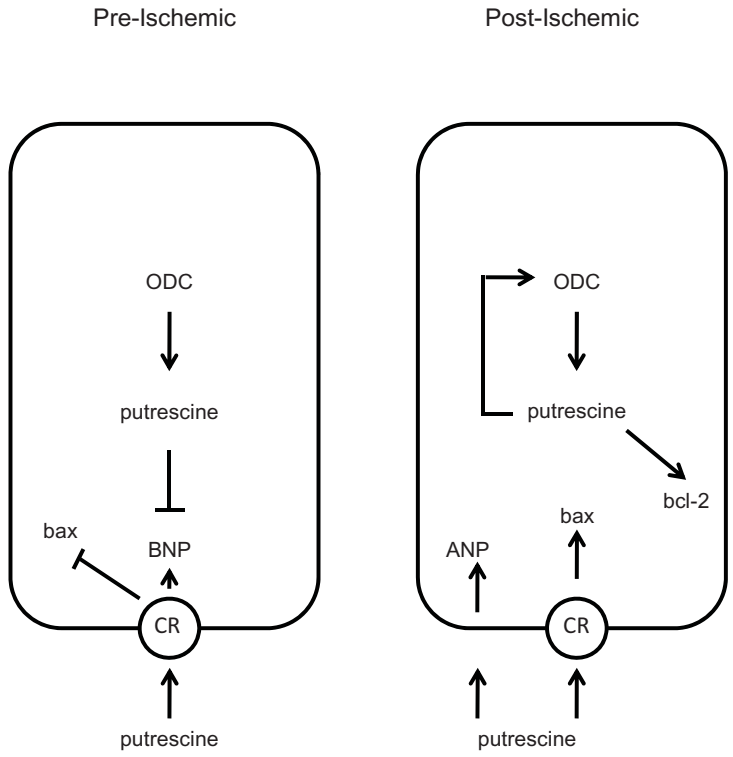

Fig. (3). Conclusive summary of the findings. Left: In pre-ischemic hearts endogenous ODC activity controls BNP expression and calcium receptor (CR)-dependent effects counterbalance the effect of ODC on BNP and attenuate bax expression. Right: In post-ischemic hearts endogenous ODC activity forms a feedback loop to its own regulation and induces bcl-2 expression whereas stimulation of calcium receptors antagonizes this by activating bax expression and reducing ANP expression.

mechanism in post-ischemic hearts but the effects of DFMO and putrescine were not additive, indicating that a cross-talk between the endogenous feedback inhibition and calcium receptor-dependent signalling.

In summary this study provides strong evidence for a significant difference in post-ischemic coupling of endogenous and exogenous polyamine metabolism. The data of the study are summarized in Fig. (**3**) where the effects of ODC inhibition and calcium receptor activation in normoxic and post-ischemic hearts were compared. Ischemia/reperfusion shifts arginine metabolism from NO to polyamine metabolism by induction of arginase [1]. In principle this leads to an elevated release of putrescine that acts in an autocrine way on heart cells by modifying bax and BNP expression. As BNP is both a cardioprotective natriuretic peptide and a cardiac risk marker these observations are of relevance for the understanding of the early post-infarct remodelling.

REFERENCES

[1] Garcia-Dorado D. Myocardial reperfusion injury: a new view. Cardiovasc Res 2004; 61: 363-4.

[2] Eefting F, Rensing B, Wigman J, *et al*. Role of apoptosis in reperfusion injury. Cardiovasc Res 2004; 61: 414-26.

[3] Fan G-C, Ren X, Qian J, *et al*. Novel cardioprotective role of a small heat-shock protein, hsp20, against ischemia/reperfusion injury. Circulation 2005; 111: 1792-9.

[4] Vila-Petroff M, Salas MA, Said M, *et al*. CaMKII inhibition protects against necrosis and apoptosis in irreversible ischemia-reperfusion injury. Cardiovasc Res 2007; 73: 689-98.

[5] Zhou X, Fan G-C, Ran X, *et al*. Overexpression of histidine-rich Ca-binding protein protects against ischemia/reperfusion-induced cardiac injury. Cardiovasc Res 2007; 75: 487-97.

[6] Zhao Y-J, Xu C-Q, Zhang W-H, *et al*. Role of polyamines in myocardial ischemia/reperfusion injury and their interactions with nitric oxide. Eur J Pharmacol 2007 ; 562: 236-46.

[7] Han L, Xu C, Jiang C, *et al.* Effects of polyamines on apoptosis induced by simulated ischemia/reperfusion injury in cultured neonatal rat cardiomyocytes. Cell Biol Int 2007; 31: 1345-52.

[8] Tantini B, Fiumana E, Cetrullo S, *et al*. Involvement of polyamines in apoptosis of cardiac myoblasts in a model of simulated ischemia. J Mol Cell Cardiol 2006; 40: 775-82.

[9] Schlüter K-D, Frischkopf K, Flesch M, *et al*. Central role for ornithine decarboxylase in b-adrenoceptor mediated hypertrophy. Cardiovasc Res 2000; 45: 410-7.

[10] Singh K, Xiao L, Remondino A, Sawyer DB, Colucci WS. Adrenergic regulation of cardiac myocyte apoptosis. J Cell Physiol 2001; 189: 257-65.

[11] Thomas T, Thomas TJ. Polyamines in cell growth and cell death: molecular mechanisms and therapeutical applications. Cell Mol Life Sci 2001; 58: 244-58.

[12] Grohé C, van Eickels M, Wenzel S, *et al*. Sex-specific differences in ventricular expression and function of parathyroid hormone-related peptide. Cardiovasc Res 2004; 61: 307-16.

[13] Livak KJ, Schmittgen TD. Analysis of relative gene expression data using real-time quantitative PCR and the 2(-delta delta C(T)). Methods 2001; 25: 402-8.

[14] Taimor G, Lorenz H, Hofstaetter B, Schlüter K-D, Piper HM. Induction of necrosis but not apoptosis after anoxia and reoxygenation in isolated adult cardiomyocytes of rat. Cardiovasc Res 1999; 41: 147-56.

[15] Durante W, Johnson FK, Johnson RA. Arginase: A critical regulator of nitric oxide synthesis and vascular function: Clin Exp Pharmacol Physiol 2007; 34: 906-11.

[16] Tastan H, Abdallah Y, Euler G, Piper HM, Schlüter K-D. Contractile performance of adult ventricular rat cardiomyocytes is not directly jeopardized by NO/cGMP-dependent induction of pro-apoptotic pathways. J Mol Cell Cardiol 2007; 42: 411-21.

[17] Wang R, Xu C, Zhao W, *et al.* Calcium and polyamine regulated calcium-sensing receptors in cardiac tissues. Eur J Biochem 2003; 270: 2680-8.

Received: October 15, 2009 Revised: November 26, 2009 Accepted: November 30, 2009

Cell-Specific Effects of Nitric Oxide Deficiency on Parathyroid Hormone-Related Peptide (PTHrP) Responsiveness and PTH1 Receptor Expression in Cardiovascular Cells

Rolf Schreckenberg, Sibylle Wenzel, Rui Manuel da Costa Rebelo, Anja Röthig, Rainer Meyer, and Klaus-Dieter Schlüter

Physiologisches Institut (R.S., S.W., R.M.d.C.R., A.R., K.-D.S.), Justus-Liebig-Universität Giessen, D-35392 Giessen, Germany; and Institut für Physiologie II (R.M.), Universitätsklinikum Bonn, D-53111 Bonn, Germany

The missing influence of estrogen on endothelial nitric oxide (NO) synthase often forms the basis for a worsening of the cardiac risk profile for women in postmenopause. Various studies have shown that decreasing estrogen levels also directly effect the expression of PTHrP and TGFβ1. PTHrP is involved in the endothelium-dependent regulation of coronary resistance and cardiac function. The current study investigates to what extent chronic NO deficit affects the cardiac effects of PTHrP. NO deficit was achieved in female adult rats by feeding them the NO synthase inhibitor *N*-omega-nitro-L-arginine methyl ester over a period of 4 wk. Isolated hearts of the conditioned animals were investigated in Langendorff technique and perfused for 3 min with 100 nM PTHrP. The contraction behavior of isolated cardiomyocytes was registered in a cell-edge detection system. Hearts from untreated animals displayed a significant drop in left ventricular developed pressure and a pronounced increase in heart rate in consequence of short term PTHrP stimulation. In hearts from NO-deficient rats PTHrP no longer affected the inotropy and chronotropy. The vasodilating effect of PTHrP on coronary vessels was, however, independent of the NO level. These changes were accompanied by a differing expression of the PTH1 receptor. TGFβ1 was identified as an important mediator for the regulation of the PTH1 receptor in myocytic but not endothelial cells. These results indicate that chronic NO deficit down-regulates the PTH1 receptor in a TGFβ1-dependent way. These findings are important with respect to the relatively new therapy of postmenopausal osteoporosis with PTHrP analogs. **(*Endocrinology* 150: 3735–3741, 2009)**

PTHrP was first identified as the cause of the syndrome hypercalcemia of malignancy in 1987 (1). In its structure as well as in its mechanism of action it displays characteristics similar to parathormone and tuberoinfundibular peptide 39. Within the cardiovascular system, PTHrP is expressed in smooth muscle cells, endothelial cells, and atrial myocardium. Through paracrine and autocrine mechanisms, it influences the contractility and proliferation of smooth muscle cells through the PTH1 receptor (2–4). At isolated endothelial cells, a PTH1 receptor mediated release of nitric oxide (NO) has been observed (5). Results from Sutliff *et al.* (6) also showed, however, that the endothelium-derived hyperpolarizing factor participates in PTHrP-mediated vasorelaxation. The specific effect of PTHrP on the ventricular function is the subject of ongoing research. It affects the inotropy as well as the chronotropy and hypertrophy. PTHrP released from the endothelium during an ischemia not only improves the intropy of the postischemic heart, but it also simultaneously induces an improvement in coronary perfusion (7, 8). Mediated by the PTH1 receptor (PTH1-R), PTHrP directly improves the parameters of cardiac function and myocardial perfusion through protein kinase A/protein kinase C-dependent activation of adenylate cyclase (9).

ISSN Print 0013-7227 ISSN Online 1945-7170
Printed in U.S.A.

doi: 10.1210/en.2008-1585 Received November 19, 2008. Accepted March 20, 2009.
First Published Online April 2, 2009

For editorial see page 3443

Abbreviations: eNOS, Endothelial NO synthase; L, animals assigned to receive L-NAME; L/H, animals assigned to receive L-NAME plus Hydralazine; L-NAME, *N*-omega-nitro-L-arginine methyl ester; LVDP, left ventricular developed pressure; L/W, animals assigned to receive L-NAME for 2 wk only and got drinking water thereafter; NO, nitric oxide; PTH1-R, PTH1 receptor.

There is little evidence regarding concrete mechanisms as to how PTHrP expression and the specific cardiovascular effects of PTHrP are regulated under physiological and pathophysiological conditions. Various studies have demonstrated that women are largely protected from cardiovascular disease up to menopause. After menopause, however, a woman's risk profile worsens dramatically (10, 11). Two studies showed, *in vivo*, that decreasing estrogen levels directly effect the expression of PTHrP (12, 13). In addition, the cardiac PTHrP effects demonstrate significant sex-specific differences that would explain a deterioration of the cardiac status during postmenopause (8).

A decrease in NO levels is considered responsible for a portion of cardiovascular disease in postmenopause. A substitution with estrogen leads to an increase in NO production due to activation and increase in the expression of endothelial NO synthase (eNOS) (14, 15). Lagumdzija *et al.* (16) demonstrated that the osteoanabolic effects of estrogen in eNOS knockout mice were largely neutralized. They postulate that IGF-I and PTHrP could be negatively affected in their functionality. Definitive results could be only demonstrated for a reduced effect of IGF-I (16).

The current study hypothesized that NO deficiency affects the cardiac effects of PTHrP. Because an NO deficiency is a common problem in postmenopausal women, this study is important for a better understanding of new therapy options of postmenopausal osteoporosis with PTHrP analogs and their cardiac cross-effects.

The NO deficit was achieved in female adult rats by feeding them the NO synthase inhibitor *N*-omega-nitro-L-arginine methyl ester (L-NAME) over a time span of 4 wk. The effectiveness of the L-NAME substitution was checked with weekly blood pressure measurement. To separate blood pressure effects from NO effects, a treatment group was additionally given the antihypertensive hydralazine. Subsequent to therapy, at Langendorff technique, the isolated hearts of the animals were perfused, stimulated with PTHrP, and then processed with biomolecular methods. To investigate the contraction behavior of the individual heart muscle cells, the cardiac myocytes were isolated from the hearts of L-NAME-treated animals and acute effects of PTHrP were registered in the cell-edge detection system.

Materials and Methods

The investigation conforms to the Guide for the Care and Use of Laboratory Animals published by the National Institutes of Health (publication 85-23, revised 1996).

Experimental model

Forty-seven 3-month-old female Wistar rats were divided into four groups and kept in individual cages. Animals were allowed food and water *ad libitum*. Animals were assigned to receive L-NAME (L; 7.5 mg/d in drinking water), L-NAME plus Hydralazine (L/H; 5.0 mg/d in drinking water), or drinking water only (age matched control) for 28 d. A fourth group received L-NAME for 2 wk only and got drinking water thereafter (L/W).

Determination of blood pressure *in vivo*

For determination of blood pressure, rats were set in a separate chamber and blood pressure (peak systolic blood pressure, and heart rate) were determined via the tail-cuff method. Briefly, the mean of 10 consecutive blood pressure readings was obtained for each animal at weekly intervals. Body weight was recorded weekly and water consumption daily.

Ovariectomy of female rats

Female rats were ovariectomized (n = 12) or sham operated (n = 6) at the age of 4 months as described previously in detail (17). Half of the ovariectomized animals received estrogen supplementation by sc pellets inserted into the dorsal neck region under local anesthesia. Five weeks after surgery, rats were anesthetized, killed by decapitation, and the hearts were excised.

Langendorff perfusion

Experiments were performed on isolated hearts from the conditioned rats. Hearts were rapidly excised, and the aorta was cannulated for retrograde perfusion with a 16-gauge needle connection to a Langendorff perfusion system. A polyvinyl chloride balloon was inserted into the left ventricle through the mitral valve and held in place by a suture tied around the left atrium. The other end of the tubing was connected to a pressure transducer for continuous measurement of left ventricular pressure. A second transducer connected to the perfusion line just before the heart was used to measure coronary perfusion pressure. The perfusion system consisted of a warmed storage container for perfusate solutions, a rotary pump, and a temperature-controlled chamber in which the hearts were mounted. Hearts were perfused with a modified Tyrode solution as described previously (8). After attachment to the Langendorff system, the hearts were allowed to stabilize for at least 20 min. The intraventricular balloon was inflated to give a diastolic pressure of 10 mm Hg, and the balloon volume was held constant thereafter. The flow was adjusted to give a perfusion pressure of 50 mm Hg and measured again at the end of the stabilization period. Parameters determined were the left ventricular developed pressure (LVDP) that was calculated as peak systolic pressure minus diastolic pressure, the perfusion pressure, and the heart rate. To avoid differences in oxygen supply due to changes in the coronary resistance, hearts were perfused at a constant flow. Hearts were allowed to beat freely. Temperature was held constant at 37 C throughout the whole experiment.

Perfusion protocols

In the present study, 32 hearts were perfused in Langendorff technique to investigate the influence of chronic nitric oxide deficiency on PTHrP stimulation. The following protocol was used: 20 min stabilization period followed by 3 min PTHrP stimulation. Synthetic PTHrP(1-36) in a final concentration of 100 nM was used in this study to stimulate the PTH1 receptor (PTH1-R).

Cell preparations

Ventricular heart muscle cells were isolated from rats treated with L-NAME alone and in combination with Hydralazine as described previously in greater detail (18). Hearts were excised under deep ether anesthesia, transferred rapidly to ice-cold saline, and mounted on the cannula of a Langendorff perfusion system. Heart perfusion and subsequent steps were all performed at 37 C. First, hearts were perfused in the noncirculating mode for 5 min at 10 ml/min (perfusate in mmol/liter: NaCl 110, KH_2PO_4 1.2, KCl 1.2, $MgSO_4$ 1.2, $NaHCO_3$ 25, glucose 11, gassed with 5% CO_2-95% O_2). Thereafter perfusion was continued with recirculation of 50 ml of the above perfusate supplemented with 0.06% (wt/vol) crude collagenase and 25 μM $CaCl_2$ at 5 ml/min. After 25 min, ventricular tissue was minced and incubated for 20 min in recirculating medium with 1% (wt/vol) BSA under 5% CO_2-95% O_2. Gentle trituration through a pipette released cells from the tissue chunks. The resulting cell suspension was filtered through a 200-μm nylon mesh. The filtered material was washed twice by centrifugation (3 min, 25 x-g) and resuspended in the above perfusate, in which the concentration of $CaCl_2$ was increased stepwise to 0.2 and 0.5 mmol/liter. After further centrifugation (3 min, 25 $\times$ *g*), the cell pellet was resuspended in serum-free

TABLE 1. Peak systolic blood pressure and heart rate *in vivo*

	$P_{syst.}$ basal (mm Hg)	$P_{syst.}$ wk 4 (mm Hg)	Heart rate basal (bpm)	Heart rate wk 4 (bpm)
Control (C)	124 ± 7	123 ± 4	367 ± 37	353 ± 13
L-NAME (L)	125 ± 6	174 ± 6[a]	352 ± 33	363 ± 16
L-NAME/H_2O (L/W)	124 ± 6	137 ± 6[a]	366 ± 28	353 ± 34
L-NAME + Hy. (L/H)	124 ± 5	126 ± 5	355 ± 24	356 ± 32

Changes in systolic blood pressure over a time span of 4 wk. Rats were given pure drinking water (C), L-NAME (L), L-NAME for the first 2wk only (L/W), or L-NAME plus Hydralazine (Hy.) (L/H). Data are means ± SD (n = 8 animals for each group). $P_{syst.}$, Systolic blood pressure.

[a] $P < 0.05$ *vs.* basal.

culture medium (medium 199 with Earle's salts, 5 mmol/liter creatine, 2 mmol/liter L-carnitine, 5 mmol/liter taurine, 100 IU/ml penicillin, and 100 μg/ml streptomycin), and cells were plated at a density of 7×10^4 elongated cells per 35-mm culture dish (type 3001; Falcon, Oxnard, CA). The culture dishes had been preincubated overnight with 4% (vol/vol) fetal calf serum in medium 199. Two hours after plating, cultures were washed with the serum-free medium 199 to remove round and nonattached cells.

Determination of cell contraction

Cells were allowed to contract at room temperature and analyzed using a cell-edge detection system as previously described (19). Cells were stimulated via two AgCl electrodes with biphasic electrical stimuli composed of two equal but opposite rectangular 50-V stimuli of 0.5 msec duration. Each cell was stimulated at 2.0 Hz for 1 min. Every 15 sec contractions were recorded. The mean of these four measurements at this frequency was used to define the cell shortening of a given cell. Cell lengths were measured via a line camera (data recording at 500 Hz). Data are expressed as cell shortening normalized to diastolic cell length [Δ Length/Length (percent)].

RNA isolation and real-time RT-PCR

Total RNA was isolated from cardiomyocytes and left ventricles using peqGold TriFast (peqlab; Biotechnologie GmbH, Germany) according to the manufacturer's protocol. To remove genomic DNA contamination, isolated RNA samples were treated with 1 U desoxyribonuclease per microgram RNA (Invitrogen, Karlsruhe, Germany) for 15 min at 37 C. One microgram of total RNA was used in a 10-μl reaction to synthesize cDNA using Superscript RNaseH reverse transcriptase (200 U/μg RNA; Invitrogen) and oligo dTs as primers. Reverse transcriptase reactions were performed for 50 min at 37 C. Real-time quantitative PCR was performed using the Icycler IQ detection system (Bio-Rad, Munich, Germany) in combination with the IQ SYBR Green real-time PCR supermix (Bio-Rad). The thermal cycling program consisted of initial denaturation in one cycle of 3 min at 95 C, followed by 45 cycles of 30 sec at 95 C, 30 sec at the individual annealing temperature for each primer, and 30 sec at 72 C. Primers used for determination had the following sequences: hypoxanthine-guanine phosphoribosyl transferase forward, CCA GCG TCG TGA TTA GTG AS, hypoxanthine-guanine phosphoribosyl transferase reverse, CAA GTC TTT CAG TCC TGT CC; PTH1-R forward, GGC TGC ACT GCA CGC GCA A, PTH1-R reverse, TTG CGC TTG AAG TCC AAA CGC; TGFβ1 forward, ATT CCT GGC GTT ACC TTG G, TGFβ1 reverse, CCT GTA TTC CGT CTC CTT GG. Quantification was performed as described before (20).

Western blot

Isolated cardiomyocytes of L-NAME-treated rats were incubated with lysis buffer as described before (2). Samples (100 μg protein) were loaded on a 12.5% SDS-PAGE and blotted onto membranes as described before. Blots were incubated first with a monoclonal antibody against the PTH1-R (antibody 05-517; Upstate Biotechnology, Lake Placid, NY) and second with an antimouse IgG antibody coupled to alkaline phosphatase. The actin band was used as a loading control.

Statistics

Data are expressed as indicated in the legends. ANOVA and the Student-Newman-Keuls test for *post hoc* analysis were used to analyze experiments in which more than one group was compared. In cases in which two groups were compared, Student's *t* test was used. $P < 0.05$ was regarded as significant.

Results

Influence of L-NAME on vital signs

After a 2-wk training phase, the basal blood pressure averaged 124 ± 6.4 mm Hg in all test groups at the start of the trial. This value did not change during the course of the trial for the animals in the control group. The animals in the L-NAME group developed an average systolic blood pressure of 174 ± 6.2 mm Hg after 4 wk. When the antihypertensive Hydralazine was added to the L-NAME feed after 2 wk of L-NAME treatment, the blood pressure fell from 160 ± 5.8 mm Hg (after 2 wk of L-NAME) to 126 ± 5.2 mm Hg. When the L-NAME substitution was ended after 2 wk, the blood pressure fell to a high-normal 137 ± 5.5 mm Hg by the end of the treatment. There was no change in heart rate in all test groups over the entire trial time period (Table 1).

Influence of PTHrP on LVDP

The isolated hearts of the conditioned animals underwent saline perfusion according to the Langendorff technique. Subsequent to the stabilization phase, the hearts were perfused for 3 min with 100 nM PTHrP. A negative inotropic effect is one of the acute cardiac effects of PTHrP. The LVDP of the control hearts decreased from 93.7 ± 3.9 to 75.8 ± 2.9 mm Hg during PTHrP perfusion. The LVDP of the L-NAME group, on the other hand, did not change. Before PTHrP perfusion, LVDP was 102.4 ± 2.8 mm Hg and after 3 min stimulation it was 100.5 ± 2.6 mm Hg. The hearts in the L/W group displayed a significant drop from 95.2 ± 3.7 to 78.9 ± 2.7 mm Hg. Through the combined L-NAME/Hydralazine treatment in the L/H group, normotensive blood pressure was achieved despite an NO deficit. The hearts from this group displayed similar behavior to the L group in that there was no change in LVDP during PTHrP stimulation (115.2 ± 4.4 *vs.* 117.0 ± 3.4 mm Hg) (Fig. 1A).

Influence of PTHrP on heart rate

The positive chronotropic effects of PTHrP were mediated by a direct stimulation of the pacemaker cells. In the control hearts

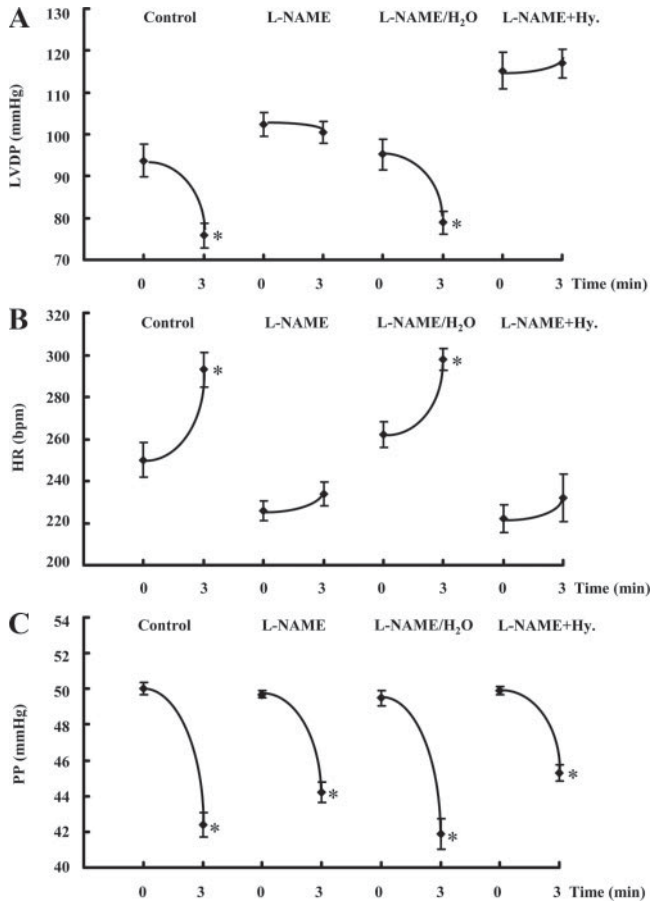

FIG. 1. Effect of PTHrP(1-36) on cardiac function. Isolated hearts of the conditioned animals were perfused for 3 min with 100 nM PTHrP. A, Impact of PTHrP on LVDP. Changes are expressed as absolute values before and 3 min after application of PTHrP. B, Impact of PTHrP on heart rate (HR). C, Impact of PTHrP on perfusion pressure (PP). Data are means ± SEM (n = 8 hearts). *, $P < 0.05$ *vs.* basal. Hy., Hydralazine.

stimulation with PTHrP lead to a 17.2% increase in the heart rate (250 ± 8 *vs.* 293 ± 8 bpm). In the L group the heart rate did not change. The heart rates of the L/W hearts increased 13.7% from 262 ± 6 to 298 ± 5 bpm. In the L/H group, there was no increase in the heart rate (Fig. 1B).

Influence of PTHrP on perfusion pressure

PTHrP exerts its vasorelaxing effects on the coronary vessels through the release of the endothelial mediator endothelium-derived hyperpolarizing factor (6). As a measure of coronary resistance, the perfusion pressure was recorded during PTHrP stimulation. Independent of the four treatment schemes, PTHrP reduced the perfusion pressure in all four groups between 9.4 and 15.1% (Fig. 1C).

PTHrP effects during acute NO blockade

Isolated hearts of untreated rats (n = 4) were perfused in Langendorff technique for 10 min with L-NAME to achieve an acute NO deficit. Subsequent to the L-NAME perfusion again, the hearts were perfused for 3 min with 100 nM PTHrP. These hearts displayed a similar behavior to the untreated control hearts in that there was a significant drop in LVDP (104.7 ± 4.3 *vs.* 86.2 ± 5.9 mm Hg), a significant increase in heart rate (223 ± 8 *vs.* 259 ± 11 bpm), and a remarkable reduction in the perfusion pressure (98.1 ± 11.3 *vs.* 58.7 ± 10.4 mm Hg).

Acute effect of PTHrP on single-cell contraction

The differing PTHrP effects on the contraction at the isolated hearts was verified in a further series of experiments on isolated heart muscle cells. Cardiomyocytes were isolated from identically preconditioned rats and stimulated after 10-min PTHrP incubation at 2 Hz with a cell-edge detection method. PTHrP reduced unloaded cell shortening in isolated myocytes from the control animals, as normalized based on the diastolic cell length, by 17 ± 1.4% (n = 49, $P < 0.01$). PTHrP had no influence, however, on the cell shortening of isolated L-NAME myocytes (Δ Length/Length, 10.1 *vs.* 10.3%, n = 49). There was also no change for the myocytes of the L/H group in relative cell shortening (Δ Length/Length, 10.0 *vs.* 10.4%, n = 28).

Changes in PTH1-R expression

To seek an explanation at the molecular level for the reduced PTHrP responsiveness of the NO-deficient rats, the entire RNA was isolated from the left ventricles, and, with the help of the real-time PCR, the expression of the PTH1-R was determined. With respect to the control group, the expression in ventricles of

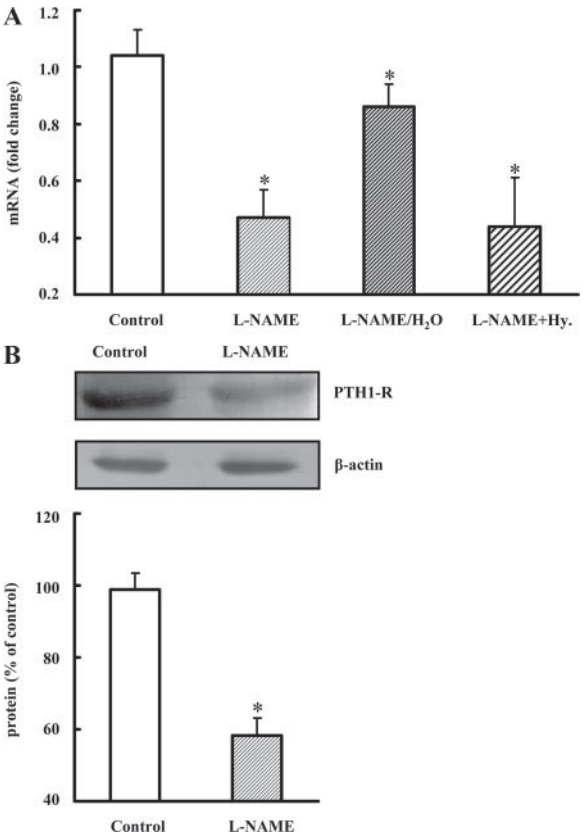

FIG. 2. Changes in PTH1-R expression. A, mRNA was isolated from the left ventricles of the Langendorff perfused hearts, and the expression of the PTH1-R was determined. Data are means ± SEM (n = 8 hearts). *, $P < 0.05$ *vs.* control. B, Representative immunoblot indicating PTH1-R immunoreactivity in isolated heart muscle cells from control and L-NAME-treated animals. PTH1-R values were normalized to actin levels. C, Densitometric analysis of immunoblots. PTH1-R was significantly decreased in myocytes from L-NAME-fed animals (*filled bar*) compared with myocytes of control animals (*open bar*). Data are means ± SEM (n = 3 hearts). *, $P < 0.05$ *vs.* control.

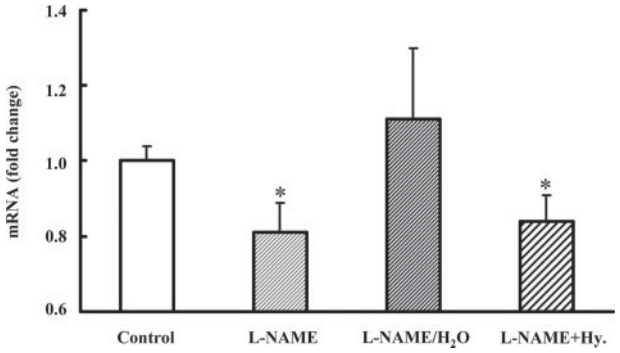

FIG. 3. TGFβ1 mRNA expression determined by quantitative RT-PCR in the left ventricles of hearts that underwent Langendorff perfusion. Data are means ± SEM (n = 8 hearts). *, $P < 0.05$ *vs.* control. Hy., Hydralazine.

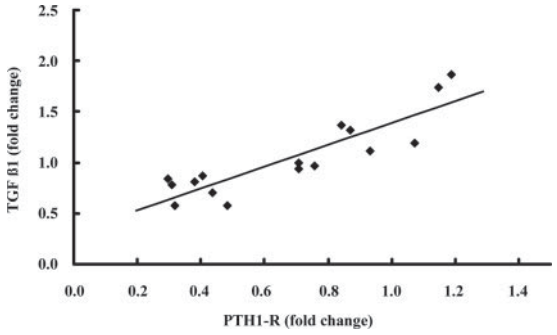

FIG. 4. Correlation between TGFβ1 and PTH1-R mRNA expression analyzed by quantitative RT-PCR. Overall, expression of TGFβ1 was significantly related to PTH1-R expression of individual rats from all test groups. Data represent values from the L/W and L/H groups (r = 0.88, $P < 0.001$).

the L-NAME group was 53 ± 1% ($P < 0.01$) lower. In ventricles of the L/W group, a reduction in PTH1-R expression of only 14 ± 1% was observed. In the left ventricle of normotensive but NO-deficient rats (L/H group), the PTH1-R was down-regulated to 44 ± 2% ($P < 0.01$) (Fig. 2A). In the Western blot, the down-regulation of the PTH1-R was also confirmed on the protein level. In isolated myocytes from L-NAME-fed animals, the PTH1-R protein levels decreased 41.7% (n = 3, $P < 0.05$) compared with the myocytes of the control animals (Fig. 2B).

TGFβ1 mediated regulation of the PTH1-R

Earlier studies indicated that TGFβ1 might possibly play a decisive role in the regulation mechanism of the PTH1-R. In the ventricles of the hearts that underwent a saline perfusion, the expression of TGFβ1 was positively correlated with the expression of the PTH1-R. In the L and L/H groups, in which the PTH1-R was down-regulated, the TGFβ1 expression was reduced to 81 ± 1% ($P < 0.05$) and 83 ± 1% ($P < 0.05$), respectively (Fig. 3). The TGFβ1 expression in the L/W group showed no change in comparison with the control group. Figure 4 shows the correlation between TGFβ1 and PTH1-R expression of individual rats from two different treatment groups (r = 0.88, $P < 0.001$).

To demonstrate a casual relationship between the expression of TGFβ1 and PTH1-R, myocytes from 3-month-old female Wistar rats were isolated and incubated over 24 h with 1 ng of TGFβ1. PTH1-R expression was subsequently ascertained. Compared with the unconditioned cells, PTH1-R expression increased by a factor of 4.1 ± 1.8 (n = 4, $P < 0.05$) in TGFβ1 stimulated myocytes (Fig. 5A).

In an identical manner, the coronary microvascular endothelial cells of female rats were stimulated for 24 h with TGFβ1 and the expression of PTH1-R was determined. In agreement with the results regarding the unchanged coronary resistance of the hearts that underwent saline perfusion, PTH1-R expression in the endothelial cells did not change (Fig. 5B).

Changes in PTH1-R expression in ovariectomized animals

To show that the regulation of the PTH1-R in hearts of L-NAME-treated animals is comparable with that in hearts of estrogen-deficient rats, entire RNA of the left ventricles was isolated and the expression of the receptor was determined. With respect to sham-operated animals, the expression in ventricles of ovariectomized rats was 39 ± 2% ($P < 0.01$) lower. In ventricles of ovariectomized animals under estrogen supplementation a reduction in PTH1-R expression of only 13 ± 1% was observed (supplemental Fig. S1, published as supplemental data on The Endocrine Society's Journals Online web site at http://endo.endojournals.org).

Discussion

Various studies have shown that sex-specific variation in PTHrP expression is caused by differences in estrogen levels (8, 12, 13).

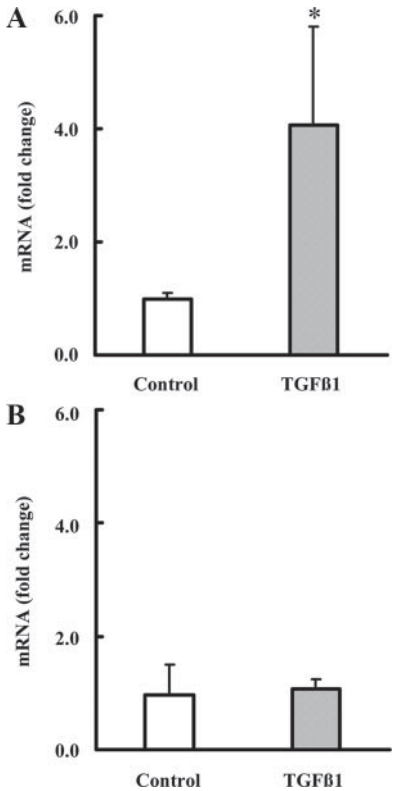

FIG. 5. Effect of TGFβ1 on PTH1-R mRNA expression. A, Isolated myocytes of female Wistar rats were incubated over 24 h with 1 ng of TGFβ1 and PTH1-R expression was ascertained by quantitative RT-PCR. B, Coronary microvascular endothelial cells of female rats were stimulated for 24 h with TGFβ1 and the expression of PTH1-R was determined. Data are means ± SEM (n = 4 hearts). *, $P < 0.05$ *vs.* control.

A falling estrogen level is also believed to be responsible for the increase in cardiovascular events for women in postmenopause. An NO deficiency, related to estrogen levels, often forms the basis for a worsening of the cardiac risk profile. The goal of this study was to more accurately characterize the cardiac effects of parathyroid hormone-related peptide under an chronic NO deficit.

The most important results show that PTHrP no longer had an effect on the inotropy and chronotropy of hearts from NO-deficient rats. The vasodilating effects on coronary vessels were, however, still present. These changes in the parameters of cardiac function are accompanied by a differing expression of the PTH1-R in the various target cells. An important mediator in the regulation mechanism of the PTH1-R is TGFβ1, whose expression is positively correlated with the expression of the receptor. However, an acute inhibition of NO synthesis did not affect the cardiac effects induced by a short-term PTHrP stimulation.

The prevalence of cardiac events rises significantly for women in menopause. This is caused by a decline in cardioprotective female sex hormones. Various studies have come to the same conclusion: hormone replacement therapy significantly reduces various risk factors for coronary heart disease. Arterial blood pressure, smooth muscle proliferation, serum lipid levels, and glucose and insulin metabolism are all affected (21–23). The effects of estrogen and progesterone, however, not only have a preventive character but also influence substantially the long-term remodeling and the progression of congestive heart failure as a result of myocardial infarct (24, 25).

In clinical studies and diverse animal models, the genomic and nongenomic effect of estrogen on eNOS was found to be responsible for a portion of the protective characteristics of hormone replacement therapy (14, 26).

In this study an NO deficit was generated in 3-month-old female Wistar rats by feeding them L-NAME. This resulted in a change, due to a variation in PTH1 receptor expression, in the response behavior of the animals' heart muscles to PTHrP. A comparable variation in PTH1-R expression could be also observed in ovariectomized animals. The estrogen deficit caused by ovariectomy induces a remarkable decrease in eNOS activity (-55%) in the myocardium as reported by Loyer *et al.* (27). TGFβ1 was identified as an important mediator for the regulation of the receptor.

The differing cardiac expression of TGFβ1 in the individual treatment groups indicates a casual relationship with the altered NO level. It has already been shown that exogenously administered NO leads to an overexpression of TGFβ1 protein and mRNA in human coronary smooth muscle cells (28). In rat cardiac fibroblasts, incubation with an NO donor or a cGMP analog also lead to a significant increase in the expression of TGFβ1 (29). An ANP-induced increase in the cytosolic cGMP concentration in mesangial cells lead to an increased biosynthesis of TGFβ1 (30). These observations lead to the conclusion that the decreased NO levels in L-NAME-fed animals lower the basal TGFβ1 expression through a reduced activation of cGMP-dependent signal pathways.

The significant correlation between TGFβ1 and PTH1-R expression, as well as the up-regulation of PTH1-R mRNA in isolated cardiomyocytes under TGFβ1 stimulation, identify TGFβ1 as an important cardiac regulation factor of the PTH1-R on a molecular level. Jongen *et al.* (31) were able to demonstrate a TGFβ2-mediated reduction in PTH1-R mRNA in fetal rat osteoblasts, which resulted in decreased PTHrP binding. McCauley *et al.* (32) reported on the influence of TGFβ1 and demonstrated an up-regulation in PTH1 receptor expression in osteoblastic cells.

The results of this study indicate a comparable mechanism in the left ventricular heart muscle cells of the rat. The complete loss of the negatively inotropic or positively chronotropic PTHrP effect cannot, however, be fully explained by a down-regulation of the receptor to 47.0% (mRNA) or 58.3% (protein). An additional desensitization or internalization of the receptor could neither be confirmed nor ruled out with the available data.

The vasorelaxing effect on the coronary vessels is one of the most important cardioprotective effects of PTHrP. At the molecular level, a contribution of the endothelium-derived hyperpolarizing factor with a subsequent cyclooxygenase-dependent release of prostaglandin could be demonstrated (33). Through the perfusion pressure of the isolated perfused hearts, it could be shown that this mechanism, independent of the corresponding therapy scheme of the test groups, was intact. As opposed to isolated cardiomyocytes, TGFβ1 also did not influence the expression of the PTH1-R in microvascular endothelial cells.

Based on the results of this study, this changed functional profile of PTHrP with a reduced NO level contributes to a worsening of postmenopausal cardioprotection. Whereas the improvement of the coronary perfusion could also be observed in NO-deficient animals, the reduced responsiveness of cardiac myocytes would have a negative effect on the postischemic functional recovery of the heart. The PTHrP, which is endothelially released during ischemia/hypoxia directly improves the contractile function of the postischemic or stunned myocardium (7, 8). A decreased expression of the myocardial PTH1-R thus weakens an important endogenous protection mechanism in reperfusion.

In summary, the results of this study demonstrate for the first time that a chronic NO deficit can influence the cardiac effects of PTHrP. A loss of the inotropic and chronotropic effect is associated with a down-regulation of the PTH1-R in left ventricular cardiomyocytes. The vessel-relaxing properties of PTHrP are not affected under these conditions. The myocytic, but not the endothelial, regulation of the PTH1-R occurs with the participation of TGFβ1.

Acknowledgments

Address all correspondence and requests for reprints to: Dr. Rolf Schreckenberg, Physiologisches Institut, Aulweg 129, D-35392 Giessen, Germany. E-mail: rolf.schreckenberg@ugcvr.de.

This work was supported by the Deutsche Forschungsgemeinschaft (SFB 547, project A1).

Disclosure Summary: The authors have nothing to disclose.

References

1. **Burtis WJ, Wu T, Bunch C, Wysolmerski JJ, Insogna KL, Weir EC, Broadus AE, Stewart AF** 1987 Identification of a novel 17,000-dalton parathyroid hormone-like adenylate cyclase stimulating protein from a tumor associated with humoral hypercalcemia of malignancy. J Biol Chem 262:7151–7156
2. **Schlüter K, Katzer C, Frischkopf K, Wenzel S, Taimor G, Piper HM** 2000 Expression, release, and biological activity of parathyroid hormone-related peptide from coronary endothelial cells. Circ Res 86:946–951
3. **Bui TD, Shallal A, Malik AN, al-Mahdawi S, Moscoso G, Bailey ME, Burton PB, Moniz C** 1993 Parathyroid hormone related peptide gene expression in human fetal and adult heart. Cardiovasc Res 27:1204–1208
4. **Deftos LJ, Burton DW, Brandt DW** 1993 Parathyroid hormone-like protein (PLP) is a secretory product of arterial myocytes. J Clin Invest 92:727–735
5. **Kalinowski L, Dobrucki LW, Malinski T** 2001 Nitric oxide as a second messenger in parathyroid hormone-related protein signaling. J Endocrinol 170: 433–440
6. **Sutliff RL, Weber CS, Qian J, Miller ML, Clemens TL, Paul RJ** 1999 Vasorelaxant properties of parathyroid hormone-related protein in the mouse: evidence for endothelium involvement independent of nitric oxide formation. Endocrinology 140:2077–2083
7. **Jansen J, Gres P, Umschlag C, Heinzel FR, Degenhardt H, Schluter K-D, Heusch G, Schulz R** 2003 Parathyroid hormone-related peptide improves contractile function of stunned myocardium in rats and pigs. Am J Physiol 284: H49–H55
8. **Grohé C, van Eickels M, Wenzel S, Meyer R, Degenhardt H, Doevendans PA, Heinemann MP, Ross G, Schlüter KD** 2004 Sex-specific differences in ventricular expression and function of parathyroid hormone-related peptide. Cardiovasc Res 61:307–316
9. **Schlüter KD, Weber M, Piper HM** 1997 Effects of PTHrP(107–111) and PTHrP(7-34) on adult cardiomyocytes. J Mol Cell Cardiol 29:3057–3065
10. **Gordon T, Kannel WB, Hjortland MC, McNamara PM** 1978 Menopause and coronary heart disease: the Framingham study. Ann Intern Med 89:157–161
11. **Lerner DJ, Kannel WB** 1986 Patterns of coronary heart disease morbidity and mortality in the sexes: a 26-year followup of the Framingham population. Am Heart J 111:383–390
12. **Holt EH, Lu C, Dreyer BE, Dannies PS, Broadus AE** 1994 Regulation of parathyroid hormone-related peptide gene expression by estrogen in GH4C1 rat pituitary cells has the pattern of a primary response gene. J Neurochem 62:1239–1246
13. **Cros M, Silve C, Graulet AM, Morieux C, Ureña P, de Vernejoul MC, Bouizar Z** 1998 Estrogen stimulates PTHrP but not PTH/PTHrP receptor gene expression in the kidney of ovariectomized rat. J Cell Biochem 70:84–93
14. **Chambliss KL, Shaul PW** 2002 Estrogen modulation of endothelial nitric oxide synthase. Endocr Rev 23:665–686
15. **Rosselli M, Imthurn B, Keller PJ, Jackson EK, Dubey RK** 1995 Circulating nitric oxide (nitrite/nitrate) levels in postmenopausal women substituted with 17ß-estradiol and norethisterone acetate. A two year follow-up study. Hypertension 25:848–853
16. **Lagumdzija A, Ou G, Petersson M, Bucht E, Gonon A, Pernow Y** 2004 Inhibited anabolic effect of insulin-like growth factor-I on stromal bone marrow cells in endothelial nitric oxide synthase-knockout mice. Acta Physiol Scand 182:29–35
17. **Nuedling S, van Eickels M, Alléra A, Doevendans P, Meyer R, Vetter H, Grohé C** 2003 17β Estradiol regulates the expression of endothelin receptor type B in the heart. BJP 140:195–201
18. **Schlüter K-D, Piper HM** 2005 Isolation and culture of adult ventricular cardiomyocytes. In: Dhein S, Mohr FM, Delmar M, eds. Practical methods in cardiovascular research. Berlin-Heidelberg: Springer Verlag; 557–567
19. **Langer M, Lüttecke D, Schlüter K-D** 2003 Mechanism of the positive contractile effect of nitric oxide on rat ventricular cardiomyocytes with positive force/frequency relationship. Eur J Physiol 447:289–297
20. **Livak KJ, Schmittgen TD** 2001 Analysis of relative gene expression data using real-time quantitative PCR and the 2[-$\delta\delta$ C(T)]. Methods 25:402–408
21. **Nabulsi AA, Folsom AR, White A, Patsch W, Heiss G, Wu KK, Szko M** 1993 Association of hormone-replacement therapy with various cardiovascular risk factors in postmenopausal women. N Engl J Med 328:1069–1075
22. **Farhat MY, Lavigne MC, Ramwell PW** 1996 The vascular protective effects of estrogen FASEB J 10:615–624
23. **Walton C, Godsland IF, Proudler AJ, Wynn V, Stevenson JC** 1993 The effects of the menopause on insulin sensitivity, secretion and elimination in non-obese, healthy women. Eur J Clin Invest 23:466–473
24. **Smith PJ, Ornatsky O, Stewart DJ, Picard P, Dawood F, Wen WH, Liu PP, Webb DJ, Monge JC** 2000 Effects of estrogen-replacement on infarct size, cardiac remodeling, and the endothelin system following myocardial infarction. Circulation 102:2983–2989
25. **Patten RD, Karas RH** 2006 Estrogen replacement and cardiomyocyte Protection. Trends Cardiovasc Med 16:69–75
26. **McNeill AM, Zhang C, Stanczyk FZ, Duckles SP, Krause DN** 2002 Estrogen increases endothelial nitric oxide synthase via estrogen receptors in rat cerebral blood vessels: effect preserved after concurrent treatment with medroxyprogesterone acetate or progesterone. Stroke 33:1685–1691
27. **Loyer X, Damy T, Chvojkova Z, Robidel E, Marotte F, Oliviero P, Heymes C, Samuel JL** 2007 17β-Estradiol regulates constitutive nitric oxide synthase expression differentially in the myocardium in response to pressure overload. Endocrinology 148:4579–4584
28. **Schmidt A, Geigenmueller S, Voelker W, Seiler P, Buddecke E** 2003 Exogenous nitric oxide causes overexpression of TGF-β1 and overproduction of extracellular matrix in human coronary smooth muscle cells. Cardiovasc Res 58: 671–678
29. **Abdelazis N, Colombo F, Mercier I, Calderone A** 2001 Nitric oxide attenuates the expression of transforming growth factor-β3 mRNA in rat cardiac fibroblasts via destabilization. Hypertension 38:261–266
30. **Wolf G, Ziyadeh FN, Stahl RA** 1995 Atrial natriuretic peptide stimulates the expression of transforming growth factor-β in cultured murine mesangial cells: relationship to suppression of proliferation. J Am Soc Nephrol 6:224–233
31. **Jongen JW, Willemstein-Van Hove EC, Van der Meer JM, Bos M, Jüppner H, Segre GV, Abou-Samra AB, Feyen J, Herrmann-Erlee MP** 1995 Down regulation of the receptor for parathyroid hormone (PTH) and PTH-related peptide by transforming growth factor-β in primary fetal rat osteoblasts. Endocrinology 136:3260–3266
32. **McCauley LK, Beecher CA, Melton ME, Werkmeister JR, Jüppner H, Abou Samara AB, Segre GV, Rosol TJ** 1994 Transforming growth factor-β1 regulates steady-state PTH/PTHrP receptor mRNA levels and PTHrP binding in ROS 17/2.8 osteosarcoma cells. Mol Cell Endocrinol 101:331–336
33. **Abdallah Y, Ross G, Dolf A, Heinemann MP, Schlüter KD** 2006 N-terminal parathyroid hormone-related peptide hyperpolarizes endothelial cells and causes a reduction of the coronary resistance of the rat heart via endothelial hyperpolarization. Peptides 27:2927–2934

British Journal of Pharmacology (2009), 156, 901–908

0007-1188/09
www.brjpharmacol.org

RESEARCH PAPER

Post-conditioning restores pre-ischaemic receptor coupling in rat isolated hearts

Rolf Schreckenberg, Thorsten Maier and Klaus-Dieter Schlüter

Justus-Liebig-University, Institute of Physiology, Aulweg, Giessen, Germany

Background and purpose: Ischaemic preconditioning (IPC) and ischaemic post-conditioning (IPoC) activate signal transduction pathways that are also involved in receptor de- and re-sensitization such as phosphatidylinositol (PI) 3-kinase. Therefore, IPC and IPoC may affect post-infarct receptor coupling.
Experimental approach: Rat isolated hearts (Langendorff mode, constant flow) were exposed to 45 min flow arrest followed by 120 min reperfusion, including IPC or IPoC. Control hearts were perfused without a 45 min flow arrest. Left ventricular developed pressure (LVdevP) was determined. Thirty min after reperfusion, hearts were exposed to parathyroid hormone-related peptide (PTHrP) or isoprenaline for 10 min to monitor receptor responsiveness. Reperfusion injury was quantified by enzyme release.
Key results: IPC and IPoC significantly reduced enzyme release compared with ischaemia and reperfusion alone by 75% and 62% respectively. Wortmannin or chelerythrine inhibiting either PI 3-kinase or protein kinase C, respectively, attenuated protection. Application of PTHrP 30 min after reperfusion did not change LVdevP in hearts exposed to ischaemia (+1 ± 11%), but IPoC restored the normal and non-ischaemic response to PTHrP characterized by a negative inotropism (–8.3 ± 3.9% and –12.9 ± 6.1%). IPC restored a small negative inotropic effect (–4.4 ± 4.7%). Application of a PTHrP receptor antagonist during the 45 min flow arrest attenuated receptor desensitization (ΔLVdevP: –6.1 ± 1.7%). Wortmannin but not chelerythrine attenuated the re-sensitizing effect of IPoC on post-ischaemic receptor coupling (ΔLVdevP: +6.2 ± 10.5 and –15.0 ± 7.7%). As observed with PTHrP receptors, IPoC restored β-adrenoceptors (ΔLVdevP: +9.3 ± 11.8% vs. 62.3 ± 15.8%).
Conclusions and implications: IPoC restores PTHrP receptor coupling in a PI 3-kinase-dependent way. A similar mechanism may allow β-adrenoceptor re-sensitization.
British Journal of Pharmacology (2009) **156**, 901–908; doi:10.1111/j.1476-5381.2008.00053.x; published online 17 February 2009

Keywords: β-adrenoceptors; parathyroid hormone-related peptide; receptor re-sensitization

Abbreviations: AUC, area under curve; I/R, ischaemia and reperfusion; IPC, ischaemic preconditioning; IPoC, ischaemic post-conditioning; LVdevP, left ventricular developed pressure; PI 3-kinase, phosphatidylinositol 3-kinase; PKC, protein kinase C; PTHrP, parathyroid hormone-related peptide; RISK, reperfusion injury salvage kinase

Introduction

Reperfusion therapy in acute myocardial infarction has significantly improved patient survival (van Domburg *et al.*, 2005). However, reperfusion alone has its limitations due to the induction of reperfusion injury and the mechanism(s) underlying reperfusion injury are matters for debate. However, it is generally accepted that several procedures reduce infarct size, when they are evoked at the onset of reperfusion (Garcia-Dorado *et al.*, 2006; Gross and Auchampach, 2007). One of the most prominent procedures is the so-called ischaemic post-conditioning (IPoC) that mimics some aspects of ischaemic preconditioning (IPC), and IPC and IPoC are safe when applied clinically (Staat *et al.*, 2005; Ramzy *et al.*, 2006). Nevertheless, many experimental studies have convincingly shown that there is negligible functional improvement of the heart, despite significant reduction of infarct size (Zhao *et al.*, 2003). Moreover, even the effect on infarct size seems to be a delay, rather than an attenuation (Watanabe *et al.*, 2006). On the other hand, this delay in the progressive loss of viable myocardium may provide a therapeutic opportunity if it offers more time in which to start post-infarct therapy that is aimed at attenuating the subsequent loss of function. In order to develop such treatment regimes, it is necessary to know more about receptor function in the post-infarcted myocardium.

We have recently identified an endothelium-derived peptide, parathyroid hormone-related peptide (PTHrP), as an endogenous cardiac protective factor that improves

Correspondence: Professor and Dr Klaus-Dieter Schlüter, Justus-Liebig-University, Institute of Physiology, Aulweg 129, D-35392 Giessen, Germany.
E-mail: Klaus-Dieter.Schlueter@physiologie.med.uni-giessen.de
Received 11 September 2008; accepted 7 October 2008

post-ischaemic function (Jansen *et al*., 2003; Grohé *et al*., 2004; Lüttecke *et al*., 2005). Ischaemia-dependent release of PTHrP from endothelial cells is sufficient to improve post-ischaemic heart function after brief periods of ischaemia (Jansen *et al*., 2003; Grohé *et al*., 2004). However, this effect is attenuated in prolonged ischaemia due to receptor desensitization because endogenously released PTHrP desensitizes PTHrP receptors (Ross *et al*., 2007). Therefore, hearts do not benefit either from endogenously released PTHrP or from PTHrP added to the perfusate after prolonged ischaemia. In the present study we hypothesized that IPC or IPoC may re-sensitize PTHrP receptors of the post-ischaemic heart. Although PTHrP is able to improve the function of post-ischaemic hearts it acts as a negative inotropic peptide in non-ischaemic hearts. Thus, even if our hypothesis is right, that PTHrP responsiveness can be reactivated by IPC or IPoC, it is an open question whether this would have beneficial effects for the functional recovery of post-ischaemic hearts.

Ischaemic preconditioning and IPoC activate multiple signal transduction pathways, called the reperfusion injury salvage kinase (RISK) pathway. Among signal transduction processes caused by IPC and IPoC, phosphatidylinositol (PI) 3-kinase activation has been identified leading to a subsequent activation of Akt and p70rsk (Hausenloy and Yellon, 2006). However, PI 3-kinase activation is also important for receptor trafficking and therefore may be involved in receptor re-sensitization (Drake *et al*., 2006). In the present study we hypothesized therefore, that IPoC may restore receptor coupling to PTHrP after long-term ischaemia. IPC activates similar kinases but at different time points, namely prior to a so-called triggering period and at reperfusion. As PI 3-kinase and other parts of the RISK pathway are involved in both receptor internalization and receptor recovery, one may assume that IPC and IPoC modify receptor trafficking. Indeed, IPC is able to induce receptor internalization and desensitization (Tong *et al*., 2004). On the other hand, IPC and IPoC also sensitize receptors as has been shown previously for the adenosine A_{2b} receptor (Philipp *et al*., 2006; Kuno *et al*., 2007). Whether IPC or IPoC modify PTHrP receptor responsiveness is not known at present and that possibility was analysed in this study. Finally, we addressed the question whether the proposed effect on post-infarct receptor coupling was more generally applicable, that is, to other receptors. For that purpose we chose to study β-adrenoceptor stimulation. As an experimental model we used a constant flow, non-working heart preparation in order to uncouple vascular resistance from perfusion-dependent oxygen supply allowing the study of myocardial function independent of corresponding vascular effects. In these non-working hearts left ventricular developed pressure (LVdevP) recovers well, in the first 30 min of reperfusion, but then falls (Grohé *et al*., 2004; Ross and Schlüter, 2005; Ross *et al*., 2007). Therefore, all hearts were treated at this time point, to provide a similar base-line function.

Methods

Animals and analysis of left ventricular developed pressure

All animal procedures in this investigation conformed to the Guide for the Care and Use of Laboratory Animals published by the US National Institute of Health (NIH Publication No. 85-23, revised 1996). Adult (5–6 months, 190–250 g) female Wistar rats were used to investigate the impact of ischaemia, IPC or IPoC on post-ischaemic receptor responsiveness. Experiments were performed on isolated hearts from these rats. Hearts were rapidly excised, and the aorta was cannulated for retrograde perfusion with a 16-gauge needle connected to a Langendorff perfusion system. A polyvinyl chloride balloon was inserted into the left ventricle through the mitral valve and held in place by a suture tied around the left atrium. The other end of the tubing was connected to a pressure transducer for continuous measurement of left ventricular pressure. A second transducer connected to the perfusion line just before the heart was used to measure coronary perfusion pressure. The perfusion system consisted of a warmed storage container for perfusate solutions, a rotary pump and a temperature-controlled chamber. Hearts were perfused with an oxygenated saline medium [composition of the perfusate (in $mmol \cdot L^{-1}$): 140.0 NaCl, 24.0 $NaHCO_3$, 2.7 KCl, 0.4 NaH_2PO_4, 1.0 $MgCl_2$, 1.8 $CaCl_2$ and 5.0 glucose, gassed with 95% O_2-5% CO_2, pH 7.4]. After attachment to the Langendorff system, hearts were allowed to stabilize for at least 20 min. The intraventricular balloon was inflated to give a diastolic pressure of 10 mmHg, and the balloon volume was held constant thereafter. The flow was adjusted to give a perfusion pressure of 50 mmHg. Parameters determined were left ventricular diastolic pressure and left ventricular systolic pressure. The developed pressure (LVdevP) was calculated as LVdevP = peak systolic pressure – diastolic pressure. To avoid differences in oxygen supply due to changes in the coronary resistance, hearts were perfused at a constant flow. Hearts were allowed to beat freely. Temperature was held constant at 37°C throughout the whole experiment.

Perfusion protocols

The study consisted of three parts. The different protocols are summarized in Figure 1. In the first part of the study the following protocols were used to investigate the effect of ischaemia and reperfusion (I/R), IPC and IPoC on post-infarct receptor coupling: I/R: 45 min flow arrest and 120 min reperfusion; IPC: three cycles of 3 min flow arrest followed by 5 min reperfusion prior to ischaemia and subsequent flow arrest for 45 min followed by reperfusion for 120 min; IPoC: 45 min flow arrest followed by three cycles of 30 s perfusion and 30 s flow arrest and reperfusion for 117 min; control (C): control experiments were performed on perfused hearts without a 45 min flow arrest as time-matched normoxic controls.

Each of the four groups consisted of 16 hearts. Eight of them were exposed to PTHrP(1–36) ($100\ nmol \cdot L^{-1}$) 30 min after reperfusion for 10 min, and the other eight hearts per group received vehicle only (Figure 1A). LVdevP was measured at the end of the stabilization period (Figure 1, arrow 'B'), after 30 min of reperfusion (Figure 1, arrow 'R1'), 10 min after the subsequent addition of PTHrP or vehicle (Figure 1, arrow 'Re') or at the end of the reperfusion period (Figure 1, arrow 'R2'). PTHrP receptor responsiveness was defined as the change in LVdevP between 'R1' and 'Re'.

In the second part of the study we investigated (i) whether ischaemia-dependent endogenously released PTHrP

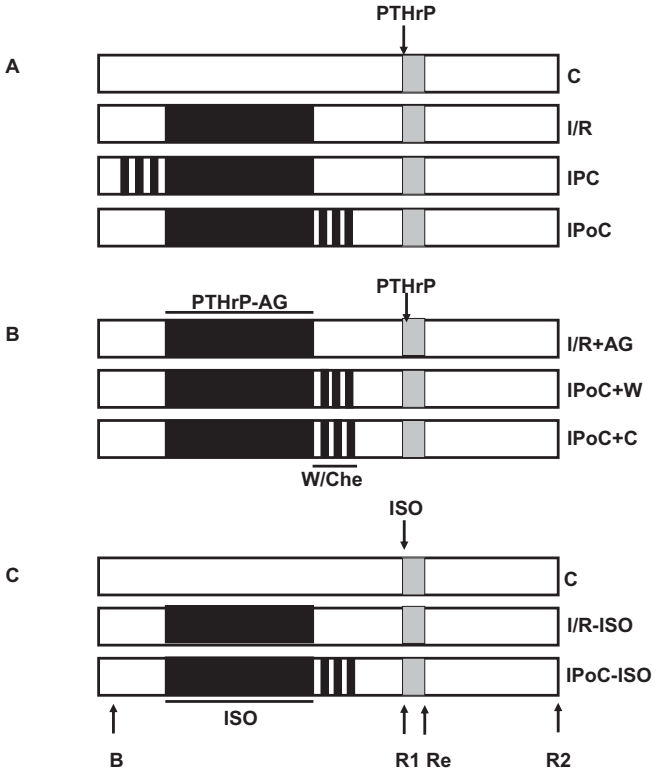

Figure 1 Schematic overview of the experimental design. The study was performed in three steps (A–C). Flow was stopped during the ischaemic periods, which are indicated in black. Functional data were recorded before any intervention (basal, B), 30 min after the onset of reperfusion (R1), 10 min after the addition of PTHrP (100 nmol·L^{-1}) or isoprenaline (ISO, 100 nmol·L^{-1}) (Response, Re) or at the end of the experiments (R2). Where indicated wortmannin (W, 100 nmol·L^{-1}) or chelerythrine (Che, 1 μmol·L^{-1}) were added. When isoprenaline was given during ischaemia, its concentration was 10 nmol·L^{-1}. When the activity of PTHrP released during ischaemia was inhibited, a PTHrP antagonist [PTHrP-AG = PTHrP(7–34), 100 nmol·L^{-1}] was given. I/R, ischaemia and reperfusion; IPC, ischaemic preconditioning; IPoC, ischaemic post-conditioning; PTHrP, parathyroid hormone-related peptide.

desensitized the PTHrP receptors; and (ii) whether the effect of IPoC on PTHrP receptor responsiveness depends on PI 3-kinase and protein kinase C (PKC) activation (Figure 1B). For this purpose, hearts received a PTHrP receptor antagonist [PTHrP(7–34), 100 nmol·L^{-1})] prior to the 45 min flow arrest. The antagonist was washed out with reperfusion. In order to show that the effect of IPoC on PTHrP receptor coupling depends on PI 3-kinase activation, the IPoC was performed in the presence of wortmannin (100 nmol·L^{-1}) or chelerythrine (1 μmol·L^{-1}) (each $n = 8$). Parameters under investigation in this part of the study were basal function (Figure 1, arrow 'B'), 30 min recovery (Figure 1, arrow 'R1') and PTHrP responsiveness (Figure 1, 'Re').

In the third part of the study we investigated whether IPoC restored β-adrenoceptor coupling (Figure 1C). For this purpose, hearts were exposed to isoprenaline (10 nmol·L^{-1}) prior to the flow arrest, and isoprenaline was washed out during reperfusion. Isoprenaline (100 nmol·L^{-1}) was reperfused, 30 min after starting reperfusion. This part of the study contained another three groups of eight hearts: control (C), which represents a normoxic control perfusion, I/R or IPoC in which isoprenaline was present during 45 min no-flow arrest. Parameters under investigation in this part of the study were basal function (Figure 1, arrow 'B'), 30 min recovery (Figure 1, arrow 'R1') and isoprenaline responsiveness (Figure 1, 'Re').

Finally, another 12 hearts were used to monitor activation of the kinase, p70rsk. For that, hearts were exposed to the I/R protocol, IPoC protocol and IPoC protocols with wortmannin or chelerythrine added at reperfusion and keeping the antagonists in the perfusate during the first 5 min of reperfusion (IPoC + W and IPoC + C, Figure 1). In these experiments, reperfusion was stopped after 15 min, and the left ventricles were excised and freeze-clamped in liquid nitrogen. Tissue samples were dissolved in lysis buffer as described previously (Ruf *et al.*, 2002). Levels of p70rsk activity were measured with a commercially available p70 S6K activity assay (Assay Designs, Inc., Ann Arbor, USA) according to the manufacturer's instructions. Briefly, tissue samples were normalized to their total protein levels and incubated with a substrate peptide of the kinase. Phosphorylation of this peptide was determined by application of an antibody directed against the phosphorylated form of the substrate peptide.

Determination of cardiac protection

In order to address the question whether the IPC and IPoC protocols described above, did protect the myocardium, we analysed perfusate samples during the first 15 min of reperfusion every 5 min. The total amount of lactate dehydrogenase (LDH) was measured, as a biochemical correlate of infarct size. The procedure to quantify LDH activity has been published before (Schlüter *et al.*, 1991). From the three different values a curve of LDH release was plotted, and the results are expressed as area under curve (AUC). Perfusate samples at later time points (30, 40, 60 and 90 after the onset of reperfusion) were also assayed for LDH activity but these values did not exceed the basal values of normoxic control hearts. Therefore, they were not included in the calculation of enzyme release.

Statistics

Quantitative results were expressed as means ± SEM as indicated. In experiments in which more than two groups were compared with each other, one-way analysis of variance was used, with Student-Newman-Keuls test for post hoc analysis. $P < 0.05$ was used as a level of significance.

Materials

Synthetic PTHrP(1–36) was used in this study in order to stimulate PTHrP receptors, and synthetic PTHrP(7–34) was used as an antagonist. These peptides were obtained from Bachem. They were dissolved in double distilled water with addition of 1% (v/v) acetic acid according to the manufacturer's suggestions. The concentration used for PTHrP was obtained from the previously established concentration–response relationship in the same model (Grohé *et al.*, 2004). Isoprenaline was obtained from Sigma/RBI and dissolved in double distilled water without further additions. Wortmannin

and chelerythrine were obtained from Calbiochem, dissolved in dimethylsulphoxide (DMSO) and stored as stock solutions (100 μmol·L^{-1}).

Results

Cardiac protective effects of IPC and IPoC

Firstly, we showed that IPC and IPoC procedures used in this study, were cardio-protective. LDH release, taken as a biochemical indicator of infarct size, was increased in I/R compared with normoxic controls, but significantly reduced in IPC and IPoC (Figure 2). These data demonstrate the well-known cardio-protective effects of IPC and IPoC on the myocardial structure in the Langendorff model used for this study. The cardio-protective effect of IPoC was attenuated if PI 3-kinase or PKC activation during IPoC was attenuated by application of wortmannin or chelerythrine respectively (Figure 2). The data confirmed the contribution of both kinases in the salvage pathway activated to reduce infarct sizes. As PI 3-kinase activation is part of a salvage pathway involving PI 3-kinase, Akt and p70rsk, we confirmed the suitability

of wortmannin to block this pathway on the biochemical levels as well. IPoC increased the p70rsk activity by 69.0 ± 8.8% (Figure 3, $n = 5$). When the PI 3-kinase inhibitor wortmannin was given during reperfusion the IPoC-induced activation of p70rsk was abolished. However, the PKC inhibitor chelerythrine did not attenuate p70rsk activation in this model (Figure 3).

Effect of IPC and IPoC on PTHrP receptor responsiveness

In order to test our hypothesis that IPoC re-sensitizes PTHrP receptors, we performed experiments in an I/R model, an IPC model and an IPoC model. These results were compared with those obtained for time-matched non-ischaemic controls (C). Hearts were either treated with PTHrP or vehicle after 30 min of reperfusion for the next 10 min. In additional experiments ischaemia was performed in the presence of a PTHrP antagonist, or IPoC was performed in the presence of either wortmannin or chelerythrine. There were no differences on baseline characteristics between the rat hearts from the 11 different groups. LVdevP ranged from 135 to 152 mmHg between these groups (data not shown). Within the first 30 min of reperfusion, the initial depression of cardiac function was improved to nearly normoxic control values in all groups undergoing 45 min flow arrest, irrespective of the treatment regime. Based on the nearly identical 30 min recovery values we decided to test receptor responsiveness at that time point. In Figure 4, these values are given for the seven groups exposed to PTHrP thereafter. When PTHrP was applied 30 min after reperfusion the peptide significantly reduced LVdevP in the IPoC group as it did in normoxic control hearts (Figure 5). However, in the I/R group, PTHrP was unable to change the LVdevP. In the

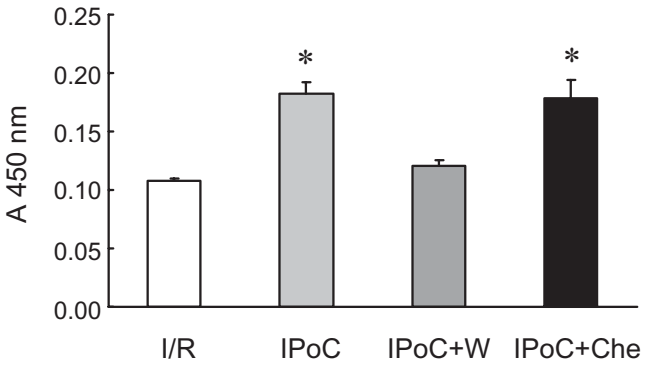

Figure 3 Effect of ischaemic post-conditioning (IPoC) and its inhibition by wortmannin (W) and chelerythrine (Che) on the activation of the reperfusion injury salvage kinase pathway as monitored by p70rsk activity, measured by phosphorylation of a p70rsk substrate peptide and quantified on a microplate reader. Data are expressed as absorbance at 450 nm and are means ± SEM ($n = 5$). *$P < 0.05$ vs. ischaemia and reperfusion (I/R).

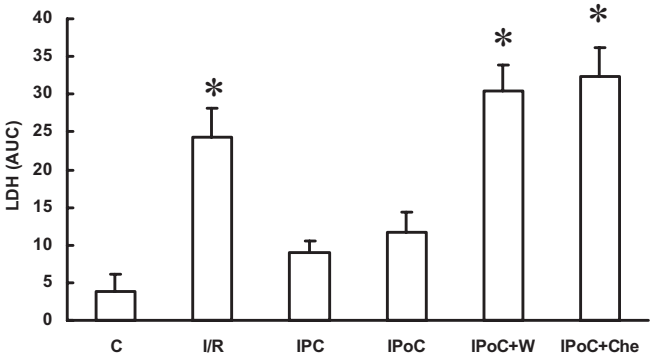

Figure 2 Effects on reperfusion injury, of ischaemia and reperfusion (I/R), ischaemic preconditioning (IPC), ischaemic post-conditioning (IPoC), IPoC with wortmannin (IPoC + W) and IPoC with chelerythrine (IPoC + Che). Reperfusion injury was determined by lactate dehydrogenase (LDH) release into the perfusate. Samples were collected after 5, 10 and 15 min and the area under curve (AUC) was calculated. Data are shown in comparison with normoxic time controls (C). Data are expressed as means ± SEM, $n = 8$ in each group. *$P < 0.05$ vs. C.

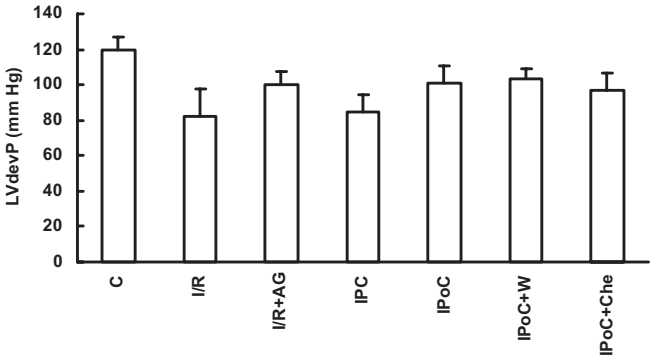

Figure 4 Functional recovery during reperfusion in groups with ischaemia and reperfusion (I/R), ischaemic preconditioning (IPC), ischaemic post-conditioning (IPoC), IPoC and wortmannin (W), IPoC and chelerythrine (Che) and normoxic controls (C). Left ventricular developed pressure (LVdevP) was measured during the first 30 min of reperfusion. Data are means ± SEM; $n = 8$–16 in each group. $P < 0.05$ n.s. vs. C. AG, antagonist.

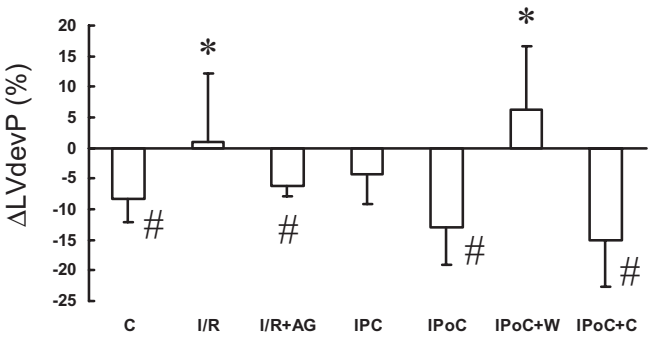

Figure 5 Acute effects of parathyroid hormone-related peptide (PTHrP) (100 nmol·L^{-1}) on functional parameters for the ischaemia and reperfusion (I/R), ischaemic preconditioning (IPC), ischaemic post-conditioning (IPoC), normoxic control (C) group, IPoC with wortmannin (W) and IPoC with chelerythrine (Che). PTHrP was perfused, 30 min after the onset of reperfusion, for 10 min. Data shown in this figure are the changes, 10 min after drug application. Data are given for left ventricular developed pressure (LVdevP) and represent means ± SEM; $n = 8$ in each group. *$P < 0.05$ vs. C; #$P < 0.05$ vs. baseline before application. For the absolute values before application of PTHrP or vehicle see Figure 4. AG, antagonist.

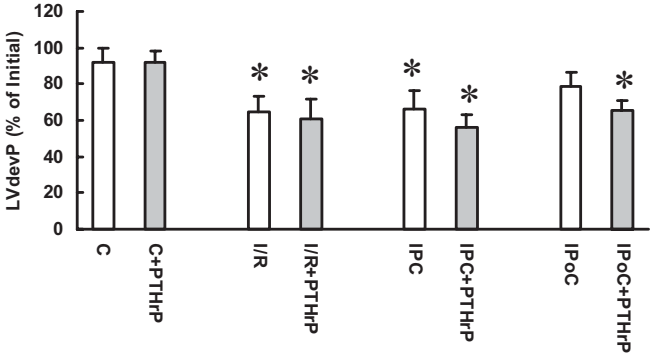

Figure 6 Effect of cardiac protection and parathyroid hormone-related peptide (PTHrP) receptor stimulation on recovery over 120 min. Left ventricular developed pressure (LVdevP) was measured for the ischaemia and reperfusion (I/R), ischaemic preconditioning (IPC), ischaemic post-conditioning (IPoC), normoxic control (C) group and expressed as percentage of initial values (mean: 145 ± 8 mmHg). In the PTHrP groups, the peptide was perfused at 30 min of reperfusion and maintained for 10 min, before the peptide was washed out again. Data are means ± SEM; $n = 8$ in each group, *$P < 0.05$ vs. C or C + PTHrP.

IPC group, a moderate decrease of LVdevP was observed (Figure 5). These data suggested that the endogenous PTHrP, released during ischaemia, desensitized PTHrP receptors and that IPoC re-sensitized the receptor responsiveness. In order to prove this assumption directly, we performed additional experiments in which the endogenously released PTHrP was antagonized by application of a PTHrP receptor antagonist during ischaemia. As expected, PTHrP responsiveness was not attenuated in this group (Figure 5; I/R + AG). In order to test directly whether PI 3-kinase activation during IPoC is responsible for the re-sensitization of PTHrP receptors in this group, we added either wortmannin or chelerythrine at the onset of reperfusion. The data show that wortmannin but not chelerythrine attenuated the recovery of receptor responsiveness induced by IPoC (Figure 5; IPoC + W and IPoC + C).

Effect of late PTHrP receptor stimulation of functional recovery

Continuation of reperfusion to 120 min revealed small differences in functional recovery between I/R, IPC and IPoC (Figure 6). In all three groups the mean LVdevP was lower than in the normoxic control group. However, in the IPoC group the mean LVdevP at the end of the reperfusion was not significantly different from normoxic controls. In normoxic controls, transient stimulation of PTHrP receptors had no sustained effect on LVdevP. In the I/R group, PTHrP receptor stimulation did not evoke an acute effect and, in line with this, it did not change LVdevP throughout the reperfusion (Figure 6). In the IPC group, PTHrP receptors were slightly responsive and these hearts showed a slight decrease in LVdevP that did not reach the level of significance. However, in the IPoC group PTHrP receptors showed a negative inotropic effect and, if IPoC was combined with PTHrP receptor stimulation, the mean LVdevP was slightly lower at the end of the experiments compared with IPoC alone (Figure 6).

Effect of IPoC on β-adrenoceptor responsiveness

To determine if the observed effect of IPoC was specific for the PTHrP receptor or if it might apply to receptors in general, we tested the hypothesis that IPoC re-sensitizes β-adrenoceptors as well. In contrast to PTHrP receptors, that rapidly desensitize by endogenously released PTHrP during 45 min flow arrest, β-adrenoceptors did not desensitize by flow arrest, per se. Subsequent addition of isoprenaline (10 nmol·L^{-1}) to the perfusate at 30 min after reperfusion caused an increase in LVdevP of 7.3 ± 1.6% in control hearts, 12.7 ± 3.4% in hearts exposed to I/R, 7.2 ± 4.2% in hearts exposed to IPC and 9.1 ± 3.7% in hearts exposed to IPoC (each $n = 6$). However, when isoprenaline (10 nmol·L^{-1}) was added prior to the 45 min flow arrest and maintained during ischaemia, a loss of post-ischaemic receptor coupling was observed for β-adrenoceptors as well (Figure 7, I/R). As expected, non-ischaemic hearts responded to isoprenaline (100 nmol·L^{-1}) with a significant increase in LVdevP. Isoprenaline responsiveness was restored in hearts pre-exposed to isoprenaline (10 nmol·L^{-1}) during the 45 min flow arrest, if an IPoC procedure was performed (Figure 7).

Discussion

The present study investigated the hypothesis that IPoC influences receptor coupling in the post-ischaemic heart. The study focused on the responsiveness of the PTHrP receptor, for the following reasons. We had previously shown that an ischaemia-dependent release of PTHrP contributed to the functional recovery of hearts after a moderate period of ischaemia *in vitro* and *in vivo* (Jansen *et al.*, 2003; Grohé *et al.*, 2004). However prolonged ischaemia leads to receptor desensitization and thereby to a loss of the cardiac protective effects of PTHrP (Ross *et al.*, 2007). IPoC activates PI 3-kinase pathways that are involved in receptor trafficking in cells. Therefore, IPoC may modify normal PTHrP receptor coupling in post-ischaemic hearts. We found that IPoC restored a

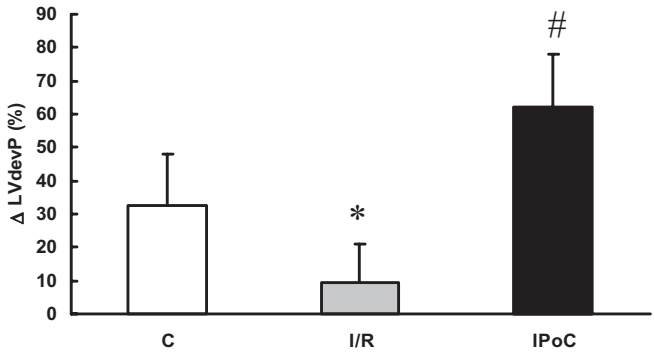

Figure 7 Effect of ischaemic post-conditioning (IPoC) on β-adrenoceptor coupling in hearts with desensitized β-adrenoceptors. Normoxic control hearts were compared with hearts undergoing 45 min flow arrest in the presence of isoprenaline (10 nmol·L^{-1}) subsequently followed by reperfusion (I/R) or IPoC and reperfusion. Isoprenaline (100 nmol·L^{-1}) was perfused 30 min after the onset of reperfusion, and changes in heart function were determined. Data shown in this figure are the changes 5 min after drug application. Data are given for left ventricular developed pressure (LVdevP) and represent means ± SEM; $n = 8$ in each group; $^*P < 0.05$ vs. C; $\#P < 0.05$ vs. I/R.

normoxic-like receptor coupling in these hearts. Moreover, we demonstrated that IPoC restored β-adrenoceptor responsiveness, too, as long as these receptors were desensitized during ischaemia. IPoC in the presence of wortmannin did not restore receptor coupling. We conclude that PI 3-kinase activation was causally involved in the restoration of receptor coupling.

The role of PTHrP in the response of the heart to I/R has been characterized in greater detail before. While PTHrP exerts a small negative contractile effect in normoxic hearts and isolated cardiomyocytes, it improves contractile performance in the post-ischaemic heart and cardiomyocytes (Jansen *et al.*, 2003; Grohé *et al.*, 2004; Lüttecke *et al.*, 2005). However, this response is lost during prolonged ischaemia, as shown before (Ross *et al.*, 2007). This was reconfirmed in our new study. In a previous study it was found that desensitization of PTHrP receptors (also known as PTH type 1 receptors) enables PTH type 2 receptors to dilate cardiac vessels. This was shown by application of the specific PTH type 2 receptor agonist, the tuberoinfundibular peptide of 39 residues (TIP39) (Ross *et al.*, 2007). However, whether TIP39 is released in the post-ischaemic heart is not known. The lack of effectiveness on cardiac contractility further reduces the ability of TIP39 to improve cardiac function in the reperfused rat heart. We therefore investigated whether we could re-sensitize PTHrP receptors in hearts after prolonged ischaemia and whether this was accompanied by a normoxic-like negative inotropic effect or with a post-ischaemia-like positive contractile effect, as found in post-ischaemic hearts with brief ischaemia. The outcome of these experiments would indicate whether or not PTHrP is a candidate to be used as a positive inotropic mimetic in post-infarcted hearts. In this study, however, a normoxic-like negative contractile effect of PTHrP receptor stimulation was restored by IPoC and no benefit in either sustained improvement or reduction of contractile function was observed, at least under these conditions.

Receptor internalization, but also receptor recovery, requires PI 3-kinase-dependent steps (Tong *et al.*, 2004; Drake *et al.*, 2006). IPoC activates PI 3-kinase, and PI 3-kinase activation induces downstream events that have been summarized as the RISK pathway and include a PI 3-kinase-dependent activation of Akt and p70rsk (Hausenloy and Yellon, 2006). Therefore, we tested the hypothesis that IPoC re-sensitizes receptors via PI 3-kinase activation. We found that IPoC activates p70rsk by approximately 15% above the value found in I/R and that this was indeed antagonized by wortmannin, a PI 3-kinase inhibitor. Another kinase that also leads to cardiac protection and is part of the RISK pathways is PKC. However, although PKC inhibition by chelerythrine significantly attenuated IPoC-induced cell protection it did not modify receptor recoupling. Thus, PI 3-kinase, but not PKC-dependent, steps are part of the receptor recoupling process. Moreover, this experiment shows that the observed effect of IPoC on re-sensitization of PTHrP receptors is not simply the effect of infarct reduction but really depends on an altered functional responsiveness of the surviving cardiomyocytes. The cardio-protective effects evoked by IPoC are elicited during the first minutes of reperfusion but are also responsible for receptor responsiveness. However, receptor re-sensitization was observed 30 min after reperfusion. This is not necessarily a paradox because receptor re-sensitization requires re-expression of receptors to the sarcolemmal membrane and this requires more time than the attenuation of hypercontraction.

The observed effect of IPoC on re-sensitization of PTHrP receptors led to an acute reduction of LVdevP. However, as we have shown previously, receptor-dependent effects evoked by PTHrP, in chronic pressure-overloaded hearts, are switched into a paradoxical positive contractile effect (Ross and Schlüter, 2005). If this holds, re-establishing PTHrP receptor responsiveness in pressure-overloaded hearts may be of greater functional relevance than in hearts from normotensive rats.

In our model, the β-adrenoceptors were affected similarly to the PTHrP receptors. However, this observation may be of academic interest but not necessarily of clinical or therapeutic impact, because the β-adrenoceptors are not desensitized in the post-ischaemic heart. In this study we added isoprenaline during ischaemia and added an excess of isoprenaline to the post-ischaemic hearts in order to demonstrate such an effect of IPoC on β-adrenoceptor re-sensitization. The concentration required to induce a positive contractile effect by isoprenaline was 10-fold higher than that used in normoxic hearts. Nevertheless, although the kinetics of receptor desensitization and recovery are low for the β-adrenoceptors compared with the PTHrP receptors, these experiments indicated that IPoC restores receptor re-sensitization of another G-protein coupled receptor as well. Without any doubt this has consequences for the functional recovery of the post-ischaemic heart and in addition to the post-infarct remodelling that is caused by receptor-dependent processes.

Like IPoC, IPC activates PI 3-kinase-dependent pathways that are involved in receptor internalization and thus in receptor desensitization. Following this suggestion, it is likely hat IPC per se would desensitize PTHrP receptors. As a

consequence of this, endogenously released PTHrP should not be able to improve the functional recovery in the IPC hearts. In the IPoC hearts, however receptor re-sensitization occurs, and this may improve the functional recovery. Indeed, the LVdevP was highest in the IPoC group and lowest in the IPC group at 30 min of reperfusion. However, although the different levels of recovery support this hypothesis, such differences did not reach the level of significance.

This IPC- or IPoC-dependent receptor re-sensitization has previously been observed for a subtype of adenosine receptors (A_{2b}) (Philipp *et al.*, 2006; Kuno *et al.*, 2007). However, there is a marked difference between the observations made in our study and those found for adenosine A_{2b} receptors. The adenosine receptors were not desensitized by I/R, but a hypersensitization was found with both IPC and IPoC. In contrast, the PTHrP receptors in this study were completely desensitized, and we observed a re-sensitization together with a restoration of a normoxic-like behaviour. Therefore, the mechanism may be different and the fact that sensitization of adenosine A_{2b} receptors was found with IPC and IPoC, but re-sensitization of PTHrP receptors only with IPoC may already indicate a different mechanism.

The fact that all hearts recovered initially quite well during reperfusion is explained by the experimental model. In non-working, Langendorff-perfused hearts, recovery is not impaired by post-ischaemic vascular resistance because the hearts were perfused under constant flow conditions. Furthermore, we used a lower perfusion pressure (50 mmHg) than those reported in some other papers, for the following reason. In these saline perfused rat hearts, a perfusion pressure of 50 mmHg was sufficient to maintain heart function in normoxic hearts for 3 h. If we increased the perfusion pressure to 80 mmHg, the functional recovery was impaired but IPoC resulted in a functional improvement, relative to the effects of I/R alone (data not shown). However, under these conditions there is a high risk for oedema formation. Thus, at such high perfusion pressures of saline-perfused hearts, it is difficult to distinguish between functional recovery due to improved cardiomyocyte function and that due to improving vascular defects.

In conclusion, this is the first study reporting the influence of IPoC on PTHrP receptor coupling in the post-ischaemic heart. Further studies are required to investigate the relevance of these findings on post-infarct remodelling, that is, altered growth responses to agonists that contribute to reactive myocardial hypertrophy. Our study shows that the effect of IPC and IPoC on infarct size is independent of effects on restoration of receptor recoupling. We need also to identify the signalling steps involved in this process, and finally these results need to be transferred from the rat heart model used in this study to models that are more closely linked to clinical practice, that is, hearts from hypertensive rats and/or aged animals.

Acknowledgement

This study was supported by the Deutsche Forschungsgemeinschaft, SFB 547, project A1.

Conflict of interest

None.

References

Drake MT, Shenoy SK, Lefkowitz RJ (2006). Trafficking of G protein-coupled receptors. *Circ Res* **99**: 570–582.

Garcia-Dorado D, Vinten-Johansen J, Piper HM (2006). Bringing preconditioning and postconditioning into focus. *Cardiovasc Res* **70**: 167–169.

Grohé C, van Eickels M, Wenzel S, Meyer R, Degenhardt H, Doevendans PA *et al.* (2004). Sex-specific differences in ventricular expression and function of parathyroid hormone-related peptide. *Cardiovasc Res* **61**: 307–316.

Gross GJ, Auchampach JA (2007). Reperfusion injury: does it exist? *J Mol Cell Cardiol* **42**: 12–18.

Hausenloy DJ, Yellon DM (2006). Survival kinases in ischemic preconditioning and postconditioning. *Cardiovasc Res* **70**: 240–253.

Jansen J, Gres P, Umschlag C, Heinzel FR, Degenhardt H, Schlüter K-D *et al.* (2003). Parathyroid hormone-related peptide improves contractile function of stunned myocardium in rats and pigs. *Am J Physiol Heart Circ Physiol* **284**: H49–H55.

Kuno A, Critz SD, Cui L, Solodushko V, Yang X-M, Krahn T *et al.* (2007). Protein kinase C protects preconditioning rabbit hearts by increasing sensititvity of adenosine A2b-dependent signaling during early reperfusion. *J Mol Cell Cardiol* **43**: 262–271.

Lüttecke D, Ross G, Abdallah Y, Schäfer C, Piper HM, Schlüter K-D (2005). Parathyroid hormone-related peptide improves contractile responsiveness of adult rat cardiomyocytes with depressed cell function irrespectively of oxidative inhibition. *Basic Res Cardiol* **100**: 320–327.

Philipp S, Yang X-M, Cui L, Davis AM, Downey JM, Cohen MV (2006). Preconditioning protects rabbit hearts through a protein kinase C-adenosine A2b receptor cascade. *Cardiovasc Res* **70**: 308–314.

Ramzy D, Rao V, Weisel RD (2006). Clinical applicability of preconditioning and postconditioning: the cardiothoracic surgeons's view. *Cardivasc Res* **70**: 174–180.

Ross G, Schlüter K-D (2005). Cardiac-specific effects of parathyroid hormone-related peptide: modification by aging and hypertension. *Cardiovasc Res* **66**: 334–344.

Ross G, Heinemann MP, Schlüter K-D (2007). Vasodilatory effect of tuberoinfundibular peptide (TIP39): requirement of receptor desensitization and its beneficial effect in the post-ischemic heart. *Peptides* **28**: 878–886.

Ruf S, Piper HM, Schlüter K-D (2002). Specific role for the extracellular signal-regulated kinase pathway in angiotensin II- but not phenylephrine-induced cardiac hypertrophy in vitro. *Pflügers Arch – Eur J Physiol* **443**: 483–490.

Schlüter K-D, Schwartz P, Siegmund B, Piper HM (1991). Prevention of the oxygen-paradox in hypoxic-reoxygenated hearts. *Am J Physiol Heart Circ Physiol* **261**: H416–H423.

Staat P, Rioufol G, Piot C, Cottin Y, Cung TT, L'Huillier I *et al.* (2005). Postconditioning the human heart. *Circulation* **112**: 143–148.

Tong H, Rockman HA, Koch WJ, Steenbergen C, Murphy E (2004). G protein-coupled receptor internalization signaling is required for cardioprotection in ischemic preconditioning. *Circ Res* **94**: 1133–1141.

Van Domburg RT, Sonnenschein K, Nieuwlaat R, Kamp O, Storm CJ, Bax JJ *et al.* (2005). Sustained benefit 20 years after reperfusion therapy in acute myocardial infarction. *J Am Coll Cardiol* **46**: 15–20.

Watanabe K, Yaoita H, Ogawa K, Oikawa M, Maehara K, Maruyama Y (2006). Attenuated cardioprotection by ischemic preconditioning in coronary stenosed heart and its restoration by carvedilol. *Cardiovasc Res* **71**: 537–547.

Zhao Z-Q, Corvera JS, Halkos ME, Kerendi F, Wang N-P, Guyton RA *et al*. (2003). Inhibition of myocardial injury by ischemic postconditioning during reperfusion: comparison with ischemic preconditioning. *Am J Physiol Heart Circ Physiol* **285**: H579–H788.

Basic Res Cardiol 104:424–426 (2009)
DOI 10.1007/s00395-009-0784-x

EDITORIAL

Klaus-Dieter Schlüter
Rolf Schreckenberg

Ischemic injury and the parathyroid hormone-related protein system: friend or foe?

Parathyroid hormone-related protein (PTHrP) is part of a peptide family consisting of a couple of structurally similar peptides such as parathyroid hormone, PTHrP, tuberoinfundibular peptide of 39 amino acids, and osteostatin. They act through signals induced by binding to one out of three distinct receptors, named PTHR1, PTHR2, and PTHR3. As the latter one has been described only in the Zebrafish PTH1R and PTH2R are the main receptors responsible for signaling in higher vertebrates. In the current issue of Basic Research of Cardiology Monego et al. [7] report about the expression of PTHrP and PTH1R in human ventricular tissue. Stimulation of PTH1R is involved in the regulation of tissue function, calcium homeostasis, and growth regulation. PTHrP acts exclusively through the PTH1R. It has initially been described as a peptide responsible for hypercalcemia of malignancy but it is now clear that it interacts in many physiological processes. Dysregulation of the PTHrP system leads to diverse diseases such as tumor formation, pulmonary defects, preeclampsia, and psoriasis. Further, mutations in the PTH1R cause severe genetic defects like the Jansen-Syndrome or the Blomstrand-Syndrome. The study of Monego et al. deals with the cardiovascular expression of PTHrP and PTH1R. With respect to cardiovascular physiology and pathophysiology PTHrP is discussed as part of the endothelium-dependent regulation of vascular flow as well as part of the endogenous response of the heart to ischemia and/or pressure overload. It is likely to assume that mechanical stress is a common mechanism leading to an activation of the PTHrP system under such conditions including an up-regulation of the peptide, of the corresponding receptor and of the release of the peptide into the circulation.

In order to understand the importance of the study provided by Monego et al. it is important to summarize the known cardiovascular effects of PTHrP. Potential mechanisms by which PTHrP acts in the cardiovascular system have been identified in animal experiments, experiments on isolated hearts, and experiments on cardiovascular cells. PTHrP protects endothelial cells against apoptosis, it reduces the vascular tone, it improves cardiac inotropy, it increases beating rates, it is able to induce hypertrophic growth, and it plays a major role in heart and vessel development [2, 10]. Therefore, an activation of the PTHrP system must be considered as an adaptive response required to maintain cardiac function. However, only few data are available investigating the role of PTHrP in human cardiovascular physiology. Based on early observations published by Bui et al. [1], ventricular expression of PTHrP seems to be neglible. Endothelial cells are considered as the main source of PTHrP formation in the heart, followed by atrial myocytes [3]. However, such an expression profile is similar to that of other peptides involved in cardiovascular regulation, i.e. ANP. Since ANP is re-expressed in hypertrophied myocytes in the ventricle it is timely to hypothesize that ventricular cardiomyocytes may re-express PTHrP in stress conditions, too. This hypothesis was tested in the study

Published online: 17 April 2009

Prof. Dr. K.-D. Schlüter (✉) · R. Schreckenberg
Physiologisches Institut
Justus-Liebig Universität
Aulweg 129
35392 Gießen, Germany
Tel.: +49-641/99-47212
Fax: +49-641/99-47219
E-Mail: klaus-dieter.schlueter@physiologie.med.uni-giessen.de

BRC 784

published in this issue of Basic Research of Cardiology [7]. A specific role for PTHrP has been shown in ischemia/reperfusion and therefore it is of specific interest to know whether PTHrP and its corresponding receptor is up-regulated in the ventricular myocardium in ischemic heart disease [6]. Further, increased cardiac formation of PTHrP in heart failure has been reported but the source of it remained unclear [8]. Based on the present study from Monego ventricular cardiomyocytes may be the source.

The new study presents the largest investigation published so far that deals with the ventricular expression of PTHrP and PTH1R in human hearts. Therefore, it improves significantly our understanding of the role of PTHrP in cardiac physiology. The authors report about a significant expression of PTHrP in ventricular cardiomyocytes in hearts depicted from patients with ischemic disease and hypertrophy. Therefore, they confirmed results suggested by animal experiments before in clinical related settings. However, as a significant extension of such studies they found that ventricular cardiomyocytes, normally not considered as a source of PTHrP, express substantial amounts of PTHrP under such conditions. Further, although the expression did not reach the level of significance they found nevertheless a greater expression in cardiomyocytes from females compared to males. This is in accordance with an estrogen-dependent regulation of PTHrP and a specific role for PTHrP in females, leading to the speculation that PTHrP may contribute to gender-specific protection of female hearts [4, 5]. Moreover, the authors report about a significant up-regulation of the corresponding receptor under the same conditions giving the observed inotropic effects of PTHrP a morphologic correlation. It should be noted that the strength of this manuscript is the high number of samples (n = 101) that were analyzed by the authors. This goes far above the levels reported so far in any comparable study.

Once the activation of the PTHrP system in ischemic heart disease cannot be ignored any more, it is time to identify the potential benefit or danger of such an activation. As the study performed by Monego and colleagues does not allow to go into this direction because of it's descriptive nature one has to speculate about consequences. Published data with animal experiments do not lead to a clear picture. PTHrP is able to improve cardiac output specifically in post-ischemic hearts [6]. However, whether this positive inotropism leads to an adaptive response of the heart at the long run is not clear. Further, recent studies on hypertensive rats argue for a different role of PTHrP in normtensive and hypertensive hearts [9]. As PTH1R is coupled to receptor activator modifying proteins (RAMPs), as do receptors for adrenomedullin as discussed by Monego et al. in their manuscript, it will be a future challenge to identify the impact of RAMPs on PTH1R activation before we can decide whether we should consider the observed activation of the cardiac PTHrP system as beneficial or detrimental and even more important to decide under which of these conditions we should improve or inhibit the activation of the PTHrP system.

References

1. Bui TD, Shallal A, Malik AN, Al-Mahdawi S, Moscoso G, Bailey ME, Burton PB, Moniz C (1993) Parathyroid hormone-related peptide gene expression in human fetal and adult heart. Cardiovasc Res 27:1024–1028
2. Clemens TL, Cormier S, Eichinger A, Endlich K, Fiaschi-Taesch N, Fischer E, Friedman PA, Karaplis AC, Massfelder T, Rossert J, Schlüter K-D, Silve C, Stewart AF, Takane K, Helwig JJ (2001) Parathyroid hormone-related protein and its receptors: nuclear functions and roles in the renal and cardiovascular systems, the placental trophoblasts and the pancreatic islets. Br J Pharmacol 134:1113–1136
3. Degenhardt H, Jansen J, Schulz R, Sedding D, Braun-Dulläus R, Schlüter K-D (2002) Mechanosensitive release of parathyroid hormone-related peptide from coronary endothelial cells. Am J Physiol Heart Circ Physiol 283:H1489–H1496
4. Grohé C, van Eickels M, Wenzel S, Meyer R, Degenhardt H, Doevendans PA, Heinemann MP, Ross G, Schlüter K-D (2004) Sex-specific differences in ventricular expression and function of parathyroid hormone-related peptide. Cardiovasc Res 61:307–316
5. Holt EH, Lu CE, Dreyer B, Dannies PS, Broadus AE (1994) Regulation of parathyroid hormone-related peptide gene expression by estrogen in GH4C1 rat pituitary cells has the pattern of a primary response gene. J Neurochem 62:1239–1246
6. Jansen J, Gres P, Umschlag C, Heinzel FR, Degenhardt H, Schlüter K-D, Heusch G, Schulz R (2003) Parathyroid hormone-related peptide improves contractile function of stunned myocardium in rats and pigs. Am J Physiol Heart Circ Physiol 284:H49–H55
7. Monego G, Arena V, Pasquini S, Stigliano E, Fiaccavento R, Leone O, Arpesella G, Potena L, Raneletto FO, di Nardo P, Capelli A (2009) Ischemic injury activates PTHrP and PTH1R expression in human ventricular cardiomyocytes. Basic Res Cardiol. doi:10.1007/s00395-008-0774-4

8. Ogino K, Ogura A, Kinugasa Y, Furuse Y, Uchida K, Shimoyama M, Kinugawa T, Tomikura Y, Igawa O, Hisatome I, Bilezikian JP, Shigemasa C (2002) Parathyroid hormone-related peptide is produced in the myocardium and increased in patients with congestive heart failure. J Clin Endocrin Metab 87:4722–4727

9. Ross G, Schlüter K-D (2005) Cardiac-specific effects of parathyroid hormone-related peptide: modification by aging and hypertension. Cardiovasc Res 66:334–344

10. Schorr K, Taimor G, Degenhardt H, Weber K, Schlüter K-D (2003) Parathyroid hormone-related peptide is induced by stimulation of α1-adrenoceptors and improves resistance against apoptosis in coronary endothelial cells. Mol Pharmacol 63:111–118

Cardiovascular Research (2009) **82**, 77–83
doi:10.1093/cvr/cvp027

Parathyroid hormone improves contractile performance of adult rat ventricular cardiomyocytes at low concentrations in a non-acute way

Ilhan Tastan, Rolf Schreckenberg, Solaiman Mufti, Yaser Abdallah, Hans Michael Piper, and Klaus-Dieter Schlüter*

Justus-Liebig-Universität Giessen, Physiologisches Institut, Aulweg 129, D-35392 Giessen, Germany

Received 16 September 2008; revised 6 January 2009; accepted 19 January 2009; online publish-ahead-of-print 24 January 2009

Time for primary review: 42 days

KEYWORDS
Heart function;
Calcium sensing receptor;
Inotropy

Aims In patients with congestive heart failure, plasma parathyroid hormone (PTH) levels are positively associated with cardiac function. PTH, used to mobilize stem cells from the bone marrow after myocardial infarction, causes an increased left ventricular ejection fraction. The aim of this study was to investigate whether low but plasma-relevant concentrations of PTH directly influence the contractile properties of cardiomyocytes.

Methods and results Isolated adult rat ventricular cardiomyocytes were exposed to PTH(1–34) or full-length PTH at picomolar concentrations for 24 h. Cell shortening was measured at 2 Hz as a cellular correlate of inotropic responsiveness. Intracellular calcium was measured in Fura-AM-loaded cells. PTH(1–3) (20–200 pM) and full-length PTH (200 pM) increased cell shortening within 24 h. PTH had no effect on cell size, but resting and peak systolic calcium concentrations were elevated. The beneficial effect of PTH was mediated via its cAMP/protein kinase A-activating domain and attenuated by addition of a protein kinase A inhibitor. In contrast, PTH peptides representing a protein kinase C-activating domain but not a cAMP/protein kinase A-activating domain or peptides that represent none of these domains had no effect on cell shortening. The effect of PTH on cell shortening was strong at low concentrations of extracellular calcium but declined at higher calcium concentrations. PTH downregulated the expression of the calcium sensing receptor, a receptor known to antagonize the action of PTH on calcium transport. Furthermore, PTH antagonized the angiotensin II-induced loss of cell function.

Conclusion Low concentrations of PTH improve cell shortening by increasing calcium load at rest. By this mechanism cardiomyocytes compensate reduced extracellular calcium levels as they occur in patients with heart failure.

1. Introduction

Ventricular cardiomyocytes are well known as potential target cells of parathyroid hormone (PTH).[1–3] PTH has been identified as a pro-hypertrophic agonist.[4] Clinical data supported these findings as cardiac hypertrophy is a common finding in patients with end-stage renal disease or hyperparathyroidism in which PTH levels are elevated.[5–8] Acute effects of PTH on cardiomyocytes required rather high concentrations of PTH, and it remained an open question whether cardiac effects of PTH really play a role in cardiac disease stages except in patients with end-stage renal disease or hyperparathyroidism. The finding that microvascular endothelial cells express PTH-related protein (PTHrP), a structurally related peptide, has led to the impression that PTHrP rather than PTH is the natural ligand of cardiac PTH/PTHrP receptors.[9] PTH and PTHrP display a strong homology in their N-terminal part. This suggests that they act in a similar way on cardiomyocytes. However, detailed analysis of the effects of PTH and PTHrP on cardiomyocytes has also revealed specific effects for each of the two hormones.[10]

There is rising interest to re-address the question whether chronic elevated plasma levels of PTH influence cardiac physiology. First, end-stage heart failure is often accompanied by reduced plasma calcium concentrations leading to a subsequent increase in plasma PTH. Such a mechanistic link was hypothesized by McCarty in 2005.[11] In heart failure, a rise in angiotensin II and subsequently in aldosterone levels must be assumed. The latter is known to increase calcium excretion, which will lead to a corresponding activation of PTH.[12] A slight reduction in plasma

This paper was guest edited by Håvard Attramdal, University of Oslo, Norway.

* Corresponding author. Tel: +49 641 99 47 212; fax: +49 641 99 47 219.
E-mail address: klaus-dieter.schlueter@physiologie.med.uni-giessen.de

sodium has been demonstrated in patients with end-stage heart failure, too.[13] Another cause for a mild but significant increase in plasma PTH seems to be vitamin D deficiency due to less outdoor activity.[14,15] The increase in PTH concentration may be small and within the so-called physiological range in patients with heart failure but normal kidney function in contrast to patients with end-stage renal disease or hyperparathyroidism, as mentioned above, but it is nevertheless significantly elevated. Thus, it needs to be analysed whether small increases in plasma PTH affect cardiac performance. Second, application of PTH has been introduced in the treatment of patients with osteoporosis, due to its anabolic effects on osteoblasts.[16] Therefore, a better understanding of chronic effects of PTH on cardiac cells must be established to judge about possible cardiac side effects of chronically applied PTH. Finally, PTH has been shown to mobilize bone-derived stem cells.[17] PTH improved post-infarct recovery, at least under experimental conditions. Nevertheless, it is difficult to decide at present whether this effect of PTH depends on direct cardiac effects evoked by PTH or whether it is indirectly mediated by stem-cell mobilization. Again, a better understanding of long-term effects on cardiac performance would help to understand the potential of PTH under these conditions.

In a previous study, we demonstrated that PTH exerts a pro-hypertrophic effect on cardiomyoctyes.[4] We were also able to demonstrate acute effects of PTH on β-adrenoceptor stimulation-dependent inotropic responses.[10] However, it has never been investigated whether PTH modifies contractile performance of cardiomyocytes when applied in a chronic way to these cells. Therefore, the renewed interest in cardiac-specific effects of PTH has prompted us to determine long-term effects of PTH on the contractile behaviour of cardiomyocytes. In the present study, we hypothesized that PTH improves contractile function of cultured adult rat ventricular cardiomyocytes exposed to PTH for 24 h and that PTH counterbalances the effect of reduced calcium and sodium as it occurs in end-stage heart failure.

2. Methods

2.1 Cell culture

Adult ventricular rat cardiomyocytes were isolated from male Wistar rats by collagenase digestion of the hearts as previously described in greater detail.[18] Rats were housed under standardized conditions with free access to food and water. The investigation conforms to the *Guide of the Care and Use of Laboratory Animals* published by the US National Institutes of Health (NIH Publication No. 85–23, revised 1996). Briefly, hearts were excised under deep ether anaesthesia, transferred rapidly to ice-cold saline and mounted on the cannula of a Langendorff perfusion system. Heart perfusion and subsequent steps were all performed at 37°C. First, hearts were perfused in the non-circulating mode for 5 min at 10 mL/min (perfusate in mM: NaCl 110, KH_2PO_4 1.2, KCl 1.2, $MgSO_4$ 1.2, $NaHCO_3$ 25, glucose 11, gassed with 5% CO_2–95% O_2). Thereafter, perfusion was continued with recirculation of 50 mL of the above perfusate supplemented with 0.06% (w/v) crude collagenase and 25 μM $CaCl_2$ at 5 mL/min. After 30 min, ventricular tissue was minced and incubated for 20 min in recirculating medium with 1% (w/v) bovine serum albumin under 5% CO_2–95% O_2. Gentle trituration through a pipette released cells from the tissue chunks. The resulting cell suspension was filtered through a 200 μm nylon mesh. The filtered material was washed twice by centrifugation (3 min, 25 *g*) and resuspended in the above perfusate, in which the concentration of $CaCl_2$ was increased stepwise to 0.2 and 0.5 mM. After further centrifugation (3 min, 25 *g*), the cells in the pellet were suspended in serum-free culture medium (medium 199 with Earle's salts, 5 mM creatine, 2 mM carnitine, 5 mM taurine, 100 IU/mL penicillin, 100 μg/mL streptomycin, and 10 μmol/l β-D-arabinofuranoside). The calcium concentration in medium 199 is 1.8 mmol/L. Cells were attached to cell culture dishes by precoating of the culture dishes with 4% (vol/vol) fetal calf serum. On average, the initial number of rod-shaped cells was $\sim 4 \times 10^4$ cells per dish. The cells were washed 2 h after preparation, and the remaining cells were incubated for 24 h with agonists as indicated in the Results section.

2.2 Determination of cell shortening

Cell shortening was determined as described before in greater detail.[19] Briefly, cells were used after 24 h. All cell-shortening experiments were performed at room temperature. Only rod-shaped cells that contracted regularly were used for quantification. Cell length was analysed using a line-camera. Cells were stimulated at 2 Hz for 1 min via two AgCl electrodes with biphasic electrical stimuli composed of two equal, but opposite rectangular 50 V stimuli at 0.5 ms duration. Every 15 s cell shortening was recorded. The median of four cell shortenings per cell was used as the average cell shortening of the individual cell.

2.3 Quantification of calcium transients

To measure cytosolic [Ca^{2+}], cardiomyocytes were loaded at 37°C with 5 μM Fura-2AM for 30 min and then washed for further 30 min as described before.[20] Alternating excitation of the fluorescence dye at wavelengths of 340/380 nm of Fura-2 was performed with a Video-Imaging-System (Till Photonics) adapted to the microscope.

2.4 Determination of cell sizes

Myocyte growth was determined on phase-contrast micrographs recorded on tape using a CCD video camera as described before.[21] Cell volumes were calculated by the following formula: volume = $(\text{radius})^2 \times \pi \times \text{length}$, assuming a cylindrical cell shape.

2.5 Real-time RT—PCR

In order to quantify the expression of the calcium-sensing receptor in cardiomyocytes, cells were homogenized and RNA was extracted to obtain total cellular RNA. Aliquots (1 μg) were used for real-time polymerase chain reaction using the I-Cycler (Bio-Rad, Germany) and SYBR green as the fluorescence signal. The expressions of the calcium-sensing receptor was normalized to hypoxanthine phosphoribosyl transferase (HPRT) as a housekeeping gene for loading control. Each sample was run in duplicate. The primer sequence is as follows: HPRT: forward CCAGCGTCGTGATTAGTGAT; reverse: CAAGTCTTTCAGTCCCTGTCC; calcium-sensing receptor: forward: ATTCCTGGCGTTACCTTGG; reverse: AGGTCTGCCATAGTCGTCATC. DNA contaminations were excluded by amplification with the following β-actin primers that cover an intron of the actin gene: forward: GGCTCCTAGCACCATGAAGA; reverse: ACTCCTGCTTGCTGATCCAC. The amplification products of actin runs were loaded on an agarose gel and the size of the product was investigated.

2.6 Determination of protein kinase A activation

In order to determine protein kinase A activity in cells exposed to PTH cells were incubated with the hormone or antagonists for 10 min. Then media were removed from plates, the plates were washed with ice-cold PBS and 1 mL of a lysis buffer (composition in mM: MOPS 20, β-glycerolphosphate 50, sodium fluoride 50, sodium vanadate 1, EGTA 5, EDTA 2, NP40 1%, dithiothreitol 1, benzamidine 1, phenylmethanesulphonylfluoride 1, leupeptin 10 μg/

mL, aprotinin 10 μg/mL) was added. Cells were scraped using a rubber policeman, transferred to a microcentrifuge tube, sonicated 3 × 20 s, and centrifuged. The remaining supernatant was used to determine the protein content and measure protein kinase A activity. Kinase activity was measured using the non-radioactive PKA kinase activity assay kit (assay Designs, Inc., Ann Arbor, USA). Samples were measured exactly according to the manufacturer's suggestions.

2.7 Statistics

Results are expressed as means ± standard deviation (SD) or standard error of the mean (SEM) as indicated. Differences were analysed by one-way ANOVA followed by Student–Newman–Keuls *post-hoc* analysis. A value of $P < 0.05$ was regarded as significant.

3. Results

3.1 Long-term effect of parathyroid hormone on cardiomyocyte cell shortening

In order to address the question whether chronic exposure of cardiomyocytes to PTH(1–34) modifies the contractile performance, adult rat ventricular cardiomyocytes were exposed to various concentrations of PTH(1–34) for 24 h. Thereafter, cells were paced at 2 Hz and cell shortenings were recorded. A bell-shaped concentration curve was observed. PTH(1–34) at 20 pM was sufficient to increase cell shortening. A maximal effect was obtained at 200 pM (*Figure 1A*). On average, PTH (200 pM) increased cell shortening normalized to diastolic cell lengths by 16.1 ± 3.6% from 6.72 ± 0.16% of diastolic cell length to 7.80 ± 0.25% of diastolic cell length. In absolute values PTH(1–34) increased the mean shortening amplitude by 16.1 ± 4.9% from 5.77 ± 0.14 μm to 6.70 ± 0.28 μm. During the whole study the effect of PTH(1–34) on cell shortening was analysed in five different preparations (221 cells in total). The mean increase of cell shortening normalized to diastolic cell length was 11.3 ± 1.8% (range: 6.5–16.1%). *Figure 1B* gives a representative single-cell recording. Experiments were also repeated in the presence of rec-hPTH(1–84) in order to address the question whether N-terminal PTH-peptides used for this study represent the bioactivity of full-length PTH. Rec-hPTH(1–84) increased cell shortening by 10.6 ± 1.9% [$n = 48$ cells from two preparations; not significantly different from PTH(1–34)].

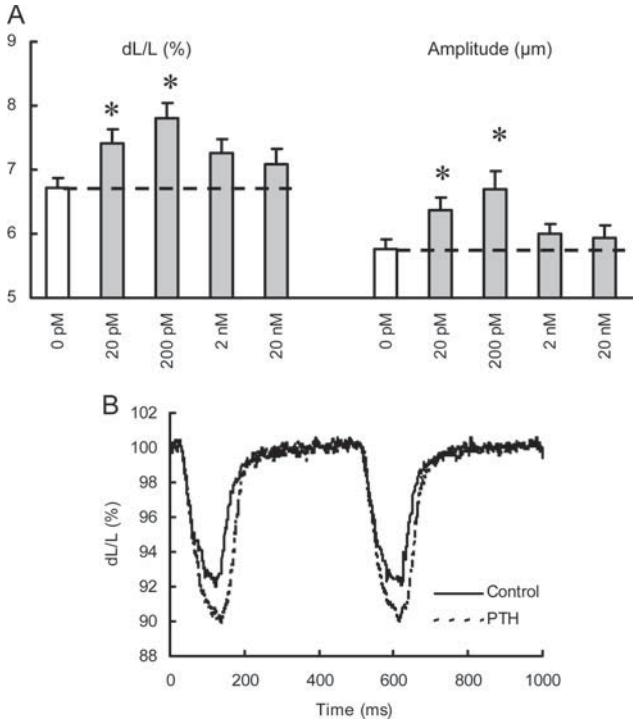

Figure 1 Effect of PTH(1–34) on cell shortening. Cardiomyocytes were exposed to parathyroid hormone for 24 h and cell shortening was measured thereafter at 2 Hz. (*A*) Concentration response curves for cell shortening expressed after normalization to diastolic cell lengths (left) or as absolute values (right). (*B*) Representative single-cell recording. Data are means ± SEM from $n = 36$ cells. *$P < 0.05$ vs. untreated controls.

The effect of PTH(1–34) at 200 pM was analysed in more detail. PTH(1–34) did not evoke any effect on cell length, cell width, or cell volume (*Figure 2A*). However, in addition to an increased cell shortening, the maximal contraction velocity and the maximal relaxation velocity were significantly accelerated by 33.3 and 26.9%, respectively. In absolute values contraction velocity increased from 123 ± 3 to 164 ± 7 μm/s and relaxation velocity from 119 ± 4 to 151 ± 5 μm/s (*Figure 2B*). Finally, we addressed the question whether PTH influences the intracellular calcium concentration. Cardiomyocytes exposed to PTH(1–34) for 24 h displayed higher resting calcium as well as a higher peak calcium. Calcium transients were not different (*Figure 2C*). PTH-dependent calcium absorption by mouse cortical ascending limbs is negatively regulated by the calcium-sensing receptor.[22] Thus, we hypothesized that PTH may increase resting calcium by down-regulating calcium-sensing receptors. Indeed, PTH(1–34) at 200 pM decreased the steady-state mRNA expression of the calcium-sensing receptor by 48 ± 13% ($n = 3$, $P = 0.019$).

3.2 Signal transduction pathways involved in the parathyroid hormone effect

PTH is known to activate either adenylyl cyclase or phospholipase C, leading to a subsequent activation of protein kinase A (PKA) or protein kinase C (PKC). We first addressed the question whether an activation of PKA is required for the PTH effects described above. For this purpose experiments were repeated in the presence of H89 (1 μM), an inhibitor of PKA. When the cells were exposed to H89 for 24 h basal contractile activity was already reduced (*Figure 3*). Moreover, PTH(1–34) was unable to increase cell shortenings in the presence of H89 (*Figure 3*). These data suggested that PTH exerts the above-mentioned effects via an activation of the adenylyl cyclase-activating domain. This hypothesis was further verified in experiments in which cells were exposed to PTH(7–34). This peptide lacks the adenylyl cyclase-activating domain but still represents an intact PKC-activating domain. As expected, PTH(7–34) was unable to increase cell shortening (*Figure 3*). These data strongly argue for a cAMP/PKA-dependent effect and against a potential role for PKC. This was further verified in experiments in which cardiomyocytes were exposed to N-truncated PTH peptides with an intact PKC-activating domain or a point mutation that destroys bioactivity of the PKC-activating domain.[23] PTH(28–48)-Asn29, representing an intact PKC-activating domain but no adenylyl cyclase-activating domain did not perform a significant effect on cell shortening (control: 10.60 ± 1.02; PTH: 11.16 ± 1.53%; $n = 52$ cells,

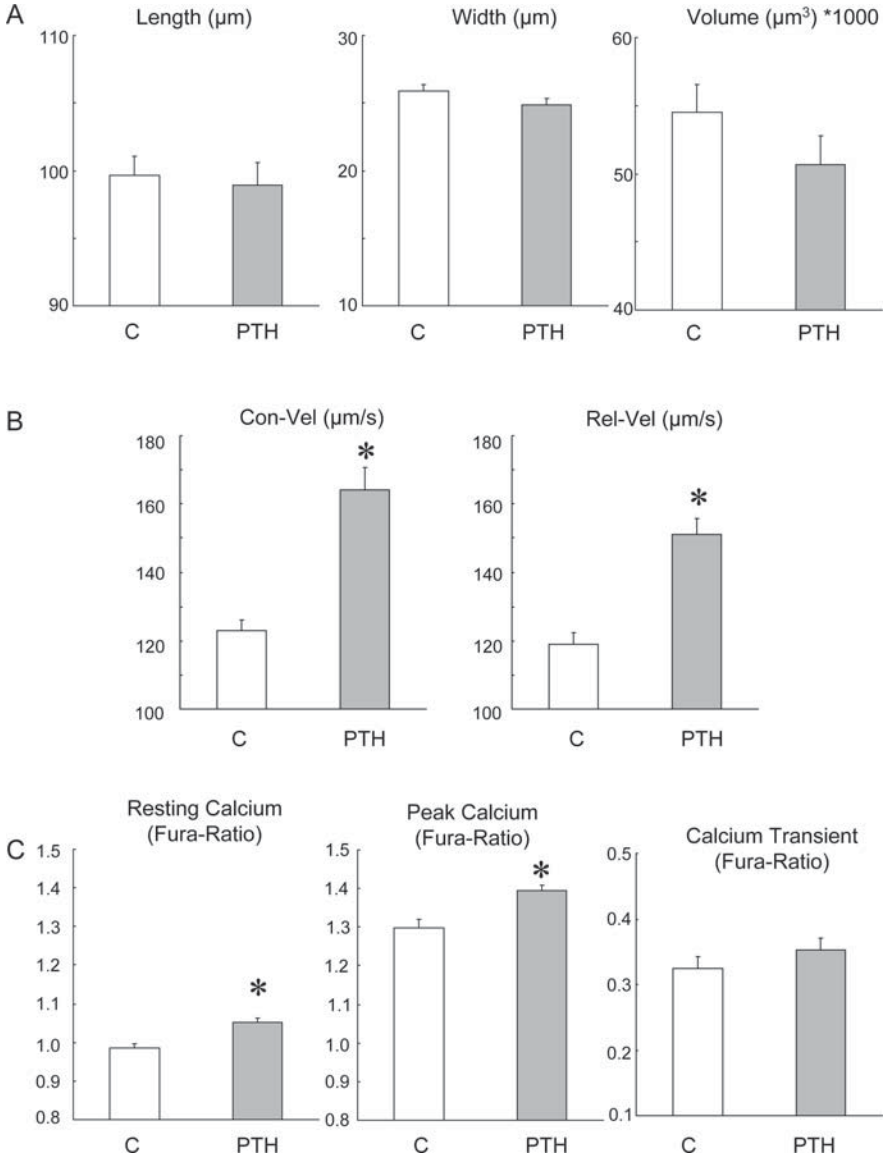

Figure 2 Effect of PTH(1–34) on cell volumes (*A*), shortening and relaxation velocities (*B*), and intracellular calcium (*C*). Cells were exposed to PTH(1–34) (200 pM) for 24 h. Thereafter cell lengths and widths were measured and the volumes were calculated as explained in the Methods section. Contraction and relaxation velocities were quantified from single-cell recordings as shown in *Figure 1*. Intracellular calcium was measured in Fura-2-AM-loaded cells and expressed as the ratio of the fluorescence at 340–380 nm. Data are means ± SEM from $n = 36$ cells. *$P < 0.05$ vs. untreated controls.

$P = 0.07$ vs. control). PTH(28–48)-Ala29, representing a peptide with neither a PKC-activating domain nor an adenylyl cyclase activating domain, did not exert any effect either (10.97 ± 1.53; $n = 52$ cells, $P = 0.229$ vs. control). Collectively, these data strongly suggest that PTH(1–34) affects cell shortening via its adenylyl cyclase/protein kinase A-activating domain.

The latter finding was confirmed by biochemical determination of protein kinase A activity. Cells were exposed to PTH(1–34), PTH(7–34), H89, or combinations of them for 10 min. Thereafter cells were harvested and the protein kinase A activity was measured. As expected, PTH(1–34) increased protein kinase A activity significantly by 26.3 ± 11.9% (*Figure 3B*). Neither PTH(7–34), nor H89 or PTH(1–34) in the presence of H89 increased protein kinase A activity. Isoprenaline (10 nM) was used as a positive control. The β-adrenoceptor agonist increased protein kinase A activity earlier (within 5 min) and to a significant higher amount (+39.9 ± 7.9%, $n = 4$) than PTH. These data confirmed the findings drawn from the cell-shortening experiments.

3.3 Effect of parathyroid hormone on maximal cell shortening

All experiments mentioned above characterize the effect of PTH on basal cell shortening. As next, we addressed the question whether PTH modifies the maximal induced cell shortening. Cardiomyocytes were again exposed to PTH(1–34) (200 pM) for 24 h. Then the cells were exposed to a buffer that contained either 1.1, 1.8, or 2.3 mM calcium. As expected, cell shortening increased by increasing extracellular calcium concentrations. However, cells pre-exposed to PTH(1–34) displayed a significant increase in cell shortening at low calcium concentration but not at high calcium concentrations (*Figure 4A*). As found for maximal

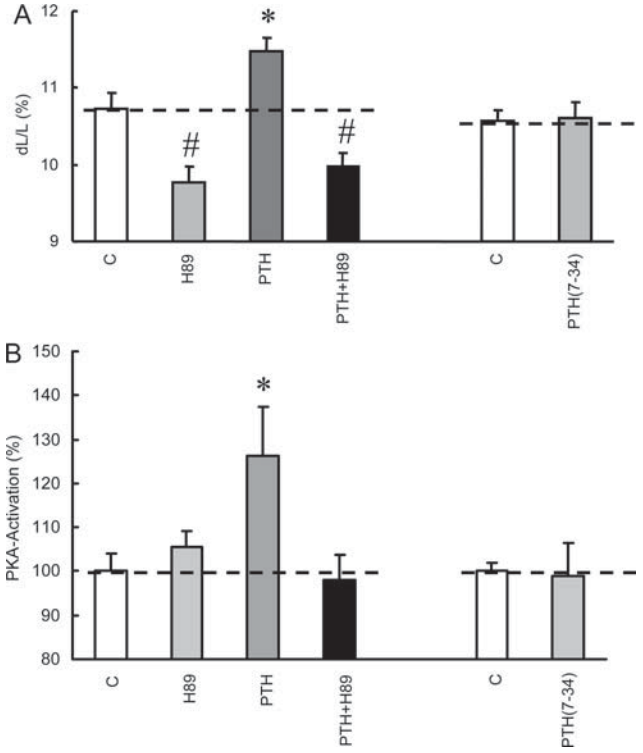

Figure 3 Effect of H89 (1 μM) on the effect of PTH(1–34) (200 pM) on cell shortening and protein kinase A activity. (*A*) Cells were exposed to H89 and parathyroid hormone for 24 h and cell shortenings were recorded thereafter. In a separate experiment cells were exposed to PTH(7–34) (200 pM). Data are means ± SEM from $n = 36$ cells. *$P < 0.05$ vs. untreated controls. (*B*) Cells were exposed to H89 and parathyroid hormone for 10 min and protein kinase A activities were recorded thereafter. In a separate experiment cells were exposed to PTH(7–34). Data are means ± SEM from $n = 4$ culture dishes. *$P < 0.05$ vs. untreated controls.

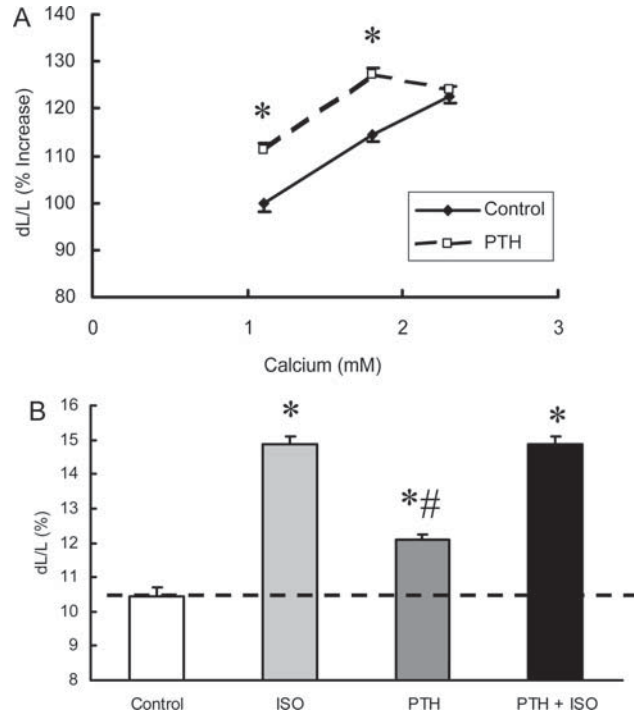

Figure 4 Effect of PTH(1–34) on maximal contractile responsiveness evoked by either increasing the extracellular calcium concentration (*A*) or stimulation with isoprenaline (10 nM) (*B*). Data are means ± SEM from $n = 36$ cells. *$P < 0.05$ vs. untreated controls.

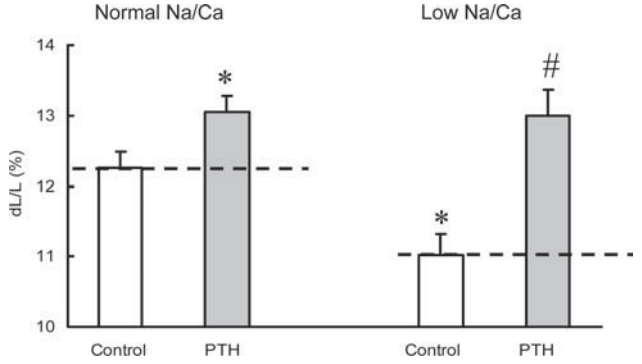

Figure 5 Effect of PTH(1–34) on maximal contractile responsiveness in cells exposed to normal sodium (143 mM) and normal calcium (1.1 mM) or reduced sodium (137 mM) and reduced calcium (0.9 mM) as it has been measured in patients with heart failure. Data are means ± SEM from $n = 36$ cells. *$P <$ 0.05 vs. untreated controls.

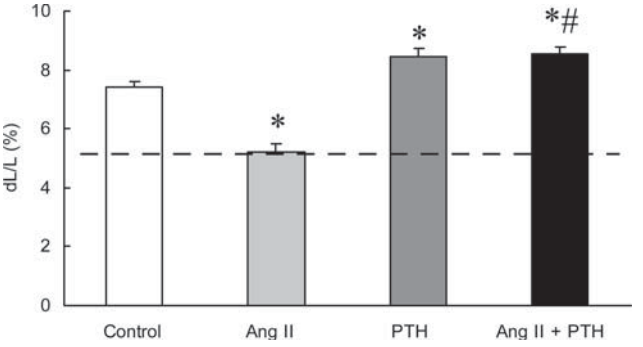

Figure 6 Effect of PTH(1–34) on angiotensin II-induced loss of function. Cells were exposed to angiotensin II (Ang II, 100 nM), PTH(1–34) (200 pM), or combinations of them for 24 h and cell shortening was measured thereafter. Data are means ± SEM from $n = 36$ cells. *$P < 0.05$ vs. untreated controls.

calcium-induced cell shortening, cells pre-exposed to PTH(1–34) for 24 h did not display a further increase in isoprenaline-induced cell shortening, too. As expected, isoprenaline increased cell shortenings of untreated control cells as well as in those pre-exposed to PTH. However, in cells pre-exposed to PTH no further increase was observed above the level of isoprenaline in untreated cells (*Figure 4B*).

3.4 Effect of parathyroid hormone on cell shortening in modified media

As indicated in the introduction, PTH concentrations are slightly elevated in patients with end-stage heart failure. Plasma concentration of calcium and sodium is slightly reduced in these patients.[13] In order to understand the relevance of the observed effect of PTH under these conditions, we performed experiments in modified media that completely mimicked this situation. Extracellular calcium was reduced from 1.1 to 0.9 mM and extracellular sodium was reduced from 143 to 137 mM. Cells exposed to PTH(1–34) for 24 h developed an increased cell shortening in the presence of normal calcium and sodium that was improved under conditions of slightly reduced calcium and sodium that represent more directly the changes in electrolyte balance of patients with heart failure. Under these

conditions, PTH(1–34) increased cell shortening by 17.7% (*Figure 5*).

3.5 Effect of parathyroid hormone on angiotensin II-induced contractile failure

The same cell-culture system was recently used to investigate the effect of angiotensin II (Ang II, 100 nM) on cell shortening.[24] As activation of the renin–angiotensin system is a key process leading to heart failure, we finally addressed the question whether PTH is able to antagonize this effect. As expected, Ang II reduced basal cell shortening by 29.7 $\pm$ 1.4% (*Figure 6*). Pre-exposure of cardiomyocytes to PTH increased cell shortening by 14.2 $\pm$ 3.8% and completely antagonized the Ang II-dependent negative contractile effect (*Figure 6*).

4. Discussion

In patients with heart failure various factors limit the contractile activity of cardiomyocytes and impair normal heart function. Among others, an elevated plasma Ang II level, electrolyte imbalance as characterized by lower free calcium and sodium, and as a result of this electrolyte imbalance slightly increased plasma values of PTH are observed.[13] Although these alterations are well known and documented it is less clear which of these changes are part of an adaptive mechanism that allows the heart to maintain normal pump activity and which of these are directly linked to the loss of function. This study was aimed to clarify the role of constitutively elevated PTH levels as they occur in patients with heart failure. We hypothesized that cardiomyocytes develop an altered function if they are constitutively exposed to PTH levels in the range of those found in plasma of patients with heart failure but without established renal disease. Indeed, the current study shows that if cardiomyocytes are exposed to low concentrations of PTH for 24 h they develop an improved mechanical response to electrical stimulation. Moreover, this effect was observed at low concentrations of PTH. At higher concentrations PTH has been shown to evoke a pro-hypertrophic effect which was evoked via its PKC-activating domain.[4] The newly described effect of picomolar concentrations of PTH on cardiomyocytes' function seemed to be cAMP/PKA-dependent. Although we did not directly measure cAMP levels, we showed that the effects of PTH described in this study require an intact cAMP/PKA-activating domain and were insensitive to peptides representing a PKC-activating domain. In a former study, we have also directly measured the accumulation of cAMP in adult rat ventricular cardiomyocytes in response to PTH(1–34).[10] The data of this former study indicated a 1.50-fold increase in total cAMP within 5 min that was nevertheless low compared with isoprenaline (29.5-fold) and that did not reach the level of significance. We also found a small increase in contraction amplitudes (10 nM PTH: +7.2%, n.s.) that declined at higher concentrations (1 μM).[10] The data of our new study suggest that the response of cardiomyocytes to cAMP-dependent signalling is slow and requires a longer time period to get significant, such as 24 h as has been used in this study. Noteworthy, the latter represents more precisely conditions of heart failure in which cardiomyocytes are exposed constitutively to small elevated plasma PTH levels.

Thus, our data suggest that slightly elevated concentrations of plasma PTH in patients with heart failure represent an adaptive response. It is in line with this assumption that patients treated for heart failure of less-advanced severity had higher circulating levels of PTH than patients with more severe heart failure.[25]

The question whether PTH modifies the contractile response of cardiomyocytes has been addressed before. However, in most of those experiments it was investigated whether PTH modifies the contractile response in an acute way. In some conditions of heart failure in which PTH is elevated to much higher values such as hyperparathyroidism or in patients with renal dysfunction requiring dialysis, PTH is considered as an agent that depresses cardiac function. As expected from these studies a marked improvement of left ventricular function after parathyroidectomy was observed in a haemodialysis patient with secondary hyperparathyroidism and left ventricular dysfunction.[26] Other studies on patients with primary hyperparathyroidism have demonstrated a long-lasting increased risk of myocardial hypertrophy and heart failure.[27]

In contrast, experiments on cardiomyocytes exposed to PTH in an acute way have not developed a clear picture. In addition the question whether cardiomyocytes chronically exposed to PTH respond in a similar way has never been considered. Our study is different from studies published previously on PTH-dependent changes in cardiomyocytes' function as the cells were exposed at least for 24 h to PTH. Such experiments have been performed before, but in those cases hypertrophy-related parameters were investigated rather than functional data. The study suggests that PTH improves cardiac function as long as the concentration is too low to activate the PKC-dependent pathways. The latter one seems to be related to myocardial hypertrophy and heart failure. On the mechanistic basis this seemed to be achieved by increased intracellular calcium. Similarly, peripheral blood mononuclear cells are characterized by elevations in intracellular calcium under conditions of aldosteroidism that go along with reduced plasma calcium. This was termed 'calcium paradox' to indicate that lower plasma calcium leads to more plasma PTH that then increase intracellular calcium.[12] The fall in plasma ionized calcium concentration seems to be the consequence of Ang II-dependent induced aldosteronism leading to an increased urinary and faecal excretion of calcium.[28] It is likely to assume that this fall in plasma calcium triggers an increase of PTH release from the parathyroid glands. PTH has been considered to be responsible for the increase of intracellular calcium in peripheral blood mononuclear cells and this could be prevented by a calcium channel blocker.[29] Alternatively, aldosterone may increase calcium channel number or open probability directly. However, PTH is able to increase intracellular calcium via activation of voltage-dependent calcium channels in cardiomyocytes.[3] Therefore, it is likely to speculate that the effect of PTH on diastolic and peak systolic calcium in cardiomyocytes is mediated by this pathway. However, the described acute effect of PTH on voltage-dependent calcium currents was independent of cAMP/PKA and full-length PTH evoked a stronger effect than PTH (1–34).[3] Thus, we proved another possibility that might explain the effect of PTH on resting calcium. Here we

demonstrate that PTH downregulates the steady state mRNA of the calcium-sensing receptor in cardiomyocytes. This receptor antagonizes PTH-dependent calcium transport at least in mouse cortical ascending limbs.[22] This indicates that on the cellular level stimulation of the calcium-sensing receptor is able to antagonize the action of PTH. Therefore, its downregulation may explain at least in part the increase in intracellular calcium observed in cells exposed to PTH. It is in line with these assumptions that in patients with congestive heart failure elevated PTH levels are associated with a better left ventricular ejection fraction and resting cardiac output.[30]

Acknowledgements

We thank the expert technical assistance of Peter Volk and Nadine Woitasky.

Conflict of interest: none declared.

Funding

Supported by grants from the Deutsche Forschungsgemeinschaft (DFG), from the Excellence Cluster Cardio-Pulmonary Sciences (ECCPS), and from the Rhön-Klinikum Giessen-Marburg.

References

1. Bogin E, Massry SG, Harary I. Effect of parathyroid hormone on rat heart cells. *J Clin Invest* 1981;**67**:1215–1227.
2. Wang R, Wu L, Karpinski E, Pang PKT. The effects of parathyroid hormone on L-type voltage-dependent calcium channel currents in vascular smooth muscle and ventricular myocytes are mediated by a cyclic AMP dependent mechanism. *FEBS Lett* 1991;**282**:331–334.
3. Smogorzewski M, Zayed M, Zhang Y-B, Roe J, Massry SG. Parathyroid hormone increases cytosolic calcium concentration in adult rat cardiac myocytes. *Am J Physiol Heart Circ Physiol* 1993;**264**:H1998–H199H.
4. Schlüter K-D, Piper HM. Trophic effects of catecholamines and parathyroid hormone on adult ventricular cardiomyocytes. *Am J Physiol Heart Circ Physiol* 1992;**263**:H1739–H1746.
5. Benardi D, Bernini L, Cini G, Brandinelli GA, Urti DA, Bonechi I. Asymmetric septal hypertrophy in uremic-normotensive patients on regular hemodialysis. *Nephron* 1985;**39**:30–35.
6. London GM, de Vernejoul M-C, Fabiani F, Marchais SJ, Guerin AP, Metivier F *et al*. Secondary hyperparathyroidism and cardiac hypertrophy in hemodialysis. *Kidney Int* 1987;**32**:900–907.
7. Hara S, Ubara Y, Arizono K, Ikeguchi H, Katori H, Yamada A *et al*. Relation between parathyroid hormone and cardiac function in long-term hemodialysis patients. *Miner Electrolyte Metab* 1995;**21**:72–76.
8. Sato S, Ohta M, Kawaguchi Y, Okada H, Ono M, Saito H *et al*. Effects of parathyroidectomy on left ventricular mass in patients with hyperparathyroidism. *Miner Electrolyte Metab* 1995;**21**:67–71.
9. Schlüter K-D, Katzer C, Frischkopf K, Wenzel S, Taimor G, Piper HM. Expression, release, and biological activity of parathyroid hormone-related peptide from coronary endothelial cells. *Circ Res* 2000;**86**:946–951.
10. Schlüter K-D, Weber M, Piper HM. Parathyroid hormone induces protein kinase C but not adenylate cyclase in adult cardiomyocytes and regulates cyclic AMP levels via protein kinase C-dependent phosphodiesterase activity. *Biochem J* 1995;**310**:439–444.
11. McCarty. Nutritional modulation of parathyroid hormone secretion may influence risk for left ventricular hypertrophy. *Med Hypothesis* 2005;**64**:1015–1021.
12. Vidal A, Sun Y, Bhattacharaya SK, Ahokas RA, Gerling IC, Weber KT. Calcium paradox of aldosteronism and the role of the parathyroid gland. *Am J Physiol Heart Circ Physiol* 2006;**290**:H286–H294.
13. Arakelyan KP, Sahakyan YA, Hayrapetyan LR, Khudaverdyan DN, Ingelman-Sundberg M, Mkrtchian S *et al*. Calcium-regulating peptide hormones and blood electrolyte balance in chronic heart failure. *Reg Peptides* 2007;**142**:95–100.
14. Alsafwah S, Laguardia SP, Nelson MD, Battin DL, Newman KP, Carbone LD *et al*. Hypovitaminosis D in african americans residing in mephis, tennessee with and without heart failure. *Am J Med Sci* 2008;**335**:292–297.
15. Laguardia SP, Dockery BK, Bhattacharya SK, Nelson MD, Carbone LD, Weber KT. Secondary hyperparathyroidism and hypovitaminosis D in african-american with decompensated heart failure. *Am J Med Sci* 2006;**332**:112–118.
16. Finkelstein JS, Hayes A, Hunzelman JL, Wylland JJ, Lee H, Neer RM. The effects of parathyroid hormone, alendronate, or both in men with osteoporosis. *N Engl J Med* 2003;**349**:1216–1226.
17. Zaruba M-M, Huber BC, Brunner S, Deindl E, David R, Fischer R *et al*. Parathyroid hormone treatment after myocardial infarction promotes cardiac repair by enhanced neovascularization and cell survival. *Cardiovasc Res* 2008;**77**:722–731.
18. Schlüter K-D, Schreiber D. Adult ventricular cardiomyocytes: Isolation and culture. *Meth Mol Biol* 2005;**290**:305–314.
19. Langer M, Lüttecke D, Schlüter K-D. Mechanism of the positive contractile effect of nitric oxide on rat ventricular cardiomyocytes with positive force/frequency relationship. *Pflügers Arch—Eur J Physiol* 2003;**447**:289–297.
20. Abdallah Y, Gkatzoflia A, Gligorievski D, Kasseckert S, Euler G, Schlüter K-D *et al*. Insulin protects cardiomyocytes against reoxygenation-induced hypercontracture by a survival pathway targeting SR Ca^{2+} storage. *Cardiovasc Res* 2006;**70**:346–353.
21. Tastan H, Abdallah Y, Euler G, Piper HM, Schlüter K-D. Contractile performance of adult ventricular rat cardiomyocytes is not directly jeopardized by NO/cGMP-dependent induction of pro-apoptotic pathways. *J Mol Cell Cardiol* 2007;**42**:411–421.
22. Motoyama HI, Friedman PA. Calcium-sensing receptor regulation of PTH-dependent calcium absorption by mouse cortical ascending limbs. *Am J Physiol Renal Physiol* 2002;**283**:F399–F406.
23. Schlüter K-D, Wingender E, Tegge W, Piper HM. Parathyroid hormone-related protein antagonizes the action of parathyroid hormone on adult cardiomyocytes. *J Biol Chem* 1996;**271**:3074–3078.
24. Mufti S, Wenzel S, Euler G, Piper HM, Schlüter K-D. Angiotensin II-dependent loss of cardiac function: Mechanisms and pharmacological targets attenuating this effect. *J Cell Physiol* 2008;**217**:242–249.
25. Zittermann A, Schleithoff SS, Tenderich G, Berthold HK, Korfer R, Stehle P. Low vitamin D status: a contributing factor in the pathogenesis of congestive heart failure? *Am J Coll Cardiol* 2003;**41**:105–112.
26. Nagashima M, Hashimoto K, Shinsato T, Ashida K, Kobayashi M, Yamashita H *et al*. Marked improvement of left ventricular function after parathyroidectomy ina hemodialysis patient with secondary hyperparathyroidism and left ventricular dysfunction. *Circ J* 2003;**67**:269–272.
27. Andersson P, Rydberg E, Willenheimer R. Primary hyperparathyroidism and heart disease—a review. *Eur Heart J* 2004;**25**:1776–1787.
28. Chokar VS, Yun S, Bhattacharya SK, Ahokas RA, Myers LK, Xing Z *et al*. Hyperparathyroidism and the calcium paradox of aldosteronism. *Circulation* 2005;**111**:871–878.
29. Ahokas RA, Sun Y, Bhattacharya SK, Gerling IC, Weber KT. Aldosteronism and a proinflammatory vascular phenotype. Role of Mg^{2+}, Ca^{2+} and H_2O_2 in peripheral blood mononuclear cells. *Circulation* 2005;**111**:51–57.
30. Shane E, Mancini D, Aaronson K, Silverberg SJ, Seibel MJ. Bone mass, vitamin D deficiency, and hyperparathyroidism in congestive heart failure. *Am J Med* 1997;**103**:197–207.

frontiers in Physiology

SYSTEMATIC REVIEW
published: 17 December 2018
doi: 10.3389/fphys.2018.01799

Review on Chamber-Specific Differences in Right and Left Heart Reactive Oxygen Species Handling

Klaus-Dieter Schlüter, Hanna Sarah Kutsche, Christine Hirschhäuser, Rolf Schreckenberg and Rainer Schulz*

Department of Physiology, Justus-Liebig-University Giessen, Giessen, Germany

Reactive oxygen species (ROS) exert signaling character (redox signaling), or damaging character (oxidative stress) on cardiac tissue depending on their concentration and/or reactivity. The steady state of ROS concentration is determined by the interplay between its production (mitochondrial, cytosolic, and sarcolemmal enzymes) and ROS defense enzymes (mitochondria, cytosol). Recent studies suggest that ROS regulation is different in the left and right ventricle of the heart, specifically by a different activity of superoxide dismutase (SOD). Mitochondrial ROS defense seems to be lower in right ventricular tissue compared to left ventricular tissue. In this review we summarize the current evidence for heart chamber specific differences in ROS regulation that may play a major role in an observed inability of the right ventricle to compensate for cardiac stress such as pulmonary hypertension. Based on the current knowledge regimes to increase ROS defense in right ventricular tissue should be in the focus for the development of future therapies concerning right heart failure.

Keywords: cardiac remodeling, heart failure, oxidative stress, pulmonary hypertension, uncoupling protein, MAO

OPEN ACCESS

Edited by:
Thao P. Nguyen,
UCLA David Geffen School of Medicine, United States

Reviewed by:
Marcos Lopez,
University of Chicago, United States
Marlin Touma,
UCLA David Geffen School of Medicine, United States

****Correspondence:***
Klaus-Dieter Schlüter
klaus-dieter.schlueter@physiologie.med.uni-giessen.de

Specialty section:
This article was submitted to Oxidant Physiology, a section of the journal Frontiers in Physiology

Received: *06 September 2018*
Accepted: *29 November 2018*
Published: *17 December 2018*

Citation:
Schlüter K-D, Kutsche HS, Hirschhäuser C, Schreckenberg R and Schulz R (2018) Review on Chamber-Specific Differences in Right and Left Heart Reactive Oxygen Species Handling. Front. Physiol. 9:1799. doi: 10.3389/fphys.2018.01799

INTRODUCTION

Oxidative stress is defined as a condition by which an imbalance occurs between the production of reactive oxygen species (ROS) and the antioxidant defense system. The term ROS includes molecules that have one or more unpaired electrons (i.e., superoxide and hydroxyl) and non-radicals that are able to generate free radicals (i.e., hydrogen peroxide). Intracellular sources of ROS are the electron transport chain of the mitochondria, monoamine oxidase (MAO), p66shc (for review, see Di Lisa et al., 2017), xanthine oxidase (XO), uncoupling proteins (UCP, depending on the mitochondrial membrane potential; for review see Cadenas, 2018), uncoupled nitric oxide (NO) synthase (NOS), sodium-potassium ATPase (NKA), and nicotinamide adenine dinucleotide phosphate (NADPH) oxidase (NOX) (for review, see Egea et al., 2017). The defense system contains enzymes such as superoxide dismutase (SOD), catalase, glutathione peroxidase, and coupled NOS. **Figures 1**, **2** give an overview about ROS sources and ROS defense systems in the heart. Whereas subtle changes in ROS act as intracellular signaling pathways (*redox signaling*) high levels of ROS can cause cell damage and dysfunction (*oxidative stress*) (for review, see Egea et al., 2017).

The following review article now summarizes our current understanding about similarities and differences in ROS handling between LV and RV. We searched the current literature (PubMed, MedLine data bank until July, 2018) using the terms "right heart and ROS," "pulmonary hypertension and ROS," "RV failure and ROS," "LV failure and ROS," "RV hypertrophy and ROS"

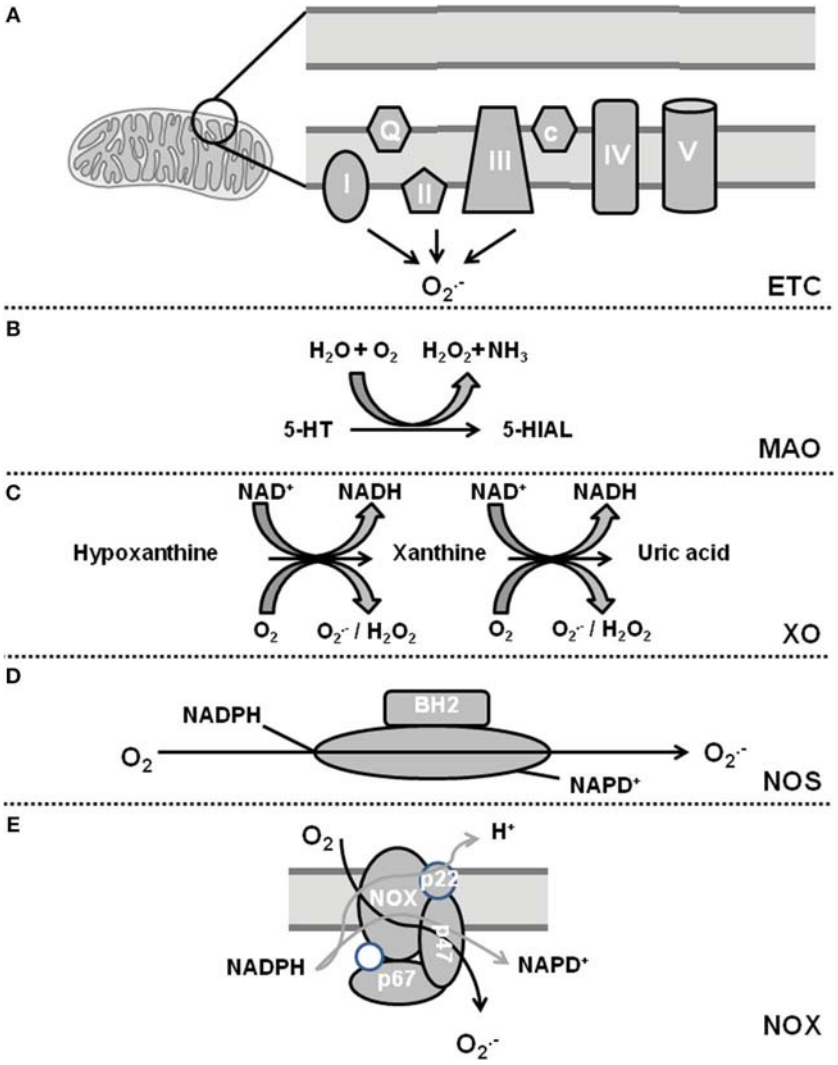

FIGURE 1 | Sources of reactive oxygen species in cardiomyocytes. **(A)** Complex I and III of the electron transport chain (ETC) constitutively release $O_2^{\cdot-}$ and complex II can be activated by NOX-dependent ROS. **(B)** Monoamine oxidase (MAO) generates H_2O_2. **(C)** Xanthine oxidase (XO) catalyzes a two-step reaction leading to additional release of H_2O_2. **(D)** Uncoupling of nitric oxide synthase (NOS) leads to generation of $O_2^{\cdot-}$. **(E)** NADPH oxidase (NOX) generates also $O_2^{\cdot-}$ upon activation.

and "LV hypertrophy and ROS." Most studies dealing with ROS and RV hypertrophy used models of pulmonary hypertension induced by banding, monocrotaline injection or chronic hypoxia. In these models ROS contribute to pulmonary hypertension and RV remodeling. In many studies, effects of ROS reduction on RV hypertrophy were secondary to reduced pulmonary pressure (reviewed by Wong et al., 2013). In the current review we therefore focus on studies directly assessing ROS and ROS-dependent effects in RV tissue and compare these results to established concepts generated from the LV.

OXIDATIVE STRESS IN THE HEART

Oxidative stress in cardiomyocytes occurs during chronic pressure or volume overload of the heart (Gladden et al., 2013; Hansen et al., 2016), cardiac ischemia/reperfusion (Riba et al., 2017), cardiomyopathy (Ishikawa et al., 2005), diabetes (Guido et al., 2017), chemotherapy-induced heart failure in the left (Mouli et al., 2015; Li et al., 2018), and right ventricle (Anghel et al., 2018), poison such as cigarette smoke (Talukder et al., 2011), chronic kidney disease (Duni et al., 2017), or aging (Chang et al., 2017), or as a response to congenital heart failure (Iacobazzi et al., 2016). Within the heart other sources of ROS are cells adjacent to cardiomyocytes such as inflammatory cells (Xu et al., 2011; Hernandez-Resendiz et al., 2018), endothelial cells (Burger et al., 2011), stem cells (Mandraffino et al., 2017), and cardiac fibroblasts (Ciulla et al., 2011). Redox signaling contributes to cardiac hypertrophy and even more important oxidative stress contributes to the transition of adaptive to maladaptive cardiac hypertrophy,

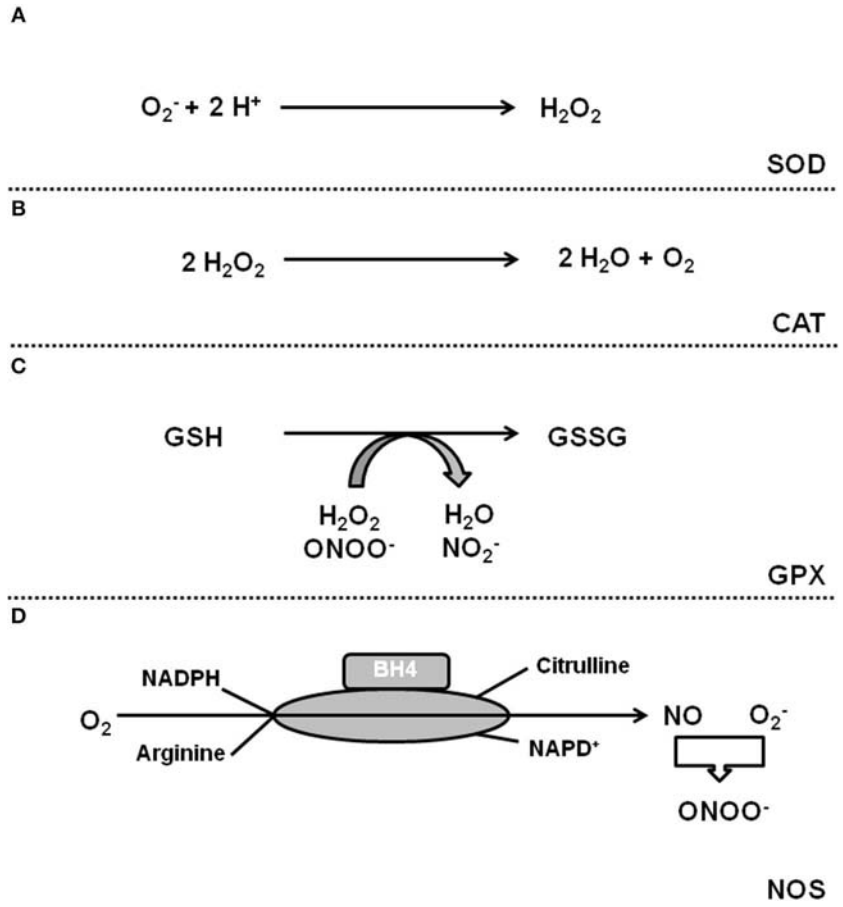

FIGURE 2 | ROS defense systems in cardiomyocytes. **(A)** Superoxide dismutases catalyze the formation of H_2O_2 that can be detoxificated by catalase **(B)**. **(C)** Gluatathione peroxidase (GPX) reduces H_2O_2. **(D)** Coupled NOS generates NO that neutralizes $O_2^{\cdot-}$.

named maladaptive remodeling. Oxidative stress can damage cells by growth factor-independent activation of cardiac growth regulation (Calamaras et al., 2015), can inactivate NO leading to loss of myocyte-specific NO function (Rassaf et al., 2006; Lüneburg et al., 2016), can directly reduce cardiomyocyte function by oxidative modification of sarcomere proteins such as tropomyosin (Heusch et al., 2010b; Canton et al., 2011) or sarcoplasmatic reticulum proteins (i.e., SERCA; Qin et al., 2017), can induce a calcium desensitization of myofibrils (Wang et al., 2008), can activate the Na-K-ATPase (Wang et al., 2017a), can damage mitochondrial function (Ide et al., 2001; Sverdlov et al., 2016), or can induce cell death (apoptosis, necrosis; Redza-Dutordoir and Averill-Bates, 2016). Therefore, ROS defense strategies of the cells are necessary for cell survival and functional stabilization in both ventricles.

DIFFERENCES BETWEEN RIGHT AND LEFT VENTRICLE

The different chambers of the heart are derived from different embryonic origin, namely the first (left ventricle, LV) and second heart field (right ventricle, RV). In rodent hearts, cardiomyocytes isolated from the LV or RV differ in size, number of mononucleated cells, cellular adaptation to culture conditions, and cell shortening (Schlüter, 2016; summarized in **Figure 3**). This gives raise to speculations that the LV and RV may differentially respond to cardiac stresses. Pressure overload is associated with adaptations performed on the transcriptional level. Many of them are similar between the RV and LV. However, some genes are upregulated in the pressure-overloaded RV only, including genes involved in Wnt signaling (Dickkopf 3, Sfrp2, and Wif1), annexin A7, clusterin/apolipoprotein J, neuroblastoma suppression of tumorigenicity 1 (Nbl1), formin-binding protein (Fnbp4), and the lectin-like oxidized low-density lipoprotein (oxLDL) receptor (LOX; Reddy and Bernstein, 2015). Differences occur also on the level of miRNA (Reddy and Bernstein, 2015). Considering the high impact of ROS for cardiac adaptation to pressure overload, it is also important to understand such differences with respect to ROS formation, ROS defense, and ROS-dependent cellular responses. Indeed, mitochondria isolated from the LV or RV of rat hearts generates different amounts of ROS (Schreckenberg et al., 2015; summarized in **Figure 3**). Treatment of isolated perfused rat hearts with serotonin, a substrate for MAO, results

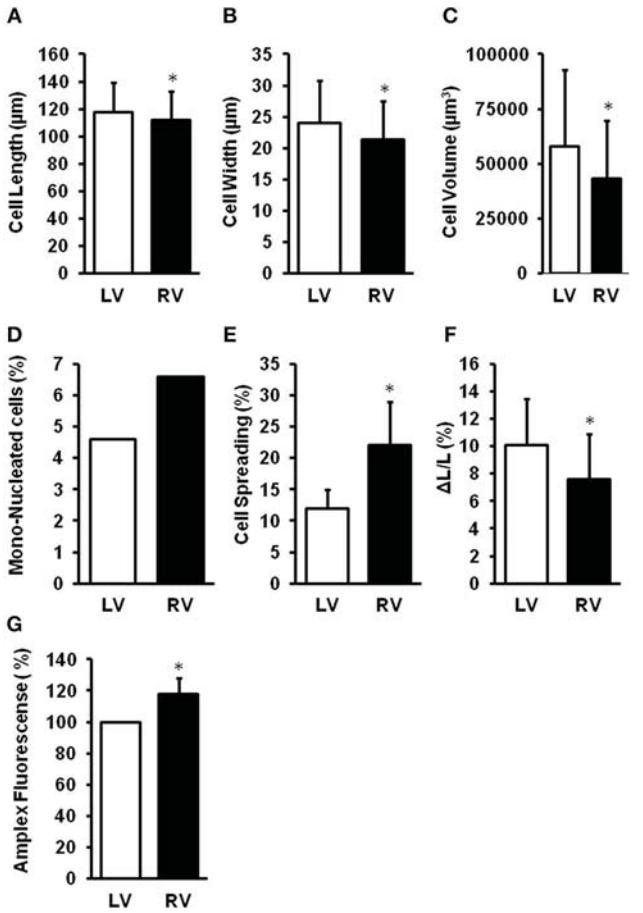

FIGURE 3 | Differences between right (RV) and left (LV) ventricular cardiomyocytes. LV cardiomyocytes are longer **(A)**, wider **(B)**, larger **(C)**, less mono-nucleated **(D)**, have a reduced cell spreading **(E)** as adaptation to culture conditions, and a stronger load-free cell shortening **(F)**. Furthermore, mitochondria from RV generate more ROS **(G)**. Data depicted from Schreckenberg et al. (2015) and Schlüter (2016). *$p < 0.05$ vs. LV.

in the promotion of protein carbonylation as evidenced by increased ROS formation, specifically in the RV but not the LV. Interestingly, no differences between RV and LV antioxidant enzymes and serotonin receptors/transporter are detected (Liu et al., 2008).

ROS IN RIGHT HEART HYPERTROPHY AND FAILURE: CYTOSOLIC ROS

Pressure overload induces the NOX subunit gp91 (Li et al., 2002; Byrne et al., 2003; Tanaka et al., 2005; Grieve et al., 2006; Liu et al., 2006, 2010; Guggilam et al., 2007; DeMarco et al., 2008; Nisbet et al., 2009; Chemaly et al., 2011; Xu et al., 2011; Ogura et al., 2013; Frazziano et al., 2014; Matsuda et al., 2015; Ma et al., 2016; Sirker et al., 2016; Zhu et al., 2017). In human right and left heart failure the p47phox subunit of NOX also translocates to the sarcrolemma (Nediani et al., 2007). Increased NOX expression is associated with increased formation of superoxide anions (Nediani et al., 2007; Ogura et al., 2013; Dos Santos Lacerda et al., 2017; Türck et al., 2018). Furthermore, hypoxia, leading to pulmonary hypertension, and RV hypertrophy, increases RV expression of NOX2/4 (Liu et al., 2014; Ye et al., 2016; Zhu et al., 2017). In the monocrotaline-induced pulmonary hypertension rat model, Nox4 expression is induced in cardiomyocytes but also in the intercellular area (mainly co-localizing with fibroblasts) (He et al., 2017). In the RV, NOX4 is also regulated by the α_{1A}-receptor (Cowley et al., 2017); stimulation of this receptor decreases NOX4 expression during pulmonary hypertension. NOX-dependent ROS modifies mitochondrial function by increased release of ROS from complex II of the mitochondria during the transition from RV hypertrophy to failure (Redout et al., 2007) (ROS induced ROS release). There are differences between the RV and LV ventricles in the primary source of ROS production. In the RV, NOX, and mitochondrial complex II activity both increase during the transition to heart failure, whereas, in the LV, NOX appears to be the primary source of ROS generation (Redout et al., 2010).

Xanthine oxidoreductase (XO) activity remains unaltered in the monocrotaline-induced RV hypertrophy model but its activity increases with the transition to RV failure. XO is mainly localized in $CD68^+$ inflammatory cells based on studies with an affinity-purified polyclonal antibody (de Jong et al., 2000). In another rat model of pulmonary hypertension-induced RV failure, metabolomics analysis revealed an increase in xanthine, and uric acid in the hypertrophied RV, suggesting the production of ROS by XO. Furthermore, the RV level of α-tocopherol nicotinate declined, consistent with oxidative stress decreasing antioxidants (Wang et al., 2017). XO also contributes to ROS formation in LV (Moris et al., 2017).

Uncoupled NOS is another protein involved in the generation of oxidative stress in the LV secondary to pressure overload (Takimoto et al., 2005). In the RV, uncoupled NOS contributes to ROS generation, too. In caveolin-1 (Cav-1) knockout mice subjected to chronic hypoxia the transition from RV hypertrophy to failure is accelerated compared to wild-type mice and caused by uncoupling of RV endothelial NOS and increased protein tyrosine nitration; all changes are prevented by re-expressing an endothelial-specific Cav-1 transgene (avoiding NOS uncoupling) or by NOS inhibition without modifying the extent of pulmonary hypertension (Cruz et al., 2012). Also, in a pharmacological model of hypertension chronic administration of L-NAME leads to uncoupling of NOS in RV (Schreckenberg et al., 2015).

Uncoupling of NOS can be caused by reduced substrate (arginine) for NOS. Reasons for substrate limitation can be an induction of arginase that leads to substrate limitation (Heusch et al., 2010; Schreckenberg et al., 2015), increased plasma concentrations of asymmetric dimethyl arginine (ADMA), a natural circulating inhibitor of NOS (Lüneburg et al., 2016), or depletion of NOS with tetrahydrobiopterin (BH_4, Shimizu et al., 2013).

ROS IN RIGHT HEART HYPERTROPHY AND FAILURE: MITOCHONDRIAL ROS

A proteomic analysis of the normal rabbit and porcine RV and LV free walls shows equivalent cellular aerobic capacity, volume

of mitochondria, mitochondrial enzyme content (cytochrome c oxidase, respiratory complexes 1 and 3–5, aconitase, SOD), and mitochondrial enzyme activities (Phillips et al., 2011). Interestingly, mitochondrial membrane potential, a surrogate of overall mitochondrial function, is lower in the resting RV compared to the LV (Nagendran et al., 2008), while—at least in rats—ROS formation in mitochondria isolated from the RV is slightly higher than in LV mitochondria (Schreckenberg et al., 2015). At last in part, the latter might be the consequence of a reduced ROS defense capacity (Borchi et al., 2010; Manni et al., 2016). Comparing mitochondria from hypertrophic RV with those of non-hypertrophic LV revealed differences in electrone transport chain activity and ATP generating enzyme expression Gupto et al., 2016.

While the mitochondrial protein profiles of the RV and LV are quite similar at rest, they diverge when subjected to an increased afterload (Phillips et al., 2011), and mitochondrial membrane potential increases with RV hypertrophy (Nagendran et al., 2008). This hyperpolarization of mitochondria, indicating reduced oxidative phosphorylation, is related to an activation of the nuclear factor of activated T cells (NFAT) pathway and is reversed by dichloroacetate, an inhibitor of pyruvate dehydrogenase kinases (PDK) (Nagendran et al., 2008). Thus, an increase in PDK activity in RV hypertrophy contributes to the decreased oxidation of pyruvate in mitochondria and an increased conversion of pyruvate to lactate in the cytosol. An increase in glycolytic hexokinase and lactate dehydrogenase activities occurs following monocrotaline-induced pulmonary hypertension at the stage of compensated RV hypertrophy (Balestra et al., 2015), further supporting the concept of a metabolic switch from mitochondrial oxidative phosphorylation to glycolysis in the compensated phase of RV hypertrophy (Paulin and Michelakis, 2014; Sutendra and Michelakis, 2014). Indeed, a decreased mitochondrial oxygen usage and an increased anaerobic glycolysis has been described in patients with pulmonary hypertension (Wong et al., 2011) (for a detailed review, see Freund-Michel et al., 2014), and the decrease in mitochondrial oxidative phosphorylation during the development of RV hypertrophy has been suggested to decrease mitochondrial ROS formation (for review, see Paulin and Michelakis, 2014).

The increase in glucose uptake and the mitochondrial hyperpolarization are lost with the progression of RV hypertrophy to failure (Nagendran et al., 2008). For the LV, ROS sensors revealed increased mitochondrial ROS in resting and contracting cardiomyocytes during the progression to heart failure. Pathway analysis of mitochondrial ROS-sensitive networks indicated that increased mitochondrial ROS in failing cardiomyocytes disrupts the normal coupling between cytosolic signals and nuclear gene programs driving mitochondrial function, calcium handling, action potential repolarization, and antioxidant enzymes (Dey et al., 2018). Indeed, in the RV, during the transition from RV hypertrophy to RV failure, mitochondrial ROS defense system (SOD-2) is down-regulated (Redout et al., 2007).

Another key regulator that is decreased during RV failure is the peroxisome proliferator-activated receptor gamma coactivator (PGC) 1α, leading to impaired fatty acid oxidation, decreased mitochondrial mass and number, and reduced oxidative capacity, potentially contributing to increased ROS production (Karamanlidis et al., 2011; Gomez-Arroyo et al., 2013). In an animal model of pulmonary hypertension-induced RV failure, fatty acid oxidation decreases secondary to the failure of palmitoylcarnitine to stimulate oxygen consumption. In humans with pulmonary hypertension, RV long-chain fatty acids and triglyceride contents are increased and ceramide, a mediator of lipotoxicity, accumulates (Brittain et al., 2016).

ROS DEFENSE SYSTEMS IN RV

In rats treated with monocrotaline to increase pulmonary artery pressure without inducing RV hypertrophy, RV hydrogen peroxide increases but SOD, catalase, and glutathione peroxidase activities are also enhanced (Siqueira et al., 2018).

During pressure overload–induced LV hypertrophy, antioxidant enzymes are activated in the compensated stage but their activity decreases during the onset of LV failure. In contrast, only the antioxidant enzyme catalase becomes activated in some (Ecarnot-Laubriet et al., 2003) but not all studies (Pichardo et al., 1999) while SOD and glutathione peroxidase are not activated at all in the compensated stage of RV hypertrophy secondary to pulmonary hypertension, predisposing the RV to ROS induced damage at an earlier stage than in the LV (Pichardo et al., 1999; Ecarnot-Laubriet et al., 2003; Schreckenberg et al., 2015). With a progression of from RV hypertrophy to failure, down-regulation of antioxidant enzymes, and increased ROS production occurs in a mice model of pulmonary hypertension (Aziz et al., 2015; Reddy and Bernstein, 2015), although in one model of monocrotaline-induced RV failure, glutathione peroxidase increases while catalase, and SOD activities are similar to sham animals (Türck et al., 2018).

Despite some controversial results the general view, however, remains that increased ROS formation and decreased ROS defense leads to increased oxidative stress driving the progression from RV hypertrophy to RV failure.

DOWNSTREAM SIGNALING

(Patho)physiological conditions known to activate p38 mitogen activated protein (MAP) kinase are often associated with increased ROS formation (Wenzel et al., 2001, 2006, 2007). Indeed, p38 MAP kinase is activated by oxidative stress (Redout et al., 2007). An activation of p38 MAP kinase pathways is linked to cardiac hypertrophy and dysfunction and in RV and LV of end-stage failing human hearts, p38 MAP kinase and extracellular-signal regulated kinase (ERK), but not c-Jun N-terminal kinases (JNK), are activated; a significant correlation between protein kinase activities is observed between LV and RV from the same heart (Nediani et al., 2007).

Increased ROS subsequently modifies tropomyosin, induces matrix metalloproteases (MMPs 2, 9, and 13), sensitizes β-adrenoceptors (via induction of protein kinase C-ε), and causes endothelial dysfunction in the right ventricle (Cheng et al., 2009; Lu et al., 2011; Cau et al., 2013; Schreckenberg et al., 2015).

In LV tissue, ROS is associated with an induction of $p90^{rsk}$ and the sodium-proton-exchanger (NHE) and furthermore, via ROS-dependent formation of lipid peroxidation-derived aldehydes (Cingolani et al., 2011). Furthermore, ROS activates the mammalian target of rapamycin (mTOR)-$p70^{s6k}$ pathway (Calamaras et al., 2015). Both pathways (NHE and mTOR-$p70^{s6k}$) are also involved in growth factor-dependent acceleration of protein synthesis (Simm et al., 1998; Schäfer et al., 2002). Commonly ROS and growth factors activate also the ERK pathway but the latter is not directly linked to the regulation of protein synthesis (Pönicke et al., 2001; Calamaras et al., 2015).

Apart from NOX, activation of the renin-angiotensin-system is apparent in the RV during pressure overload (for review, see Ameri et al., 2016). Compared to normal hearts, however, angiotensin II binding is diminished in the failing RV of pulmonary artery hypertension patients due to angiotensin II type 1 receptor down-regulation, despite RV myocardial angiotensin converting enzyme (ACE) activity being increased (Zisman et al., 1998). Interestingly, the ACE DD genotype, associated with an increased myocardial ACE activity, is more frequent in patients with pulmonary hypertension than in healthy individuals, but it is also associated with preserved RV function in pulmonary hypertension patients (Abraham et al., 2003).

A specific role for LOX-1 in RV hypertrophy and failure has been suggested. First, oxLDL receptors cross react with NOX (Ogura et al., 2013). Furthermore, ventricular expression of oxLDL receptors is induced under hypoxia leading to pulmonary hypertension and RV hypertrophy (Zhu et al., 2017). Cross-reactivity of oxLDL receptors with angiotensin II receptors type 1 has also been reported. In all these cases, NOX is subsequently activated favoring oxidative stress. It seems that this mechanism plays an important role in right heart failure.

THERAPEUTIC IMPLICATIONS

In general, attenuation of mitochondrial-derived oxidative stress is a reasonable therapeutic concept to attenuate RV hypertrophy and transition to RV failure (for review, see Maarman et al., 2017).

As expected from the findings that ROS is increased in RV hypertrophy and transition to RV failure, trapping molecules targeting mitochondrial ROS (mitoTEMPO), folic acid, EUK-134, a synthetic antioxidant mimicking the activity of SOD, attenuate RV hypertrophy (Redout et al., 2010; Qipshidze et al., 2012; Datta et al., 2015).

Regulation of SOD, in particular SOD-1 (located in the cytosol), and SOD-2 (located in mitochondria), has been proven to attenuate hypertrophy and even more important transition to heart failure. In a pharmacological rat model of hypertension (L-NAME induced hypertension) SOD-2 was induced in the LV but not in the RV (Schreckenberg et al., 2015). Up-regulation of SOD-2 in the LV was associated with less oxidative stress and preserved function in the presence of hypertrophy. Similarly, induction of SOD-2 activity has repeatedly reported to improve cardiac

TABLE 2 | Differences between LV and RV in ROS handling leading to hypertrophy and failure.

(A) ROS formation		
NOX gp91	LV ↑	RV ↑
NOX p47phox	LV ↑	RV ↑
NOX2/4		RV ↑
NOX-dependent ROS	LV ↑	
NOX-dependent Complex II		RV ↑
XO		RV ↑
NOS uncoupling	LV ↑	RV ↑
PDK		RV ↑
(B) ROS defense		
α-tocopherol nicotinate		RV ↓
Non-oxidative glucose metabolism		RV ↑
SOD-2	LV ↑	RV ↓
PGC-1α		RV ↓
Catalase	LV ↑	
Glutathione peroxidase	LV ↑	
(C) ROS-associated remodeling		
AT-1 receptor		RV ↓
ACE		RV ↑
LOX-1		RV↑

↑, *activated or induced during hypertrophy and/or transition to failure.*
↓, *deactivated or reduced during hypertrophy and/or transition to failure.*

TABLE 1 | Treatment of the angiotensin-NOX-ROS axis and effects on hypertrophy.

Drug	Species	Tissue	Target	Read-out	References
Isoflavone	Mice	LV	Ang-II-dependent	Hypertrophy	Chen et al., 2014
Taxofilin	Mice	LV	Ang-II-dependent	Hypertrophy	Guo et al., 2015
Spironolacton	Rats	LV	Renin-dependent	Hypertrophy	Habibi et al., 2011
Amlodipine/Atorvastatin	Rats	LV	Hypertension	Hypertrophy	Lu et al., 2009
Green Tea	Rats	LV	Ang-II-dependent	Hypertrophy	Papparella et al., 2008
AT1/ACE-I	Rats	LV	SHR	Hypertrophy	Tanaka et al., 2005
ACE inhibition	Rats	LV	Salt-induced BP	Cardiac function	Tsutsui et al., 2001
Atorvastatin	Rats	LV	Pressure overload	Hypertrophy	Li et al., 2013
Apocynin	Rats	LV	Pressure overload	Hypertrophy	Liu et al., 2010

function. Interestingly, at least for the LV multiple strategies to improve SOD activity work, such as the natural product Sheng-Mai-San (Chai et al., 2016), inhibition of the renin-angiotensin-system (Tanaka et al., 2005), calcium antagonists (Umemoto et al., 2004), or resveratrol (Danz et al., 2009). Whether any of these mechanisms is sufficient to increase SOD activity in RV remains unclear. As mentioned above, SOD is induced during hypertrophy in LV tissue (Date et al., 2002; Lu et al., 2010; Qiao et al., 2014; Aziz et al., 2015; Schreckenberg et al., 2015). Failure to increase SOD as an adaptive mechanism to rescue mitochondrial and cytosolic ROS is associated with heart failure (Redout et al., 2007; Koga et al., 2013). In a model of bronchopulmonary dysplasia, SOD-2 expression but not activity is induced leaving ROS formation unchanged. This underlines the importance of SOD-2 activity for protection against ROS-derived damage. Failure of the RV to up-regulate SOD-2 expression and activity might be a key step for right heart failure.

Other treatment using secoisolariciresinol diglucoside (Puukila et al., 2017), dehydroepiandrosterone (Alzoubi et al., 2013; Rawat et al., 2014), trimethoxystilbene (Liu et al., 2014), pterostilbene (Dos Santos Lacerda et al., 2017), trapidil (Türck et al., 2018), and α_{1A}-adrenoceptor stimulation with A61603 (Cowley et al., 2017) and finally fenofibrate (Galhotra et al., 2018) attenuate both RV hypertrophy and dysfunction and decreases RV ROS levels at the same time; however, a causality between changes in ROS and preservation of RV morphology and/or function could not be proven.

In contrast to the pharmacological approaches, neither the genetic deletion of sirtuin 3 (Waypa et al., 2013) nor the up-regulation of thioredoxin 2 (Adesina et al., 2017) affected RV hypertrophy during pulmonary hypertension. Sirtuin-3 is a nicotinamide adenine dinucleotide–dependent deacetylase that activates forkhead box O3a (FOXO3)-dependent up-regulation of SOD-2 (Sundaresan et al., 2009). Thioredoxin 2 is a mitochondrial located protein involved in ROS defense of the organelle (Dunn et al., 2010).

β-Blockers may also considered as a therapeutic option in right heart failure. β-Adrencoeptor signaling is sensitized by ROS. At least in the left ventricle carvedilol, a β-blocker with antioxidative properties, was able to attenuate the hypertrophic response to anthracylines (Arozal et al., 2011). In rats with monocrotaline-induced pulmonary hypertension bucindolol treatment decreases RV necrosis, fibrosis, and infiltration of inflammatory cells and improves RV systolic function. In addition, bucindolol promotes a decrease in the cardiac sympathovagal balance by reducing sympathetic drive and increasing parasympathetic drive (Lima-Seolin et al., 2017). Changes in ROS were not measured. In a model of hypertension (two-kidney one-clip), β-blockers attenuated ROS and MMP2, a ROS-dependent regulated MMP, independent of its antioxidative property suggesting that direct stimulation of β-adrenoceptors increases ROS in ventricular tissue (Rizzi et al., 2014).

There are multiple reports that treatment regimes affecting the angiotensin-NOX-ROS axis attenuate hypertrophy and heart failure, but also few examples showing no effects (**Table 1**).

CONCLUSION

A coupling between ROS, cardiac hypertrophy and heart failure has been established for the LV. Concerning the RV only few data are available that directly analyzes right heart hypertrophy in the context of ROS signaling. As it stands there is consensus that RV tissue has a reduced oxidative defense capacity thereby favoring oxidative stress especially during the transition from RV hypertrophy to failure. Whether ROS targets in the RV include those proteins that are directly linked to cardiac growth is unclear and questionable. In contrast, oxidative modification of proteins leading to failure seems to be similar between both ventricles. **Table 2** highlights the findings on ROS formation, defense, and targets in RV in comparison to LV.

AUTHOR CONTRIBUTIONS

K-DS and RaS wrote the manuscript, performed literature search, and work on the conception. HK and CH provided data to **Figure 3** and read and improved the manuscript. RoS read and added conceptional ideas and data to the chapter defense system.

FUNDING

K-DS and RaS received funding from the German Research Foundation (SFB/CRC 1213 B05).

ACKNOWLEDGMENT

We thank Claudia Lorenz (Alcedis GmbH) for proofreading of our manuscript.

REFERENCES

Abraham, W. T., Raynolds, M. V., Badesch, D. B., Wynne, K. M., Groves, B. M., Roden, R. L., et al. (2003). Angiotensin-converting enzyme DD genotype in patients with primary pulmonary hypertension: increased frequency and association with preserved haemodynamics. *J. Renin. Angiot. Aldoster. Syst*. 4, 27–30. doi: 10.3317/jraas.2003.003

Adesina, S. E., Wade, B. E., Bijli, K. M., Kang, B. Y., Williams, C. R., Ma, J., et al. (2017). Hypoxia inhibits expression and function of mitochondrial thioredoxin 2 to promote pulmonary hypertension. *Am. J. Physiol. Lung Cell. Mol. Physiol.* 312, L599–L608. doi: 10.1152/ajplung.00258.2016

Alzoubi, A., Toba, M., Abe, K., O'Neill, K. D., Rocic, P., Fagan, K. A., et al. (2013). Dehydroepiandrosterone restores right ventricular structure and function in rats with severe pulmonary arterial hypertension. *Am. J. Physiol. Heart Circ. Physiol.* 304, H1708–H1718. doi: 10.1152/ajpheart.00746.2012

Ameri, P., Bertero, E., Meliota, G., Cheli, M., Canepa, M., Brunelli, C., et al. (2016). Neurohormonal activation and pharmacological inhibition in pulmonary arterial hypertension and related right ventricular failure. *Heart Fail. Rev*. 21, 539–547. doi: 10.1007/s10741-016-9566-3

Anghel, N., Herman, H., Balta, C., Rosu, M., Stan, M. S., Nita, D., et al. (2018). Acute cardiotoxicity induced by doxorubicin in right ventricle is associated with increase of oxidative stress and apoptosis in rats. *Histol. Histopathol*. 33, 365–378. doi: 10.14670/HH-11-932

Arozal, W., Sari, F. R., Watanabe, K., Arumugam, S., Veeraveedu, P. T., Ma, M., et al. (2011). Carvedilol-afforded protection against daunorubicin-induced

cardiomyopathic rats *in vivo*: effects on cardiac fibrosis and hypertrophy. *ISRN Pharmacol*. 8:430549. doi: 10.5402/2011/430549

Aziz, A., Lee, A. M., Ufere, N. N., Damiano, R. J., Townsend, R. R., and Moon, M. R. (2015). Proteomic profiling of early chronic pulmonary hypertension: evidence for both adaptive and maladaptive pathology. *J. Pulm. Respir. Med*. 5:1000241. doi: 10.4172/2161-105X.1000241

Balestra, G. M., Mik, E. G., Eerbeek, O., Specht, P. A., van der Laarse, W. J., and Zuurbier, C. J. (2015). Increased *in vivo* mitochondrial oxygenation with right ventricular failure induced by pulmonary arterial hypertension: mitochondrial inhibition as driver of cardiac failure? *Respir. Res*. 16:6. doi: 10.1186/s12931-015-0178-6

Borchi, E., Bargelli, V., Stillitano, F., Giordano, C., Sebastiani, M., Nassi, P. A., et al. (2010). Enhanced ROS production by NADPH oxidase is correlated to changes in antioxidant enzyme activity in human heart failure. *Biochim. Biophys. Acta* 1802, 331–338. doi: 10.1016/j.bbadis.2009.10.014

Brittain, E. L., Talati, M., Fessel, J. P., Zhu, H., Penner, N., Calcutt, M. W., et al. (2016). Fatty acid metabolic defects and right ventricular lipotoxicity in human pulmonary arterial hypertension. *Circulation* 133, 1936–1944. doi: 10.1161/CIRCULATIONAHA.115.019351

Burger, D., Montezano, A. C., Nishgaki, N., He, Y., Carter, A., and Touyz, R. M. (2011). Endothelial microparticle formation by angiotensin II is mediated via Ang II receptor type I/NADPH oxidase/Rho kinase pathways targeted to lipid rafts. *Arterioscler. Thromb. Vasc. Biol*. 31, 1898–1907. doi: 10.1161/ATVBAHA.110.222703

Byrne, J. A., Grieve, D. J., Bendall, J. K., Li, J. M., Gove, C., Lambeth, J. D., et al. (2003). Contrasting roles of NADPH oxidase isoforms in pressure-overload versus angiotensin II–induced cardiac hypertrophy. *Circ. Res*. 93, 802–804. doi: 10.1161/01.RES.0000099504.30207.F5

Cadenas, S. (2018). Mitochondrial uncoupling, ROS generation and cardioprotection. *Biochim. Biophys. Acta* 1859, 940–950. doi: 10.1016/j.bbabio.2018.05.019

Calamaras, T. D., Lee, C., Lan, F., Ido, Y., Siwik, D. A., and Colucci, W. S. (2015). Lipid peroxidation product 4-hydroxy-trans-2-nonenal (HNE) causes protein synthesis in cardiac myocytes via activated mTORC1-P70S6K-RPS6 signaling. *Free Radic. Biol. Med*. 82, 137–146. doi: 10.1016/j.freeradbiomed.2015.01.007

Canton, M., Menazza, S., Sheeran, F. L., Polverino de Laureto, P., Di Lisa, F., Pepe, S., et al. (2011). Oxidation of myofibrillar proteins in human heart failure. *J. Am. Coll. Cardiol*. 57, 300–309. doi: 10.1016/j.jacc.2010.06.058

Cau, S. B., Barato, R. C., Celes, M. R., Muniz, J. J., Rossi, M. A., and Tanus-Santos, J. E. (2013). Doxycycline prevents acute pulmonary embolism-induced mortality and right ventricular deformation in rats. *Cardiovasc. Drugs Ther*. 27, 259–267. doi: 10.1007/s10557-013-6458-9

Chai, C. Z., Mo, W. L., Zhuang, X. F., Kou, J. P., Yan, Y. Q., and Yu, B. Y. (2016). Protective effects of Sheng-Mai-San on right ventricular dysfunction during chronic intermittent hypoxia in mice. *Evid. Based Complement. Alternat. Med.* 2016:4682786. doi: 10.1155/2016/4682786

Chang, Y. M., Chang, H. H., Lin, H. J., Tsai, C. C., Tsai, C. T., Chang, H. N., et al. (2017). Inhibition of cardiac hypertrophy effects in D-galactose-induced senescent hearts by alpinate oxyphyllae fructus treatment. *Evid. Based Complement. Alternat. Med.* 2017:2624384. doi: 10.1155/2017/2624384

Chemaly, E. R., Hadri, L., Zhang, S., Kim, M., Kohlbrenner, E., Sheng, J., et al. (2011). Long-term *in vivo* resistin overexpression induces myocardial dysfunction and remodeling in rats. *J. Mol. Cell. Cardiol*. 51, 144–155. doi: 10.1016/j.yjmcc.2011.04.006

Chen, G., Pam, S. Q., Chen, C., Pan, S. F., Zhang, X. M., and He, Q. Y. (2014). Puerarin inhibits angiotensin II-induced cardiac hypertrophy via the redox-sensitive ERK1/2, p38 and NF-κB pathways. *Acta Pharmacol. Sin.* 35, 463–475. doi: 10.1038/aps.2013.185

Cheng, Y. S., Dai, D. Z., and Dai, Y. (2009). Isoproterenol disperses distribution of NADPH oxidase, MMP-9, and pPKCε in the heart, which are mitigated by endothelin receptor antagonist CPU0213. *Acta Pharmacol. Sin.* 30, 1099–1106. doi: 10.1038/aps.2009.104

Cingolani, O. H., Pérez, N. G., Ennis, I. L., Alvarez, M. C., Mosca, S. M., Schinella, G. R., et al. (2011). *In vivo* key role of reactive oxygen species and NHE-1 activation in determining excessive cardiac hypertrophy. *Pflugers Arch. Eur. J. Physiol*. 462, 733–743. doi: 10.1007/s00424-011-1020-8

Ciulla, M. M., Paliotti, R., Carini, M., Magrini, F., and Aldini, G. (2011). Fibrosis, enzymatic and non-enzymatic cross-links in hypertensive heart disease. *Cardiovasc. Hematol. Disord. Drug Targets* 11, 61–73. doi: 10.2174/187152911798347025

Cowley, P. M., Wang, G., Joshi, S., Swigart, P. M., Lovett, D. H., Simpson, P. C., et al. (2017). α1A-Subtype adrenergic agonist therapy for the failing right ventricle. *Am. J. Physiol. Heart Circ. Physiol*. 313, H1109–H1118. doi: 10.1152/ajpheart.00153.2017

Cruz, J. A., Bauer, E. M., Rodriguez, A. I., Gangopadhyay, A., Zeineh, N. S., Wang, Y., et al. (2012). Chronic hypoxia induces right heart failure in caveolin-1-/- mice. *Am. J. Physiol. Heart Circ. Physiol*. 302, H2518–H2527. doi: 10.1152/ajpheart.01140.2011

Danz, E. D., Skramsted, J., Henry, N., Bennett, J. A., and Keller, R. S. (2009). Resveratrol prevents doxorubicin cardiotoxicity through mitochondrial stabilization and the Sirt1 pathway. *Free Radic. Biol. Med*. 46, 1589–1597. doi: 10.1016/j.freeradbiomed.2009.03.011

Date, M. O., Morita, T., Yamashita, N., Nishida, K., Yamaguchi, O., Higuchi, Y., et al. (2002). The antioxidant N-2-mercaptopropionyl glycine attenuates left ventricular hypertrophy in *in vivo* murine pressure-overload model. *J. Am. Coll. Cardiol*. 39, 907–912. doi: 10.1016/S0735-1097(01)01826-5

Datta, A., Kim, G. A., Taylor, J. M., Gugino, S. F., Farrow, K. N., Schumacker, P. T., et al. (2015). Mouse lung development and NOX1 induction during hyperoxia are developmentally regulated and mitochondrial ROS dependent. *Am. J. Physiol. Lung. Cell Mol. Physiol*. 309, L369–L377. doi: 10.1152/ajplung.00176.2014

de Jong, J. W., Schoemaker, R. G., de Jonge, R., Bernocchi, P., Keijzer, E., Harrison, R., et al. (2000). Enhanced expression and activity of xanthine oxidoreductase in the failing heart. *J. Mol. Cell. Cardiol*. 32, 2083–2089. doi: 10.1006/jmcc.2000.1240

DeMarco, V. G., Habibi, J., Whaley-Connell, A. T., Schneider, R. I., Heller, R. L., Bosanquet, J. P., et al. (2008). Oxidative stress contributes to pulmonary hypertension in the transgenic (mRen2)27 rat. *Am. J. Physiol. Heart Circ. Physiol*. 294, H2659–H2668. doi: 10.1152/ajpheart.00953.2007

Dey, S., DeMazumder, D., Sidor, A., Foster, D. B., and O'Rourke, B. (2018). Mitochondrial ROS drive sudden cardiac death and chronic proteome remodeling in heart failure. *Circ. Res*. 123, 356–371. doi: 10.1161/CIRCRESAHA.118.312708

Di Lisa, F., Giorgio, M., Ferdinandy, P., and Schulz, R. (2017). New aspects of p66Shc in ischaemia reperfusion injury and other cardiovascular diseases. *Br. J. Pharmacol*. 174, 1690–1703. doi: 10.1111/bph.13478

Dos Santos Lacerda, D., Türck, P., Gazzi de Lima-Seolin, B., Colombo, R., Duarte Ortiz, V., Poletto Bonetto, J. H., et al. (2017). Pterostilbene reduces oxidative stress, prevents hypertrophy and preserves systolic function of right ventricle in cor pulmonale model. *Br. J. Pharmacol*. 174, 3302–3314. doi: 10.1111/bph.13948

Duni, A., Liakopoulos, V., Rapsomanikis, K. P., and Dounousi, E. (2017). Chronic kidney disease and disproportionally increased cardiovascular damage: does oxidative stress explain the burden? *Oxidat. Med. Cell. Longevity*. 2017:9036450. doi: 10.1155/2017/9036450

Dunn, L. L., Buckle, A. M., Cooke, J. P., and Ng, M. K. (2010). The emerging role of the thioredoxin system in angiogenesis. *Arterioscler. Thromb. Vasc. Biol.* 30, 2089–2098. doi: 10.1161/ATVBAHA.110.209643

Ecarnot-Laubriet, A., Rochette, L., Vergely, C., Sicard, P., and Teyssier, J. R. (2003). The activation pattern of the antioxidant enzymes in the right ventricle of rat in response to pressure overload is of heart failure type. *Heart Dis*. 5, 308–312. doi: 10.1097/01.hdx.0000089836.03515.a9

Egea, J., Fabregat, I., Frapart, Y. M., Ghezzi, P., Görlach, A., Kietzmann, T., et al. (2017). European contribution to the study of ROS: a summary of the findings and prospects for the future from the COST action BM1203 (EU-ROS). *Redox Biol.* 13, 94–162. doi: 10.1016/j.redox.2017.05.007

Frazziano, G., Al Ghouleh, I., Baust, J., Shiva, S., Champion, H. C., and Pagano, P. J. (2014). Nox-derived ROS are acutely activated in pressure overload pulmonary hypertension: indications for a seminal role for mitochondrial Nox4. *Am. J. Physiol. Heart Circ. Physiol*. 306, H197–H205. doi: 10.1152/ajpheart.00977.2012

Freund-Michel, V., Khoyrattee, N., Savineau, J. P., Muller, B., and Guibert, C. (2014). Mitochondria: roles in pulmonary hypertension. *Int. J. Biochem. Cell Biol*. 55, 93–97. doi: 10.1016/j.biocel.2014.08.012

Galhotra, P., Prabhakar, P., Meghwani, H., Mohammed, S. A., Banerjee, S. K., Seth, S., et al. (2018). Beneficial effects of fenofibrate in pulmonary hypertension in rats. *Mol. Cell. Biochem.* 449, 185–194. doi: 10.1007/s11010-018-3355-3

Gladden, J. D., Zelickson, B. R., Guichard, J. L., Ahmed, M. I., Yancey, D. M., Ballinger, S., et al. (2013). Xanthine oxidase inhibition preserves left ventricular systolic but not diastolic function in cardiac volume overload. *Am. J. Physiol. Heart Circ. Physiol.* 305, H1440–H1450. doi: 10.1152/ajpheart.00007.2013

Gomez-Arroyo, J., Mizuno, S., Szczepanek, K., Van Tassell, B., Natarajan, R., dos Remedios, C. G., et al. (2013). Metabolic gene remodeling and mitochondrial dysfunction in failing right ventricular hypertrophy secondary to pulmonary arterial hypertension. *Circ. Heart Fail.* 6, 136–144. doi: 10.1161/CIRCHEARTFAILURE.111.966127

Grieve, D. J., Byrne, J. A., Siva, A., Layland, J., Johar, S., Cave, A. C., et al. (2006). Involvement of the nicotinamide adenosine dinucleotide phosphate oxidase isoform Nox2 in cardiac contractile dysfunction occurring in response to pressure overload. *J. Am. Coll. Cardiol.* 47, 817–826. doi: 10.1016/j.jacc.2005.09.051

Guggilam, A., Haque, M., Kerut, E. K., McIlwain, E., Lucchesi, P., Seghal, I., et al. (2007). TNF-α blockade decreases oxidative stress in the paraventricular nucleus and attenuates sympathoexcitation in heart failure rats. *Am. J. Physiol. Heart Circ. Physiol.* 293, H599–H609. doi: 10.1152/ajpheart.00286.2007

Guido, M. C., Marques, A. F., Tavares, E. R., Tavares de Melo, M. D., Salemi, V. M. C., and Maranhão, R. C. (2017). The effects of diabetes induction on the rat heart: differences in oxidative stress, inflammatory cells, and fibrosis between subendocardial and interstitial myocardial areas. *Oxidat. Med. Cell. Longevity* 2017:5343972. doi: 10.1155/2017/534397

Guo, H., Zhang, X., Cui, Y., Zhou, H., Xu, D., Shan, T., et al. (2015). Taxifolin protects against cardiac hypertrophy and fibrosis during biomechanical stress of pressure overload. *Toxicol. Appl. Pharmacol.* 287, 168–177. doi: 10.1016/j.taap.2015.06.002

Gupto, A. A., Cordero-Reyes, A. M., Youker, K. A., Matsunami, R. K., Engler, D. A., Li, S., et al. (2016). Differential mitochondrial function in remodeled right and nonremodeled left ventricles in pulmonary hypertension. *J. Card. Fail.* 22, 73–81. doi: 10.1016/j.cardfail.2015.09.001

Habibi, J., DeMarco, V. G., Ma, L., Pulakat, L., Rainey, W. E., Whaley-Connell, A. T., et al. (2011). Mineralocorticoid receptor blockade improves diastolic function independent of blood pressure reduction in a transgenic model of RAAS overexpression. *Am. J. Physiol. Heart Circ. Physiol.* 300, H1484–H1491. doi: 10.1210/endo-meetings.2011.PART4.P2.P3-440

Hansen, T., Galougahi, K. K., Celermajer, D., Rasko, N., Tang, O., Bubb, K. J., et al. (2016). Oxidative and nitrosative signalling in pulmonary arterial hypertension — implications for development of novel therapies. *Pharmacol. Therap.* 165, 50–62. doi: 10.1016/j.pharmthera.2016.05.005

He, J., Li, X., Luo, H., Li, T., Zhao, L., Qi, Q., et al. (2017). Galectin-3 mediates the pulmonary arterial hypertension-induced right ventricular remodeling through interacting with NADPH oxidase 4. *J. Am. Soc. Hypertens.* 11, 275–289.e2. doi: 10.1016/j.jash.2017.03.008

Hernandez-Resendiz, S., Chinda, K., Ong, S. B., Cabrera-Fuentes, H., Zazueta, C., and Hausenloy, D. J. (2018). The role of redox dysregulation in the inflammatory response to acute myocardial ischaemia-reperfusion injury - adding fuel to the fire. *Curr. Med. Chem.* 25, 1275–1293. doi: 10.2174/0929867324666170329100619

Heusch, P., Aker, S., Boengler, K., Deindl, E., van de Sand, A., Klein, K., et al. (2010). Increased inducible nitric oxide synthase and arginase II expression in heart failure: no net nitrite/nitrate production and protein S-nitrosylation. *Am. J. Physiol. Heart Circ. Physiol.* 299, H446–H453. doi: 10.1152/ajpheart.01034.2009

Heusch, P., Canton, M., Aker, S., van de Sand, A., Konietzka, I., Rassaf, T., et al. (2010b). The contribution of reactive oxygen species and p38 mitogen-activated protein kinase to myofilament oxidation and progression of heart failure in rabbits. *Br. J. Pharmacol.* 160, 1408–1416. doi: 10.1111/j.1476-5381.2010.00793.x

Iacobazzi, D., Suleiman, M. S., Ghorbel, M., George, S. J., Caputo, M., and Tulloh, R. M. (2016). Cellular and molecular basis of RV hypertrophy in congential heart disease. *Heart* 102, 12–17. doi: 10.1136/heartjnl-2015-308348

Ide, T., Tsutsui, H., Hayashidani, S., Kang, D., Suematsu, N., Nakamura, K., et al. (2001). Mitochondrial DNA damage and dysfunction associated with oxidative stress in failing hearts after myocardial Infarction. *Circ. Res.* 88, 529–535. doi: 10.1161/01.RES.88.5.529

Ishikawa, K., Kimura, S., Kobayashi, A., Sato, T., Matsumoto, H., Ujiie, Y., et al. (2005). Increased reactive oxygen species and anti-oxidative response in mitochondrial cardiomyopathy. *Circ. J.* 69, 617–620. doi: 10.1253/circj.69.617

Karamanlidis, G., Bautista-Hernandez, V., Fynn-Thompson, F., Del Nido, P., and Tian, R. (2011). Impaired mitochondrial biogenesis precedes heart failure in right ventricular hypertrophy in congenital heart disease. *Circ. Heart Fail.* 4, 707–713. doi: 10.1161/CIRCHEARTFAILURE.111.961474

Koga, K., Kenessey, A., and Ojamaa, K. (2013). Macrophage migration inhibitory factor antagonizes pressure overload-induced cardiac hypertrophy. *Am. J. Physiol. Heart Circ. Physiol.* 304, H282–H293. doi: 10.1152/ajpheart.00595.2012

Li, J. M., Gall, N. P., Grieve, D. J., Chen, M., and Shah, A. M. (2002). Activation of NADPH oxidase during progression of cardiac hypertrophy to failure. *Hypertension* 40, 477–484. doi: 10.1161/01.HYP.0000032031.30374.32

Li, M., Sala, V., De Santis, M. C., Cimino, J., Cappello, P., Pianca, N., et al. (2018). Phosphoinositide 3-kinase gamma inhibition protects from anthracycline cardiotoxicity and reduces tumor growth. *Circulation* 138, 696–711. doi: 10.1161/CIRCULATIONAHA.117.030352

Li, R., Fang, W., Cao, S., Li, Y., Wang, J., Xi, S., et al. (2013). Differential expression of NAD(P)H oxidase isoforms and the effect of atorvastatin on cardiac remodeling in two-kidney two-clip hypertensive rats. *Pharmazie* 68, 261–269. doi: 10.1691/ph.2013.2782

Lima-Seolin, B. G., Colombo, R., Bonetto, J. H. P., Teixeira, R. B., Donatti, L. M., Casali, K. R., et al. (2017). Bucindolol improves right ventricle function in rats with pulmonary arterial hypertension through the reversal of autonomic imbalance. *Eur. J. Pharmacol.* 798, 57–65. doi: 10.1016/j.ejphar.2016.12.028

Liu, B., Luo, X. J., Yang, Z. B., Zhang, J. J., Li, T. B., Zhang, X. J., et al. (2014). Inhibition of NOX/VPO1 pathway and inflammatory reaction by trimethoxystilbene in prevention of cardiovascular remodeling in hypoxia-induced pulmonary hypertensive rats. *J. Cardiovasc. Pharmacol.* 63, 567–576. doi: 10.1097/FJC.0000000000000082

Liu, J., Zhou, J., An, W., Lin, Y., Yang, Y., and Zang, W. (2010). Apocynin attenuates pressure overload-induced cardiac hypertrophy in rats by reducing levels of reactive oxygen species. *Can. J. Physiol.Pharmacol.* 88, 745–752. doi: 10.1139/Y10-063

Liu, J. Q., Zelko, I. N., Erbynn, E. M., Sham, J. S., and Folz, R. J. (2006). Hypoxic pulmonary hypertension: role of superoxide and NADPH oxidase (gp91phox). *Am. J. Physiol. Lung Cell. Mol. Physiol.* 290, L2–L10. doi: 10.1152/ajplung.00135.2005

Liu, L., Marcocci, L., Wong, C. M., Park, A. M., and Suzuki,Y. J. (2008). Serotonin-mediated protein carbonylation in the right heart. *Free Radic. Biol. Med.* 45, 847–854. doi: 10.1016/j.freeradbiomed.2008.06.008

Lu, J. C., Cui, W., Zhang, H. L., Liu, F., Han, M., Liu, D. M., et al. (2009). Additive beneficial effects of amilodipine and atorvastatin in reversing advanced cardiac hypertophy in elderly spontaneously hypertensive rats. *Clin. Exptl. Pharmacol. Physiol.* 36, 1110–1119. doi: 10.1111/j.1440-1681.2009.05198.x

Lu, X., Dang, C. Q., Guo, X., Molloi, S., Wassall, C. D., Kemple, M. D., et al. (2011). Elevated oxidative stress and endothelial dysfunction in right coronary artery of right ventricular hypertrophy. *J. Appl. Physiol.* 110, 1674–1681. doi: 10.1152/japplphysiol.00744.2009

Lu, Z., Xu, X., Hu, X., Fassett, J., Zhu, G., Tao, Y., et al. (2010). PGC-1a regulates expression of myocardial mitochondrial antioxidants and myocardial oxidative stress after chronic systolic overload. *Antiox. Redox. Signal.* 13, 1011–1022. doi: 10.1089/ars.2009.2940

Lüneburg, N., Siques, P., Brito, J., Arriaza, K., Pena, E., Klose, H., et al. (2016). Long-term chronic intermittent hypobaric hypoxia in rats causes an imbalance in the asymmetric dimethylarginine/nitric oxide pathway and ROS activity: a possible synergistic for altitude pulmonary hypertension? *Pulm. Med.* 2016:6578578. doi: 10.1155/2016/6578578

Ma, L., Ambalavanan, N., Liu, H., Sun, Y., Jhala, N., and Bradley, W. E. (2016). TLR4 regulates pulmonary vascular homeostasis and remodeling via redox signaling. *Front. Biosci.* 21, 397–409. doi: 10.2741/4396

Maarman, G. J., Schulz, R., Sliwa, K., Schermuly, R. T., and Lecour, S. (2017). Novel putative pharmacological therapies to protect the right ventricle in pulmonary hypertension: a review of current literature. *Br. J. Pharmacol.* 174, 497–511. doi: 10.1111/bph.13721

Mandraffino, G., Aragona, C. O., Cairo, V., Scuruchi, M., Lo Gullo, A., D'ascola, A., et al. (2017). Circulating progenitor cells in hypertensive subjects: effectiveness of a treatment with olmesartan in improving cell number and miR profile in addition to expected pharmacological effects. *PLoS ONE* 12:e0173030. doi: 10.1371/journal.pone.0173030

Manni, M. E., Rigacci, S., Borchi, E., Bargelli, V., Miceli, C., Giordano, C., et al. (2016). Monoamine oxidase is overactivated in left and right ventricles from ischemic hearts: an intriguing therapeutic target. *Oxidat. Med. Cell. Longevity* 2016:4375418. doi: 10.1155/2016/4375418

Matsuda, S., Umemoto, S., Yoshimura, K., Itoh, S., Murata, T., and Fukai, T. (2015). Angiotensin II activates MCP-1 and induces cardiac hypertrophy and dysfunction via Toll-like receptor 4. *Atheroscler. Thromb*. 26, 833–844. doi: 10.5551/jat.27292

Moris, D., Spartalis, M., Tzatzaki, E., Spartalis, E., Karachaliou, G. S., Triantafyllis, A. S., et al. (2017). The role of reactive oxygen species in myocardial redox signaling and regulation. *Ann. Transl. Med.* 5:324. doi: 10.21037/atm.2017.06.17

Mouli, S., Nanayakkara, G., AlAlasmari, A., Eldoumani, H., Fu, X., Berlin, A., et al. (2015). The role of frataxin in doxorubicin-mediated cardiac hypertrophy. *Am. J. Physiol. Heart Circ. Physiol.* 309, H844–H859. doi: 10.1152/ajpheart.00182.2015

Nagendran, J., Gurtu, V., Fu, D. Z., Dyck, J. R., Haromy, A., Ross, D. B., et al. (2008). A dynamic and chamber-specific mitochondrial remodeling in right ventricular hypertrophy can be therapeutically targeted. *J. Thorac. Cardiovasc. Surg.* 136, 168–178. doi: 10.1016/j.jtcvs.2008.01.040

Nediani, C., Borchi, E., Giordano, C., Baruzzo, S., Ponziani, V., Sebastiani, M., et al. (2007). NADPH oxidase-dependent redox signaling in human heart failure: relationship between the left and right ventricle. *J. Mol. Cell. Cardiol.* 42, 826–834. doi: 10.1016/j.yjmcc.2007.01.009

Nisbet, R. E., Graves, A. S., Kleinhenz, D. J., Rupnow, H. L., Reed, A. L., Fan, T. H., et al. (2009). The role of NADPH oxidase in chronic intermittent hypoxia-induced pulmonary hypertension in mice. *Am. J. Respir. Cell Mol. Biol.* 40, 601–609. doi: 10.1165/2008-0145OC

Ogura, S., Shimosawa, T., Mu, S., Sonobe, T., Kawakami-Mori, F., Wang, H., et al. (2013). Oxidative stress augments pulmonary hypertension in chronically hypoxic mice overexpressing the oxidized LDL receptor. *Am. J. Physiol. Heart Circ. Physiol.* 305, H155–H162. doi: 10.1152/ajpheart.00169.2012

Papparella, I., Ceolotto, G., Montemurro, D., Antonello, M., Garbisa, S., Rossi, G. P., et al. (2008). Green tea attenuates angiotensin II-induced cardiac hypertrophy in rats by modulating reactive oxygen species production and the Src/Epidermal growth factor receptor/Act signalling pathway. *J. Nutr.* 138, 1596–1601. doi: 10.1093/jn/138.9.1596

Paulin, R., and Michelakis, E. D. (2014). The metabolic theory of pulmonary arterial hypertension. *Circ Res.* 115, 148–164. doi: 10.1161/CIRCRESAHA.115.301130

Phillips, D., Aponte, A. M., Covian, R., Neufeld, E., Yu, Z. X., and Balaban, R. S. (2011). Homogenous protein programming in the mammalian left and right ventricle free walls. *Physiol. Genom.* 43, 1198–1206. doi: 10.1152/physiolgenomics.00121.2011

Pichardo, J., Palace, V., Farahmand, F., and Singal, P. K. (1999). Myocardial oxidative stress changes during compensated right heart failure in rats. *Mol. Cell. Biochem.* 196, 51–57. doi: 10.1023/a:1006914111957

Pönicke, K., Schlüter, K. D., Heinroth-Hoffmann, I., Seyfarth, T., Goldberg, M., Piper, H. M., et al. (2001). Naunyn Schmiedebergs. *Arch. Pharmacol.* 364, 444–453. doi: 10.1007/s002100100469

Puukila, S., Fernandes, R. O., Türck, P., Carraro, C. C., Bonetto, J. H. P., de Lima-Seolin, B. G., et al. (2017). Secoisolariciresinol diglucoside attenuates cardiac hypertrophy and oxidative stress in monocrotaline-induced right heart dysfunction. *Mol. Cell. Biochem*. 432, 33–39. doi: 10.1007/s11010-017-2995-z

Qiao, W., Zhang, W., Gai, Y., Zhao, L., and Fan, J. (2014). The histone acetyltransferase MOF overexpression blunts cardiac hypertrophy by targeting ROS in mice. *Biochem. Biophys. Res. Commun.* 448, 379–384. doi: 10.1016/j.bbrc.2014.04.112

Qin, F., Siwik, D. A., Pimentel, D. R., Morgan, R. J., Biolo, A., Tu, V. H., et al. (2017). Cytosolic H_2O_2 mediates hypertrophy, apoptosis, and decreased SERCA activity in mice with chronic hemodynamic overload. *Am. J. Physiol. Heart Circ. Physiol.* 306, H1453–H1463. doi: 10.1152/ajpheart.00084.2014

Qipshidze, N., Tyagi, N., Metreveli, N., Lominadze, D., and Tyagi, S. C. (2012). Autophagy mechanism of right ventricular remodeling in murine model of pulmonary artery constriction. *Am. J. Physiol. Heart Circ. Physiol.* 302, H688–H696. doi: 10.1152/ajpheart.00777.2011

Rassaf, T., Poll, L. W., Brouzos, P., Lauer, T., and Totzeck, M., Kleinbongard, P., et al. (2006). Positive effects of nitric oxide on left ventricular function in humans. *Eur. Heart J.* 27, 1699–1705. doi: 10.1093/eurheartj/ehl096

Rawat, D. K., Alzoubi, A., Gupte, R., Chettimada, S., Watanabe, M., Kahn, A. G., et al. (2014). Increased reactive oxygen species, metabolic maladaptation, and autophagy contribute to pulmonary arterial hypertension-induced ventricular hypertrophy and diastolic heart failure. *Hypertension* 64, 1266–1274. doi: 10.1161/HYPERTENSIONAHA.114.03261

Reddy, S., and Bernstein, D. (2015). Molecular mechanisms of right ventricular failure. *Circulation* 132, 1734–1742. doi: 10.1161/CIRCULATIONAHA.114.012975

Redout, E. M., van der Toorn, A., Zuidwijk, M. J., van de Kolk, C. W. A., van Echteld, C. J. A., Musters, R. J. P., et al. (2010). Antioxidant treatment attenuates pulmonary arterial hypertension-induced heart failure. *Am. J. Physiol. Heart Circ. Physiol.* 298, H1038–H1047. doi: 10.1152/ajpheart.00097.2009

Redout, E. M., Wagner, M. J., Zuidwijk, M. J., Boer, C., Musters, R. J. P., van Hardeveld, C., et al. (2007). Right-ventricular failure is associated with increased mitochondrial complex II activity and production of reactive oxygen species. *Cardiovasc. Res.* 75, 770–781. doi: 10.1016/j.cardiores.2007.05.012

Redza-Dutordoir, M., and Averill-Bates, D. A. (2016). Activation of apoptosis signalling pathways by reactive oxygen species. *Biochim. Biophys. Acta* 1863, 2977–2992. doi: 10.1016/j.bbamcr.2016.09.012

Riba, A., Deres, L., Sumegi, B., Toth, K., Szabados, E., and Halmosi, R. (2017). Cardioprotective effect of resveratrol in a postinfarction heart failure model. *Oxidative Med. Cell. Longevity* 2017:6819281. doi: 10.1155/2017/6819281

Rizzi, E., Guimaraes, D. A., Ceron, C. S., Prado, C. M., Pinheiro, L. C., Martins-Oliveira, A., et al. (2014). β1-Adrenergic blockers exert antioxidant effects, reduce matrix metalloproteinase activity, and improve renovascular hypertension-induced cardiac hypertrophy. *Free Radical. Biol. Med.* 73, 308–317. doi: 10.1016/j.freeradbiomed.2014.05.024

Schäfer, M., Schäfer, C., Piper, H. M., and Schlüter, K. D. (2002). Hypertrophic responsiveness of cardiomyocytes to α- and β-adrenoceptor stimulation requires sodium-proton-exchanger-1 (NHE-1) activation but not cellular alkalization. *Eur. J. Heart Fail.* 4, 249–254. doi: 10.1016/S1388-9842(02)00016-8

Schlüter, K. D. (ed.). (2016). "Ways to study the biology of cardiomyocytes," in *Cardiomyocytes – Active Players in Cardiac Disease* (Cham: Springer International Publishing), 3–23. doi: 10.1007/978-3-319-31251-4_1

Schreckenberg, R., Rebelo, M., Deten, A., Weber, M., Rohrbach, S., Pipicz, M., et al. (2015). Specific mechanisms underlying right heart failure: the missing upregulation of superoxide dismutase-2 and its decisive role in antioxidative defense. *Antioxdi. Redox Signal.* 23, 1220–1232. doi: 10.1089/ars.2014.6139

Shimizu, S., Ishibashi, M., Kumagai, S., Wajima, T., Hiroi, T., Kurihara, T., et al. (2013). Decreased cardiac mitochondrial tetrahydrobiopterin in a rat model of pressure overload. *Int. J. Mol. Med.* 31, 589–596. doi: 10.3892/ijmm.2013.1236

Simm, A., Schlüter, K. D., Diez, C., Piper, H. M., and Hoppe, J. (1998). Activation of p70S6 kinase by β-adrenoceptor agonists on adult cardiomyocytes. *J. Mol. Cell. Cardiol.* 30, 2059–2067. doi: 10.1006/jmcc.1998.0768

Siqueira, R., Colombo, R., Conzatti, A., de Castro, A. L., Carraro, C. C., Tavares, A. M. V., et al. (2018). Effects of ovariectomy on antioxidant defence systems in the right ventricle of female rats with pulmonary arterial hypertension induced by monocrotaline. *Can. J. Physiol. Pharmacol.* 96, 295–303. doi: 10.1139/cjpp-2016-0445

Sirker, A., Murdoch, C. E., Protti, A., Sawyer, G. J., Santos, C. X. C., Martin, D., et al. (2016). Cell-specific effects of Nox2 on the acute and chronic response to myocardial infarction. *J. Mol. Cell. Cardiol.* 98, 11–17. doi: 10.1016/j.yjmcc.2016.07.003

Sundaresan, N. R., Gupta, M., Kim, G., Rajamohan, S. B., Isbatan, A., and Gupta, M. P. (2009). Sirt3 blocks the cardiac hypertrophic response by augmenting Foxo3a-dependent antioxidant defense mechanisms in mice. *J. Clin. Invest.* 119, 2758–2771. doi: 10.1172/JCI39162

Sutendra, G., and Michelakis, E. D. (2014). The metabolic basis of pulmonary arterial hypertension. *Cell Metab.* 19, 558–573. doi: 10.1016/j.cmet.2014.01.004

Sverdlov, A. L., Elezaby, A., Qin, F., Behring, J. B., Luptak, I., Calamaras, T. D., et al. (2016). Mitochondrial reactive oxygen species mediate cardiac structural, functional, and mitochondrial consequences of diet-induced metabolic heart disease. *J. Am. Heart. Assoc.* 5:e002555. doi: 10.1161/JAHA.115.002555

Takimoto, E., Champion, H. C., Li, M., Ren, S., Rodriguez, E. R., Tavazzi, B., et al. (2005). Oxidant stress from nitric oxide synthase−3 uncoupling stimulates

cardiac pathologic remodeling from chronic pressure load. *J. Clin. Invest*. 115, 1221–1231. doi: 10.1172/JCI21968

Talukder, M. A., Johnson, W. M., Varadharaj, S., Lian, J., Kearns, P. N., El-Mahdy, M. A., et al. (2011). Chronic cigarette smoking causes hypertension, increased oxidative stress, impaired NO bioavailability, endothelial dysfunction, and cardiac remodeling in mice. *Am. J. Physiol. Heart Circ. Physiol*. 300, H388–H396. doi: 10.1152/ajpheart.00868.2010

Tanaka, M., Umemoto, S., Kawahara, S., Kubo, M., Itoh, S., Umeji, K., et al. (2005). Angiotensin II type 1 receptor antagonist and angiotensin-converting enzyme inhibitor altered the activation of Cu/Zn-containing superoxide dismutase in the heart of stroke-prone spontaneously hypertensive rats. *Hypertens. Res*. 28, 67–77. doi: 10.1291/hypres.28.67

Tsutsui, H., Ide, T., Hayashidami, S., Kinugawa, S., Suematsu, N., Utsumi, H., et al. (2001). Effects of ACE inhibition on left ventricular failure and oxidative stress in Dahl salt-sensitive rats. *J. Cardiovasc. Pharmacol*. 37, 725–733. doi: 10.1097/00005344-200106000-00010

Türck, P., Lacerda, D. S., Carraro, C. C., de Lima-Seolin, B. G., Teixeira, R. B., Poletto Bonetto, J. H., et al. (2018). Trapidil improves hemodynamic, echocardiographic and redox state parameters of right ventricle in monocrotaline-induced pulmonary arterial hypertension model. *Biomed. Pharmacother*. 103, 182–190. doi: 10.1016/j.biopha.2018.04.001

Umemoto, S., Tanaka, M., Kawahara, S., Kubo, M., Umeji, K., Hashimoto, R., et al. (2004). Calcium antagonist reduces oxidative stress by upregulating Cu/Zn superoxide dismutase in stroke-prone spontaneously hypertensive rats. *Hypertens. Res*. 27, 877–885. doi: 10.1291/hypres.27.877

Wang, L., Lopaschuk, G. D., and Clanachan, A. S. (2008). H_2O_2-induced left ventricular dysfunction in isolated working rat hearts is independent of calcium accumulation. *J. Mol. Cell. Cardiol*. 45, 787–795. doi: 10.1016/j.yjmcc.2008.08.010

Wang, X., Liu, J., Drummond, C. A., and Shapiro, J. I. (2017a). Sodium potassium adenosine triphosphatase (Na/K-ATPase) as a therapeutic target for uremic cardiomyopathy. *Exp. Opin. Ther. Targets* 21, 531–541. doi: 10.1080/14728222.2017.1311864

Wang, X., Shults, N. V., and Suzuki, Y. J. (2017). Oxidative profiling of the failing right heart in rats with pulmonary hypertension. *PLoS ONE* 12:e0176887. doi: 10.1371/journal.pone.0176887

Waypa, G. B., Osborne, S. W., Marks, J. D., Berkelhamer, S. K., Kondapalli, J., and Schumacker, P. T. (2013). Sirtuin 3 deficiency does not augment hypoxia-induced pulmonary hypertension. *Am. J. Respir. Cell Mol. Biol*. 49, 885–891. doi: 10.1165/rcmb.2013-0191OC

Wenzel, S., Abdallah, Y., Helmig, S., Schäfer, C., Piper, H. M., and Schlüter, K.-D. (2006). Contribution of PI 3-kinase isoforms to angiotzensin II- and α-adrenoceptor-mediated signaling pathways in cardiomyocytes. *Cardiovasc. Res*. 71, 352–362. doi: 10.1016/j.cardiores.2006.02.004

Wenzel, S., Rohde, C., Wingerning, S., Roth, J., Kojda, G., and Schlüter, K. D. (2007). Lack of endothelial nitric oxide synthase-derived nitric oxide formation favors hypertrophy in adult ventricular cardiomyocytes. *Hypertension* 49, 193–200. doi: 10.1161/01.HYP.0000250468.02084.ce

Wenzel, S., Taimor, G., Piper, H. M., and Schlüter, K. D. (2001). Redox-sensitive intermediates mediate angiotensin II-induced p38 MAP kinase activation, AP-1 binding activity, and TGF-β expression in adult ventricular cardiomyocytes. *FASEB J*. 15, 2291–2293. doi: 10.1096/fj.00-0827fje

Wong, C. M., Bansal, G., Pavlickova, L., Marocci, L., and Suzuki, Y. J. (2013). Reactive oxygen species and antioxidants in pulmonary hypertension. *Antioxid. Redox Signal*. 18, 1789–1796. doi: 10.1089/ars.2012.4568

Wong, Y. Y., Ruiter, G., Lubberink, M., Raijmakers, P. G., Knaapen, P., Marcus, J. T., et al. (2011). Right ventricular failure in idiopathic pulmonary arterial hypertension is associated with inefficient myocardial oxygen utilization. *Circ. Heart Fail*. 4, 700–706. doi: 10.1161/CIRCHEARTFAILURE.111.962381

Xu, Q., Dalic, A., Fang, L., Kiriazis, H., Ritchie, R. H., Sim, K., et al. (2011). Myocardial oxidative stress contributes to transgenic β_2-adrenoceptor activation induced cardiomyopathy and heart failure. *Br. J. Pharmacol*. 162, 1012–1028. doi: 10.1111/j.1476-5381.2010.01043.x

Ye, J. X., Wang, S. S., Ge, M., and Wang, D. J. (2016). Suppression of endothelial PGC-1α is associated with hypoxia-induced endothelial dysfunction and provides a new therapeutic target in pulmonary arterial hypertension. *Am. J. Physiol. Lung. Cell Mol. Physiol*. 310, L1233–L1242. doi: 10.1152/ajplung.00356.2015

Zhu, T. T., Zhang, W. F., Luo, P., Qian, Z. X., Li, F., Zhang, Z., et al. (2017). LOX-1 promotes right ventricular hypertrophy in hypoxia-exposed rats. *Life Sci.* 174, 35–42. doi: 10.1016/j.lfs.2017.02.016

Zisman, L. S., Asano, K., Dutcher, D. L., Ferdensi, A., Robertson, A. D., Jenkin, M., et al. (1998). Differential regulation of cardiac angiotensin converting enzyme binding sites and AT_1 receptor density in the failing human heart. *Circulation* 98,1735–1741. doi: 10.1161/01.CIR.98.17.1735

Conflict of Interest Statement: The authors declare that the research was conducted in the absence of any commercial or financial relationships that could be construed as a potential conflict of interest.

ANTIOXIDANTS & REDOX SIGNALING
Volume 23, Number 15, 2015

DOI: 10.1089/ars.2014.6139

Discoveries

ORIGINAL RESEARCH COMMUNICATION

Specific Mechanisms Underlying Right Heart Failure: The Missing Upregulation of Superoxide Dismutase-2 and Its Decisive Role in Antioxidative Defense

Rolf Schreckenberg,[1] Manuel Rebelo,[1] Alexander Deten,[2] Martin Weber,[1] Susanne Rohrbach,[1] Márton Pipicz,[3,4] Csaba Csonka,[3,4] Péter Ferdinandy,[3,5] Rainer Schulz,[1] and Klaus-Dieter Schlüter[1]

Abstract

Aims: Research into right ventricular (RV) physiology and identification of pathomechanisms underlying RV failure have been neglected for many years, because function of the RV is often considered less important for overall hemodynamics and maintenance of blood circulation. In view of this, this study focuses on identifying specific adaptive mechanisms of the RV and left ventricle (LV) during a state of chronic nitric oxide (NO) deficiency, one of the main causes of cardiac failure. NO deficiency was induced in rats by L-NAME feeding over a 4 week period. The cardiac remodeling was then characterized separately for the RV/LV using quantitative real-time polymerase chain reaction, histology, and functional measurements. ***Results:*** Only the RV underwent remodeling that corresponded morphologically and functionally with the pattern of dilated cardiomyopathy. Symptoms in the LV were subtle and consisted primarily of moderate hypertrophy. A massive increase in reactive oxygen species (ROS) (+4.5 ± 0.8-fold, *vs.* control) and a higher degree of oxidized tropomyosin (+46% ± 4% *vs*. control) and peroxynitrite (+32% ± 2% *vs*. control) could be identified as the cause of both RV fibrosis and contractile dysfunction. The expression of superoxide dismutase-2 was specifically increased in the LV by 51% ± 3% and prevented the ROS increase and the corresponding structural and functional remodeling. ***Innovation:*** This study identified the inability of the RV to increase its antioxidant capacity as an important risk factor for developing RV failure. ***Conclusion:*** Unlike the LV, the RV did not display the necessary adaptive mechanisms to cope with increased oxidative stress during a state of chronic NO deficiency. *Antioxid. Redox Signal.* 23, 1220–1232.

Introduction

For a long time, the right ventricle (RV) was viewed to play a marginal role in the maintenance and stability of global hemodynamics of adults. As a consequence, research into RV physiology, including the identification of specific pathomechanisms, has been a neglected subject of study, and only a few randomized clinical trials on RV failure have been carried out (29).

In this way, the range of therapeutic interventions available for RV failure corresponds largely to those for left ventricular (LV) failure. These interventions primarily target vasodilatation and thus at reducing cardiac afterload (34). However, the National Heart, Lung, and Blood Institute described the situation in a special report on the RV as follows: ''… right ventricular failure cannot be understood simply by extrapolating data and experience from left ventricular failure…The right ventricle is different from the left ventricle''(50).

The inadequate understanding of the RV pathophysiology, however, stands in sharp contrast to the frequency of RV failure, which does not differ from that of LV failure. The results of the CORE trial have also demonstrated that isolated RV failure or involvement of the RV in the cardiac symptoms

[1]Physiologisches Institut, Justus-Liebig-Universität Gießen, Giessen, Germany.
[2]Fraunhofer-Institut für Zelltherapie und Immunologie, Leipzig, Germany.
[3]Pharmahungary Group, Szeged, Hungary.
[4]Cardiovascular Research Group, Department of Biochemistry, University of Szeged, Szeged, Hungary.
[5]Department of Pharmacology and Pharmacotherapy, Semmelweis University, Budapest, Hungary.

Innovation

The results of the study demonstrate the inability of the right ventricular (RV) to cope with oxidative stress caused by a chronic deficiency in nitric oxide. The limited potential of the RV to increase its endogenous antioxidive capacity must be taken into consideration during the targeted development of new treatment stategies for RV insufficiency. The central role of the RV and its frequent involvement in numerous cardiovascular conditions underscore the necessity of viewing the RV pathophysiology as an independent entity, as it cannot simply be deduced from observations of the left ventricle.

is associated with a poorer prognosis compared with purely LV dysfunction (35).

However, the well-documented molecular and cellular mechanisms identified in the LV cannot readily be translated to the right heart. This situation can be substantiated by the specific cardiogenesis of the RV, the cellular origin of which can be traced back to the secondary or anterior heart field along with the septum and the outflow tract. In contrast, the atria and the entire LV originate from a population of progenitor cells that formed the primary heart field (49, 51).

At a molecular and cellular level, the pathogenesis and progression of chronic cardiac insufficiency can often be attributed to a reduced bioavailability of nitric oxide (NO), increased radical stress, and cardiac fibrosis (13, 27, 31).

In particular, the increased rate of cardiovascular events associated with chronic kidney diseases, type 2 diabetes mellitus, or women after menopause is ascribed to a general deficit of NO, among other factors (7, 48).

The effects of NO within the cardiovascular system are not solely attributed to its vasodilatory and thus antihypertensive properties. NO interacts far more ubiquitously at cellular and subcellular levels, in part, by nitrosation of cystein residues within signaling pathways of the renin-angiotensin-aldosterone system (RAAS), the sympathetic nervous system, and the mitochondria, and thus directly and indirectly influences the function and structure of the myocardium (21, 39, 45).

The primary research aim of this study is to identify the key enzymes and pathomechanisms that are specific and are regulated differently for the RV and LV during a state of systemic NO deficiency.

Chronic NO deficiency was induced in this study in female adult rats by feeding them the NOS inhibitor L-NAME over a period of 4 weeks. The effects of reduced NO levels on molecular and cellular parameters were studied for both ventricles.

During long-term application of L-NAME, the symptoms in experimental animals could only, in part, be attributed to the immediate reduction in the NO-dependent effects. Over the further course, a chronic deficiency in NO led to increased formation of reactive oxygen species (ROS) that not only favor the development of hypertension but also directly affect cell and organ functions. For this reason, the pure L-NAME substitution was supplemented by two additional applications. One treatment group also received the angiotensin-converting enzyme (ACE)-inhibitor captopril, while another was given the radical scavenger and superoxide dismutase (SOD)-mimetic tempol in the form of a therapeutic intervention in the third and fourth week of L-NAME application. Along with its interaction with the RAAS and the subsequent reduction in angiotensin-II-dependent effects, captopril also has direct antioxidant properties *via* a cleavable sulfhydryl group (36). The use of tempol allowed the identification of protective effects that can be attributed solely to a reduction in ROS.

Signal mechanisms and their effect on the contractile behavior after chronic exposure to L-NAME were also analyzed *in vitro* in cardiomyocytes isolated from the RV or LV independent of systemic influences and blood pressure.

Results

Effect of L-NAME on systemic hemodynamics

The systolic blood pressure averaged 126 ± 7 mm Hg with no group differences between all test groups at the start of the experimental protocol. This value did not change throughout the entire course of the experiment for the animals in the control group. In the L-NAME group (L), systolic blood pressure increased to 173 ± 7 mm Hg after 4 weeks. On addition of the ACE-inhibitor captopril to the L-NAME feed after 2 weeks of treatment (LC) for the remaining 2 weeks, the blood pressure fell from 159 ± 5 mm Hg (after 2 weeks of L-NAME) to 135 ± 5 mm Hg at 4 weeks. The supplemental application of the SOD-mimetic tempol (LT) did not result in a fall in blood pressure but prevented a further increase during the last 2 weeks of the treatment period (161 ± 4 mm Hg). The heart rate did not change significantly in the entire collective throughout the observation period (Supplementary Fig. S1 and Supplementary Table S1; Supplementary Data are available online at www.liebertpub.com/ars).

Consequences of chronic NO deficiency on the cardiac remodeling

The wet weights of the RV and LV were standardized to the body weight (BW) of the particular animal. Compared with the control group, the animals in the L and LT groups developed low-grade LV hypertrophy based on a moderate increase in the LV/BW ratio. Captopril normalized the ratio to the level of the control animals (Fig. 1A).

No significant difference could be detected compared with the drinking-water controls for the RV/BW ratio independent of the particular application scheme (Fig. 1A).

The raw data obtained for BW, the RV and LV, and lungs and kidneys are listed in Supplementary Table S2.

However, the geometry of the RV changed in L-NAME-fed animals and corresponded to the clinical picture of dilated cardiomyopathy. The supplemental application of captopril or tempol was able to positively affect the structural remodeling of the RV—the RV dilatation was reduced, and the decrease in the wall thickness was almost prevented (Fig. 1B, C).

On a molecular level, the remodeling of the RV and LV was characterized by re-expression of fetal genes. Brain natriuretic peptide and myosin heavy-chain beta were induced to a comparable level by L-NAME in both the RV and the LV. The induction of atrial natriuretic peptide (ANP), which is primarily re-expressed in response to cardiac pressure load, was increased only in the LV by 7.8 ± 1.3 fold (Supplementary Fig. S2).

Functional consequences of the structural remodeling

The consequences of the L-NAME-induced remodeling on cardiac function were analyzed at the end of the 4-week

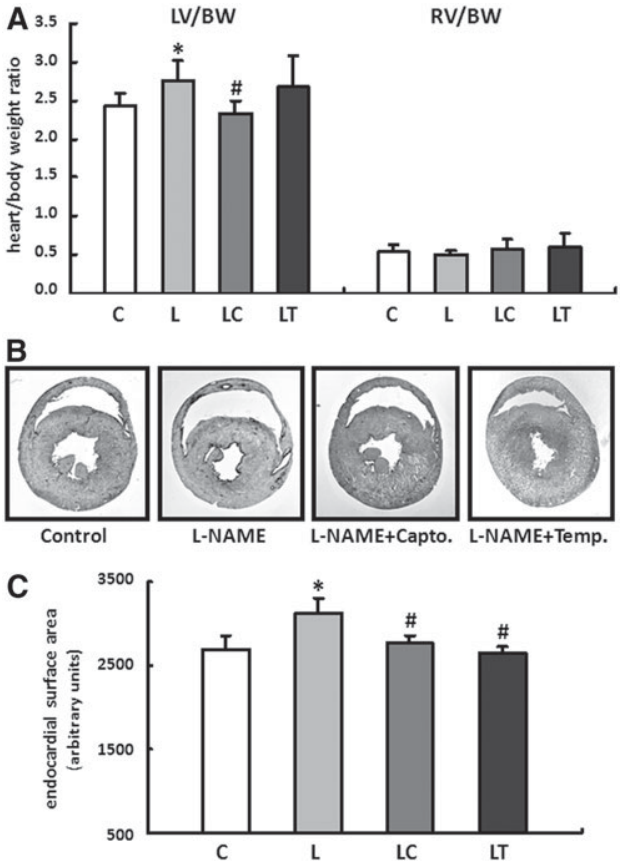

FIG. 1. L-NAME induced changes in cardiac remodeling. (A) Effects of the different treatment strategies on myocardial hypertrophy. The wet weight of the right ventricle (RV) and left ventricle (LV) were normalized to the body weight (BW) of the particular animal. Data are means ± S.D. of $n = 8$ hearts. **(B)** Representative images of horizontal heart sections from each treatment group. The geometry of the RV changed in L-NAME fed animals and corresponded with the pattern of dilated cardiomyopathy. **(C)** Endocardial surface area of the RV was determined from histological sections. Data are means ± SD of $n = 5$ hearts. $^{*}p < 0.05$ *versus* control, $^{\#}p < 0.05$ *versus* L-NAME.

substitution using a Millar tip catheter that was advanced on the right side to the RV *via* the jugular vein and atrium. The stabilized signal was then recorded continuously over a period of 30 min.

The peak RV pressure was reduced as a result of the L-NAME application and was affected only by captopril treatment. However, both therapy strategies significantly improved the RV dp/dt max or RV dp/dt min and thus specifically reduced the contractile dysfunction of the RV (Table 1).

As the cardinal symptom of impaired RV function, the blood accumulation was determined using the liver wet weight (LW) and the liver transaminases glutamate-oxaloacetate transaminase/glutamate-pyruvate transaminase (GOT/GPT). In animals fed L-NAME, the LW/BW ratio increased by 9.2% ± 0.6% (C *vs.* L, 29.4 g/kg *vs.* 32.1 g/kg, $p = 0.10$) while the transaminases rose by 14.8% ± 1.7% (C *vs.* L, 85.8 U/L *vs.* 98.4 U/L, $p = 0.01$).

The LV function, represented by the LV-developed pressure (LVDP), was determined using a balloon catheter. Regardless of the particular application scheme, no significant differences in the LVDP, the LV dp/dt max, or LV dp/dt min could be detected (Supplementary Table S3). Uniform lung wet weights largely rule out a restrictive functional disorder (Supplementary Table S2).

Regulation of the ROS in the right and left ventricles

As previously stated in the introduction, chronic deficiency in NO is often associated with an increase in oxidative stress.

The fluorescence microscopy images of the dihydroethidium (DHE) staining showed only a slight radical load for the LV independent of the particular application scheme with no significant differences between the treatment groups.

In contrast to this, the RV had an elevated radical load even in untreated controls compared with the LV, and this was further increased till 4.5 ± 0.8-fold during L-NAME substitution. The two therapy options, captopril and tempol, significantly reduced the concentration of ROS in the RV to a comparable level (Fig. 2A, B).

It could already be seen that an increased accumulation of ROS contributes to contractile dysfunction by oxidative modification of tropomyosin (Tm) (14, 15). The formation of disulphide cross-bridges (DCB) at the level of cystein residues leads to an enhanced dimerization of Tm, which could be detected as high-molecular-weight peptide (~80 kDa) under non-reducing conditions in immunoelectrophoresis. L-NAME application did not have any effects on DCB formation in the LV; however, in the RV, a significant increase in cross-linking processes was detected, leading to a 46% ± 4% increase in oxTm/Tm ratio (Fig. 3A, B).

Given the specific changes in oxidative stress measured by DHE staining, a specific powerful oxidant species, peroxynitrite ($ONOO^-$), was quantified in the tissues from the RV and LV. The formation of $ONOO^-$ is based on the reaction between ROS and NO. The molecule itself does not have any free radical properties, but it can dissociate rapidly into highly reactive decomposition products.

Comparable to the results obtained for radical staining, no group difference could be detected for the LV concentration of $ONOO^-$. Likewise, the RV had a higher concentration of $ONOO^-$ compared with the left even in the control group. L-NAME substitution led to a further significant increase in peroxynitrite in the RV that could be reduced by tempol to the level of the controls. Captopril, by contrast, led to an additional increase in the $ONOO^-$ concentration in the RV myocardium in the LC group (Fig. 4).

The concentration of malondialdehyde (MDA) in the blood plasma was determined as a general indicator of oxidative stress. The 4-week application of L-NAME led to a 24.2% ± 4.9% (C *vs.* L, $p < 0.05$) increase in plasma MDA levels.

To identify a potential mechanism that explains the different formation in ROS in both ventricles, the expression pattern of antioxidative enzymes was analyzed. In their role as oxidoreductases, SODs catalyze the conversion of superoxide into hydrogen peroxide (H_2O_2) and oxygen and thus perform important antioxidant functions. The expression patterns of the three isoforms SOD1, 2, and 3 were each determined separately for the RV and LV of the C and L groups. Only the expression of SOD2 was specifically increased in the LV of L-NAME-substituted animals by 51% ± 3%. In contrast, this isoform was downregulated in the RV by 30% ± 4%. No significant changes could be detected in

TABLE 1. HEART RATE AND RIGHT VENTRICULAR CONTRACTILITY ASSESSMENT *IN VIVO* UNDER ANESTHESIA

	Heart rate (bpm)	*RVSP (mm Hg)*	*RVEDP (mm Hg)*	*RV dp/dt max (mm Hg/s)*	*RV dp/dt min (mm Hg/s)*
Control (C)	422 ± 27	37.0 ± 5.4	2.6 ± 1.6	2292 ± 355	− 2105 ± 395
L-NAME (L)	391 ± 25	30.7 ± 4.6[a]	0.9 ± 2.2	1608 ± 98[a]	− 1363 ± 136[a]
L-NAME + captopril (LC)	397 ± 28	35.9 ± 1.0	1.8 ± 0.2	1925 ± 109[a,b]	− 1486 ± 82[a,b]
L-NAME + tempol (LT)	425 ± 24	30.5 ± 1.9[a]	1.4 ± 1.1	1929 ± 47[a,b]	− 1737 ± 90[a,b]

Changes in RV contractility after 4 weeks. Rats were given pure drinking water (C) $n = 10$, L-NAME (L) $n = 9$, L-NAME plus captopril (LC) $n = 5$ or L-NAME plus tempol (LT) $n = 6$. Data are means ± SD.
[a] $p < 0.05$ *versus* control.
[b] $p < 0.05$ *versus* L-NAME.
bpm, beats per minute; RV, right ventricle; RVEDP, right ventricular end-diastolic pressure; RVSP, right ventricular systolic pressure.

the expression of SOD1 and SOD3 (Fig. 5A). The selective upregulation of SOD2 in the LV of animals fed L-NAME was then confirmed in Western blots (Fig. 5B, C).

An increase in the expression of the transcription factors PGC-1α and nuclear respiratory factor-2 (Nrf-2), which are involved in the regulation of SOD2, was only seen in the LV of the L group. Other downstream targets of Nrf-2 such as glutamate-cysteine ligase, catalytic subunit (Gclc), and thioredoxin reductase 1 (TXNRD1) were also selectively induced in the LV in animals fed L-NAME (Fig. 6A–D).

The catalase, which is also an oxidoreductase that converts any H_2O_2 that accumulates to oxygen and water, was upregulated only in the LV similar to SOD2. L-NAME had no effect on the expression of the glutathione peroxidase (Gpx) in either the RV or the LV (Fig. 6E, F).

That there is no change in the expression of the mitochondrial uncouplers UCP2 and UCP3 as well as the hydroxyacyl-CoA dehydrogenase, alpha subunit (HADHA) of the trifunctional protein (MTP) and the transcription factor Nrf-1 indicates that applying L-NAME has no effect on the mitochondrial biogenesis in either the RV or the LV (Supplementary Fig. S3A–D).

Of the two subunits of NADPH oxidase, p22phox and NOX2, only the expression of NOX2 was increased in the LV of rats fed L-NAME (Fig. 6G, H).

Effect of L-NAME on cell shortening and SOD2 expression in isolated cardiomyocytes

To investigate the effect of L-NAME on the contractile behavior and SOD2 expression at a cellular level, cardiomyocytes

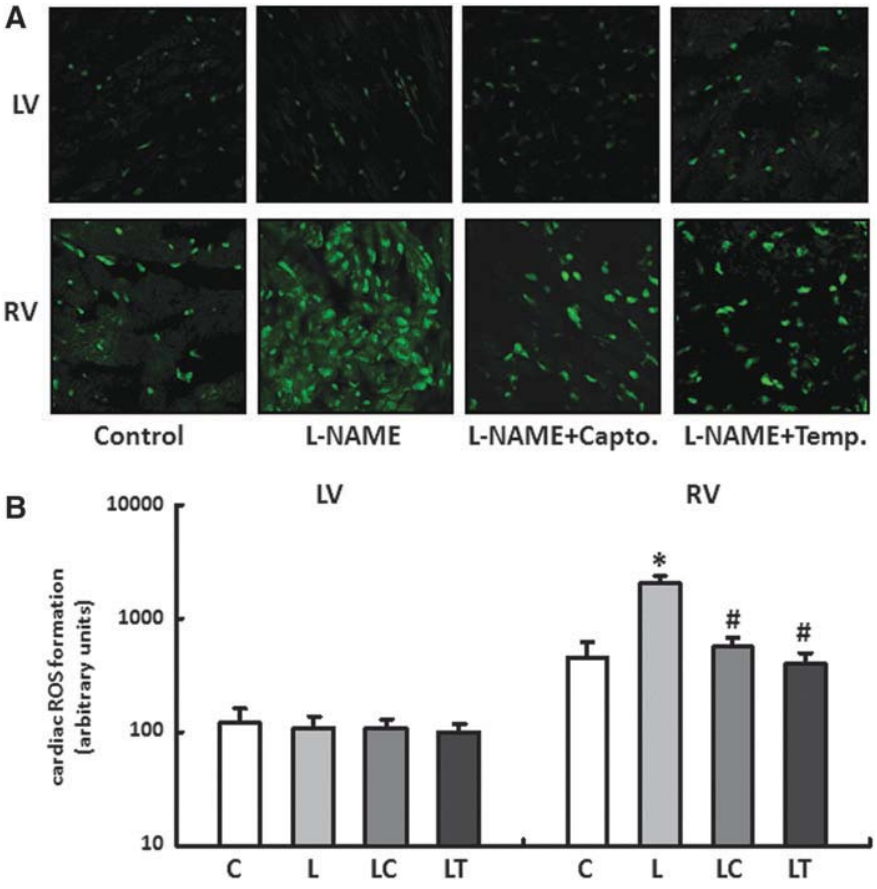

FIG. 2. (A, B) Generation of superoxide in right and left ventricles. Dihydroethidium (DHE) staining was performed to measure the formation of reactive oxygen species in heart tissue from RV and LV of all treatment groups (control [C], L-NAME [L], L-NAME plus captopril [LC] and L-NAME plus tempol [LT]). Slides were imaged by confocal microscopy using an excitation wavelength of 488 nm and an emission wavelength of 540 nm. Data are means ± SD of $n = 5$ hearts. $^{*}p < 0.05$ *versus* control, $^{\#}p < 0.05$ *versus* L-NAME.

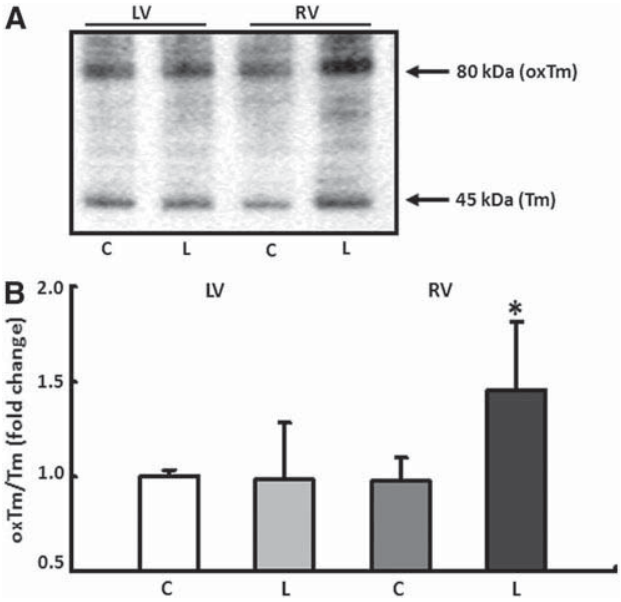

FIG. 3. Conformational changes of tropomyosin (Tm) induced by oxidative stress. (A) Quantification of disulphide cross-bridge formation in tropomyosin (Tm) under non-reducing conditions. Oxidative modification of Tm (oxTm) leads to dimerization of the protein and was detected as a high-molecular-weight peptide of ~80 kDa. **(B)** Protein expression was analyzed in the RV and LV of control (C) and L-NAME fed animals (L). Results are given as ratio of oxTm to Tm. Data are means ± SD of $n = 4$ hearts. *$p < 0.05$ *versus* control.

were isolated separately from the RV and LV of untreated rats and incubated for 24 h with L-NAME. Compared with untreated control cells, L-NAME led to a significant reduction in the relative cell shortening only in the RV myocytes. The expression of SOD2 corresponded to the *in vivo* results previously described (Fig. 7A–C). Accordingly, L-NAME led to an increase in mitochondrial ROS formation only in RV myocytes as detected by mitochondria-targeted superoxide fluorescent indicator MitoSOX Red (Supplementary Fig. S4).

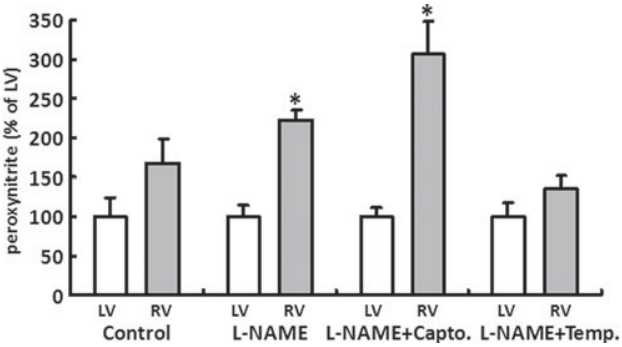

FIG. 4. L-NAME induced changes in the formation of peroxynitrite ($ONOO^-$). $ONOO^-$ was measured in heart tissue from RV (*gray bars*) and LV (*white bars*) of all treatment groups (control [C], L-NAME [L], L-NAME plus captopril [LC], and L-NAME plus tempol [LT]). Average LV concentration of $ONOO^-$ was 0.65 ± 0.21 ng/mg protein. Values of RV are displayed as percent of LV. Data are means ± SD of $n = 4$ hearts. *$p < 0.05$ *versus* LV.

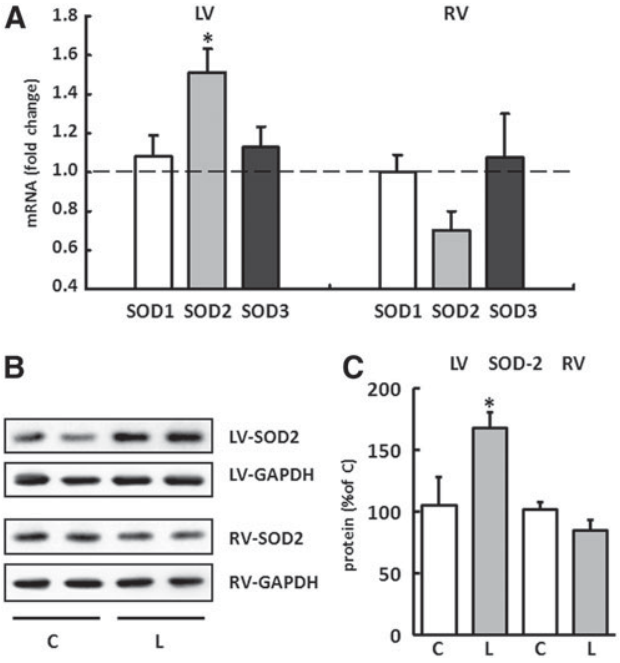

FIG. 5. Expression pattern of superoxide dismutases (SOD) in right and left ventricles. (A) The expression for SOD1, SOD2, and SOD3 was analyzed separately for the RV and LV of drinking-water controls and L-NAME-fed animals. Results are displayed as fold change for each isoform normalized to the control group (*dashed line*). The expression of hypoxanthine-guanine phosphoribosyltransferase (HPRT) was used for normalization. Data are means ± SEM of $n = 8$ hearts. **(B)** Representative immunoblots indicating SOD2 immunoreactivity in the RV and LV from control (C) and L-NAME (L)-treated animals. SOD2 values were normalized to GAPDH levels. **(C)** Densitometric analysis of immunoblot bands. SOD2 was significantly increased in the LV from L-NAME fed animals (*gray bar*) compared with control animals (*white bar*). Data are means ± SD of $n = 5$ hearts. *$p < 0.05$ *versus* control.

The cell shortening seen in the LV cardiomyocytes was significantly reduced if the myocytes incubated with L-NAME were also incubated with the translation inhibitor cycloheximide, the transcription inhibitor actinomycin D, or the Sirt1 inhibitor Ex-527 (Fig. 7D). Under these conditions, the induction of the SOD2 expression failed to materialize (Fig. 7A, B). The MAP kinase inhibitor PD98059 did not have any effect on the cell contraction.

Effect of L-NAME on the cardiac remodeling of the extracellular matrix

Finally, the development and induction of cardiac fibrosis was analyzed in response to the different level of ROS in the RV and LV.

The causal involvement of the cytokine transforming growth factor beta1 (TGF-beta1) in the progression of chronic cardiac insufficiency has already been well documented. It also plays a critical role in the development and maintenance of cardiac fibrosis.

The expression patterns for TGF-beta1 and the extracellular matrix proteins collagen I and collagen III were analyzed separately for the RV and LV using real-time reverse transcription polymerase chain reaction (RT-PCR). In the LV, only the

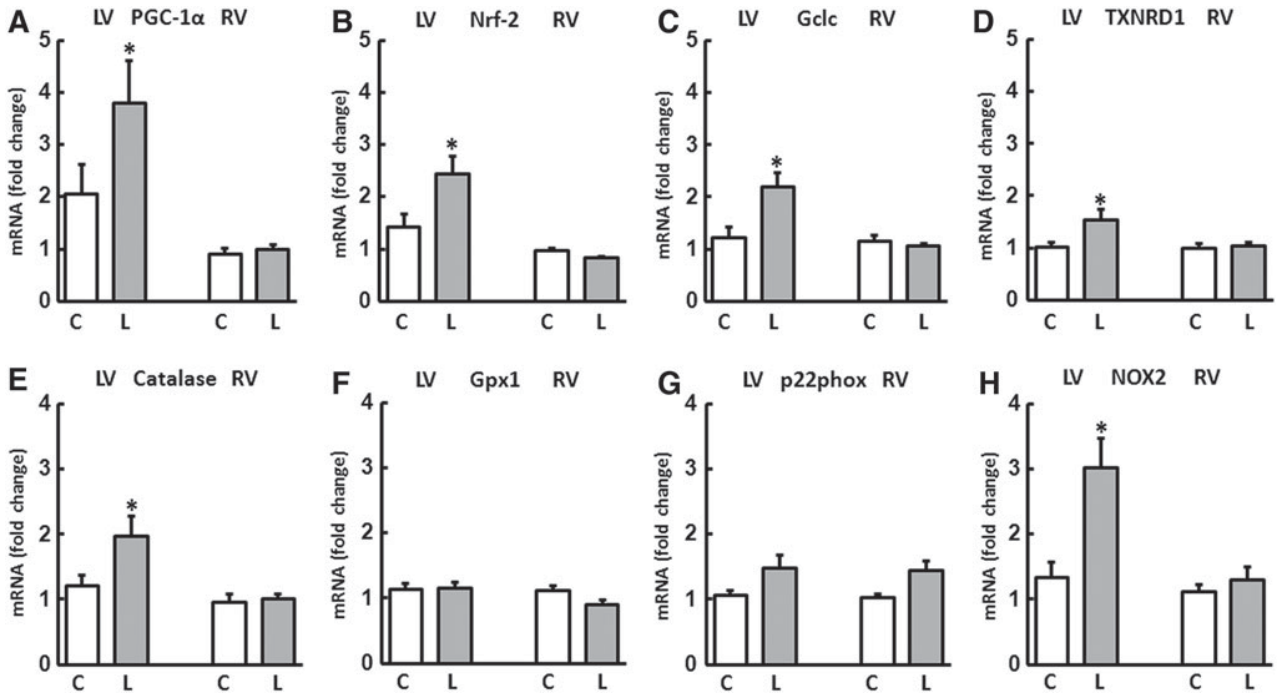

FIG. 6. Regulation of genes involved in redox homeostasis and antioxidative defense. The expression of mRNA was analyzed in the RV and LV of control (C) and L-NAME (L)-fed animals. The transcription factors **(A)** PGC-1α and **(B)** nuclear respiratory factor-2 (Nrf-2) as well as their downstream targets **(C)** glutamate cysteine ligase (Gclc) and **(D)** thioredoxin reductase 1 (TXNRD1) were selectively induced in the LV of L-NAME fed animals. L-NAME also induced the expression of **(E)** catalase in the LV but had no effect on the expression of **(F)** glutathione peroxidase 1 (Gpx1). Expression of **(G)** p22phox was not influenced but that of **(H)** NOX2 was induced by L-NAME in the LV. Data are means ± SD of $n = 8$ hearts. *$p < 0.05$ *versus* control.

expression of TGF-beta1 was reduced in L-NAME fed animals by 19% ± 3% compared with their drinking-water controls. In the LC and LT groups, no change could be detected in the expression of any of the genes investigated. In contrast to the normal finding in the LV, TGF-beta1 was upregulated in the RV in the L group by 102% ± 6%. The expression of collagen I was increased by 156% ± 16%, and that of collagen III was increased by 280% ± 26%. Both the increase in the TGF-beta1 and the induction of the two collagen isoforms could be significantly reduced by captopril and tempol (Fig. 8A–C).

The massive upregulation of the collagen in the RV of L-NAME-fed animals could subsequently be confirmed using Sirius Red staining in histological sections. Qualitatively, the areas close to the interventricular septum were particularly affected by an increased incorporation of extracellular matrix proteins. Localization of the fibrosis along the RV circumference was limited primarily to endocardial and epicardial compartments (Fig. 8D, E).

However, when the antihypertensive hydralazine was combined with L-NAME after 2 weeks of L-NAME treatment, the blood pressure fell from 160 ± 6 mm Hg (after 2 weeks of L-NAME) to 126 ± 5 mm Hg. However, due to the inability of hydralazine to prevent L-NAME-induced $O_2^{-\bullet}$ production, the hearts from this group also displayed a significant upregulation of TGF-beta1 only in the RV (Supplementary Fig. S5).

The structural remodeling of the RV and LV in eNOS$^{-/-}$ mice

To validate results obtained from L-NAME experiments, eNOS$^{-/-}$ mice were used as another model for a chronic deficiency in NO. Comparable to the mRNA expression pattern in the RV and LV of L-NAME fed animals, SOD2 was upregulated only in the LV of eNOS$^{-/-}$ mice, whereas the expression of TGF-beta1 and collagen I did not change in the LV but was significantly increased in the RV (Supplementary Fig. S6).

Discussion

The state of chronically reduced bioavailability of NO is a risk factor for the entire cardiovascular system, which can be attributed to the increased hemodynamic, oxidative, and fibrotic stress. In this study, the conditions were created for a corresponding scenario in 3-month-old female Wistar rats by feeding them the nonspecific NOS inhibitor L-NAME. Once the 4-week treatment period was complete, the cardiac remodeling was characterized separately for the RV and LV while considering the structural and functional adaptive responses.

Unlike the LV, the RV did not display the necessary adaptive mechanisms to cope with increased oxidative stress, the main and new finding of this study. The radical load induced by L-NAME in the RV myocardium led to the formation of a dilated cardiomyopathy with pronounced contractile dysfunction and cardiac fibrosis. The endogenous antioxidant potential prevented a corresponding structural and functional remodeling in the LV. Using adjuvant therapy with the SOD-mimetic tempol or captopril, which also has an antioxidative effect, the vicious cycle of free radical generation, fibrosis, and contractile dysfunction could be disrupted in the RV. Using the model of isolated cardiomyocytes, it

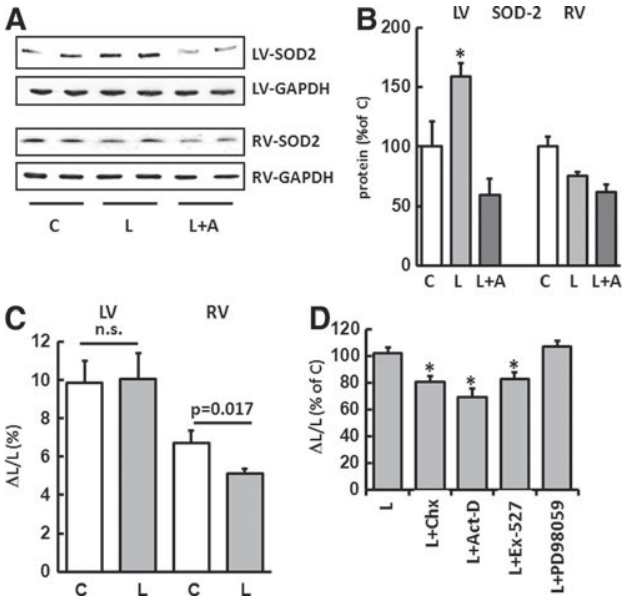

FIG. 7. Effects of L-NAME on SOD2 expression and cell shortening at a cellular level. (A) Representative immunoblots indicating SOD2 immunoreactivity in isolated cardiomyocytes from untreated control cells (C), cells incubated for 24 h with L-NAME (L) and L-NAME plus actinomycin D (L + A). SOD2 values were normalized to GAPDH levels. **(B)** Densitometric analysis of immunoblot bands. SOD2 was upregulated only in myocytes isolated from the LV. Data are means ± SD of $n = 4$ hearts. **(C)** Effect of L-NAME on cell shortening. Cardiomyocytes were isolated separately from the RV and LV of untreated rats and incubated with L-NAME for 24 h. L-NAME led to a significant reduction in relative cell shortening only in RV myocytes. Data are means ± SD of $n = 4$ hearts. **(D)** Cell shortening of LV cardiomyocytes was significantly reduced if myocytes were co-incubated with L-NAME (L) and the translation inhibitor cycloheximide (L + Chx), the transcription inhibitor actinomycin D (L + Act-D), or the Sirt1 inhibitor Ex-527 (L + Ex-527). PD98059 (L + PD98059) did not have any effect on cell contraction. Data are means ± SD of $n = 4$ hearts. $^*p < 0.05$ *versus* control.

could also be shown that the specific endogenous properties of RV myocytes were critically involved in the diagnosed RV dysfunction.

In general, the RV is characterized by a high degree of plasticity. If it detects systemic perfusion due to a patent arterial duct while still in the uterus, this function is transferred from birth onward to the left half of the heart (26). The myocardium of the RV adjusts postpartum to its new function and is characterized from this point on by a high degree of elasticity due to the low wall thickness. The structure and geometry are designed for volume work and can adjust more easily to an increased preload than to an increase in the afterload (26).

The contribution of the RV to maintaining appropriate blood circulation was underestimated for many years, and research into its specific physiology was neglected. However, its importance for the entire cardiovascular system can be explained solely by the fact that physical performance correlates more strongly with RV function than with LV function (4).

Gulati *et al.* diagnosed an RV dysfunction in 30% of patients with nonischemic dilated cardiomyopathy and identified this as an independent risk factor that was associated with a fourfold higher total mortality (24). Comparable results were obtained by Mehta *et al.* for the involvement of the RV in LV myocardial infarction, and they describe an increased rate of postischemic complications and fatalities (35). For pulmonary hypertension, the right heart function was even identified as a critical predictor for premature mortality, although the RV has the potential to adjust in the long term to a pathologically increased afterload by means of compensatory hypertrophy (25).

The chronic application of L-NAME in drinking water is an established model for arterial hypertension. The increased vascular resistance and the vascular remodeling are induced by a lowering of the NO level and activation of the systemic and local renin–angiotensin systems as well as greater oxidative stress (23). The therapeutic use of the ACE-inhibitor captopril led to a significant fall in the systolic blood pressure, while the antioxidant tempol was only able to prevent a further increase in the last 2 weeks.

The involvement of ROS in cardiovascular effects induced by L-NAME has already been demonstrated by Kumar *et al.*, who were even able to significantly lower the blood pressure using oral application of syringic acid, a naturally occurring antioxidant (30). A reduction of oxidative stress through selective inhibition of xanthine oxidase by allopurinol had no effect on hypertension but significantly improved the L-NAME-induced cardiac remodeling (28). The significantly elevated plasma MDA levels, which can be attributed to an increase in the lipid peroxidation, suggest that chronic application of L-NAME also led to an increase in radical stress in the model used here.

However, histological and molecular results indicate that the cause of the RV dysfunction is a massive increase in oxidative stress. NADPH oxidase, xanthine oxidase, and the renin–angiotensin system were identified as potential sources of excessive radical production under chronic L-NAME application (46). ROS, generated by NADPH oxidases, also induce the formation of ROS in mitochondria, which, in turn, stimulate radical production in the cytosol, thus inducing a self-sustaining vicious cycle (17, 38, 40). A targeted pharmacological intervention using substances with an antioxidant potential specific for mitochondrial ROS disrupts this feed-forward cycle efficiently (44).

This therapeutic approach corresponds to the endogenous upregulation of SOD2 in the LV of animals treated with L-NAME. The type 2 isoform of SOD, which is also known as manganese superoxide dismutase (Mn-SOD), catalyzes the formation of H_2O_2 from superoxide anions, specifically in the mitochondria.

As a direct consequence of the RV radical load, the induction of the cytokine TGF-beta is a key mechanism that is responsible for the development of fibrosis and RV failure (12, 27, 31).

In addition to RV fibrosis, which primarily affects ventricular stiffness and thus diastolic filling, a higher degree of oxidized Tm (oxTm) could be identified in RV of animals fed L-NAME. The formation of DCB induced by oxidative stress leads to a conformational change of Tm protein, which directly affects contractile function. However, the observed modification of Tm in RV of L-NAME-fed animals is likely to be responsible for the deterioration in RV systolic pressure as well as for the reduction in dp/dt max and dp/dt min (14, 15).

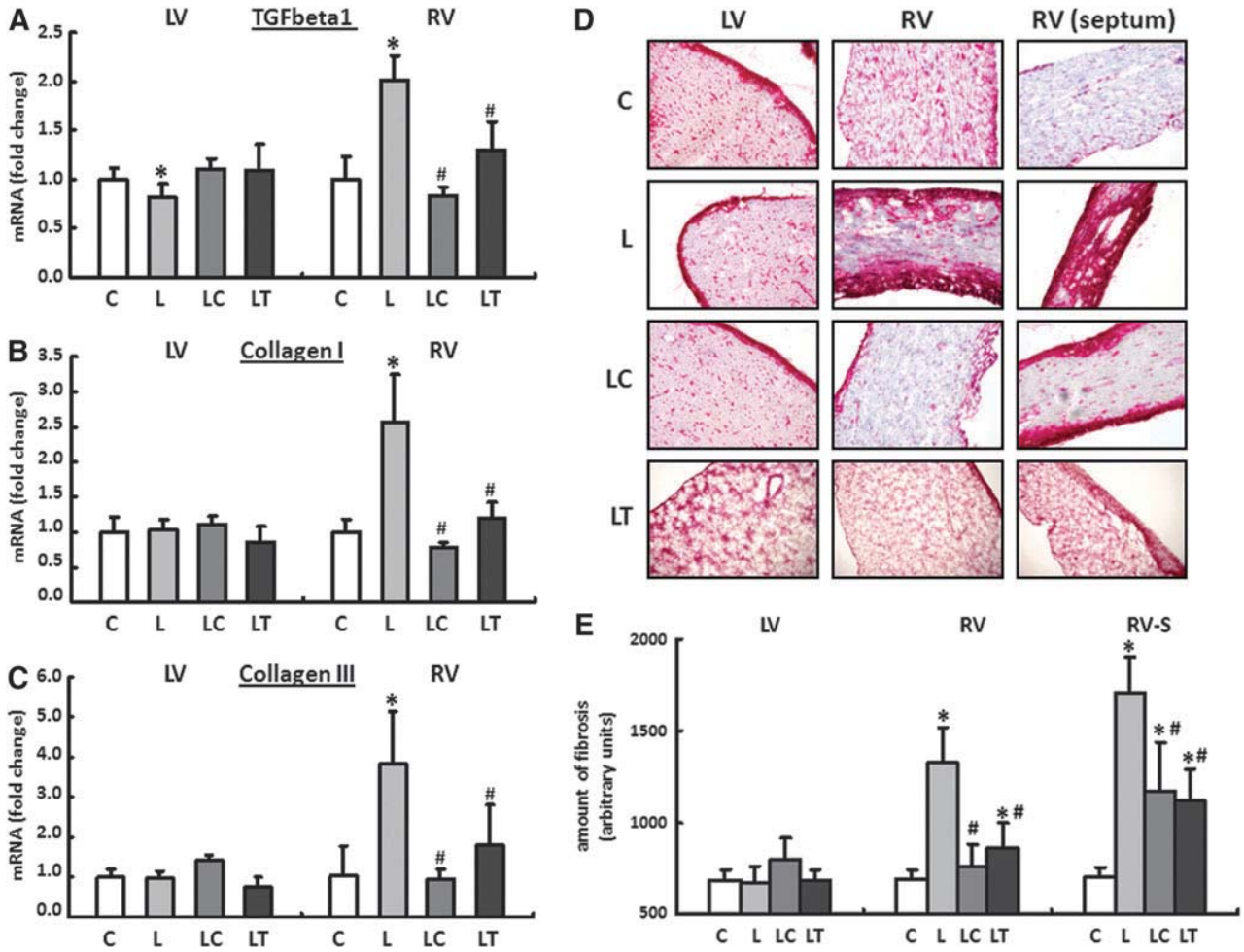

FIG. 8. Cardiac remodeling of the extracellular matrix. The mRNA expression for **(A)** transforming growth factor beta1 (TGF-beta1), **(B)** collagen I, and **(C)** collagen III was analyzed in all four treatment groups separately for the RV and LV using real-time reverse transcription polymerase chain reaction (RT-PCR). Rats were given pure drinking water (C), L-NAME (L), L-NAME plus captopril (LC), and L-NAME plus tempol (LT). The expression of HPRT was used for normalization. Data are means ± SEM of $n = 8$ hearts. **(D, E)** The massive upregulation of collagen I and III in the RV of L-NAME-fed animals (L) could be confirmed subsequently in histological sections with the help of Sirius Red staining. RV fibrosis could be significantly reduced by captopril (LC group) or tempol (LT group). RV (septum): RV close to the septum interventricularis. Data are means ± SD of $n = 5$ hearts. $^{*}p < 0.05$ *versus* control, $^{\#}p < 0.05$ *versus* L-NAME.

The missing upregulation of SODs in the RV together with the accumulation of $O_2^{-\bullet}$ have also led to a selective increase in peroxynitrite in the RV of animals fed L-NAME.

The intrinsically higher RV $ONOO^-$ concentration compared with the LV conforms to the results obtained with the DHE-based radical staining. The induction of the LV TXNRD1 expression described is critically involved in the detoxification of $ONOO^-$ by making peroxiredoxin available.

The significant reduction in free radicals achieved by tempol, therefore, also led to a normalization of the $ONOO^-$ concentration in the RV in the LT group. Because both ROS and NO are required for the formation of $ONOO^-$, the increase in peroxynitrite in the RV of the LC group could possibly be explained by the stimulatory effect of captopril on NO production. The inhibitory effect on the RAS, direct antioxidative effects, and the increased formation of NO are some of the protective properties of captopril that can generally contribute to a reduction in oxidative stress (9, 22). To what extent the increased formation of $ONOO^-$ in the RV of the LC group influences structural or functional remodeling cannot be determined based on the current data. Furthermore, the significance of $ONOO^-$ as an exclusively harmful compound is in doubt, and its involvement in the maintenance of the redox homeostasis and stress adaptation is the subject of ongoing discussion (3, 19, 20).

The inability of the RV to appropriately adjust its antioxidant capacity under pathophysiological conditions caused by L-NAME or an eNOS knockout led to an increase in the formation of free radicals (DHE staining, MitoSox Red), an increased percentage of oxTm, and a rise in the formation of peroxynitrite. The causes of the resultant cardiac dysfunction are based on a structurally remodeled ventricle with a significantly increased quantity of collagen and the impaired function of the RV cardiomyocytes themselves. The restrictive components of the cardiac symptoms led to an increase in the liver transaminases GOT/GPT *via* blood accumulation in the liver.

The LV was able to critically elevate its antioxidant potential by inducing PGC-1α and its downstream target Nrf-2 (10). Nrf-2 dependent genes, which include the cytoprotective proteins Gclc and TXNRD1 along with SOD2, prevented both the structural remodeling and the impaired function of the LV myocardium (11, 18). The transcription of PGC-1α is, in turn, regulated by Sirt1, the inhibition of which by Ex-527 led to a reduction in the cell shortening of LV isolated myocytes as did the inhibition of transcription by actinomycin D (Act-D) and the inhibition of translation by Chx. The previously described upregulation of SOD2 was prevented by a blockade of this signaling pathway.

Both therapeutic interventions, captopril and tempol, had an equally positive effect on the cardiac remodeling of the RV independent of their antihypertensive efficiency. Moreover, hydralazine with strong antihypertensive but no antioxidative properties was unable to prevent the induction of the RV remodeling (6). These results support the conjecture that neither the blood pressure nor an elevated afterload but rather ROS is the cause of the RV symptoms. This situation is supported by the results of the cell culture experiments that confirmed the impaired adaptation mechanisms (reduced SOD2 expression) and the resulting impaired function of the RV myocardium independent of systemic influences and blood pressure.

To what extent the application of L-NAME affected the pulmonary arterial pressure was not determined in this study. Sekiguchi *et al.* compared the peripheral and pulmonary arterial blood pressure in spontaneously hypertensive rats and rats fed L-NAME (2 weeks, 50 mg/100 ml). Systemic hypertension was recorded in both models. An increase in the pulmonary arterial pressure could, however, only be diagnosed in the spontaneously hypertensive rats (SHR), while the chronic application of L-NAME did not have any effect on the pressure ratios in the pulmonary circulation system (43). These results correspond to the expression pattern described in this study for the natriuretic peptide ANP. The increased afterload in the LV, associated with a moderate hypertrophy, led to a significant increase in the LV ANP expression. The lack of induction of ANP expression in the RV myocardium indicates that the pressure conditions in the pulmonary circulation are unchanged.

In light of this, the results of this study can be translated to cardiac diseases that are associated with elevated oxidative stress and, subsequently, can induce the development of RV failure (10). Without itself being the starting point of the symptoms, for the RV there is an elevated risk of being secondarily damaged due to increased accumulation of ROS during LV failure or LV infarction.

In summary, the results of this study show for the first time that oxidative stress is a vastly greater risk factor for the RV than for the LV. Molecular and cellular results indicate that critical signaling pathways and key enzymes in the RV and LV are activated and regulated in different ways, which may lead to the development of targeted therapy against RV failure. Indeed, our results suggest that the prognosis for RV failure can be greatly improved by using ACE inhibitors with high antioxidant capacity.

Materials and Methods

The investigation conforms the Guide for the Care and Use of Laboratory Animals published by the US National Institute of Health (NIH Publication No. 85-23, revised 1996). The study was approved by the local authorities for animal experiments (V54-19c 2015 (I) GI 20/1 Nr. 58-2005).

Experimental model

Eighty-two 3-month-old female wistar rats were divided into four groups and kept in individual cages. Animals had free access to food and water *ad libitum*. Animals were assigned to receive L-NAME (7.5 mg/day in drinking-water), L-NAME plus captopril (5.0 mg/day in drinking-water) (2), L-NAME plus tempol (1.0 m*M* in drinking-water) (5), L-NAME plus hydralazine (5.0 mg/day in drinking-water) (42), or drinking-water only (age-matched control) for 28 days (Supplementary Fig. S1A). As an alternative model for a chronic deficiency in NO, 6-month-old female $eNOS^{-/-}$ mice and their wild-type littermates were used.

The health status of the experimental animals was determined weekly using a ''distress score'' (33). Over the entire experimental period, no animals died or had to be excluded from the study based on the exclusion criteria.

Determination of the blood pressure and heart rate

Peak systolic blood pressure and heart rate were measured weekly using the non-invasive tail-cuff method (TSE-Systems, 209000Series). Before the start of the study, the animals were adjusted to the experimental procedure over 1 week. The mean of 10 consecutive blood pressure readings was obtained for each animal at weekly intervals.

RNA isolation and real-time RT-PCR

Total RNA was isolated from RV and LV using peqGold TriFast (peqlab; Biotechnologie GmbH) according to the manufacturer's protocol. To remove genomic DNA contamination, isolated RNA samples were treated with 1 U DNase/μg RNA (Invitrogen) for 15 min at 37°C. One μg of total RNA was used in a 10 μl reaction to synthesize cDNA using Superscript RNaseH Reverse Transcriptase (200 U/μg RNA; Invitrogen) and oligo dTs as primers. RT reactions were performed for 50 min at 37°C. Real-time quantitative PCR was performed using the MyiQ® detection system (Bio-Rad) in combination with the iTaq Universal SYBR Green Real-Time PCR Supermix (Bio-Rad). Quantification was performed as described earlier (32). Primer sequences are listed in Supplementary Table S4.

Picrosirius red staining

Samples were embedded with Tissue-Tek® (Sakura) and sectioned in 10 μm slices. Histological sections were fixed in Bouin solution and subsequently stained in 0.1% (wt/vol) Sirius Red solution (Sigma-Aldrich Chemie). Sections were washed by 0.01 N HCl, Aqua dest. and counterstained for nuclei by Mayers hemalaun solution, washed with Aqua dest. for 5 min, and dehydrated with ethanol. Total collagen content was quantified by digital image analysis using Leica Confocal Software Lite Version (LCS Lite). The mean of $n = 5$ preparations was used to quantify the extent of interstitial fibrosis.

Measurement of superoxide

To perform DHE staining, cryosections of RV and LV were incubated with DHE (dissolved in 1 X PBS) for 10 min

at 37°C in a light-protected humidity chamber, then fixed with Dako Fluorescent Mounting Medium (Dako, North America, Inc.). Slides were then imaged by confocal microscopy (LSM 510 META; Carl Zeiss) using an excitation wavelength of 488 nm; emission was recorded at 540 nm (37).

Analysis was performed by digital image analysis using Leica Confocal Software Lite Version (LCS Lite). The mean fluorescence intensity of $n = 5$ ventricles was used to quantify the extent of superoxide.

Mitochondrial ROS analysis

Formation of ROS in mitochondria was detected with MitoSOX Red, a mitochondrial superoxide fluorescence indicator. Briefly, isolated cardiomyocytes were incubated with 1 μM MitoSOX Red at 37°C for 30 min and then washed twice for 10 min in CCT medium. The loaded cells were excited at 510 nm, and the emitted light was collected at 580 nm (1).

Detection of MDA using a TBARS Assay Kit

The formation of MDA was used as a well-established indicator of oxidative stress in plasma samples. Shortly, blood samples from treated and untreated rats were centrifuged (1500 *g*) at 4°C for 15 min to obtain plasma. One hundred microliters sample was incubated with TBA under acid conditions for 60 min at 95°C. Sample vials were then placed on ice for 10 min and centrifuged for 10 min at 1600 *g*. One hundred fifty microliters reaction mixture was measured fluorometrically in duplicate at an excitation wavelength of 530 nm and an emission wavelength of 550 nm. The tests were carried out using TBARS Assay Kit purchased from Cayman Chemical Company.

Measurement of peroxynitrite

To estimate peroxynitrite formation in the RV and LV, we measured peroxynitrite marker nitrotyrosine by ELISA (components from Cayman Chemical) in ventricular homogenates as previously described (8, 16). Briefly, RV and LV tissue samples were pulverized in liquid nitrogen, sonicated in 4× homogenization buffer, and centrifuged. Supernatants were then incubated overnight with anti-nitrotyrosine rabbit IgG and nitrotyrosine acetylcholinesterase tracer in precoated (mouse anti-rabbit IgG) microplates followed by development with Ellman's reagent. Protein concentration of the samples was measured by the bicinchoninic acid assay.

Western blot

Total protein was extracted from RV and LV using Cell Lysis Buffer (10×) (Cell Signaling) according to the manufacturer's protocol. Briefly, the homogenate was centrifuged at 14,000 g at 4°C for 10 min and the supernatant was treated with Laemmli buffer. Protein samples were loaded on NuPAGE Bis-Tris Precast gels (10%; Life Technology) and, subsequently, transferred onto nitrocellulose membranes. Blots were incubated with one of the following antibodies: anti-Tm purchased from Sigma-Aldrich (product T9283) or anti SOD2 purchased from Merck Millipore (product 06-984). Secondary antibodies [horseradish peroxidase (HRP)-conjugated] directed against rabbit IgG or mouse IgG were purchased from Sigma-Aldrich, respectively Affinity Biologicals.

Hemodynamic measurements

Heart function was measured in closed-chest spontaneously breathing rats anesthetized with thiopental sodium (Trapanal® 60 mg/kg i.p.) using ultraminiature catheter pressure transducers (3 F; Millar Instruments, Inc.). Briefly, the rats were placed in supine position on a heating pad and the RV catheter (model SPR-291) was inserted into the right jugular vein and advanced into the RV *via* the right atrium. Heart rate, RV systolic pressure, and the rate in rise and fall of ventricular pressure (RV dp/dt) were recorded continuously on a PC at a sampling rate of 1 kHz using PowerLab 16/30 with Quad Bridge Amp and LabChart 7 software (all ADInstruments) for 10–15 min.

Langendorff perfusion

To analyze LV function, conditioned rats were anaesthetized by isoflurane and killed by cervical dislocation. Thereafter, hearts were rapidly excised and the aorta was cannulated for retrograde perfusion with a 16-gauge needle connected to a Langendorff perfusion system. A polyvinyl chloride balloon was inserted into the LV through the mitral valve and held in place by a suture tied around the left atrium. The other end of the tubing was connected to a pressure transducer for continuous measurement of LV pressure, dp/dt max, and dp/dt min (41).

Measurements of transaminases (GOT/GPT) in blood plasma

To quantify GOT/GPT levels in plasma samples, the rat aspartate aminotransferase ELISA Kit from Bioassay Technology Laboratory was used. The test procedure was performed according to the manufacturer's instructions. Briefly, blood samples from treated and untreated rats were centrifuged (1500 *g*) for 15 min to obtain plasma. Forty microliters of plasma were then incubated in duplicate with 10 μl biotin-labeled anti GOT/GPT antibodies and streptavidin-HRP. The liquid turned blue after adding chromogen solution and yellow with the effect of acid. The color intensity correlates positively with the concentration of GOT/GPT.

Isolation and cultivation of cardiomyocytes from the RV and LV

Heart muscle cells from the RV and LV were isolated from 3-month-old male wistar rats. Briefly, hearts were excised, transferred rapidly to ice-cold saline, and mounted on the cannula of a Langendorff perfusion system. Heart perfusion and subsequent steps were performed at 37°C. First, hearts were perfused in a non-circulating manner for 5 min at 10 ml/min. Thereafter, perfusion was continued with recirculation using 50 ml perfusate supplemented with 0.06% (w/v) crude collagenase and 25 μM $CaCl_2$ at 5 ml/min for 25 min. Then, the RV was dissected from the LV and septum and processed separately in the next few steps (47).

Isolated cardiomyocytes were then incubated with L-NAME (1.0 mM; Sigma-Aldrich, product N5751) alone and in the presence of cyclohexemide (35.0 μM; Sigma-Aldrich, product C-7698), actinomycin D (5.0 μM; Sigma-Aldrich, product A5142), Ex-527 (10.0 μM; Sigma-Aldrich, product E7034), or PD98059 (10.0 μM; Merck Millipore, product 513000) for 24 h.

Determination of cell contraction

Cell shortening was measured as described earlier in greater detail (47). Briefly, isolated cardiomyocytes were allowed to contract at room temperature and analyzed using a cell-edge detection system. Cells were stimulated *via* two AgCl electrodes with biphasic electrical stimuli composed of two equal but opposite rectangular 50-V stimuli of 0.5 ms duration. Each cell was stimulated for 1 min at a frequency of 2.0 Hz. Every 15 s contractions were recorded. The mean of these four measurements was used to define the cell shortening of a given cell. Cell lengths were measured *via* a line camera (data recording at 500 Hz). Data are expressed as cell shortening normalized to diastolic cell length (dL/L [%]).

Statistics

Data are expressed as indicated in the legends. ANOVA and the Student–Newman–Keuls test for *post hoc* analysis were used to analyze experiments in which more than one group was compared. In cases in which two groups were compared, Student's *t*-test or Mann–Whitney test was employed, depending on a normal distribution of samples (Levene test). $p < 0.05$ was regarded as significant.

Acknowledgments

The study was supported by the Deutsche Forschungsgemeinschaft (DFG) and received funding through the Excellence Cluster Cardio-Pulmonary System (ECCPS, Giessen). C.C. holds a János Bolyai fellowship; P.F. is a Szentágothai Fellow of the National Program of Excellence (Grant TAMOP 4.2.4.A/2-11-1-2012-0001).

Author Disclosure Statement

No competing financial interests exist.

References

1. Abdallah Y, Kasseckert SA, Iraqi W, Said M, Shahzad T, Erdogan A, Neuhof C, Gündüz D, Schlüter KD, Tillmanns H, Piper HM, Reusch HP, and Ladilov Y. Interplay between Ca^{2+} cycling and mitochondrial permeability transition pores promotes reperfusion-induced injury of cardiac myocytes. J Cell Mol Med 15: 2478–2485, 2011.
2. Amazonas R, de Almeida Sanita R, Kawachi H, and Lopes de Faria J. Prevention of hypertension with or without renin-angiotensin system inhibition precludes nephrin loss in the early stage of experimental diabetes mellitus. Nephron Physiol 107: 57–64, 2007.
3. Andreadou I, Iliodromitis EK, Rassaf T, Schulz R, Papapetropoulos A, and Ferdinandy P. The role of gasotransmitters NO, H_2S, CO in myocardial ischemia/reperfusion injury and cardioprotection by preconditioning, postconditioning, and remote conditioning. Br J Pharmacol 2014 doi: 10.1111/bph.12811.
4. Baker BJ, Wilen MM, Boyd CM, Dinh H, and Franciosa JA. Relation of right ventricular ejection fraction to exercise capacity in chronic left ventricular failure. Am J Cardiol 54: 596–599, 1984.
5. Banday AA, Marwaha A, Tallam LS, and Lokhandwala MF. Tempol reduces oxidative stress, improves insulin sensitivity, decreases renal dopamine D1 receptor hyperphosphorylation, and restores D1 receptor-G-protein coupling and function in obese Zucker rats. Diabetes 54: 2219–2226, 2005.
6. Bauersachs J, Bouloumié A, Fraccarollo D, Hu K, Busse R, and Ertl G. Hydralazine prevents endothelial dysfunction, but not the increase in superoxide production in nitric oxide-deficient hypertension. Eur J Pharmacol 362: 77–81, 1998.
7. Baylis C. Nitric oxide deficiency in chronic kidney disease. Am J Physiol Renal Physiol 294: 1–9, 2008.
8. Bencsik P, Kupai K, Giricz Z, Görbe A, Pipis J, Murlasits Z, Kocsis GF, Varga-Orvos Z, Puskás LG, Csonka C, Csont T, and Ferdinandy P. Role of iNOS and peroxynitrite-matrix metalloproteinase-2 signaling in myocardial late preconditioning in rats. Am J Physiol Heart Circ Physiol 299: 512–518, 2010.
9. Benzie IF and Tomlinson B. Antioxidant power of angiotensin-converting enzyme inhibitors *in vitro*. Br J Clin Pharmacol 45: 168–169, 1998.
10. Borchi E, Bargelli V, Stillitano F, Giordano C, Sebastiani M, Nassi PA, d'Amati G, Cerbai E, and Nediani C. Enhanced ROS production by NADPH oxidase is correlated to changes in antioxidant enzyme activity in human heart failure. Biochim Biophys Acta 1802: 331–338, 2010.
11. Buelna-Chontal M, Guevara-Chávez JG, Silva-Palacios A, Medina-Campos ON, Pedraza-Chaverri J, and Zazueta C. Nrf2-regulated antioxidant response is activated by protein kinase C in postconditioned rat hearts. Free Radic Biol Med 74: 145–156, 2014.
12. Bujak M and Frangogiannis NG. The role of TGF-β signaling in myocardial infarction and cardiac remodeling. Cardiovasc Res 74: 184–195, 2007.
13. Cannon RO 3rd. Role of nitric oxide in cardiovascular disease: focus on the endothelium. Clin Chem 44: 1809–1819, 1998.
14. Canton M, Skyschally A, Menabò R, Boengler K, Gres P, Schulz R, Haude M, Erbel R, Di Lisa F, and Heusch G. Oxidative modification of tropomyosin and myocardial dysfunction following coronary microembolization. Eur Heart J 27: 875–881, 2006.
15. Canton M, Menazza S, Sheeran FL, Polverino de Laureto P, Di Lisa F, and Pepe S. Oxidation of myofibrillar proteins in human heart failure. J Am Coll Cardiol 57: 300–309, 2011.
16. Csont T, Csonka C, Onody A, Gorbe A, Dux L, Schulz R, Baxter GF, and Ferdinandy P. Nitrate tolerance does not increase production of peroxynitrite in the heart. Am J Physiol Heart Circ Physiol 283: 69–76, 2002.
17. Dikalov S. Cross talk between mitochondria and NADPH oxidases. Free Radic Biol Med 51: 1289–1301, 2011.
18. Do MT, Kim HG, Choi JH, and Jeong HG. Metformin induces microRNA-34a to downregulate the Sirt1/Pgc-1α/Nrf2 pathway, leading to increased susceptibility of wild-type p53 cancer cells to oxidative stress and therapeutic agents. Free Radic Biol Med 74: 21–34, 2014.
19. Ferdinandy P. Peroxynitrite: just an oxidative/nitrosative stressor or a physiological regulator as well? Br J Pharmacol 148: 1–3, 2006.
20. Ferdinandy P and Schulz R. Nitric oxide, superoxide, and peroxynitrite in myocardial ischaemia-reperfusion injury and preconditioning. Br J Pharmacol 138: 532–543, 2003.
21. Gaucher C, Boudier A, Dahboul F, Parent M, and Leroy P. S-nitrosation/denitrosation in cardiovascular pathologies: facts and concepts for the rational design of S-nitrosothiols. Curr Pharm Des 19: 458–472, 2013.
22. Gauthier KM, Cepura CJ, and Campbell WB. ACE inhibition enhances bradykinin relaxations through nitric oxide

and B1 receptor activation in bovine coronary arteries. Biol Chem 394: 1205–1212, 2013.
23. Gonzalez W, Fontaine V, Pueyo ME, Laquay N, Messika-Zeitoun D, Philippe M, Arnal JF, Jacob MP, and Michel JB. Molecular plasticity of vascular wall during N(G)-nitro-L-arginine methyl ester-induced hypertension: modulation of proinflammatory signals. Hypertension 36: 103–109, 2000.
24. Gulati A, Ismail TF, Jabbour A, Alpendurada F, Guha K, Ismail NA, Raza S, Khwaja J, Brown TD, Morarji K, Liodakis E, Roughton M, Wage R, Pakrashi TC, Sharma R, Carpenter JP, Cook SA, Cowie MR, Assomull RG, Pennell DJ, and Prasad SK. The prevalence and prognostic significance of right ventricular systolic dysfunction in nonischemic dilated cardiomyopathy. Circulation 128: 1623–1633, 2013.
25. Handoko ML, de Man FS, Allaart CP, Paulus WJ, Westerhof N, and Vonk-Noordegraaf A. Perspectives on novel therapeutic strategies for right heart failure in pulmonary arterial hypertension: lessons from the left heart. Eur Respir Rev 19: 72–82, 2010.
26. Hines R. Right ventricular function and failure: a review. Yale J Biol Med 64: 295–307, 1991.
27. Jain M, Rivera S, Monclus EA, Synenki L, Zirk A, Eisenbart J, Feghali-Bostwick C, Mutlu GM, Budinger GR, and Chandel NS. Mitochondrial reactive oxygen species regulate transforming growth factor-β signaling. J Biol Chem 288: 770–777, 2013.
28. Kasal DA, Neves MF, Oigman W, and Mandarim-de-Lacerda CA. Allopurinol attenuates L-NAME induced cardiomyopathy comparable to blockade of angiotensin receptor. Histol Histopathol 23: 1241–1248, 2008.
29. Kevin LG and Barnard M. Right ventricular failure. Contin Educ Anaesth Crit Care Pain 7: 89–94, 2007.
30. Kumar S, Prahalathan P, and Raja B. Syringic acid ameliorates (L)-NAME-induced hypertension by reducing oxidative stress. Naunyn Schmiedebergs Arch Pharmacol 385: 1175–1184, 2012.
31. Lijnen PJ, Petrov VV, and Fagard RH. Induction of cardiac fibrosis by transforming growth factor-beta(1). Mol Genet Metab 71: 418–435, 2000.
32. Livak KJ and Schmittgen TD. Analysis of relative gene expression data using real-time quantitative PCR and the 2(-delta delta C(T)). Methods 25: 402–408, 2001.
33. Lloyd MH and Wolfensohn SE. *Practical Use of Distress Scoring Systems in the Application of Humane Endpoints. Humane Endpoints in Animal Experiments for Biomedical Research*. London: Royal Society of Medicine Press, 1999, pp. 48–53.
34. Markel TA, Wairiuko GM, Lahm T, Crisostomo PR, Wang M, Herring CM, and Meldrum DR. The right heart and its distinct mechanisms of development, function, and failure. J Surg Res 146: 304–313, 2008.
35. Mehta SR, Eikelboom JW, Natarajan MK, Diaz R, Yi C, Gibbons RJ, and Yusuf S. Impact of right ventricular involvement on mortality and morbidity in patients with inferior myocardial infarction. J Am Coll Cardiol 37: 37–43, 2001.
36. Misík V, Mak IT, Stafford RE, and Weglicki WB. Reactions of captopril and epicaptopril with transition metal ions and hydroxyl radicals: an EPR spectroscopy study. Free Radic Biol Med 15: 611–619, 1993.
37. Nazarewicz RR, Bikineyeva A, and Dikalov SI. Rapid and specific measurements of superoxide using fluorescence spectroscopy. J Biomol Screen 18: 498–503, 2013.
38. Nediani C, Borchi E, Giordano C, Baruzzo S, Ponziani V, Sebastiani M, Nassi P, Mugelli A, d'Amati G, and Cerbai E. NADPH oxidase-dependent redox signaling in human heart failure: relationship between the left and right ventricle. J Mol Cell Cardiol 42: 826–834, 2007.
39. Pacher P, Beckman JS, and Liaudet L. Nitric oxide and peroxynitrite in health and disease. Physiol Rev 87: 315–424, 2007.
40. Queliconi BB, Wojtovich AP, Nadtochiy SM, Kowaltowski AJ, and Brookes PS. Redox regulation of the mitochondrial K(ATP) channel in cardioprotection. Biochim Biophys Acta 1813: 1309–1315, 2011.
41. Schreckenberg R, Maier T, and Schlüter KD. Post-conditioning restores pre-ischaemic receptor coupling in rat isolated hearts. Br J Pharmacol 156: 901–908, 2009.
42. Schreckenberg R, Wenzel S, da Costa Rebelo RM, Röthig A, Meyer R, and Schlüter KD. Cell-specific effects of nitric oxide deficiency on parathyroid hormone-related peptide (PTHrP) responsiveness and PTH1 receptor expression in cardiovascular cells. Endocrinology 150: 3735–3741, 2009.
43. Sekiguchi F, Yamamoto K, Matsuda K, Kawata K, Negishi M, Shinomiya K, Shimamur K, and Sunano S. Endothelium-dependent relaxation in pulmonary arteries of L-NAME-treated Wistar and stroke-prone spontaneously hypertensive rats. J Smooth Muscle Res 38: 131–144, 2002.
44. Shen X, Zheng S, Metreveli NS, and Epstein PN. Protection of cardiac mitochondria by overexpression of MnSOD reduces diabetic cardiomyopathy. Diabetes 55: 798–805, 2006.
45. Soetkamp D, Nguyen TT, Menazza S, Hirschhäuser C, Hendgen-Cotta UB, Rassaf T, Schlüter KD, Boengler K, Murphy E, and Schulz R. S-nitrosation of mitochondrial connexin 43 regulates mitochondrial function. Basic Res Cardiol 109: 433, 2014.
46. Suda O, Tsutsui M, Morishita T, Tanimoto A, Horiuchi M, Tasaki H, Huang PL, Sasaguri Y, Yanagihara N, and Nakashima Y. Long-term treatment with Nw-nitro-l-arginine methyl ester causes arteriosclerotic coronary lesions in endothelial nitric oxide synthase-deficient mice. Circulation 106: 1729–1735, 2002.
47. Tastan I, Schreckenberg R, Mufti S, Abdallah Y, Piper HM, and Schlüter KD. Parathyroid hormone improves contractile performance of adult rat ventricular cardiomyocytes at low concentrations in a non-acute way. Cardiovasc Res 82: 77–83, 2009.
48. Tessari P, Cecchet D, Cosma A, Vettore M, Coracina A, Millioni R, Iori E, Puricelli L, Avogaro A, and Vedovato M. Nitric oxide synthesis is reduced in subjects with type 2 diabetes and nephropathy. Diabetes 59: 2152–2159, 2010.
49. Verzi MP, McCulley DJ, De Val S, Dodou E, and Black BL. The right ventricle, outflow tract, and ventricular septum comprise a restricted expression domain within the secondary/anterior heart field. Dev Biol 287: 134–145, 2005.
50. Voelkel NF, Quaife RA, Leinwand LA, Barst RJ, McGoon MD, Meldrum DR, Dupuis J, Long CS, Rubin LJ, Smart FW, Suzuki YJ, Gladwin M, Denholm EM, Gail DB; National Heart, Lung, and Blood Institute Working Group on Cellular and Molecular Mechanisms of Right Heart Failure. Right ventricular function and failure: report of a National Heart, Lung, and Blood Institute working group on cellular and molecular mechanisms of right heart failure. Circulation 114: 1883–1891, 2006.

51. Zaffran S, Kelly RG, Meilhac SM, Buckingham ME, and Brown NA. Right ventricular myocardium derives from the anterior heart field. Circ Res 95: 261–268, 2004.

Address correspondence to:
Dr. Rolf Schreckenberg
Physiologisches Institut
Justus-Liebig-Universität Gießen
Aulweg 129
Gießen D-35392
Germany

E-mail: rolf.schreckenberg@physiologie.med.uni-giessen.de

Date of first submission to ARS Central, September 30, 2014; date of final revised submission, April 24, 2015; date of acceptance, May 13, 2015.

Abbreviations Used

ACE = angiotensin-converting enzyme
Act-D = actinomycin D
ANP = atrial natriuretic peptide
BNP = brain natriuretic peptide
bpm = beats per minute
BW = body weight
C = control group
Chx = cyclohexemide
DCB = disulphide cross-bridges
DHE = dihydroethidium
$eNOS^{-/-}$ = homozygous eNOS knockout
Gclc = glutamate-cysteine ligase, catalytic subunit
GOT/GPT = glutamate-oxaloacetate transaminase/glutamate-pyruvate transaminase
Gpx1 = glutathione peroxidase 1
H_2O_2 = hydrogen peroxide
HADHA = hydroxyacyl-CoA dehydrogenase, alpha subunit
HPRT = hypoxanthine-guanine phosphoribosyltransferase
HRP = horseradish peroxidase
L = L-NAME group
LC = L-NAME/captopril group
LT = L-NAME/tempol group
LV = left ventricle
LVDP = left ventricular developed pressure
LW = liver wet weight
MHC-α = myosin heavy chain alpha
MHC-β = myosin heavy chain beta
NO = nitric oxide
NOX2 = cytochrome b-245 heavy chain
Nrf(-1,-2) = nuclear respiratory factor (-1, -2)
$ONOO^-$ = peroxynitrite
oxTm = oxidized tropomyosin
P22phox = cytochrome b-245 light chain
PGC-1α = peroxisome proliferator-activated receptor gamma coactivator 1-alpha
RAAS = renin-angiotensin-aldosterone system
ROS = reactive oxygen species
RT-PCR = reverse transcription polymerase chain reaction
RV = right ventricle
RVEDP = right ventricular end-diastolic pressure
RVSP = right ventricular systolic pressure
SHR = spontaneously hypertensive rats
SOD (1-3) = superoxide dismutase (1-3)
TGF-beta1 = transforming growth factor beta1
Tm = tropomyosin
TXNRD1 = thioredoxin reductase 1
UCP(-2,-3) = mitochondrial uncoupling protein (-2, -3)

„Hiermit erkläre ich, dass ich die vorliegende Arbeit bzw. die mir zuzuordnenden Teile im Rahmen einer kumulativen Habilitationsschrift, selbstständig und ohne unzulässige Hilfe oder Benutzung anderer als der angegebenen Hilfsmittel angefertigt habe. Alle Textstellen, die wörtlich oder sinngemäß aus veröffentlichten oder nichtveröffentlichten Schriften entnommen sind, und alle Angaben, die auf mündlichen Auskünften beruhen, sind als solche kenntlich gemacht. Ich versichere, dass ich für die nach §2 (3) der Habilitationsordnung angeführten bereits veröffentlichten Originalarbeiten als Erst- oder Seniorautor fungiere, da ich den größten Teil der Daten selbst erhoben habe, für das Design der Arbeiten verantwortlich bin und die Manuskripte maßgeblich gestaltet habe. Für alle von mir erwähnten Untersuchungen habe ich die in der „Satzung der Justus-Liebig-Universität zur Sicherung guter wissenschaftlicher Praxis“ niedergelegten Grundsätze befolgt. Ich versichere, dass alle an der Finanzierung der Arbeiten beteiligten Geldgeber in den jeweiligen Publikationen genannt worden sind. Ich versichere außerdem, dass die vorgelegte Arbeit weder im Inland noch im Ausland in gleicher oder ähnlicher Weise einer anderen Prüfungsbehörde vorgelegt wurde oder Gegenstand eines anderen Prüfungsverfahrens war. Mit der Überprüfung meiner Arbeit durch eine Plagiatserkennungssoftware bzw. ein internetbasiertes Softwareprogramm erkläre ich mich einverstanden.“

Gießen, 01.08.2020

_____

Dr. Rolf Schreckenberg